Proceedings of 1st NATIONAL V/STOL AIRCRAFT SYMPOSIUM

Contd

3-4 NOVEMBER 1965

WRIGHT-PATTERSON AFB, OHIO

Proceedings of 1st NATIONAL V/STOL AIRCRAFT SYMPOSIUM

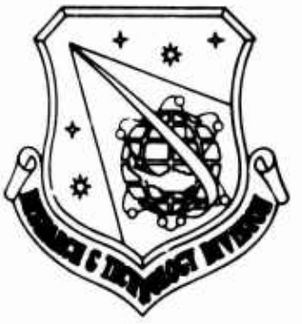

3-4 NOVEMBER 1965

WRIGHT-PATTERSON AFB, OHIO

FOREWARD

This document contains the complete text of the papers presented at the First National V/STOL Aircraft Symposium held at Wright Patterson Air Force Base, Ohio on 3 - 4 November 1965. This Symposium was sponsored by the American Helicopter Society and was co-hosted by the Aeronautical System Division and Systems Engineering Group, Research and Technology Division, of the Air Force Systems Command.

With the ever rising interest and activity in V/STOL aircraft throughout the free world, the Aeronautical Systems Division and American Helicopter Society are especially pleased to make available to our readers this collection of outstanding and timely papers.

TABLE OF CONTENTS

V/STOL Aircraft Design

The Influential Variables of V/STOL Propulsion
by Bill Rodenbaugh, and L. B. Veno,
General Electric Company I-1

Hot Cycle Rotor/Wing High Speed VTOL Aircraft
by M. S. Harned, and R. E. Head,
Hughes Tool Company I-29

A Comparative Study of Propeller Driven VTOLs for the Tri-Service Four Ton Requirement
by G. J. Howard, and H. D. Ulisnik,
Sikorsky Aircraft Company I-82

Impact of Jet VTOL Attitude Control on Mission Performance
by J. Patierno, and H. Asdurian,
Northrop Norair I-97

Effect of Size on VTOL Aircraft Hover and Low Speed Handling Qualities
by J. F. Johnson, and C. F. Friend,
Lockheed Aircraft Company I-133

V/STOL Subsystem Design

V/STOL Visual Flight Simulation Techniques
by R. J. Heintzman, JSAF II-1

The XC-142A Wing and Flap Control System
by G. K. Fling,
Ling Temco Vought II-40

X-22A Variable Stability System
by J. L. Beilman,
Cornell Aeronautical Laboratory II-51

Preliminary Development of a Trailing Rotor System
by J. A. DeTore,
Bell Helicopter Company II-105

ABSTRACT

The proceedings of the First National V/STOL Aircraft Symposium held at Wright Patterson Air Force Base, Ohio on 3 - 4 November 1965 are presented in this report. This Symposium was sponsored by the American Helicopter Society and was co-hosted by the Aeronautical Systems Division and Systems Engineering Group, Research and Technology Division, of the Air Force Systems Command.

The proceedings as set forth in this report are in the same order as presented during the meetings. The technical papers presented are grouped into the following three categories: (1) V/STOL Aircraft Design, (2) V/STOL Subsystem Design, and (3) V/STOL Aircraft Testing and Operation.

The Breguet 941/McDonnell 188 Cross-Shaft System
by H. J. DeGarcia,
McDonnell Aircraft Company II-118

V/STOL Aircraft Testing & Operation

The Canadair CL-84 V/STOL Tilt-Wing Prototype
by F. C. Phillips,
Canadair Limited III-1

Escape and Recovery Systems for V/STOL Aircraft
by James McCormack, and S. Blair Poteate Jr.,
USAF III-45

The XC-142A Flight Test Program
by T. W. Shepard,
Ling Temco Vought III-78

Lift Fan, V/STOL
by S. H. Spooner, and D. R. Geehring,
US Army and General Electric Company III-97

X-22A Flight Test Program
by R. L. Pfeiff,
Bell Aerosystems Company III-98

V/STOL AIRCRAFT DESIGN

Bernard Lindenbaum, USAF

Technical Session Chairman

THE INFLUENTIAL VARIABLES OF V/STOL PROPULSION

L. B. Veno

Bill Rodenbaugh

General Electric Company

THE INFLUENTIAL VARIABLES OF V/STOL PROPULSION

W. L. Rodenbaugh
Advanced Product Planning Operation

L. B. Veno
Manager, Aircraft Systems, Small Aircraft Engine Department
Flight Propulsion Division, General Electric Company,
Lynn, Massachusetts.

INTRODUCTION

This paper on VTOL influence factors presents the results and summary conclusions of a wide scope study for a number of contemporary types of V/STOL systems. The purpose of this paper is to highlight influential factors in the area of propulsion and propulsion-associated items and to point out for comment and consideration the common and uncommon items which should guide our future design efforts for propulsion specifically directed to V/STOL applications.

As is the case with most papers, much of the discussion will deal with those items and assumptions which are necessary to form a somewhat generalized background upon which to base the actual point of the study. It was our purpose, when formulating this paper, to show a fundamental approach which encompasses the span of V/STOL's. We hope to show that although helicopters and V/STOL supersonic fighters appear initially as widely divergent types, to the propulsion planner there are a significant number of areas that we can isolate with common requirements and a number of areas of advancement in propulsion technology which will benefit most V/STOL designs.

We shall begin with a broad definition of what we mean by an "influential variable." In the view of the authors, this is some precisely measurable design criteria, such as engine weight or SFC, which significantly influences the overall mission performance of the V/STOL system. Conversely, the "sensitivity" of a system is the quantitative change in mission performance with a change in the "influential variable."

Another objective of this paper is to illustrate what is of first importance; a ranking of the influential variables, if you will. From the standpoint of propulsion designers, it is important for all of us to realize that advancement in propulsion technology alone will not provide a satisfactory solution in terms of minimum penalty for VTOL.

Finally, by our presentation of the subject, we hope to emphasize the approach being taken by General Electric across the broad spectrum of VTOL configurations, thereby emphasizing our diverse interests and activities in this area.

SCOPE

Present-day applications for V/STOL are numerous. For example, the roles of logistics, close support, attack, surveillance, etc., are all envisioned as possible V/STOL systems. Actually, more V/STOL's are in various stages of design and development than new, conventional aircraft systems.

On each type, for each application, one can find elements which we have selected as important influence factors. They are shown on Figure I.

We recognize that dollars, downwash, operating cost, etc., are also important. However, in order to be more objective we have confined our studies to the values shown. Each of the influence variables will be discussed separately and the basis of their representative values established. It should be noted that a majority of propulsion items are listed; however, some items, such as time in lift, reaction control allowance and lift margin, are included to emphasize the critical nature of system requirements as well.

Figure 2 illustrates some of the V/STOL types of the day from the helicopter to the supersonic VTOL fighter. We recognize that there are in addition to those shown many more, such as the X19/X22/P1127 types. Although these are all valid members of the V/STOL family, we have confined our analysis to principally account for the types shown. In Figure 2 we have noted the characteristics of each by their respective flat plate drag area, wing loading and disc loading. We have found, as have others, that the parameter disc loading is a good fundamental measurement criteria for V/STOL systems.

As a first example, we show the respective lifting efficiencies of the five propulsion systems on Figure 3 over the range of disc loadings from 7 to beyond 2000 lbs/sq. ft. We have further designated the disc loading of 7-10 lbs/sq. ft. to represent the helicopter and compound types, we have presumed the area between 30-50 lbs/ sq. ft. as the province of the tilt-wing design; the lift fan, fixed-wing airplane is given 400-600 lbs/ sq. ft.; and finally, a fixed-wing airplane utilizing direct lift with deflected cruise propulsion is plotted between 2000-4000 lbs/sq. ft. These particular designs form a continuous curve of lift per unit power required which varies inversely with disc loading. This curve is based, of course, on the familiar relationship $F = m\ V$. The value of disc loading is more significant since it determines the relative size of the vehicle. It is also fundamental to the design when considering its influence on such things as downwash, erosion, noise, reingestion, etc. One must remember that low disc loading is achieved by use of lifting devices; i.e., rotors, propellers, fans, jets, which are part of the total propulsion system. As we all know, this curve shows the sacrifice in lifting efficiency made to achieve the compact installation for high speed flight.

Usually, the vertical flight requirement is most critical in defining the total propulsion requirements; however, agility, STO limits or high speed requirements can occasionally override in setting the amount of installed power. In general, because of the relative efficiencies in forward flight, we considered that design cruise speed tends to vary with disc loading as shown (Figure 4). In the lower disc loading devices, the lifting system is jointly used for cruise propulsion or with some modification, such as rotor-unloading on a compound. However, on most of these types, including the tilt-propeller

and tilt-wings, speed potential is somewhat limited by this all-purpose utilization. These vehicles tend to balance the power required for hover and the power required for cruise. The trend toward the "composite" powerplant is recognized for a high speed design. This is true of the lift fan type and in the fighter having both specialized lift and cruise powerplants. The P1127 is, of course, an exception which returns to a single propulsion system for both lift and cruise. You will note that high disc loading V/STOL's may be designed for both subsonic and supersonic operation.

In Figure 5 data is presented to document the principal characteristics of the baseline designs selected. Because of their particular characteristics, low disc loading devices (helicopters, compounds) tend to be short range, high payload devices. The steady downward trend of payload and reversed trend of fuel carried (range) versus disc loading is noted. Therefore, on the high end of the spectrum the lift-supported vehicle is generally longer in range with a relatively small payload.

Obviously, we recognized that each of the various types have a particular kind of use; that the efficient lifting system, like helicopters and compounds, will fulfill missions requiring a significant time im hover, whereas the high speed systems will be asked to utilize their VTOL capability for little more than vertical take-off and landing, minimizing "inefficient lift system" effects. Certainly this and other baseline assumptions are argumentative and will be, therefore, one of the influence factors evaluated. Most of the baseline vehicles shown on Figure 5 are representative of today's flying V/STOL hardware or extrapolations to the baseline gross weight of 30,000 lbs.

DISCUSSION

The first influence factor to be considered is "time in lift." This is shown on Figure 6, as mentioned earlier, to decrease rather steadily with disc loading. It reflects that when one is good at something, he is asked to do it more frequently. The interesting thing about time in lift is that when it is combined with lifting efficiency, the result is a rather constant amount of hover fuel on board regardless of type (refer back to data in Figure 5).

The second influence factor selected is also one established by the system/mission requirement and not by design. It is referred to in this paper as the "lift margin." In order to explain the lift margin, it is best first to review the characteristics of gas turbine engines. We are aware that thrust or horsepower output is adversely affected by ambient temperature and altitude. The first is fundamentally a Mach number effect; the second is related to density. The rate of deterioration of thrust or power is shown on Figure 7a as a function of sea level temperature and altitude.

Classically, the V/STOL system requirements are being written with capability required on some non-standard day. In effect, a vehicle designed for a condition such as 6000 ft, 95°F VTO will have a large reserve of power or thrust on a standard day.....we call this <u>lift margin</u>.

Figure 7b plots lift margin versus disc loading and for reference purposes, we have superimposed the non-standard day condition grid. It should be noted that this margin includes, for all types studied, a fixed 10% allowance for ground effect, vertical acceleration, etc. Again the more efficient

lifting machines are called upon to meet the more stringent requirements. It is evident that a substantial margin is being built into the low disc loading types by present practices. We don't attempt, in this paper, to justify these choices, nor do we allow ourselves the luxury of ignoring the fact that these are, in the end, the likely military design conditions. The influence of these assumptions will also be one of the prime items investigated as regards its effect on performance.

There is an element in lift margin which, though included in the data of Figure 7a, we have elected to examine separately; that is, the excess of power or lift for allowance of satisfactory control of the aircraft in hover; "reaction control." The variation of reaction control lift allowance with disc loading is shown on Figure 8.

This reserve is based on traditional requirements for minimum acceptable flying qualities for stability, maneuvering, and engine-out emergency. In the case of each type, the most optimum configuration was assumed. For example, in the case of the lift fan, the gas-power transfer system was used (References 4, 5, 6, 9, 10, and 11).

Now, the lifting efficiency, lift margins and reaction control, as well as cruise speed, manifest themselves in determining the size, and hence weight, of the propulsion system. As noted earlier, we have elected to segregate those portions of the aircraft system which we consider part of the lift propulsion group. Under this heading come such things as rotors, transmissions, propellers, gearboxes, fans, vectoring systems and lift engines. Further, we try to separate the propulsion devoted to cruise from that used exclusively for lift. This gets to be "arbitrary" in rotary-wing vehicles.

The lifting system lift/weight ratio is shown as one of the curves on Figure 9. This curve includes the total installed weight of the various lifting systems. It reflects, in part, the lifting efficiency trend when plotted versus disc loading and yet still shows that the higher disc loading devices are the lightest per pound of thrust output. In opposition to this trend, the cruise engine weight is seen to be increasing as a result of higher cruise speeds expected with the high disc loading vehicles. In the case of both lift and cruise systems, suitable weight penalties have been included for installation, ducting, control and accessory arrangements (see Reference 5 for example).

The surprising and quite significant thing about these plots is in the summation of these weights denoted by the "lift and cruise systems." This shows that regardless of the VTOL type (disc loading), the total effective lift-to-weight ratio is very nearly a constant across the spectrum. This tells us that it takes weight to generate lift and provide thrust, and that we must look to the trade-offs which take place within the total propulsion package.

The concept of using the term L/W (the ratio of total installed hover lift to installed propulsion weight) is useful since it provides an immediate index of the amount of propulsion on board any vehicle:

$$\% \text{ Propulsion Weight} = \frac{\text{Propulsion Weight}}{\text{Gross Weight}} = \frac{\text{Lift Margin}}{\text{Total Inst. L/W}}$$

As an example from the previous:

$$\text{For Low Disc Loading} = W/GW = \frac{1.7}{5} = 34\% \text{ Gross Weight}$$

$$\text{For High Disc Loading} = W/GW = \frac{1.2}{5} = 24\% \text{ Gross Weight}$$

The direct influence of lift margin on installed engine weight should be noted.

The propulsion system performance with "representative" state-of-the-art is best shown by curves of specific fuel consumption on an equivalent thrust basis for both lift and cruise powerplants when operating in their respective environments. These are shown as trends on Figure 10a. The lift SFC increases directly with disc loading, as we would expect from Figure 3. The cruise SFC, on the other hand, levels out at the disc loadings where turbofan or turbojet cruise propulsion is used.

Even though the cruise SFC increases with disc loading, this is counter-balanced by the higher cruise speeds and produces a rather constant variation in specific range $\left(\frac{\text{N. Miles}}{\text{lb fuel}} = \frac{\text{Velocity}}{(\text{SFC})\ (\text{Drag})}\right)$ as shown on Figure 10b. The reduction in cruise efficiency shown for the helicopter and compound designs is due primarily to supporting the weight of the vehicle on a rotor in flight, as opposed to the more efficient use of a fixed wing (we know, of course, that many other advantages exist for this rotor-supported design). Specific range, as reflected by the specific fuel consumption in cruise, will be one of the significant influence factors investigated.

RESULTS

The overall performance of the various V/STOL types is shown on Figure 11 wherein mission performance is plotted versus disc loading for our series of 30,000 lb vehicles. The strong trend of increasing radius with disc loading is partially the result of decreasing payload. Thus, the capability, measured by ton-miles flown (radius x payload), is perhaps the best measure of overall ability.

It is interesting that although many diverse assumptions were made, the capability of VTOL types is surprisingly insensitive to the choice of disc loading and design cruise speed. Slight compromises shown in productivity at either end of the disc loading spectrum are in favor of either greater time in lift or greater cruise speeds. Remember that the lower disc loading end of the curve can be altered to somewhat higher productivity simply by reassigning the fuel, here assumed for lift, to fuel available for cruise. Variations in influence factors will be measured by their effect on the radius (hence productivity). Recall, as we discuss the factors that the desire is to show a relative change, not to isolate the absolute capability of any one of the systems, nor to establish one type as superior to others. This, then, gets us to the point of this paper -- how do propulsion factors influence capability in these "base"designs.

Figure 12 plots the percent change in radius versus percent change in the selected variables for the tilt-wing design. We have chosen to describe in detail the tilt-wing since it lies part way between the limits of disc loading covered. The plot illustrates relative effects of arbitrarily altering the variables from the base value (Figures 3-10), one at a time to present the effect on capability (radius) and also the relative sensitivity (slope of the lines) of the variables compared to each other.

We further chose to plot the curves such that the change in variable is in the direction to decrease radius. The relations are for a constant gross weight design, requiring, for example:

- Reduction in cruise fuel available with increases in propulsion size; hence, weight due to greater total lift for changes in control or lift margin.
- Reduction in cruise fuel available with increases in propulsion weight (lift or cruise) or increased time in lift.
- Reduction in radius by poorer specific range resulting from increased cruise SFC for unchanged fuel load.

Certainly, radius capability could have been retained as a constant and the gross weight adjusted. However, we feel that for the purpose of description in the paper, the trends determined are accurate and descriptive.

Specifically, from the data for the tilt-wing, we see that the propulsion weight, lift or cruise, is of similar importance to the cruise efficiency (SFC). This group is somewhat more critical to productivity than lift margin and significantly more influential than assignment of control requirements or lift time or lift SFC. As an example of the use of the curve: Assume a 20% change in each variable and read the resulting effect in capability as a percent change in radius:

	Variable Change 20%			Radius n. mi.	
	Base	New	% Change	Old	New
Cruise SFC, Lb/Hr/Lb Thrust	.55	.66	20	250	200
Lift System Weight, Lb	4500	5400	30		175
Cruise Engine Weight, Lb	3000	3600	19		203
Lift Margin, % Lift	37	44	14		215
Time in Lift, Minutes	10	12	7		232
Reaction Control, % Lift	12	14.4	5		237

One concludes from the above that a 20% increase in the lift system weight would be the most costly, accounting for 75 miles of range decrease. To propulsion people, these data provide some guidance as to where to place emphasis in our design work.

Figure 13 is a collection of plots similar to Figure 12 for each of the systems studied. Reference is made to the legend to follow the effects of the variables.

one constant value being cruise SFC, which remains a 1:1 line in each case. The figures are presented here primarily for the reader's perusal on detail questions and as a documented step to the final summary curve of the paper which follows.

Figure 14 summarizes the effects of the chosen influence parameters against disc loading. The ordinant of the curve is presented as the slope of the lines of Figure 13 (change in radius with change in variable) so that the results then are compared on the basis of radius sensitivity as a function of disc loading (type of system) for each selected influence factor.

CONCLUSIONS

Using the curve interrelations, some revealing trends can be brought out:

1. All variables but cruise SFC have a downward trend with disc loading. This implies that the lower disc loadings are more sensitive (in capability) to different values of influential factors than higher disc loading systems.

2. At the disc loadings above 100 lb/ft^2, the cruise SFC is from 1 to 2.5 times as influential as propulsion weight and approaches eight times the importance of lift time (or SFC), reaction control or establishment of some required lift margin. Thus, any minimization of weight at the expense of cruise efficiency would appear to be erroneous.

3. At disc loadings generally associated with high speed designs -- 500 lb/ft^2 up, the change in sensitivity of the parameters with change in disc loadings is small.

4. In the range of rotary wing or propeller lift designs -- disc loadings below 100 lb/ft^2 -- the weight of the lift system becomes the dominant variable (due perhaps to the fact that the lift systems, as we view it, is the majority of the propulsion group). The importance of weight reduction in the large multipurpose discs thus appears to be of paramount importance. Also, in this type small changes in lift margin assumed are significant because of the large initial amount of lift tradtionally having been reserved.

5. The reverse in the sensitivity trend for the designs at very low disc loadings (below 10 lb/ft^2) is brought about by the very rapid increase in lifting efficiency at these low disc loadings which tend to mask propulsion variations.

6. A second striking characteristic which is due to the high lift efficiency at low disc loading is the relative insensitivity of time in lift even though the basic designs had more than 10:1 ratio of assigned time across the spectrum (2 mins. to more than 20 minutes).

All these variations are certainly affected by the initial assumptions. Our purpose was to be adequately consistent across this broad spectrum thereby to give insight to the relative importance of influential propulsion parameters. We have attempted to study in the "real world" as regards

required margins, time in lift, reaction control level and current propulsion weight and SFC state-of-the-art. Other assumptions, other missions, other sizes, other propulsion schemes can skew or may even reverse some trends. Notwithstanding, the basic conclusions drawn from the work in this paper will still remain useful. They are summarized below.

SUMMARY

The purpose behind this work was to investigate and highlight propulsion-oriented influence factors for a wide spectrum of V/STOL designs. Let's review and summarize the study:

1. Relating the various types of systems to their disc loading proved to be a useful way of obtaining meaningful relations in the family of V/STOL aircraft.

2. Relating change in capability (radius) with change in variable is a direct and useful method to evaluate both influence and sensitivity of designs to influential parameters.

3. Although there is a wide variation in division of total propulsion weight, between lift and cruise engine, across the spectrum of designs, there is a surprisingly constant installed lift-to-weight ratio for the total propulsion system. This definitely underlines the need to discuss V/STOL propulsion "in total" -- not to concentrate exclusively on only a portion of the system, nor to neglect the weight of installation. This is equally true not only for the high disc loading vehicle where the engine manufacturer has been nominally responsible for the entire system, but also for the rotary wing machines where the "lift system" is traditionally the airframer's province.

4. Recognizing the existence of a nearly constant value of weight per unit of lift, the capability of the various systems is strongly influenced by the amount of lift margin which then establishes the percent of the gross weight which will be taken up by the total propulsion group.

5. The design point lift margin is strongly influenced by the altitude/temperature condition at which VTO is required. The penalties of choosing a stringent combination -- because of precedent or as a "hedge" against marginal utility -- are significant. In low disc loading systems, this choice can far outweigh the influence of advances in propulsion performance and weight.

6. Considering the variation in roles and aerodynamic configuration in the the systems studied, the consistency of the TON-MILE capability is significant. If there is indeed a penalty for V/STOL, it apparently is uniform across the disc loading spectrum.

7. The study illustrates again the fundamental principal that propulsion efficiency -- as manifested in SFC at cruise power -- is extremely important. There would seem to be little to gain by compromising propulsion performance to reduce weight or otherwise favor the lifting task (i. e. oversizing the cruise engine for large margins or control, etc.).

8. **Propulsion advancements that will contribute most directly to progress in V/STOL are suggested by the sensitivity relations:**

- **Reduction in total installed engine weight without compromise in the goals of improved cruise performance.**

- **Engines designed to be "rated" such that the decay in lift potential with takeoff altitude and temperature and by generation of reaction control is minimized.**

- **Reduction in weight without cruise efficiency compromise in rotary wings and propellers are at least as important to capability as the expected advancements in "engines."**

Speaking as V/STOL propulsion system planners, data such as this emphasizes the fact that the adequacy of a propulsion scheme cannot be assessed without involving the aircraft and mission; neither can it be assessed "piece at a time." Most important, basic propulsion advancements which benefit a particular V/STOL vehicle are likely to be applicable and beneficial across the spectrum of V/STOL aircraft. W_e plan to remember this.

REFERENCES

1. Denning, R. M.: "Extensions of the Lift/Thrust Engine Principle in V/STOL Aircraft," SAE Paper No. 587B, October 1962.

2. Hazen, D. C.: "Applications and Engineering Problems of VTOL-STOL Military Aircraft," SAE Paper No. 629B, January 1963.

3. Lombard, A. A. and Heyworth, A. J.: "Powerplant System for V/STOL Aircraft," SAE Paper No. 635B, January 1963.

4. Goldsmith, Robert H. and Hickey, David H.: "Characteristics of Aircraft with Lifting-Fan Propulsion Systems for V/STOL," IAS Paper No. 63-27, January 1963.

5. Rodenbaugh, W. L.: "An Approach to the Evaluation of Propulsion Systems in V/STOL Aircraft," SAE Paper No. 860D, April 1964.

6. McKinney, M. O. Jr., Kuhn, R. E., and Reeder, J. P.: "Aerodynamics and Flying Qualities of Jet V/STOL Airplanes," SAE Paper No. 864A, April 1964.

7. Albers, R. R., Rodenbaugh, W. L., and Veno, L. B.: "The Case for STOL with V-Capable Aircraft," Joint AIAA/CASI Paper No. 64-792, October 1964.

8. Stepniewski, W. Z. and Young, M. I.: "Helicopters and Propeller-Type VTOL Aircraft in the Light of Technologies," SAE Paper No. 650193, April 1965.

9. Peterson, John M.: "Tailoring the Lift Fan V/STOL Concept to Mission Requirements," SAE Paper No. 650196, April 1965.

10. Klingloff, Robert F, Sardanowsky, Wladimir, and Baker, Robert C; "The Effect of VTOL Design Configuration on Power Required for Hover and Low Speed Flight," Journal of the American Helicopter Society, July 1965.

11. "V/STOL's - Turning Promise to Reality" - September 1965 issue of Astronautics and Aeronautics, pages 26 through 56.

Brown, Harold, "The Military Potential of V/STOL Aircraft"
Miller, Rene H., "V/STOL Technology - Problems and Perspective"
Jacobson, D. H. and Hockert, C. E., "VTOL Propulsion"
Greene, L. P. and Cotter, W. E., "Lift Jet Technology"
Swan, Gail H., "Tilt-Wing Deflected-Slipstream Aircraft"
Goldsmith, Robert H., "Lift-Fan Technology"
Wood, Carlos C., "Helicopter Prospects"

TABLE OF INFLUENCE VARIABLES

- Time in Lift
- Lift Margin
- Reaction Control Margin
- Lift System Weight
- Cruise Engine Weight
- SFC/Specific Range

LIST OF FIGURES

Figure 1 Table of Influence Factors

2 Typical V/STOL Configurations

3 Lift Efficiency vs Disc Loading

4 Cruise Speed vs Disc Loading

5 Table of Design Data

6 Time in Lift vs Disc Loading

7 a) Lift Decay
b) Lift Margin vs Disc Loading

8 Reaction Control Reserve vs Disc Loading

9 Installed Propulsive Weight vs Disc Loading

10 a) SFC vs Disc Loading
b) Specific Range vs Disc Loading

11 Radius/Capability vs Disc Loading

12 Influence of Key Variables - Explanation

13 Influence of Key Variables
a) Helicopter
b) Compound
c) Tilt Wing
d) Lift-Fan
e) Composite

14 Mission Sensitivity vs Disc Loading-Summary

LIFT EFFICIENCY
Lift/Unit Power
0
1
2
3
4
5
6
7
8
1
10
100
1000
10,000
Disc Loading - Lb/Ft 2
Helicopter
Compound
Tilt Wing
Lift Fan
Composite

TYPICAL CONFIGURATIONS

Gross Weight for All Designs = 30,000#

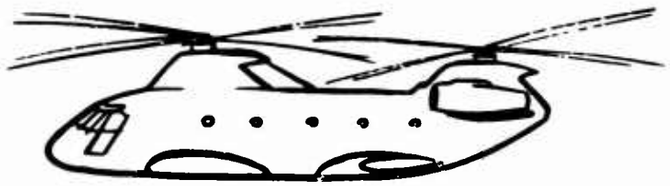

HELICOPTER

$f = 30\ FT^2$

DISC LOADING = 7.5 LB/FT^2

COMPOUND HELICOPTER

$f = 25\ FT^2$

WING LOADING = 100 LB/FT^2
DISC LOADING = 10 LB/FT^2

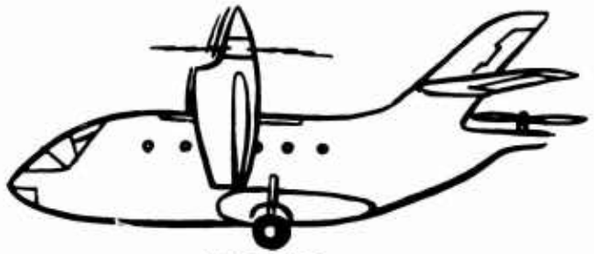

TILT WING

$f = 17\ FT^2$

WING LOADING = 60 LB/FT^2
DISC LOADING = 40 LB/FT^2

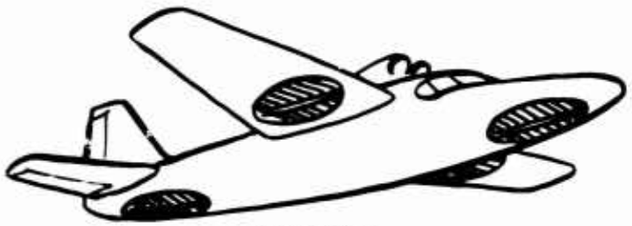

LIFT FAN

$f = 10\ FT^2$

WING LOADING = 60 LB/FT^2
DISC LOADING = 500 LB/FT^2

COMPOSITE VTOL

$f = 6\ FT^2$

WING LOADING = 120 LB/FT^2
DISC LOADING = 2500 LB/FT^2

DESIGN DATA

VEHICLE TYPE		HELICOPTER	COMPOUND	TILT WING	LIFT FAN	COMPOSITE
GROSS WEIGHT		←		30,000 LBS	→	
STRUCTURE & EQUIP.		8650	10,300	13,500	13,600	12,000
EMPTY WEIGHT		18,000	19,000	22,000	17,600	18,000
USEFUL LOAD		12,000	11,000	8,000	12,400	12,000
PAYLOAD + CREW		8,000	8,000	5,000	2,000	1,500
FUEL		4,000	3,000	4,000	8,400	10,500
CRUISE ENGINE	WT.	1450	1900	3000	3000	3300
LIFT AUGMENTATION SYSTEM	ROTOR/PROP	5040	2700	1600		
	DRIVE	2860	4100	2900		
	TOTAL	7900	6800	4500	3000	2700
TOTAL PROPULSION	WT	9350	8700	7500	6000	6000
TIME IN LIFT	MIN	30.0	20.0	10.0	4.0	2.5
HOVER FUEL	LB	1200	900	940	1000	1250
CRUISE SPEED	MACH	.25	.40	.60	.80	.90
	KNOTS	165	250	350	470	520
MISSION RADIUS N. Mi.		130	140	265	650	790
TON-MILES		1040	1120	1325	1300	1180
DISC LOADING		7.5	10	40	500	2500

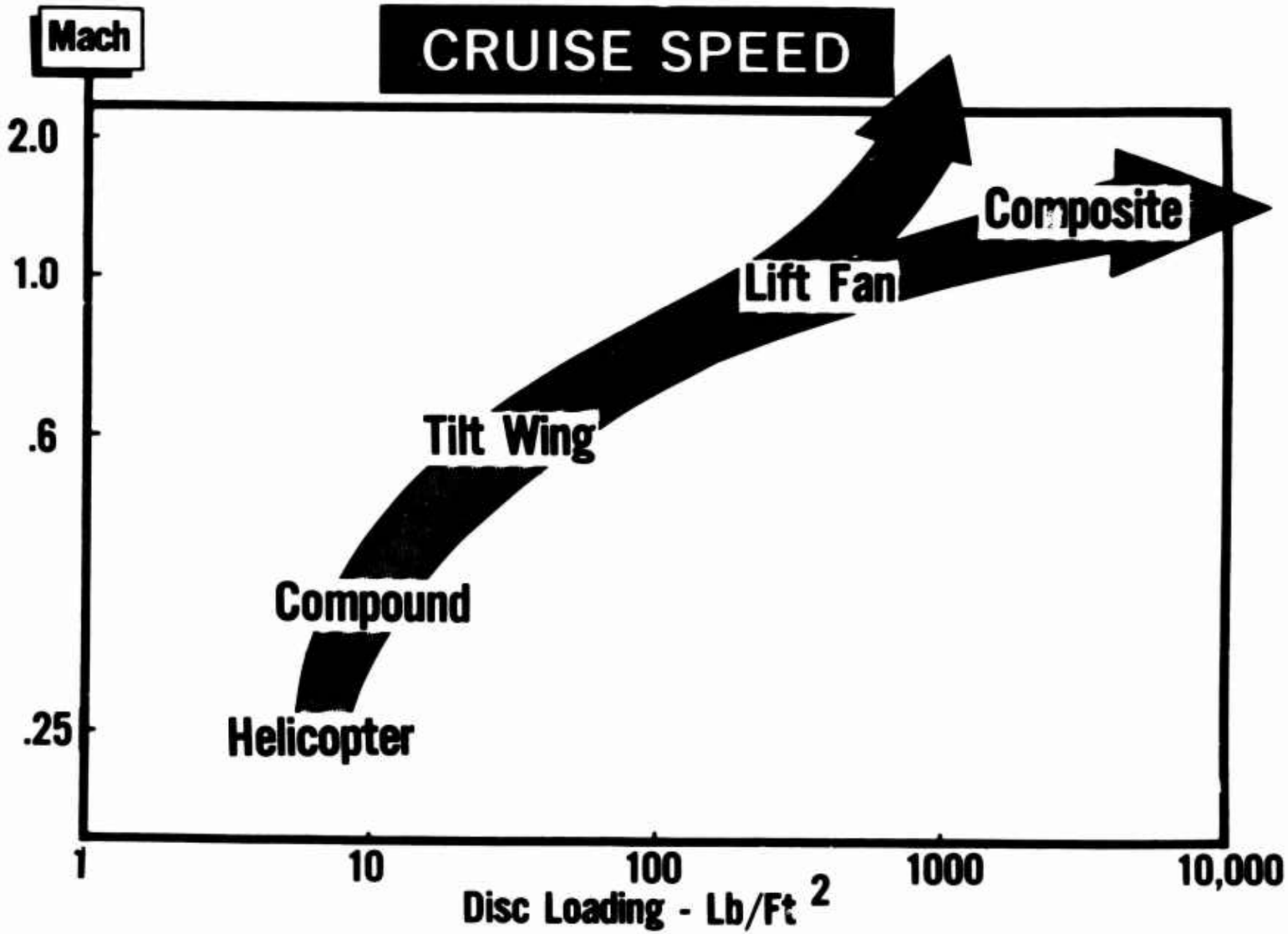
CRUISE SPEED
Mach
2.0
1.0
.6
.25
Helicopter
Compound
Tilt Wing
Lift Fan
Composite
1
10
100
1000
10,000
Disc Loading - Lb/Ft 2

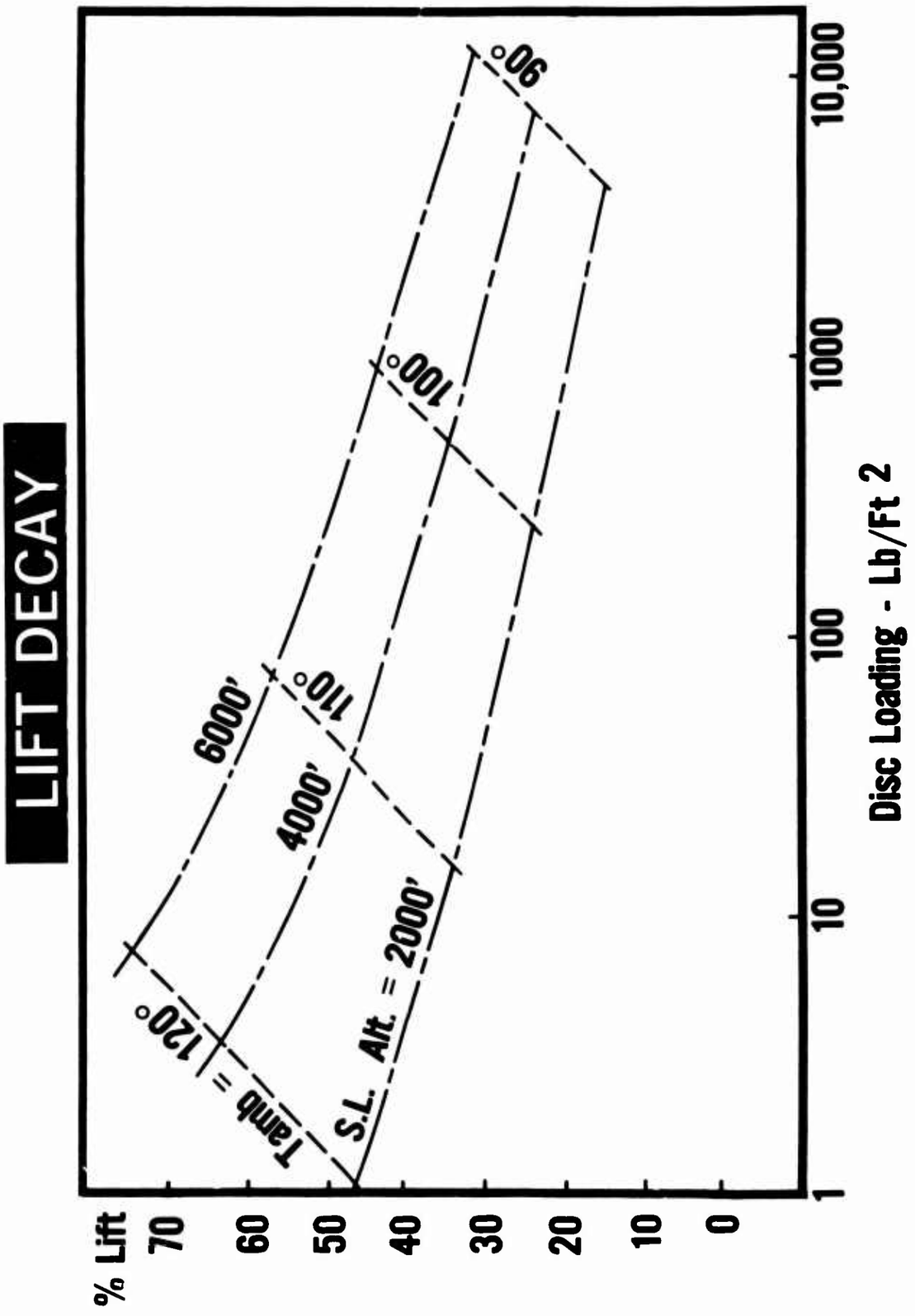
LIFT DECAY
% Lift
70
60
50
40
30
20
10
0
1
10
100
1000
10,000
Disc Loading - Lb/Ft 2
90°
100°
110°
120°
Tamb =
S.L.
4000'
6000'
Alt. = 2000'

TIME IN LIFT
Min.
0
4
8
12
16
20
24
28
32
Helicopter
Compound
Tilt Wing
Lift Fan
Composite
10
100
1000
10,000
Disc Loading - Lb/Ft 2

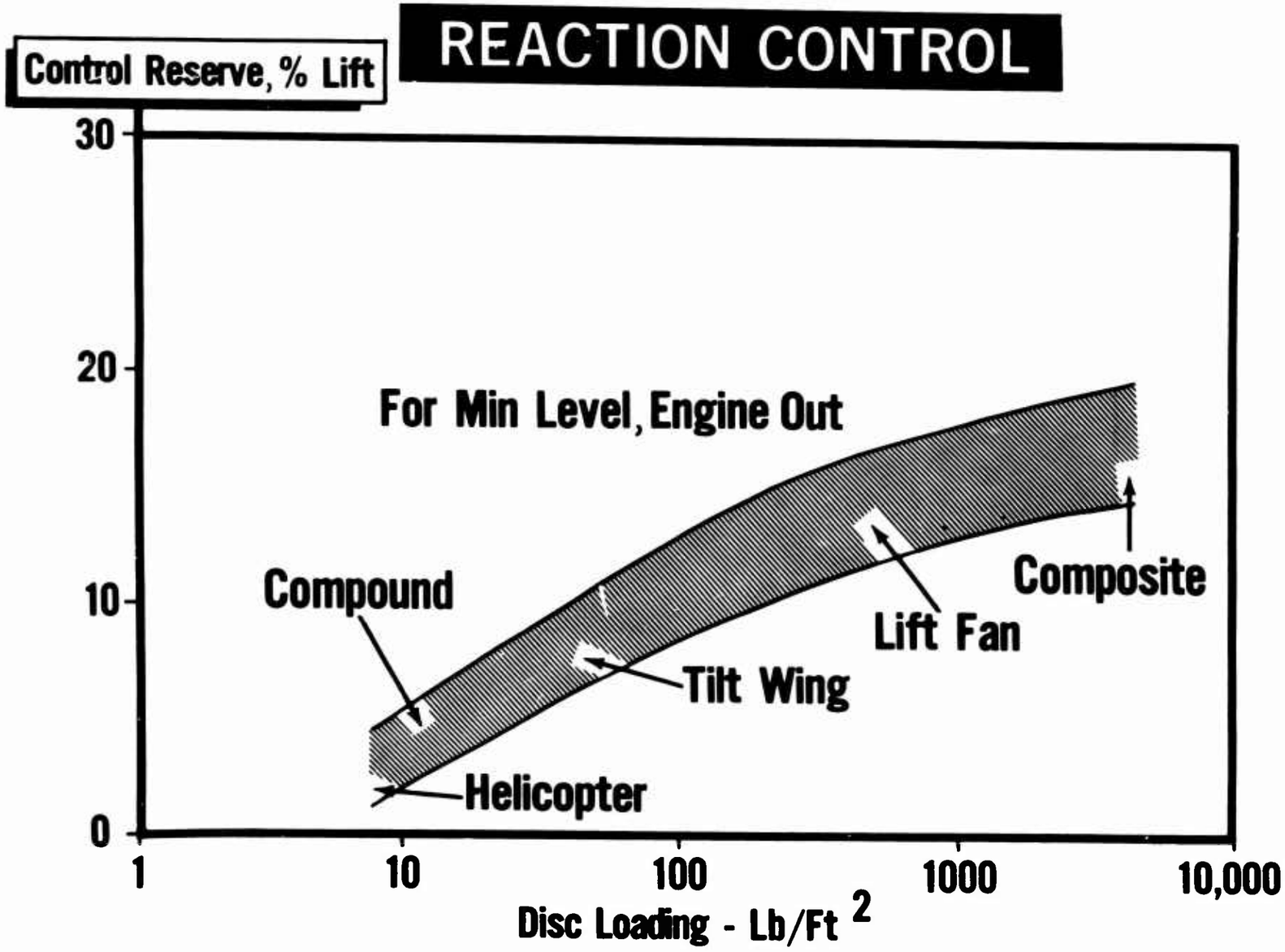
REACTION CONTROL
Control Reserve, % Lift
30
20
10
0
For Min Level, Engine Out
Compound
Tilt Wing
Lift Fan
Composite
Helicopter
1
10
100
1000
10,000
Disc Loading - Lb/Ft 2

LIFT MARGIN

% Lift
70
60
50
40
30
20
10
0
1
10
100
1000
10,000
Disc Loading - Lb/Ft 2
Resulting Margin @ SL, 59°F
Includes Losses & Control
Helicopter
Compound
Tilt Wing
Lift Fan
Composite
Design Pt. Margin
Basic Margin at Design

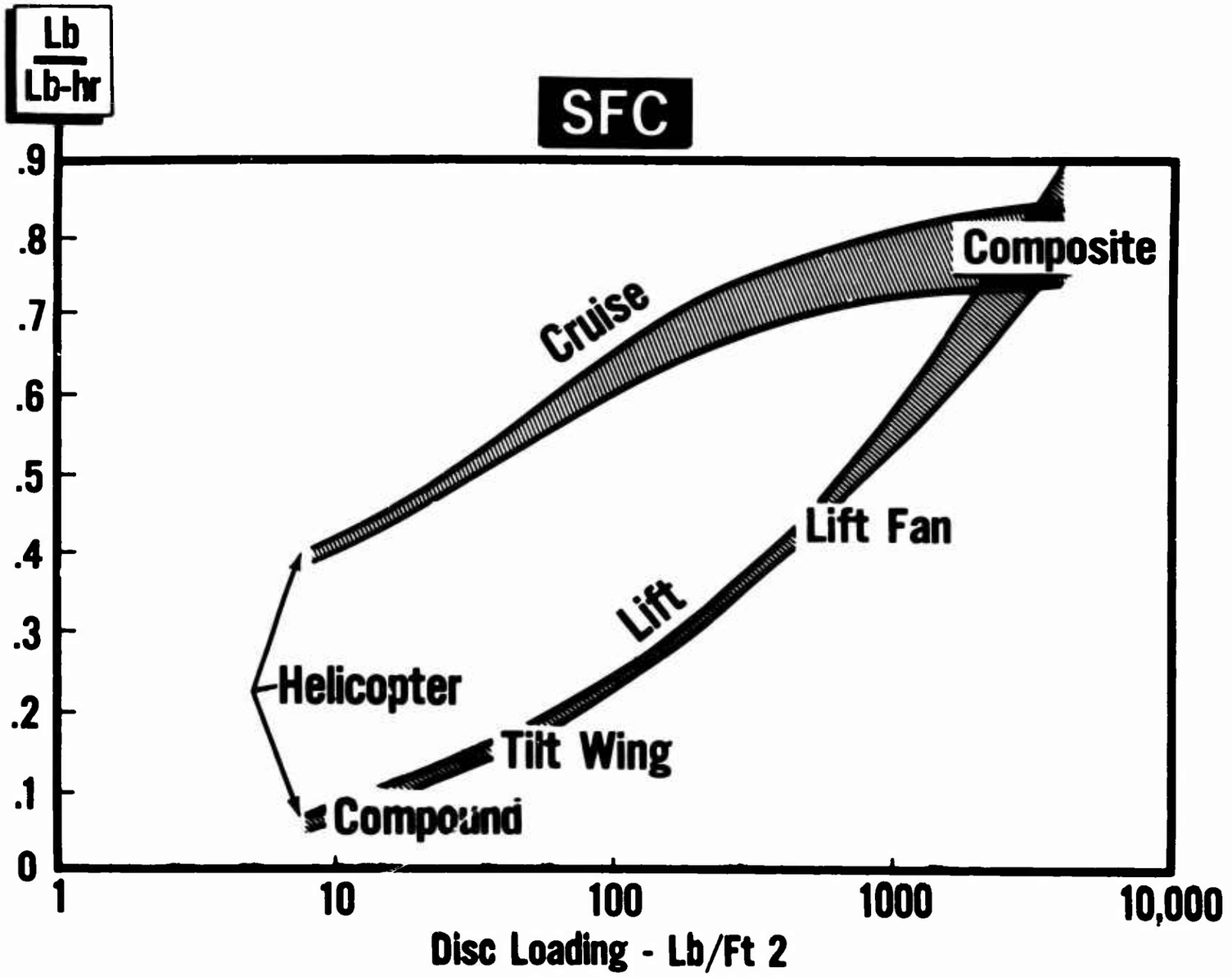
Lb
Lb-hr
SFC
.9
.8
.7
.6
.5
.4
.3
.2
.1
0
Composite
Cruise
Lift Fan
Lift
Helicopter
Tilt Wing
Compound
1
10
100
1000
10,000
Disc Loading - Lb/Ft 2

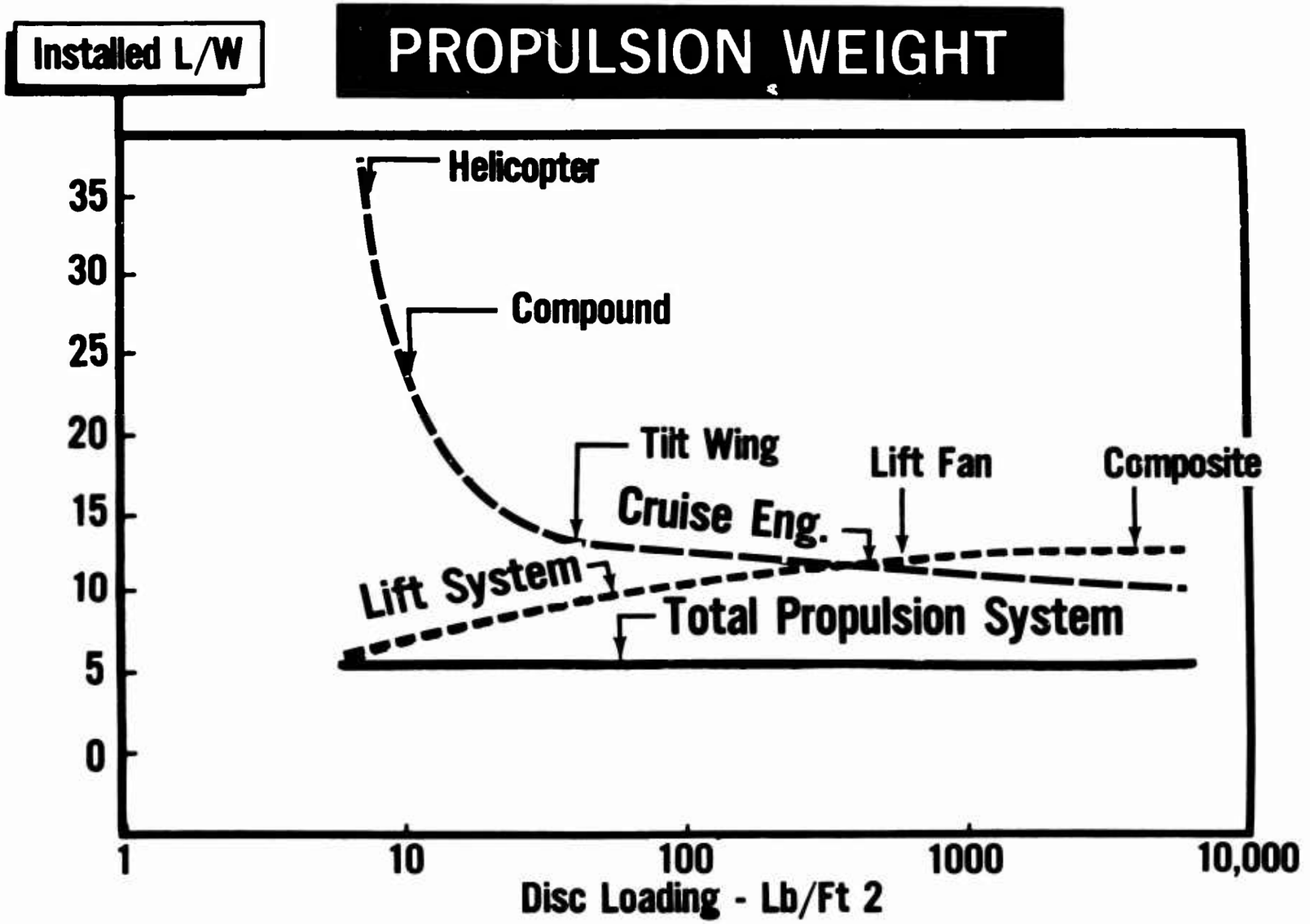
PROPULSION WEIGHT
Installed L/W
35
30
25
20
15
10
5
0
Helicopter
Compound
Tilt Wing
Lift Fan
Composite
Cruise Eng.
Lift System
Total Propulsion System
1
10
100
1000
10,000
Disc Loading - Lb/Ft 2

MISSION PERFORMANCE
Radius
N. Miles
Capability
Ton-Miles
GW = 30,000 Lbs
Helicopter
Compound
Tilt Wing
Radius
Capability
Lift Fan
Composite
Disc Loading - Lb/Ft 2
0
100
200
300
400
500
600
700
800
200
400
600
800
1000
1200
1400
1600
1800
1
10
100
1000
10,000

SPECIFIC RANGE
S.R. = V / Thrust × SFC
N. Miles / Lb. Fuel
.24
.22
.20
.18
.16
.14
.12
.10
Helicopter
Compound
Tilt Wing
Lift Fan
Composite
1
10
100
1000
10,000
Disc Loading - Lb/Ft 2

COMPARISON OF INFLUENCE FACTORS

Constant GW = 30000#

(a)

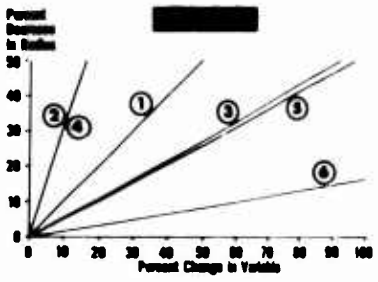

(b)

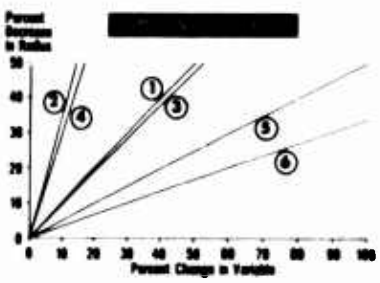

LEGEND

1. Cruise SFC
2. Lift System Wgt.
3. Cruise Engines Wgt.
4. Lift Margin
5. Time in Lift or Lift SFC
6. Reaction Control

INFLUENCE OF KEY VARIABLES (c)

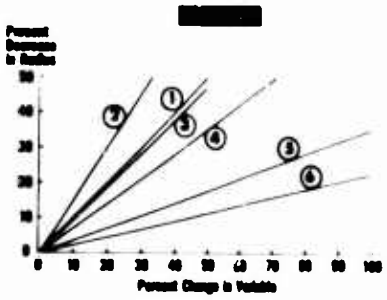

(d)

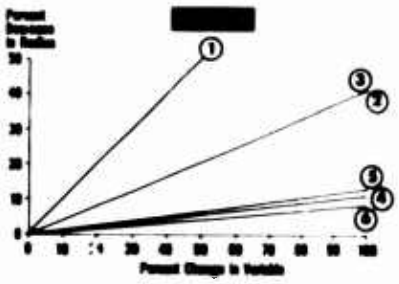

(e)

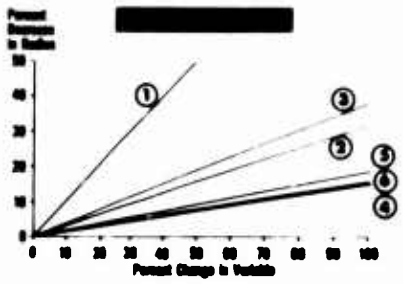

INFLUENCE OF KEY VARIABLES

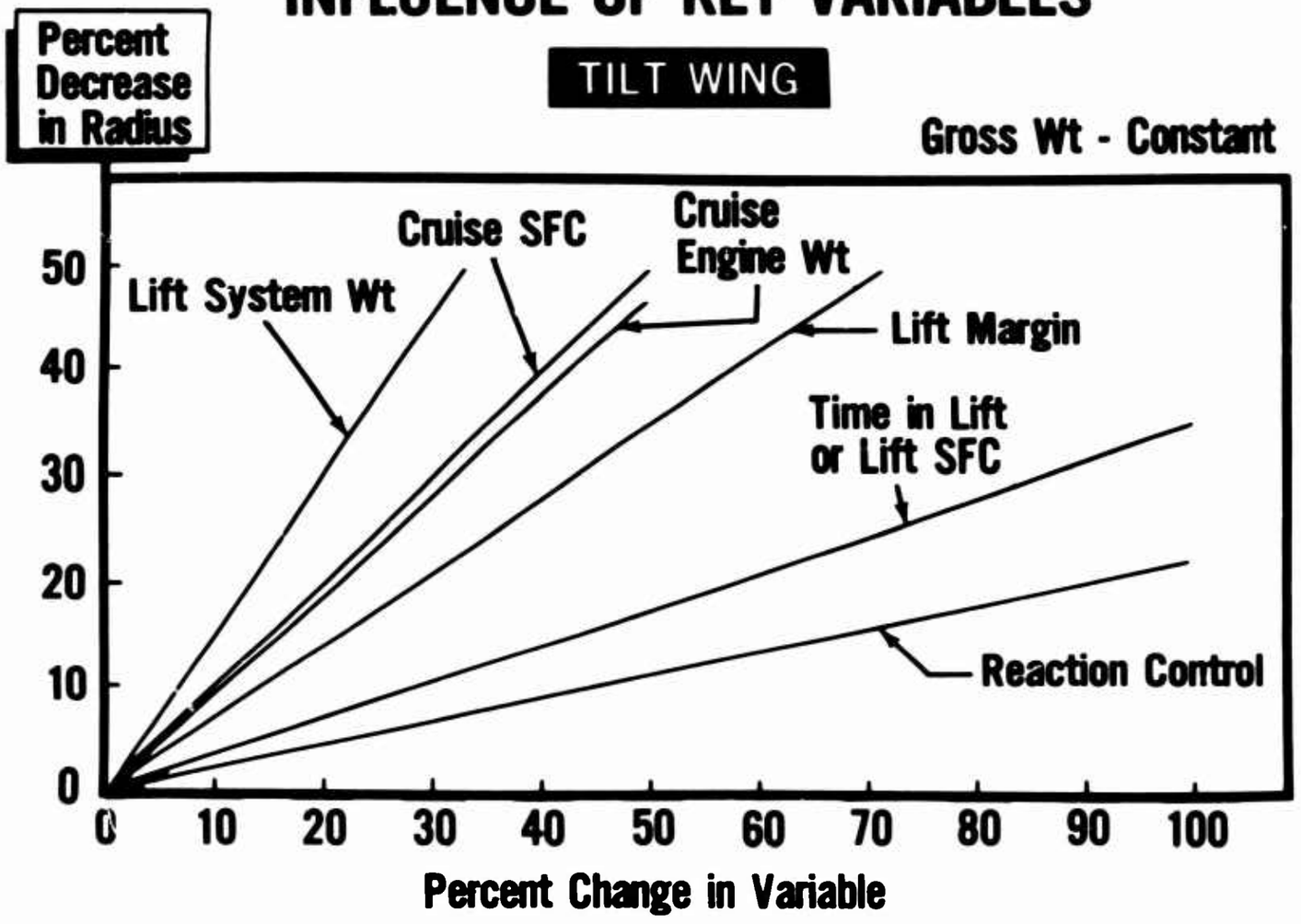

HOT CYCLE ROTOR/WING HIGH SPEED VTOL AIRCRAFT

M. S. Harned

R. E. Head

Hughes Tool Company

EFFECTS OF INFLUENCE FACTORS

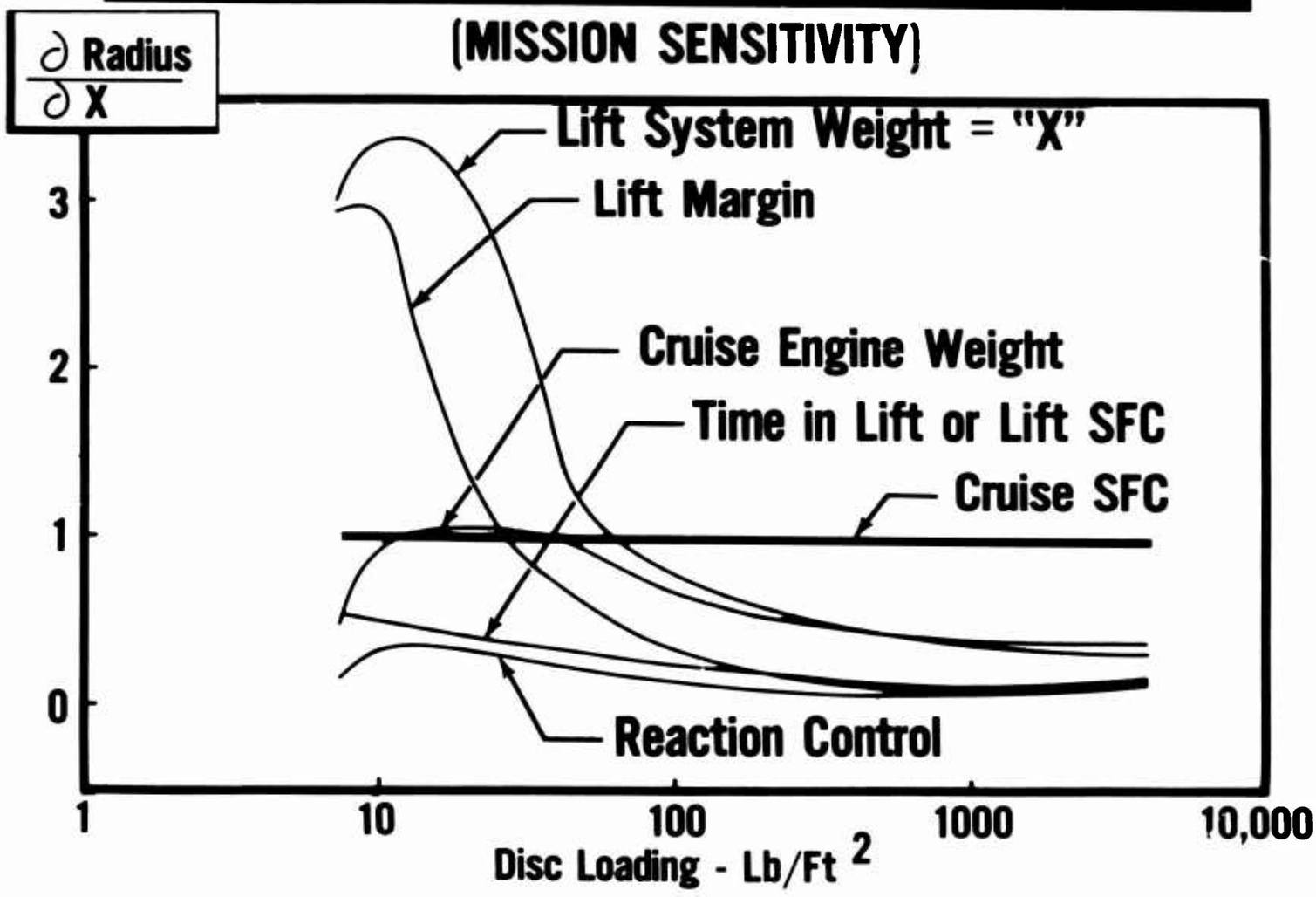

ABSTRACT

HOT CYCLE ROTOR/WING HIGH-SPEED VTOL AIRCRAFT

M. S. Harned, Vice President - Operations, and R. E. Head, Project Engineer - Advance Design

The Hot Cycle Rotor/Wing is a new concept for a high-speed VTOL aircraft that approaches the high-speed capability and cruise efficiency of a fixed-wing jet airplane, combined with hover efficiency and operational advantages approaching those of a helicopter. The concept embodies a simple and lightweight lift/propulsion system and provides high payload capability with corresponding economic benefits. The Rotor/Wing is a unique, dual-purpose lifting device that is basically a Hot Cycle rotor with an unusually large hub. It functions as a helicopter rotor with tip-jet drive for vertical and low-speed flight and stops during flight to become a low-aspect-ratio, fixed-wing for cruise. By stopping the rotor for forward flight, the speed limitations of the helicopter are removed. The feasibility of the Hot Cycle propulsion system has been proven by the successful flight testing of the XV-9A helicopter. The practicability of the Rotor/Wing concept has been demonstrated through wind tunnel tests and Hughes-sponsored whirlstand tests. The Air Programs Branch of the Office of Naval Research and the Airframe Design Section of the Bureau of Naval Weapons have jointly supported a wind tunnel research program. These tests provide basic information on all flight regimes of the Rotor/Wing aircraft and are described in detail. A typical Rotor/Wing vehicle is also described. At the end of September 1965, the Hughes Hot Cycle Rotor/Wing entry was named as one of the winners in the U. S. Army AVLABS Composite Research Aircraft competition.

SUMMARY

The Hot Cycle Rotor/Wing is a new concept for high-speed vertical takeoff aircraft. It is a unique, dual-purpose lifting device that is basically a Hot Cycle helicopter rotor with an unusually large hub. It acts as a tip-jet-powered rotor for vertical and low-speed flight, and stops during flight to become a low-aspect-ratio, swept wing for cruise. By stopping the rotor in forward flight, the speed limitations of the helicopter rotor are removed, enabling more efficient cruise and operation at speeds up to 500 knots as a jet airplane. The single, dual-purpose lifting device combined with the simplicity and light weight of the Hot Cycle propulsion system holds promise of high payload capability superior to that of any other high-speed VTOL aircraft concept.

The Hot Cycle Rotor/Wing promises:

Hover efficiency and low-speed flying qualities comparable to those of conventional helicopters.

Cruise lift/drag ratio superior to a delta wing.

Universal operational suitability due to low downwash velocity and low noise level in hover.

Safety of flight due to simple and straightforward conversion procedure and capability to initiate an autorotational landing from any flight mode.

Simplicity, low support requirements, low empty weight, high payload capacity, good cruise efficiency, and high productivity.

INTRODUCTION

For many years there has been an intensive search by much of the airplane and helicopter industry for a high-speed VTOL aircraft. This effort has produced a large variety of concepts, most of which have had serious deficiencies in complexity, cost, or operational unsuitability.

Our approach at Hughes was to restrict our research to vehicle types that would have a high enough lift per horsepower to be economically practical and have a low enough noise level and downwash velocity to be operationally practical. This quickly limited our field of lifting systems to the low-disc-loading helicopter rotor. This is illustrated first in Figure 1, where the ratio of lift/horsepower is plotted as a function of downwash velocity. Here you see that the helicopter rotor typically provides twice the lift per horsepower of the propeller and thirty times that of the turbojet. This is quite important, because fuel consumption in

hover and engine weight are directly related to the power requirement in low-speed flight. If it is assumed that operation without specially prepared surfaces and protection for ground personnel is a requirement, the downwash also should have less than hurricane velocity; this further limits the choice to the helicopter rotor. Figure 2 clearly points to the selection of either a turbine shaft-driven or Hot Cycle-driven helicopter rotor on a noise level basis. Although our studies were much more detailed than this, these two charts show the basic reasons why we concluded that any useful VTOL aircraft must use a helicopter rotor to provide the vertical rising capability.

Fortunately, the Hot Cycle tip-jet rotor drive had already been developed, providing the ability for a helicopter to carry a useful load approaching twice its empty weight. The XV-9A Research Vehicle is shown in Figure 3 flying with the first successful Hot Cycle rotor. The propulsion system is illustrated in Figure 4.

This simple, lightweight rotor drive clearly offered great potential for an efficient VTOL aircraft. Consequently, the remaining step was to adapt the rotor to permit a high subsonic cruise capability. Systems for retracting the rotor appeared complex, heavy, and expensive; therefore, our efforts were directed toward stopping the rotor and using it as a wing. Our final solution was that of incorporating a large "trisector" hub fairing, intermediate in shape between a circle and a triangle, as illustrated in Figure 5. This fairing accomplishes the following:

1. Supports the blade, with a very small weight penalty, far enough out so that the rotor can be slowed down and stopped at a speed of 150 knots. Our studies showed that a conventional rotor that depends on centrifugal force to support the blades at high forward speeds would become excessively heavy if it were strong enough to stop turning at 150 knots.

2. Exposes enough of the outer portion of the rotor blade to provide good hovering capability.

3. Fairs out completely the hub and rotor mechanisms that are major drag factors on the helicopter.

4. Provides a fixed-wing shape having a high sweep angle at the root decreasing at the blade with a better aspect ratio than that of a delta wing.

5. Provides a fixed-wing shape with a center of pressure close to the rotor mast. This feature is quite important for balancing the aircraft in both the running-rotor and stopped-rotor flight modes.

Having developed a very promising concept, we proceeded to test[1] the hover characteristics and verified predictions of hovering efficiency based on rotor theory[2,3]. At this point, ONR, and BuWeps became interested, and sponsored a wind tunnel test program. These tests[1] demonstrated the ability to stop and start the rotor at 150 knots and showed the Rotor/Wing to have an acceptable fixed-wing lift/drag ratio. This paper describes in detail the test results and some of the potential applications of the Hot Cycle Rotor/Wing.

HOT CYCLE ROTOR/WING CONCEPT

The proven Hot Cycle propulsion system[4], shown schematically in Figure 4 for the XV-9A, offers a mechanically simple system to power rotary-wing aircraft, and is used to drive the Rotor/Wing. High-energy gases from turbine gas generators are ducted out through the blades to tip-jets that drive the rotor like a pinwheel. The rotor itself becomes the power turbine, converting the energy of the gases directly to rotary power. Because all the power is transmitted pneumatically through light-weight ducting, all gearboxes, shafting, and the tail rotor are eliminated. The last is possible because there is no shaft torque to counteract. This makes possible nearly doubling the useful load to empty weight ratio of a shaft-driven helicopter.

The application of the Hot Cycle drive to the Rotor/Wing is illustrated in Figure 6. For vertical takeoff, the rotor is driven by the tip-jets, the same as the XV-9A. For forward flight when the rotor is stopped, diverter valves direct the gases straight out the tailpipe for direct propulsive thrust.

Figure 7 pictorially illustrates the various flight regimes available to the Hot Cycle Rotor/Wing aircraft and the associated speed ranges. The Hot Cycle Rotor/Wing aircraft takes off, hovers, flies at slow speeds, and lands in the helicopter mode, during which the rotor is powered by its tip-jets, and the aircraft is controlled principally by rotor-blade cyclic and collective pitch control. To increase flight speed, the power is shifted from the rotor to airplane-type thrust nozzles, and the rotor autorotates; primary control is still through rotor cyclic pitch, aided by the rudder and elevators. As the speed reaches approximately 150 knots, the rotor is slowed until it stops turning, and the rotor hub acts as a fixed wing for pure airplane flight; control now is provided by the rudder and the elevators, acting in unison for pitch control and differentially for roll control. In the airplane configuration, high subsonic speeds are achievable.

The conversion from helicopter flight to airplane flight can be accomplished manually in a very straightforward manner, and this has been demonstrated in wind tunnel tests. Analysis has shown that no stability

augmentation system is required during conversion. The conversion process can be reversed at any time at the desire of the pilot, and can be accomplished in level flight, during climb, or in descent, at the option of the pilot.

The improved cost-effectiveness of the Rotor/Wing aircraft with respect to other high-speed VTOL concepts is most easily shown by comparing plots of the payload-to-empty weight ratio versus range. Data taken from the trade press is used in Figure 8 to compare a number of aircraft concepts for hover out of ground effect at standard day sea level conditions. The payload/empty weight ratio basically compares the work that a craft can do with what it costs, since the initial and operating costs are nearly proportional to the empty weight for a class of similar aircraft. The Rotor/Wing has considerably better payload-to-empty-weight for ranges up to 1700 nautical miles than the other types for VTO at standard sea level. The greater cost-effectiveness of the Rotor/Wing is even more pronounced, as shown in Figure 9, for VTO at 6000 feet 95° F. The main reasons for this improved cost-effectiveness lie in the simple and lightweight Hot Cycle propulsion system, in the hovering performance of the helicopter-type rotor, and in the use of a dual-purpose lifting device, that avoids duplication of lift and propulsion systems for various flight regimes.

A most important advantage of the Hot Cycle Rotor/Wing aircraft over many other low-disc-loading, high-speed VTOL's is its safety of flight aspect with regard to entering autorotation in case of complete engine power failure. The Rotor/Wing is a single lifting device that is not folded or retracted to attain aerodynamic cleanness for high-speed flight, and it can be quickly and simply unlocked and brought up to speed, using only aerodynamic forces, so that an autorotational landing may be made.

DESIGN STUDIES FOR HOT CYCLE ROTOR/WING VTOL AIRCRAFT APPLICATIONS

The Hot Cycle Rotor/Wing is adaptable to a wide range of vehicles that require high cruise speed capability with the hovering efficiency and operational advantages approaching those of the helicopter. A number of applications that have been studied are illustrated in Figure 10. Details of one, the recovery/transport aircraft, will suffice to demonstrate the potentialities of the concept.

This general-purpose vehicle has a design gross weight of 45, 500 pounds based on hot day hovering performance and is powered by a pair of General Electric GE1/J1 gas generators. It is designed for search and rescue operations or, alternatively, for general cargo transport. Figure 11 shows the general arrangement, while Tables 2 and 3 list the basic characteristics and weight breakdown, respectively.

This aircraft is intended to spend most of its flying time in the stopped-rotor regime. In this mode the Rotor/Wing is locked with one blade pointing forward and the others swept back. As shown in Figure 12, a streamlined, well-sealed aircraft configuration is obtained by means of fairing doors on the fuselage that close tightly against the forward blade, a turtleback fairing that raises to fair the rear of the hub into the aft fuselage, and pneumatic seals that close the gap between the bottom of the hub and top of the fuselage. For the short-term powered or autorotating rotor modes, these fairings and seals open to allow rotor clearance.

The performance of this aircraft is calculated for the MIL-STD-210A hot atmosphere. Figure 13 is a plot of its hover performance and Figure 14 shows its speed-altitude and rate of climb characteristics for its design gross weight.

Its mission capability is best shown by Figures 15 and 16. The former shows its potential for search and rescue operations. In these, the aircraft takes off initially in an overload condition and arrives at the rescue site at its design gross weight, so that it can hover at once if required to pick up personnel. Figure 16 is a plot of its payload-range characteristics. The VTO curves are, of course, for vertical takeoff; the STO curves are for a helicopter-type running takeoff in ground effect; the CTO curves are for an airplane-type takeoff with the rotor locked and a long runway available. A payload limit line is included, to indicate the payload restriction for the shorter ranges if vertical landing at the destination is a requirement. This chart indicates that the recovery transport aircraft can easily ferry itself to any point in the world, since the longest range required is the 2500* nautical miles from California to Hawaii.

HOT CYCLE PROPULSION SYSTEM RESEARCH AND DEVELOPMENT RESULTS

Recognizing the potential improvement in rotor system characteristics offered by the Hot Cycle system, the Army, Navy, and Air Force sponsored, with Hughes, an investigation to establish feasibility and to provide technical data for application of the concept. This program culminated in late 1961 and early 1962 in successful whirl tests of the 55-foot diameter Hot Cycle rotor. Gas was supplied to the rotor by a J57 turbojet at the conditions and flow rate of two T64 gas generators, for which the rotor was designed. A total of 60 hours of whirl testing was performed.

Following the successful completion of a 60-hour whirl test program, a flight research program was initiated under the sponsorship of the U. S. Army (AVLABS), with the U. S. Navy participating by furnishing YT64-6 gas generators to power the XV-9A Hot Cycle research vehicle. Starting

*Including allowance for headwinds.

in late 1964, a series of ground and flight tests was begun. These included 15 hours of whirlstand testing, 50 hours of ground testing, and 35 hours of flight testing and were successfully completed in the summer of 1965[4]. Figure 3 shows the XV-9A in flight, and Figure 4 is a schematic of its propulsion system.

As a result of the extensive whirl tower, ground test, and flight test experience,

1. The feasibility of the Hot Cycle system is proven.

2. The predicted performance capability is verified.

3. The low noise level is confirmed.

4. All basic data needed for operational applications are available.

The verification of performance predictions by the flight tests of the XV-9A helicopter, as shown in Figure 17, is indicative of the accuracy of the performance prediction method. This same method is used in all the performance predictions for the Hot Cycle applications and design studies.

ROTOR/WING RESEARCH AND DEVELOPMENT WORK ACCOMPLISHED

Rotor/Wing research and development work began at Hughes in late 1962 and has continued to date. Three major activities have been completed[1]:

Hover tests

Rotor/Wing alone wind tunnel tests

Complete model Rotor/Wing wind tunnel tests

ROTOR/WING HOVER TESTS

The Rotor/Wing concept requires the lifting rotor to have a centerbody large enough to support the weight of the aircraft when acting as a fixed wing at a reasonable conversion air speed. Because no data were available to show the effect of so large a centerbody on the hovering performance of a rotor, a series of tests was conducted by Hughes during the winter of 1962-63 to experimentally investigate the Rotor/Wing, Figure 18.

The test program was set up to determine four characteristics:

1. The hovering efficiency of the rotor with a large centerbody

(and to find if an optimum centerbody planform shape exists)

2. The efficiency of symmetrical (fore and aft) blade airfoil sections, since in the stopped-rotor flight one blade is in reversed flow (compared with helicopter flight) and symmetry of configuration was thought necessary.

3. The effect of the ratio of centerbody area to rotor area.

4. The ground effect for hovering near the ground.

Three centerbodies, of the relative size* and shape shown in Figure 19, were built for these tests, and a number of blade airfoil sections, all of 15-percent thickness ratio, were tested with each hub: NACA 0015, circular arc with parabolic leading and trailing edges, elliptical, and elliptical with camber. A rotor diameter of 80 inches was established so that the model could be used later in a low-speed wind tunnel.

Since rotor testing is a difficult art at best, and the results are affected by wind gusts, the test setup, the proximity of buildings, and so forth, it was decided to test a standard or reference rotor of conventional geometry along with the Rotor/Wing configurations. In this way, the test facility could be completely checked out, and an accurate comparison could be made with conventional helicopter performance. The outline of the reference rotor is indicated in Figure 19.

All models were powered by a pneumatic drive, using high-pressure, cold air to simulate tip-jet effects on the rotor performance.

As one would suspect, the thrust produced in hovering was proportional to the exposed length of the blades; thus the rotor with circular hub was most efficient, followed closely by the trisector hub, and then by the triangular hub. The circular arc airfoil section proved to be the most efficient of the double-ended sections. The configuration selected as the best compromise for hover and cruise flight was the trisector hub and circular arc blades. Extended blades that were 20 percent longer than the original blades were tested, to permit investigating the effect of hub-to-disc-area ratio, and showed a 10-percent increase in thrust going from a hub/disc ratio of 0.24 to 0.30, as indicated in Figure 20. Figure 20 also shows the thrust and torque characteristics of the Rotor/Wing compared with the reference rotor. In the thrust region where we want to operate the Rotor/Wing, there is a power penalty for constant thrust of 25 percent for the extended blade version. This is considered to be an acceptable price to pay for a VTOL system that has the promise of high subsonic flight speeds and outstanding payload-carrying ability.

*Each hub had the same planform area: 11.9 square feet.

Preliminary analysis indicated the possibility of an adverse ground effect caused by evacuating air from the bottom side of the centerbody. It was also thought that this effect might have hysteresis with ground plane height; that is, show different augmentation effects depending on whether the Rotor/Wing was approaching or leaving the ground.

Figure 21 shows the effect of ground plane height for thrust data reduced to a common torque coefficient and plotted as the ratio of thrust in ground effect to thrust out of ground effect. No noticeable hysteresis occurred between the ground plane moving up and ground plane moving down, and the Rotor/Wing exhibited a ground effect somewhat improved over that of a conventional helicopter rotor[5].

WIND TUNNEL TESTS OF ROTOR/WING ALONE

In the spring of 1964, Hughes loaned two of the Rotor/Wing models used in the hovering tests to the Navy (BuWeps) for subsonic wind tunnel tests at the David Taylor Model Basin Aerodynamics Laboratory (Figure 22). These stopped-rotor tests were made using the triangular and circular hub models with elliptical and NACA 0015 airfoil section blades. The data (Figure 23) showed that the Rotor/Wing configuration has lift and drag characteristics similar to those of other low aspect ratio wings. One important finding was that one blade should point forward and the other two sweep back for best stability in pitch.

WIND TUNNEL TESTS OF COMPLETE ROTOR/WING MODEL

After completion of the hover model tests and the stopped-rotor tests of the Rotor/Wing alone, the main area of investigation remaining was the feasibility of the conversion procedure from running- to stopped-rotor and back again. To study this, as well as powered-rotor, autorotating-rotor, and stopped-rotor characteristics of the complete model, the model shown in Figure 24 was built under contract to the Office of Naval Research, with the Bureau of Naval Weapons participating. This model, which was of approximately one-sixth scale compared with a proposed full-scale Rotor/Wing ASW aircraft, completed two series of wind tunnel tests in the spring of 1965 at the David Taylor Model Basin Aerodynamics Laboratory.

The powered-rotor aerodynamic characteristics were measured over a forward flight speed range corresponding to approximately 60 to 150 knots for a full-scale aircraft, and are plotted in Figure 25*. The lift

*Conventional rotor blade pitch terminology is used:
$\theta = A_0 - A_1 \cos\psi - B_1 \sin\psi - A_2 \cos 2\psi - B_2 \sin 2\psi - \ldots$
however, unlike the conventional flapping rotor, the A_n terms make the Rotor/Wing develop pitching moments, and B_n terms make it roll.

developed by the Rotor/Wing is less than would be expected from a conventional rotor, because of the small blade span and download on the hub. Figure 26 shows a comparison between the Rotor/Wing and a helicopter in hovering and in forward flight[2,3].

The Rotor/Wing, which has no flapping hinges at the blade roots, develops a strong tendency to roll toward the retreating side of the rotor, but this is easily cancelled by application of lateral cyclic pitch.

Autorotation is planned to be a transitory step between the helicopter and airplane modes of flight, although extended flight could be performed in this mode. The aerodynamic characteristics of the Rotor/Wing aircraft in autorotation are given in Figure 27.

In airplane flight with the Rotor/Wing stopped and locked, one of the main points of interest is the lift-to-drag ratio. As Figure 28 shows, the maximum trimmed L/D of the model is 8.6. To convert to full-scale lift/drag ratio, we correct first for Reynolds number effects[6], and then for a low-drag fuselage configuration. The model fuselage was contoured to enclose the internal mechanisms without trying to achieve minimum drag. These corrections indicate a maximum L/D of approximately 10 for the basic Rotor/Wing geometry, and this occurs at an indicated airspeed of 210 knots – a value high enough to result in good cruise speeds at high altitudes.

If we go to longer blades than the basic model had, the resulting increase in aspect ratio should increase the maximum lift/drag ratio as shown in Figure 29, and it is intended that a full-scale Rotor/Wing aircraft could achieve a maximum lift/drag ratio of 12. A second benefit arising from the longer blades would be a lowered disc loading and increased hovering efficiency, as shown in Figure 30, which indicates that the hovering figure of merit will be somewhat less than 0.6 for a full-scale aircraft. This is thought to be an acceptable penalty for a VTOL aircraft that can cruise at speeds approaching 500 knots.

It is planned to use an all-movable horizontal tail for both pitch and roll control in stopped-rotor flight – the two halves used in unison for pitch and differentially for roll, as in the manner of the X-15 and the F-111. Tests in the wind tunnel showed this to be a satisfactory method of control.

Conversion tests were made in the wind tunnel using two techniques. The first was a pseudoconversion in which the rotor was powered to run at various rpm's while the tunnel speed was held constant and the rotor blade pitch controls and model angle of attack were manipulated to maintain a constant lift force and zero rolling moment. From these data, a map, such as Figure 31, was drawn and paths selected through it to make

the rotor accelerate and decelerate. The second technique used a completely unpowered rotor and an automatic programming device that sensed rotor speed and followed the predetermined schedule of collective pitch, cyclic pitch, and fuselage angle of attack shown in Figure 32. This resulted in aerodynamic moments that would start or stop the rotor while maintaining constant lift, zero rolling moment, and a small pitching moment that could easily have been compensated by the horizontal tail if the proper incidence were used. Figure 33 shows the pitch, roll, and lift response of the model during a conversion.

While automatic conversions were demonstrated in the wind tunnel, manual conversions were also made, with results indistinguishable from the automatic runs – indicating that a pilot could easily fly the aircraft through conversion without help from automatic programming devices.

The details of the response of the Rotor/Wing at very low rpm's are quite interesting. Figure 34 shows a time history of the Rotor/Wing shaft bending moments transferred into pitching and rolling moments in the nonrotating fuselage coordinate system for the first three revolutions of the rotor during an automatic conversion, starting from zero rpm. Because of the extreme stiffness of this particular model, it ran at rpm's well below the three-per-rev resonance speed, and the rotor airloads could be measured by reading the shaft bending moments without being confused by the phase shifts, resonances, and so forth, that usually obscure airload data in more conventional rotor models. During the first half of the first revolution, a nose-down trim change occurred. Before the beginning of the second revolution, an equilibrium was established, and only a nominal amount of three-per-rev moment was delivered by the rotor from then on. Converting these alternating moments to angular displacements of a full-scale aircraft, we see in Figure 35 that the response is small and should be felt as no more than a short-duration shudder as the rotor starts or stops. The lateral acceleration felt by the pilot's head at a point three feet above the center of gravity is approximately ± 0.15 g – no more than the steady-state lateral acceleration allowed by military specification[7].

CONCLUSIONS

The Hot Cycle Rotor/Wing high-speed VTOL aircraft is a unique new concept that promises a high subsonic speed aircraft that has:

1. Cruise efficiency superior to that of a delta-wing jet airplane.

2. Vertical takeoff and landing capability approaching the efficiency and operational advantages of a helicopter.

3. Simplicity and low empty weight.

Sufficient test data have been established in the Hot Cycle XV-9A program and in the Rotor/Wing whirl-test and wind tunnel test programs to indicate that such a performance potential exists and to make it possible to proceed to the next step in the design and development of a full-scale aircraft with good assurance of success.

REFERENCES

1. Head, R. E., Summary Technical Report, Rotor/Wing Concept Study, Hughes Tool Company-Aircraft Division Report 65-15, August 1965 (Available to qualified DDC users only through ONR code 461).

2. LaForge, S., Performance Handbook, Hughes Tool Company-Aircraft Division Report XA-8016.

3. Gessow, A. and Tapscott, R. J., Charts for Estimating Performance of High Performance Helicopters, NACA Report 1266, 1956.

4. Cohan, S. and Hirsh, N. B., Summary Report, XV-9A Hot Cycle Research Aircraft Program, Hughes Tool Company-Aircraft Division Report 65-27.

5. Gessow, A. and Myers, G. C., Jr., Aerodynamics of the Helicopter, The Macmillan Company, 1952.

6. Frost, R. C. and Rutherford, R., Subsonic Wing Span Efficiency, AIAA Journal, April 1963.

7. Anon. Helicopter Flying and Ground Handling Qualities; General Requirements for, Military Specification MIL-H-8501A, September 1961.

LIST OF ILLUSTRATIONS AND TABLES

Figure

1 Hover Lift Efficiency
2 Hot Cycle Rotor System Noise Comparison
3 XV-9A Hot Cycle Research Aircraft
4 XV-9A Propulsion System Schematic
5 Rotor/Wing with Trisector Hub
6 Propulsion System Schematic
7 Rotor/Wing Flight Modes
8 Payload Versus Range – (High-Speed VTOL Aircraft) - Standard Sea Level
9 Payload Versus Range – (High-Speed VTOL Aircraft) - 6000 ft 95° F
10 Rotor/Wing Aircraft Design Studies
11 Recovery/Transport Aircraft General Arrangement
12 Rotor/Wing Retractable Fairings
13 Hover Ceiling Out of Ground Effect
14 Speed and Climb Performance
15 Basic Recovery Mission
16 Payload-Range
17 XV-9A Propulsion System Performance
18 Rotor/Wing Hover Test Models
19 Model Components
20 Hovering Test Results
21 Ground Effect
22 Rotor/Wing Alone Wind Tunnel Model
23 Stopped Rotor Aerodynamic Characteristics
24 Complete Rotor/Wing Wind Tunnel Model
25 Helicopter Aerodynamic Characteristics
26 Ratio of Power Required by Rotor/Wing Model and Power Required by Conventional Helicopter
27 Autorotation Aerodynamic Characteristics
28 Complete Model Lift/Drag Ratio
29 Estimated Maximum Trimmed Lift/Drag Ratio
30 Hovering Figure of Merit
31 Pseudoconversion Test
32 Control Time History - Automatic Conversion
33 Model Response During Automatic Conversion
34 Model Rotor/Wing Low RPM Characteristics - Automatic Conversion
35 Aircraft Rolling Amplitudes During Conversion

Table

1 Symbols and Nomenclature
2 Basic Characteristics, Recovery/Transport VTOL Aircraft
3 Weight Summary

TABLE 1
SYMBOLS AND NOMENCLATURE

A_1	Longitudinal cyclic pitch control angle, degrees
A_2	Second harmonic longitudinal cyclic pitch angle, degrees
b	Number of rotor blades
B	Rotor blade tip loss factor
B_1	Lateral cyclic pitch control angle, degrees
c	Rotor blade chord, feet
D	Drag force, pounds
i_H	Horizontal tail incidence angle, degrees
Δi_H	Differential horizontal tail incidence angle, degrees
L	Lift force, pounds
$\mathcal{L}$	Rolling moment, foot-pounds
M	Pitching moment, foot-pounds
N	Yawing moment, foot-pounds
N_R	Rotor speed, rpm
PPF	Profile power factor
Q	Torque, foot-pounds
q	Dynamic pressure, pounds/square foot
R	Rotor radius, feet
V	Airspeed, knots
Y	Side force, pounds
Z	Rotor plane height above ground, feet
α	Fuselage angle of attack, degrees
β	Fuselage side-slip angle, degrees
θ	Rotor collective pitch angle, degrees
θ_1	Rotor blade twist angle, degrees
μ	Rotor advance ratio, $\left(\frac{60\ V}{2\pi N_R R}\right)$
ξ	Ratio of rotor blade root radius to blade tip radius
σ	Rotor solidity ratio, $\left(\frac{b\ c}{\pi R}\right)$

ϕ Fuselage roll angle, degrees

Ω Rotor rotational speed, radius/second

C_Q Torque coefficient $\left(\frac{Q}{\rho \pi R^3 (\Omega R)^2}\right)$

C_T Thrust coefficient $\left(\frac{T}{\rho \pi R^2 (\Omega R)^2}\right)$

C_D Drag Coefficient $\left(\frac{D}{q \pi R^2}\right)$

C_L Lift coefficient $\left(\frac{L}{q \pi R^2}\right)$

C_M Pitching moment coefficient $\left(\frac{M}{q \pi R^3}\right)$

$\overline{\overline{\mathcal{L}}}$ Rotor shaft bending moment coefficient transferred into fuselage coordinate system, rolling component $\left(\frac{\mathcal{L}}{L\ R}\right)$

$\overline{\overline{M}}$ Rotor shaft bending moment coefficient transferred into fuselage coordinate system, pitching component $\left(\frac{M}{L\ R}\right)$

$\overline{\overline{M}}_s$ Rotor shaft bending moment coefficient $\left(\frac{M_s}{L\ R}\right)$

M Figure of merit $0.707 \frac{C_T^{3/2}}{C_Q}$

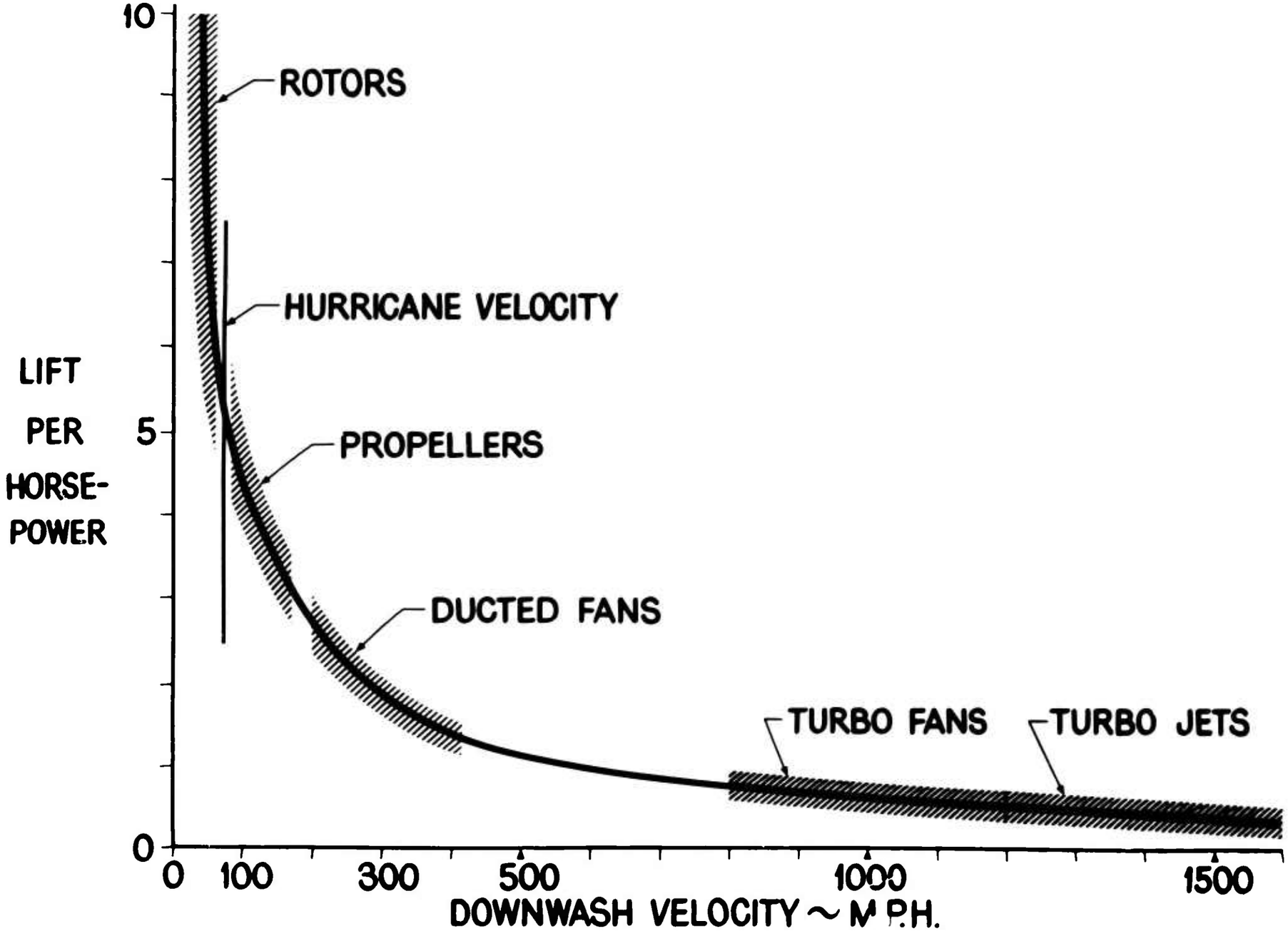

Figure 1 Hover Lift Efficiency

TABLE 2
BASIC CHARACTERISTICS, RECOVERY/TRANSPORT VTOL AIRCRAFT

Rotor/Wing diameter, ft	70
Disc area, sq ft	3850
Number of blades	3
Wing area (Locked), sq ft	1300
Span (locked), ft	63
Aspect ratio	3.3
Length overall, ft	106
Height, ft	21
Cabin volume, cu ft	2000
Crew accommodations for pilot, copilot, crew chief	
General Electric GE1/J1 gas generators	2
General Electric cruise fans	2

TABLE 3
WEIGHT SUMMARY, RECOVERY/TRANSPORT VTOL AIRCRAFT

	Pound
Rotor/Wing group	7990
Tail group	1590
Body group	5900
Landing gear group	2040
Flight controls group	1920
Yaw control system	140
Miscellaneous propulsion system	1050
Engines	1310
Cruise fans	1300
Instruments	150
Hydraulic equipment group	460
Electrical equipment group	610
Electronic equipment group	290
Furnishings equipment group	680
Air conditioning and anti-icing group	800
WEIGHT EMPTY	26,230
Crew	600
Rescue equipment	350
Oil and unusable fuel	180
Fuel (basic mission)	18,140
DESIGN GROSS WEIGHT (VTO)	45,500
MAXIMUM GROSS WEIGHT (overload at load factor = 2.0)	68,000

Figure 3 XV-9A Hot Cycle Research Aircraft

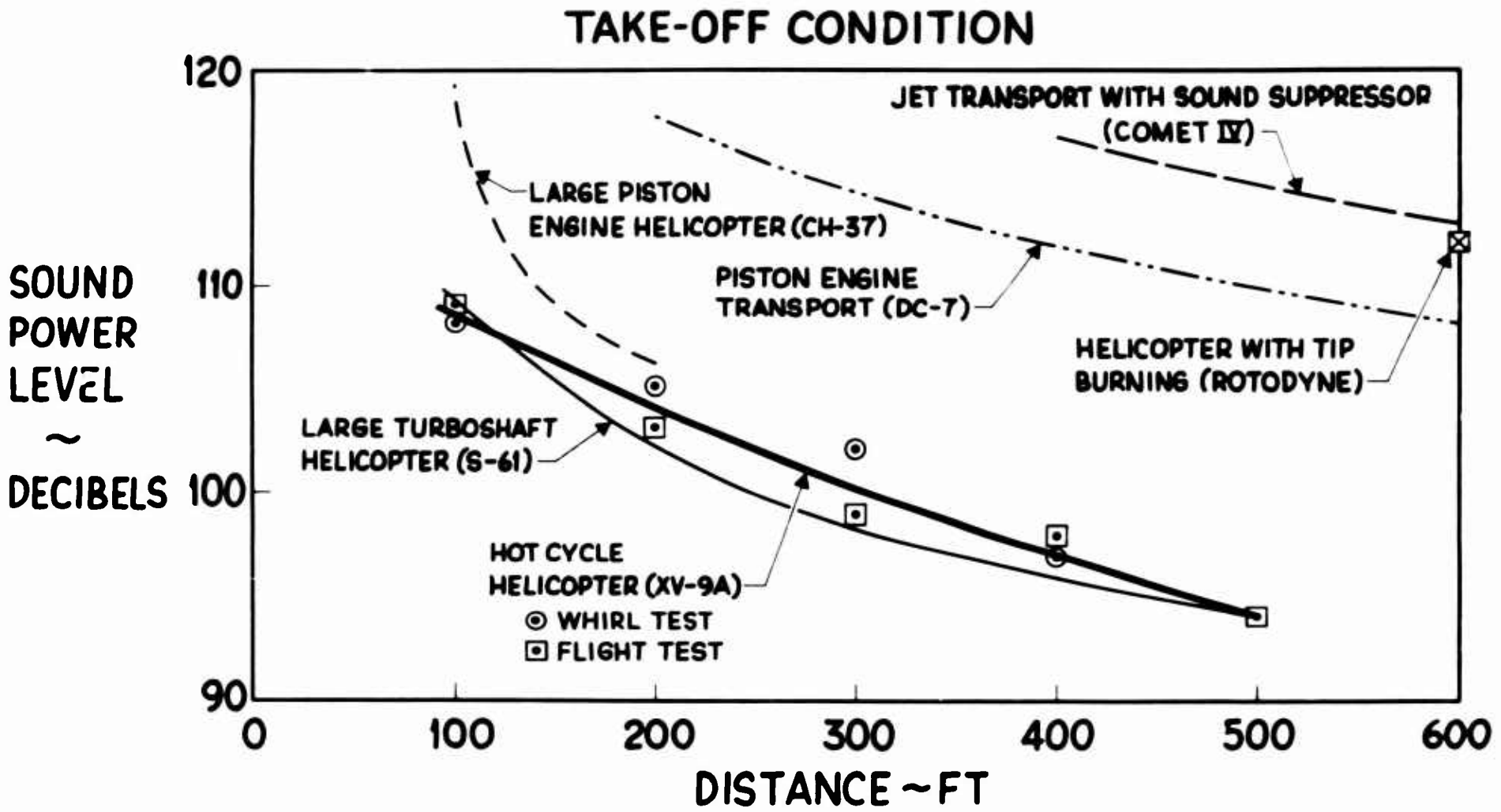

Figure 2. Hot Cycle Rotor System Noise Comparison

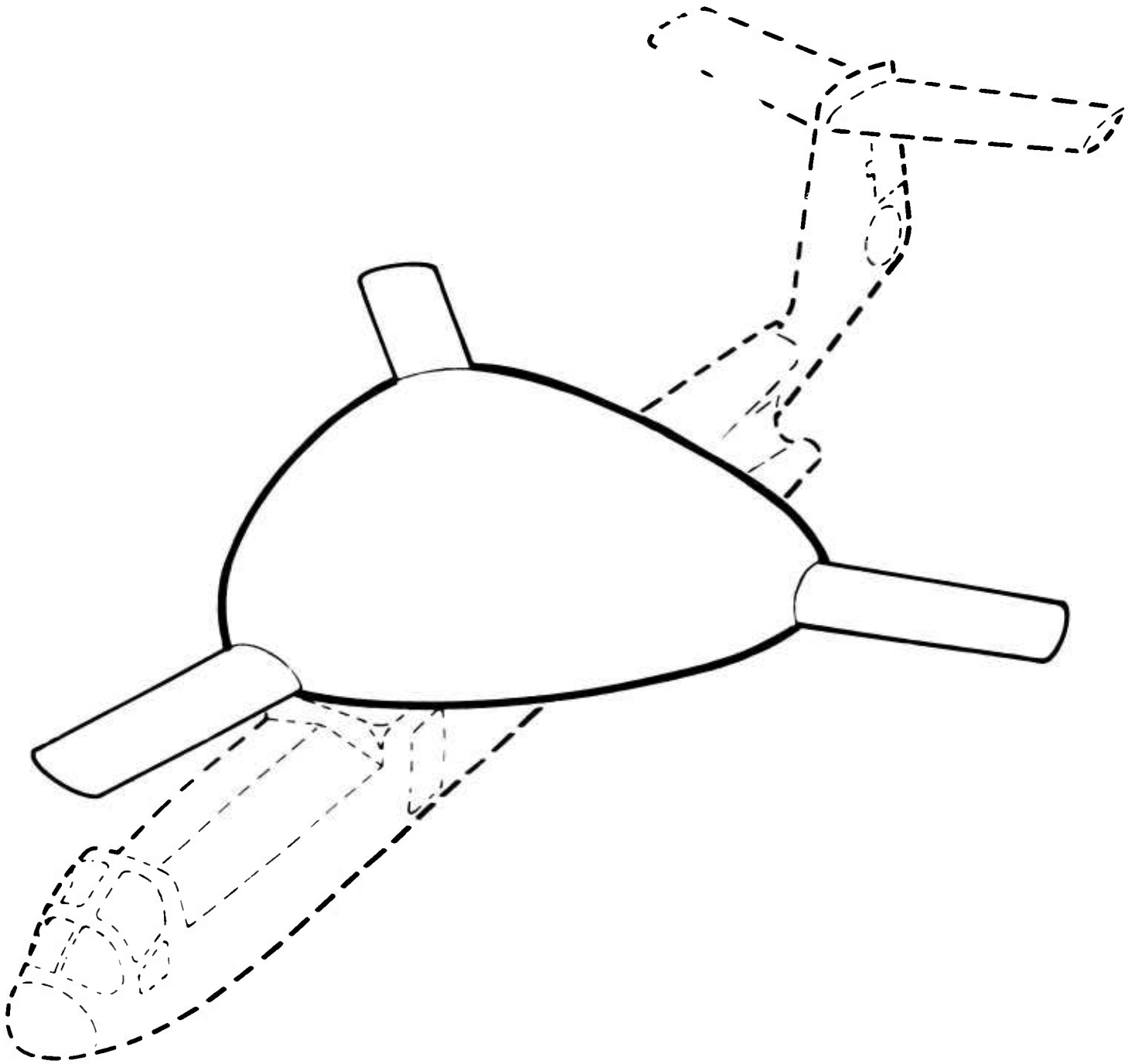

Figure 5. Rotor/Wing With Trisector Hub

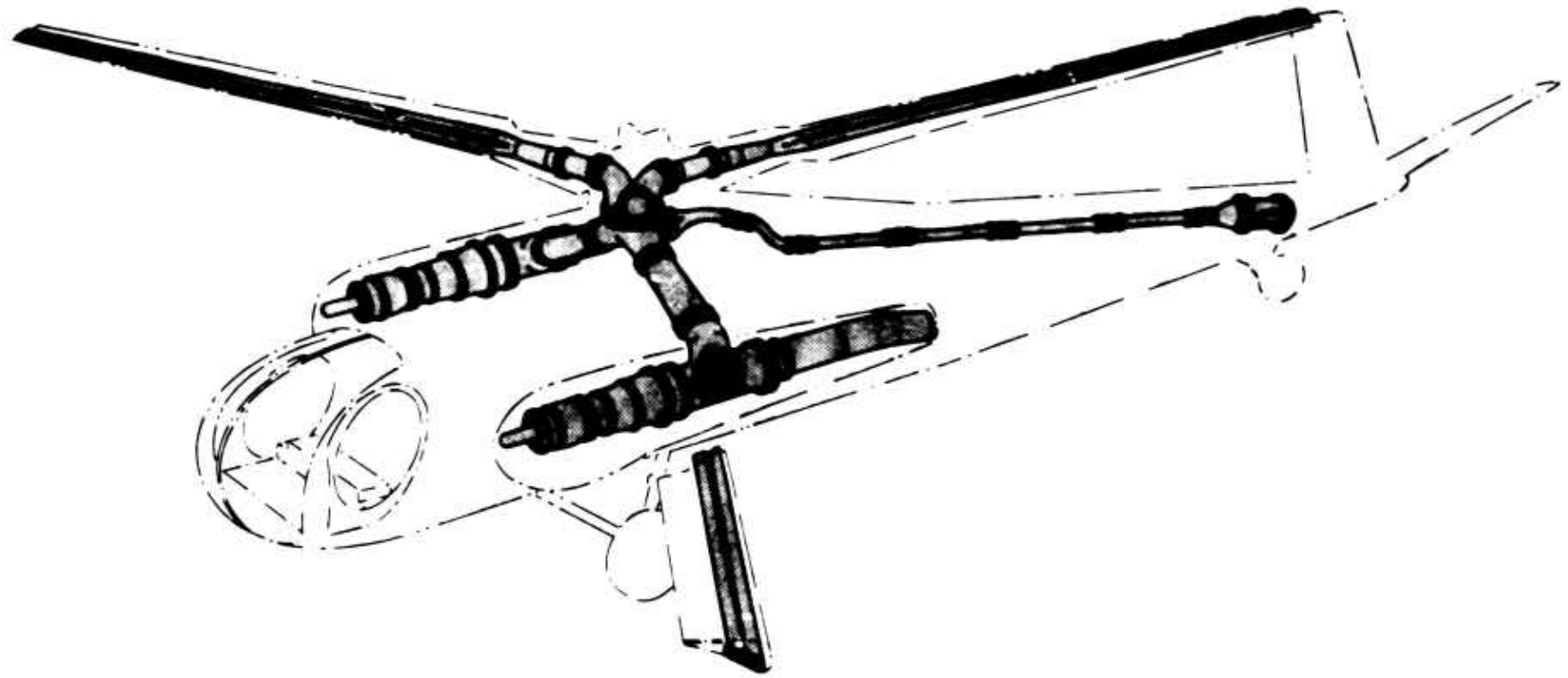

Figure 4. XV-9A Propulsion System Schemati

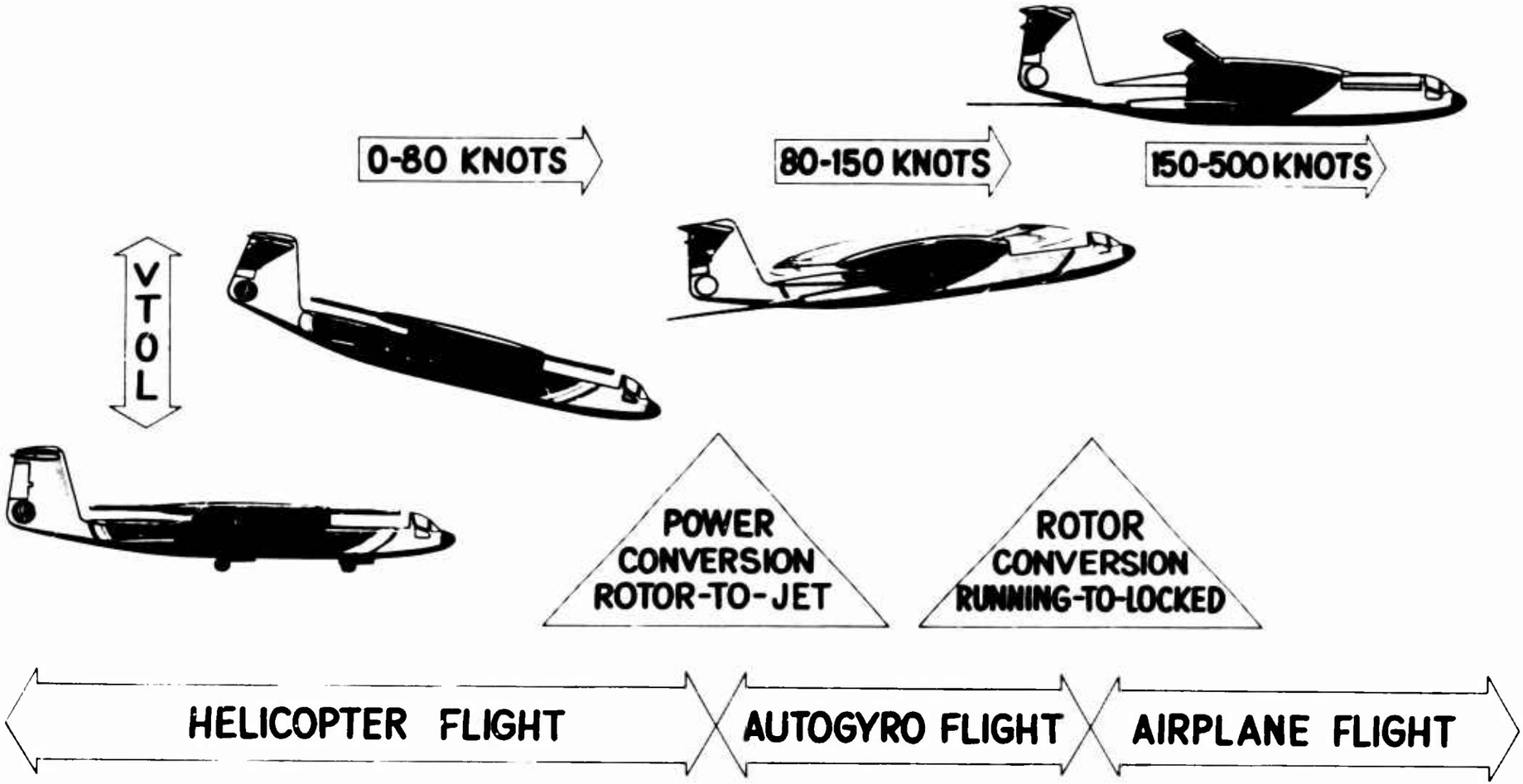

Figure 7. Rotor/Wing Flight Modes

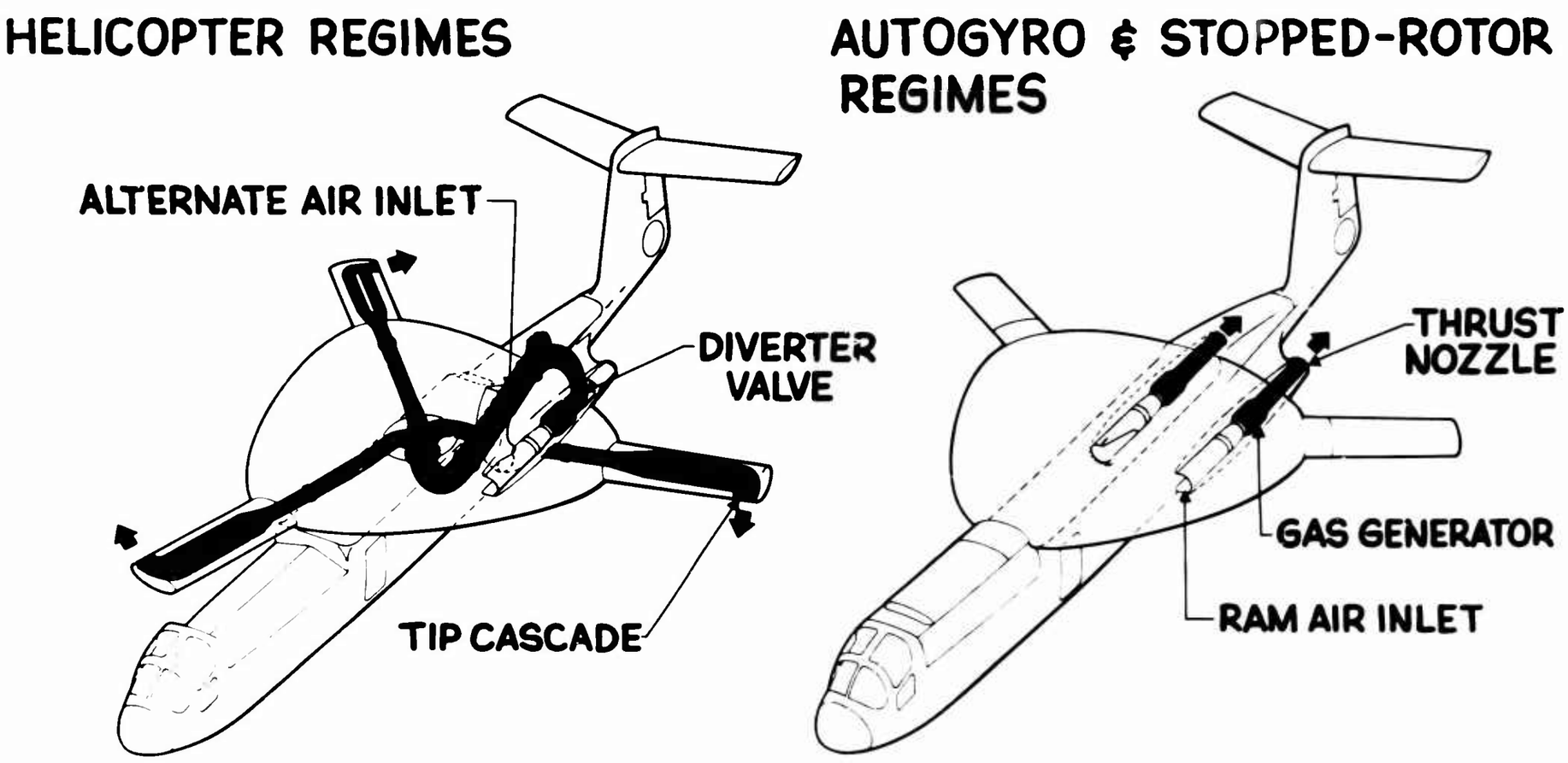

Figure 6. Propulsion System Schematic

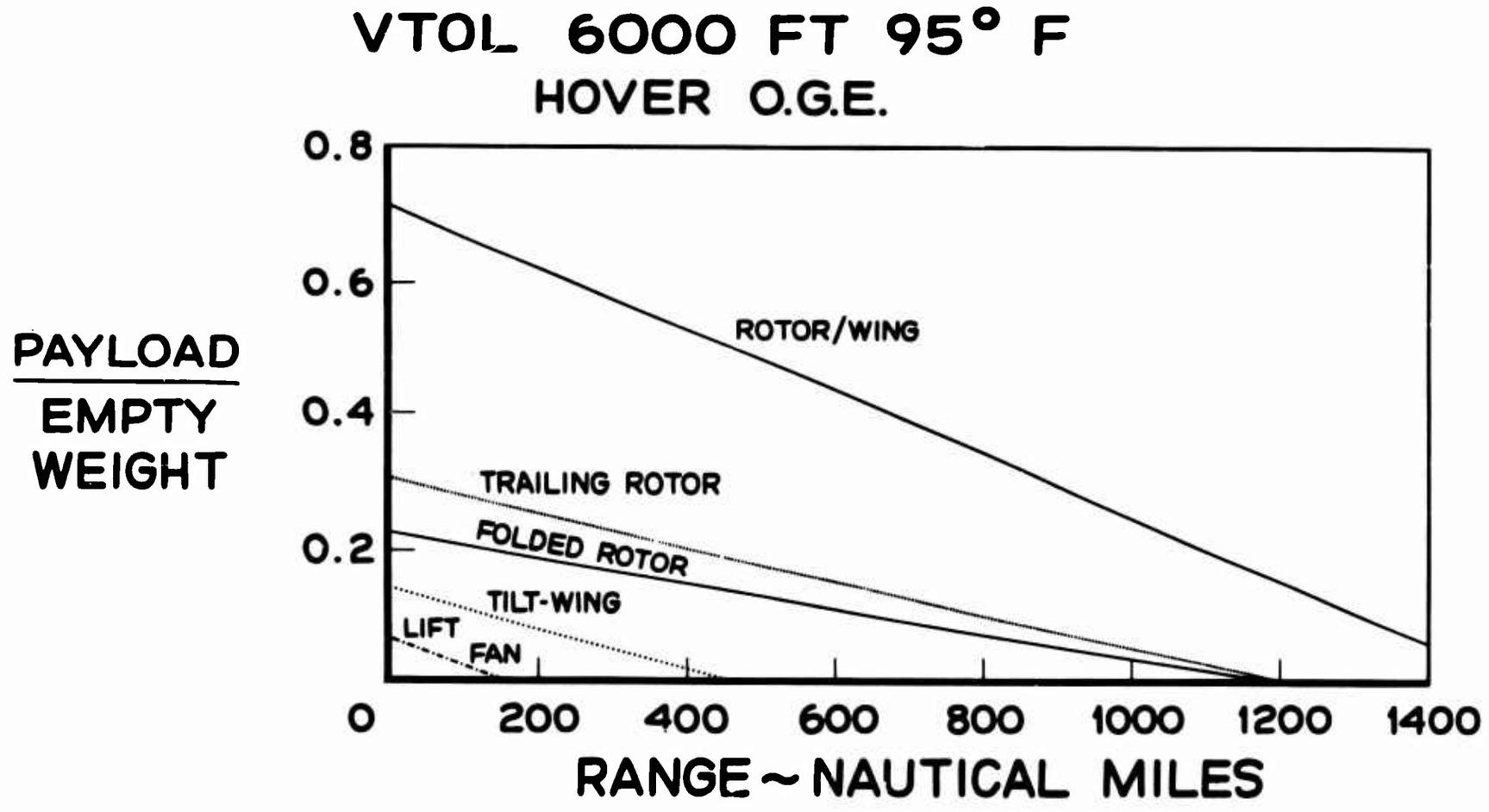

Figure 9. Payload Versus Range - High-Speed VTOL Aircraft - 6000 Feet, 95° F

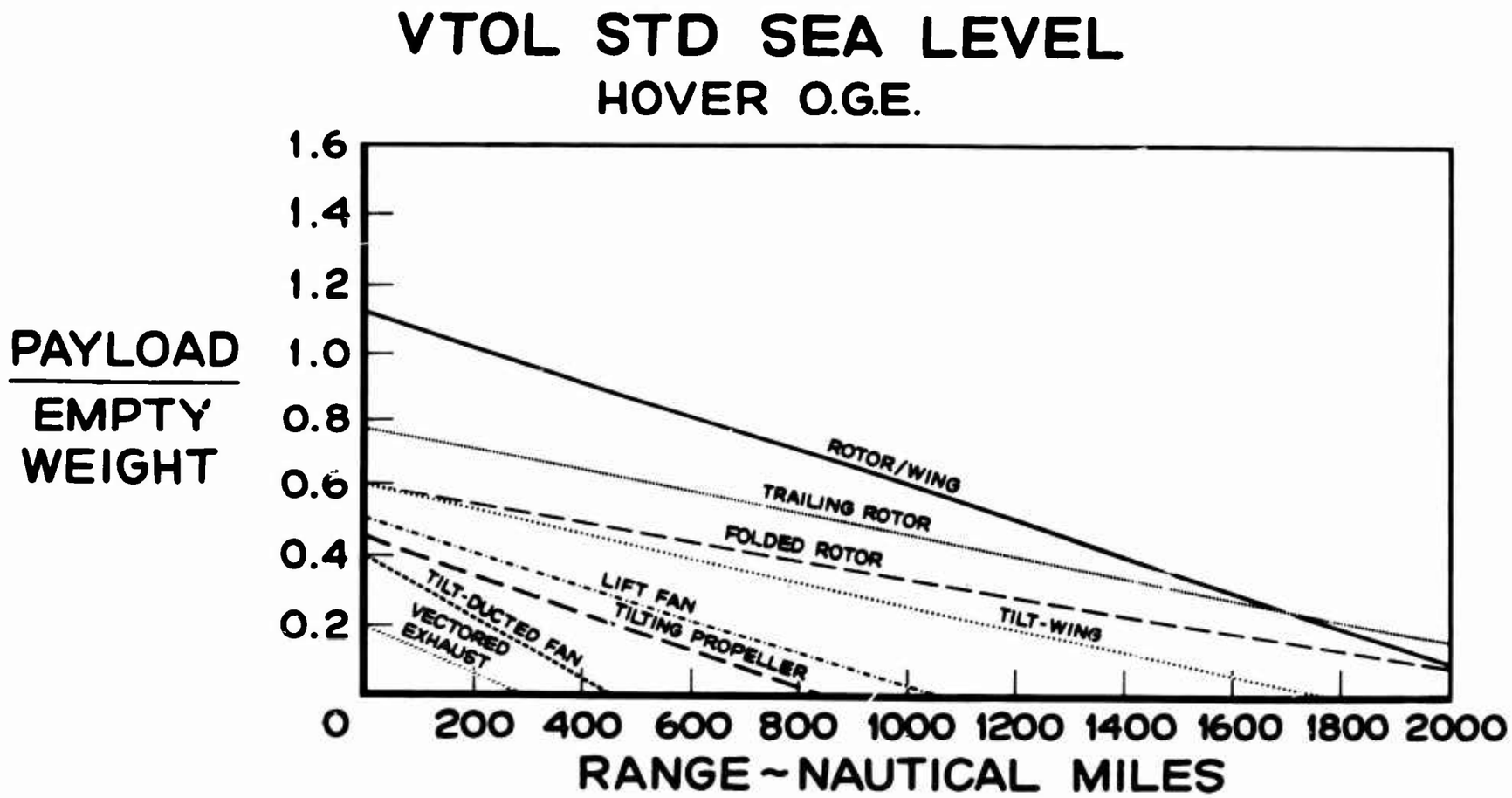

Figure 8. Payload Versus Range - High-Speed VTOL Aircraft - Standard Sea Level

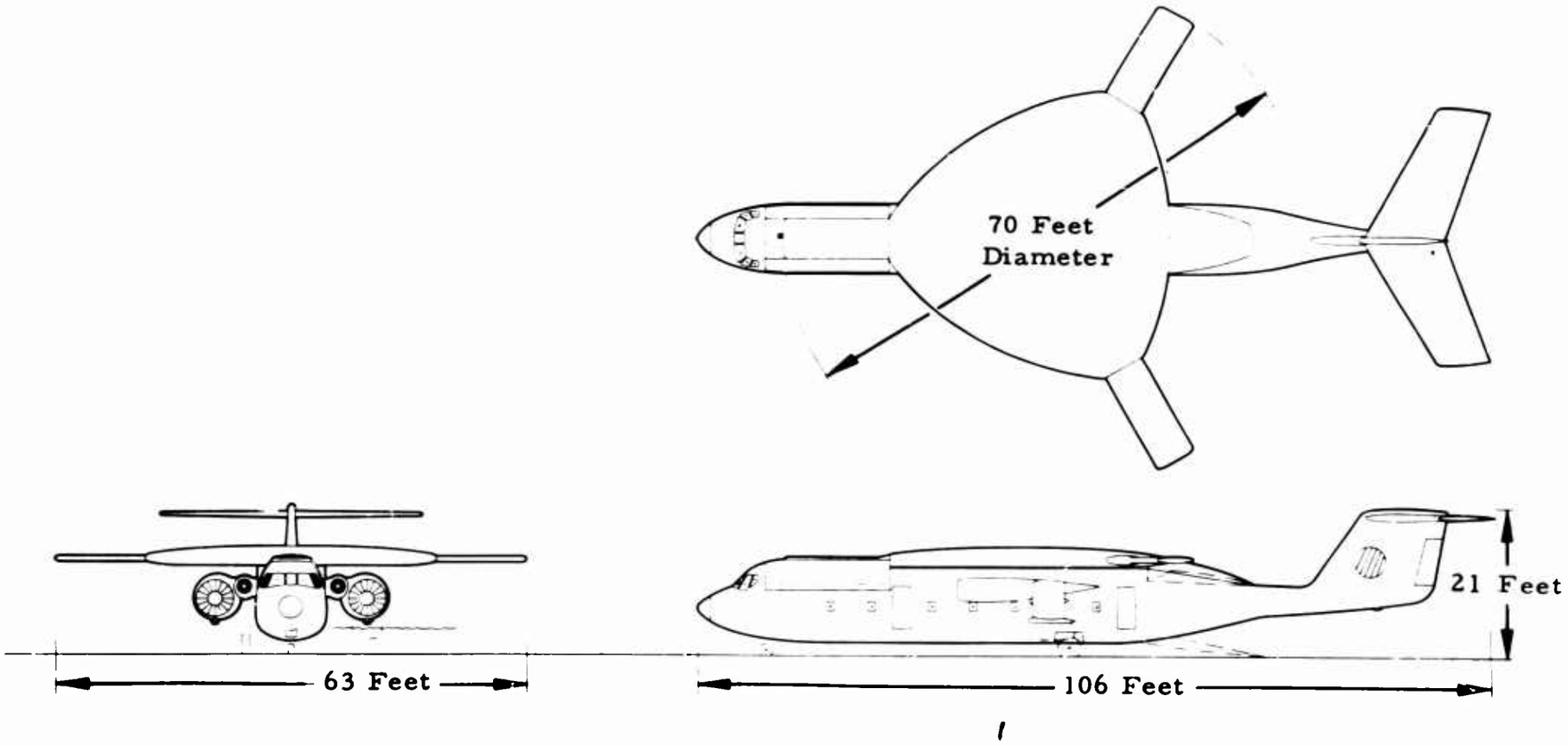

Figure 11. Recovery/Transport Aircraft General Arrangement

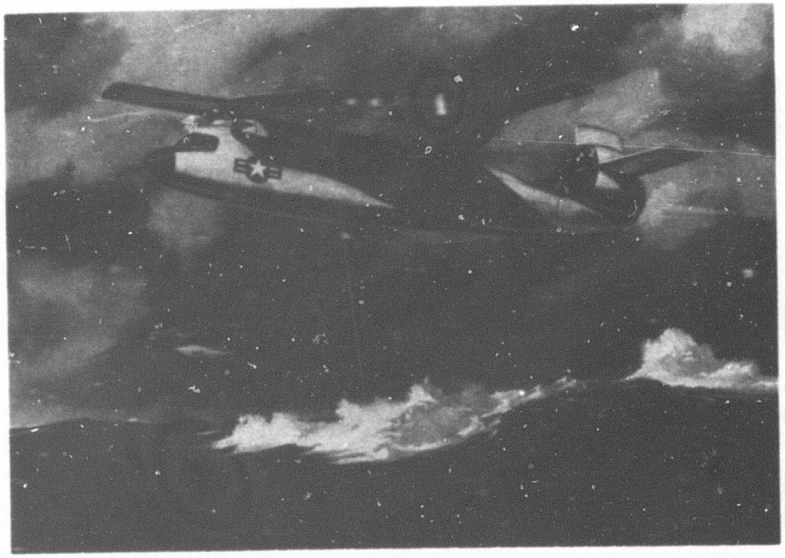

Anti-Submarine Warfare

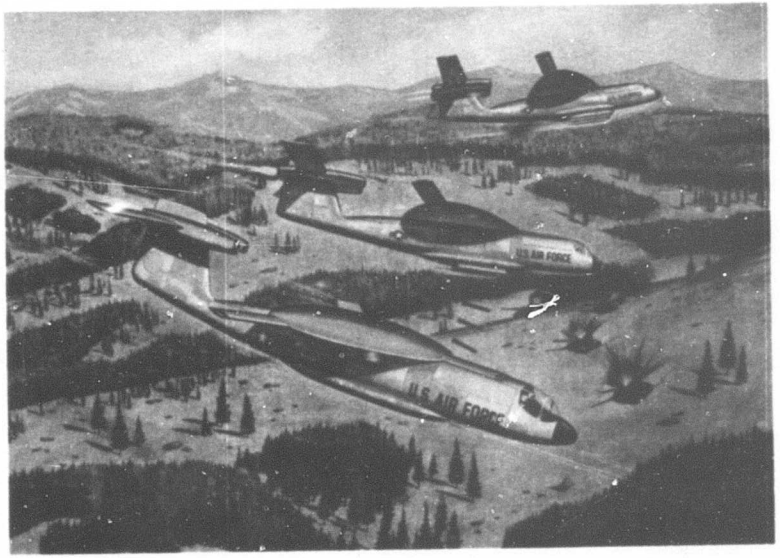

Fire Support

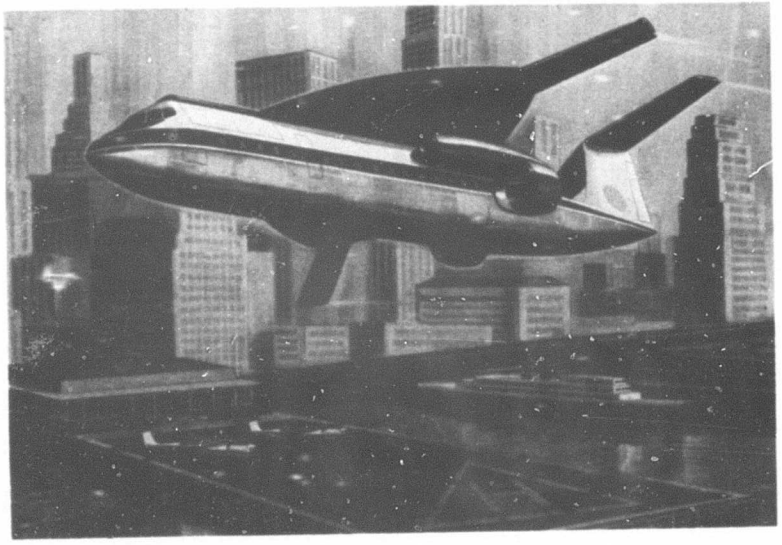

City Center Transport

Recovery/Transport

Figure 10. Rotor/Wing Aircraft Design Studies

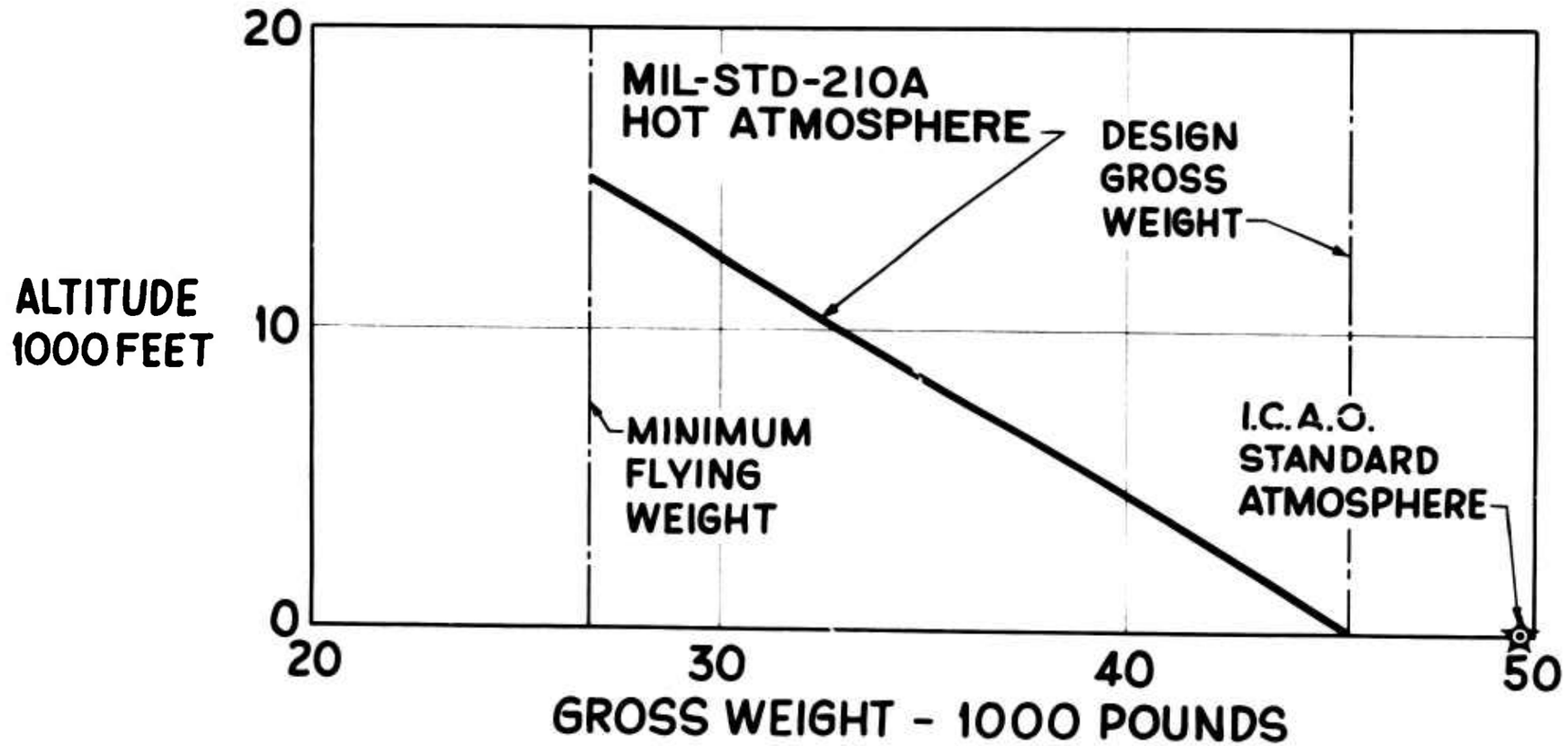

Figure 13. Hover Ceiling Out of Ground Effect

Figure 12. Rotor/Wing Retractable Fairings

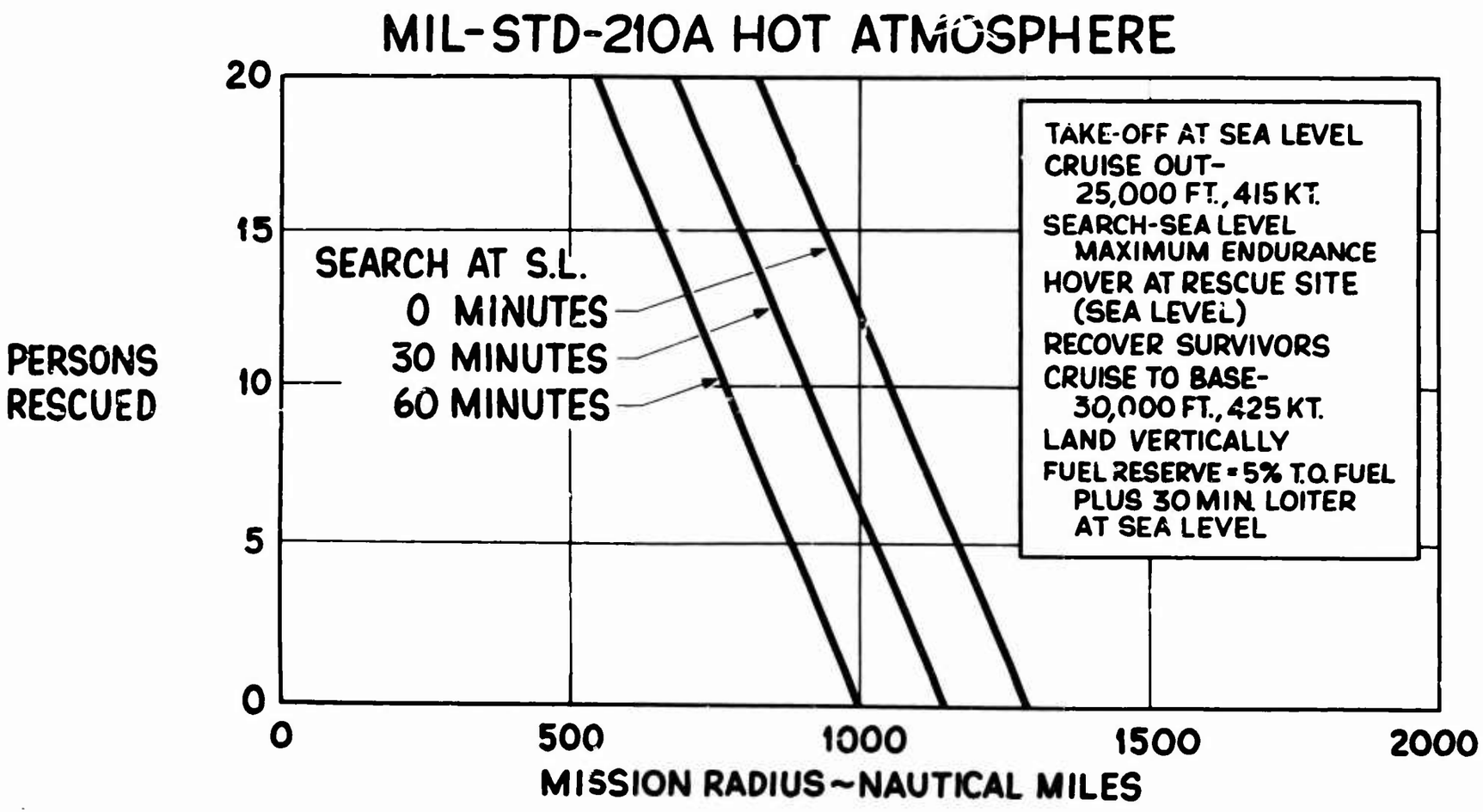

Figure 15. Basic Recovery Mission

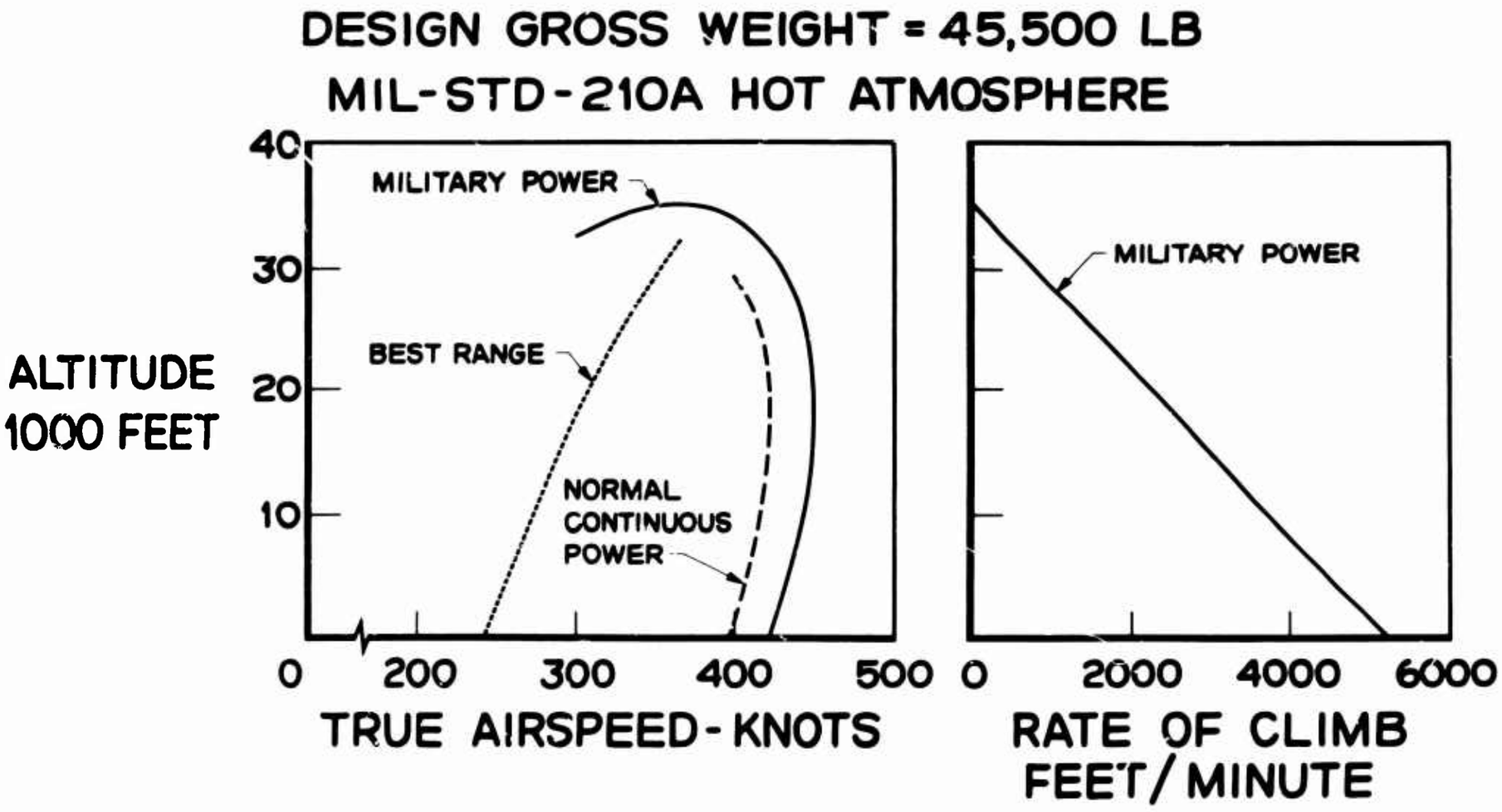

Figure 14. Speed and Climb Performance

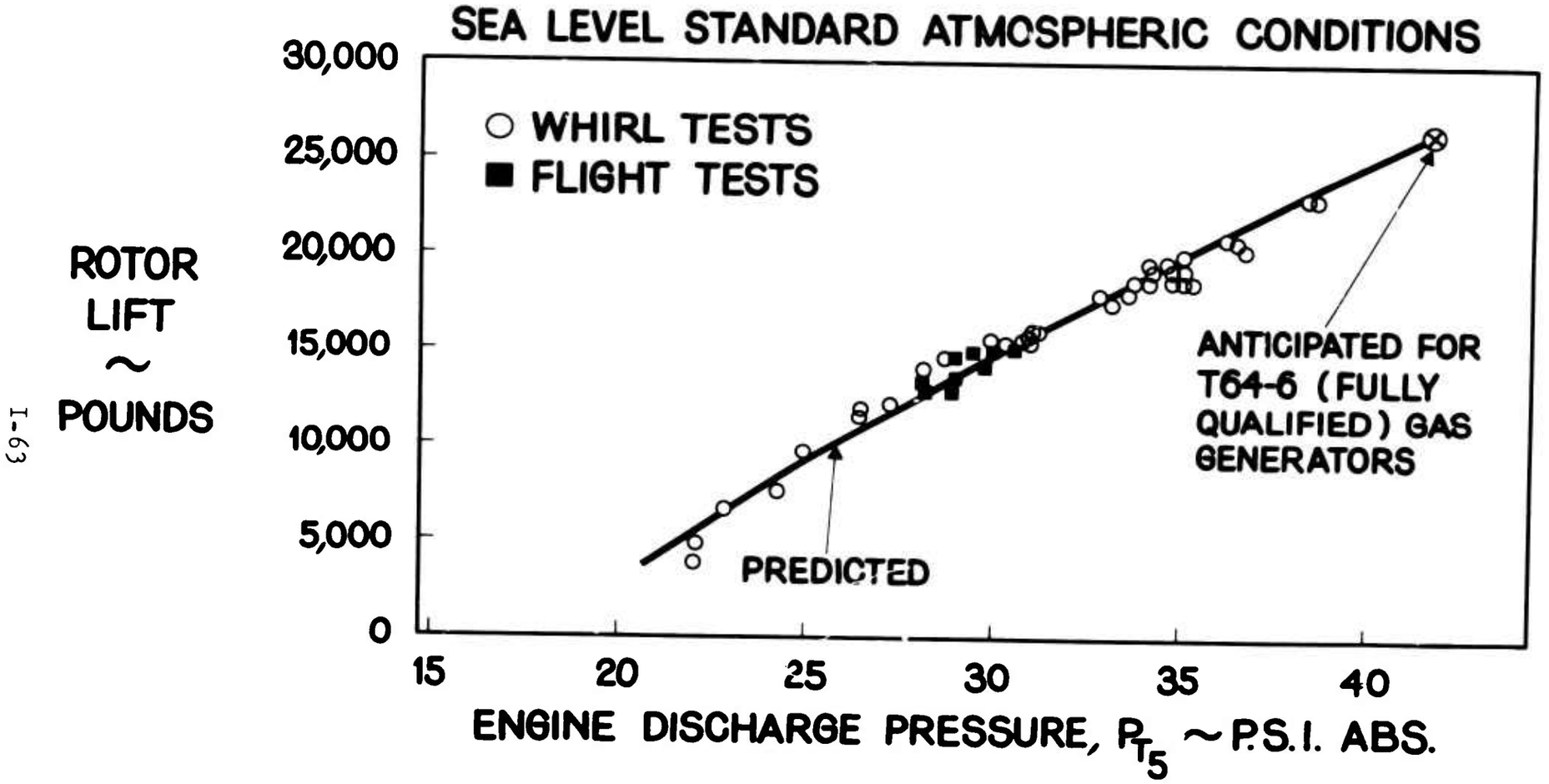

Figure 17. XV-9A Propulsion System Performance

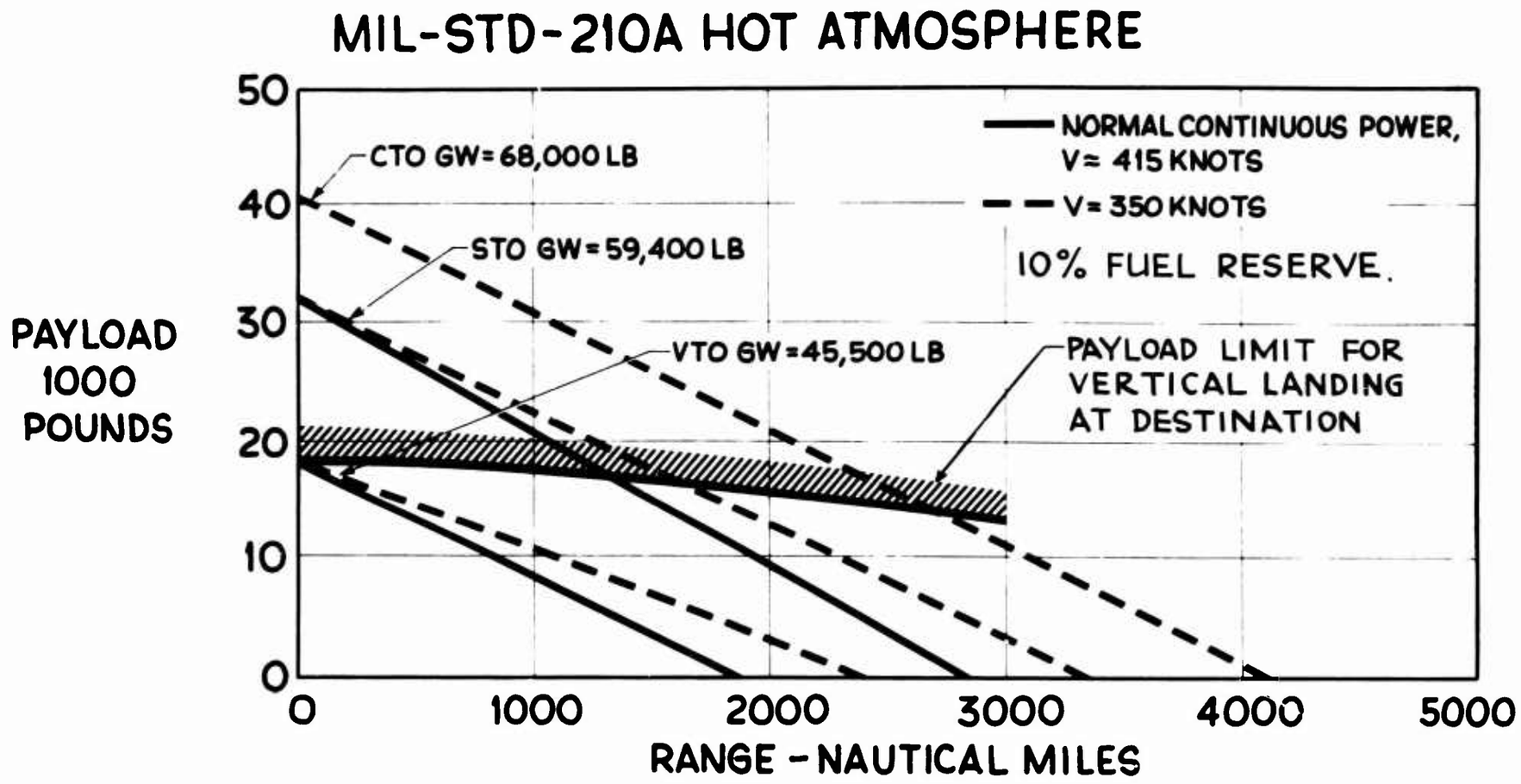

Figure 16. Payload-Range

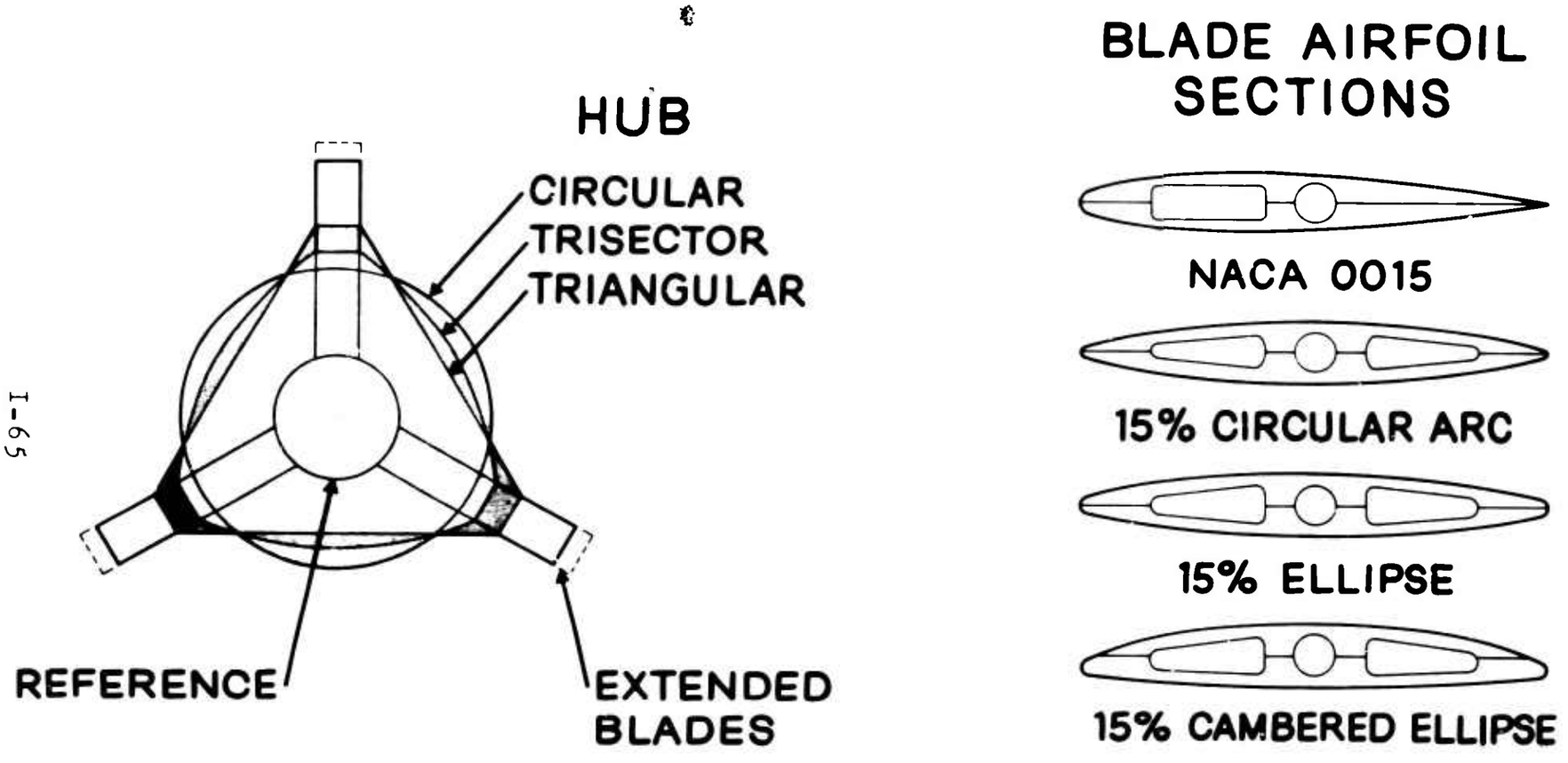

Figure 19. Model Components

Figure 18. Rotor/Wing Hover Test Models

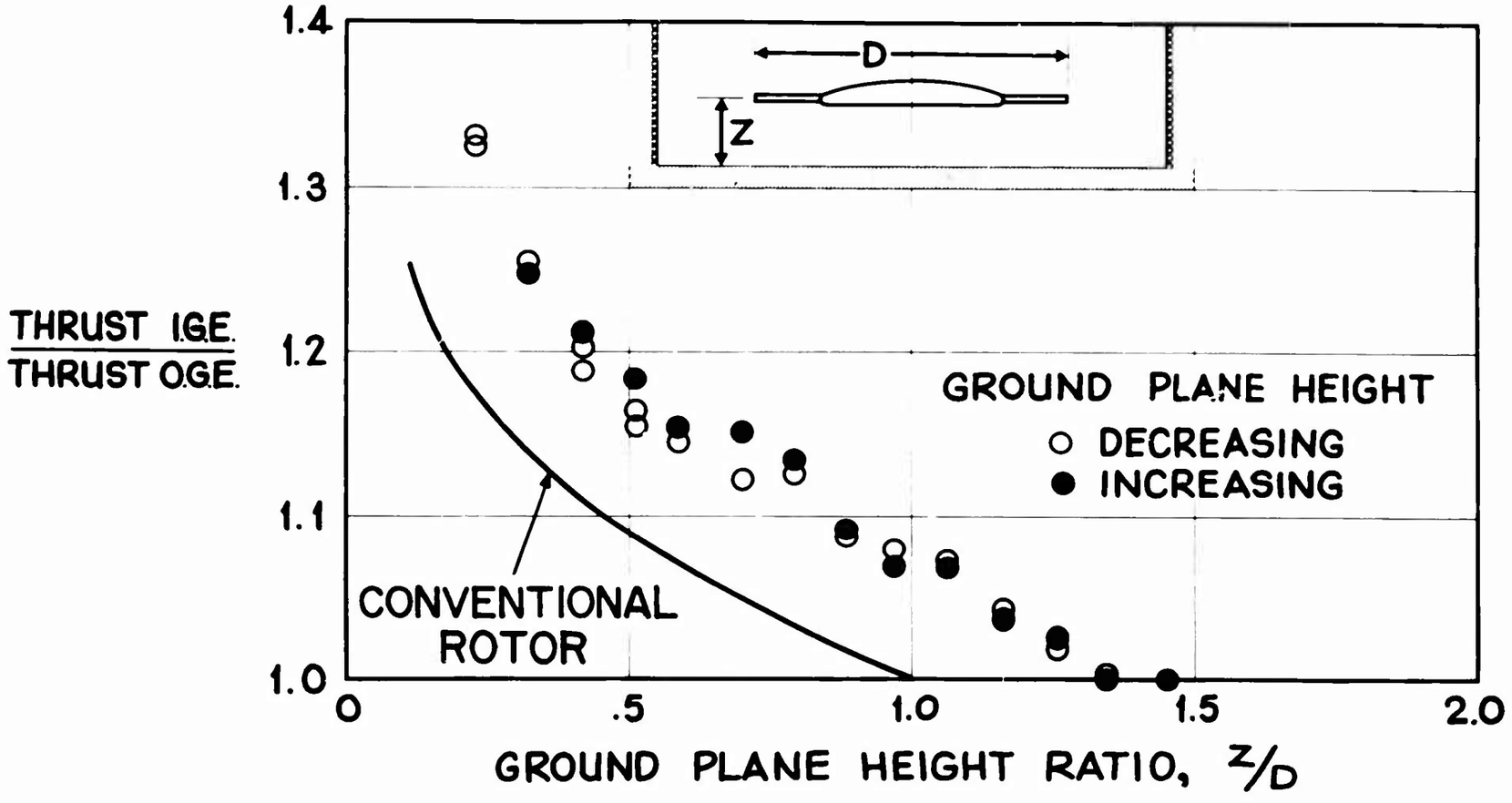

Figure 21 Ground Effect

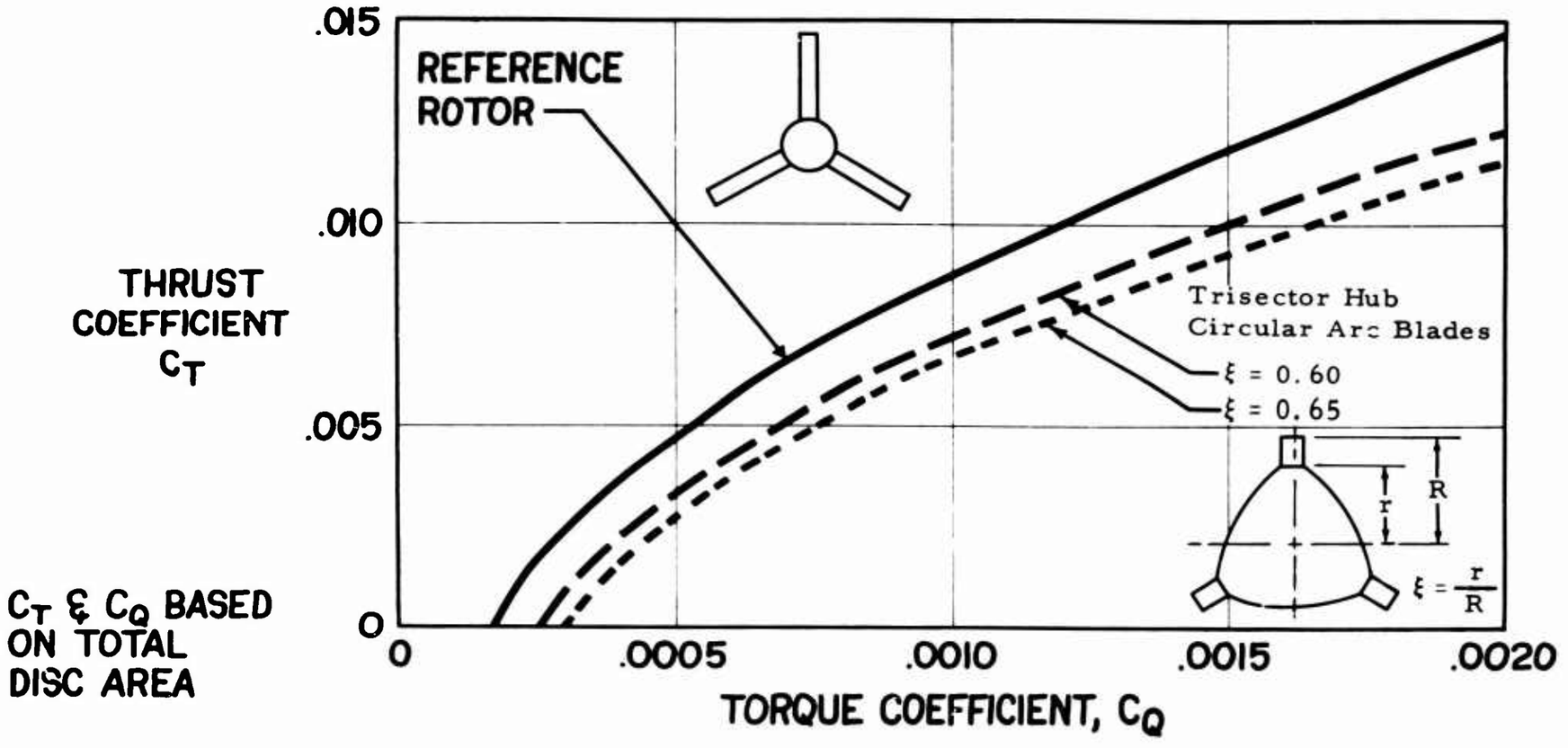

Figure 20. Hovering Test Results

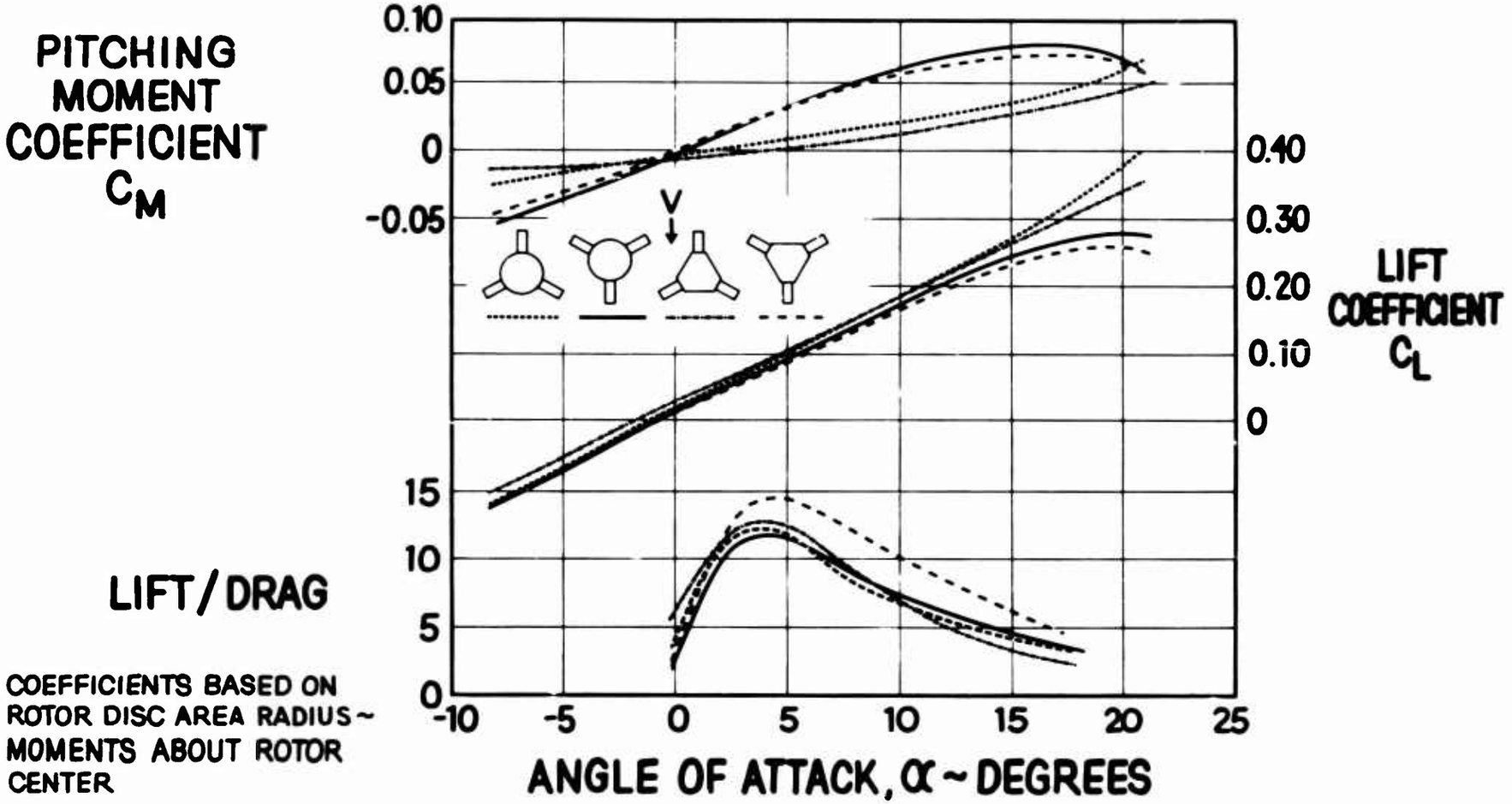

Figure 23. Stopped Rotor Aerodynamic Characteristics

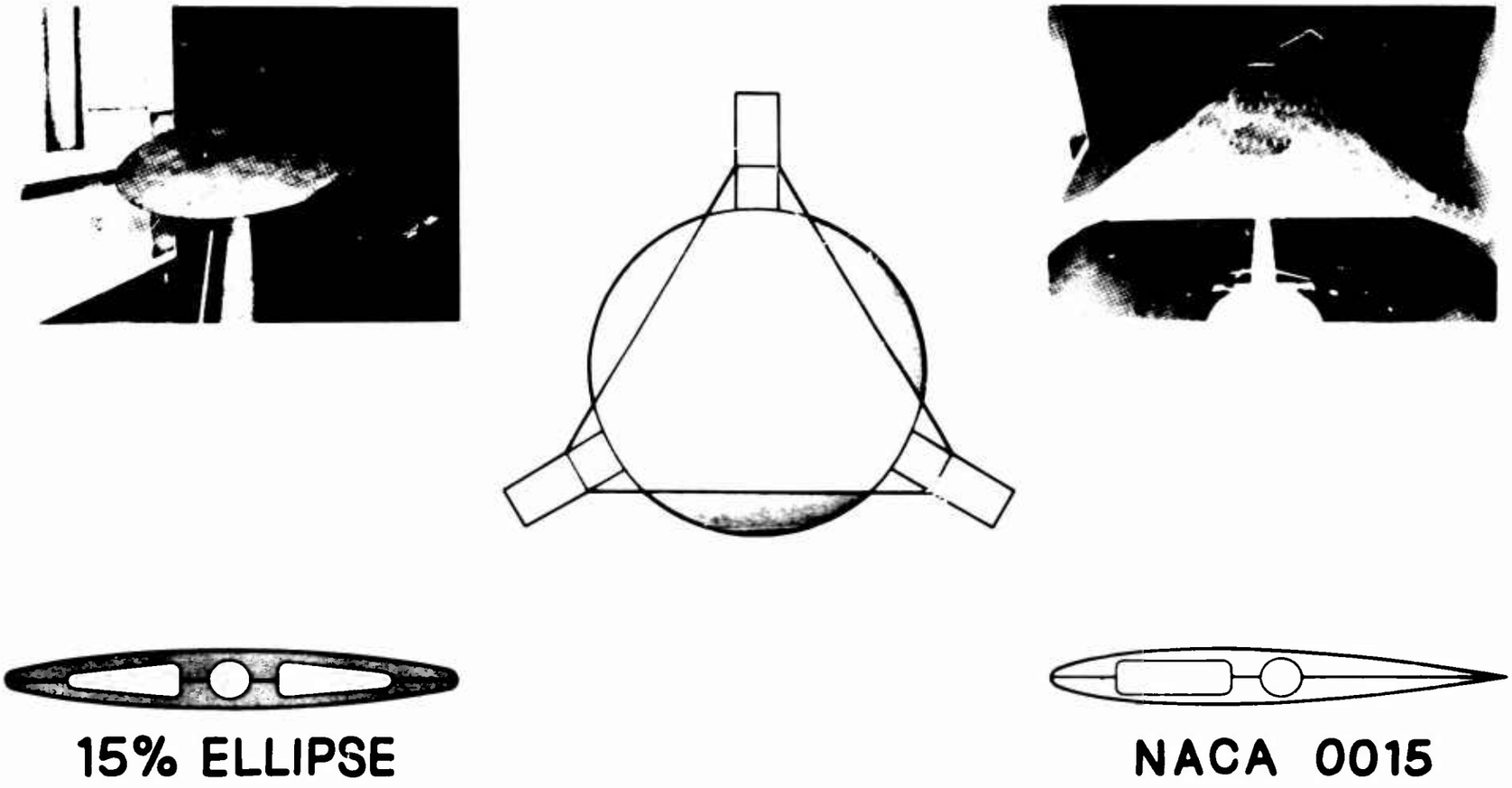

Figure 22. Rotor/Wing Alone Wind Tunnel Model

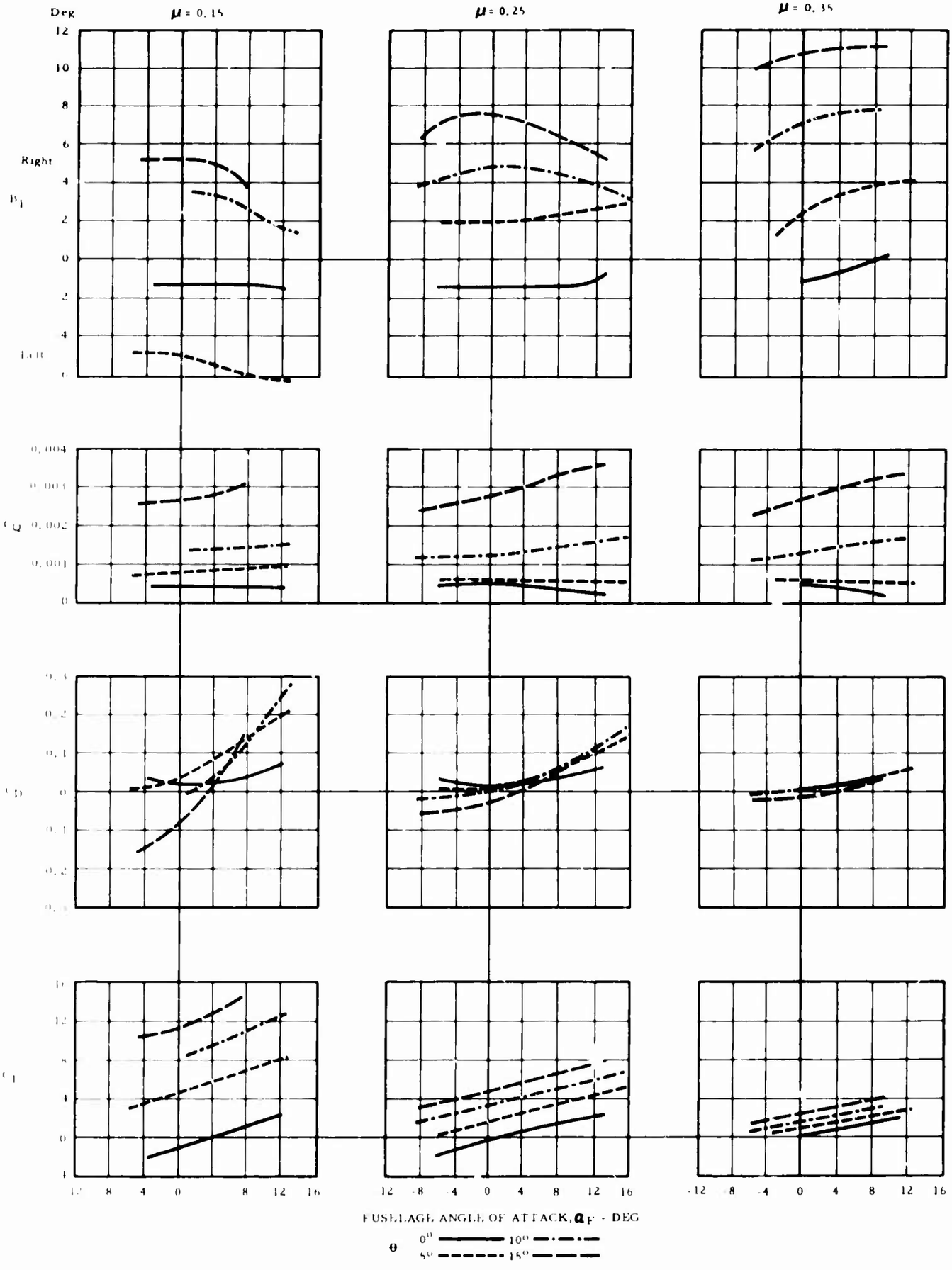

Figure 25. Helicopter Aerodynamic Characteristics

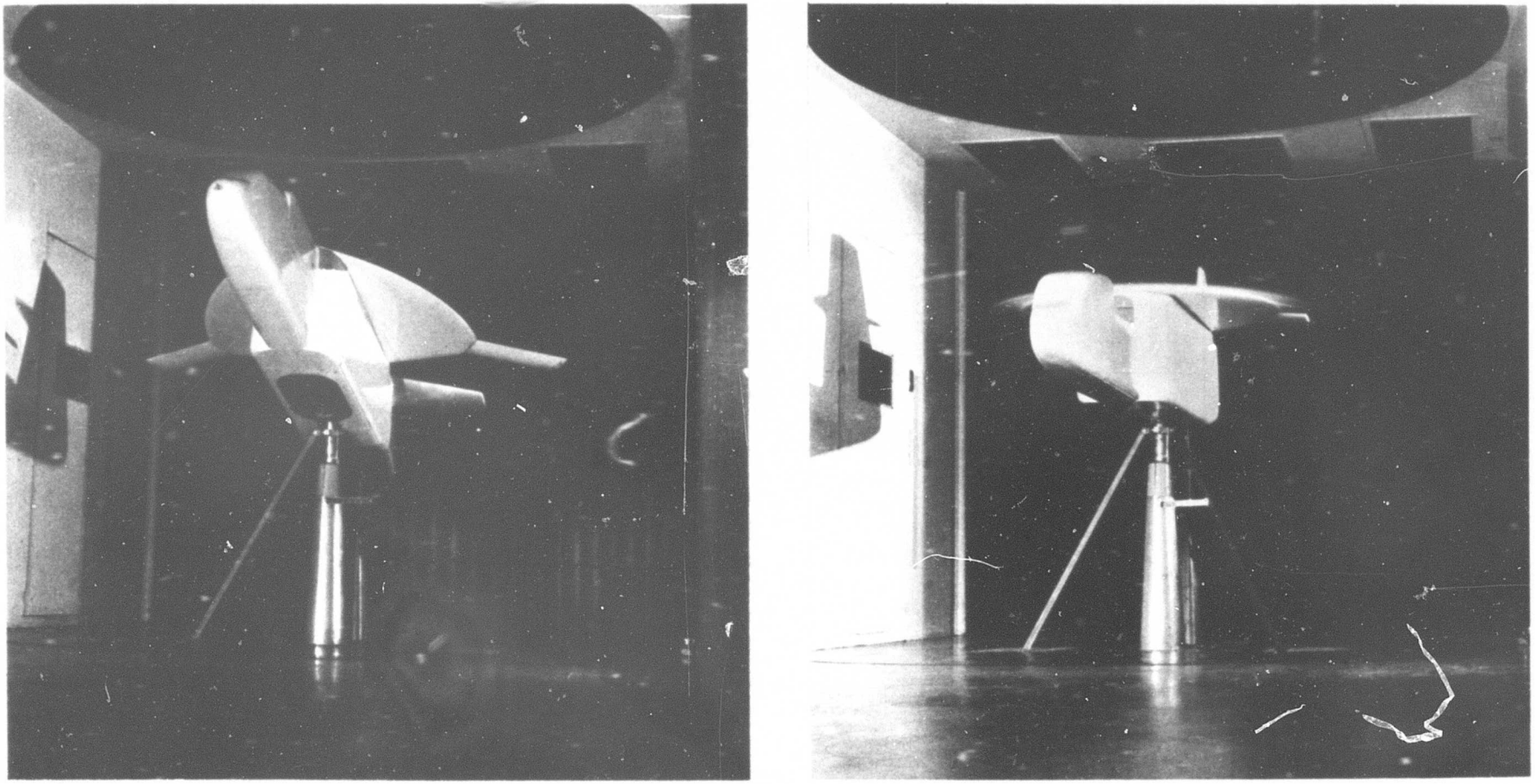

Figure 24. Complete Rotor/Wing Wind Tunnel Model

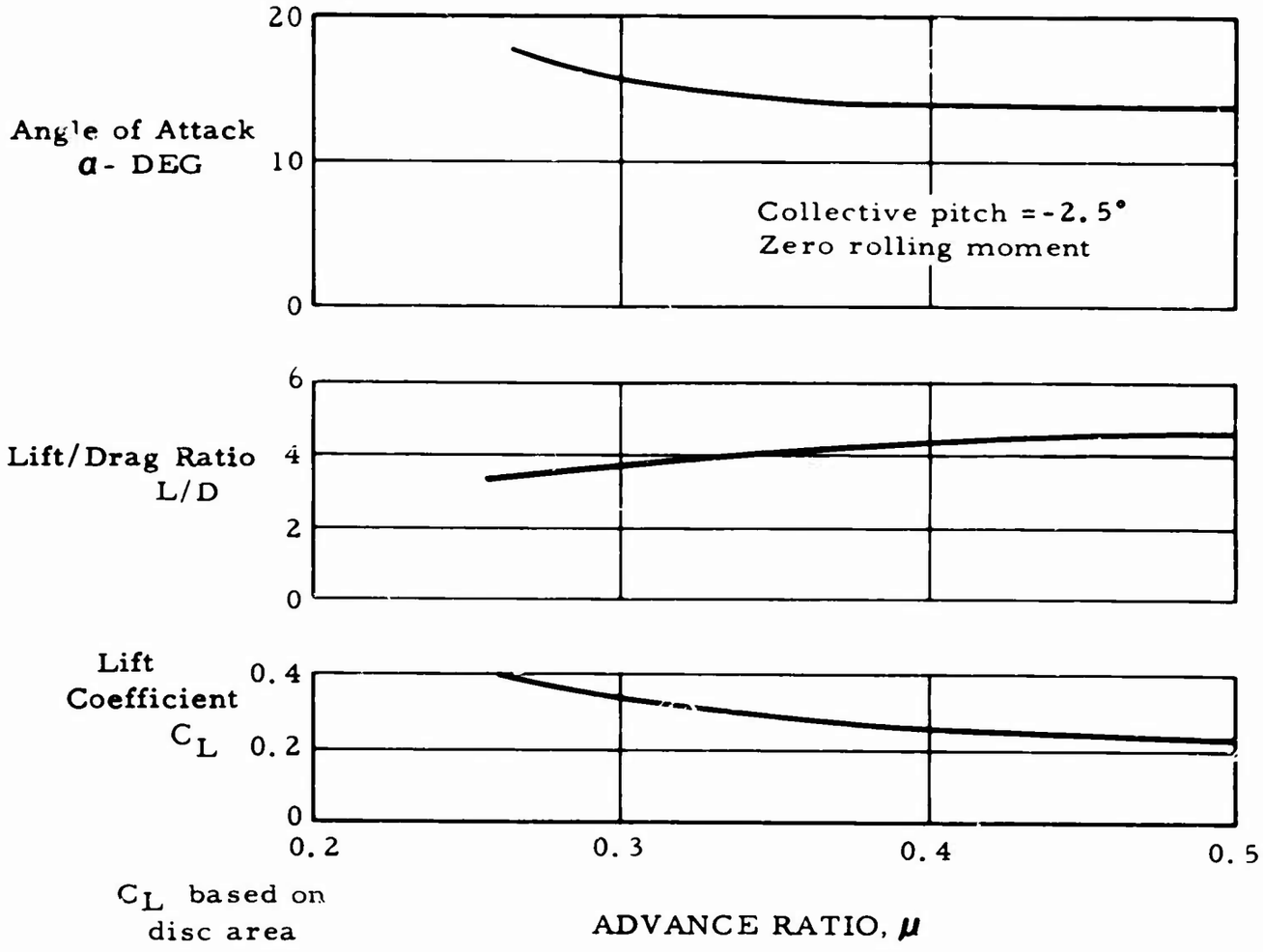

Figure 27. Autorotation Aerodynamic Characteristics

Figure 26. Ratio of Power Required by Rotor/Wing Model to Power Required by Conventional Helicopter

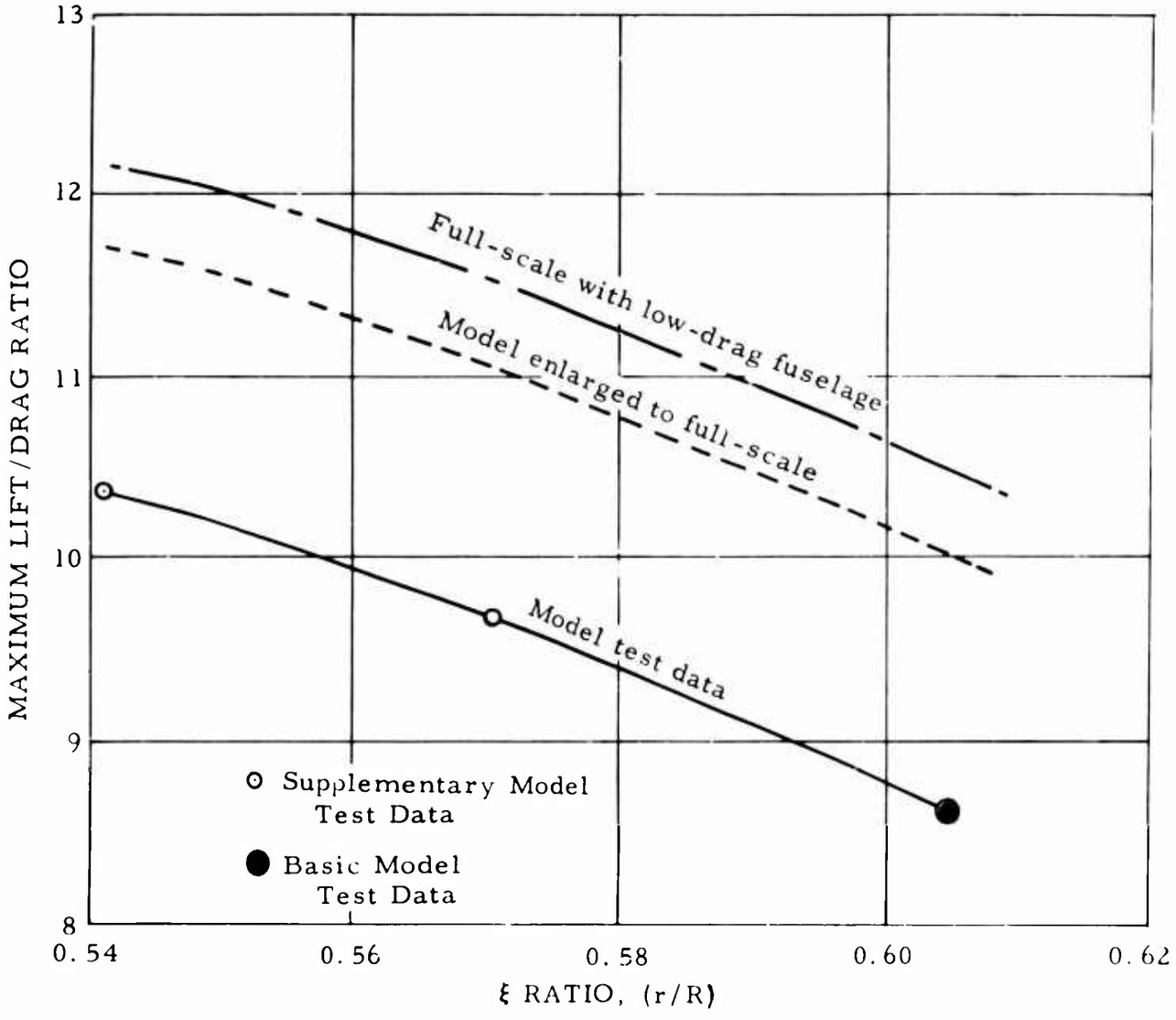

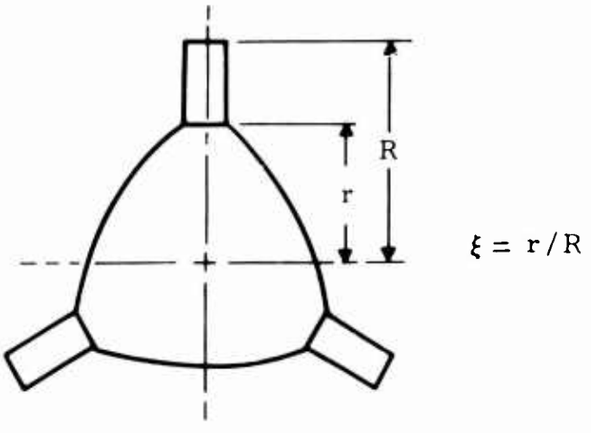

Figure 29. Estimated Maximum Trimmed Lift/Drag Ratio

Figure 28. Complete Model Lift/Drag Ratio

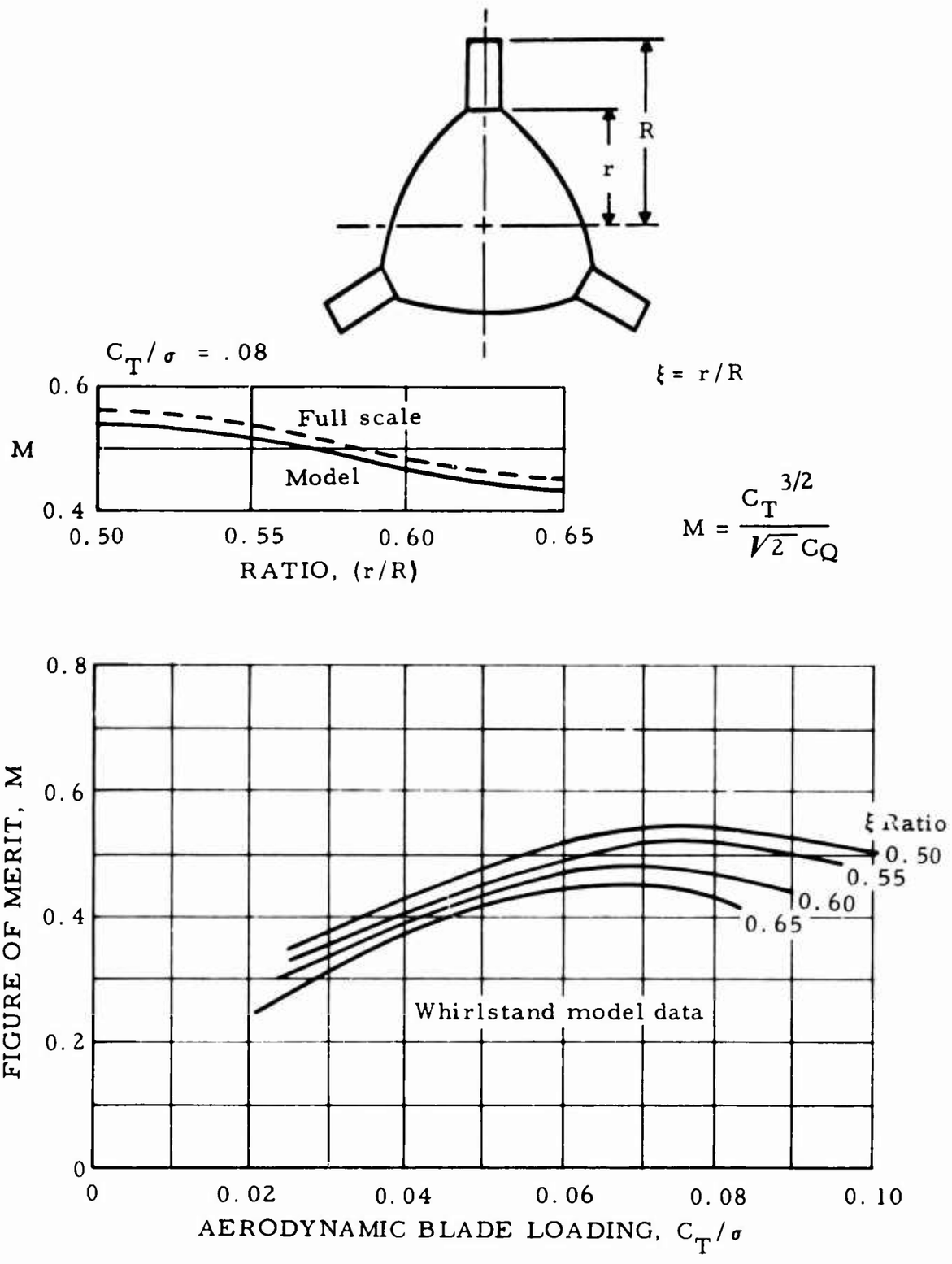

Figure 30. Hovering Figure of Merit

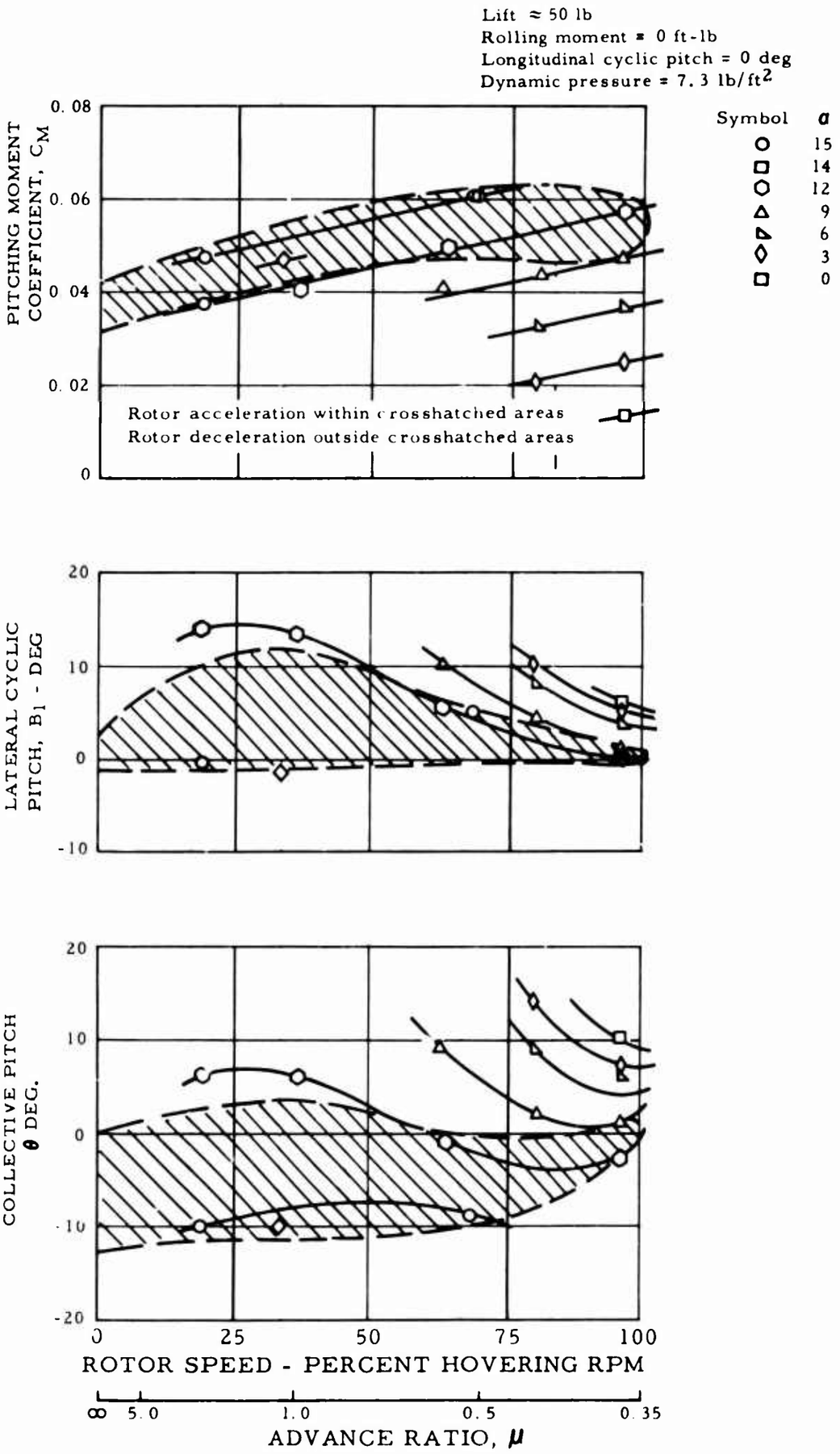

Figure 31. Pseudoconversion Test

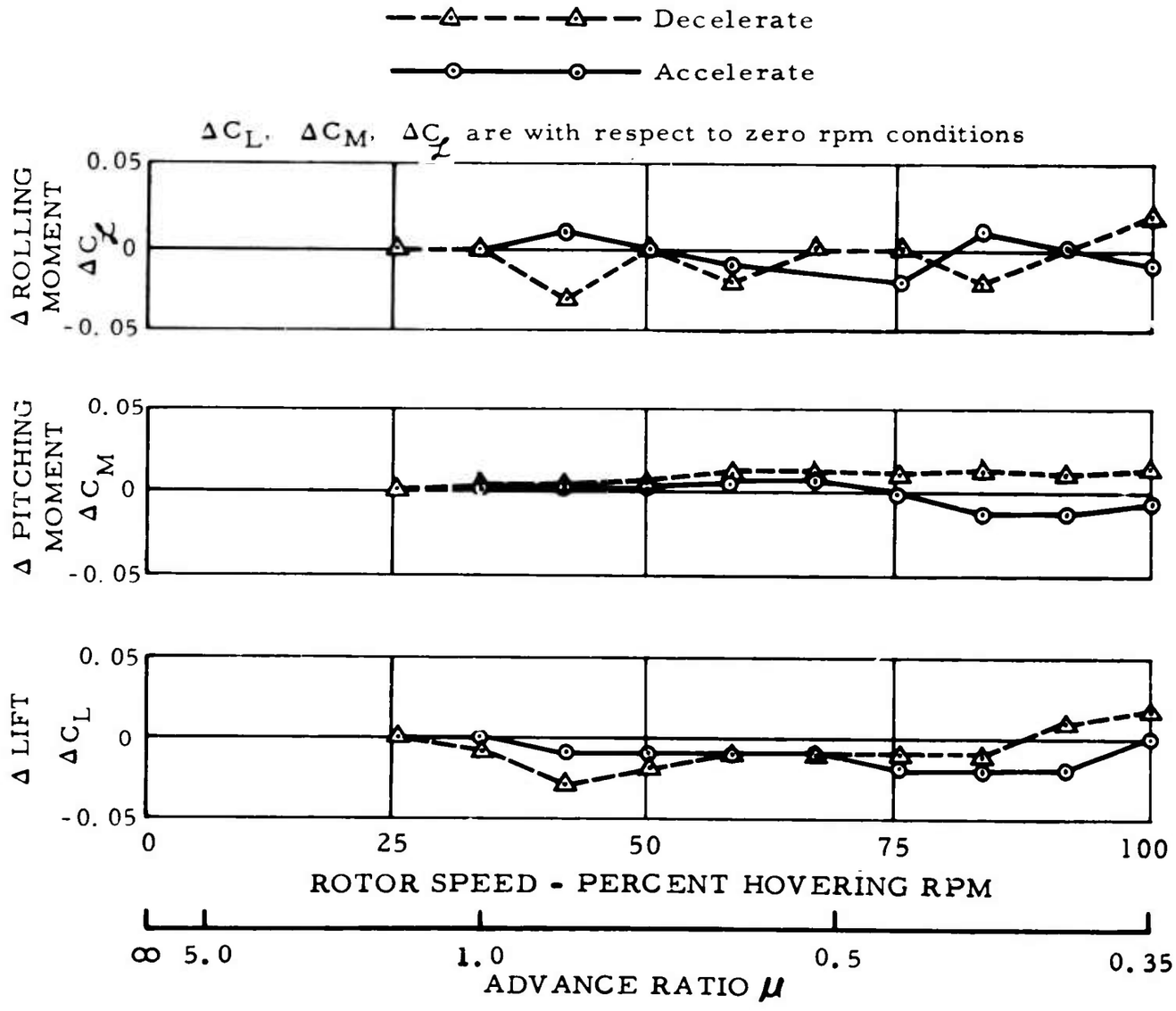

Figure 33. Model Response During Automatic Conversion

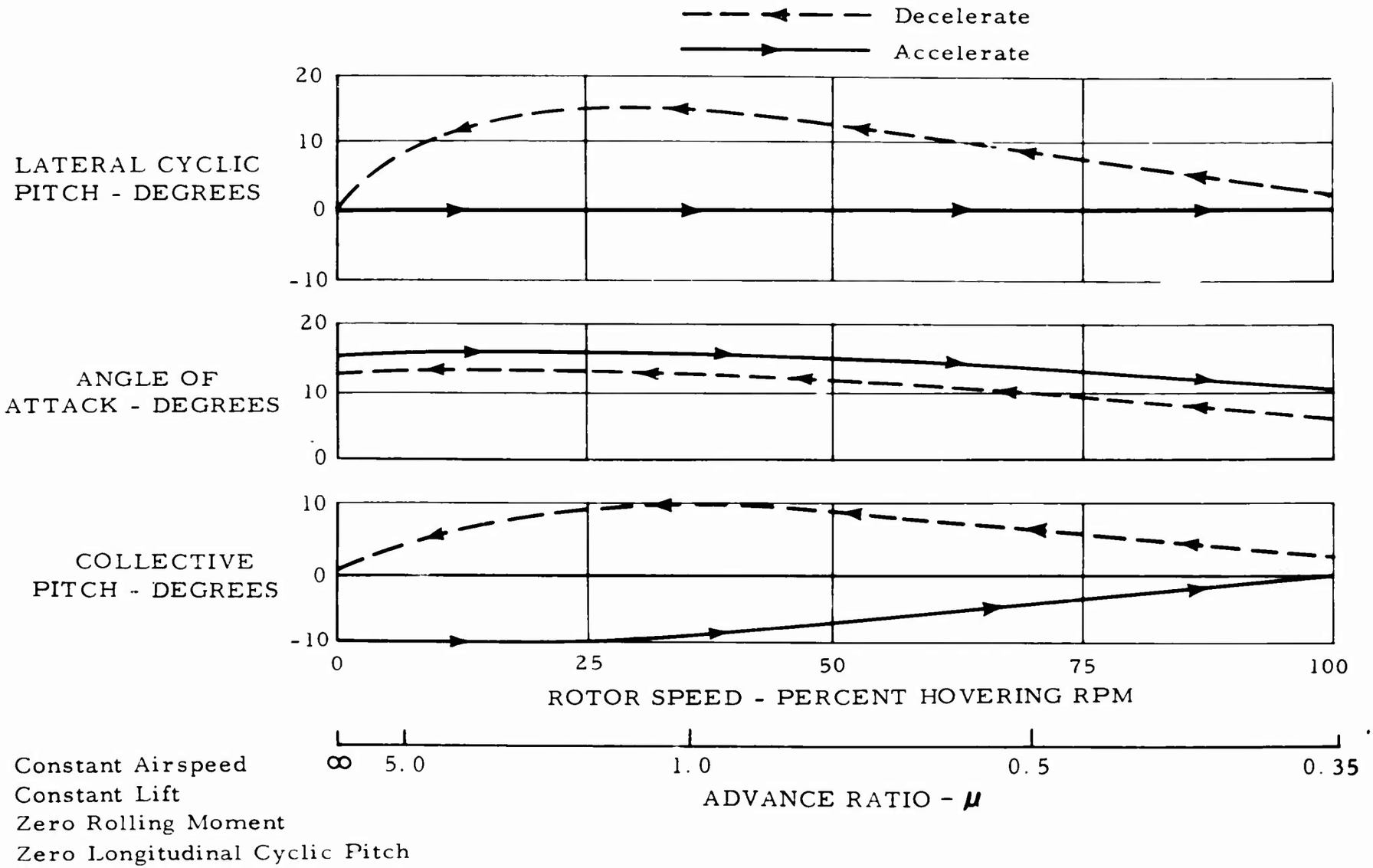

Figure 32. Control Time History - Automatic Conversion

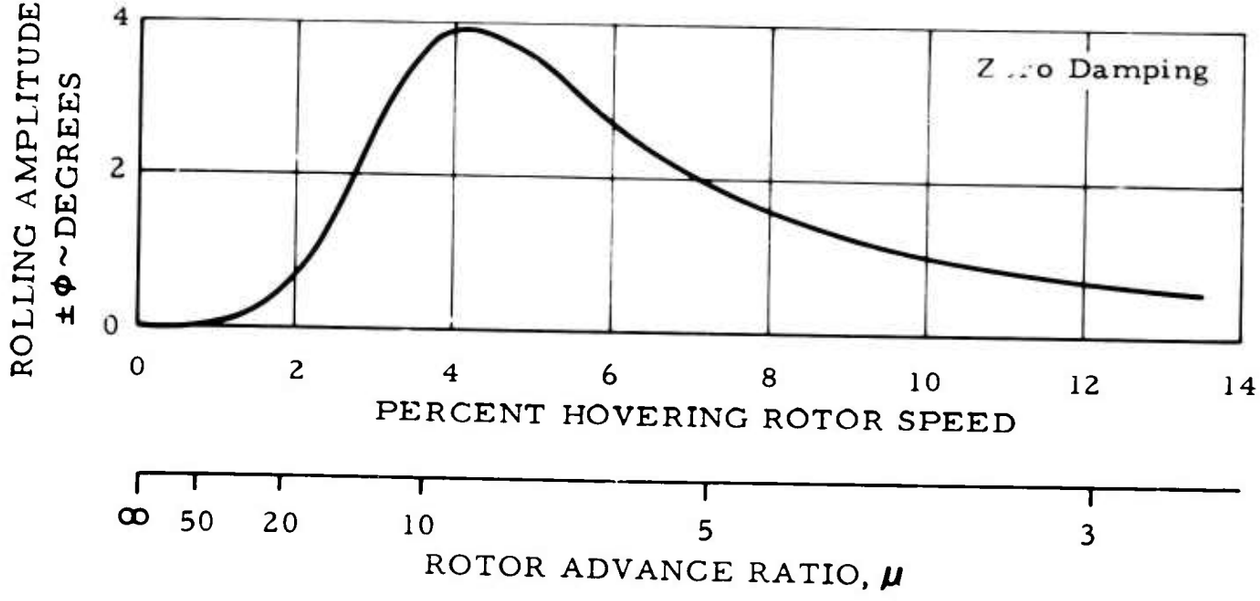

Figure 35. Aircraft Rolling Amplitudes During Conversion

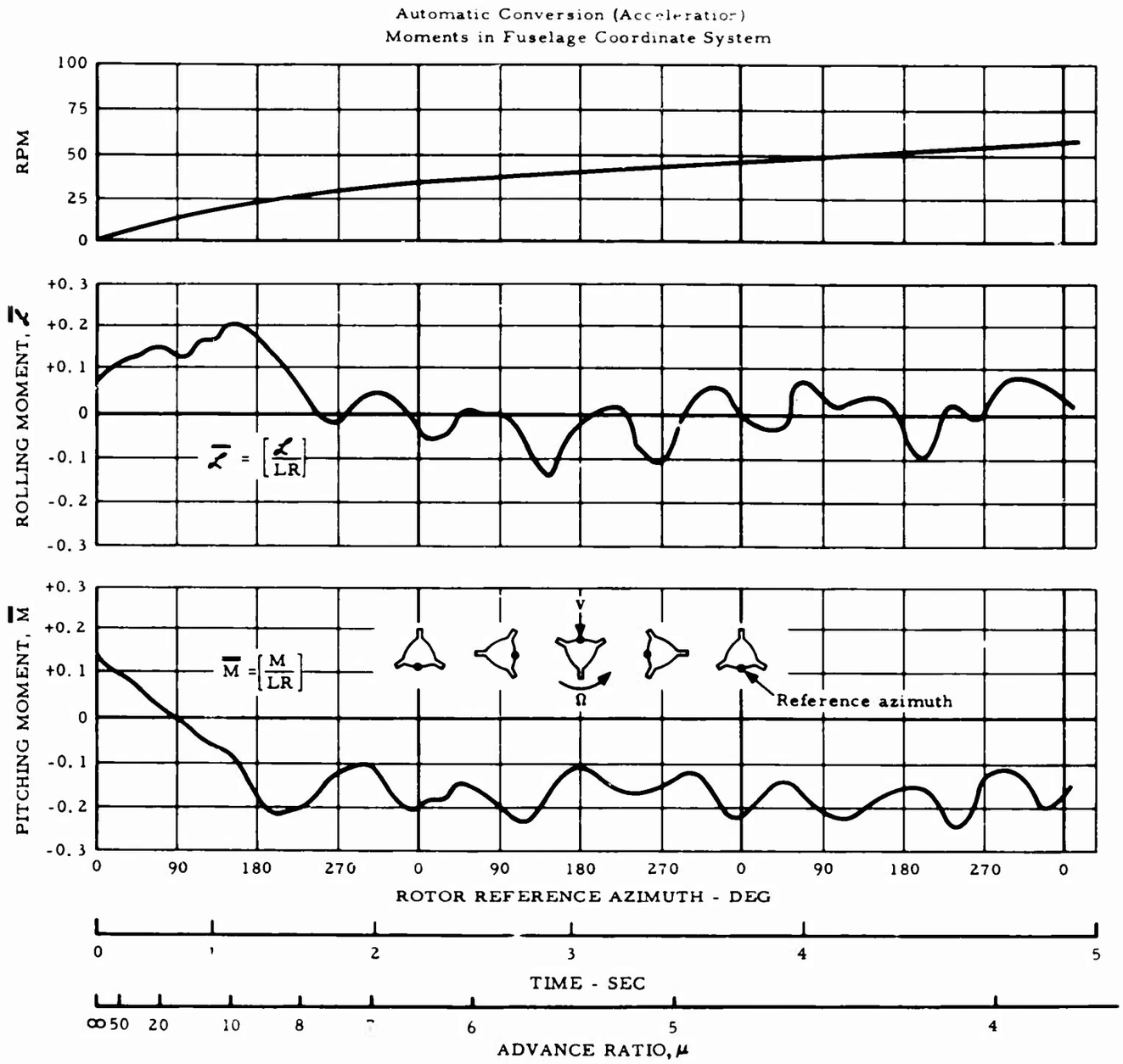

Figure 34. Model Rotor/Wing Low RPM Characteristics - Automatic Conversion

A COMPARATIVE STUDY OF PROPELLER DRIVEN VTOLS FOR THE TRI-SERVICE FOUR TON REQUIREMENT

G. J. Howard

H. D. Ulisnik

Sikorsky Aircraft Company

A COMPARATIVE STUDY OF PROPELLER DRIVEN V/STOL FOUR TON ASSAULT TRANSPORTS

G. J. Howard, Supervisor, Advanced Concepts
H. D. Ulisnik, Senior Design Engineer,
Advanced Concepts

Division of United Aircraft Corporation
Stratford, Connecticut U. S. A.

ABSTRACT

A comparative design study is presented of four fundamentally different VTOL types which utilize propellers as their primary cruise system. The Tri-Service four-ton mission forms the basis against which a quad tilt propeller, tilt prop/rotor, and two direct lift jets, one with cruise thrust vectoring and the other without, are compared.

Results of a parametric analysis, based on current state-of-the-art capabilities, are discussed with particular emphasis placed on mission performance and evaluations are made on the basis of productivity and vehicle empty weights as these parameters are held to be good indexes of system costs. In addition, some design problems are discussed in the context of current technology.

The direct lift jet with cruise thrust vectoring is seen to emerge from the design study as the design concept possessing the highest mission effectiveness.

INTRODUCTION

During the past ten years many studies and investigations of VTOL aircraft have been made and a large number of experimental aircraft built and tested. The scope of this work has been extremely broad--but one fact is clear. Feasibility of vertical takeoffs and landings with aircraft having both satisfactory payload to gross weight ratios and the speed and range of conventional aircraft is no longer a prime question. Current VTOL technology is such that the question of feasibility is being replaced by questions of economics and operational suitability. Consequently, the problem of what form a VTOL will take for a given requirement is more important than the question of will it work? No single VTOL is pre-eminent for all operational requirements, and thus a variety of VTOL forms can be expected as a result of a great variety in mission requirements. Conversely a particular set of mission requirements can be expected to lead to a particular form of VTOL.

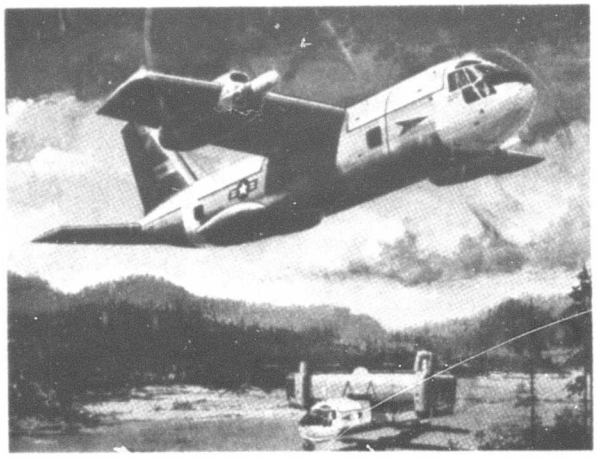

Figure 1. TRI-SERVICE SUBMITTAL

Figure 2. SIKORSKY CH-53A

This study used a mission similar to the Tri-Service four-ton mission as the operational requirement against which a broad spectrum of VTOL's were parametrically synthesized, then optimized and finally evaluated against each other. The parametric analysis was greatly facilitated by the extensive data available from our own Tri-Service submittal (figure 1), as well as the large amount of information published throughout the aerospace industry on aircraft of similar capabilities. The Sikorsky CH-53A (figure 2) helicopter served as an additional source of data particularly in such areas as the fuselage, undercarriage, and subsystem weights. This helicopter, currently the most advanced VTOL assault transport in volume production, has the same payload and volume characteristics as those required in the study.

As expected, a particular generic type of VTOL emerged as "best suited" to the low altitude, low subsonic speed requirements of the Tri-Service mission. Characterized by their propeller cruise propulsion systems, four design solutions form the subject matter of this paper.

The mission requirements used in this study are generally similar to those against which the XC-142 tilt wing is currently being evaluated.

A. Performance:

1. Hover ceiling, OGE, 6,000' 82° F. at military power.
2. Cruise speed S.L. Std. - 250 knot minimum at normal rated power.
3. Maximum speed S.L. Std. - as limited by military power and/or structural strength-weight tradeoffs.

B. Mission Profile:

1. Warm up, conventional take off, and accelerate to speed - 5 minutes at S.L. Std. normal rated power. (T64-ST159 engines only)
2. Cruise out 200 nautical miles at S.L. Std. conditions, with four tons payload
3. Hover at design gross weight OGE for five minutes at S.L. Std.
4. Land and reduce payload to two tons (no fuel consumed).
5. Cruise back 200 nautical miles at S.L. Std. conditions.
6. Land - (no fuel consumed).

C. Additional Requirements:

1. Ten percent of total mission fuel to be held in reserve.
2. 105% of engine manufacturer's guaranteed specific fuel consumptions to be used in all fuel computations.
3. Cargo compartment to be 30 feet long x 7.5 feet wide x 6.5 feet high.
4. Fuel tanks to be self-sealing on bottom third.
5. Propellers, rotors, engine inlets, aerodynamic surfaces, and cockpit windshield glass to be anti-iced.
6. A limit load factor of +3 to -1.0 g to be applied.
7. Certain group weights to be maintained as invariant, such as, cockpit, furnishings, electronics, navigation, cargo floor, crew, air conditioning, and auxiliary equipment.
8. Control at 6000' 82.° F. OGE must meet AGARD specifications as a minimum, with 100% application on critical axis plus a 15% simultaneous application on remaining two axes.
9. Vehicle must be capable of continued level flight at design gross weight in the event of loss of one cruise powerplant.

This mission was chosen for a company funded study because of Sikorsky's long standing interest in all forms of VTOL transports. It was also felt that a large number of configuration choices existed in the assault transport area and that these require sorting out.

TECHNICAL APPROACH

The design data presented in this paper has been generated by synthesizing families of VTOL transports with parametric techniques. The fundamental aircraft operating characteristics used as inputs are: hovering altitude, hovering ambient air temperature, hovering time, cruise speed, cruise altitude, and range. Gross weight is assumed and payload is computed as a function of gross weight. The assumed gross weight is varied until the desired payload is exceeded. This procedure is one of continuous iteration

in which payloads are determined at each gross weight with fixed installed power and mission capability. A continuous variation of payload with gross weight similar to figure 3 is generated. Illustrated here is the fact that for constant available power, the payload capability will increase with gross weight up to a point beyond which payload will diminish. Every point along the gross weight scale has a corresponding set of lift system parameters determined by the required performance. Since the available power is constant, lift system size and weight becomes disproportionately large and heavy as gross weight is continuously increased. This trend, plus the influence the lift system growth has on other aspects of the vehicle, results in the payload capability eventually decreasing. Point B of figure 3 is therefore trivial since it represents a grossly inefficient solution. The lightest gross weight and the smallest vehicle that will completely perform the mission is at point A. The determination of this point for each vehicle form is the object of the parametric synthesis.

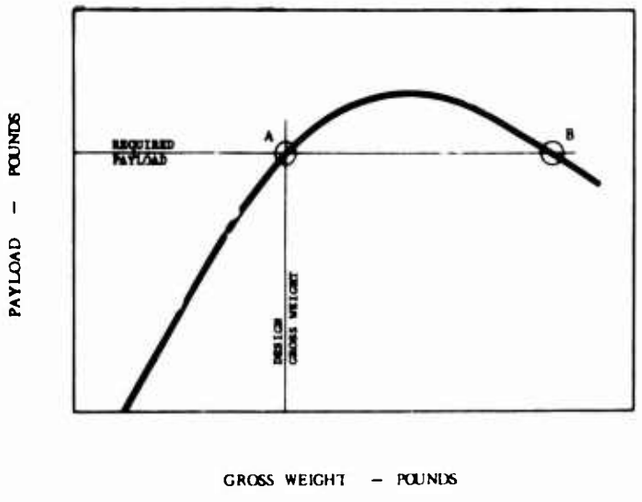

Figure 3. PAYLOAD VS GROSS WEIGHT

With the vehicle now defined (by the solution at point A) the unavoidable assumptions which must be made in any parametric study are tested for realism by a closely coordinated design study. This involves design layouts supported by performance refinement calculated on digital computers; and stability, control, and handling qualities examined in six degrees of freedom on an analog flight simulator. Deficiencies uncovered in this manner are corrected, parametric assumptions are modified, and the process of design iteration is continued until a closed solution is obtained.

DISCUSSION

The four solutions selected for comparative evaluation in this paper are: a tilt prop/rotor, a tandem wing quad tilt propeller, and two direct lift jets, one of which uses its propeller cruise propulsion system in the vertical flight mode and one which does not. All of these aircraft make multiple use of the General Electric T64-ST159A turboshaft engine having characteristics as defined in Ref 1. In the two jet configurations, the lift engine installations are made up of multiple Continental model 465 turbofans as described in Ref 2.

TILT PROP/ROTOR

The tilt prop/rotor (figure 4) utilizes two 28.2 foot diameter, four bladed cyclic feathering, offset hinge, articulated prop/rotors for both the hovering mode and the cruise mode. Power is provided by four turboshaft engines mounted close inboard and cantilevered off the rear spar of the wing. This location was selected to provide both good engine access as well as to minimize yaw and roll inertia. Coupling gear boxes containing free wheeling units

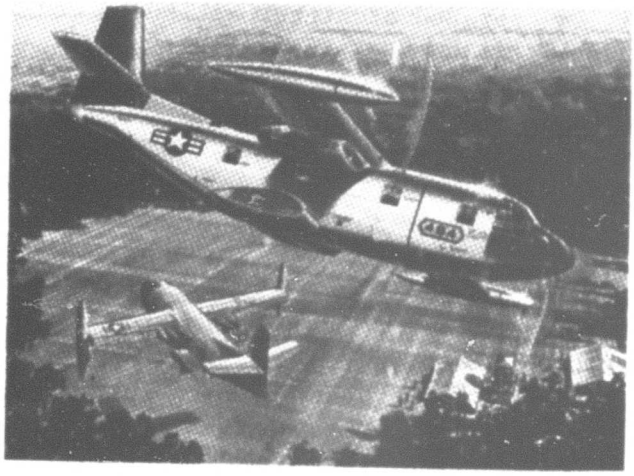

Figure 4. TILT PROP/ROTOR

connect the engines to the cross shafting. The AR = 6 wing has an area loading of 106 pounds per square foot and represents a design trade-off between cruise efficiency and transition characteristics. As can be seen in figure 4, the large flaperons which serve both as ailerons and flaps are deflected downward 90 degrees to minimize the hovering vertical drag. These surfaces are programmed with the prop/rotor tilt angle and are also connected via a combination mechanical phasing/mixing unit to the pilot's control and the prop/rotor cyclic pitch system.

The desirable features of a flapping prop/rotor, such as strong control and light weight, have been retained by giving careful consideration to the problems of dynamic stability (Ref 4), rotor induced vibration, and elastic coupling between the wing and the prop/rotor which it supports. It was found for example that the weight penalty in the wing could be minimized by a structural tuning process, particular attention being given to the wing's torsional modes. Dimensions and weights of the tilt prop rotor design are shown in table 1.

Table 1. Tilt Prop/Rotor

Engines	
Four turboshaft engines	G.E. T64-ST159
Rotors	
Diameter	28.2 ft.
Activity factor	100
Integrated design lift coefficient	0.5
Overall length	58.7 ft.
Overall height	26.0 ft.
Wing	
Span	47.6 ft.
Area	377.0 sq.ft.
Taper ratio	0.7
Horizontal tail area	151.0 sq.ft.
Vertical tail area	95.6 sq.ft.
Weight	Weight, lbs
Rotor group	3,556
Tail group	710
Wing	2,320
Transmission system	2,830
Fuselage	4,086
Controls	1,450
Electrical	576
Hydraulics	130
Landing gear	1,429
Powerplant group	3,963
Fuel system	475
Invariant items *	2,744
Weight empty	24,269
Crew; oil and trapped fluids	760
Fuel	7,800
Payload	8,000
Gross Weight	40,829

* electronics, instrumentation, navigation equipment, furnishings, anti-icing provisions, air conditioning and auxiliary gear

The tilt prop/rotor is faced with a dilemma. It is, when applied to the ground rules of this study, forced to operate well below its maximum obtainable productivity. The principle reason for this being the hovering altitude and temperature requirements imposed, which in turn lead to a propulsion system mismatch with the sea level cruise requirement. This mismatch can be reduced by the use of relatively low disc loadings thereby reducing the installed power. However, the larger diameter prop/rotors so required adversely effect the wing span and wing weight as well as becoming disproportionality heavy in themselves. Shut down of two engines to provide a power match is considered untenable from a flight safety standpoint since the mission profile must be flown at tree top level. Shut down of one engine helps somewhat as does lowered prop/rotor tip speeds. Multispeed gearing was examined and found too heavy. In short, no panacea could be found and it is concluded that the tilt prop/rotor vehicle must accept, for this mission, a relatively poor cruise efficiency. It should

be pointed out through, that improved cruise efficiencies can be obtained from the tilt prop/rotor configuration when it is operated at higher altitudes and airspeeds. In other words a different set of mission requirements.

An interesting aspect of this power mismatch though is the relatively high sea level dash speed capability of the tilt prop/rotor vehicle. This could well be a very desirable attribute from the standpoint of survivability since an assault transport will be called upon to operate in the zone of combat.

Figure 5. QUAD TILT PROPELLER

Table 2. Quad Tilt Propeller

Engines	
Four turboshaft engines	G.E. T64-ST159
Propellers	
Diameter	18.5 ft.
Activity factor	90
Integrated design lift coefficient	0.5
Overall length	51.6 ft.
Overall height	22.4 ft.
Forward wing	
Span	30.0 ft.
Area	138.0 sq.ft.
Aft wing	
Span	34.0 ft
Area	275.0 sq.ft.
Vertical tail area	106.0 sq.ft.
Weight	Weight, lbs
Propellers	2,960
Tail	266
Wing group	2,248
Transmission system	2,733
Fuselage	4,030
Controls	1,192
Electrical	576
Hydraulics	130
Landing gear	1,381
Powerplant group	4,019
Fuel system	478
Invariant items	2,744
Weight empty	22,757
Crew; oil and trapped fluids	760
Fuel	7,930
Payload	8,000
Gross Weight	39,447

QUAD TILT PROPELLER

The tandem wing, tandem tilt propeller aircraft illustrated in figure 5 is supported in the vertical mode and propelled in the cruise mode by four 18.5 foot diameter, four bladed, conventional propellers. Four turboshaft engines, two forward and two aft provide the power. In hovering and low speed flight, pitch control is obtained by differential propeller pitch between the fore and aft pairs. Roll control is similarly obtained by differential pitch between lateral pairs. Adequate low speed yaw control was obtained only after differential propeller tilting was employed. Differential thrusting with diagonal pairs or aerodynamic surfaces operating in the propeller wakes were both found to be unsatisfactory (Ref 5). In cruise flight, control about all three axes is by use of conventional aerodynamic surfaces. Transition control is obtained by a combination of propeller pitch and aerodynamic surfaces, propeller control being phased out as the nacelles are tilted forward to the cruise position. Clean axis control is insured by control programming through a mechanical mixing unit. The principal characteristics of the quad tilt propeller are shown in table 2.

The quad tilt propeller configuration suffers from much the same problem as does the tilt prop/rotor machine. There is still the mismatch between hover power and cruise power requirements and again a careful tradeoff between propulsion system weights and fuel weights resulted in the best solution being inferior to the configurations which

use lift engines from the standpoints of cruise efficiency and transport productivity.

DIRECT LIFT JET

This form of VTOL is characterized by the fact that it obtains most or all of its zero airspeed lift by means of directing the exhaust gases from lightweight turbojets or turbofans downward. These take the form of specialized engines designed for relatively short time operation at a particular set of conditions or of a more universal engine designed so as to be capable of vectoring its thrust for either lift or cruise. A lift system is made up of one or the other or a combination of both types of engines.

In the course of this study several design approaches to the direct lift jet assault transport were examined. Early concepts had the lift engines mounted in wing pods that also housed the cruise propulsion system and the main under carriage. A large cruise drag penalty is associated with this approach due to the nacelle bulk and cross sectional area dictated by the turbofan lift engines. Pod structural weight is also significant and so alternate arrangements were examined. Great freedom in configuration design is possible within the direct lift concept and subsequent effort led to installing the lift engines in the fuselage itself, disposed fore and aft of the cargo compartment. With this arrangement the cruise drag attributable to the hovering lift system is negligible and the lift engine installation weight is minimized. In cruise, this configuration presents the outward appearance of a conventional modern turboprop transport. Its principal characteristics are shown in table 3.

Table 3. Direct Lift (No Cruise Thrust Vectoring)

Engines	
Two turboprop engines	G.E. T64-ST159
Eight turbofan lift engines	Continental 465
Propellers	
Diameter	13.0 ft.
Activity factor	80
Integrated design lift coefficient	0.5
Overall length	60.0 ft.
Overall height	22.0 ft.
Wing	
Span	58.3 ft.
Area	418.0 sq.ft.
Taper ratio	0.34
Horizontal tail area	120.0 sq.ft.
Vertical tail area	106.0 sq.ft.
Weight	Weight lbs
Propellers	792
Tail group	710
Lift engine group	3,964
Wing	2,460
Fuselage	4,470
Controls	855
Electrical	460
Hydraulics	145
Landing gear	1,447
Powerplant group	2,971
Fuel system	402
Invariant items	2,744
Weight empty	21,420
Crew, oil and trapped fluids	760
Fuel	5,990
Payload	8,000
Gross Weight	36,170

The sea level, 250 knot cruise requirement of the study mission makes propeller propulsion an obvious engineering choice. With lift engines used as thehovering lift system, the cruise propulsion system becomes entirely independent of the hovering altitude and temperature requirements. Hence no compromise is necessary and a cruise mismatch need not be accepted. Both the propellers and the installed power can be selected to provide peak performance in cruise. Propulsive efficiencies approaching 90% are possible, and significant improvements in specific range as compared to, the tilting category of VTOL are obtained.

The iterated direct lift design solution of this study has two turboprop engines each driving a 3 way, 13 foot diameter, propeller. The eight turbofan lift engines in two groups of four are differentially thrusted for hovering pitch control. Compressor bleed air from these engines is ducted to wing tip variable area nozzles to provide roll control. Yaw control is obtained by differential thrust from the cruise propellers. In this manner the three axes are essentially uncoupled and efficient use can be made of the cruise

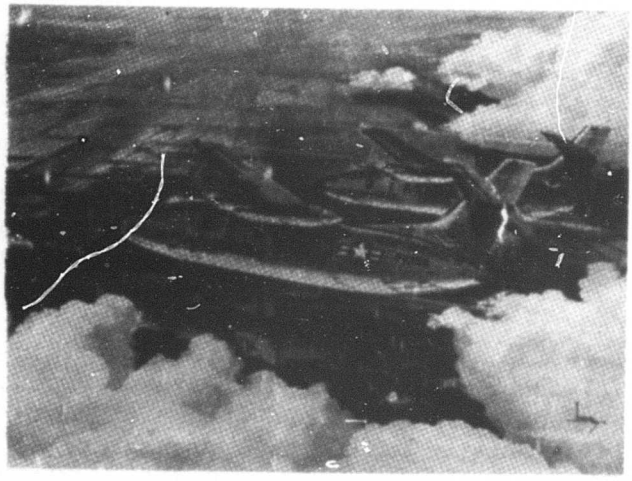

Figure 6. DIRECT LIFT JET

propulsion system while in the hover mode. No cross shafting is employed since it is possible to retain control even in the event of a cruise engine failure while hovering. In this event however, control is degraded and the pitch and yaw axis become coupled.

As with any type of VTOL, loss of an engine during hover can not be permitted to result in an uncontrollable situation. With a lift jet supported transport this is a particularly difficult thing to achieve. A flight simulator study clearly demonstrated the need for automatic failure sensing and power management following a lift engine malfunction. The reason for this is that in a transport, the lift engine banks are not located on or very near the aircraft's center of gravity. Hence loss of an engine means, in addition to a loss in vertical thrust, an upsetting control moment. Depending on such factors as engine location and number of engines used, this upsetting control moment can be quite substantial. Time histories of aircraft response following a lift engine failure have shown that the time between failure and corrective action is critical. Simulation studies are continuing at Sikorsky on this aspect but this much is already clear; a high installed thrust to weight ratio is not in itself sufficient to provide the degree of safety required in a transport VTOL in the advent of a lift engine failure.

DIRECT LIFT JET--WITH CRUISE THRUST VECTORING

Several earlier Sikorsky Aircraft studies in which direct lift vehicles were examined had concluded that in the category of transports it was highly desirable to vector the cruise propulsion system. In this manner the cruise propulsion engines supply a share of the lift thrust and only the remainder is provided by lift engines. The aircraft in these studies had, however, all used turbofans or turbojets for cruise propulsion while for this low altitude low speed mission, a propeller was the desirable choice. Figure 7 shows a qualitative comparison of the manner in which thrust capability will vary as a function of speed for a turbojet, a turbofan and a propeller all designed to provide identical thrust at a particular set of cruise conditions. Shown here is that a propeller is a good static thrust producer and hence its use in hover should be worthwhile providing that vectoring its static thrust through ninety degrees can be accomplished efficiently. A number of schemes for

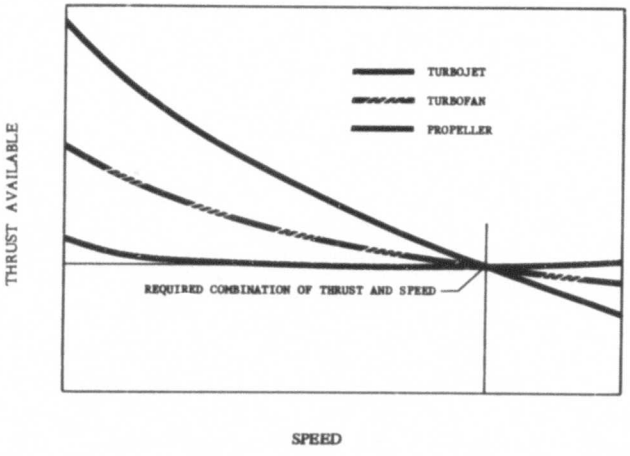

Figure 7. PROPULSION CHARACTERISTICS

doing this were examined. Included were: slipstream vectoring by means of a flap system in the propeller wake, rotating wing tip mounted propeller nacelles (similar to those on the tandem wing quad tilt propeller configuration), and lastly rotating the outer portion of the wing which carry the propeller nacelles. In all cases the engines were mounted at some distance from the propellers, are not tilted, and are shaft interconnected. The first two of the above schemes were eventually discarded as being either, inefficient, too heavy, possessed of serious control problems, or all three. The last scheme, however, proved to be a particularly attractive arrangement and it is this configuration that emerged from the design study as "best of lot."

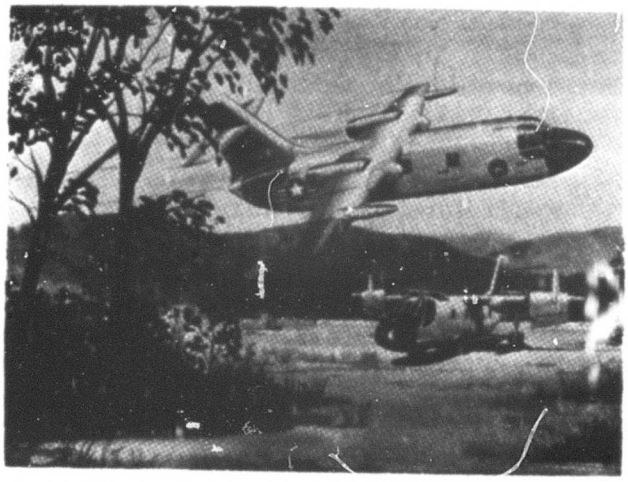

Figure 8. DIRECT LIFT JET
(with cruise thrust vectoring)

Table 4. Direct Lift (With Cruise Thrust Vectoring)

Engines	
Two turboshaft engines	G.E. T64-ST159
Six turbofan lift engines	Continental 465
Propellers	
Diameter	14.0 ft.
Activity factor	120.0
Integrated design lift coefficient	0.65
Overall length	55.5 ft.
Overall height	19.3 ft.
Wing	
Span	58.3 ft.
Area	418.0 sq.ft.
Taper ratio	0.34
Horizontal tail area	120.0 sq.ft.
Vertical tail area	97.0 sq.ft.
Weight	Weight, lbs
Propellers	1,030
Tail	700
Lift engine group	2,988
Wing	2,920
Transmission system	1,298
Fuselage	4,330
Controls	850
Electrical	576
Hydraulics	160
Landing gear	1,231
Powerplant group	2,115
Fuel system	365
Invariant items	2,744
Weight empty	21,307
Crew, oil and trapped fluids	760
Fuel	5,100
Payload	8,000
Gross Weight	35,167

This aircraft, illustrated in Figure 8., utilizes two turboshaft engines driving two 14 foot diameter, interconnected, propellers and six turbofan lift engines mounted in fore and aft banks of three engines each. The propellers have been sized to provide optimum performance in cruise. During hover and low speed operation they are tilted with the outer wing panel to a vertical position to provide a portion of the lift and control required. The lift engines have only to supply the remaining portion. Pitch control in hover is provided by differential thrusting of the lift engine groups, longitudinal stick being coupled to the engine fuel controls. Roll control is by means of differential propeller pitch, and yaw control is by means of differential ailerons operating in the propeller slip streams. Thus, by making use of the propellers the hovering control system is made simpler and more efficient by eliminating the need for a reaction control system. Adequate control is obtained without the use of lift engine bleed air and its associated penalties in vertical thrust and pneumatic system complexity. The net required installed thrust-to-weight ratio is therefore minimized by virtue of the reduced demand this control configuration places on the available power. In addition this configuration provides a large stall margin during a decelerating transition because maximum propeller thrust can be maintained throughout the maneuver while the lift engines provide the vertical control. Table 4. presents the principal characteristics of the direct lift jet with cruise thrust vectoring.

This arrangement of tilting wing-propeller units combined with lift engines provides a lower system hovering SFC than that associated with a purely jet lifted VTOL. Shown in Figure 9. is the sensitivity of these two approaches to lift engine operating time per flight, as measured by aircraft design gross weight. The gross weights are parametric solution weights and represent a continuous variation in aircraft parameters. For almost any conceivable flight profile, lift engine operating time can be expected to exceed two minutes. Thus it can be seen from Figure 9. that the weights associated with tilting the propellers will be more than offset by the lower fuel requirements, and the simpler and lighter lift engine installation that results. Simpler because of the absence of a bleed air reaction control system and lighter because of the lower installed thrust necessary to meet the hovering thrust and control requirements.

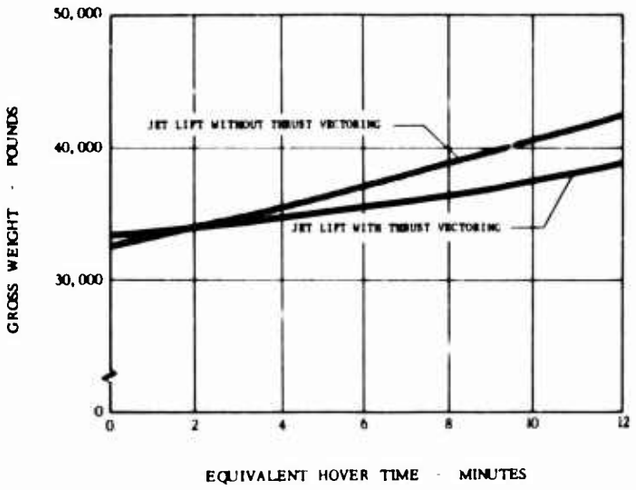

Figure 9. SENSITIVITY TO HOVER TIME

COMPARISONS

Figure 10. which illustrates cruise efficiency in terms of nautical miles per pound of fuel consumed, graphically shows the effect of cruise mismatch. The tandem wing quad tilt propeller vehicle and the tilt prop/rotor vehicle have approximately twice the power installed than that required for sea level 250 knots cruise. This results from the 6000 foot ANA hot day hover capability to which they are designed. Since shut down of two engines is considered as impractical for safety reasons, the specific ranges shown in Figure 10. have been based on allowing only one engine to be shut down at the mission speed of 250 knots. The non-optimum power settings result, then, in relatively poor engine SFC's. In addition the low blade loading of these tilting types results in a comparatively low prop/rotor or propeller efficiency. These aspects combine to produce a specific range for the tilt prop/rotor which is 23% less than that of the jet lift VTOL's (at the mission speed of 250 knots). The tandem wing quad tilt propeller has a specific range 24% less. The slight advantage of the tilt prop/rotor over the quad is due to its lower span loading. High altitude cruise increases this advantage.

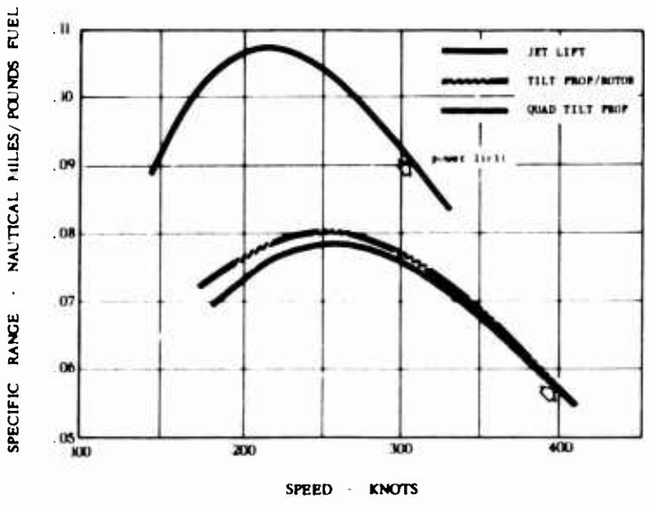

Figure 10. SEA LEVEL, SPECIFIC RANGE

As a result of the excess power available in cruise to either the tilt prop/rotor or the quad, high rates of climb or high dash speeds are possible.

These aircraft do not become power limited until 400 knots. However, the design study solutions presented in tables 1. and 2. would be somewhat different for any sea level speed above 310 knots. Structural considerations reflecting the increased aerodynamic loads as a result of the sea level gust environment would necessitate increases in weight in several areas of the basic airframe.

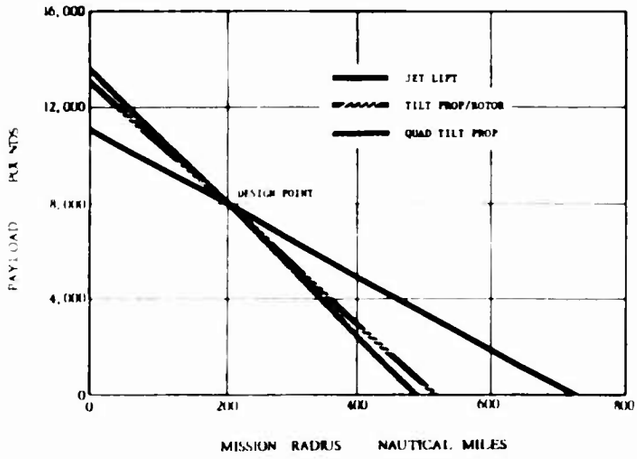

Figure 11. PAYLOAD VS RADIUS

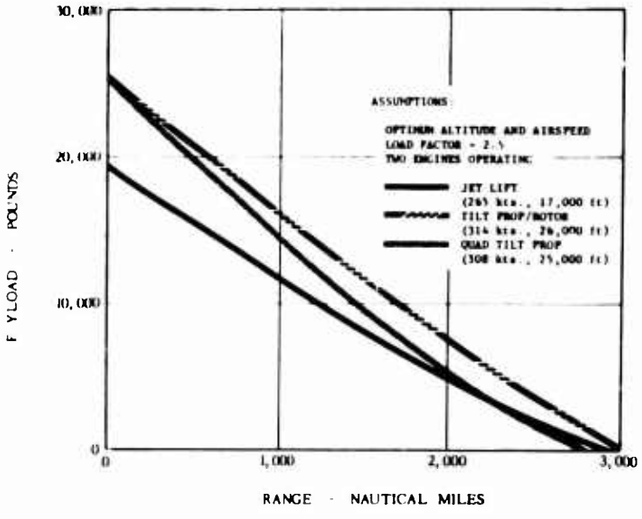

Figure 12. PAYLOAD VS RANGE
OPTIMUM ALTITUDE AND AIRSPEED

Again confining our comparisons to the 250 knots sea level case with take-off at design gross weight, we find that the higher total L/D (includes propulsion efficiencies) of the jet lifted types results in either higher payload or greater mission radius capability than the tilt types for any mission radius exceeding 200 nautical miles. This is illustrated in Figure 11. where the comparative cruise efficiencies of the study aircraft characterize the slope of their respective payload versus mission radius plots.

What happens when these aircraft are operated each at their own optimum cruise altitude and airspeed? Figure 12. is a comparison of payload versus range at optimum cruise conditions. The tilting forms, because they are now operating at altitude rather than sea level, are allowed to shut down two engines. Thus we find all four study aircraft exhibiting essentially the same absolute range. In this plot the take-off is STOL at a reduced load factor of 2.5, and thus the absolute range shown is also the ferry range. All four aircraft are thus seen to be self-deployable.

It is interesting to observe the higher optimum cruise speeds and cruise altitudes the tilting forms possess over the jet lifted aircraft. The reason for this can be found in the low blade loading associated with the prop/rotors or propellers of the tilt types. Operation at high advance ratios and low air densities tends to bring the blade section lift coefficients closer to their L/D maximums and hence high propulsion efficiencies (Ref. 6). On the other hand, the propellers on the jet lifted configurations were selected on the basis of 250 knot sea level cruise.

Even under optimum conditions of cruise however, neither the tilt prop/rotor or the tandem wing quad tilt propeller attain the specific range of the jet lifted VTOL's. They are still suffering from too much blade area and non optimum blade twist distributions. Thus for a 3000 nautical mile ferry flight, it is necessary for the tilt types to take off with over 5000 pounds more fuel on board than the direct lift jets require.

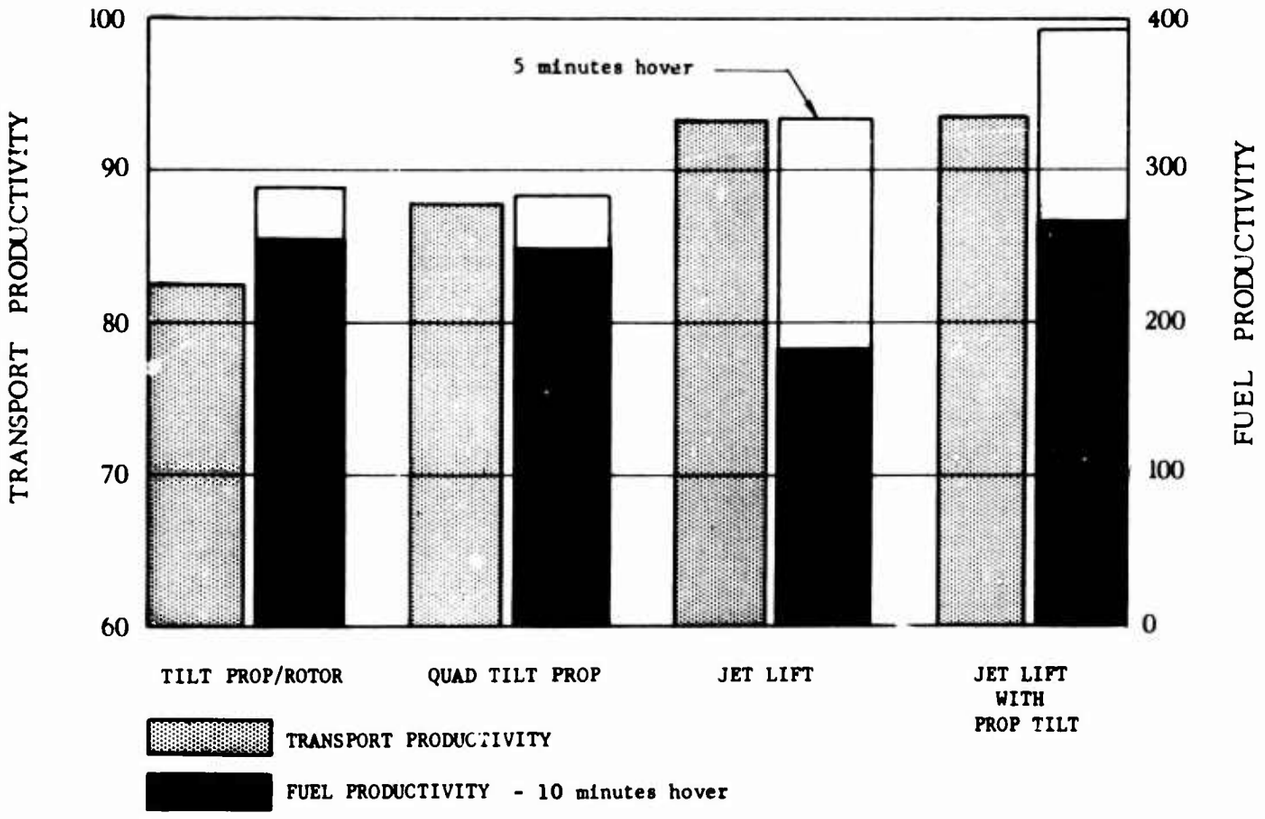

Figure 13. SUMMARY COMPARISON ON THE BASIS OF PRODUCTIVITY

Productivity for a transport can be expressed as:

productivity = (payload x cruise speed)/weight empty

This relates the two most important aspects of a transport mission with aircraft cost by assuming that initial cost is to a first approximation, proportional to weight empty. Perhaps of equal interest because of its bearing on operating cost and logistics is productivity per pound of fuel consumed.

fuel productivity = (payload x cruise speed)/fuel load

A configuration that exhibits a high numerical value of these two indexes is a better choice than a configuration exhibiting low values. Shown in Figure 13. are these indexes for the four aircraft types discussed in this paper. This figure is held to be a summary of all that has been previously said. Clearly the direct lift jet which uses its cruise propellers for vertical thrust emerges as the concept possessing the highest mision effectiveness.

CONCLUSIONS

For the low level, low speed, transport mission used as the basis of this study, propeller driven configurations have the capability required to provide competitive design solutions.

1) Of the four fundamentally different types presented in this paper, the tilting wing-propeller with auxiliary turbofan lift engines for hovering and

low speed flight emerges as the most promising concept. It is a well-balanced solution possessing good off-design performance plus good hovering and low speed control characteristics. Its vertical flight capability does not adversely effect cruise efficiency and no cruise mismatch results from the imposed combination of hovering altitude and temperature with the sea level 250 knot cruise speed requirement. In fact the complete flexibility of load sharing between the the lift engines and the propellers during the design optimization process, allows for both the cruise power and cruise thrust producers to be matched precisely to any imposed cruise requirement.

2) The latitude of design freedom opened up by the lift engine and the attractiveness of the solutions obtained assures future designs for operational VTOL aircraft the moment availability of a "second generation" lift engine can be forecast.

3) The marriage of tilting propellers with auxiliary lift engines extends the domain of jet supported aircraft into the low speed sea level assault transport category. Thus the lift engine has application across the entire spectrum of flight and is not limited to purely high speed VTOL strike aircraft as several investigations have concluded.

4) The desirability of recovering the static thrust of the cruise propulsion system has been found to remain true even when cruise propulsion is provided by propellers. For the case of the design solutions presented in this paper the benefits accrued from tilting the propellers as compared to not tilting the propellers on the jet lifted configurations include:

a) lower hovering SFC
b) fewer lift engines required
c) lighter design solution
d) more efficient control

5) The tandem wing quad tilt propeller and the tilt prop/rotor vehicles are both found to be inferior design approaches as applied to the selected study mission. Other mission requirements such as longer hover time, higher cruise speed requirements or less stringent hover conditions would make these forms more attractive. Also their relatively low downwash velocities and temperatures may be desirable from the standpoint of suitability for operating from unprepared landing sites. However, the aerodynamics of these forms, particularly during transition, pose a difficult control and handling qualities problem. Finally, the weight penalties originating from lightly loaded lift systems will be difficult to justify, unless hover times exceeding 15 minutes are necessary or unless a low velocity downwash is mandatory.

References

1. General Electric Brochure - T64 Growth Engines, July 10, 1962

2. Continental Aviation and Engineering Corporation - Engine Specification No. 2241-A, Engine, Aircraft, Lift, Continental Model 465, Preliminary

3. AGARD Report 408, Recommendations for V/STOL Handling Qualities, October, 1962

4. H. C. Quigley and D. G. Koenig - The Effect of Blade Flapping on the Dynamic Stability of a Tilting Rotor Convertiplane - NASA conference on V/STOL aircraft - November 17-18, 1960

5. R. C. Baker - Yaw Control Power Capability of a Tandem Wing - Tilt Propeller VTOL Aircraft in Hover. Sikorsky Engineering Memo 1157, May 17, 1963

6. R. Hafner - Domain of the Convertible Rotor - Journal of Aircraft Vol. 1, No. 6 - November-December, 1964

IMPACT OF JET VTOL ATTITUDE CONTROL ON MISSION PERFORMANCE

J. Patierno

H. Asdurian

Northrop Norair

IMPACT OF CONTROL PROVISIONS ON MISSION PERFORMANCE OF JET VTOL AIRCRAFT USING REACTION CONTROL SYSTEMS

John Patierno
Haig Asdurian

Northrop Norair

ABSTRACT

Control power composition and usage are characterized. It is demonstrated that handling quality considerations dictate large control power margins over minimum levels for performing maneuvers, but control utilization distributions show that these large control demands are sporadic. A fully variable bleed reaction control system which capitalizes on this characteristic is compared with various constant bleed systems. The thrust losses associated with control provisions with each system are presented for a typical transonic jet VTOL design employing the composite propulsion system concept. The radius penalty associated with the increased lift engine size required to maintain a constant takeoff gross weight is presented for each system and the gross weight increase required to maintain a given close support mission radius is defined. In addition, the radius capability afforded by a given propulsion system size is defined for each system.

It is shown that fully variable bleed system with the engine tailored to match control demands has substantial advantages over other systems, particularly as the mission performance requirements are increased.

INTRODUCTION

The design of a flight control system for VTOL aircraft for hover and transition flight requires careful consideration to assure that maximum mission performance is achieved while providing the control power and handling qualities necessary to assure mission success. Nothing short of excellent controllability should be accepted and a control system that efficiently provides this capability must be sought. Since the provision of control power entails extraction of energy from the lifting system, the lifting capability of the aircraft is penalized in the process. This results in a loss in fuel or payload capability. In order to minimize this penalty the engine design must be tailored to match the demands of the control system. A concentrated joint effort on the part of both the airframe and engine manufacturer is essential to achieve an optimum system. However, it is the authors' opinion that insufficient effort has been directed toward the problem. While much attention has been focused on defining control power requirements and desirable control modes, and a wealth of information has been published, design approaches for efficient provision of control power have not been set forth. Yet, few design areas provide the aircraft designer with as fertile a field for improvement in VTOL aircraft performance.

This paper is presented in order to indicate the effect on mission performance of various system approaches for jet powered vehicles utilizing engine compressor bleed for reaction control. Initially, control power requirements and control utilization are discussed and where appropriate, recommendations for establishing design criteria are made. This discussion provides the background necessary for assessing various constant bleed and variable bleed concepts. A typical transonic VTOL design employing the composite propulsion system concept is then exercised in order to compare the concepts in terms of the radius capability at a constant design takeoff gross weight. The results for this design are then generalized to indicate the mission radius capability as a function of design takeoff gross weight for each concept. In addition, the radius capability afforded by a given propulsion system size is determined for each concept.

CONTROL POWER REQUIREMENTS

Prerequisite to the design of an efficient reaction control system is a basic understanding of control power requirements. It is not the intent of this paper to present a thorough treatment of control power requirements, but to characterize the composition and usage of control power in order that a reaction control concept tailored to these characteristics to minimize penalties for control provisions can be defined. As proposed in Reference 1, control power requirements can logically be grouped into maneuvering, trim, and restoring requirements.

Maneuvering requirements are those associated with controlling the movement of the vehicle to a degree allowing satisfactory performance of required flight tasks. Basically, the vehicle must be capable of being oriented sufficiently rapidly to allow performance of required takeoff and landing trajectories in the most severe operational environment envisioned for the airplane. Isolated task analyses indicate that relatively low control powers are sufficient to provide the response necessary to maneuver the airplane to a degree allowing performance of practical flight profiles with minimal penalties in fuel consumption. However, many flight simulation programs and flight test investigations have shown that handling quality considerations and attention sharing significantly increase the control power required over that indicated by the isolated task analyses. The pilot demands complete confidence in the vehicle and margins over minimum requirements to perform the tasks. He prefers large control inputs for short periods to small control inputs for long periods, even though the latter approach can theoretically allow adequate performance of flight tasks. With rapid response to his commands, corrections can be performed quickly allowing attention to be devoted elsewhere.

For example, a number of research investigations have indicated that the control power levels required for emergency operation are substantially lower than those required for normal operation. The lateral control data obtained with the variable stability X-14A (Reference 2) is shown on Figure 1 to demonstrate the point. The damping-control power relationship is shown for Cooper pilot ratings of 3-1/2 and 6-1/2 corresponding to minimum acceptable systems for normal operation and emergency operation respectively. A Pilot rating of 6-1/2 implies that the aircraft can successfully complete its required flight tasks, and Figure 1 indicates that a control power as low as

.70 rad/sec.^{2} is sufficient. However, the pilot desires a substantial margin over this level for acceptable handling qualities for normal operation as evidenced by a minimum acceptable control power of 1.75 rad/sec.^{2} for a pilot rating of 3-1/2. These data reveal two significant points. First of all, maximum maneuvering commands must, by necessity, be sporadic in nature. For example, if a control power level of 1.75 rad/sec.^{2} is commanded for as long as 1 second, a 100 degree attitude change would result, which is obviously higher than practical. If the reaction control system can be designed to provide these sporadic commands without penalizing the lifting capability of the vehicle during normal control usage, the performance losses associated with control provision would be minimized. Secondly, since handling qualities considerations are important in determining maximum requirements, potential reductions in pilot acceptance of control power margins are possible by optimizing the functional characteristics of the control system (force gradients, stick sensitivities, stability augmentation system characteristics, etc.). For example, data presented in reference 3 and 4 indicate that high stick sensitivity can result in substantial reductions in required control power.

Also, it is the authors' opinion that it is unrealistic to define maneuvering control power requirements while isolating the effects of gusts, disturbances in ground proximity and gyroscopic coupling, although these considerations should rigorously be included under restoring requirements. These factors directly influence the ability to perform precise maneuvers and reflect on the pilot's judgment of acceptable maneuvering control power levels. It seems clear that maneuvering control power requirements must be defined with simultaneous consideration to all interrelated factors that effect the characteristics of the vehicle while maneuvering.

Trim requirements are those necessary to cope with center-of-gravity travel, thrust unbalance (during vectoring), engine or stability augmentation system (SAS) failures, jet induced aerodynamic pitching moments during transition, and aerodynamic moments in steady winds at hover or in transition principally due to jet induced effects. These requirements are all very much dependent on configuration, and with proper configuration design are minimal compared to the maneuvering control power requirements. In addition to the capability of trimming engine failures, restoring control power margins are necessary for arresting motion, and to return the vehicle to initial conditions. Restoring capability must also be available to override stability augmentation system (SAS) failures and defines the limit of SAS authority. These restoring requirements need not necessitate additional control power over trim and maneuvering requirements depending on the configuration design.

In order to determine the total control power requirements, the maneuvering, trim, and restoring requirements must be combined in a rational manner. Table 1 shows a recommended approach for establishing the critical total reaction control power requirements for normal and emergency operation. Two alternatives are shown for emergency operation. If the mission is to be aborted upon engine failure, the control power to restore the airplane to a safe attitude for pilot escape or a favorable impact attitude is critical. However, if the mission is to be continued, satisfactory control for maneuvering under emergency conditions must be available and the more critical of the maneuvering or restoring requirements should be provided. The total control

power required for each pertinent flight condition must be determined to identify the critical design condition. It is not the purpose of this paper to elaborate on definition of total control power requirements. The salient point that is intended to be conveyed is that maneuvering requirements are a major portion of the total control power required and are greatly influenced by handling quality considerations. These requirements are a consequence of the pilot's desire for relatively high control power margins over minimum levels to perform tasks, but for normal attitude changes the maximum levels are required for durations substantially less than a second.

CONTROL POWER UTILIZATION

Since maneuvering control inputs are time variant with large inputs of short duration, determination of the utilization characteristic of maneuvering control demands is an important consideration for the design of the control system and for determination of VTOL takeoff performance. A control system design approach which properly matches the spectrum of maneuvering control demands to the engine bleed source should provide the most efficient airplane. Trim requirements are essentially constant with time for a particular flight condition. Restoring requirements represent emergency situations and are of very short duration when they do occur. Therefore, the normal control utilization is primarily the superimposition of maneuvering inputs over the trim requirements. In order to demonstrate the typical time variant characteristic of maneuvering control power demands, a representative attitude change will be considered. In hovering flight, attitude changes are primarily confined to a range of ± 20 degrees in pitch and roll which implies that large inputs for maneuvering are introduced for extremely short periods of time. Figure 2 shows a time history for a pitch attitude change of 20 degrees from a hover condition with a rate command system and the airplane represented as a "pure inertia." (Aerodynamic and gyroscopic coupling effects are neglected.) A maximum control power of .90 rad/sec.^{2} and a damping level of -1.5 1/sec. were used for the example. The pilot input, SAS input, and the resultant pitch attitude and rate versus time are shown. In addition, the net acceleration (sum of absolute magnitude of the pilot and SAS acceleration input) is shown. The results show that a steady state pitch angle of 20 degrees is attained in approximately 2.5 seconds. The net acceleration time history indicates that the pilot input is washed out rapidly by the SAS input, and the mean control power required for the maneuver is only .26 rad/sec.^{2}. A control power utilization distribution for the maneuver can be defined and is shown in Figure 3. The distribution is defined by determining the percent time at or above a given net acceleration level during the maneuver. Examination of the distribution indicates that large control power levels are introduced for a small percentage of the total maneuver time.

Utilization distributions representing the accumulation of all maneuvers performed during takeoff, landing, hovering, and transition would be expected to be lower than the example since a majority of attitude changes are somewhat smaller in magnitude. However, there is insufficient data presently available to adequately define accumulated utilization distributions. In order to gain some insight as to the order of magnitude of accumulated utilization characteristics a review of unpublished flight test data and

flight simulation results with jet powered vehicles was made. Based on these data, Figure 4 presents estimated utilization distributions for the roll, pitch and yaw axes. The mean utilization levels for each axis are shown. These data are not the result of a systematic investigation aimed specifically toward development of utilization data with close control of test conditions, and should not be interpreted as a rigorous set of design guides. A concerted research program directed toward establishing utilization data is strongly recommended. However, the estimated data should be a good first approximation and demonstrate that the control power inputs are nominally quite low. The data are basically pertinent to VFR hovering and takeoff and landing tasks where pilot workload is highest and therefore critical in terms of utilization. Flight simulation studies have shown that control power utilization for IFR tasks is lower than for VFR. Due to a reduced rate of flight information input to him, the pilot is less willing to make gross attitude changes for maneuvering under IFR conditions. The estimated data are associated with a rate command control mode, but it is not anticipated that control mode has any significant effect.

Figure 5 is presented to illustrate this point. Time histories are shown for an attitude command system with essentially the same response as the rate command system of Figure 2 (20 degrees attitude change in 2.5 seconds). The pilot and stability augmentation system inputs as a function of time are again shown. The attitude command feedback gains were 4.0 1/sec. and 4.3 1/sec.^{2} for the rate and attitude loops respectively, and a control power of 1.5 rad/sec.^{2} is required to achieve the same response. The control power utilization curve for this system is presented in Figure 6 and compared with the rate command system shown on Figure 3. Although the maximum control power is higher with the attitude system, there is no indication that there is a significant effect of control mode on mean utilization. It is not the purpose of this paper to elaborate on the pros and cons of rate command versus attitude command modes. However, a significant point demonstrated in Figure 5 is that with an attitude command system the SAS input must be higher than the pilot input. Therefore, the authority of the SAS cannot be limited to allow pilot override of system failures. This implies that extremely reliable systems with multiple redundancy must be provided. In the authors' opinion, redundancy notwithstanding, the elimination of pilot override capability is not good design practice if there is any possibility of providing an acceptable system approach which gives the pilot this ability. With a rate command system the authority of the SAS can be limited without significantly altering response characteristics. In any case, the control utilization characteristics should not be appreciably effected regardless of the control mode employed.

In addition to the utilization of control power for each axis, it is equally important to define the combined utilization of all axes simultaneously. The mean reaction force utilization for each axis is directly additive to define the total mean utilization, but definition of the total utilization distribution is difficult. An approximate method is to assume that inputs for each axis are randomly distributed and the reaction forces for each axis can be added in a statistically random manner. This should be a good assumption for flight in the hovering regime where there is negligible coupling between axes. The approximation is probably not quite as good for

maneuvers at high transition speeds where coordination for banked turns is required due to aerodynamic coupling between the roll and yaw axes. It is recommended that the requirement for maximum simultaneous application of control be established on the basis of the predicted total reaction force utilization distribution. A design criteria which requires the capability of achieving the total reaction force commanded perhaps 1 to 5 percent of the time should be adequate. Reference 5 states that the pilot should be able to obtain full control power about all axes simultaneously. It is felt that this requirement is unreasonable and results in unnecessarily severe penalties to the design. In order to demonstrate the suggested approach, the approximate method for defining the total reaction force utilization described above will be applied to a typical aircraft later in the paper.

Reference 5 also requires that; to provide sufficient height control during vertical takeoffs, vertical thrust available out of ground effect should be at least 1.05 times the aircraft takeoff weight assuming that 50 percent of the available control power is being used simultaneously about all axes. This requirement is judged to be unrealistic on two counts. Definition of a 5 percent thrust margin out of ground effect may not allow takeoff depending on the ground effect characteristics of the vehicle. Therefore, it is suggested that the 5 percent margin also apply to vertical thrust in ground effect. In addition, the 50 percent simultaneous control power utilization is much too severe and unduly penalizes airplane performance. Inputs of that magnitude are used for extremely short periods as will be demonstrated for the typical application below. Even if the thrust loss associated with a control demand of that magnitude is relatively high with the particular reaction control system employed, the durations are so short that the effect on the takeoff trajectory would be insignificant. It is recommended that the thrust margin requirement apply at the mean utilization of maneuvering control power in each axis simultaneously plus the trim requirements.

TYPICAL APPLICATION

The typical transonic close support VTOL aircraft shown in Figure 7 will be exercised to demonstrate the basis for the recommendations noted above and to provide a base vehicle for a comparative evaluation of various reaction control system concepts. The airplane is designed for a takeoff gross weight of 30,000 pounds with full internal fuel and a 3000 pound payload. Pertinent characteristics are given in Table 2. The composite propulsion system consists of four lift turbojets rated at 6250 pounds each, and two lift/cruise turbofans rated at 5000 pounds each. The installed thrust indicated in Table 2 reflects a 10 percent thrust loss accounting for pressure recovery, exhaust gas re-ingestion, and ground effects but no penalty for control provisions. (The weight of the reaction control ducting and nozzles are accounted for in defining the fuel capability.) An installed thrust to gross weight ratio of 1.05 in ground effect is used. The increase in rated engine thrust to accommodate control provisions, and the corresponding reduction in fuel capability will be determined for each of the reaction control systems that will be applied. Only the lift turbojets are used as the bleed source for the reaction control systems. Control nozzles are located at the wing and fuselage extremities of the vehicle and all roll and pitch reaction forces are directed upward (downward efflux) to maximize the net vertical force. The maximum control power levels for the airplane are

shown in Table 2 and should be representative of excellent handling qualities. The trim control power levels are based on the estimated critical center-of-gravity location for the pitch axis and hover in a 35 knot side wind for the roll and yaw axes.

Using the control ppwer utilization curves of Figure 4, the maneuvering reaction force utilization curves for the typical airplane are given in Figure 8. The total reaction force utilization for all three axes is shown in Figure 9 based on a statistically random distribution of inputs for each axis as previously discussed. The reaction forces corresponding to 50 and 100 percent simultaneous application of maneuvering control power for each axis are shown. Control demands greater than 50 percent simultaneous application only occur approximately 2 percent of the time. A 50 percent simultaneous application would appear to be a good basis for a design requirement and is used for this analysis. With the reaction force data defined in Figures 8 and 9, the reaction control system concepts described below will be applied, and the net vertical force available at takeoff after provisions for control will be determined for each. Using these results the increase in rated engine thrust required to maintain a 30,000 pound design takeoff weight will be defined for each. The most efficient approach is to hold the lift/cruise engine size and increase the size of the lightweight lift engines since this results in minimum penalty to fuel capability. An estimate of the ratio of incremental lift engine thrust to incremental airplane empty weight of 8.0 is employed. This is based on a bare engine thrust to bare engine weight ratio of 17.0 and accounts for additional installation weight, including fuselage structure, associated with the increased engine size.

The mission selected is a close support profile with optimum cruise out and back at an altitude of 500 feet and 30 minutes of loiter for a combat allowance.

Reaction Control System Concepts

Several methods of engine control and operation are possible to accommodate compressor bleed air extraction. Turbine inlet temperature (TIT) must be held within the capability of the engine design and stall free operation of the compressor preserved. As compressor discharge air is taken from the cycle, engine thrust decreases with the magnitude of the decrease dependent on the mode of engine operation. Consequently, it is important to minimize the required bleed air quantity and to select a mode of engine operation that is least penalizing to the aircraft as a whole.

Following is a brief description of some of the possible modes of engine operation along with the incurred jet nozzle thrust penalties. Figure 10 exhibits typical turbojet lift engine jet nozzle thrust decay characteristics for different modes of engine operation as compressor bleed air is extracted. Figure 11 presents a typical characteristic of reaction force available as a function of percent bleed airflow. Figure 10 indicates that highest thrust losses occur when a fixed exhaust area engine rated at zero bleed is operated to stay within TIT limits. A reduction of rpm is required with attendant thrust losses as shown by Curve 1. Curve 2 repersents the same engine operating at rated rpm with exhaust area varied to maintain rated TIT. This curve represents the locus of an infinite number of fixed exhaust area engines

set up for specific percentages of bleed. Curve 3 represents the thrust variation for variable bleed extraction from a fixed exhaust area engine set up to operate at rated turbine inlet conditions at a preselected bleed quantity. This engine would operate under temperature at bleed flows lower than rated and overtemperature above rated bleed. Thermal lag permits operation at temperatures above rated on a transient basis. Figure 12 presents the transient overtemperature exposure capability of a representative uncooled turbine lift turbojet engine. In view of the fact that aircraft control demands are time dependent, and that increasing control magnitudes are associated with decreasing demand durations, the engine transient turbine temperature capability may be used to advantage.

Various reaction control systems that can be formulated on the basis of these engine characteristics are described below. Each of these systems is applied to the typical aircraft to determine the engine bleed air requirements and the effect on the net vertical force at takeoff (the sum of the jet nozzle thrust and the net upward acting reaction control forces). The results are discussed below with the system descriptions and summarized on Figure 13.

Variable Bleed System A: This system employs fully variable compressor bleed air extraction from the lift engines with the nozzles or valves in the control lines serving to meter only that flow required to meet the instantaneous aircraft control demands. In this way, the fully variable bleed system lends itself to the simplest aircraft plumbing system consistent with minimum bleed flow. It is not necessary to control the discharge of a constant quantity of flow and bleed flow is available to any control axis. As such, utilization of the minimum quantity of bleed air is insured. Bleed air demand from the engine is effected simply by opening of the appropriate control nozzles. The engine bleed air ports, air distribution ducting and control nozzles are all sized to provide the maximum required control capability in each axis. The rated bleed level corresponding to rated TIT must be selected to provide an acceptable turbine temperature environment for demands higher than the rated bleed level. There is insufficient data at this time for a rigorous selection. For this analysis the rated bleed level is selected to provide the mean utilization reaction force level. Preliminary indications are that this should result in an acceptable temperature environment as will be illustrated. For the example airplane, a total of 2000 pounds of reaction force is required to satisfy the mean utilization plus trim reaction control requirements (Figure 9). With the lift engines rated at the bleed level required to produce this force level Figure 13 indicates that an installed jet nozzle thrust loss of 3600 pounds will result. However, a reaction force of 1600 pounds is recovered vertically. These results are shown on Figure 13. An increase of 8.9 percent in lift engine size is required to provide the 2000 pound additional net vertical force to maintain a takeoff gross weight of 30,000 pounds. With the increased lift engine size the percent bleed required to provide the mean utilization plus trim reaction forces is determined to be 8.8 percent from Figure 11 ($F_{Reaction}/F_{Rated\ Zero\ Bleed}$ = 2000/27200 = .074). With the engine trimmed at this level the TIT variation with bleed extraction for a typical lift turbojet is as shown in Figure 14. The maximum bleed level corresponding to application of 50 percent of the control power in each axis simultaneously plus trim is 17.9 percent. The maximum potential overtemperature is shown to be 215 degrees Fahrenheit. In order to show the distribution of TIT

variations, Figures 9, 11, and 14 are combined to define Figure 15. The resulting distribution indicates that the overtemperature excursions constitute a small percentage of time. Since this distribution represents a composite of numerous individual bleed demands with periods of below rated temperature operation interspersed with overtemperature periods, the overtemperature excursions should be well within the transient capability illustrated on Figure 12. It should be noted that this exposure will only occur during operation at takeoff power settings. At lower power settings, such as that required for hover at takeoff weight, and reduced weights, little or no operation above rated turbine inlet conditions will result as illustrated on Figure 16.

Variable Bleed System B: This system employs a fixed auantity of bleed air which is extracted continuously plus a variable quantity for intermittent use. The engine is operated at rated conditions at the fixed quantity of bleed and overtemperature at higher bleed flows. This system is less taxing on the engine compressor design as a result of smaller bleed air transient extractions. If the fixed quantity corresponds to that required for mean control utilization, the same performance as indicated for Variable Bleed System A would result. However, the engine temperature environment is more severe than the fully variable system since engine temperature would not drop below rated for control demands less than mean utilization. Therefore, for an acceptable turbine operating environment, rated conditions must be established at a substantially higher bleed level resulting in larger thrust losses than the fully variable bleed system. Also, in order to supply the maximum control demands for each axis the complication of providing for bleed air transfer between axes is necessary, or higher maximum bleed levels than the fully variable system are required.

Constant Bleed System A: This system is the simplest constant bleed concept that can be applied. The bleed air required for maximum control power in each axis is delivered continuously and control moments are effected simply by modulating flow within each axis. However, since the design requirement for simultaneous application of control is only 50 percent of the maneuvering control power in each axis plus trim, the 7600 pound total reaction force required (Figure 9) is somewhat higher than the 4100 pound minimum reaction force possible. The net vertical force is defined by adding the 5000 pound reaction force for maximum pitch and roll control power (Figure 8) to the jet nozzle thrust for rated temperature at the 7600 pound reaction force corresponding to 100 percent simultaneous control application. Figure 13 shows the net vertical force for this system and indicates that an increase of 37.0 percent in lift engine size is required for a 30,000 pound takeoff weight. Also, the bleed required is approximately 26.5 percent which may be higher than practical.

Constant Bleed System B: This system reduces the required bleed air extraction from the engines for Constant Bleed System A by supplying bleed air corresponding to full control power in pitch and roll only, and rotating the pitch nozzles for yaw control. Pitch and roll control moments are again effected by modulating flow within each axis. This system is relatively simple and does not require a substantially higher total reaction force (5000 pounds) than the minimum to achieve the design requirement for simultaneous control application (4100 pounds). The net vertical force is defined

by adding the maximum roll reaction force, and the vertical component of the pitch-yaw nozzle reaction force at the rotation required for yaw mean utilization to the jet nozzle thrust for rated temperature at the 5000 pound total reaction force level. Figure 13 shows the net vertical force for this system and indicates that a sizeable improvement is obtained over Constant Bleed System A. The lift engine size increase required is 18.0 percent. Bleed requirements are also reduced to 20.1 percent against 26.5 percent for Constant Bleed System A.

Constant Bleed System C: This system concept is based on minimizing the constant bleed air extraction from the engines to a level corresponding to the design requirement for maximum simultaneous application of control power (50 percent of the maneuvering requirement in each axis plus trim). However, a system complexity penalty must be paid to achieve this minimum bleed in that large control demands is one axis require flow to be diverted from the other axes or from a neutral nozzle. The total control nozzle area must be held constant as variations in control inputs are introduced necessitating a complex system design. The total reaction force required for this system is 4100 pounds (Figure 9). The net vertical force capability is defined by adding the total reaction force less the 450 pound yaw reaction force corresponding to mean utilization (Figure 8) to the jet nozzle thrust at rated temperature at the bleed level for the total reaction force required. Figure 13 shows that only a small additional advantage over Constant Bleed System B is obtained. A 17.0 percent increase in lift engine size is required. The maximum bleed requirement can also be reduced to 17.9 percent but these gains are not significant in the light of the associated increased system complexity.

Mission Performance Trade-Offs

The lift engine sizes required for a 30,000 pound takeoff gross weight for the reaction control systems described above, are summarized in Table 3. Also presented, are the effect on fuel capability and the resultant mission radii. These results show that the variable bleed system results in approximately half the radius penalty for control provisions as the best of the constant bleed systems. In addition, the lift engine development and unit cost would be higher as a consequence of the larger engine size required.

In addition to the comparative radii for each system at a given gross weight, a comparison of the gross weights required for a given radius is also of interest. In order to accomplish this, a family of aircraft of varying gross weight and the same general arrangement as the typical 30,000 pound airplane was defined, and the variation of inertia characteristics and control moment arms with gross weight determined. Since the inertias increase more than the control moment arms with increasing gross weight, the resultant reaction forces required are a higher percentage of the gross weight resulting in higher percentage thrust losses with increased airplane size. Figure 17 presents the rated lift engine thrust increase required for control provisions as a function of takeoff gross weight for each reaction control system concept. The lift/cruise engine thrust is held constant at 33 percent of the takeoff gross weight to maintain the same design maximum speed capability. Based on these data, the variation of mission radius with design gross weight is presented in Figure 18 for each concept. From Figure 18, the gross weight increase required to maintain the

215 nautical mile radius of the basic 30,000 pound airplane with no control provisions is defined for each of the reaction control system concepts. The results are summarized in Table 4. The required lift engine size for each system is also presented. Although the gross weight required for the best of the constant bleed systems is not appreciably higher than that required for the variable bleed system a significant increase in lift engine size is required, which together with a larger lift/cruise engine, and larger airframe size, result in a significant increase in cost. Figure 18 also shows that with increasing radius the effect of control system on gross weight required is somewhat greater. Figure 19 presents the percent increase in gross weight required to maintain a given radius for each of the reaction control system concepts. The advantages of a variable bleed system become more pronounced as the mission radius requirement is increased.

In some applications the objective is to achieve maximum radius performance with existing engine sizes. Table 5 is presented to show the gross weight and radius capability provided by each of the control concepts using the lift and lift/cruise engine sizes for the typical 30,000 pound airplane. Substantial reductions in performance for control provisions result and the need for an efficient control system is greatly amplified. Again the variable bleed system results in approximately half the radius penalty of the best constant bleed system.

CONCLUSIONS

1. A major portion of the total control power required is for maneuvering and is substantially influenced by handling quality considerations. The handling quality considerations are manifested in pilot demands for large margins over minimum control power levels for performing tasks. Much of the control power required is only utilized sporadically, and therefore a reaction control concept which produces minimum penalty to the airplane lifting capability, considering these sporadic demands, provides the most efficient system.

2. A fully variable bleed system with the engine exhaust area trimmed to achieve rated turbine inlet temperature at mean utilization of control, and operated overtemperature for larger control demands, provides minimum loss in thrust for control provisions. Indications are that the overtemperature and transient bleed environment that an engine operated in this manner would be exposed to should not be prohibitive or result in a reduction in engine life.

3. Control provisions have a significant impact on mission performance, but a variable bleed system results in approximately half the radius penalty at a given gross weight as the most efficient constant bleed system that can be employed. Also, the increase in gross weight required to maintain a given radius utilizing a variable bleed system is less than half the increase required for the most efficient constant bleed system.

4. A concerted research effort should be undertaken to define control utilization characteristics in order to support development of variable bleed control systems, allow establishment of requirements for maximum

simultaneous control application, and provide a basis for definition of required thrust margins for vertical takeoff. Preliminary data indicate that the Reference 5 requirement for simultaneous application of control power is not realistic. A simultaneous requirement corresponding to 50 percent of the maximum maneuvering control power in each exis plus critical trim is recommended. Also, the definition of thrust margins required for takeoff in Reference 5 is judged to be unrealistic. It is recommended that a thrust/weight ratio of 1.05, in or out of ground effect (whichever is critical), and mean utilization of control, be used to define VTOL takeoff weight.

5. Designs of future lift engines should take into consideration the requirement for transient bleed and temperature excursions as exhibited by a variable bleed system, and engine qualification requirements should reflect these transient capabilities.

REFERENCES

1. C.F. Friend, "A Fundamental Study of Reaction Control Criteria for Jet VTOL Aircraft," AIAA Paper No. 64-787, September 1964.

2. L. Stewart Rolls and Fred J. Drinkwater III, "A Flight Determination of the Attitude Control Power and Damping Requirements for a Visual Hovering Task in the Variable Stability and Control X-14A Research Vehicle," N.A.S.A. TN D 1328, May 1962.

3. J. Patierno and J. Isca, "Instrument Flight Simulator Study of the VTOL Control Power-Controllability Relationship," IAS Paper No. 61-118-1812, June 1961.

4. Kliner, W. J. and Craig, S. J., "Study of VTOL Control Requirements During Hovering and Low-Speed Flight Under IFR Conditions," IAS Preprint 61-60, January 1960.

5. Recommendations for V/STOL Handling Qualities, AGARD Report 408, October 1962.

TABLE INDEX

Table	Title
1	Total Control Power Requirements.
2	Typical Close Support Airplane Characteristics.
3	Mission Radius Performance Comparison (Gross Wt.= 30,000 Lb.).
4	Gross Weight Required for Given Mission Radius (Radius = 215 n.mi.)
5	Mission Radius Performance Comparison (Fixed Engine Sizes).

FIGURE INDEX

Figure	Title
1	Typical Lateral Control Requirements.
2	Time History of a Pitch Attitude Change (Rate Command System).
3	Control Power Utilization for a Pitch Attitude Change (Rate Command System).
4	Estimated Control Power Utilization (Roll, Pitch and Yaw).
5	Time History of a Pitch Attitude Change (Attitude Command System).
6	Control Power Utilization for a Pitch Attitude Change (Attitude Command System).
7	Typical VTOL Close Support Airplane.
8	Reaction Force Utilization (Roll, Pitch and Yaw).
9	Total Reaction Force Utilization.
10	Typical Lift Turbojet Characteristics as a Bleed Source.
11	Reaction Forces Available.
12	Typical Lift Turbojet Transient Overtemperature Capability.
13	Net Vertical Force at Takeoff for Various Reaction Control Systems.
14	Engine Turbine Inlet Temperature Variation for Variable Bleed System.
15	Distribution of Engine Turbine Inlet Temperature for Variable Bleed System.
16	Effect of Thrust Level on Percent Time over Rated Temperature for Variable Bleed System.
17	Increase in Lift Engine Thrust Required for Control Provisions.
18	Effect of Reaction Control System on Radius Versus Gross Weight.
19	Effect of Reaction Control System on Percent Increase in Gross Weight for Control Provisions.

Control Power Requirement	Normal Operation	Emergency Operation	
		Aborted Mission	Mission Cont'd.
Maneuvering			
Normal Operation	X		
Emergency Operation			X*
Trim	X	X	X
Restoring		X	X*
TOTAL	X	X	X

* Whichever is Critical

TABLE 1 TOTAL CONTROL POWER REQUIRED

Gross Weight	30,000 Lb.	
Fuel Weight	8,000 Lb.	
Payload (1[illegible] Lb. Bombs)	3,000 Lb.	
Engine Thrust	Rated (Sea Level, Std.Day)	Installed (In Grd.Effect, No Bleed)
(2) Lift/Cruise Turbofans	5,000 Lb. Each	4,500 Lb.
(4) Lift Turbojets	6,250 Lb. Each	5,625 Lb.
Moments of Inertias (With Stores)		
Roll	18,200 slg. - ft^2	
Pitch	82,000 slg. - ft^2	
Yaw	90,300 slg. - ft^2	
Moment Arms to Reaction Nozzles (From Center-of-Gravity)		
Roll	15.5 Ft.	
Pitch	23.0 Ft.	
Yaw	23.0 Ft.	
Maximum Reaction Control Power		
Roll		
Maneuver	1.50 Rad/Sec.^{2}	
Trim	.15 Rad/Sec.^{2}	
Total	1.65 Rad/Sec.^{2}	
Pitch		
Maneuver	.89 Rad/Sec.^{2}	
Trim	.05 Rad/Sec.^{2}	
Total	.85 Rad/Sec.^{2}	
Yaw		
Maneuver	.60 Rad/Sec.^{2}	
Trim	.06 Rad/Sec.^{2}	
Total	.66 Rad/Sec.^{2}	

TABLE 2 TYPICAL CLOSE SUPPORT AIRPLANE CHARACTERISTICS

Control System	Lift Engine Thrust/Eng. Lb.	Fuel Weight Lb.	Radius N.Mi.
No Control Provisions	6250	8000	215
Variable Bleed A	6810	7720	198
Constant Bleed A	8560	6840	144
Constant Bleed B	7390	7440	181
Constant Bleed C	7310	7475	183

TABLE 3 MISSION RADIUS PERFORMANCE COMPARISON

(Gross Wt. = 30,000 Lb.)

Control System	Lift Engine Thrust/Eng. Lb.	Fuel Weight Lb.	Gross Weight Lb.
No Control Provisions	6250	8000	30,000
Variable Bleed A	7040	8300	30,900
Constant Bleed A	10200	9550	35,000
Constant Bleed B	7940	8680	32,100
Constant Bleed C	7810	8600	31,900

TABLE 4 GROSS WEIGHT REQUIRED FOR GIVEN MISSION RADIUS

(Radius = 215 N.Mi.)

Control System	VTOL Gross Wt. Lb.	Fuel Weight Lb.	Radius N.Mi.
No Control Provisions	30,000	8000	215
Variable Bleed A	28,200	6680	158
Constant Bleed A	23,100	2670	0
Constant Bleed B	26,450	5320	95
Constant Bleed C	26,650	5600	104

TABLE 5 MISSION RADIUS PERFORMANCE COMPARISON

(FIXED ENGINE SIZES)

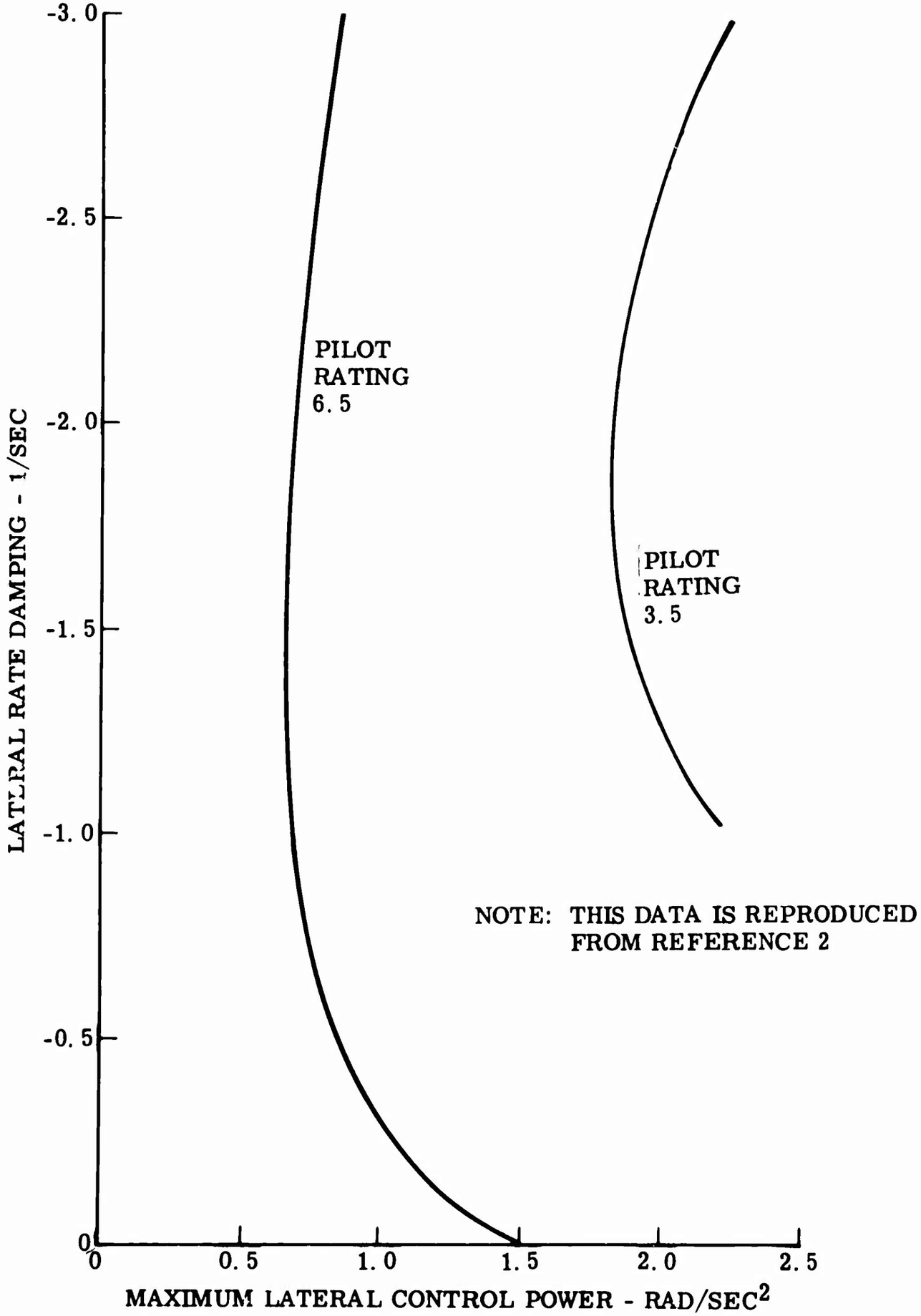

FIGURE 1 TYPICAL LATERAL CONTROL REQUIREMENTS

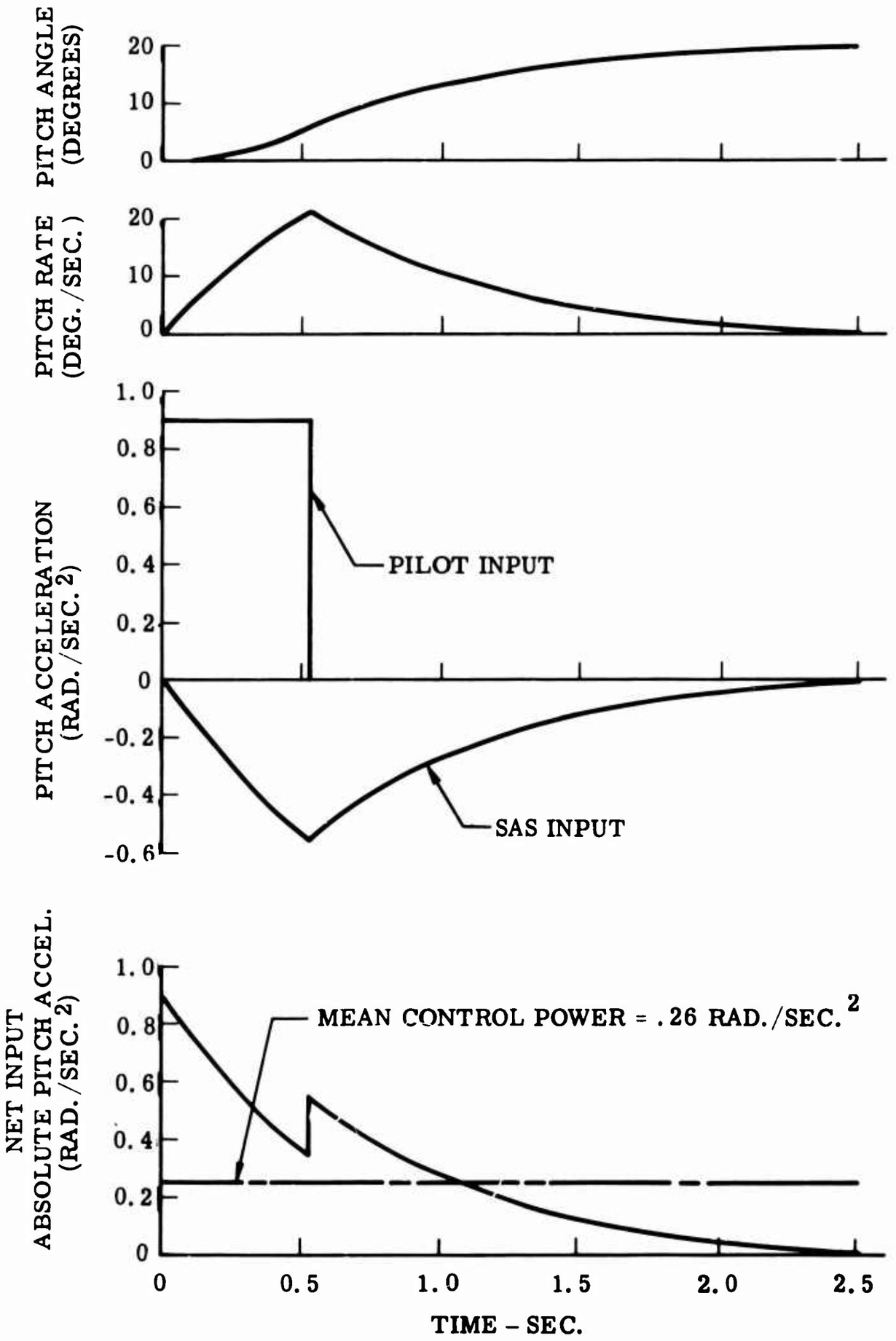

FIGURE 2. TIME HISTORY OF A PITCH ATTITUDE CHANGE (RATE COMMAND SYSTEM)

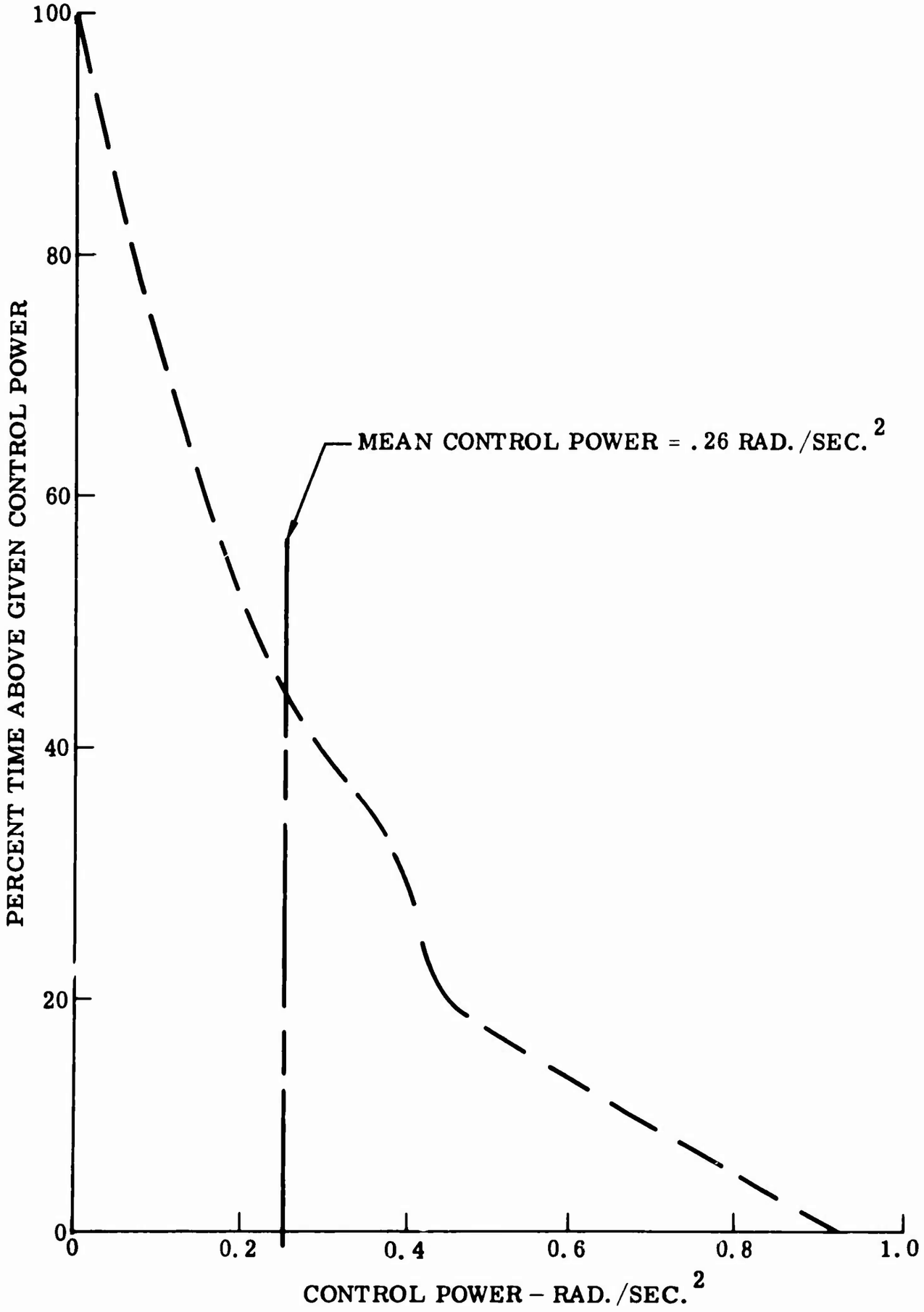

FIGURE 3. CONTROL POWER UTILIZATION DISTRIBUTION FOR A PITCH ATTITUDE CHANGE (RATE COMMAND SYSTEM)

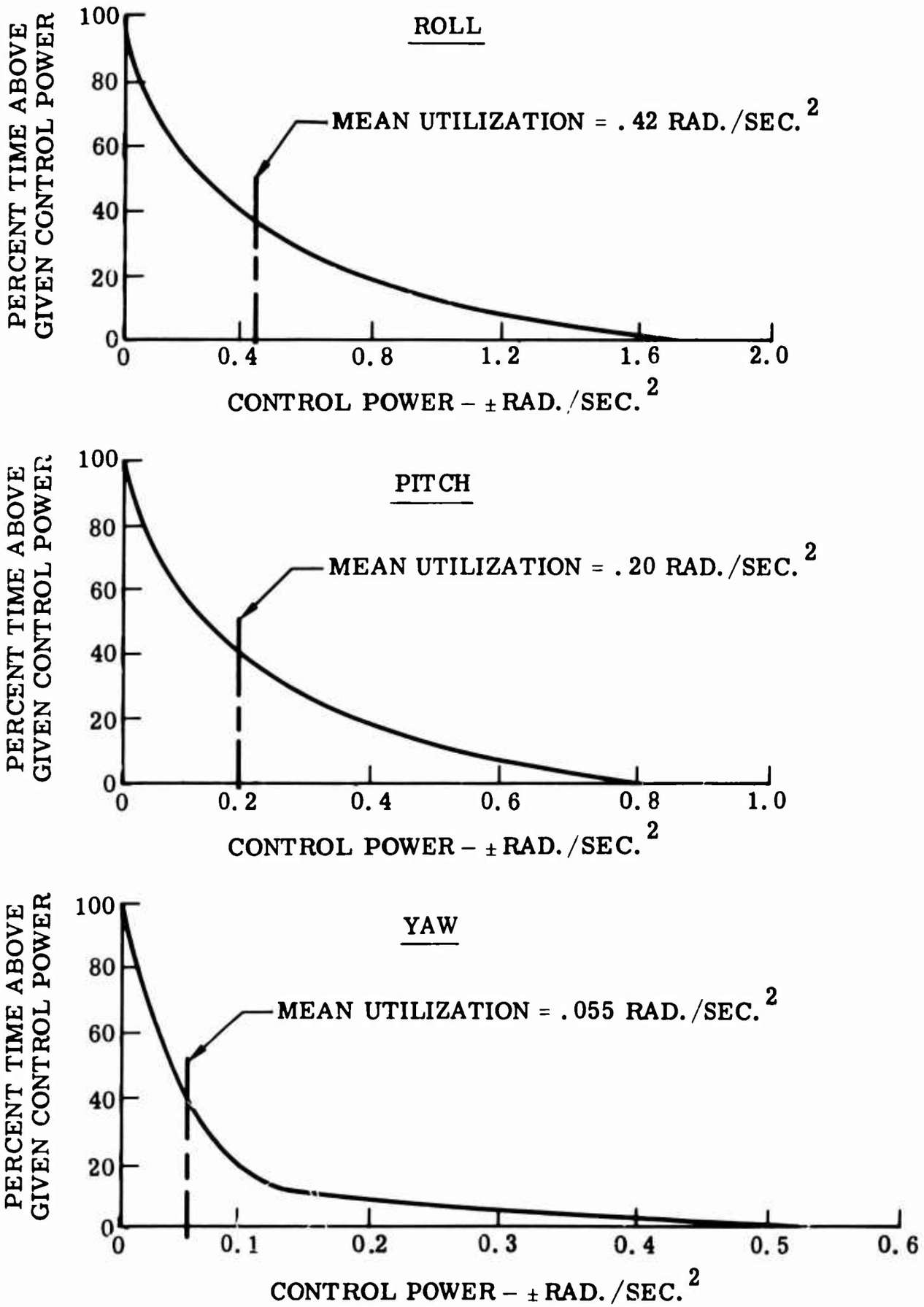

FIGURE 4. ESTIMATED CONTROL POWER UTILIZATION (ROLL, PITCH AND YAW)

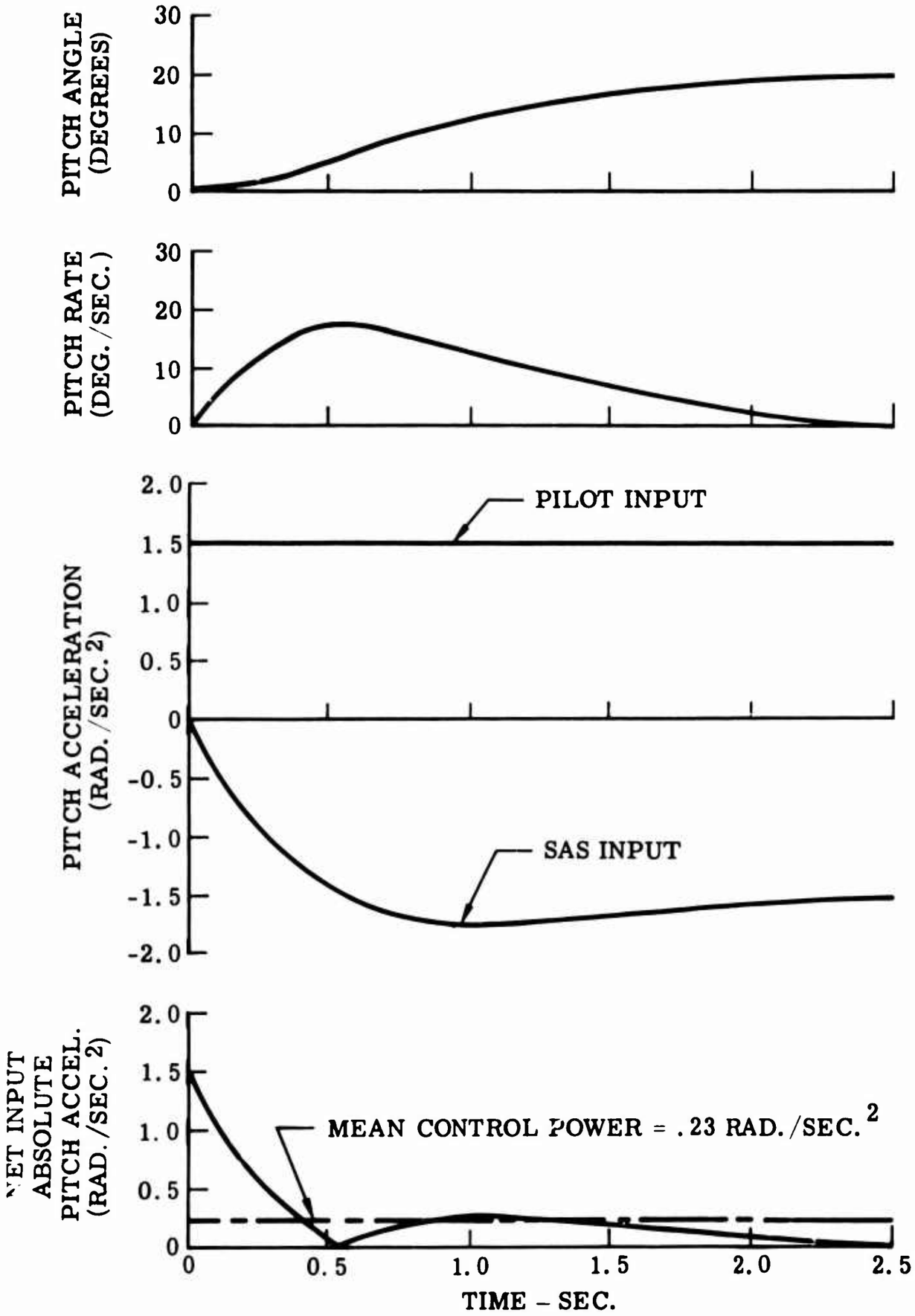

FIGURE 5. TIME HISTORY OF A PITCH ATTITUDE CHANGE (ATTITUDE COMMAND SYSTEM)

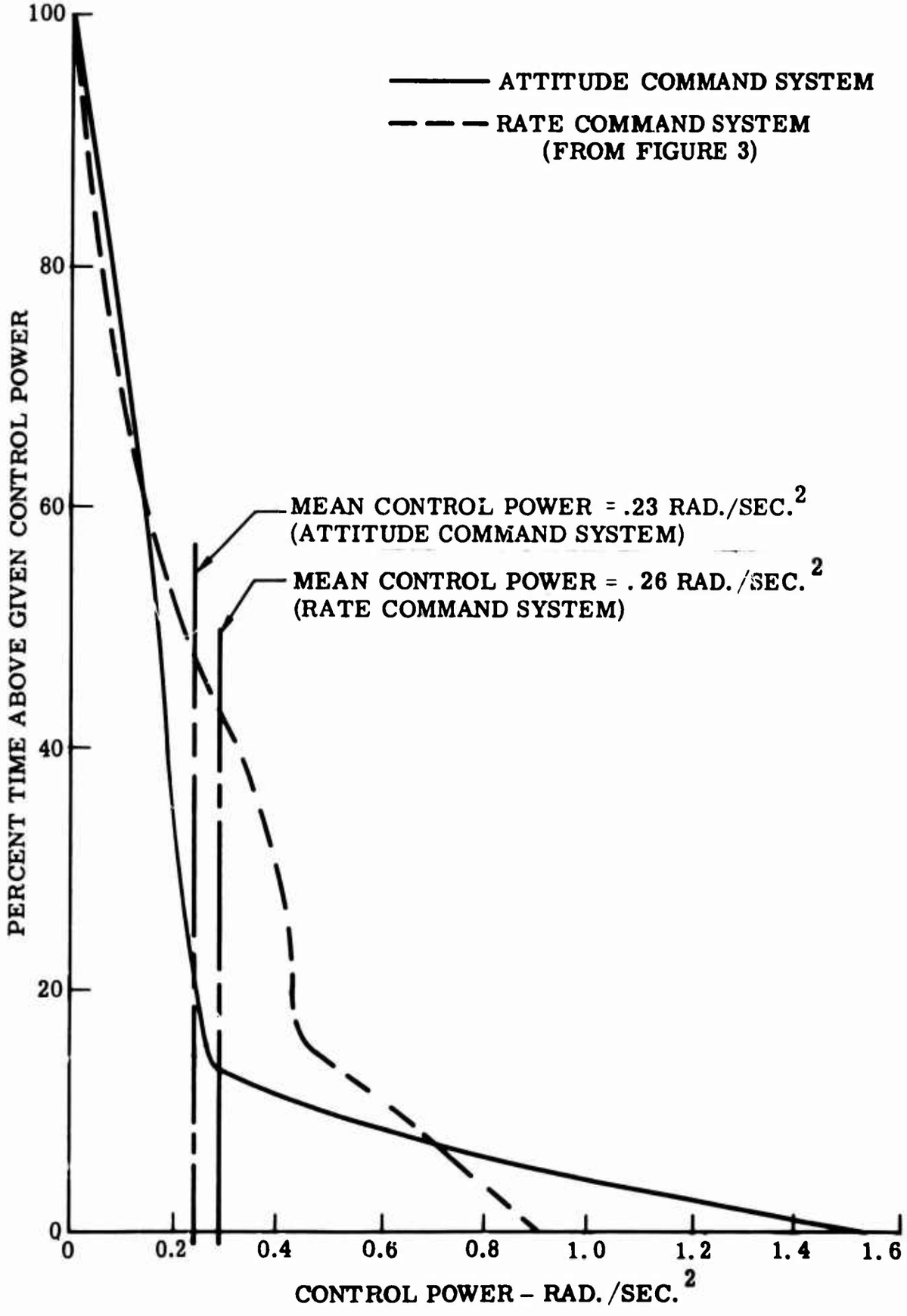

FIGURE 6. CONTROL POWER UTILIZATION DISTRIBUTION FOR A PITCH ATTITUDE CHANGE (ATTITUDE COMMAND SYSTEM)

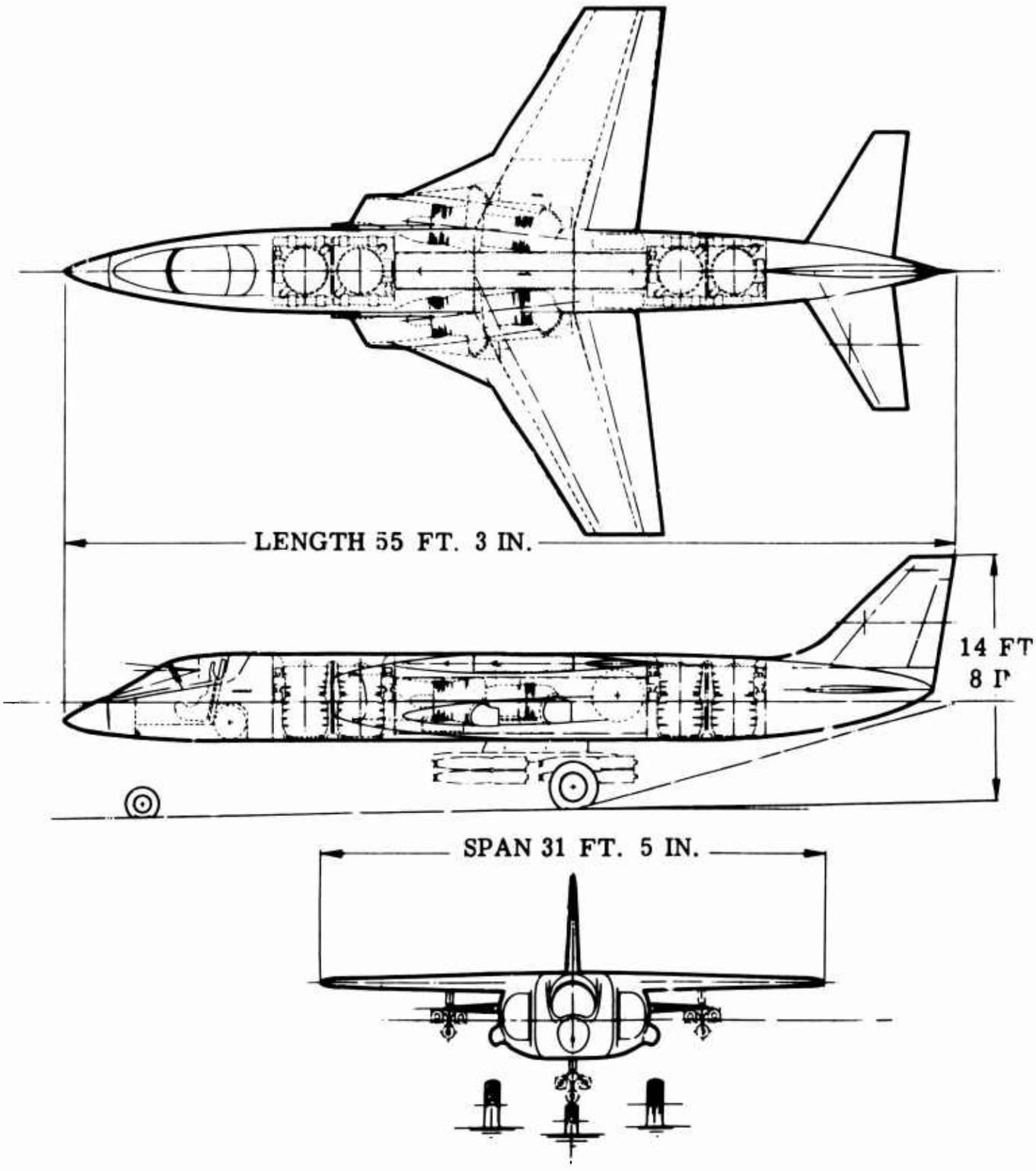

FIGURE 7. TYPICAL VTOL CLOSE SUPPORT AIRPLANE

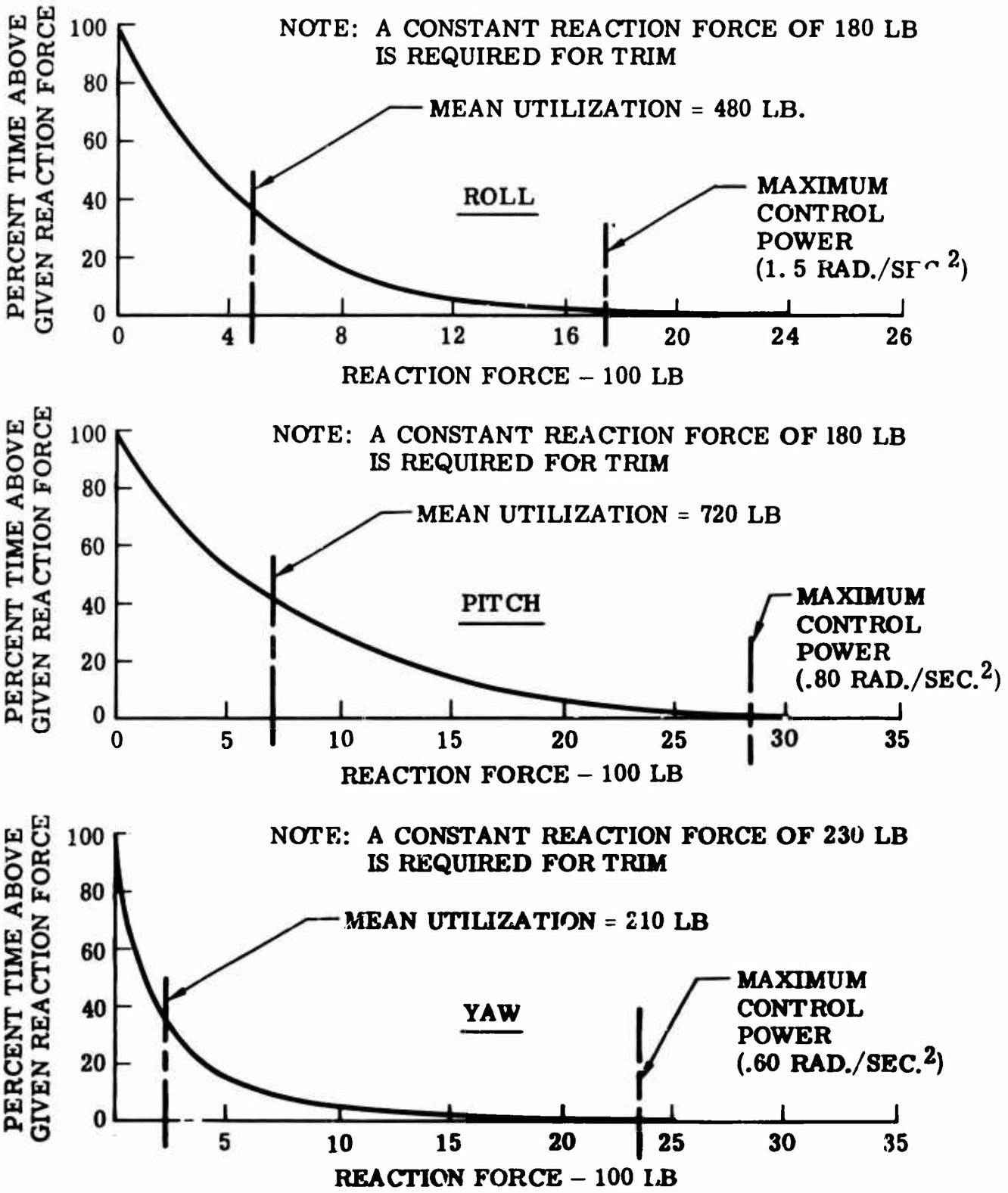

FIGURE 8. REACTION FORCE UTILIZATION (ROLL, PITCH AND YAW)

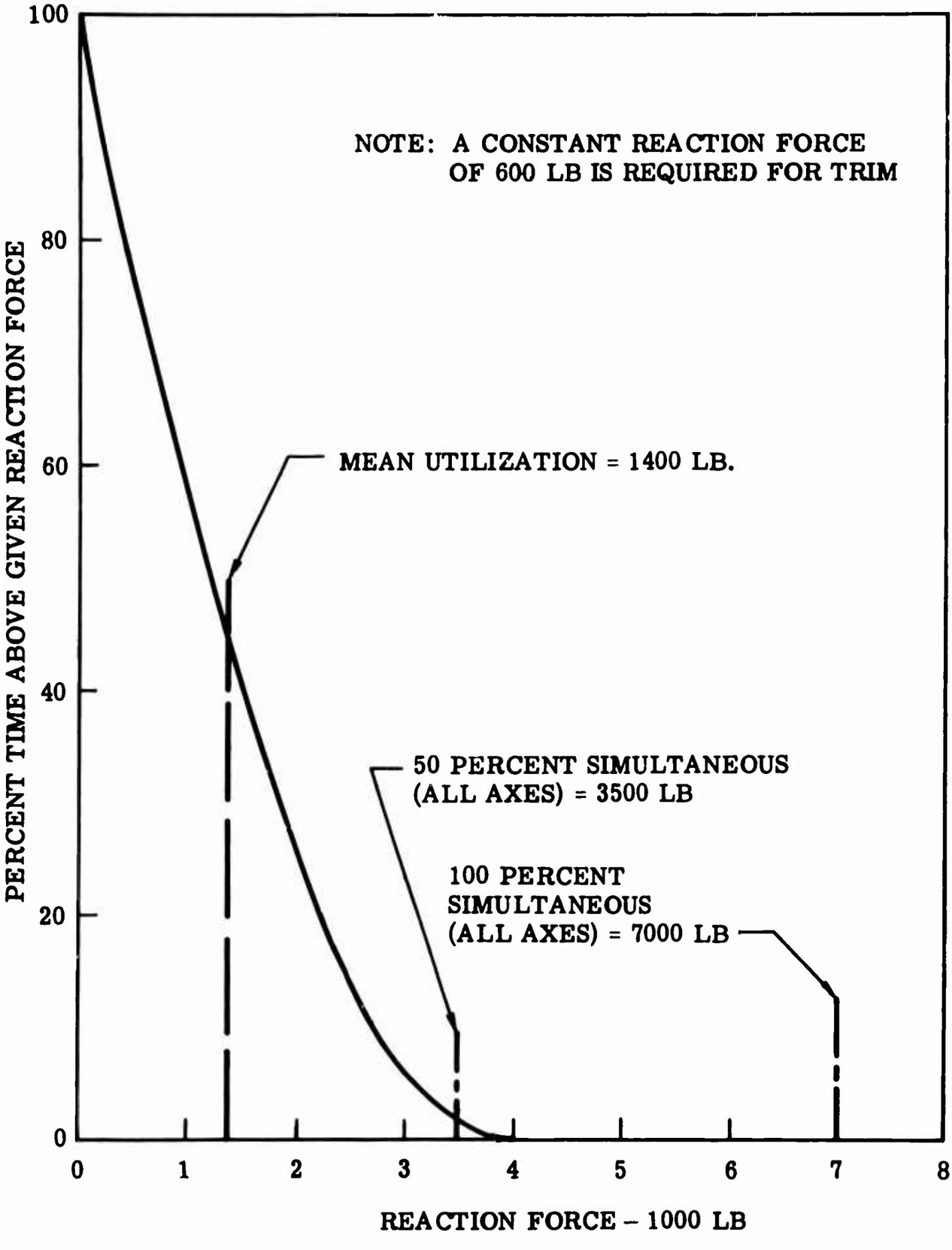

FIGURE 8. TOTAL REACTION FORCE UTILIZATION

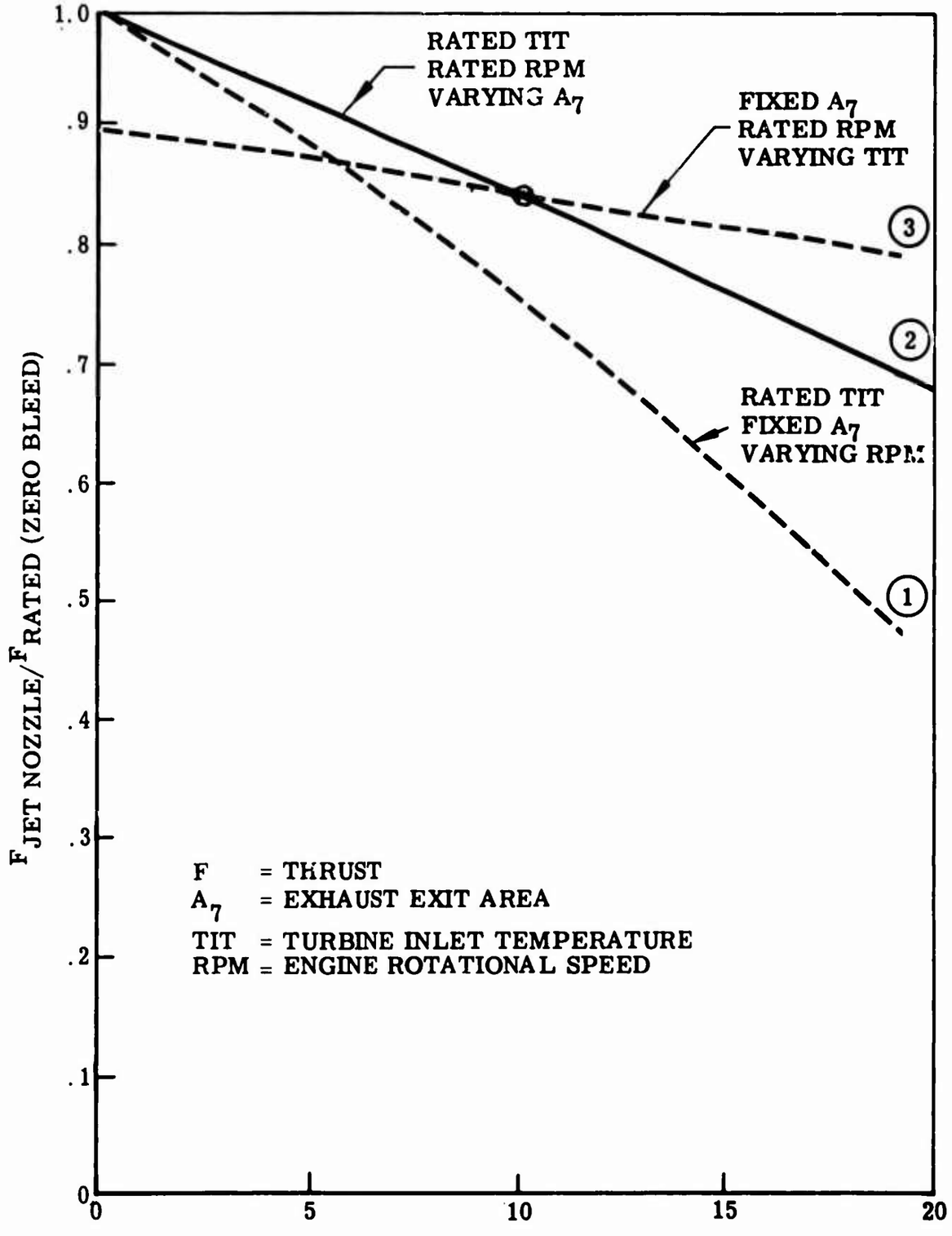

FIGURE 10. TYPICAL LIFT TURBOJET CHARACTERISTICS AS A BLEED AIR SOURCE

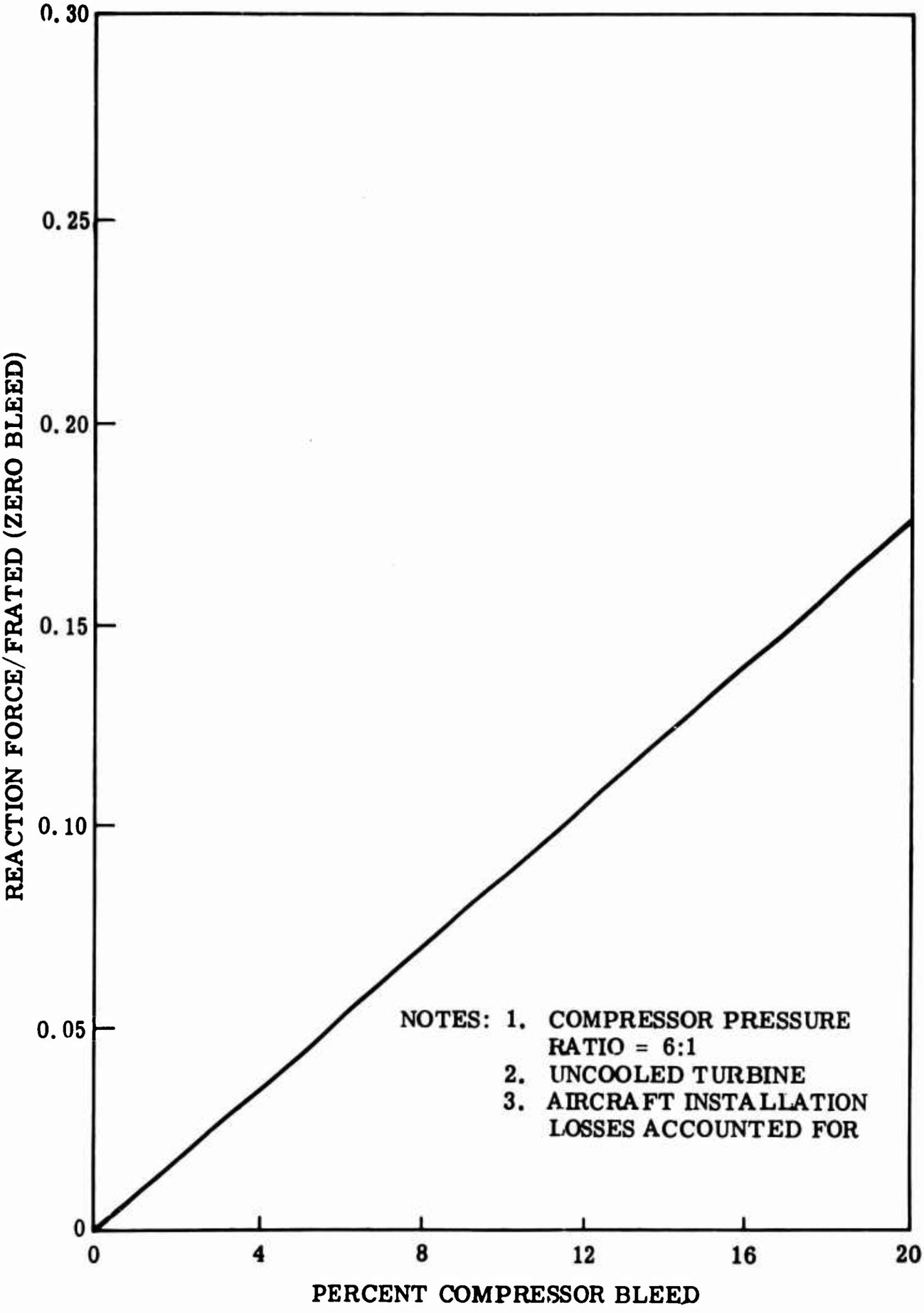

FIGURE 11. REACTION FORCE AVAILABLE

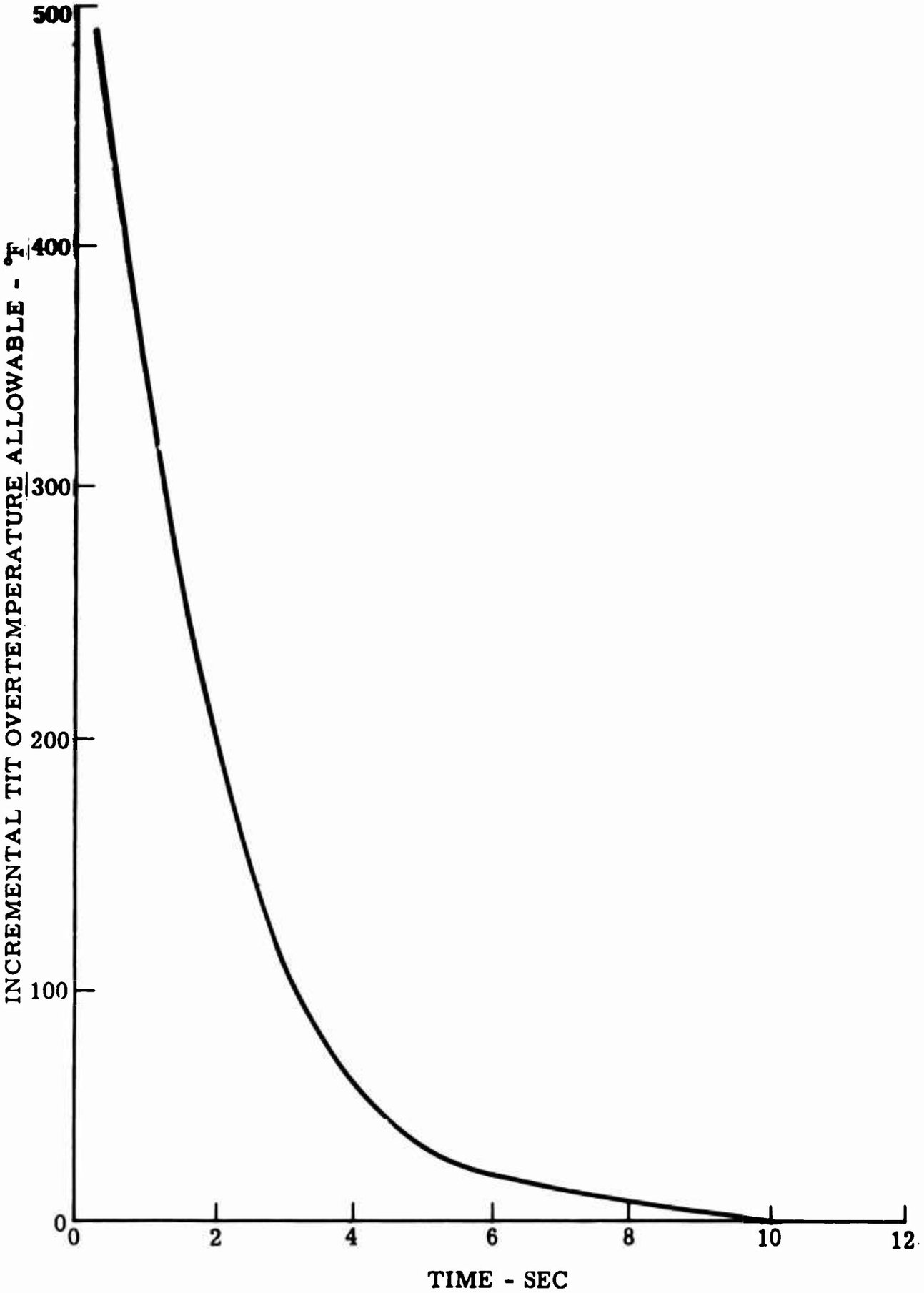

FIGURE 12 TYPICAL LIFT TURBOJET TRANSIENT OVERTEMPERATURE CAPABILITY

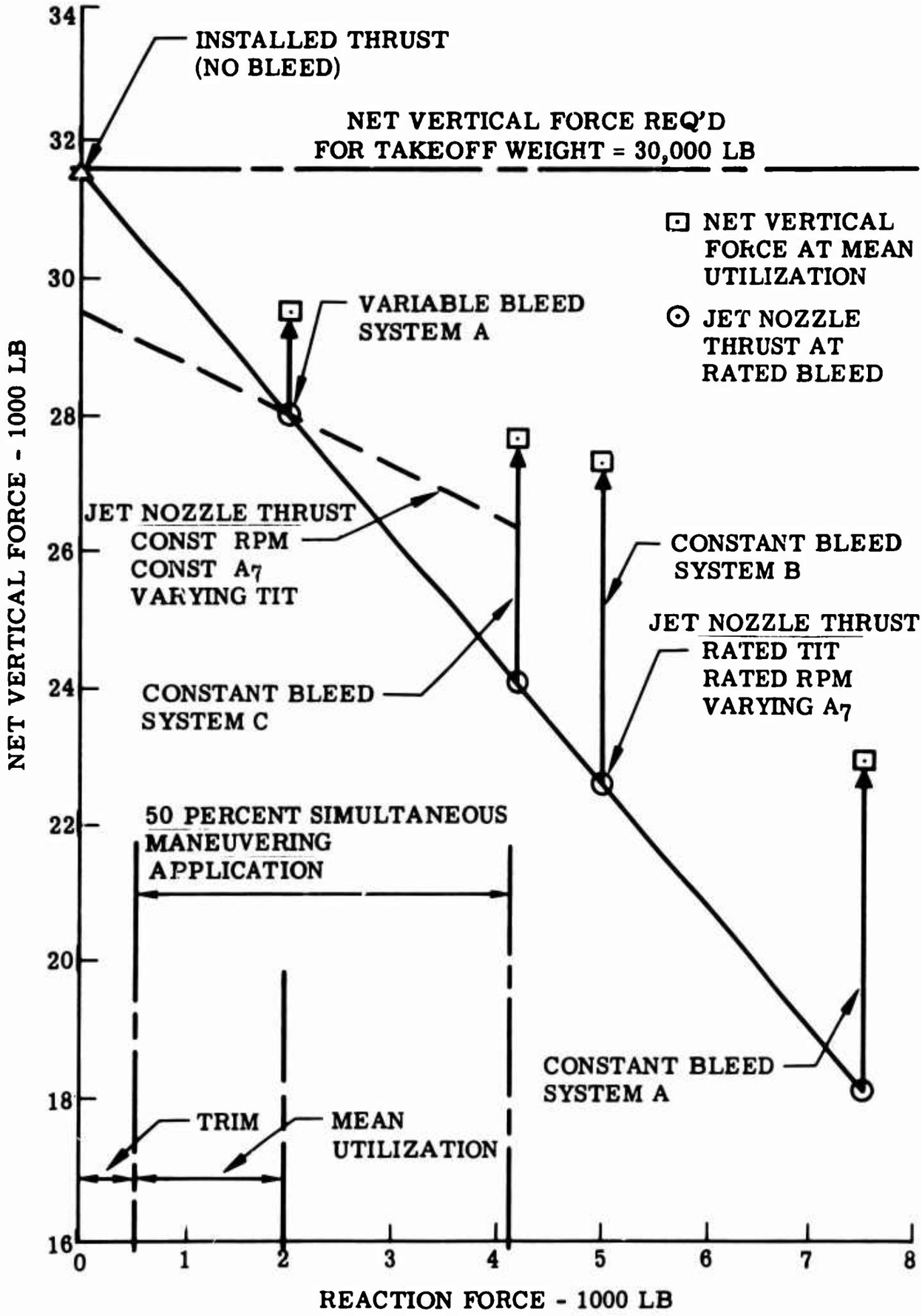

FIGURE 13 NET VERTICAL FORCE AT TAKEOFF FOR VARIOUS REACTION CONTROL SYSTEMS

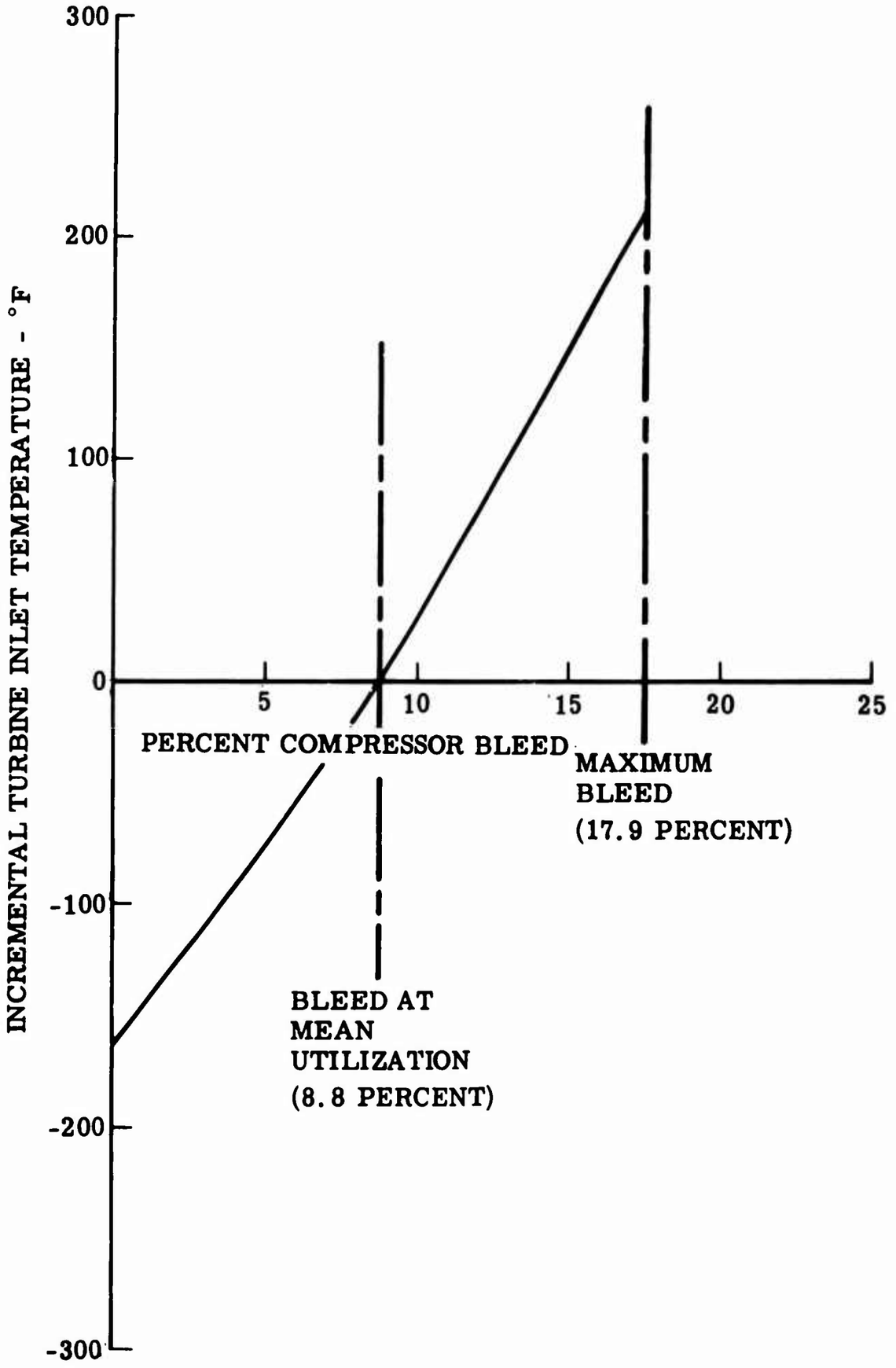

FIGURE 14 ENGINE TURBINE INLET TEMPERATURE VARIATION FOR VARIABLE BLEED SYSTEM

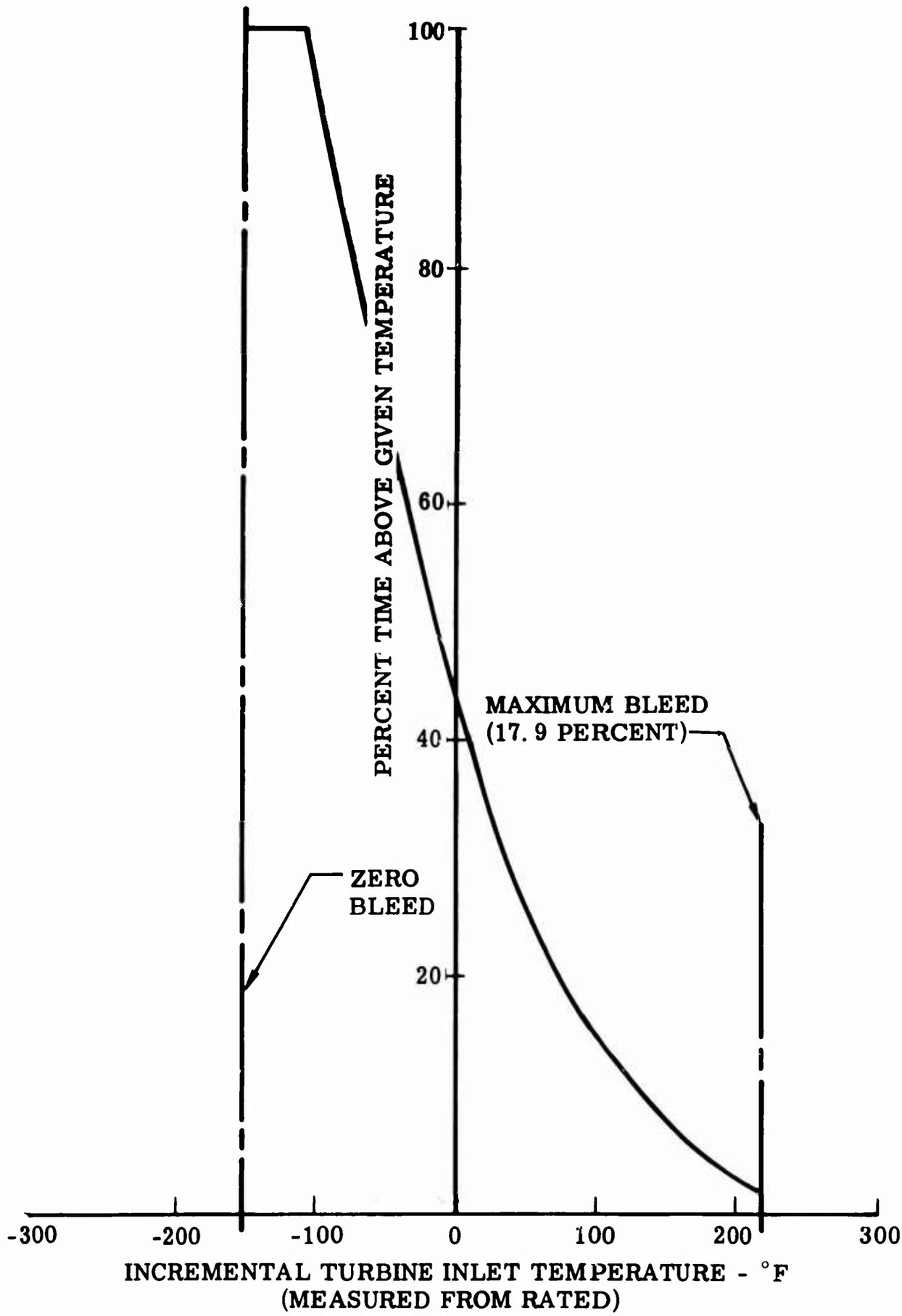

FIGURE 15 DISTRIBUTION OF ENGINE TURBINE INLET TEMPERATURE FOR VARIABLE BLEED SYSTEM

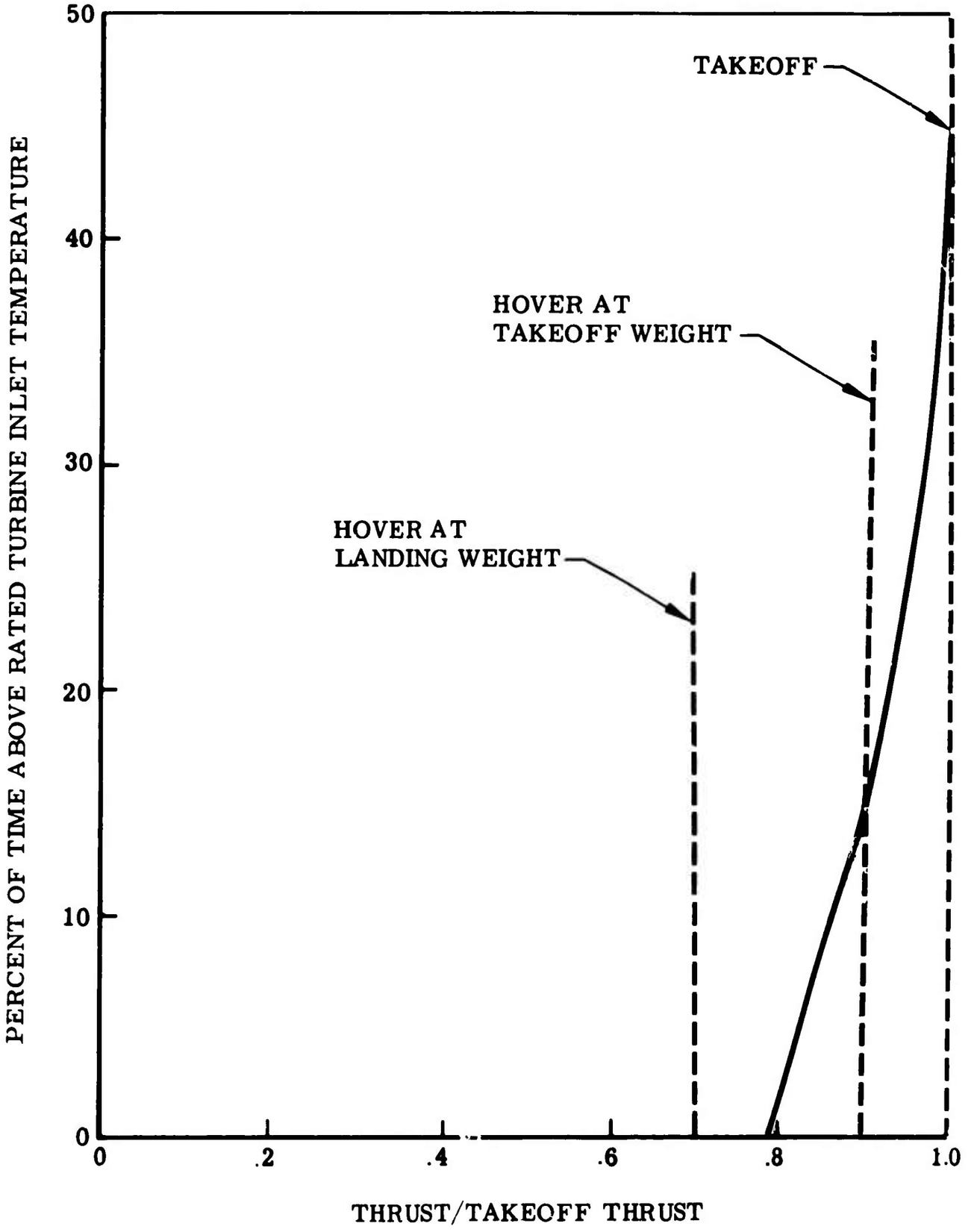

FIGURE 16. EFFECT OF THRUST LEVEL ON PERCENT TIME OVER RATED TEMPERATURE FOR VARIABLE BLEED SYSTEM

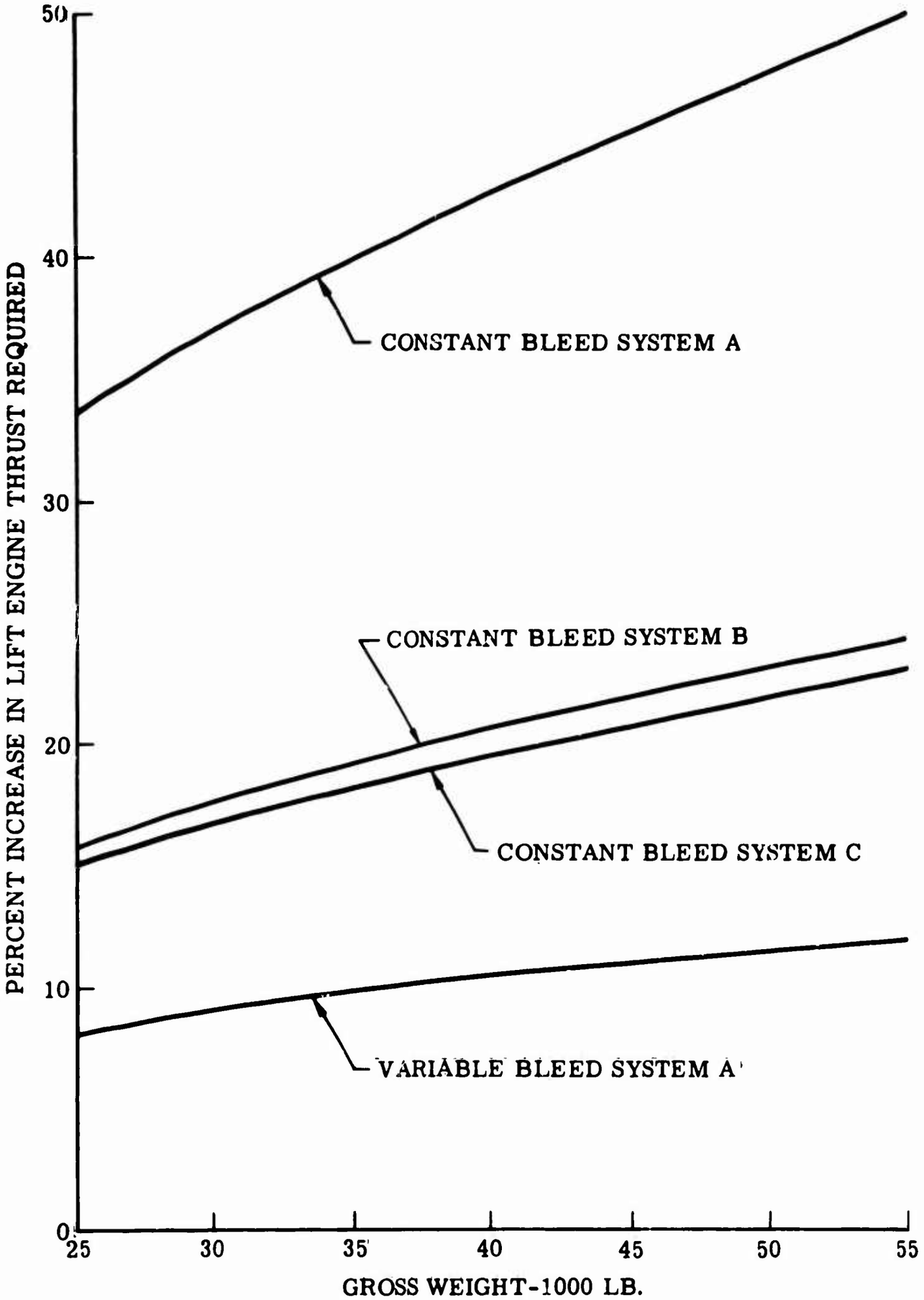

FIGURE 17. INCREASE IN LIFT ENGINE THRUST REQUIRED FOR CONTROL PROVISIONS

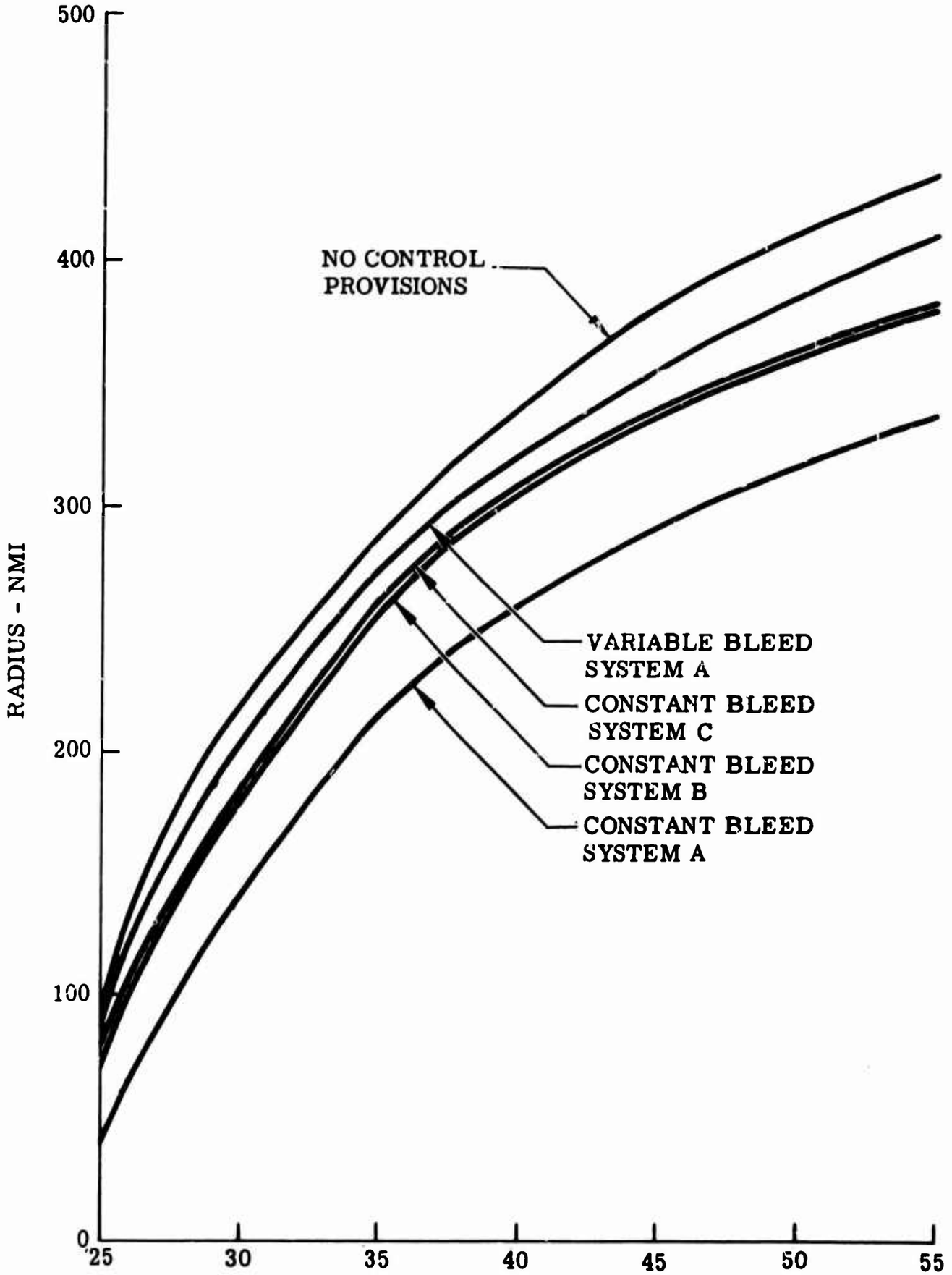

FIGURE 18. EFFECT OF REACTION CONTROL SYSTEM ON RADIUS VS. GROSS WEIGHT

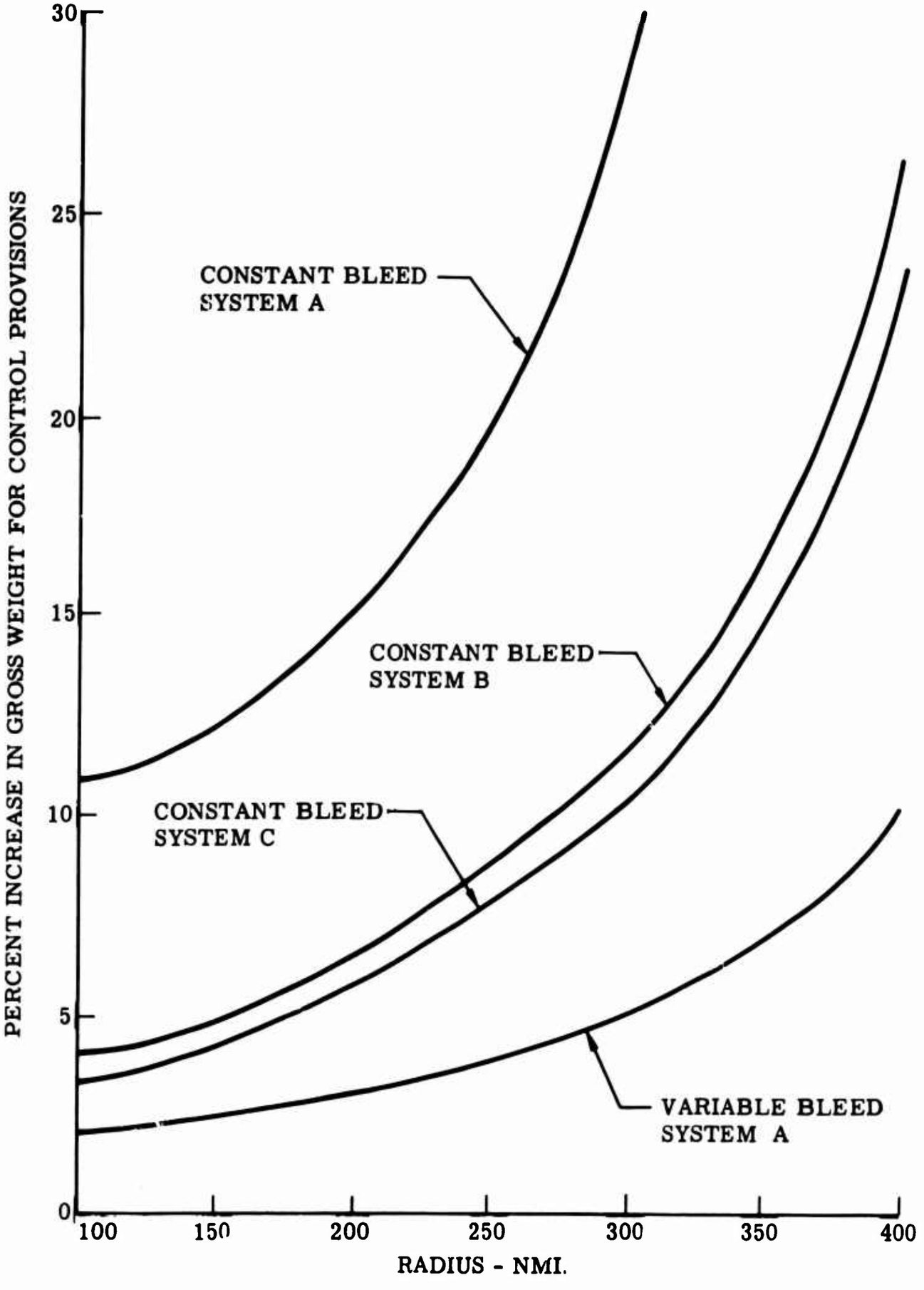

FIGURE 19. EFFECT OF REACTION CONTROL SYSTEM ON PERCENT INCREASE IN GROSS WEIGHT FOR CONTROL PROVISIONS

EFFECT OF SIZE ON VTOL AIRCRAFT HOVER AND LOW SPEED HANDLING QUALITIES

J. F. Johnson

C. F. Friend

Lockheed Aircraft Company

EFFECT OF SIZE ON VTOL AIRCRAFT HOVER AND LOW SPEED HANDLING QUALITIES

J. Ford Johnston; Chief Engineer, Research Division, Filper Corp.
Carl F. Friend; Senior Research and Development Engineer,
Lockheed-California Company

ABSTRACT

A fundamental investigation of the effect of size on VTOL aircraft hover and low speed handling qualities is presented. Both helicopter and jet VTOL are treated. Formulae for determination of size effects (with size referred to a characteristic linear dimension) on VTOL vehicle handling qualities capabilities are developed through dimensional anslyses. Hypotheses are drawn regarding effect of size on pilot-vehicle compatibility.

Some of these pertinent handling quality-capability-size relationships for similar VTOL vehicles are summarized as follows. Similar VTOL vehicles are defined as those geometrically similar configurations with constant total thrust/weight. The thrust/weight available for control of jet VTOL vehicles is also considered to be invariant with size. Although thrust/weight can be varied with size, this would effect changes in vehicle performance and weight. Aircraft having different thrust/weight may be considered as separate series with revised constants of proportionality effecting basic trends only slightly. Capability is defined as the inherent flight handling ability of the vehicle without regard to whether such capabilities are consistent with flight handling requirements.

1. Angular control power/inertia and damping/inertia decrease with increasing size.

2. Final angular velocities (except tail rotor helicopters in yaw) are invariant with size.

3. Linear accelerations and motions are nearly invariant with size.

4. Effects of external disturbances and trim changes with speed on jet VTOL are found to decrease at least as rapidly as the control power/inertia with increasing size.

5. Rotor tilt rate to external disturbances is invariant with size but angular accelerations decrease with increasing size.

6. Mission capability (the ability to perform maneuvers essential to normally assigned VTOL tasks) is not diminished appreciably by the above-stated variations with increasing size.

7. Hovering or maneuvering precision in the presence of disturbances improves with increasing size, although angular control power/inertia is decreased.

INTRODUCTION

This investigation was performed under Contract DA 44-177-AMC-236(T) sponsored by the U. S. Army Aviation Materiel Command. Assistance was provided by the VTOL Branch, Flight Mechanics and Technology Division, Langley Research Center, NASA. The authors also wish to express their appreciation to Mr. R. R. Piper (the authorized representative of U. S. Army Contracting Officer,) and his staff for their patience and guidance. The complete work by Messers. J. F. Johnston, (a Lockheed-California Company employee at the time of this work), I. H. Culver, and C. F Friend (both currently L.C.C.) is contained in USAAML Technical Report 65-24 "Study of Size Effects on VTOL Handling Qualities Criteria" (Reference 1) available through the U. S. Department of Commerce.

This paper is intended as a fundamental study aimed primarily at effect of size, but necessarily including some studies of pilot vehicle relationships. Established laws of similitude, aerodynamics, and pilot-vehicle relationships developed by other investigators are used. The approach taken is to review first the variation of inherent capabilities of VTOL vehicles, then study how these fit the pilot and the mission.

Evaluation of theoretical and experimental documentary material relative to current VTOL handling qualities criteria, References 2, 3, and 4, has shown evidence of the need for further investigation of the applicability of these criteria. A particular area of interest is the effect of vehicle size on the criteria. Provisional AGARD recommendations (Reference 3) for V/STOL aircraft in general and U. S. Military Specification MIL-H-8501A for helicopters are based on the assumption that the linear displacement of the vehicle extremity (wing tip, nose, or tail) resulting from rotational motion commanded by a unit of control input in a unit time should be constant (irrespective of vehicle size). Other authorities, References 5 and 6, contend that this assumption is not valid and suggest other criteria such as the maintenance of constant angular velocity for a unit of pilot applied control force and unit time.

Principal handling qualities requirements or recommendations of published References 2, 3, 4, and 5 are summarized in Table 1. In order to compare these criteria effectively, it is necessary to transform parameters of some of these references to parameters common to all four as is shown in Reference 1, Figures 1 through 13. Damping/inertia and control power/inertia were selected as common basic parameters because these terms are readily comprehensible. These parameters are directly related to other characteristics such as response time, angular acceleration, angular rate. Effects of control power/inertia and damping/inertia on operation and design can easily be determined.

EFFECT OF SIZE ON FLIGHT HANDLING CAPABILITY

The basic handling qualities characteristics to be considered are:

Linear acceleration, $\ddot{x}$, $\ddot{y}$, $\ddot{z}$ (equal to force/mass, F/m, feet/seconds).

Linear rate damping/mass, Fv/m, (1/seconds).

Angular acceleration, $\ddot{\theta}$, $\ddot{\phi}$, $\ddot{\psi}$, (equal to the control power/inertia, M_c/I, radians/second^2).

Angular rate damping/inertia, C/I, (1/seconds).

Angular rate time constant, I/C, (time to obtain 63 percent of the final angular rate, seconds). This is the reciprocal of the damping/inertia.

Final angular rate, M_c/C, (radians/second).

The various handling qualities criteria are stated in terms of one or more of the above characteristics. Such factors as natural frequency occurring in the pilot's frequency band or time lags in control response of the vehicle are properties of a particular design and the variation with size can also be handled by the similitude approach.

To determine the inherent variation of these two basic handling qualities characteristics with vehicle size it is first necessary to state the basic characteristic associated with size variation; that is, vehicle weight is generally proportional to the cube of a characteristic dimension as shown in Figures 17 and 18, Reference 1:

$$W \approx L^3.$$

This is a statement that the vehicle densities are relatively invariant. An associated statement is that the wing loading or disc loading tends to increase with size, Figure 22, Reference 1:

$$\frac{W}{L^2} \approx L.$$

This is the variation that satisifies the ancient square-cube law while achieving operationally feasible vehicles of large size. Vehicles of given planform family will generally follow these relations. The constant of proportionality will vary for radical changes in planform.

The vehicle inertia is $I \sim WL^2$ where L is the characteristic dimension appropriate to the axis about which the inertia is computed. Inasmuch as $W \sim L^3$, this leads to $I \sim L^5$, which is essentially in agreement with Figure 23, Reference 1.

It is recognized that vehicles can have significantly different variations of weight and moments of inertia with the major dimensions, particularly for special purpose vehicles. Other characteristics too may not closely fit assumed functions of size. In general such deviations merely change constants of proportionality and the trends will be only slightly affected.

Relations describing the effect of size on basic handling qualities capabilities are presented in Table 2. The expressions in Table 2 were derived using dimensional analysis, laws of similitude, and basic aerodynamics as given in detail in Reference 1.

EFFECT OF SIZE ON CONTROL REQUIREMENTS

The vehicle and its control systems must be capable of overcoming external disturbances acting on the vehicle and performing desired motions directed by the human pilot. The control system characteristics and vehicle motions must be compatible with the limitations of the human pilot.

EFFECT OF DISTURBANCES

The effect of size on the ability of external disturbances to produce undesirable motions and the capability of the vehicle and control system to cope with these disturbances have been analyzed in Reference 1. These disturbances include winds and gusts, ground proximity, and engine failure. Equations relating the effect of size on angular acceleration caused by a wind or gust, control displacement to cope with a wind or gust, and angular acceleration caused by an engine failure are shown in Table 2. These show that the effects of external disturbances decrease as rapidly as the control power/inertia with increasing size.

PILOT-VEHICLE COMPATBILITY

Pilot Characteristics

Inasmuch as the pilot characteristics are inherently involved in flying qualities criteria, certain basic assumptions as to the pilot characteristics should be made in considering size effect (these assumptions are not new and are frequently considered by other investigators, as reported in Reference 7):

1. The pilot is experienced in the type.

2. The pilot is an adaptive servo.

3. For motions larger than the minimum perceptible the pilot is a semilinear servo with appropriate phasing for the vehicle.

4. A requirement that the pilot augment the damping of the vehicle (by providing lead phasing, or anticipatory control) increases the learning time and the susceptibility to error.

   a. The error susceptibility increases as the time available for correction decreases: that is, as the pilot-vehicle motion frequency increases.

   b. The pilot is unable to provide damping for vehicle motion frequencies (in radians/second) in the order of $\omega \sim 1/t_p$, the inverse of the pilot perception-reaction time.

5. For motion magnitude of the order of the pilot's minimum perception the pilot's response is nonlinear.

6. For small motions the pilot adapts to find a control input which gives a vehicle motion response that is of the order of magnitude of the pilot's minimum perception level.

To which two corollaries may be added:

7. The type of control deflection giving minimal response is generally an impulsive (force-time or deflection-time integral) type of control.

8. If the minimum control pulse provides excessive response the pilot will be unable to avoid a continued oscillation.

Size Effect on Pilot-Vehicle Dynamic Stability

The above-stated pilot characteristics, in combination with the previous discussions of the control power/inertia and disturbance susceptibility variations with size, would indicate that very small VTOL vehicles might be difficult to fly. The smaller vehicles inherently have high control power relative to their inertia, and require this control power to offset external disturbances. This characteristic implies that the minimum control input available to the pilot may be excessive, leading to his over-correcting observed angular rates and being unable to reduce them to less than his perception level. This characteristic will be aggravated by friction in the control system, which tends both to increase the over-correction and to introduce lag in the control application.

The time to achieve a perceptible angular rate $\dot{\theta}_p$ due to a disturbance of control input is:

$$t = \frac{\dot{\theta}_p}{\ddot{\theta}} .$$

For the jet VTOL aircraft, $\ddot{\theta} \sim 1/L$. Therefore $t \sim \theta_p L$. The time will increase even more rapidly with size for other vehicles (as seen by the equations for acceleration in Table 2). This indicates that the time available to the pilot to perceive and react to an angular rate increment is less with small vehicle size. Thus the possibility of pilot-coupled oscillations tends to be greater in smaller vehicles.

Limitations in Providing Damping

The limitations of the pilot function in providing damping may be examined quantitatively in terms of a linear damper servo mechanism. Flight experience with these systems has shown that the allowable damper gain is limited by the occurrence of sustained oscillations at a frequency corresponding to that at which the phase lag of the damper system just exceeded 90 degrees. The criterion for stability of the system is that the gain C/I at the frequency for 90-degree system lag be less than that frequency in radians per second. This follows from the fact that at 90 + ϵ degrees lag, the "damper" acts as a spring with negative damping. The equivalent spring constant K_e is determined from $K_e = (C\dot{\theta})_{\phi=90^\circ} = (C\omega\theta)_{\phi=90^\circ}$. Therefore $K_e/I = (C\omega/I)_{\phi=90^\circ}$. But $K_e/I = \omega^2$, the square of the oscillation frequency producible by the damper gain. Therefore if $(C\omega/I)_{\phi=90^\circ} > \omega^2_{\phi=90^\circ}$, giving $(C/I)_{\phi=90^\circ} > \omega_{\phi=90^\circ}$, then the damper system gain is high enough to produce an unstable oscillation at the frequency for 90-degree system lag. The criterion for stability is then

$$(C/I)_{\phi=90^\circ} < \omega_{\phi=90^\circ}.$$

This criterion assumes that the vehicle frequency without servo is negligible relative to $\omega_{\phi=90^\circ}$. The allowable gain decreases rapidly as the vehicle basic frequency approaches the servo system 90-degree lag frequency, becoming zero when the two frequencies are equal.

In terms of the pilot, it may be assumed that, for normal control involving only small control motions, $\omega_{p_{\phi=90^\circ}} \approx 1/\tau_p \approx 4$ rad/sec. This relation implies that the pilot's contribution to damping a vehicle cannot exceed $(\Delta C/I) \approx 4$ radians/second and that this contribution must be decreased as the vehicle basic frequency approaches 4 radians/second, or if there are additional sources of phase lag in the control system. In the vehicle frequency range from 4 to about 9 radians/second, the pilot inputs can be expected to be dynamically destabilizing if the pilot assumes he must control these motions. Experience has led to recommendations such as shown in Reference 5, Figure 8 requiring high damping ratios for any vehicle modes in this frequency range.

With respect to damper gains for jet VTOL aircraft, those using thrust modulation will be limited in allowable gain by the time constant of the lift engines. This limitation applies to height and/or attitude control for all jet or fan lift VTOL craft using engine or fan speed to control left and/or attitude. A typical jet engine in the 2000-pound thrust class may have a first-order time constant of about 0.25 second. The inverse of the time constant is the circular frequency ω_e at which the lag is 45 degrees, in this case $\omega_e = 4$ rad/sec. In view of other lags in the system, it may be assumed that the frequency for 90-degree phase lag will be not greater than $\omega_{90^\circ} = 2\omega_e$, in this case about 8 rad/sec. This result would indicate a maximum vertical damping gain C_V/m somewhat less than 8 for engines in this size class. For an engine of twice the diameter (8000-pound thrust), the time constant is twice as great, indicating a maximum vertical damping gain C_V/m less than 4.

If the same thrust modulation is alsc used for attitude control, the maximum angular damping gain C/I is related to the height damping gain C_V/m by the square of the ratio of the engine distance ℓ_e from the applicable axis to the vehicle radius of gyration k about that axis.

That is, $C/I = (C_V/m)\,\Sigma\left(\frac{\ell_e}{k}\right)^2$. This relation would indicate that engines placed further out than the vehicle radius of gyration could provide a higher angular damping than linear damping, and that engines inside the vehicle radius of gyration would provide a lower damping ratio. For example, lift engines in wing tip pods could be expected to provide a reasonable value of C/I in roll, but poor C/I in pitch, since the engines are further out laterally than the roll radius of gyration, but the fore-and-aft spread of the engines is small relative to the pitch radius of gyration. It has been shown in Table 2 (as derived in Reference 1) that damping/inertia of jet VTOL aircraft is decreased with increased size.

Accuracy of Control

The question of accuracy of maneuvering is related to vehicle size in terms of both dynamic stability of the pilot-vehicle combination and of vehicle susceptibility to external disturbances. Accuracy is particularly involved in hovering/flying near obstacles, aiming or firing guns, and in IFR flight.

Aiming or firing and IFR flight are examples of maneuvers requiring angular accuracy. This accuracy is reduced by response to external disturbances and by excessive response to controls, and is increased by increased damping. On

Figure 1 - Relative Error Following a Disturbance

this basis it would appear that very small vehicles, having excessive control power (poor pilot-vehicle compatibility) and gust sensitivity would be relatively less accurate than larger vehicles having better compatibility and less gust sensitivity. In vehicles large enough for satisfactory pilot-vehicle compatibility, the effects of reducing gust sensitivity tend to increase accuracy with increasing size. On the other hand the reducing inherent damping with size tends to reduce accuracy.

In the absence of external disturbances, the maximum angular error occurs if the angular error and error rate reach their respective perception thresholds at the same time. The maximum angular error is:

$$\theta_{\epsilon_{max}} = \theta_{\epsilon_p} + K_{13} \dot{\theta}_{\epsilon_p} \tau_p$$

where

θ_{ϵ_p} is the perceived angular error

$\dot{\theta}_{\epsilon_p}$ is the perceived angular velocity.

K_{13} will have a value between 1 and about 2, depending on the magnitude of the corrective control impulse which is applied at time τ_p after the threshold error occurs. The accuracy in the a sence of disturbances then depends primarily on the perception accuracy and is independent of size, unless the size can be used to increase the perception accuracy.

In the presence of external disturbances giving displacements appreciably larger than the threshold, the angular displacement at the time τ_p at which the pilot takes corrective action is:

$$\theta_{\tau_p} = (\Delta M/I) \left[\tau_p \tau_v - \tau_v^2 (1-e^{-\tau_p/\tau_v}) \right] = (\Delta M/I) f(\tau_v)$$

where τ_v is the vehicle time constant, and $\Delta M/I$ is the step disturbance magnitude relative to the vehicle inertia; i.e., the initial angular acceleration. The total excursion is expected to be not much greater than θ_{τ_p}, inasmuch as the corrective impulse is assumed to be applied at time τ_p and to be properly sized to correct and return the vehicle. The value θ_{τ_p} is therefore reasonably proportional to the maximum excursion. The factor in brackets, $f(\tau_v)$, is plotted on Figure 1 as a function of vehicle time constant τ_v for two values of the pilot time constant τ_p. These values are τ_p = 0.25 sec, representative of normal small-deflection control, and τ_p = 0.5 sec, representative of large control deflections or of poor motion cues and visual cues by which to control. It is apparent from these plots that little reduction of the excursion magnitude is obtained from the vehicle damping if the vehicle time constant τ_v is greater than the pilot time constant τ_p.

On the other hand, large reductions in the excursion magnitude are obtainable if τ_v is made less than τ_p; that is, if the vehicle damping is made larger than that which the pilot can supply. It is of interest that conventional aircraft have time constants less than that of the pilot and generally require no auxiliary damping, whereas VTOL vehicles (except the rigid rotor helicopter with stabilizing gyro) have time constants greater than that of the pilot and benefit from additional damping.

The effects of size on the angular accuracy in the presence of gust disturbances may be evaluated from the variations of $\Delta M/I$ and of $f(\tau_v)$ with size. The initial acceleration $\Delta M/I$ has been shown to decrease with increasing size as a function between first and second power. The vehicle time constant has been shown to increase with the first power of size. A reasonable curve fit indicates that $f(\tau_v) \sim K_{\tau_v}^{0.1}$ from $\tau_v = 0.25$ to $\tau_v = 1.0$. Therefore,

$$\theta_{max} \sim \theta_{\tau_p} \sim \frac{\Delta M}{I} f(\tau_v)$$

$$\frac{\Delta M}{I} \sim \frac{1}{K_{14}L + K_{15}L^2} \quad \text{where } K_{14},\ K_{15} \text{ depend on configuration,}$$

$$f(\tau_v) \sim \tau_v^{.1} \sim L^{.1},$$

then

$$\theta_{max} \sim \frac{L^{.1}}{K_{14}L + K_{15}L^2} \sim \frac{1}{K_{14}L^{.9} + K_{15}L^{1.9}} .$$

Therefore, it is concluded that the maximum angular error due to a disturbance decreases with size, and is not significantly reduced by augmenting the vehicle damping unless the augmented damping is greater than that which the pilot can supply. Exceptions to this statement follow:

1. In the case of very large disturbances such as those caused by failure of an offset lift engine, there is an additional pilot lag associated with the pilot's adaptive mechanism: he must adapt suddenly from use of small control inputs to much larger inputs, and this creates an appreciable additional lag which may be called the adaptive lag. The total pilot lag in applying sufficient control in such cases may vary from 0.5 sec to 1.0 sec. In this case augmented damping will be of great benefit in reducing the vehicle response.

2. In normal operation, vehicle damping of the same order as or greater than that otherwise supplied by the pilot relieves the pilot work load, permitting more attention to mission and reducing susceptibility to error due to fatigue.

IFR Control

The outstanding characteristic of flight by reference to instruments is the lack of the instantaneous attitude and position information which is available by direct or peripheral vision under visual flight conditions (as noted by the authors and other observers). The use of his peripheral vision under VFR conditions allows the pilot to maintain quick reactions for flight control while conducting other tasks. The VFR reaction time is necessarily slowed under IFR conditions by the fact that

1. A minimum of two instruments - artificial horizon and direction gyro - is usually required for attitude control, and a third, the turn/bank, is also scanned. Time is lost in shifting and focusing on each instrument in turn.

2. Some percentage of the time is unavailable for attitude and position control while scanning engine condition instruments, etc.

3. In the VTOL mode, three-axis linear position information and control assume equal importance with attitude information and control. If past practice were followed, at least two instruments would be added for this purpose, making it necessary to scan at least four essential instruments to control the aircraft. Assuming that 80 percent of the time is devoted to the four essential instruments, each instrument would get 20-percent attention. This fact indicates that the pilot's perception-reaction time may be increased nearly fivefold relative to VFR by the mode of information presentation.

From previous discussions, large increases in pilot reaction time indicate corresponding decreases in his ability to provide vehicle damping and increases in the vehicle attitude errors due to external disturbances. In the VTOL mode, the corresponding linear position and velocity errors would be unacceptable. This decrement in capability can be compensated for by vehicle damping, which in the VTOL mode may need to include linear damping in height and horizontal translation as well as angular damping in pitch and roll.

An interesting alternative suggested by other investigators (such as those given in Reference 8) is the possibility of providing all attitude and position information in one presentation. This may be a head-up presentation involving projection of a simulated ground with landing target, or an instrument presentation on one dial requiring no eye shifting. The pilot IFR reaction times may be shortened to the order of VFR times, and accuracy could conceivably be increased. Thus it appears that completely blind takeoffs and landings would be practicable with the proper form of data presentation to the pilot. Emphasis should be given toward development to this end.

The effect of size in IFR operation is most apparent in the response to external disturbances. In conventional aircraft, pilots report that large transport aircraft are easier to fly IFR than light planes because of their slower response to disturbances. This slow response makes long pilot reaction times more acceptable, and is presumably one of the reasons why good data presentation for the pilot has not been adopted. More importantly, however, conventional aircraft have not required fast reactions for damping about any axis, or for control about any axis other than roll.

Hovering

The task of hovering normally involves small control motions wherein maximum control power is not involved unless the vehicle is highly susceptible to external disturbances or has attitude instability in ground effect. If maximum control power requirements are determined from vehicle flight tests in hover and low-speed maneuvers, care should be taken in attempting to apply these requirements to vehicles of other sizes in view of the rapid variation of vehicle susceptibility to trim changes, external disturbances, and attitude instability with vehicle size.

Control power requirements in the absence of two of these effects (gusts and ground effect instability) can be investigated by use of variable-stability aircraft which can be adjusted to cancel vehicle angular accelerations, due to any causes other than pilot inputs. If adequate airspeed sensors are available, trim changes due to speed can also be canceled.

More important to the experimental investigation of the effects of size on handling qualities criteria, however, is the fact that such a variable-stability VTOL research vehicle can be adjusted to represent the acceleration response to disturbances and the trim changes with speed of any size vehicle from very small to very large. Control power and damping criteria appropriate to these characteristics can then be determined.

It is recommended that such experimental investigations of the effects of size on handling qualities criteria be conducted before definitive criteria are adopted. The NASA Ames X-14A VTOL research vehicle and th NASA Langley variable-stability helicopter are adaptable to this research. With each change in simulated vehicle size, sufficient flight time should be allowed for the pilot to adapt to the "feel" of the vehicle before quantitative evaluation is undertaken.

Pilot Acceleration Effects

It has been shown that the vehicle angular accelerations due to control inputs decrease linearly with increasing vehicle size,

$$\ddot{\theta} \sim 1/L.$$

Since the pilot distance from the vehicle center of gravity is proportional to size (Figure 19, Reference 1), his linear acceleration due to an angular control input,

$$\ddot{z}_p \sim \ddot{\theta} L = \text{constant},$$

is independent of size. This initial linear acceleration of the pilot will not be properly simulated in a fixed-size research vehicle simulation of size effects, nor will pilot linear accelerations due to external disturbances. The ratio between linear accelerations due to control inputs and those due to external angular disturbances will, however, be preserved.

Effect of size on the centrifugal acceleration applied to the pilot by vehicle rotation velocity is derived as follows. It has been shown that the angular velocity is:

Jet VTOL aircraft

$$\dot{\theta}, \dot{\phi}, \dot{\psi} = \text{constant}$$

Helicopters

$$\dot{\theta}, \dot{\phi} = \text{constant}$$

$$\dot{\psi} \sim 1/L.$$

Then using the relation that pilot's distance to the vehicle center of gravity is proportional to characteristic length, his centrifugal acceleration due to angular rate is:

Jet VTOL aircraft

$$\ddot{x} \sim \dot{\theta}^2 L \sim L$$

$$\ddot{x} \sim \dot{\psi}^2 L \sim L$$

$$\ddot{z} \sim \dot{\phi}^2 L \sim L.$$

Helicopters

$$\ddot{x} \sim \dot{\theta}^2 L \sim L$$

$$\ddot{x} \sim \dot{\psi}^2 L \sim 1/L$$

$$\ddot{z} \sim \dot{\phi}^2 L \sim L.$$

Optical Effects

The large VTOL vehicle hovers with the pilot higher off the ground than does the small vehicle. The pilot's accuracy in perceiving position and velocity is diminished in proportion to his height, but remains in proportion to the vehicle size. Inasmuch as he will tend to maintain his clearance of any near obstacles in proportion to vehicle size, his relative accuracy is independent of size. A noticeable effect of larger size, however, is that greater time is used in acquiring a perceptible velocity or position error following a given attitude change. This lengthening of the time scale with increasing size eases the pilot task in hovering, just as has been observed for the size effect in IFR flight.

It should be noted that optical effects associated with size occur only in relatively close proximity to ground or obstacles. At distances beyond about twice the vehicle characteristic dimension, judgement of distance and speed is based on binocular vision, apparent size of familiar objects, perspective effects, etc.

MISSION-ORIENTED CONTROL REQUIREMENTS

The most obvious limitations of increased size are associated with flight near obstacles. The large vehicle cannot land in all the same clearings available to the smaller vehicle, nor can it fly in all the same channels. For a given twisting channel that both can fly through, the larger vehicle must fly slower because its turns are necessarily sharper than those of the smaller vehicle. The larger vehicle must also fly slower in contact flight with severely restricted visibility, inasmuch as the vehicle extends to a larger percentage of the visible field.

The jet VTOL, because of its limited hover time, has no mission at low speeds other than to take off and accelerate to flight speed, then to convert to hover and land at the end of its flight. Typical maneuvers associated with these

tasks are discussed in References 9 and 10. The associated control power requirements are relatively low. Because of its higher wing loading, the large vehicle covers a greater speed range from the stall speed to hover,

$$\Delta q \sim \frac{W}{S} \sim L$$

$$\therefore \Delta V \sim \sqrt{L}.$$

where S is the wing area.

Since linear deceleration or acceleration is invariant with size, the time to accelerate or decelerate, is

$$\Delta t \sim \Delta V \sim \sqrt{L}.$$

The deceleration time (and distance) increase with size. The trim changes are proportional to

$$\Delta M \sim C_m qSc \sim LL^2L \sim L^4$$

and

$$\frac{\Delta M}{I} \sim \frac{L^4}{L^5} \sim \frac{1}{L}.$$

The control power/inertia required to trim center of gravity changes to allow for expendable load items such as fuel and military items, and to give some flexibility in loading the aircraft (based on center of gravity limits as a constant percentage of characteristic length as is normal practice) is:

$$\frac{\Delta M}{I} \sim \frac{WL}{WL^2} \sim \frac{1}{L}.$$

These relations show that the control power/inertia required to balance trim changes decreases with increasing size and (in the case of speed changes) that the time available to compensate for these reduced trim changes is greater. These variations are in balance with the variation of capability with size.

RECOMMENDATIONS

This brief fundamental study has indicated a number of areas for further research and a methodology for guiding and interpreting such research. It is recommended that:

1. The primary effects of size (control power/inertia, damping/inertia, and response to external disturbances) be simulated on existing variable-stability jet and helicopter VTOL aircraft

by methods indicated herein for experimental determination of desirable and minimum handling qualities criteria as a function of vehicle size. Although some experimental data have been obtained showing the effects of external disturbances (especially aerodynamic moment derivatives/inertia), much more is required to properly define criteria for regulations covering a broad spectrum of aircraft. Particularly, information is lacking on the effect of aerodynamic moments with respect to vertical velocity/inertia and the effect of higher wind and gust velocities (higher than 25 knots). In addition, the effect of physical size in such terms as distance to visible extremities, pilot distance to center of gravity, etc., should be investigated.

2. Applications and extensions of the method of examining the pilot function as an adaptive servo limited by his (variable) time lag should be further developed by investigators in the various fields to which it may be applicable. These include vehicle handling quality criteria (regulations), including effect of size, data presentation, IFR flight, learning time, error susceptibility, etc.

   a. Research should be conducted on the magnitude and variation of the pilot time constant and adaptive lag under a wide variety of simulated flight conditions and vehicle characteristics, including size effects.

   b. Adequacy of data presentation should be evaluated by its effectiveness in reducing pilot time constant and adaptive lag under multiaxis control conditions.

   c. An integrated IFR data presentation should be developed to permit blind takeoffs and landings of VTOL aircraft.

BIBLIOGRAPHY

1. Culver, I. H., Johnston, J. F., and Friend, C. F., Study of Size Effects on VTOL Handling Qualities Criteria USAAML Technical Report 65-24, U.S. Army Aviation Materiel Laboratories, Fort Eustis, Virginia (Available thru U.S. Dept. of Commerce).

2. Helicopter Handling Qualities, General Military Specification, MIL-H-8501A, Republican Press, Hamilton, Ohio, November 1952.

3. Recommendations for V/STOL Handling Qualities, AGARD Report 408 Advisory Group for Aeronautical Research and Development, Paris, France, October 1962.

4. Rolls, L. S., and Drinkwater III, F. J., A Flight Determination of the Attitude Control Power and Damping Requirements for a Visual Hovering Task in the Variable Stability and Control X-14A Research Vehicle, NASA TN D-1328, National Aeronautics and Space Administration, Washington, D.C., May 1962.

5. Curry, Maj. P. R., and Matthews, Jr., J. T., Advanced Rotary Wing Handling Qualities, Proceedings of the Twentieth Annual National Forum, American Helicopter Society, Inc., Washington, D.C., May 13, 1964, pp. 20-27.

6. Lynn, R. R., New Control Criteria for VTOL Aircraft, Aerospace Engineering, Volume 21, August 1962, pp. 31-40.

7. McRuer, T., and Krendel, A., Dynamic Response of Human Operators, WADC Technical Report 56-524, Wright Air Development Center, Wright-Patterson AFB, Ohio October 1957.

8. Kelly, Jr., F. X., A New Technique for Steep Angle Approach Guidance, Proceedings of Twentieth Annual National Forum, American Helicopter Society, Inc., Washington, D.C., May 13, 1964, pp. 117-126.

9. Edenborough, K., and Wernicke, K., Theory and Flight Research on Control and Maneuverability Requirements for Nap-of-the-Earth Helicopter Operation, Proceedings of Twentieth Annual National Forum, American Helicopter Society, Inc., Washington, D.C., May 13, 1964, pp. 193-206.

10. Friend, C. F., A Fundamental Study of Reaction Control Criteria for Jet VTOL Aircraft, American Institute of Aeronautics and Astronautics, AIAA Paper No. 64-787, New York, New York, Sept. 1964.

TABLE I

PRINCIPAL HANDLING QUALITIES CRITERIA FOR VTOL VEHICLES (1)

AXIS	Source	MIL-H-8501A, Ref. 2 (2)		AGARD 408, Ref. 3 (5)		TM D-1328, Ref. 4 (7)		
	Condition	Control	Damping	Control	Damping	Control	Damping (8)	
LONGITUDINAL	IFR	$\theta_1 \geq \frac{5.10}{(W+1000)^{1/3}}$	$C \geq 15I_y$	$\phi_1 \leq \frac{5.24}{(W+1000)^{1/3}}$ $\dot{\phi} \geq 0.2$	$C \geq 15I_y$	(6)	(6)	$\dot{\theta}_D =$ 0.175
	VFR	$\theta_1 \geq \frac{3.14}{(W+1000)^{1/3}}$	$C \geq 8I_y$	(6)	(6)	$M_q/I \geq .6$ $M_q/I \leq 2.2$ (9)	$C/I = 0.5$ (9)	
	EMERGENCY (3)	(6)	(6)	$\theta_1 \geq \frac{3.14}{(W+1000)^{1/3}}$	$C \geq 8I_y$	(6)	(6)	
LATERAL	IFR	$\phi_1 \geq \frac{1.67}{(W+1000)^{1/3}}$ $\dot{\phi} \leq 0.349$, $\delta_a = 1$	$C \geq 85I_x$	$\phi_1 \geq \frac{5.24}{(W+1000)^{1/3}}$ $\phi_1 \geq 0.175$ $\phi_1 \leq 0.349$, $\delta_a = 1$	$C \geq 85I_x$	(6)	(6)	$\dot{\phi}_D =$ 0.367
	VFR	$\phi_1 \geq \frac{1.41}{(W+1000)^{1/3}}$ $\dot{\phi} \leq 0.349$, $\delta_a = 1$	$C \geq 18I_x$	(6)	(6)	$M_p/I \geq 1.8$ $M_p/I \leq 4.0$ (9)	$C/I = 2.0$ (9)	
	EMERGENCY (3)	(6)	(6)	$\phi_1 \geq \frac{5.24}{(W+1000)^{1/3}}$ $\phi_1 \geq 0.175$ $\phi_1 \leq 0.349$, $\delta_a = 1$	$C \geq 18I_x$	$M_p/I \geq 0.7$ $M_p/I \leq (6)$ (10)	$C/I = 2.0$ (10)	
DIRECTIONAL	IFR	$\psi_1 \geq \frac{5.76}{(W+1000)^{1/3}}$ (4) $\psi_1 \geq 0.873$, $\delta_r = 1$	$C \geq 27I_z$	$\psi_1 = \frac{3.14}{(W+1000)^{1/3}}$	$C \geq 27I_z$	(6)	(6)	$\dot{\psi}_D =$ 1.046
	VFR	$\psi_1 \geq \frac{5.76}{(W+1000)^{1/3}}$ (4) $\psi_1 \geq 0.873$, $\delta_r = 1$	$C \geq 27I_z$	(6)		$M_r/I \geq 0.7$ $M_r/I \leq (6)$ (9)	$C/I = 0.7$ (9)	
	EMERGENCY (3)	(6)	(6)	$\psi_1 = \frac{3.14}{(W+1000)^{1/3}}$	$C \geq 14I_z$	$M_r/I \geq 0.25$ $M_r/I \leq (6)$ (10)	$C/I = 0.7$ (10)	

R VTOL VEHICLES (1)

	NASA TN D-1328, Ref. 4 (7)		Curry & Matt., Ref. 5 (11)	
	Control	Damping (8)	Control	Damping
	(6)	(6)	$\dot{\theta}_D = 0.349$ (5) $0.175 \leq \dot{\theta} \leq 0.699$	$\tau_D = 0.5$ (5) $0.1 \leq \tau \leq 1.0$
	.6 (9) 2.2	C/I = 0.5 (9)	(6)	(6)
	(6)	(6)	(6)	(6)
	(6)	(6)	$\dot{\phi}_D = 0.611$ $0.367 \leq \dot{\phi} \leq 0.916$	$\tau_D = 0.4$ $0.1 \leq \tau \leq 1.0$
	1.8 (9) 4.0	C/I = 2.0 (9)	(6)	(6)
	0.7 (10) (6)	C/I = 2.0 (10)	(6)	(6)
	(6)	(6)	$\dot{\psi}_D = 1.570$ (2) $1.046 \leq \dot{\psi} \leq 2.617$	$\tau_D = 0.5$ (2) $0.1 \leq \tau \leq 1.5$
	0.7 (9) (6)	C/I = 0.7 (9)	(6)	(6)
	0.25 (10) (6)	C/I = 0.7 (10)	(6)	(6)

NOTES

(1) Expressions define the control power and damping required to produce vehicle motion with full control (obviously control power required for equilibrium trim is additional to these criteria), unless noted.

(2) For hover.

(3) For safe operation including landing.

(4) $\phi_1 = 192/(W + 1000)^{1/3}$ starting at $\dot{x} = \dot{y} = \dot{\psi} = 0$ with 35 KN critical wind.

(5) $0 \leq \dot{x} \leq$ Conversion.

(6) Unspecified.

(7) -30 KN $\leq \dot{x} \leq 30$ KN and 20 KN $\leq \dot{y} \leq 20$ KN.

(8) C/I for M_c/I = MINIMUM.

(9) Cooper Pilot Rating = 3.5.

(10) Cooper Pilot Rating = 6.5.

(11) Helicopter $0 \leq \dot{x} \leq$ Conversion, Modified CPR = 3.5.

(12) All expressions were taken directly from the sources listed except angles are expressed in radians to provide consistency.

SYMBOLS

C	Damping	1/se
M_c	Control Moment	ft l
I_x, I_y, I_z	Moment of Inertia x, y, z axes respectively	ft l
θ_1	Pitch displacement in one second	rad
$\dot{\theta}$	Pitch velocity	rad/
$\dot{\theta}_D$	Desired pitch velocity	
$\phi_{\frac{1}{2}}$	Roll displacement in one half second	rad
ϕ_1	Roll displacement in one second	rad
$\dot{\phi}$	Roll velocity	rad/
ψ_1	Yaw displacement in one second	rad
τ_D	Desired response time	
δ_a	Lateral stick displacement	inch
δ_r	Rudder control displacement	inch

B

TABLE 2

EFFECT OF SIZE ON VEHICLE BASIC HANDLING CHARACTERISTICS

VEHICLE		JET VTOL				
CHARACTERISTICS \ Axis		Vertical (Yaw)	Longitudinal and Lateral (Pitch and Roll)		Vertical (Yaw)	
			Jets Located Proportional to Jet Diameter	Jets Located Proportional to Vehicle Size		Articul Rotor
CAPABILITIES						
CONTROL POWER / MASS	Ft/Sec^2	Constant	Constant	Constant	$1/(K_1 + L^{\frac{1}{2}})$ (4)	$1/(K_1 + L^{\frac{1}{2}})$
					Constant (5)	Const
DAMPING / MASS	1/Sec	$K + 1/L$	$K + 1/L$	Constant (8)	$1/(K_2 + L^{\frac{1}{2}})$ (4)	$K_3 + K_4 L^{\frac{1}{2}} + K_5 L$
} LINEAR MOTIONS		Constant(8)	Constant (8)	$K + 1/L$		
					Constant (5)	$K_3 + K_4 + K_5 + L^{\frac{1}{2}}$
RESPONSE TIME	Sec	$1/(K + 1/L)$	Constant (8)	Constant (8)	$K_1 + L^{\frac{1}{2}}$ (4)	$1/(K_3 + K_4 L^{\frac{1}{2}} + K_5$
		Constant(8)	$1/(K + 1/L)$	$1/(K + 1/L)$		
					Constant (5)	$1/(K_3 + K_4 + K_5$
ANGULAR CONTROL POWER / INERTIA	Rad/Sec^2	$1/L$	$1/L$	$1/L$	$1/(K_6 L + L^{3/2})$ (4)	$1/L + K_9/L^2$
					$1/L$ (5)	
ANGULAR DAMPING / INERTIA	1/Sec	$1/L$	$1/L$	$1/L$	$1/(K_6 + L^{\frac{1}{2}})$ (4)	$1/L + K_9/L^2$
					Constant (5)	
ANGULAR RESPONSE TIME	Sec	L	L	L	$K_6 + L^{\frac{1}{2}}$ (4)	$L^2/(K_8 + L)$
					Constant (5)	
ANGULAR VELOCITY	Rad/Sec	Constant	Constant	Constant	$1/L$	Const
DISTURBANCE EFFECTS						
ANGULAR ACCELERATION CAUSED BY A WIND OR GUST	Rad/Sec^2 / Ft/Sec	$1/L^2$	$K_9/L^2 + K_{11}/L^{\frac{1}{2}}$	$K_9/L^2 + K_{10}/L$	$1/(K_6 L + L^{3/2})$ (4)	$1/L + K_9/L^2$
					$1/L$ (5)	
CONTROL DISPLACEMENT TO COUNTER A WIND OR GUST	Rad	-	-	-	Constant	Const
ACCELERATION CAUSED BY ENGINE FAILURE	Rad/Sec^2	-	$1/L^{\frac{1}{2}}$	$1/L$	-	-

ING CHARACTERISTICS					
HELICOPTERS					
	Vertical (Yaw)		Longitudinal and Lateral (Pitch and Roll)		
			Articulated Rotor		Rigid Rotor
	$+ L^{\frac{1}{2}})$	(4)	$1/(K_1 + L^{\frac{1}{2}})$	(4)	$1/(K_1 + L^{\frac{1}{2}})$ (4)
	nt	(5)	Constant	(5)	Constant (5)
	$+ L^{\frac{1}{2}})$	(4)	$K_3 + K_4 L^{\frac{1}{2}} + K_5 L + L^2$	(4)	$K_3 + K_4 L^{\frac{1}{2}} + K_5 L + L^2$ (4)
	nt	(5)	$K_3 + K_4 + K_5 + L^2$	(5)	$K_3 + K_4 + K_5 + L^2$ (5)
	$^{\frac{1}{2}}$	(4)	$1/(K_3 + K_4 L^{\frac{1}{2}} + K_5 L + L^2)$	(4)	$1/(K_3 + K_4 L^{\frac{1}{2}} + K_5 L + L^2)$ (4)
	nt	(5)	$1/(K_3 + K_4 + K_5 + L^2)$	(5)	$1/(K_3 + K_4 + K_5 + L^2)$ (5)
	$+ L^{3/2})$	(4)	$1/L + K_6/L^2$	(7)	$1/L + K_6/L^2$ (7)
		(5)			
	$+ L^{\frac{1}{2}})$	(4)	$1/L + K_6/L^2$	(7)	$1/L + K_6/L^2$ (7)
	nt	(5)			
	$^{\frac{1}{2}}$	(4)	$L^2/(K_8 + L)$	(7)	$L^2/(K_8 + L)$ (7)
	nt	(5)			
	1/L		Constant		Constant
	$+ L^{3/2})$	(4)	$1/L + K_6/L^2$	(6)	$1/L + K_6/L^2$ (6)
	1/L	(5)			
	ant		Constant		Constant
	•		•		•

(1) For translational motions.
(2) L is the characteristic length.
(3) Independent of rotor disk loading unless otherwise noted.
(4) Rotor disk loading proportional to size.
(5) Rotor disk loading constant.
(6) Rotor precession velocity invariant.
(7) K_6 proportional to equivalent hinge offset.
(8) For hovering
(9) K, K_1, K_2 ETC. ARE CONSTANTS

B

V/STOL SUBSYSTEM DESIGN

Larry Hewin, USA

Technical Session Chairman

BLANK PAGE

V/STOL VISUAL FLIGHT SIMULATION TECHNIQUES

R. J. Heintzman

USAF

ABSTRACT

V/STOL VISUAL FLIGHT SIMULATION TECHNIQUES

A continuing demand exists within industry and Government for devices which will simulate an aircraft system. Such equipment is utilized for evaluation of system design, checking vehicle response, evaluating flight controls and instrument lay-out, and training flight personnel in the operation of the aircraft. Technical developments in the visual area have not kept up with the other areas that constitute a complete flight simulator. Past achievements in visual flight simulation have been largely centered around the takeoff and landing phase of conventional flight. Simulation of the V/STOL flight envelope will require many advancements, since the V/STOL visual device must have wide-angle out-the-window viewing, good low altitude image detail, and excellent response to the dynamics of the simulated vehicle. Several recent visual simulation developments are described which offer possibilities for achieving these requirements. Virtual image type displays utilize mirrors or lens to focus the image at infinity. Transparency image storage techniques provide greater visual area coverage and flexibility. Developments in optical probes or pickups offer new possibilities for the model type system of image generation. Continuing developments in television promise camera and display techniques offering better contrasts, less noise and greater bandwidth for better resolution and transmission of picture information.

V/STOL VISUAL FLIGHT SIMULATION TECHNIQUES

INTRODUCTION

A continuing demand exists within Industry and Government for devices which will simulate an aircraft system. Such equipment is utilized for evaluation of system design by simulating flight based upon theoretical and wind tunnel data, for evaluation of flight control and flight instrument layout and design, and for training aircrew personnel in operation of the aircraft system.

With the advent of the Vertical and Short Field Takeoff and Landing (V/STOL) Aircraft, new demands on simulation technology become apparent. The purpose of this paper is to analyze visual simulation requirements for V/STOL and discuss devices that may fulfill the simulation requirements for the V/STOL Aircraft System. However, before we discuss V/STOL visual simulation, we will first review flight simulation in general, and analyze the various components which make up a visual simulation device. Also, we will attempt to point out some of the pitfalls which have been experienced in visual simulation. The material presented herein will be oriented more toward simulation for training. However, techniques and hardware are adaptable to the other mentioned applications.

A flight simulation system may be divided into several interrelated subsystems.

1. Flight, which would include the cockpit with controls and instrumentation.

2. Motion, which would support the cockpit and provide motion cues to the crew.

3. Visual, which would provide the pilot with a dynamic representation of the outside world as viewed out the simulated cockpit.

4. Tactics, which applied to the military aircraft system, would include tactical radar, ECM, and fire control systems.

Figure One shows the relationship of the various areas of the system including the man-machine loop. The computer is the nerve center of the simulator. However, all data flow originates and terminates with the aircrew. The pilot may make a decision to change the attitude or position of the aircraft. He exercises this decision through the aircraft controls. The computer calculates the change in aircraft position and attitude, and feeds information to the simulated controls and instruments, motion system and visual image generator. The pilot then reads

out the information from the flight instruments or the displayed image, or both.

SIMULATING THE AIRCRAFT

Simulation of flight dates back to the original Link Instrument Trainers of some thirty years ago. The driving equipment of these devices would more nearly represent the player piano than present day flight simulation equipment. The early Link Trainers were used only for training and were limited to practicing instrument crosscheck and flight procedures. The beginning of today's flight simulators started some years later when Dr. Richard Dehmel invented the first electronic instrument trainer.

The first United States Air Force Aircraft Flight Simulator was the B-50. This simulator was designed and built by Curtiss-Wright Corporation in 1949. It was an analog system and the design was based upon the work done by Dr. Dehmel.

The U. S. Air Force first evaluated digital flight simulation techniques with the UDOFT (Universal Digital Operational Flight Trainer) Program. UDOFT was a joint U. S. Navy - U. S. Air Force program for studying the feasibility of digital flight simulation. This device was capable of being programmed to simulate different aircraft systems. The results of this program were very successful and formed a basis for the development of Digital Flight Simulators. Digital flight simulation did not come into U. S. Air Force use until the C-135A (Boeing 707) Flight Simulator in 1962.

SIMULATING THE WORLD OUTSIDE

One task which early flight simulation devices could not simulate was low visibility approach, landing, and takeoff. Since this was a very critical part of aircraft flight, it was not long before it became apparent that the flight simulator should portray a non-programmed dynamic visual display of the breakout and transition to VFR in order to simulate the low visibility approach.

The first attempt at visual flight simulation by the U. S. Air Force was performed under contract to the Rheem Company in 1954. The goal of this program was to design and develop an all-optical, full-color visual simulation device which could be used as an attachment to flight simulators. The design concept pursued used mirrors and lenses to relay an image from a three-dimensional model to a spherical screen in front of the cockpit. (Figure Two) Three models, each with a different scale, were to simulate the airfield complex.

The direct optical approach was chosen because of the resolution limitations of closed circuit television. However, during the design phase, it became apparent that this type of system was extremely inefficient and, at best, would provide only a very dim image.

Two visual simulation devices developed almost simultaneously, utilized closed circuit television.

A device designed by Dalto Electronics Corporation was aimed strictly toward simulating a low visibility night approach. (Figure Three) The image was generated by viewing, with a television camera, an airfield lighting pattern laid out on a moving belt. Display to the pilot was accomplished by a TV monitor or a television projector and screen. Pitch, roll, altitude, and lateral displacement were simulated by motion of the television camera. Longitudinal velocity was a function of belt motion. The operational range of this device was very limited.

The Curtiss-Wright visual system was developed with greater operating parameters than the Dalto. (Figure Four) This device, dubbed the "Visulator" by Curtiss-Wright, and a name to which visual devices are sometimes referred today, utilized a vertical, rigid model. Design of this device was based upon picking up the image from the model with a small optical pickup probe, relaying the image optically to a television camera, and displaying the image in front of the simulator windscreen by a television projector and screen. Image dynamics were provided by movement of elements of the optical pickup and motion of the television camera relative to the fixed model.

Two devices, developed subsequent to the Dalto belt device and the Curtiss-Wright "Visulator", were the U. S. Air Force SMK-22/F37A-T, and the SMK-23/F37A-T Visual Simulator Trainer Attachments. Fairchild Stratos Company developed the SMK-22, a night visual simulation device, for the U. S. Air Force. The SMK-22 was similar to the Dalto device in that the image was generated by a moving belt and TV camera. (Figure Five)

The SMK-23 was designed and fabricated by Link Group, General Precision, Incorporated. It was similar to the Curtiss-Wright "Visulator" except that it utilized a vertical moving belt model rather than a fixed vertical model. (Figure Six) This device was the first visual simulation device to include closed circuit color television.

A more recently developed visual system utilizes a flat transparency scanned by a flying spot scanner to generate the image. (Figure Seven) The flying spot scanner scans the transparency in the form of a television raster. The information is read out with photo-multipliers. Perspective, pitch, and altitude information are generated by shaping of the raster. A device of this type developed by Dalto Electronics Corporation

for the U. S. Air Force, designated the SMK-43 Visual Attachment, provides full color, both daylight and night visual simulation. (Figure Eight) The transparency for this device is eight inches in diameter and is scaled at 50,000:1. The visual envelope* is approximately five miles in diameter and may be changed by changing transparencies. The image is viewed by the pilot at infinity through a large acrylic plastic lens.

All the visual simulation devices just discussed, suffered limitations or deficiencies. First, image quality was marginal because of poor resolution and picture noise. Second, the operating parameters were considered too limited in viewing angle, area of the visual envelope, and on ground picture fidelity. Last, the visual system tended to emphasize the inability of the simulator to duplicate aircraft flight response. This is particularly true during the terminal stages of landing and during takeoff.

ANALYZING THE VISUAL SYSTEM

Figure One illustrated the relationship of the various areas of the flight simulator. The portion related to visual simulation includes image generation and image display. In Figure Nine we divide the visual system into four areas - image storage, image pickup, image relay, and image display. Figure Nine lists various types of devices for each area.

Many considerations must be weighed in choosing a visual system. Figure Ten outlines some of the factors to be considered. Since limitations exist, compromise is required. As an example, if a very large visual envelope is required, a larger and more costly image generator is necessary. On the other hand, if we settle for a smaller visual envelope, the size and cost of the image generator may be rather low. In order to weigh each factor and analyze the types of visual equipment which would fulfill the requirements, we must first understand the capabilities and limitations of equipment available.

IMAGE STORAGE

Image storage is the first item to be considered. The three-dimensional model would be recommended if faithful reproduction of detail and changes in perspective during simulated flight is required. The model, however, usually means high initial cost and excessive floor space requirements. This may not be important if floor space is not at a premium or if the size of the visual envelope is limited. Size of the model may be restricted by using

*Visual envelope refers to the terrain area to be simulated.

a high scale factor; however, this creates problems in fabrication, model lighting and approaching close enough to the model with a suitable pickup probe.

The high resolution transparency is a widely utilized method of image storage. Transparencies have been used for visual simulation with several types of image pickup including direct projection systems, point light sources, and flying spot scanners. Scale ratios for a transparency storage system usually are many times the scale ratio for a model system. The transparency concept has several definite advantages over the model. The three most important are cost, size, and flexibility. The cost advantage is apparent. Size is an advantage because higher scale factors are possible with comparable resolution; flexibility, because any terrain area can be simulated merely by reading out transparency of that area.

Although transparency image storage has advantages, it also has disadvantages. The greatest disadvantage is that the transparency is two-dimensional and as such, cannot display terrain relief. Another disadvantage is that at lower simulated altitude when the pilot's line of sight begins to approach parallellism with the simulated terrain of the transparency, the resolving power falls off very rapidly. This problem is noticeable at the terminal stages of landing simulation. The SMK-43 Visual Attachment is plagued by this problem. A further disadvantage of the transparency concept is that the resolving power of the system is reduced with altitude because of the reduction of the area of the transparency being read out. The transparency system may be film resolution limited at low altitudes.

A core memory of a computer is a third type of image storage to be considered. With this type of device the stored image is a synthetically generated mathematical model of the terrain. A system of computer generated display such as the one designed by General Electric Company for NASA Manned Spacecraft Center, at Houston, Texas, can provide three-dimensional changes in perspective. Figure Eleven shows some typical geometric patterns which can be generated by such a device. The two aircraft carrier drawings show perspective changes during a typical approach.

Attempting to store real world information by this method would not be practical. If we were to attempt storing information comparable to a typical two-dimensional ten-inch color transparency, approximately 3.75×10^9 bits of information would be required, based upon assuming film resolution at 50 lines per millimeter, eight shades of gray, and three colors.

Another technique to be considered involves mixing digital computer and transparency or model storage. Such a storage system would circumvent the problem of excessive computer storage capacity and would make it possible to concentrate terrain storage in particular areas of interest.

IMAGE PICKUP

Image pickup is the second item to be considered in visual simulation.

The model system of image storage usually will have an optical pickup which is referred to as an optical probe. In addition to picking up the image, the optical probe provides simulation of aircraft roll, pitch and yaw. This is accomplished by driving various optical elements within the probe. Optical probes also have been used for picking up an image from a transparency.

The problems of the optical probe image pickup are severe and usually result in system compromises. These compromises may result in marginal system performance. The bead lens pickup, used on the U.S. Air Force SMK-23 Visual Attachment, is a good example. (Figure Twelve) A 3,000:1 model scale was chosen for the SMK-23 in order to obtain maximum visual area with minimum model size. This dictated a very small pickup element for the optical probe in order to obtain normal landing elevation. (Vertical distance from pilot's eye to runway.) The bead lens was very slow optically. Resolution on axis was marginal, and dropped rapidly off axis. Although the lens was designed for a viewing angle of approximately 50 degrees, the effective viewing angle was much less because of the fall off in resolution away from the optical axis.

Whereas the bead lens may portray a rather dismal picture for the optical probe pickup, other optical probes have been somewhat more successful. As an example, recently developed probes have a "T"* number as low as 14, as compared to T = 60 for the bead lens. Such probes have acceptable resolution and a wide field of view.

A fish eye type lens recently considered for visual simulation has a 360 degree field of view and an almost infinite depth of field. This type of lens, however, would require considerable optical correction for use in the simulation application. Photographs taken with the fish eye type lens are commonly found in magazines. The gross distortion can be seen readily in such photographs.

Another wide field of view optical probe utilizes a hyperbolic mirror for pickup. This system, being developed by the Marquardt Corporation, has a field of view which approaches 360 degrees.

A point light source projection system is a direct projection wide angle image pickup for visual simulation. This device images picture information from a flat transparency on a screen with a point source of light. (Figure Thirteen) Although this system has the advantage of direct projection and a wide field of view,

*The "T" number is the effective aperture. It is the same as the "F" number except that it takes into account the efficiency of the Optical train.

it suffers from such problems as distortions, low light level, limited visual envelope, and marginal resolution.

A recently developed method of image pickup uses a flying spot scanner cathode ray tube to read out a transparency. This method was discussed earlier in this paper and a diagram of such a device is shown in Figure Seven. Although this method of image pickup is limited to two-dimensional imaging, considerations recently have been given to provide terrain relief information by a separate image storage medium for elevation information. Such a system is being developed by Link Group, General Precision, Inc.

IMAGE RELAYING

Image relaying, the third area to be considered in visual simulation, may be all important in the design of the system. With any system utilizing television techniques, it becomes the hub around which the system is designed. Although the television loop is not necessarily the limiting factor in the performance of a visual system, it is doubtful that major improvements could be made without considering its performance.

Resolution and noise are the two most important factors in judging the performance of a television system. Resolution of the system involves the ability of the system to resolve, transmit, and display picture information. Resolution of a television image relaying system is limited by the bandwidth of the system. Bandwidth is a measure of the quantity of picture information the television system is able to process in a given unit of time.

System noise, the other factor of consideration, is a measure of the amount of superfluous or non-related picture information as compared to the related picture information. Ideally, picture quality increases with increased bandwidth and decreased noise level. However, in a television system, noise level increases with increased bandwidth.

Many portions of a visual system affect the television system. Resolution may be affected by model or transparency resolution, optical probe resolution, or spot size of the flying spot scanner. The bandwidth requirement of the system will be greater for a system with a greater field of view. Illumination of the model and optical speed of the probe will affect the ability of the television system to process the image. If the light level of the image at the photocathode of the camera is too low, the television system will have difficulty processing the image and the noise level of the picture will be very high.

The television image relaying system may be thought of as a valve through which all picture information must pass. The size

of the valve would be compared to the amount of bandpass* of the television system. In the design of a visual system, the valve or bandpass must be sized to the system. If it becomes apparent the bandpass requirements are too high, it may be necessary to compromise some area of the system design. In order to illustrate how such a compromise may be dictated, let us take a typical visual requirement and analyze the tradeoffs which may be required.

First, let us assume the requirement is for a wide field of view system, with good resolution and dynamic response. From this description the operating parameters must be established for the system. As a starting point, let us choose a 180 degree field of view in the horizontal direction, and 50 degrees in the vertical direction. If we were to match the resolution of the image to the resolution of the human eye, it would be logical to design the system on the basis of being able to discern three minutes of arc within the field of view.

If we now calculate the number of vertical and horizontal picture elements within the field of view which must be processed, we arrive at a figure of 3,600 in the horizontal direction, and 1,000 in the vertical direction. If we take the product of the horizontal and vertical elements, we find the total picture elements to be resolved is 3.6 million. In order to obtain a dynamic image, the picture information or elements must be updated at a very rapid rate. Most closed circuit television systems update the picture at a rate of 30 frames per second. If we choose 30 frames per second for this system, we find the total picture elements to be processed is over 100 million per second. A television system with a bandpass of this magnitude would be far in excess of present state-of-the-art in television. If we look for a place to cut requirements, we would find three possible areas - field of view, angular resolution, and frame rate. In actual practice, we probably would compromise either field of view or angular resolution or, quite possibly, both. A sacrifice of frame rate would not be recommended for a system which requires any degree of dynamic response.

Another solution would be to provide multiple television channels and divide the picture between channels. Such a system requires edge registering the picture similar to "Cinerama". Sometimes it is possible to provide a separate channel for each window of the cockpit rather than to edge register the display.

In establishing the configuration for a television image relaying system, the decision must be reached concerning whether the system shall be monochrome or color. Although color adds realism, and

*Bandwidth and bandpass are used synonymously throughout this paper.

may provide picture information not shown with monochrome, problems arise which do not exist with the monochrome system. A color system tends to have poorer resolution, higher noise, and less density or brightness steps. Also, a color system is less reliable and is more difficult to align and maintain.

Color television systems are either simultaneous or sequential. The simultaneous system requires duplication of circuitry and is plagued with problems in alignment and registering the primary colors. The sequential color system is plagued with poor light transfer efficiency*, color wheel synchronization, and high bandpass requirements. The bandpass must be greater because the system must process one each red, green, and blue frame to make up a composite color frame. Often after weighing the advantages and disadvantages, it may become apparent that color is not worth the sacrifices which must be made.

An example of the number of factors which can affect the performance of the image relaying portion of a visual system is the U. S. Air Force SMK-23 Visual Attachment. Because of scaling of the model, it was difficult to provide proper lighting. Scaling made it necessary to use an extremely small pickup element on the optical pickup probe. This accounted largely for the extremely slow optical speed of the probe. The sequential color wheel further reduced the light efficiency of the system. With all of these factors affecting the light level of the system, the amount of light reaching the photocathode of the camera was very low. This, along with the high bandpass of the system, contributed to producing a very noisy picture.

IMAGE DISPLAY

The image display system is the fourth area to be considered for a visual simulation device. The type of display is dictated by the basic visual requirements and the design of the other areas of the simulation system.

The television monitor is a simple and cheap method of display for a visual device having a television image relaying system. The television monitor is highly reliable and may be mounted on the cockpit of the simulator. This type of display, however, very often is considered inadequate for one or more reasons. A basic disadvantage of the TV monitor is that, in order to maintain the proper angular relationship between the viewer's eye and the displayed image, the monitor must be placed very close to the viewer. Usually, this is difficult because of the configuration of the cockpit.

*The color wheel is only 20 percent efficient.

Often it is necessary to position the monitor too high and too far away from the observer's eye. Another disadvantage is that because of the close proximity between the viewer's eye and the screen of the monitor, any slight head movement on the part of the viewer causes an exaggerated change in look angle between the viewer and the image. (Figure Fourteen) A further shortcoming of the monitor display is that the viewer is not required to re-accommodate or refocus his eyes when switching from the near focus of the instruments in the cockpit to the far focus of the outside world. Re-accommodation is a critical part of transition from instruments to visual when making a low visibility approach.

The television projector and screen is a second type of display system which is utilized with television image relaying. This type display has several advantages over the television monitor. First, it is more flexible in adapting to the flight simulator. Second, the viewing distance usually is several times that of a monitor. At this distance the look angle will not change enough to be a significant problem for normal simulation. (Figure Fourteen) Further, this distance will require some re-accommodation by the viewer.

Although the projector-screen display has advantage over the TV monitor, several serious disadvantages are apparent. This type of display is not readily adaptable to simultaneous pilot and co-pilot display. If the pilot and copilot were to view the same image on a screen with one projected source, the apparent location of objects being imaged will be different because of the difference in the look angle of the two viewers. It is possible, however, to overcome this problem by projecting two different images with different projectors on the same screen. This type of display requires a very high gain or highly directional screen.

Several types of television projectors are used for visual simulation. The light valve projector has the greatest light output and customarily has the highest resolution. However, this type projector is higher in cost and is difficult and expensive to maintain. The light valve projector combines the instantaneousness of the cathode ray tube with the light efficiency of a film projector. The system consists of a high intensity light source, a pair of schlieren stops, a rotating glass disc which carries a thin layer of transparent oil, an electron gun and deflection system, a schlieren lens, and a projection lens. (Figure Fifteen)

In operation, the electron gun writes on the oil film by laying down a charge pattern in the form of a television raster. The oil surface is deformed by the electrostatic charge pattern forces. While the transparency of the oil film remains unchanged, its refraction properties vary with the deformations. The refraction produced in conjunction with the schlieren stops permits a light image to be produced by the projection lens.

A second type of television projector uses a Schmidt type

optical system to project the image from the face of a cathode ray tube. (Figure Fifteen) This type of projector is less expensive than the light valve, and is simpler to maintain. Although it has a lower light output, the light output is acceptable for most applications. The Schmidt projector often has limited resolution. In some cases, the resolution is limited by resolution of the Schmidt optics.

A third type of projector, referred to as a refractive projector, uses a cathode ray projection tube and refractive optics, to project the image. This type of projector is the least expensive and is simple to maintain; however, it is extremely inefficient in terms of light output.

Many types of screens are available for displaying the projected image. Screens can be categorized into front or rear projection. Front projection screens are considered more desirable. However, positioning the projector may dictate use of a rear projection screen. Rear projection screens are inefficient, reduce image resolution, and a hot spot (greater brightness) will appear in the center of the screen.

Several types of front projection screens, which are highly efficient and readily adaptable to the simulation application are available. Such screen materials as the retro-reflective, the semi-spherical or the lenticular, may have a gain up to 1,000, as compared to flat white surface. These highly directional screens have a limited viewing area. However, this may not be a problem in visual simulation devices where the viewing audience is limited.

When a screen is used in conjunction with a direct projection or optical relaying visual system, a high gain screen is sometimes of extreme importance. Such visual systems are quite limited in light output with success being dependent upon the screen's efficiency.

The virtual image is a type of display system which has been given consideration for several years, but only recently has become widely utilized in visual simulation. Whereas the monitor or screen type of display images the picture on the surface of the display device, the virtual image display images the pictures at, or near infinity. The advantages of this type of display are many. First, by focusing the image at, or near infinity, the viewer's look angle will not change if he changes the position of his head. (Figure Fourteen) Second, the viewer is required to re-accommodate his eyes when changing attention from the near focus of the instrument panel to the far focus of the image out the windscreen. By viewing the image as a virtual image, the sense of presence of a screen is eliminated.

The virtual display directs most of the light in the direction of the viewer. Therefore, minimum light output is required. Virtual image displays can be compact and light weight for direct

mounting on a cockpit. They may be adapted for wide angle display. Also, it is possible to display more than one image source simultaneously at different focus distances. A three-dimension effect may be displayed by providing a separate image for each eye of the viewer.

Two types of virtual image displays are generally used for visual simulation. One type has a planar-convex lens, the other a spherical mirror. (Figure Sixteen)

The lens type is the cheapest and simplest virtual image device. A large lens is placed in front of the viewer for imaging the presentation at infinity. The lens usually is 24 inches or greater in diameter and, for economic reasons, may be made of an acrylic plastic. An additional lens is sometimes used to correct aberrations. A plastic lens can be cut to fit the configuration of the cockpit. Several lenses may be used for a wide angle display system; however, with such an arrangement, the distortions are rather excessive. Disadvantages to the lens type of virtual image display include marginal performance of plastic optics, reflections from the front surface of the lens, and physical presence of the lens at a distance close to the viewer's eye. These disadvantages, however, are not considered critical in many visual simulation applications.

The spherical mirror type of virtual image display will have considerably higher fidelity than the lens type. This type of display is considered more acceptable for the critical types of applications such as those which use the display for navigation. The cost of the optical elements for the spherical mirror virtual image system may be very high.

A synthetically fabricated mirror has been used to form a virtual image. The Marquardt "Vuemarq" has been demonstrated with such a mirror. The fabricated mirror may not compare optically with the glass mirror; however, it is satisfactory for most simulator applications. It is possible to produce fabricated, light weight, large mirrors at a considerably lower cost than the glass counterparts.

V/STOL FLIGHT SIMULATION

The requirements of the conventional aircraft system tax simulation technology to a point where compromise is necessary. The V/STOL Aircraft system will require optimum simulation of the areas required by the conventional system, plus additional parameters peculiar to the V/STOL System.

V/STOL VISUAL SIMULATION CONSIDERATIONS

The material which was presented earlier in this paper pointed out that, at its best, visual simulation is a series of compromises whereby we arrive at a system which, as near as possible, fulfills the requirements of the particular simulation mission. Design of the visual system will be even more critical for the V/STOL Flight Simulator. It will be necessary to restrict operating parameters in some areas in order to insure maximum fidelity of simulation. Success may depend upon the use of two or more different systems of image generation where several tasks are to be simulated.

Figure Seventeen divides V/STOL Visual Simulation tasks into three groups.

Conventional visual flight simulation tasks include landing and takeoff, circling, and for the military aircraft system low level, high speed flight, target identification, and target acquisition. New tasks created by V/STOL include vertical takeoff and landing, hovering, conversion from vertical-to-horizontal flight and horizontal-to-vertical flight, and short field takeoff and landing.

Considerations dictated by these new tasks are many. Short field and vertical takeoff and landing may be from any area within the visual envelope of the simulator rather than a particular airfield complex. Dynamic response of the visual system and the flight system is critical for simulation of vertical flight. Correlation of the dynamics of the various systems is even more critical. Faithful reproduction of changes in perspective and terrain relief information, while operating near ground elevation, is very important. The simulation devices should provide as many real world visual cues as practicable, since control of the aircraft during vertical flight will be highly visually oriented. As an example, peripheral vision is highly desirable.

The second group of tasks listed in Figure Seventeen includes conventional and short field takeoff and landing. Since these tasks are more instrument oriented, and are less rigorous as far as control of the vehicle, the visual simulation requirements should not be as critical.

Low level terrain following and avoidance is a third possible task to be simulated for the V/STOL System. The degree of simulation required for this task depends upon several factors. The requirement may be a simulation for checkout of vehicle design or for a training low level mission. In either case, the amount of image detail may not be of extreme concern. Therefore, such an application will require only portrayal of gross changes in terrain elevation. Another training requirement may necessitate considerable detail in terrain information in order to identify a target or a drop zone.

THE V/STOL VISUAL SIMULATION DEVICE

It has been stated that establishing the configuration of a V/STOL Visual Simulation Device requires many tradeoffs. In order to demonstrate the manner in which various tradeoffs are considered, we will analyze a typical visual requirement. Let us assume the requirement is for V/STOL Flight Simulation Device capable of providing visual flight training for pilots in vertical takeoff and landing, hovering, conventional and short field low visibility approach, landing, and takeoff, low level terrain following, and terrain avoidance.

It would be almost impossible for one system, or even one type of image generation system, to fulfill these requirements.

The low visibility approach landing and takeoff portion may be accomplished either by transparency or model. The transparency-flying spot scanner would be the most practicable type of image generation for this portion of the visual requirement. This type of image generation is flexible, both in simulating the low visibility approach and in providing simulation of different airfield complexes. The model would provide more faithful reproduction of terrain relief and perspective information but would be more costly and would not have the flexibility of the transparency system.

If the low level requirement is strictly for flying the low level mission, and no visual identification of objects within the display is required, the transparency-flying spot scanner, with means for generating and displaying elevation information, may be the solution. On the other hand, if the requirement includes identifying targets, a model may be considered. It is possible, however, that if the scale is not too high, targets can be resolved with the transparency system. The most practical method of providing targets for such a system would be to use insetting techniques or superposition of targets. This involves superposing another image on the display from a separate image generator. Cost and floor space requirements probably would rule out the model system in favor of some form of transparency system for this part of the visual system.

Considerations for establishing configuration of the vertical and hovering flight portion to the visual system will be the most difficult, as evidenced by the material presented throughout this paper. It has been stated these tasks are highly visually oriented and require careful attention to fidelity of the displayed image. It is, therefore, doubtful that any type of image storage, with the exception of the model, is capable of fulfilling the requirements. Although the model does not provide the desired flexibility, it may be more feasible to compromise this consideration until the time a more flexible image storage device is capable of providing the required fidelity. Let us, therefore, assume that model image storage is to be used for simulation of the

vertical flight tasks.

The scale ratio of a model should be as low as possible. Final decision regarding model scaling should consider model detail, dynamic response demands upon the image pickup, model lighting and possible interference at low altitudes, between image pickup and model. A moving belt model will provide some conservation of floor space for a visual simulation device. However, for the V/STOL Visual Device the disadvantages may far outweigh the advantages. First, it is difficult to construct the belt model with the same degree of detail as the rigid model. Second, the moving belt tends to flutter during operation. Third, it almost precludes any flexibility as far as changing the visual area without major physical equipment change. A fourth disadvantage is that only half of the model belt area is exposed to the image pickup at one time. Consequently, the increased model area would be of little advantage in terms of increased visual area.

In constructing a model, the amount of detail that it is possible to provide, depends largely upon the scale. However, it would be foolish to provide more detail than the visual system is capable of processing and displaying to the viewer. Model lighting should be uniform since, at reduced scales, it is almost impossible to duplicate natural shading created by real world lighting. Shading should be created by varying contrasts on the model.

As has been stated, the image pickup device used with a model type of image storage device is the optical probe. A wide angle probe is required since the device in question requires peripheral vision. Conventional optical probes may provide 90 degrees of viewing. A pickup device such as the Marquardt "Vuemarq" will provide almost 360 degrees of viewing. (Figure Eighteen) However, the amount of viewing processed by the visual system probably would be limited to much less than 360 degrees. The size of the viewing field will depend upon visual system requirements and limitations of the image relaying system and the display system. It need not be more than can be seen by the pilot when seated in the cockpit, with possibly some additional area to take care of normal head movements.

Requirements for the V/STOL Visual System, almost certainly dictate the use of television image relaying. The television system will require tradeoffs in angular resolution of the displayed image and size of the field of view. Increased requirements will be possible only by use of a wider bandwidth system and multiple television channels. It is conceivable that one channel of television will transmit an acceptable 110 degree image; however, angular resolution would be compromised if compared to the human eye. A field of view, much greater than this, will require more than one television channel or considerable compromise in angular resolution.

If we are to assume the Flight Simulator in question will be

on a moving base or motion system, it is apparent that some type of virtual image device is desirable for image display. The mirror type of virtual image device is recommended for this application. It is readily adaptable to wide angle display, provides the most realistic out the window viewing, and can be used to display multiple image inputs. A spherical mirror type display, such as the one designed and developed by Farrand Optical Company for the United States Air Force T-27 Space Flight Simulator, provides 110 degrees of viewing, multiple image input and excellent visual fidelity. (Figure Nineteen) If the Marquardt "Vuemarq" were chosen for the image pickup, the eliptical mirror type virtual image display will be required. As mentioned before, the Marquardt system has a synthetically fabricated light weight eliptical mirror. The light weight mirror may be considered more desirable because of reduced loading requirements on the cockpit motion system.

SPECIFYING A VISUAL SYSTEM

This paper has stressed the inability of present technology to approach duplicating the real world for visual simulation. It is, therefore, difficult to establish the parameters for a visual system when preparing a performance specification for such a device. Past experience has proven the difficulty in refraining from over-specifying requirements in a field requiring so much compromise.

Specifying image quality is extremely important. Testing for compliance with requirements, whenever possible, should be on the basis of analytical methods and criteria, rather than subjective evaluation. Subjective evaluation requires an opinion on the part of personnel conducting the testing. Such criteria as equivalent system bandpass, signal-to-noise ratio, geometric distortion, high-light brightness, and contrast ratio, should be specified. Methods of measuring these criteria should be defined.

Certain areas of the device will require subjective evaluation. This is especially true in the area of human factor considerations such as overall fidelity of the system and representation of the cues required for detection of impending conditions.

CONCLUSIONS

Visual Flight Simulation provides a challenge to anyone working in the field. Problems with a visual simulation device begin with defining the requirement. Since it is impossible to duplicate the real world, a visual system must be designed with many tradeoffs. Such tradeoffs are based upon the tasks to be simulated, visual simulation technology, and final cost of the system.

V/STOL Visual Flight Simulation presents even more of a challenge. The tasks to be simulated are both more numerous and more critical.

Specifying the requirement for a visual device is extremely important. Since the final system cannot be evaluated by using the real world as a standard, operating parameters for the system must be specified.

Testing of the device should be on the basis of pre-established analytical methods and criteria. Subjective testing should be limited to those areas which cannot be checked analytically.

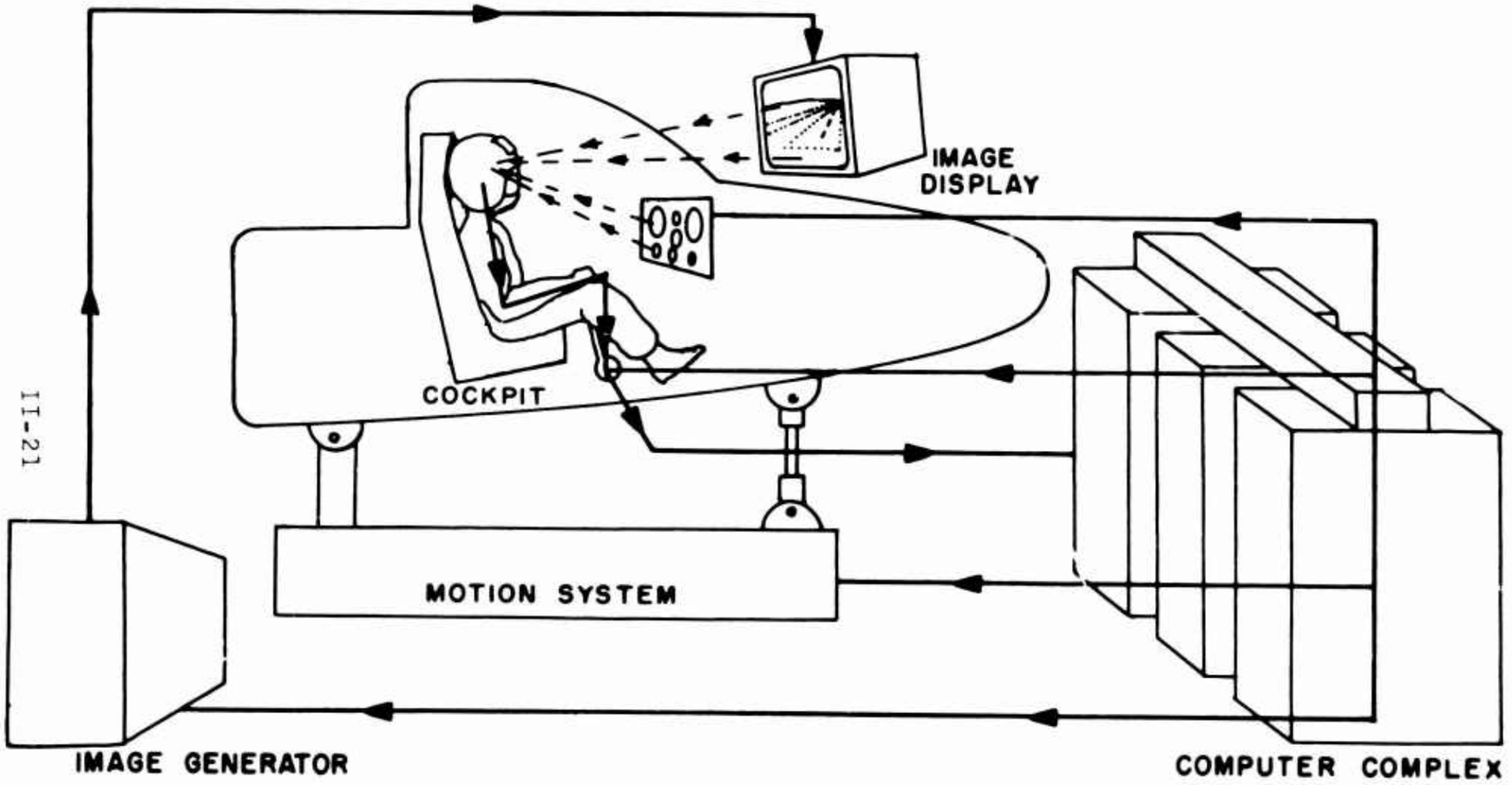
IMAGE
DISPLAY
COCKPIT
MOTION SYSTEM
IMAGE GENERATOR
COMPUTER COMPLEX

FIGURE 1

BIOGRAPHY

RICHARD J. HEINTZMAN

Mr. Richard J. Heintzman is Project Engineer on various United States Air Force Visual Simulation Programs in the Flight Simulator Branch, Systems Engineering Group, Wright-Patterson Air Force Base, Ohio. He holds a Bachelor of Science degree in Mechanical Engineering from Bradley University, Peoria, Illinois.

Prior to joining the United States Air Force, he was Project Engineer on electro-mechanical fusing devices for Eureka Williams Company, Bloomington, Illinois. He also worked in Product Engineering for Caterpillar Tractor Company, Peoria, Illinois. He was a pilot in the United States Air Force.

Mr.Heintzman's current responsibilities include in-house efforts in visual simulation and advanced visual simulation systems. He has been Project Engineer on the development of various U. S. Air Force Visual Simulation Attachments for Flight Simulators.

Removable Belt Magazine
TV Camera Control Unit
Transverse Servo
Azimuth Servo
Pitch Servo
Roll Servo
Altitude Servo
Remote Control Variable Visibility Filter
Belt with Approach and Runway Lights
Ultraviolet Flood Lamps
TV Camera
Actuating Parallelogram

FIGURE 2

FIGURE 5

FIGURE 4

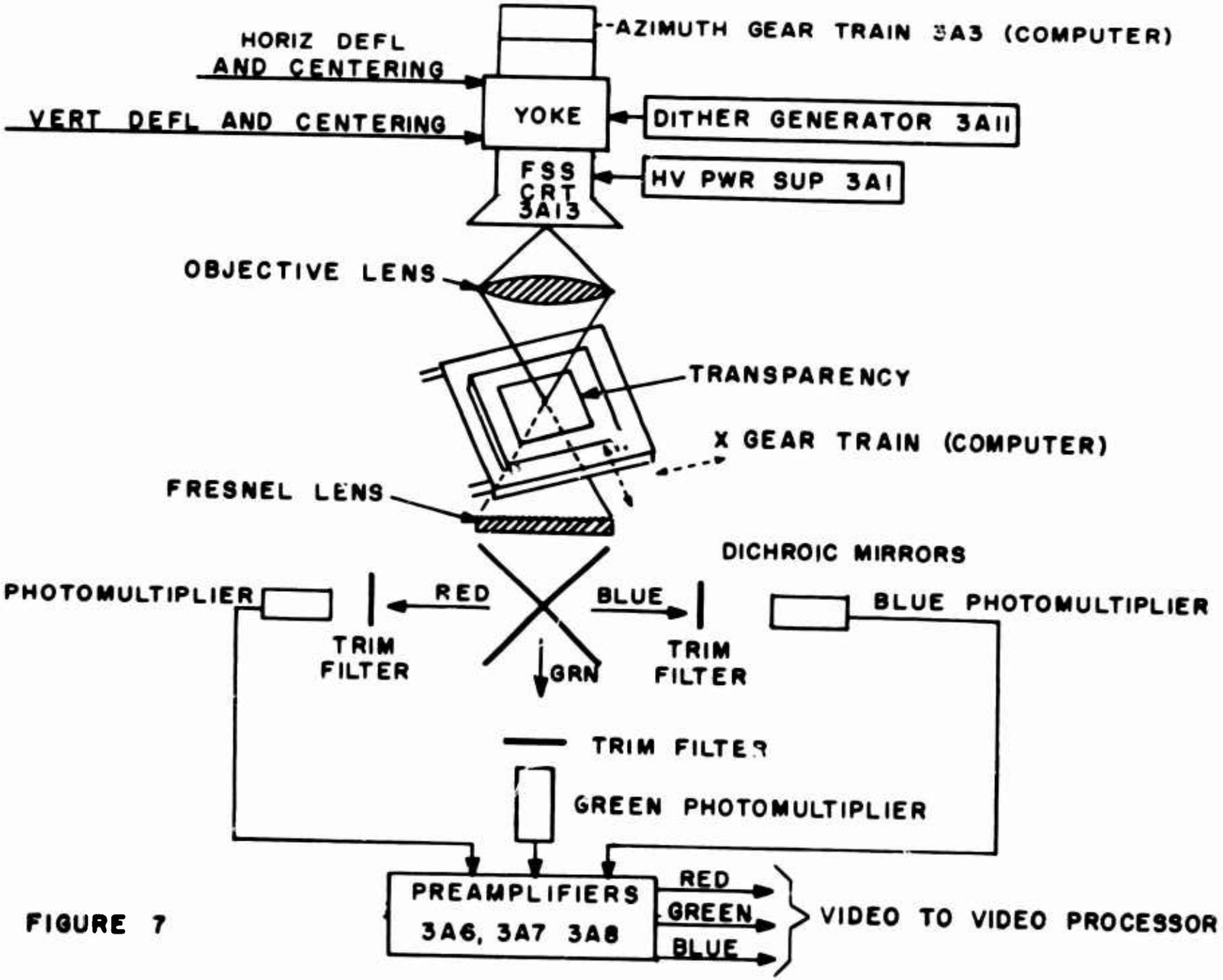
HORIZ DEFL AND CENTERING
VERT DEFL AND CENTERING
AZIMUTH GEAR TRAIN 3A3 (COMPUTER)
YOKE
DITHER GENERATOR 3A11
FSS CRT 3A13
HV PWR SUP 3A1
OBJECTIVE LENS
TRANSPARENCY
X GEAR TRAIN (COMPUTER)
FRESNEL LENS
DICHROIC MIRRORS
RED PHOTOMULTIPLIER
RED
BLUE
BLUE PHOTOMULTIPLIER
TRIM FILTER
GRN
TRIM FILTER
TRIM FILTER
GREEN PHOTOMULTIPLIER
PREAMPLIFIERS 3A6, 3A7 3A8
RED
GREEN
BLUE
VIDEO TO VIDEO PROCESSOR

FIGURE 7

FIGURE 6

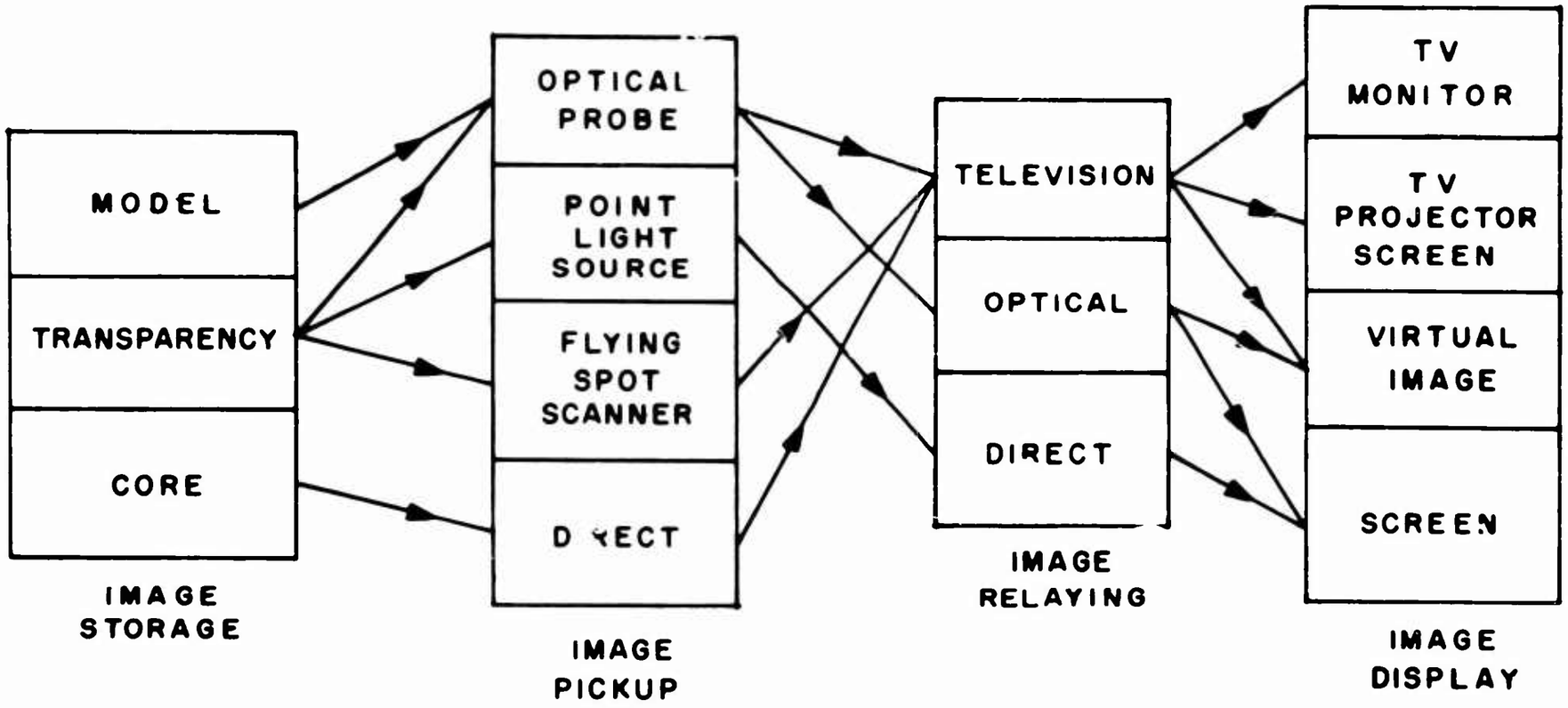
MODEL
TRANSPARENCY
CORE
IMAGE STORAGE
OPTICAL PROBE
POINT LIGHT SOURCE
FLYING SPOT SCANNER
D ECT
IMAGE PICKUP
TELEVISION
OPTICAL
DIRECT
IMAGE RELAYING
TV MONITOR
TV PROJECTOR SCREEN
VIRTUAL IMAGE
SCREEN
IMAGE DISPLAY

FIGURE 9

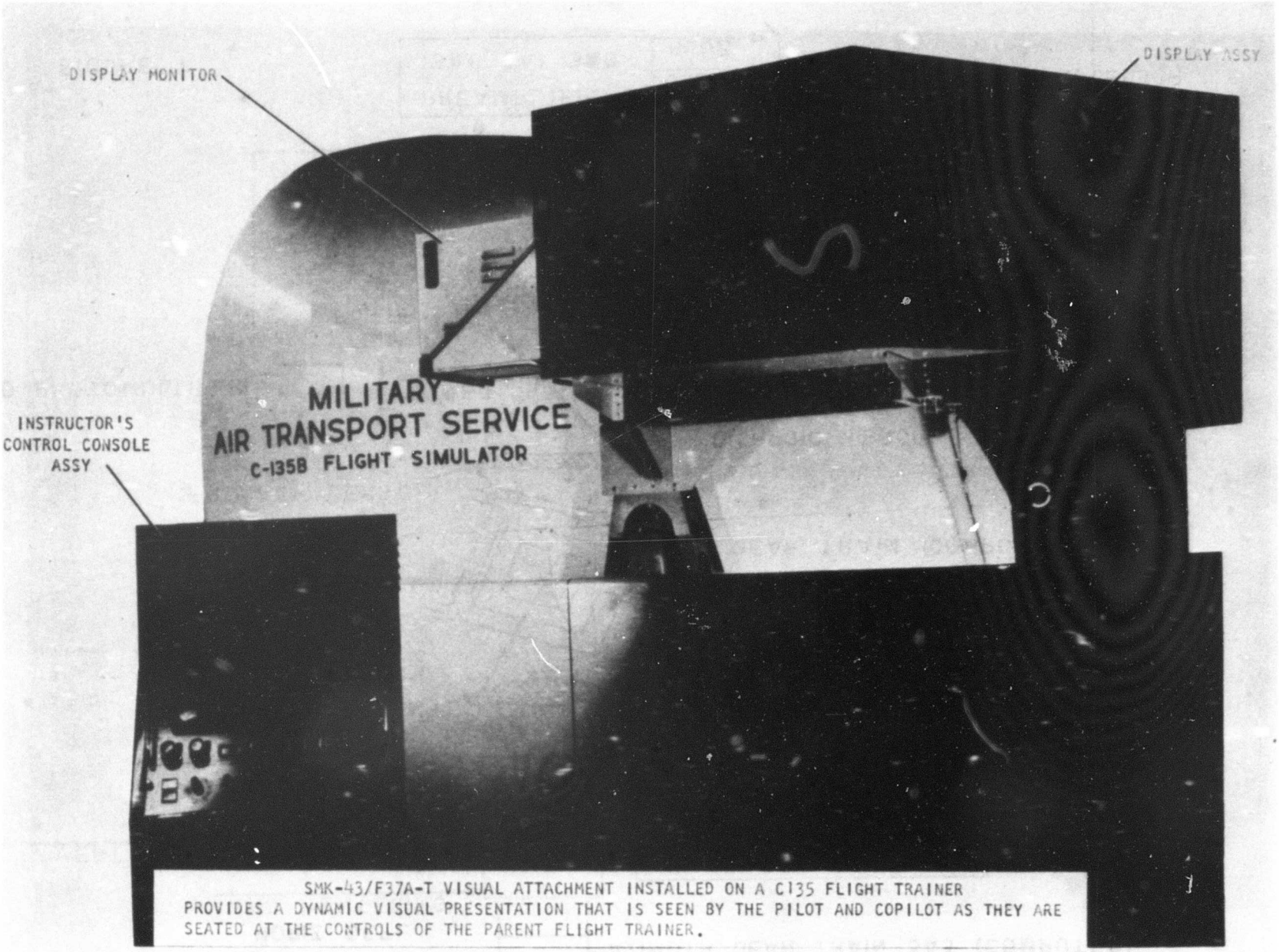

SMK-43/F37A-T VISUAL ATTACHMENT INSTALLED ON A C135 FLIGHT TRAINER PROVIDES A DYNAMIC VISUAL PRESENTATION THAT IS SEEN BY THE PILOT AND COPILOT AS THEY ARE SEATED AT THE CONTROLS OF THE PARENT FLIGHT TRAINER.

FIGURE 8

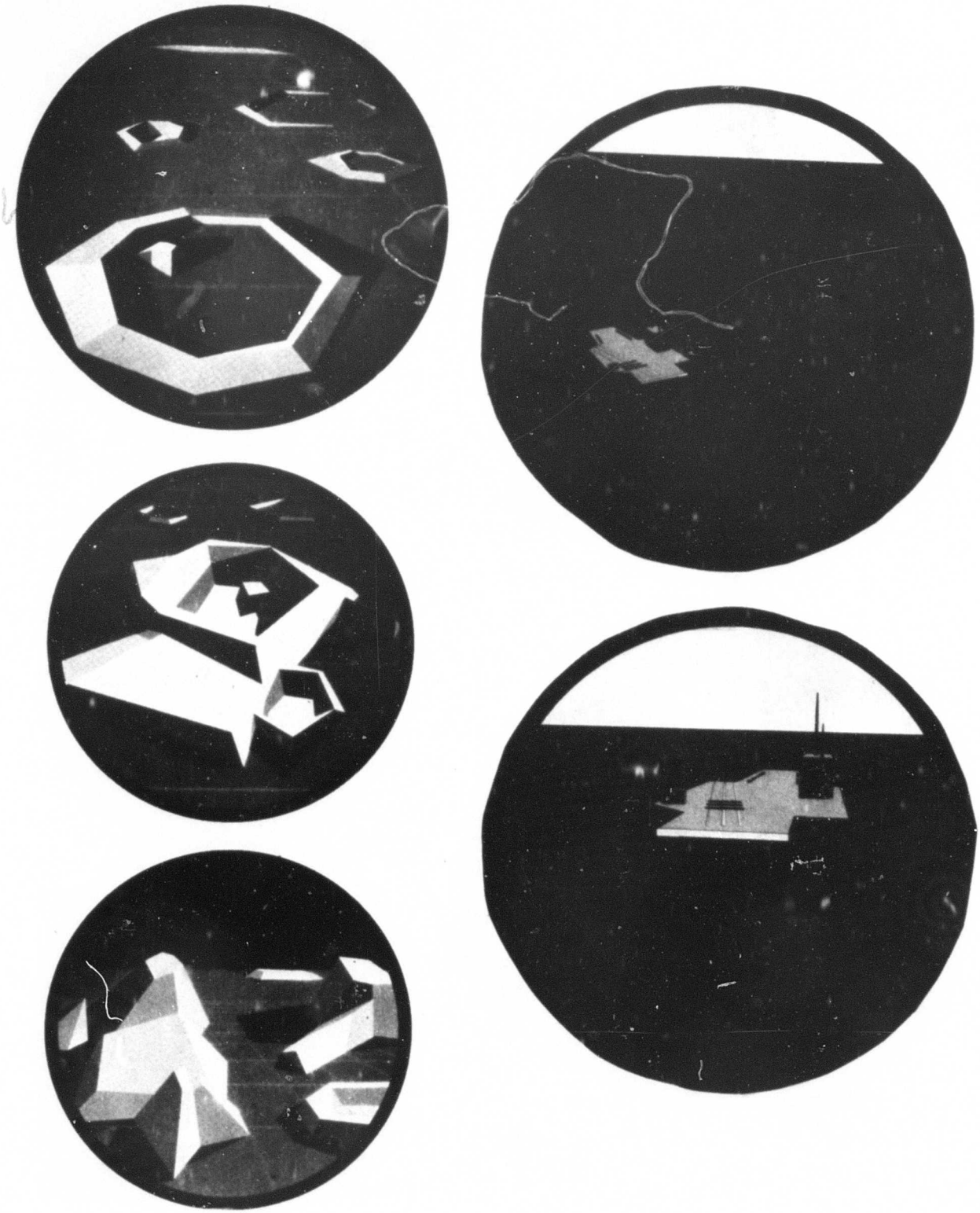

FIGURE 11

FACTORS EFFECTING DESIGN OF VISUAL DEVICE

AREA	FACTORS TO BE CONSIDERED
IMAGE STORAGE	SIZE VISUAL ENVELOPE COLOR OR MONOCHROME TWO OR THREE DIMENSIONAL IMAGE PHYSICAL SIZE STORAGE DEVICE IMAGE DETAIL
IMAGE PICKUP	RESOLUTION PHYSICAL SIZE PICKUP ELEMENT FIELD OF VIEW DYNAMIC RESPONSE
IMAGE RELAY	RESOLUTION BANDWIDTH (CAPACITY) COLOR OR MONOCHROME
IMAGE DISPLAY	FIELD OF VIEW RESOLUTION COMPATIBILITY WITH COCKPIT AND MOTION SYSTEM IMAGE FOCUS DISTANCE

FIGURE 10

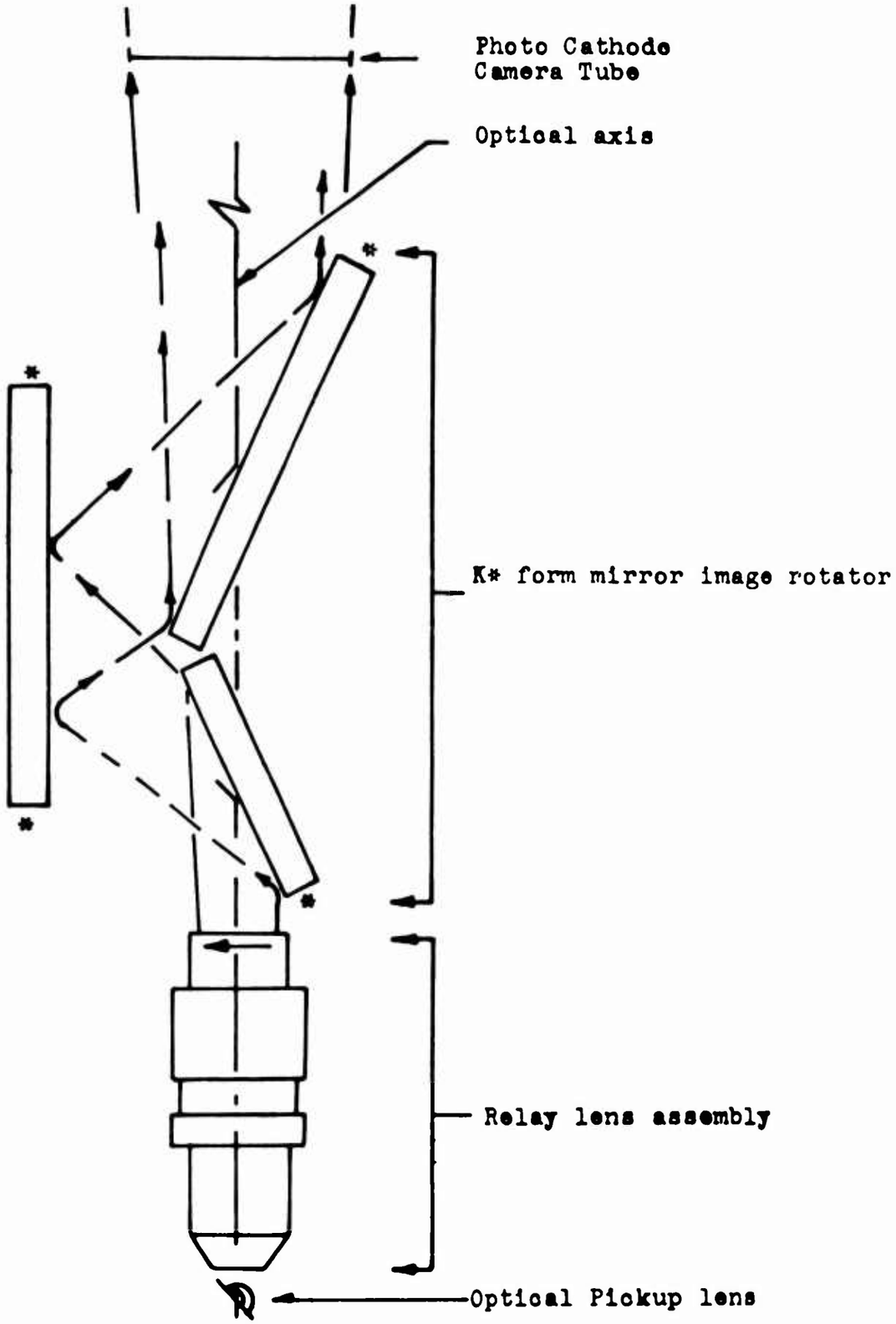

PHYSICAL CONFIGURATION BEAD LENS OPTICAL PROBE

FIGURE 12

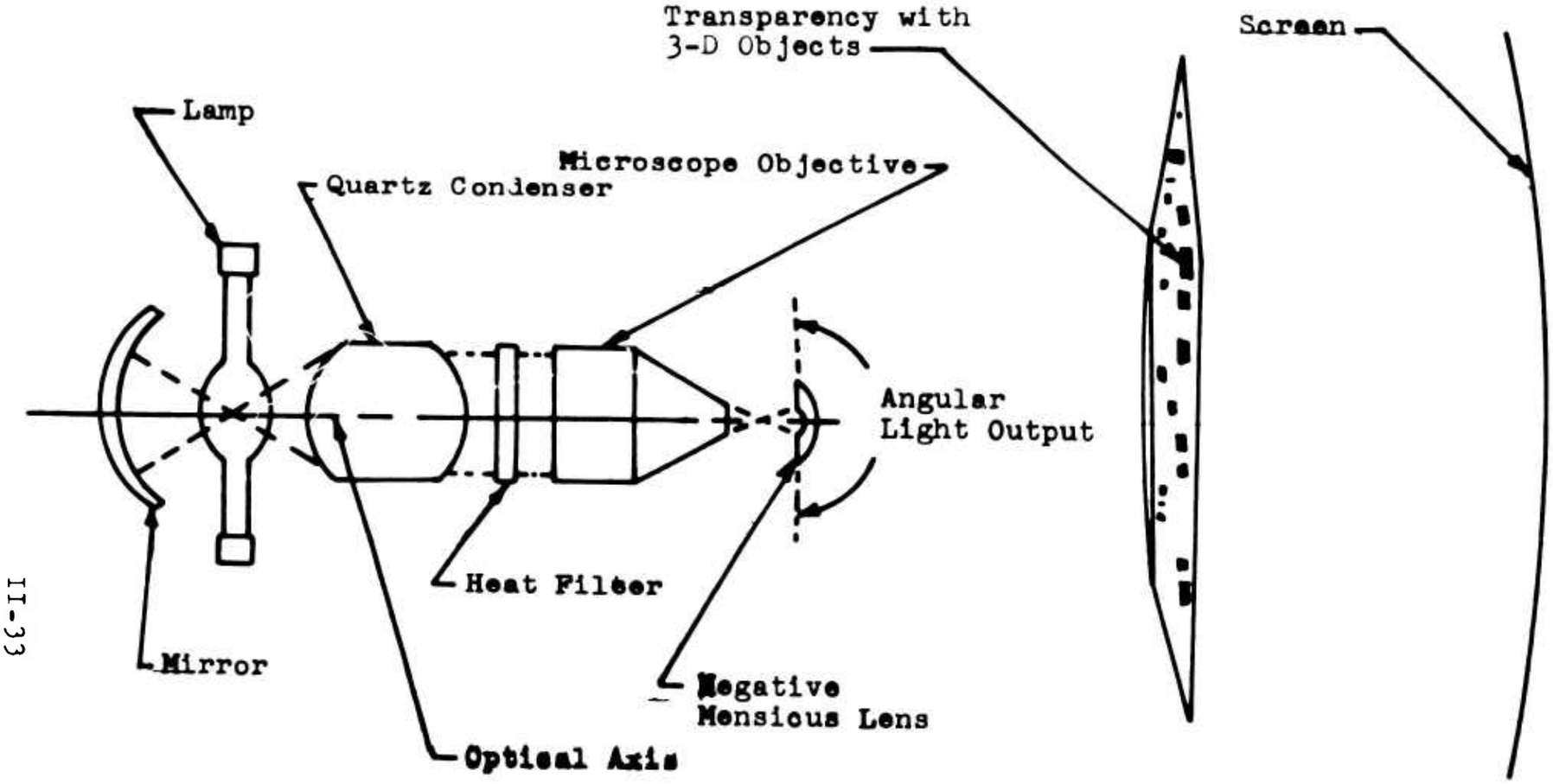

Schematic of Point Light Source

FIGURE 13

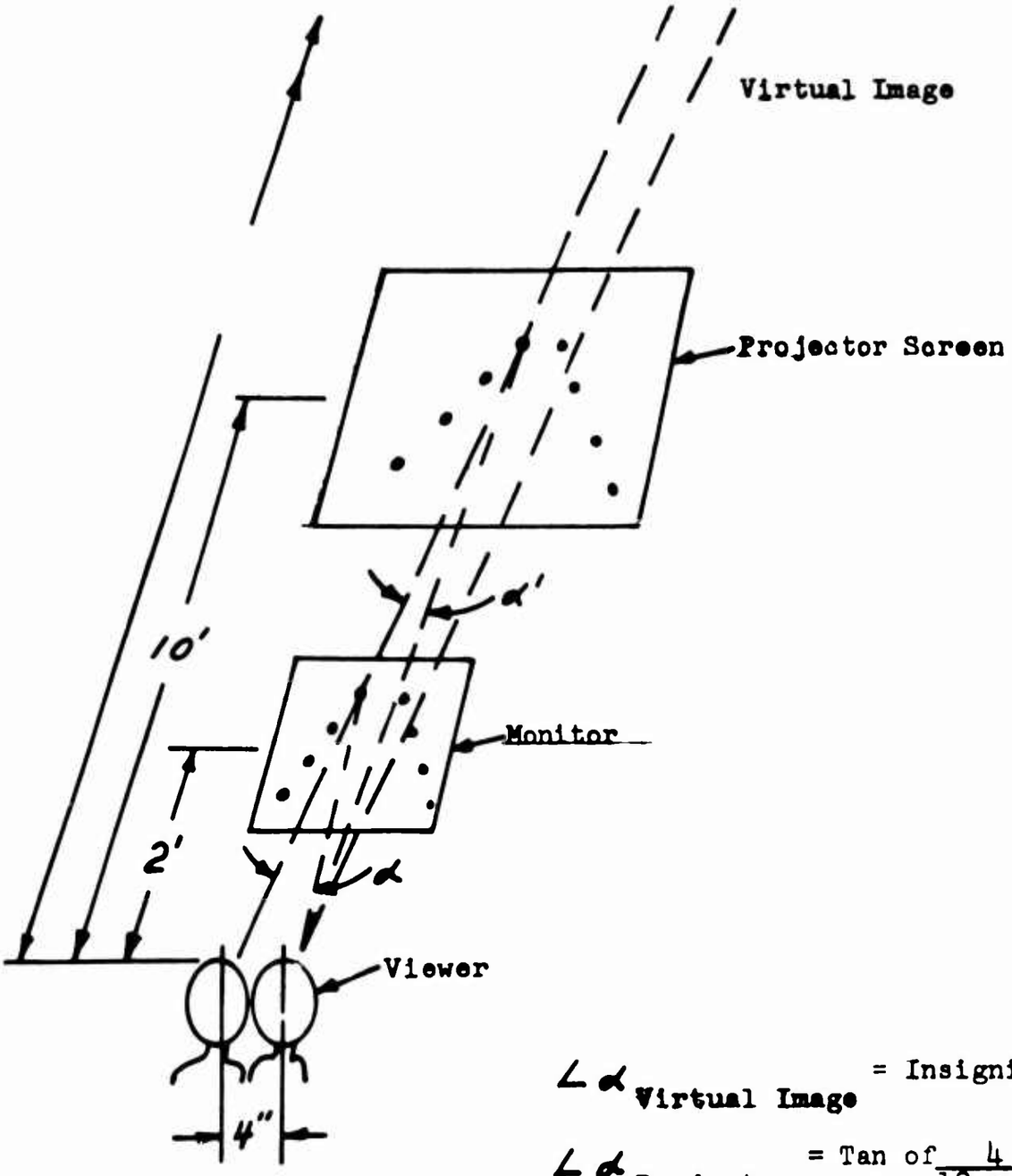

$\angle \alpha_{\text{Virtual Image}}$ = Insignificant

$\angle \alpha_{\text{Projector}}$ = Tan of $\frac{4}{12 \times 10}$ = 2°

$\angle \alpha_{\text{Monitor(2')}}$ = Tan of $\frac{4}{12 \times 2}$ = 10°

Changes in Look Angle - 4" Head Movement

FIGURE 14

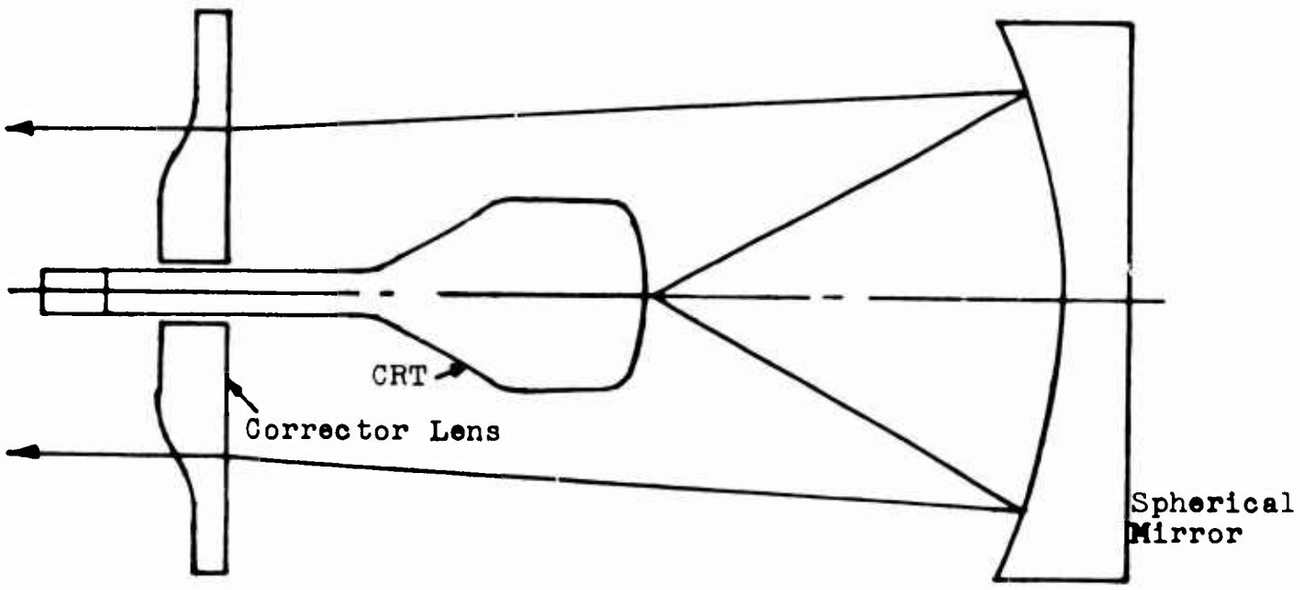

SCHMIDT PROJECTOR

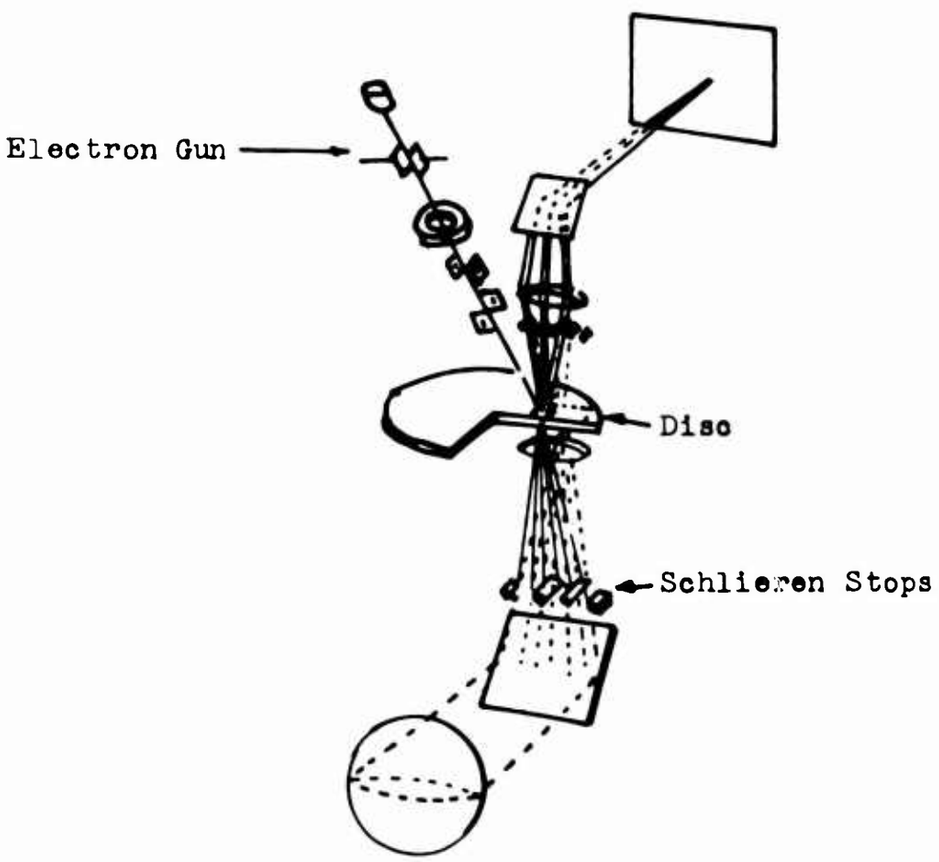

LIGHT VALVE PROJECTOR

FIGURE 15

V/STOL VISUAL SIMULATION CONSIDERATIONS

TASK	SPECIAL CONSIDERATIONS
I. A. VERTICAL TAKEOFF B. VERTICAL LANDING C. HOVER D. CONVERSION VERTICAL-TO-HORIZONTAL FLIGHT E. CONVERSION HORIZONTAL-TO-VERTICAL FLIGHT	WIDE ANGLE DISPLAY EXCELLENT DYNAMIC RESPONSE ACCURATE DISPLAY OF PERSPECTIVE POSSIBLE LIMITED VISUAL AREA EXCELLENT LOW ALTITUDE RESOLUTION
II. A. CONVENTIONAL TAKEOFF B. CONVENTIONAL LANDING C. SHORT FIELD TAKEOFF D. SHORT FIELD LANDING	GOOD DYNAMIC RESPONSE
III. A. LOW LEVEL TERRAIN AVOIDANCE B. LOW LEVEL TERRAIN FOLLOWING	GOOD DYNAMIC RESPONSE PORTRAY TERRAIN ELEVATION INFORMATION LARGE VISUAL AREA

FIGURE 17

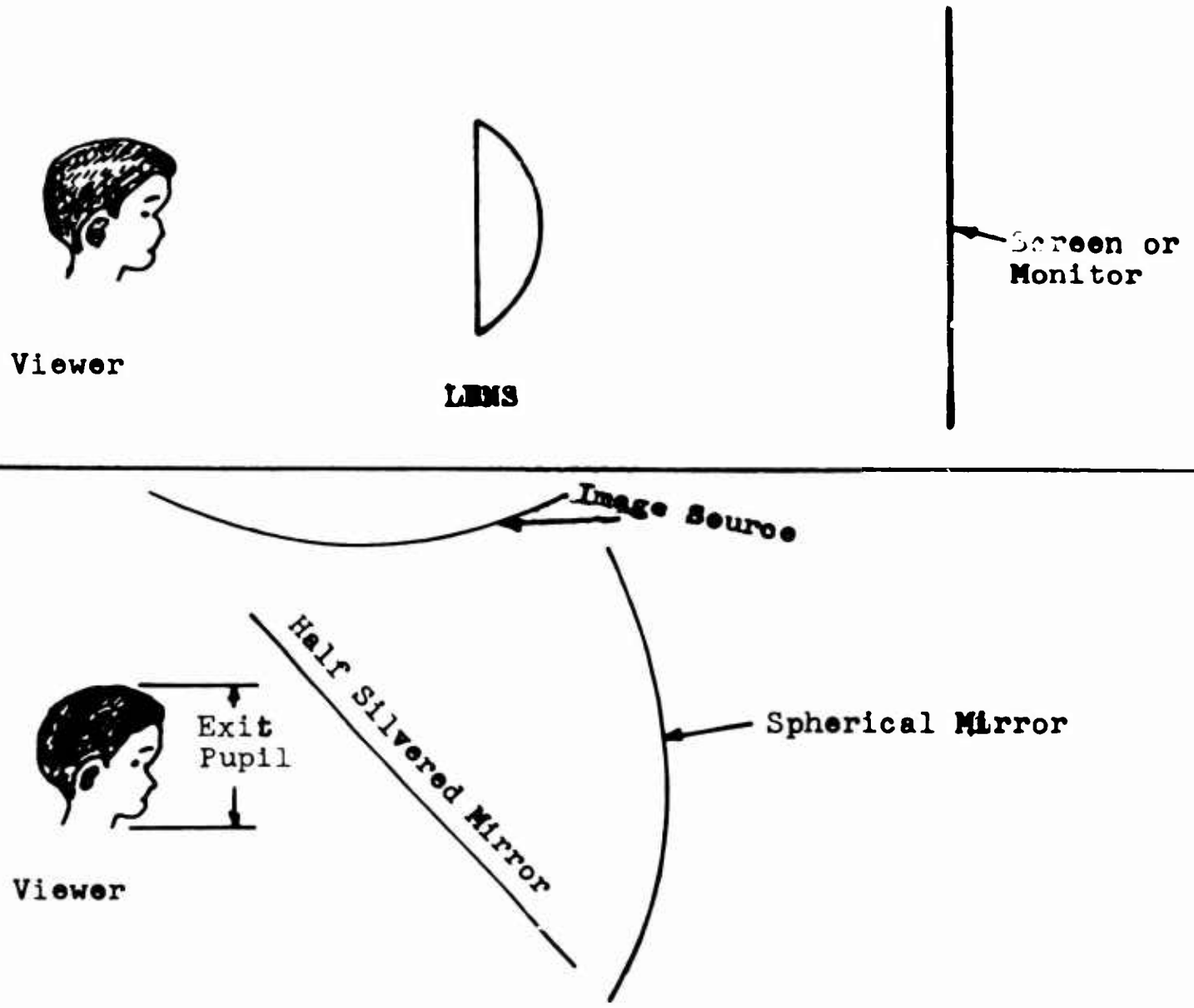

TYPES OF VIRTUAL IMAGE DISPLAY

FIGURE 16

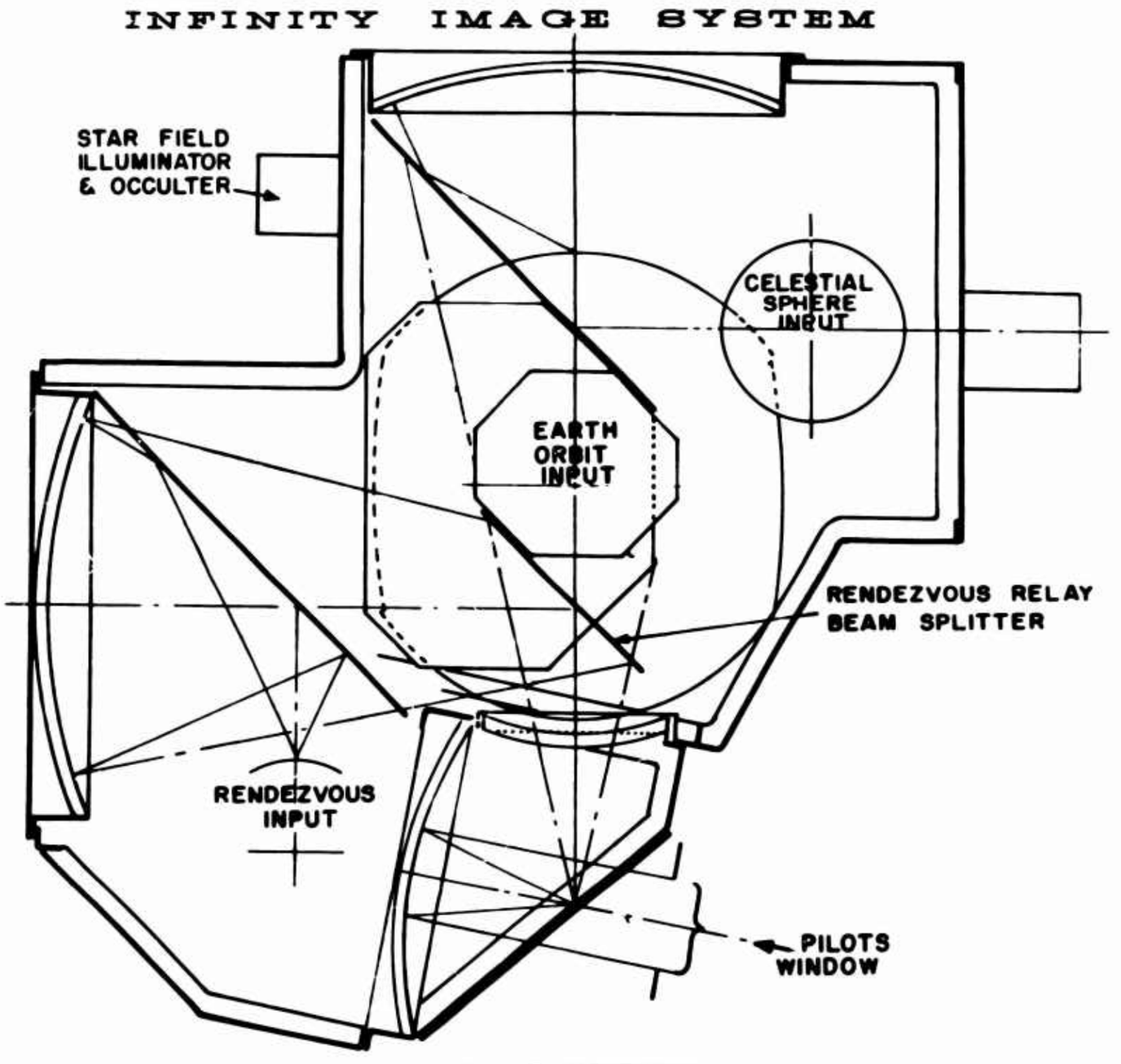

FIGURE NINETEEN

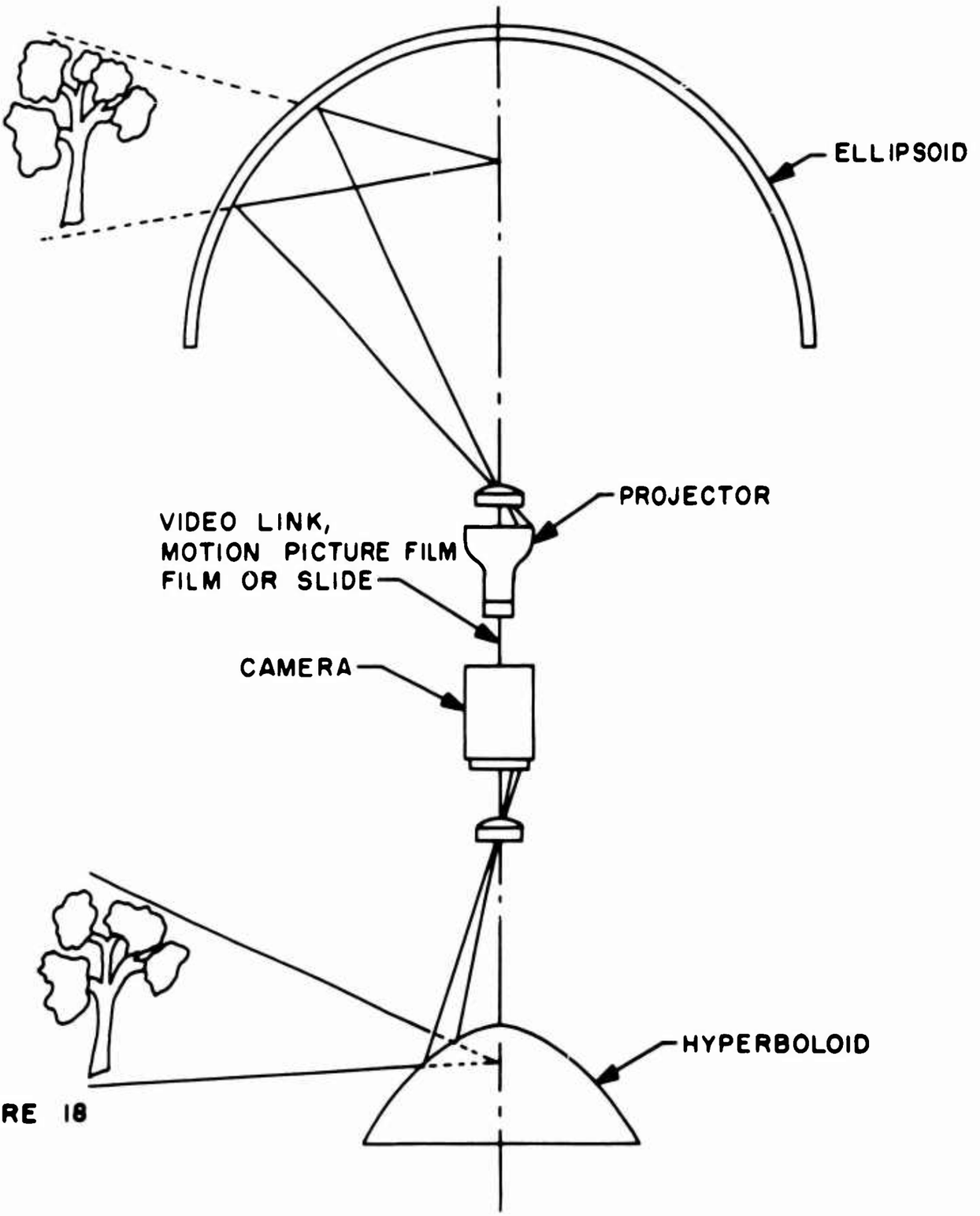
ELLIPSOID
PROJECTOR
VIDEO LINK,
MOTION PICTURE FILM
FILM OR SLIDE
CAMERA
HYPERBOLOID

FIGURE 18

THE XC-142A WING AND FLAP CONTROL SYSTEM

G. K. Fling

Ling Temco Vought

THE XC-142A WING AND FLAP CONTROL SYSTEM

by George K. Fling

Product Design Department
LTV Aerospace Corporation

ABSTRACT

A brief discussion of the tilt wing XC-142A flight controls is presented. The mechanization and operation of the wing and flap control system is described. Other control functions which are dependent upon wing or flap positions are cited.

****

The XC-142A is a cargo assault aircraft using the tilt-wing concept to provide STOL and VTOL capability. The variable incidence wing rotates from zero degrees incidence for cruise flight to 90 degrees incidence for hover flight. Pilot controls for cruise flight are conventional rudder pedals for directional control and stick for lateral and longitudinal control. Engine control is by conventional throttles. Feel forces are provided by constant rate springs in the lateral and directional control systems. Longitudinal feel is obtained from a trim programmed variable rate feel spring. In the low speed flight regime, pitch control is augmented by a tail propeller. Lateral and directional control is obtained by proper phasing with wing incidence of differential main propeller blade angle and the ailerons. Thrust is controlled by a collective lever. In vertical flight or hover, pitch control is provided by the tail propeller, lateral control by differential main propeller blade angle, and yaw control by aileron deflection.

The wing rate is controlled from a linear variable differential transformer on each collective. A fixed rate control is also located on the throttle quadrant. The trailing edge flaps are normally programmed with wing position according to the schedule shown in Figure 1. When transition from cruise flight to hover is begun, the flaps move to 27° before the wing moves. Then the flaps move on down to 60° as the wing moves up to 13°. There is no further flap movement until the wing reaches 42°. At this time the flaps begin retracting as the wing goes on up. The wing-flap program follows the reverse procedure in transitioning from hover to cruise flight. Wing-flap relationships other than that shown in Figure 1 can be obtained by operating the flap over-ride lever on the right hand throttle quadrant or by operating a flap programmer over-ride switch on the collective lever.

A block diagram of the wing-flap system is shown in Figure 2. The pilot input positions a dual linear variable differential transformer, the outputs of which are amplified to drive a dual electric motor. The motor drives two cams - one which determines wing position and one which establishes a corresponding flap position. The cam followers then position the wing and

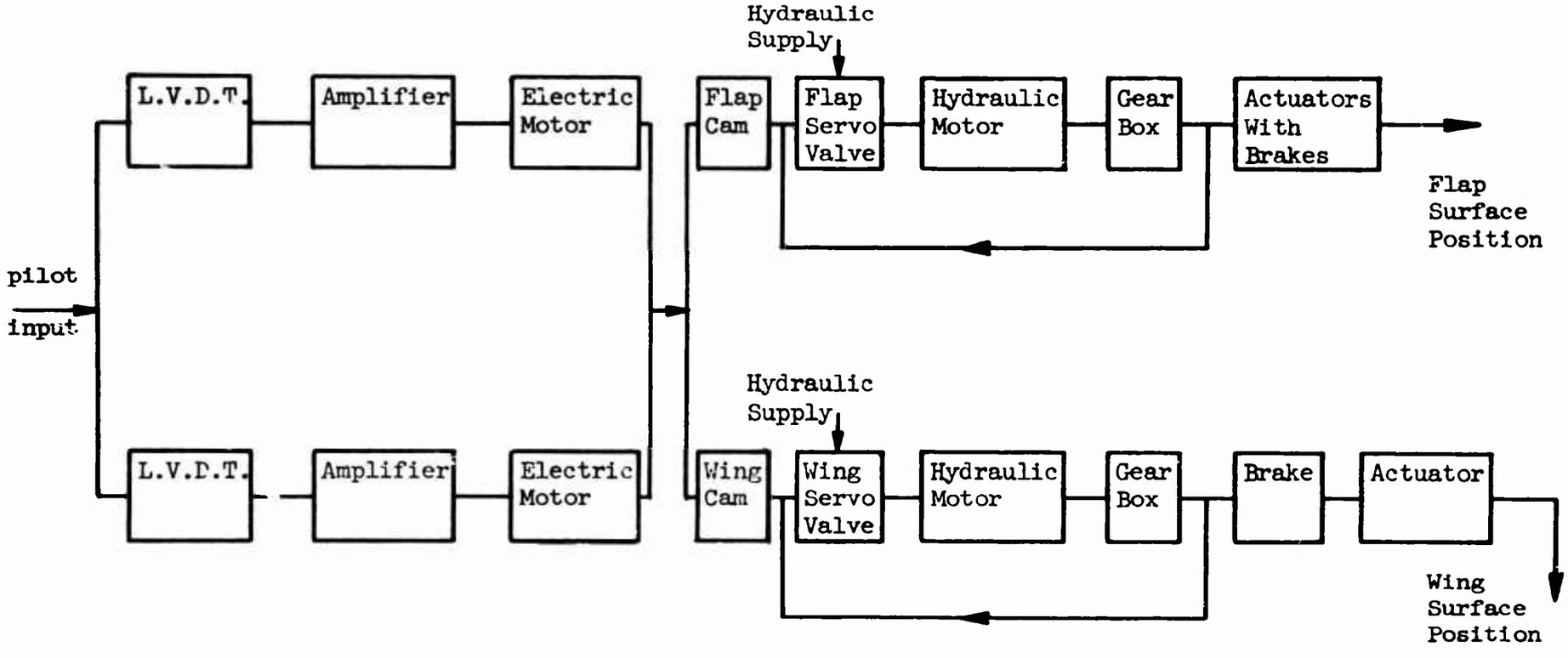

Figure 2

Block Diagram of XC-142A Wing - Flap System

Figure 1

Wing - Flap Program

FIGURE 3- XC-142A WING ACTUATORS

flap servo valves. The servo valve position determines the flow rate and direction of flow to the hydraulic motors. The hydraulic motor torque is multiplied through a reduction gear box and transmitted through torque tubes to efficient ball screw actuators.

The wing is positioned by two actuators as shown in Figure 3. Either actuator is capable of holding the maximum wing load. The normal operating load reverses direction during transition - going from compression with the wing down to tension when the wing is tilted up. Since these actuators are reversible, a torque sensitive brake is incorporated inboard of each actuator to provide a fail safe system. A hydraulic system failure or a failure of the torque tube drive would cause the wing to lock in the position where the failure occurred. The brakes are unlocked when torque is applied to the input shaft by the drive system. The torque tubes are designed to rotate at 2000 revolutions per minute which is equivalent to a wing rate of approximately 9 degrees per second. Under load the wing will travel at any rate up to a maximum of approximately 7 degrees per second.

There are six separate trailing edge flap surfaces as shown in Figure 4. The outer pair of flap surfaces on each side support the ailerons. Synchronization of all six flap surfaces is assured by the torque tube drive system. The shafting in the flap drive system is designed to rotate at a maximum speed of 2450 revolutions per minute. This is equivalent to a flap rate of approximately 22 degrees per second which could be demanded by using the programmer over-ride if a wave off was given during landing approach. Each ball screw actuator contains its own "no back" or friction brake so that a fail safe system is provided. A failure in the hydraulic system would cause all flap surfaces to lock in the position they were in when the failure occurred. A failure in one of the drive torque tubes would cause any flaps outboard of the failure to lock in the position the surfaces were in when the failure occurred. Asymmetry of the flaps would then develop slowly until the pilot recognized the situation and quit commanding a change in flap position. The pilot could then reverse the command and wash out whatever asymmetry had developed in the flaps.

The mechanization just described for the wing and flap system was chosen over other possible designs because of the following features offered:

1. relatively safe conditions which would exist following any failure in the system
2. synchronization of the multiple actuators which is inherent in such a system
3. light weight of system

Figure 5 shows the hydraulic power system for control of the wing and flaps. A pump on an auxiliary power unit normally supplies the hydraulic power for both wing and flaps. A shut-off valve or isolation valve keeps hydraulic pressure off of the servo valve so that the wing cannot be raised inadvertently. The valve is opened when the pilot places a handle in the "on-wing unlock" position. In an emergency caused by loss of the A.P.U. power source, hydraulic power is supplied to the wing and flap system by the power control No. 2-utility system.

Figure 5

Hydraulic Schematic - XC-142A Wing and Flap System

FIGURE 4

XC-142A FLAP DRIVE SYSTEM

Several other functions are operated as a function of wing or flap positions:

1. Leading edge slats
2. Unit horizontal tail automatic trim
3. Tail propeller automatic trim
4. Longitudinal feel forces and lateral feel forces
5. Forward and aft air deflectors
6. Roll-yaw integrator

The leading edge slats prevent wing stall at high angles of attack, providing the capability for a high rate of descent. The slats are extended anytime the trailing edge flaps are down more than 27° and are retracted when the trailing edge flaps are down less than 27°.

The unit horizontal tail and the tail propeller are automatically trimmed as a function of wing position to minimize transition trim changes and to prevent U.H.T. stall at lower wing incidences. Figure 6 shows the automatic trim schedule for the unit horizontal tail propeller.

Longitudinal feel forces are programmed with the unit horizontal tail trim position by the pilot's trim actuator. The maximum feel force gradient is provided at the most positive (nose down) trimmed U.H.T. incidence. Lateral feel forces are made a function of wing position by varying the ground point of the roll feel spring as a function of wing position. Lateral feel forces are greatest in the cruise configuration.

Forward and aft air deflectors are provided to keep air separation from the wing to a minimum during transition. Both air deflectors are raised by the wing. The forward air deflector is mechanically lowered by the wing while the aft air deflector is hydraulically lowered.

The roll-yaw integrator interconnects the lateral and directional control systems in such a way that the rudder pedals provide yaw control and the stick provides roll control for any wing position. This mechanical linkage receives pilot inputs, stabilization inputs, trim inputs, wing position and flap position inputs. Output signals are directed to propellers and ailerons in the direction and magnitude required to achieve pure rolling or yawing moments about the fuselage axes during transition and hover. The flap position input to the integrator is in series with the wing incidence input to the lateral differential collective phasing. When the flaps are extended beyond $7\text{-}1/2^{\circ}$ with the wing at 0°, an increment of differential collective authority is phased in to counteract adverse yaw caused by aileron deflection.

The XC-142 has undergone more than a year of flight testing at the LTV plant in Dallas. Two of the five prototype airplanes have been delievered to Edwards Air Force Base where they are now being evaluated.

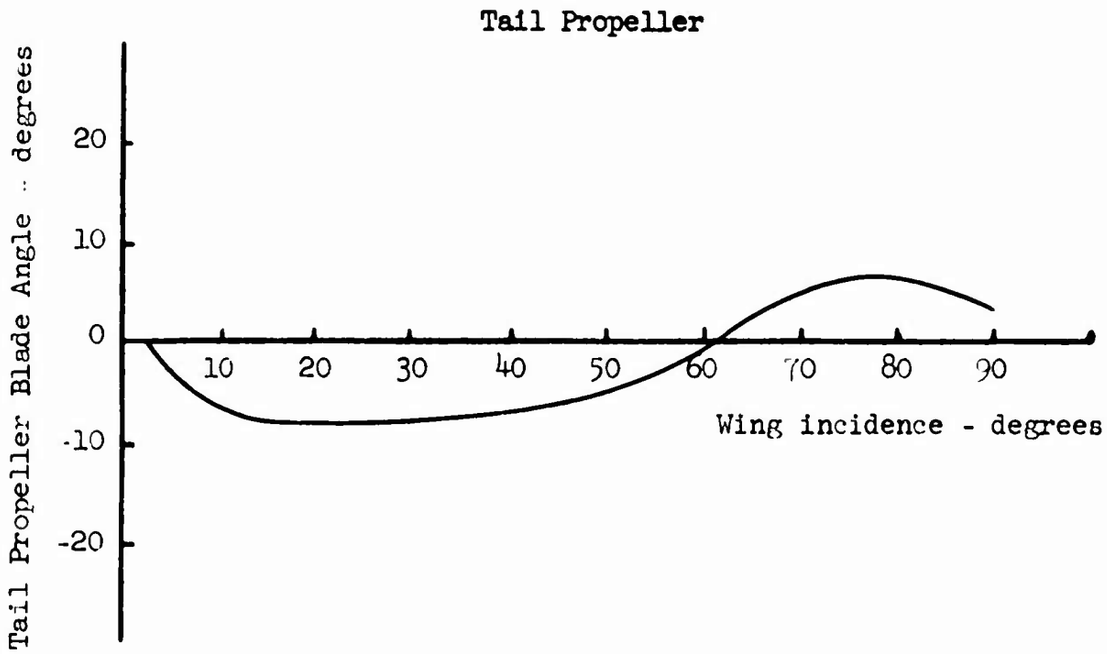

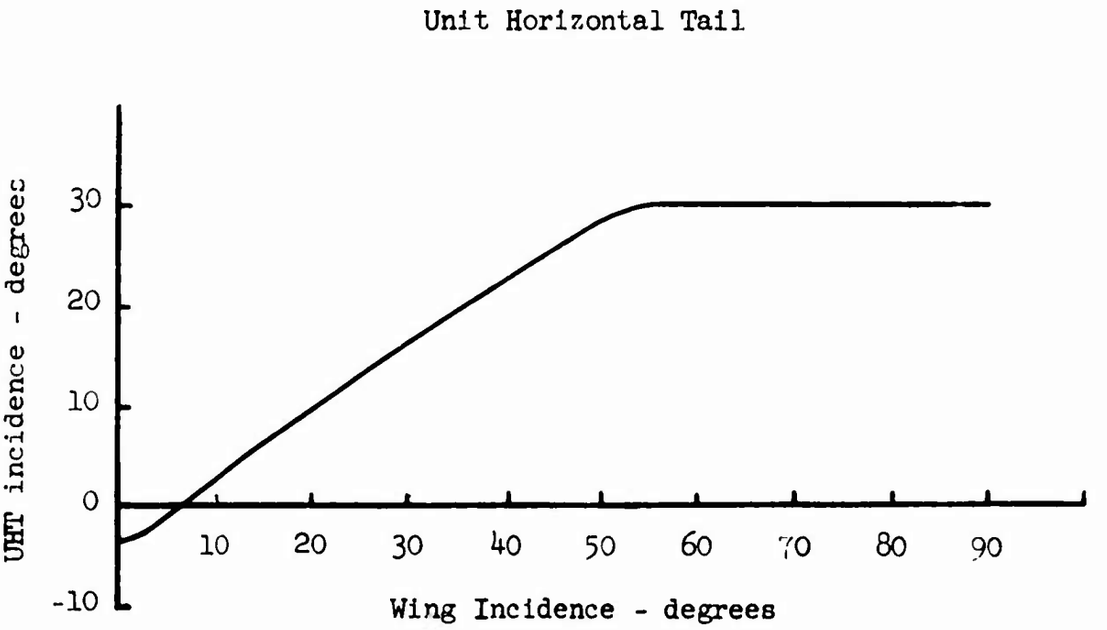

Figure 6

UHT and Tail Propeller Automatic
Trim Schedule

LIST OF ILLUSTRATIONS

1. Figure 1 - Wing-Flap Program
2. Figure 2 - Block Diagram of XC-142A Wing-Flap System
3. Figure 3 - XC-142A Wing Actuators
4. Figure 4 - XC-142A Flap Drive System
5. Figure 5 - Hydraulic Schematic - XC-142A Wing and Flap System
6. Figure 6 - U.H.T. and Tail Propeller Automatic Trim Schedule

X-22A VARIABLE STABILITY SYSTEM

J. L. Beilman

Cornell Aeronautical Laboratory

X-22A VARIABLE STABILITY SYSTEM

By John L. Beilman

Cornell Aeronautical Laboratory, Inc.

INTRODUCTION

Of all the present crop of VTOL research aircraft, only the X-22A will have a variable stability and control system, designed and constructed as an integral part of the basic airplane. In fact, this is the first time that a new type of aircraft has been planned from the beginning to be a variable stability and control airplane.

The variable stability and control capability, in conjunction with the high control power of the basic airplane, will make the X-22A unique and a highly useful and versatile tool for research into the flying qualities of the VTOL class of aircraft.

Experience with variable stability airplanes has shown that many engineering test-pilots do not appreciate the effectiveness of the "variable stability" concept until they have flown a variable stability airplane. Since flying qualities research is a highly specialized field and, for the most part, only pilots have observed the variable stability airplane in operation, it seems reasonable to assume that many engineers in the aeronautical field may not appreciate the variable stability concept. Therefore it may be profitable to begin this presentation with a functional definition of a "variable stability airplane", a brief enumeration of its possible uses, advantages and limitations and a description of the general features of mechanization.

DESCRIPTION OF A VARIABLE STABILITY AIRPLANE

A variable stability airplane may be defined as an airplane equipped with an automatic-control system in such a way that significant parameters of the airplane's motion and control, in or about one or more axes, may be altered in flight in a predictable manner. An auxiliary but very necessary part of the automatic-control system is an adjustable "artificial-feel" system for each axis of variable stability.

For example, a three-axis variable stability airplane might be capable of changing the frequencies and damping of the controlled airplane about the pitching, rolling and yawing axes and at the same time changing the coupling that exists between these axes from that which exists in the basic airplane. The artificial feel system is important because it provides coupling between the pilot and the airplane and it is the closed-loop pilot-airplane system that is of primary interest in the use of a variable stability airplane, whether that use be research, training or education. "Flying qualities" is the term used to describe the suitability, from the pilot's viewpoint, of a closed-loop pilot-airplane system for a specified task.

Uses

The research use of a variable stability airplane generally involves the evaluation of the suitability of a specified set of flying qualities for a designated mission or task. The specified flying qualities, in turn, may be related to a basic research program or evaluation of a particular airplane design. For example, Cornell Aeronautical Laboratory, Inc. has done programs to establish minimum flying qualities and to evaluate flying qualities for re-entry vehicles, but has also done programs to simulate and evaluate the B-58, TSR.2, C-5A and SST.

The training use of a variable stability airplane may be related to learning new techniques to control a new vehicle or to perform a new task. For example, a CAL variable stability airplane has been used for X-15 pilot training in the re-entry task.

The educational use of a variable stability airplane is illustrated by the CAL owned B-26's which provide flight demonstrations to student test-pilots and engineers of the Air Force, Navy and FAA. These flight demonstrations are closely correlated with classroom instruction in airplane stability and control.

Advantages and Limitations

The chief advantage of a variable stability airplane is the high fidelity of simulation which it provides. The proprioceptive cues are present and, in VFR flight, all of the visual cues external to the airplane are present. The environment is real - that is, the forces which are pushing the pilot down in the seat are also bending the wings - and this can have a significant effect on the pilot as a controller. For these reasons, the pilot evaluations are more likely to be the same for the flying qualities of the simulated airplane as for the real airplane.

As with any type of simulation, the variable stability airplane has its limitations. If very high gains are required there may be objectionable noise in the flight control system or other distracting side effects. If the true speed of the variable stability airplane and that of the simulated airplane differ by too much the simulation will be imperfect (unless direct control of lift is provided) because the pitching rate and normal acceleration cannot be matched properly at the same time. In most of the variable stability work done to date this has not been a significant limitation. Another imperfection of the variable stability airplane as a simulator is that usually the cockpit environment, i.e. location of instruments and controls, field of view, etc., is not the same as in the airplane being simulated. However, this is usually a matter of cost and not a fundamental limitation.

Mechanization

So far, a functional definition of a variable stability airplane has been given and some of its uses, advantages and limitations have been cited. To complete the introduction, the general features of mechanization of a variable stability system (VSS) will be described. (Figure 1).

First, there must be a provision, in each controlled axis, for taking hold of the airplane's flight control system with a servo of adequate power. This servo, usually electro-hydraulic, should have a natural frequency an order of magnitude higher than the highest frequency at which one anticipates forcing the airplane. This is necessary because it is important that the time lags at maneuvering frequencies be insignificant. The servo must be capable of responding to VSS electrical signals.

Secondly, there must be a system of sensors and signal processing equipment, adequate for the design goals of the VSS, which can measure all of the airplane response variables of interest. These response variables are the rigid body motions, aerodynamic quantities, and the time derivatives of these variables as required for each controlled axis. There must then be a means for selecting, proportioning and phasing, within the variable stability system, those variables which it is desired to control in a closed-loop manner. This selection, proportioning and phasing (±180°) may be done manually by the pilot or programmed automatically with some airplane variable, e.g. velocity.

Finally, as stated earlier, there must be an artificial feel system which permits changing control force gradients, nonlinearities such as breakout forces or preload, and gearing between the aerodynamic flight controls and the pilot's inputs.

DESIGN CONSIDERATIONS FOR THE X-22A VSS

It is not the purpose of this paper to discuss the many detailed flying qualities considerations from which the design criteria for a VTOL VSS can be derived. However, a few general considerations will be described which have a major influence on the functional configuration of the X-22A VSS.

Wind tunnel model tests and flight tests have proven the vertical take-off capability of several VTOL configurations. These tests have also revealed new dynamic and flying qualities problems peculiar to these vehicles in hovering and transition flight. The proposed flying qualities requirements for VTOL's rely chiefly on the results of fixed-base simulator studies and extrapolations from helicopter flying qualities specifications.

Hovering and Conventional Flight

To be most useful as a research airplane, the Bell X-22A must be capable of varying all of the significant flying qualities parameters over a range of values sufficient to represent VTOL's as a class of airplanes. The design ranges of selected stability and control parameters which have been shown to be significant to flying qualities are listed in Table I for hovering flight and Table II for conventional flight. Both tables refer to Figure 2 for boundaries defining frequencies, damping ratios and time constants shown to be significant to flying qualities.

An elementary point that may not be obvious should be noted in connection with these tables, i.e., the VSS cannot force the airplane to operate outside of its performance envelope. The fact that the parameters listed can be varied over wide ranges and to large values is due to the large amount of control power available in the X-22A. These control powers, in hovering flight, exceed 3 rad/sec^2 about the pitch and roll axes and 2 rad/sec^2 about the yaw axis. For comparison, Table III lists the maximum control powers available in a number of current VTOL airplanes.

Transition Flight

The transition from hovering, thrust-supported flight to conventional aerodynamic flight represents the newest area in which flying qualities requirements need to be defined. Since this task is unique to the VTOL airplane, the X-22A VSS must be capable of simulating those aspects of airplane motion and control which are characteristic of transition. Consequently, major emphasis in the X-22A VSS design was placed upon the transition capabilities. The capabilities listed earlier of varying the control gearing, the statics and dynamics of the longitudinal and lateral modes and of varying the control forces, in hovering and conventional flight, come about as special cases of a VSS designed to operate continuously over the velocity range represented by these types of flight. In addition, however, it is important that the X-22A VSS have the capability of:

1. varying transition time histories, both accelerative and decelerative. The prime parameters are airspeed and percent conversion.
2. varying the longitudinal trim change that can occur during transition.
3. varying lateral and longitudinal control power during transition.
4. varying time lags in the response of power plant to an order for thrust change.
5. varying the control cross-coupling and phasing during transition.

The requirement to modify the flying qualities during transition imposes the additional requirement that the VSS must incorporate an airspeed sensor capable of operating down to zero and even negative values of airspeed (hovering in a tailwind).

Response-Feedback vs. Model-Following

A major decision affecting the mechanization of the X-22A VSS was the choice between two techniques of closed-loop control: response-feedback or model-following. In the response-feedback approach, control surfaces respond to signals proportional to perturbations from some reference flight condition of chosen airframe flight variables (for example, $\Delta\alpha$, ΔV , q) as well as pilot commands. The closed-loop airframe response or dynamic characteristics depend on the particular flight variables fed back, and on the amount they affect the existing characteristics of the basic airplane. Response feedback gains alter airplane derivatives. Thus, the response-feedback approach is in essence a derivative-matching approach; that is, feedback gains are used to alter derivatives of the basic airplane in order to match the simulated airplane in some sense. The model-following approach differs in that the closed-loop research airplane tries to match the responses of a model whose equations are programmed on an airborne computer. The computer is flown by the test pilot and its outputs are the desired responses of the research airplane. In this case the control surfaces respond to error signals that are the difference between model flight variables and the corresponding airplane flight variables. The model-following approach is essentially a response-matching approach.

Both the response-feedback and the model-following systems have their advantages and disadvantages. The response-feedback system, in general, weighs less since no computer for the model is involved. However, the response-feedback system requires careful calibration if it is to be used effectively for in-flight simulations. The model-following system, by contrast, weighs more because it requires an airborne computer but this minimizes calibration problems because desired model dynamics can be programmed on the computer in a straightforward and consistent manner.

The response-feedback technique was chosen for the X-22A VSS for the following reasons.

(1) The weight and space advantage.

(2) The model-following approach was a relatively new and unproven approach. No flight experience existed to show that the hoped-for ease of calibration of a model following system could actually be realized. The response-feedback system has been proved through many hours of flight experience, and many problems, unforeseen in designs of early systems, have now been uncovered and solved.

(3) A response-feedback system can be used quite simply to alter a few, or even just one, of the characteristics of an airplane. For example, two gains, δ_e/α and $\delta_e/\dot{\alpha}$, can be used to vary short period frequency and damping (or just static stability) without affecting the rest of the basic airplane. Before this can be done with a model-following system all the characteristics of the airplane must be included in the model, and no advantage can be taken of inherent characteristics. The implications relative to the computer are staggering for a VTOL like the X-22A

which has extremely complicated and not well defined aerodynamic characteristics. The computer for the model would require a very large capacity -- perhaps only a large digital computer would suffice.

(4) Speed of response. A model-following system requires that the bandwidth of the closed-loop airplane be considerably higher than that of the model (by a factor of at least 1.5 and preferably 3). For example, one of the more difficult tasks for a model-following system is to follow a model of the basic research airplane. Because of the broad range of natural frequencies found in VTOL's, and because they are usually slow responding airplanes at low speeds, it was felt that adequate bandwidth or speed of response would be hard to obtain with the X-22A. Furthermore, the high vibration levels in the X-22A would make it doubly difficult to realize the higher gains required in a model-following system.

The design of the X-22A variable stability system, once response-feedback was selected as the approach, depended on selecting appropriate variables to be fed back to the controls. Here, past experience became a valuable asset. Numerical calculations were performed to determine whether selected gains will, for realizable values, modify the basic airplane characteristics to the desired degree. For this purpose linear analysis techniques, mostly root-locus analyses, were used. These were supported by analog computer simulation to obtain transient response records and to allow incorporation of nonlinearities.

DESCRIPTION OF X-22A VSS

The X-22A VSS can be characterized, in terms of the various functional features it incorporates, as follows:

FLIGHT CONTROL SYSTEM

In hovering flight the X-22A employs fore and aft differential blade pitch for pitching moments, left and right differential blade pitch for rolling moments and left and right differential vane (elevon) deflection for yawing moments. In forward flight fore and aft differential vane deflection is used for pitching moments, left and right differential vane deflection for rolling moments and left and right differential blade pitch for yawing moments. A mechanical mixer is used to direct and proportion the pilot's commands to the appropriate propellers and vanes as a function of the duct angle.

There are four VSS control axes - thrust, pitch, roll and yaw. Electrohydraulic servos are employed in each axis. When rigged for VSS flight the left hand flight controls are mechanically disconnected from the right hand flight controls and the primary flight control system. This is accomplished by a ground removable linkage. The evaluation pilot occupies the left hand seat; the safety pilot and airplane commander occupies the right hand seat. The VSS thrust servo operates the boost servo for the collective pitch system. The VSS pitch, roll and yaw servos operate the right hand

flight controls, moving the same linkages which are moved manually by the right hand pilot in normal non-VSS flight. In fact these same actuators serve a dual role by providing artificial feel for the primary flight control system. Phasing of these control motions to the blades and vanes is accomplished by the mechanical mixer as for normal flight.

When the evaluation pilot's flight controls are disconnected from the primary system for VSS flight, they are connected to a set of VSS pitch, roll and yaw artificial feel servos.

GAIN PROGRAMMING

The most significant new feature of the X-22A VSS is the capability of automatically and continuously adjusting the response-feedback and control system gains with airspeed. This is accomplished by a system of function generators which track velocity. The additional system complexity required to do this is justified by the overriding importance of having a variable stability VTOL capable of performing flying qualities investigations in transition flight.

The airspeed envelope of the X-22A extends from -35 to +300 knots, and transition occurs in the lower half of this range. In general, the stability and control derivatives change most rapidly between -35 and +60 knots, a range of airspeed in which conventional airspeed systems are incapable of operating. Thus, the emphasis on transition flight capabilities for the X-22A VSS created the demand for an accurate low-range airspeed system, compatible with the configuration of the X-22A airplane. The airspeed system which has been developed for this purpose, given the acronym LORAS, will be described later.

The upper velocity limit of transition for the X-22A is generally in excess of 100 knots and may be as high as 160 knots. Since the maximum velocity which can be measured by the LORAS is approximately 100 knots, it is necessary to obtain velocity information from a conventional airspeed system at the higher transition velocities.

Velocity Mixing

Because different airspeed systems are used for low-speed and high-speed measurements, there is a crossover region where both systems are capable of making the necessary measurements. The velocity function generators must operate smoothly and continuously at all airspeeds from hover through transition. This requires that the outputs from the two systems be mixed to obtain a single airspeed signal usable at all speeds. Figure 3 is a functional block diagram of this velocity mixing system.

It is difficult to say, in advance of flight tests, just what the optimum crossover airspeed will be, but it will probably be in the vicinity of 60 to 70 knots. Furthermore, the weighting functions $F_1(u_V)$ and $F_2(u_V)$ are not unique, but once either one is arbitrarily selected the other is defined in accordance with the equation for the static gain given in Figure 3. Criteria have been developed for the stability of the system shown in Figure 3.

Although they are not inside the closed loop of the function generator, as the two airspeed signals are, there are other analogous phasings between signal sources which must be made during transition, e.g., between the lateral component of velocity, v, derived from the LORAS at low speeds and the sideslip angle, β, as measured by an airstream direction vane at high speeds, or between the vertical component of velocity, w, obtained by integrating incremental normal acceleration at low speeds and the angle of attack, α, also measured by a vane at high speeds.

Circuit Details

The X-22A function generator system consists of 48 channels of gain programming in 4 drawers of 12 channels each. One drawer is the master unit, providing the mixing of the two velocity signals and tracking the weighted signal. The other drawers are slaved to the master unit.

A block diagram of a typical function generator channel is given in Figure No. 4. The multi-tap potentiometers are servo driven by the velocity signal u. The function generator input voltage E_{IN} is impressed across a string of fifty resistors which forms a voltage divider with 2% steps of the total input voltage. The function can reverse sign since any point along the voltage divider can be grounded. The function is programmed on a special printed circuit card, Figure 5. Each vertical conducting strip on the card, corresponding to a tap on the potentiometer and therefore to a particular value of u, is connected to the horizontal strip on the card which provides the desired gain. The design of the card is such that the physical arrangement of the connections becomes the geometrical analog of the function.

The required functions are generated by 18 straight line segments corresponding to equal intervals of velocity. The potentiometer provides linear interpolation between the gains corresponding to the end points of each interval. Loading errors are minimized by a 1000 to 1 step-up in impedance levels from the resistance network to the amplifier input. However, a special test board and x-y recorder facilitate experimental determination of the optimum fit to any desired function.

The unity-gain conducting segment at one end of the tapped potentiometer (Figure 4) permits bypassing the function generators by introducing a command signal to the servo which is greater than that to which the actual velocity signal is diode limited. This feature will be very convenient for flying qualities investigations in hovering and conventional flight. It eliminates the task of compensating for the function card in each channel when setting up the required VSS gains for different hovering and conventional flight configurations. The functions on these cards would change with the transition trajectories being investigated so that the required compensation would be intractable.

LOW RANGE AIRSPEED SYSTEM

Although the LORAS is undoubtedly of considerable interest as a basic measuring system, a highly detailed account of its design and construction features would represent too great a digression from the

description of the X-22A VSS. Consequently only a brief discussion of its theory of operation will be undertaken, delineating its significant features and presenting some of the experimental data in order to illustrate the kind of performance so far obtained.

Theory of Operation

The accuracy of conventional airspeed measurement systems deteriorates at low speeds because they rely on a pressure difference, Δp, from a pitot-static tube, which is proportional to the square of the velocity, V^2. The sensitivity, in terms of $\Delta p/V$, becomes very poor as the velocity approaches zero. To circumvent this problem in the X-22A, i.e. to get an accurate measurement of velocity down to zero and even negative airspeeds, an arrangement is utilized in which the pressure sensor dynamically operates at a higher level of pressure than that due to the airplane velocity alone.

Figure 6 shows the LORAS installed on the vertical tail of the X-22A. Figure 7 is a schematic view of the tube with the pertinent velocity vectors. A horizontal tube, two feet long, is mounted so that it can spin about a vertical axis. It is driven by a motor at a spin rate of 1600 rpm. At each end, it has a shielded pitot tube. The two pitot pressures are transmitted to a differential pressure gage located on the spin axis.

At zero airspeed, each pitot tube senses the pressure due to the rotational velocity. There is no pressure difference, and the output of the transducer is zero.

If the aircraft is moving forward, the advancing pitot tube will sense an increased pressure, while the retreating tube will sense a reduced pressure. Thus the transducer will sense a pressure difference. This difference will vary sinusoidally, and the magnitude of the variation will be a measure of airspeed.

To see this, we refer to Figure 7 and write

$$V_{h_1}^2 = (V_\omega + V\sin\theta)^2 + (V\cos\theta)^2$$
$$= V_\omega^2 + 2VV_\omega \sin\theta + V^2$$

Similarly,

$$V_{h_2}^2 = V_\omega^2 - 2VV_\omega \sin\theta + V^2$$

The pressure difference sensed by the transducer is

$$\Delta p = \frac{1}{2}\rho V_{h_1}^2 - \frac{1}{2}\rho V_{h_2}^2$$
$$\Delta p = 2\rho V V_\omega \sin\theta$$

The significant point to be noted is that Δp is linearly proportional to V, so that the system maintains a constant sensitivity all the way down to zero airspeed.

To illustrate what this sensitivity is for the X-22A LORAS configuration we divide both sides of the above equation by V and get

$$\frac{\Delta p}{V} = 2\rho V_\omega \sin\theta$$

Since $\theta = \omega t$, this term can be ignored as the cyclic variation in the sensitivity. We then have for the amplitude of this function

$$\frac{\Delta p}{V} = 2\rho V_\omega = 2\rho \mathcal{R}\omega = 4\pi\rho\mathcal{R}f$$

Using values for a standard atmosphere, we substitute

$$\rho = .002378 \text{ slugs/ft}^3, \quad \mathcal{R} = 1.13 \text{ ft}, \quad f = 25.5 \text{ cps}$$

and get

$$\frac{\Delta p}{V} = 0.86 \frac{\text{psf}}{\text{ft/sec}} = \frac{.006 \text{ psi}}{\text{ft/sec}}$$

Although the preceding analysis and Figure 7 are greatly simplified, it can be shown for the general case that the system will measure the component of the total velocity vector in the plane of rotation, for any angle between this vector and the longitudinal axis of the airplane. Furthermore the measurement is independent of the angle of attack since any component of velocity perpendicular to the plane of rotation does not produce a cyclic variation in pressure.

A resolver which is synchronous with the rotating tube provides the body-axis components of forward and lateral velocity. The system is omnidirectional and measures rearward as well as forward airspeed.

Additional theoretical features of the operation of the LORAS are as follows:

1. Both sides of the differential pressure gage sense ambient static pressure when the tubes are rotating and the translational velocity of the system is zero. This is so because a pressure drop equal to the impact pressure occurs across the radius of the system. This pressure drop is not due to air flow but is just that which is required to counteract the centrifugal forces acting on the entrapped column of air.
2. Cyclic variations in pressure, due to translational velocity, are propagated down the tubes at the speed of sound and it is these variations which the gage senses. Since the radius is about one foot there is an acoustic time delay of about one millisecond. This results in about 10 degrees of phase shift at the spin rate used in the X-22A system, but the directional error due to this is cancelled out by the initial phasing of the resolver.

3. The tip Mach numbers are low enough that incompressible flow relations can be used to analyze the system.

Some of the operational features of the LORAS are as follows:

1. Temperature and static pressure corrections are introduced in such a way that the crossover requirements between the LORAS and pitot-static airspeed measurements are independent of altitude. That is, the compensation has the form of $\sqrt{\sigma}$ so that the LORAS output is indicated airspeed instead of true airspeed.
2. A 2000-cps suppressed carried system is used because the information frequency is about 25 cps.
3. The use of a single transducer on the axis of rotation avoids the problems of operating transducers in the large centrifugal force field at the tips (800 g acceleration).
4. It is important that the angular frequency of the LORAS spinning tubes be well separated from the structural mode frequencies of the mounting location to avoid extraneous inputs.

Figure 8 shows the station wagon which was used to conduct tests on the LORAS and Figure 9 shows the data obtained from a typical test run.

VSS BLOCK DIAGRAMS

To illustrate the X-22A VSS control axes the functional block diagrams of Figure 10 and 11 will be discussed. These show, respectively, the pitch axis, which is the most complex of the four VSS axes of control in the X-22A, and the thrust axis.

After passing through the function generators and manual gain controls, signals corresponding to the various airplane response and control system variables are summed to provide the signal Δ'_e. This signal represents the incremental command to the VSS pitch servo with two different compensations available. The derivative term $\dot{\Delta}'_e$ provides compensation for control system lags while the term $\Delta'_e \cdot f(u) \cdot \Delta B_c$ provides a variable static gain to account for changes in elevon effectiveness with duct exit dynamic pressure. The other two input signals summed with the compensated Δ'_e signal, are alternate methods provided to eliminate control system transients and airplane trim disturbances when the VSS is engaged. These signals remain constant after engaging the VSS. The manual balance circuit provides a backup for the automatic balance system and also has considerable utility for system monitoring and troubleshooting. During VSS operation the SAS is effectively locked out by causing the two servos of the dual-redundant system to cancel at the mechanical summing point downstream from the VSS servo. By this means, failures in the locked out SAS will be detected if the cancellation is not within tolerances, yet for normal operation the VSS will not have to compensate for the SAS.

The upper right corner of Figure 10 shows the generation of the reference duct angle $\lambda_o(u)$ for transition and $\Delta\alpha$ for fixed operating point operation.

When the VSS-FBW switch in the input of the summing amplifier is in the FBW (Fly by Wire) position, the pitch servo is commanded only by the evaluation pilot's stick position without any feedback of response variables.

The source of each response feedback and control system signal shown on Figure 10 and its purpose is given in Table IV.

The thrust-axis block diagram, Figure 11, shows the various airplane response and control system variables being summed to provide the signal, Δ'_B. This signal plus its derivative are then fed through the switch path "VSS" as the incremental command to the collective pitch servo. As in the pitch axis, automatic and manual balance signals are also summed at this point and, when the switch is in the "FBW" position, the only command to the thrust servo is from the evaluation pilot's collective-pitch stick. There is no SAS cancellation requirement in the thrust axis.

In addition to the response-feedback signals, whose source and purpose are listed in Table V, two special signal computations are shown on the block diagram. These are the computations of $\delta_{avg}{}^2$ and ΔB_c. Each vane has a dual-potentiometer position transducer, and the output of the first element provides the excitation for the second element. The average of these four squared signals is then obtained, giving $\delta_{avg}{}^2$. For the second computation a signal proportional to incremental collective-pitch, ΔB_c, is obtained by summing the reference angle, B_{c_o}, and that measured as the average of the four individual blade angles. The reference angle is generated by a function generator channel and modulated by the gain W/W_o. This gain is adjusted by the safety pilot, according to program, during flight in order to compensate for changes in weight due to fuel consumption.

Block diagrams for the roll and yaw axes are given in Figures 12 and 13 and the signal sources and purposes are given in Tables VI and VII. These will not be discussed in detail since the only significant difference from the axes already discussed is the inclusion of internal control-system cross-coupling (or decoupling), i.e. aileron servo per rudder servo and rudder servo per aileron servo.

ARTIFICIAL FEEL SYSTEM

Yaw Axis

The yaw axis artificial feel system, Figure 14, is the simplest and will be discussed first. There are three cockpit gain controls associated with the yaw axis:

1. Control K_{RP} provides adjustment of the force gradient in the rudder pedals. The second section of this control provides automatic adjustment of the servo loop gain so that stable operation can be achieved at the lowest stick force gradients (highest force loop gains) required by the VSS specification.
2. Control K_{BOF} provides adjustment of the breakout force or preloading of the rudder pedals.

3. The "trim sensitivity" control governs the sensitivity of the evaluation pilot's VSS yaw trim control. For any given setting of the trim sensitivity, the pedal trimming force is proportional to the displacement of the yaw trim control from its indexed position. This is independent of the force gradient on the pedals.

The force gradient and breakout force controls are located on the right-hand console for the safety pilot whereas the yaw trim sensitivity control (and yaw trim control) is located on the left-hand console for the evaluation pilot.

Filter

The notch and low-pass filter is included in the design of the force loop to eliminate or reduce structural and inertial resonances. The pedal position differentiator is included to provide damping or undamping of the pedal servo system, as dictated by the test results on the control system test stand.

Function Generator

The function generator $f(u)$ shown in the force signal chain is provided to automatically adjust the pedal force gradient with speed. It is analogous in function to the first section of the cockpit control for setting the force gradient except that it is automatically programmed with speed. It would be desirable to program the loop gain with speed also (analogous to the second section of the cockpit force gradient control) except that there are not enough function generator channels available to do this. Tests on the Control System Test Stand will indicate whether it is in fact feasible to proceed as the diagrams indicate or whether it is imperative that the servo loop gain be programmed by a function generator. If the latter should be the case, a function generator channel will have to be taken from some other signal channel considered at such time to be of lower priority.

VSS-FBW

The VSS-FBW (Fly-by-Wire) switch bypasses the rudder pedal and yaw control characteristics set up on the right-hand console and provides a set of rudder pedal and yaw control characteristics suitable for flying the basic, non-VSS X-22A. Two discrete sets of FBW yaw control characteristics will be provided, depending on the duct angle when the FBW system is engaged. This FBW feature is included in the design so that the evaluation pilot can assist the safety pilot on VSS flights by flying the airplane while the safety pilot is setting up gains on the VSS console. The aircraft should not be flown through transition on the FBW system because of switching effects in the artificial feel system and it is not the purpose of the FBW feature to make the X-22A a two-place or two-control airplane when it is rigged for VSS flights.

Roll Axis

The roll-axis artificial feel system (Figure 15) is similar to the yaw axis artificial-feel system in all respects except trimming characteristics. Therefore, only the roll-axis trimming characteristics will be discussed here.

Two types of trimming are provided for the roll (and pitch) axis so that both airplane and helicopter type trim systems can be simulated and evaluated. These two types are referred to as rate trim and nulling trim, respectively. A selector switch on the left-hand console will permit the evaluation pilot to select either type, but roll and pitch will always be alike (i.e., rate trim on both or nulling trim on both). Whichever type of trim is selected, the normal trim button on the top of the stick grip will always be used for actual trimming of the airplane. Furthermore, the roll (and pitch) trimming systems will be automatically reset or balanced each time the feel system is disengaged.

A considerable amount of circuitry is required to implement the trimming systems and for the following discussions the diagram of Figure 15 is, at best, a rough guide.

Rate Trim

When the trim mode selector switch is in the rate position and the pilot actuates the trim button on the stick grip, the out-of-trim force will be relieved at a rate determined by the setting of the trim rate control. For any given setting of this control the trimming rate, in pounds per second, will be independent of the force gradient in the stick. Setting in a breakout force with the breakout force circuit will introduce a nonlinearity in the trimming system. The magnitude of this nonlinearity will be proportional to the magnitude of the breakout force and inversely proportional to the force gradient, but any trimming difficulty which this causes will be the same difficulty which exists in trimming any control system with similar force gradients and breakout forces.

Nulling Trim

When the trim selector switch is in the "nulling" position the pilot needs only to actuate the trim button on the stick grip for about one second. When he releases the trim button the stick will automatically be in trim.

Either rate or nulling trim may be selected when aileron stick displacement has been selected as the command signal to the rolling moment producer. However, selection of aileron stick force as the command signal to the rolling moment producer overrides the trim selector switch and only rate trim is then available. The reason for this is that the nulling type trim is associated only with a soft or low force gradient (ergo large displacement) as in helicopters, and the selection of stick force as a command signal implies a stiff or high force gradient stick configuration. Since the type of trim is always the same for both pitch and roll, this means that nulling trim can be had only when stick displacement signals have been selected as moment

command signals for both pitch and roll. Conversely, if a stick force signal has been selected as a command signal on either axis, then both axes will have only rate trim available.

Finally, it should be noted that the roll trimming system operation is such that regardless of the configuration (i.e., rate of nulling trim, stick force or displacement command) forces are trimmed off the stick without changing the stick position. Note also that, to simplify the system, it is assumed that the amount of roll trim required will in general be so small that the change in aileron stick position with speed, due to the function generator, will be negligible.

Pitch Axis

The pitch-axis artificial-feel system (Figure 16) is similar to the roll-axis artificial-feel system discussed above, with the following exceptions:

1. Normal acceleration and pitching acceleration signals can be introduced to change the forces on the stick.
2. A stick position trim control is provided so the zero-force position of the stick can be changed without altering the airplane trim. This feature will be useful for VSS studies involving very low gearing between the stick and pitching moment producers.
3. The trimming system is mechanized differently because the simplifying assumption made for the roll axis - that very little trim will be required - cannot be made for the pitch axis. Very large changes in pitch trim will be required during transition, for example. However, so far as the pilot is concerned, operation of the pitch trim system will be just like the roll trim system with the one exception that, when force signals have been selected as commands to the pitching moment producer, the stick position will change as the airplane is trimmed.

The design changes which result in the pitch axis then, as a result of accommodating large trim changes but still satisfying the criteria that the stick position should not change with speed, are as follows:

a. Summing of trim signals and stick force signals is done at the stick servo summing amplifier. Since the only signal going through the function generator (FG 2-6) is the stick force signal, which will be zero in trim flight, there will be no change in stick position due to speed alone.

b. To maintain trimming rate constant and a function only of the trim rate control setting, compensation must now be introduced to keep a fixed relationship between volts due to force and volts due to trim at the stick servo summing amplifier. This requires addition of a third section (18-3) to the force gradient control (18-1) and the use of another function generator channel (FG 2-7) which will be the inverse of the function in FG 2-6.

VSS EQUIPMENT

The equipment required for the VSS is located throughout the X-22A, from the angle of attack and sideslip vanes on the boom ahead of the nose to the LORAS rotating tubes on top of the vertical fin. Indicators, controls and switches are located on the instrument panel and all three cockpit consoles. An attitude gyro and 3-axis rate-gyro and accelerometer units are located in the fuselage near the C.G. Position pickoffs are located on all four vanes in the ducts, all four blade-pitch mechanisms, and on the ducts themselves. There are also position pickoffs, servovalves and hydraulic actuators for pitch, roll and yaw control and for artificial feel in each of these control axes. Strain gages are installed on the evaluation pilot's flight controls to sense control forces.

Major Units

The three main electronics chassis of the VSS are installed on the right hand side of the airplane immediately aft of the pilot.

The first of these is the VSS Equipment Center, Figures 17 and 18. In Figure 17, reading left to right and top to bottom, the first five drawers of equipment perform the dual function of providing signals which are required for the flight test of the basic airplane as well as for the VSS. Along with Drawer No. 10, the VSS power drawer, this equipment is known as the "shared instrumentation" because of its dual role.

The remaining six drawers of the equipment center contain specialized VSS equipment, including the electronics for the four VSS servos and the three artificial feel servos.

Figure 19 shows the second major electronics chassis, the Function Generator Unit. Figure 20 shows the third major electronics chassis, the Recording Control Unit. This unit facilitates calibrating and monitoring the VSS operation. A patch panel permits selection of 50 signals out of 80 signals available for recording. These signals can be recorded on FM tape as well as on oscillograph paper. An integral part of the Recording Control Unit is a dual 60-point commutator which permits recording, in analog form, the setting of every switch and gain control in the VSS. Thus each VSS flight record will automatically contain all the pertinent data as to VSS configuration, gains and recording system scale factors.

Figure 21 shows the LORAS rotating head unit which mounts on top of the X-22A vertical fin. Figure 22 shows the cockpit gain control which consists of one panel each for thrust, pitch, roll and yaw. Figure 23 is a close-up of the pitch axis panel showing the controls (Digitrols) which are color coded to identify the axis - green for thrust, gold for pitch, blue for yaw and gray for roll. The signal affected is denoted by the engraved black button.

Equipment Details

Many detailed items of equipment developed at CAL for variable stability airplanes have been employed or further refined for use in the X-22A VSS.

The Digitrols shown in Figure 23 are one such example. Conserving panel space and providing a digitized readout, they can quickly be set with a gloved hand to an accuracy of 0.25% of full scale.

The angle of attack and angle of sideslip vanes are another example. The lifting surfaces on these vanes are foamed plastic molded onto a hollow aluminum tube. In combination with a size 8 synchro, this arrangement results in a very low moment of inertia vane. A low moment of inertia is necessary to get a short response time. For the X-22A VSS it is desirable to achieve a short response time down to the lowest airspeeds at which the flow around the airplane permits using the vanes to measure the angles of attack and sideslip.

Electrically, the VSS is a 400-cps suppressed carrier system requiring about 500 VA of power. Many of the basic solid-state circuits, developed by CAL, have been in use for nearly four years in various CAL operated variable stability airplanes. For the X-22A program, principally to reduce weight and volume, these circuits were repackaged in a standard module form. Five of these modules are shown in Figure 24. Many new circuits were developed for the X-22A and there are approximately 30 different modules used in the VSS. Figure 25 shows a typical equipment drawer with the modules installed.

All of the modules have been tested and operate satisfactorily:

1. throughout the temperature range of -54°C to +85°C
2. in a 10-g vibration environment (zero to 500 cps) and
3. in an acoustical noise level of 148 db.

The weight of the VSS electronics was kept about 10% below the target value by strict attention to all detail parts as well as major units. Use of a 300-volt, aluminized-mylar shielded cable also resulted in a significant reduction in weight.

FLIGHT OPERATION OF VSS

To complete the picture of the X-22A VSS it will be helpful to consider how it will be operated in flight. Certain modifications are required to change from the basic X-22A to the VSS X-22A.

X-22A VSS Configuration

When the X-22A is rigged for VSS flight the thrust control system is set to operate in the "collective-pitch control" mode as contrasted with the "throttle control" mode. In the collective-pitch control mode the pilot's collective-stick inputs command blade angle directly and the engine master-governor acts to maintain constant rpm. In the throttle control mode the pilot controls the engine fuel and the blade angle adjusts to absorb the power at the selected rpm. It is necessary to use the collective-pitch control mode for VSS operation because of its significantly shorter response time.

As pointed out earlier, the flight controls for the L.H. or evaluation pilot are mechanically disconnected from the primary flight control system and are restrained by the VSS artificial feel system. This means that the R.H. pilot must be airplane commander and safety pilot since only he can fly the airplane through the primary flight control system. Therefore, until sufficient experience is obtained with the X-22A and its VSS in flight, take offs and landings will be made by the pilot in the R.H. seat. It is worth noting that the interest in the vertical take off and landing task, from a flying qualities viewpoint, will provide a greater impetus for early use of the VSS during take offs and landings than has existed in the past with more conventional VSS airplanes.

Operating Modes of VSS

There are two basic modes of operation for the X-22A VSS. One is called the "transition mode" and the other is called the "fixed-operating-point" mode (F.O.P.).

Transition Mode

In the transition mode the appropriate response feedback gains and control gains are programmed with velocity. Once the VSS is engaged in hovering flight, the airplane can be flown through an accelerative transition to forward flight and then through a decelerative transition to hovering flight without any adjustment of the VSS gains by the safety pilot. Furthermore the acceleration can be high or low and can be terminated at intermediate transition velocities. A basic X-22A limitation on VSS transition flights is that the collective-pitch control cannot be used about 160 knots. This effectively means that the X-22A is a four control-axis VSS airplane in the speed range of 0 to 160 knots. If it is desired to use the VSS for flight investigations about 160 knots the airplane must be rigged for the "throttle-control" mode of engine operation in advance of flight. The X-22A is then a three control-axis VSS airplane throughout the entire speed range and has no thrust-axis control in hovering flight.

Fixed-Operating-Point Mode

In the F.O.P. mode of VSS operation the airplane is flown to a particular flight condition as defined by altitude, airspeed and duct angle. The required VSS gains are then set by the safety pilot and the VSS is engaged, giving control of the airplane to the evaluation pilot. The evaluation pilot then looks at the flying qualities for small perturbations from the trim flight or F.O.P. conditions. If the trim flight conditions deviate very far from the prescribed conditions, the configuration examined by the safety pilot will not be the desired configuration. It is the duty of the safety pilot to monitor the trim flight conditions.

Attitude Hold

A third mode of VSS operation, which is a special case of either the transition or F.O.P. modes, is one which provides an attitude-hold autopilot function. Any desired initial condition can be selected for heading angle, pitch angle and bank angle and any desired level of position and rate gains can be set for each channel. To keep within the space allotment for the VSS it was necessary to eliminate a nulling servo from the bank angle channel. Since the voltage in this channel is proportional to the sine of the bank angle the operation of this channel will become increasingly nonlinear as the initial bank angle exceeds 30 degrees but this is not a significant restriction.

Fly-By-Wire

A fourth mode of VSS operation is provided as a convenience and a safety feature. It is called the Fly-By-Wire (FBW) mode. Everytime the VSS is engaged it is automatically engaged in the FBW mode unless the evaluation pilot or safety pilot has pressed the magnetically reset "FBW-VSS" switch to the VSS position just prior to engagement. In the FBW mode the evaluation pilot flies the basic X-22A plus SAS through normal X-22A gearing between the vanes and blades and the L.H. control stick and pedals. However, only two discrete sets of control force gradients are available for FBW operation - one for low speed flight and one for high speed flight. Selection between these two levels of force gradients is automatically accomplished by a switch which is actuated at a duct angle of +5°

The FBW feature is convenient because it enables the evaluation pilot to fly the aircraft while the safety pilot is setting up a VSS configuration on the gain console. This enables the safety pilot to devote full attention to setting up the gains, which may still take several minutes, without having to navigate and clear the aircraft with other traffic. Accomplishment of both of these tasks by the safety pilot would represent a severe work load because setting the gains requires that he have his head and gaze down in the cockpit while the flying obviously requires that he have his head up.

An additional safety bonus of the FBW mode is that it provides at least a limited "two-place" capability for the X-22A in the event of disablement of the safety pilot during VSS flight operations.

VSS Flight Procedures

During a typical VSS flight the activities of the flight crew will be as follows. At the conclusion of evaluating a configuration the evaluation pilot will tell the safety pilot to take the airplane. Either pilot can disengage the VSS by pressing a button on the stick grip. The safety pilot will then ask the evaluation pilot to re-engage his feel servos and trim as necessary. If the VSS nullmeter on the instrument panel indicates all servos are properly nulled the safety pilot will then ask the evaluation pilot to take the airplane in the FBW mode while a new VSS configuration is being set up on the console. In addition to the gain console, the safety pilot will set the various switches as required to select control displacements or control forces as pilot inputs, to select the transition or F.C.P. mode, and, if the F.C.P. mode is selected, to select the LORAS or pitot-static system as the source of airspeed information.

After the new VSS configuration is set up, the safety pilot will then take control of the airplane, momentarily press the "FBW-VSS" switch to the VSS position, and ask the evaluation pilot to re-engage and trim his feel servos. The feel servo characteristics will now be determined by the settings on the gain console. When the evaluation pilot is ready to take the airplane, and if the servo error signal is zero on the nullmeter, the safety pilot will engage the VSS by pushing the "engage" button on his stick grip. While the VSS is engaged the nullmeter indicates the out-of-trim condition in the pitch-axis of the primary flight control system. The safety pilot can monitor this signal and retrim the primary flight control system to keep this signal small. This will not change the trim of the VSS airplane but will insure that the airplane will be in trim when control reverts to the primary system. Reversion to the primary system will occur when the L.H. pilot has completed his evaluation of a configuration or when one of the safety monitor limits has been exceeded as a result of maneuvering or turbulence.

Safety Monitoring

An automatic safety monitor circuit in the VSS will disengage the VSS, including the feel servos, whenever anyone of the following parameters exceeds a preset limit:

1. normal acceleration
2. lateral acceleration
3. longitudinal acceleration
4. sideslip angle
5. rolling acceleration
6. pitching acceleration
7. yawing acceleration
8. pitch servo amplifier voltage
9. roll servo amplifier voltage
10. yaw servo amplifier voltage
11. thrust servo amplifier voltage

In addition, the safety pilot will hold in his hand at all times during VSS operation a disengage switch on an extension cord. He will use this to disengage the VSS upon observation of any operation of the flight control system or condition of the airplane which he considers unsafe.

Whenever the VSS has been disengaged by operation of the safety monitor circuit both a visual cue and an auditory cue are given to the safety pilot to alert him to take control of the airplane.

VSS FLIGHT TEST PROGRAM

In conclusion, a brief outline of the initial VSS flight test program will be given. This is the program which precedes delivery of the two X-22A airplanes to the U.S. Navy Bureau of Weapons. Aside from calibrations of the LORAS and angles of attack and sideslip vanes, the purpose of this flight test program is to demonstrate that each response feedback loop can be closed at the required level of gain. The required level is that which is predicted to be necessary in order to vary the stability and control parameters listed in Tables I and II over the ranges indicated.

The first phase of the response feedback tests is called the open loop tests. For these tests very high sensitivities will be used in the recording system and all low pass filters will be switched out. Records will then be obtained in flight for an input pulse on each control axis. It is necessary that the input pulse contain frequencies at least as high as the highest structural frequencies expected. For this reason it will be convenient to use control force inputs on the VSS with no feedback of response variables. These records can then be analyzed to get the frequency response of each sensor to the control input. Each loop can then be closed analytically through the VSS to obtain the maximum gains obtainable before the onset of structural mode instability.

The next phase of the response feedback flight tests is called the closed loop tests. In these tests each loop is closed in flight and the gain is gradually increased to the specification value (related to Tables I and II) or to two-thirds of the maximum allowable gain predicted from the open loop tests, whichever is smaller. The closed loop tests must be done selectively and sometimes in combinations. For example, it may not be possible to get closed-loop records of a high VSS value of M_α without also using enough VSS $M_{\dot{\alpha}}$ or M_q to make the airplane flyable.

As a result of the open-loop and closed loop tests it may be necessary to relocate certain sensors (gyros, accelerometers, vanes etc.), to introduce additional filtering (low-pass, band-reject or notch) or, failing in these remedial efforts, simply to accept lower gain limitations than the ideal.

LIST OF ILLUSTRATIONS

Figure	
1	Basic Loops of a Variable Stability System
2	Boundaries Defining Frequencies, Damping Ratios, and Time Constants Shown Significant to Flying Qualities
3	Functional Block Diagram of the Velocity Mixing System
4	Function Generator
5	Function Generator Card
6	LORAS Installed on the X-22A Fin
	Diagram for Finding Relative Airspeed at Tips of Spinning Tube
8	LORAS Test Vehicle
9	Low Range Airspeed System Test Results
10	Variable Stability and Control System Functional Block Diagram - Pitch Control
11	Variable Stability and Control System Functional Block Diagram - Thrust Control
12	Variable Stability and Control System Functional Block Diagram - Roll Control
13	Variable Stability and Control System Functional Block Diagram - Yaw Control
14	Artificial Feel System Yaw Axis
15	Artificial Feel System Roll Axis
16	Artificial Feel System Pitch Axis
17	VSS Equipment Center - Front View
18	VSS Equipment Center - Rear View
19	Function Generator
20	Recording Control Unit
21	LORAS Rotating Head Assembly
22	Right Hand Cockpit Console Gain Controls
23	VSS Cockpit Gain Controls - Pitch Axis Panel
24	VSS Modules
25	Typical Equipment Drawer

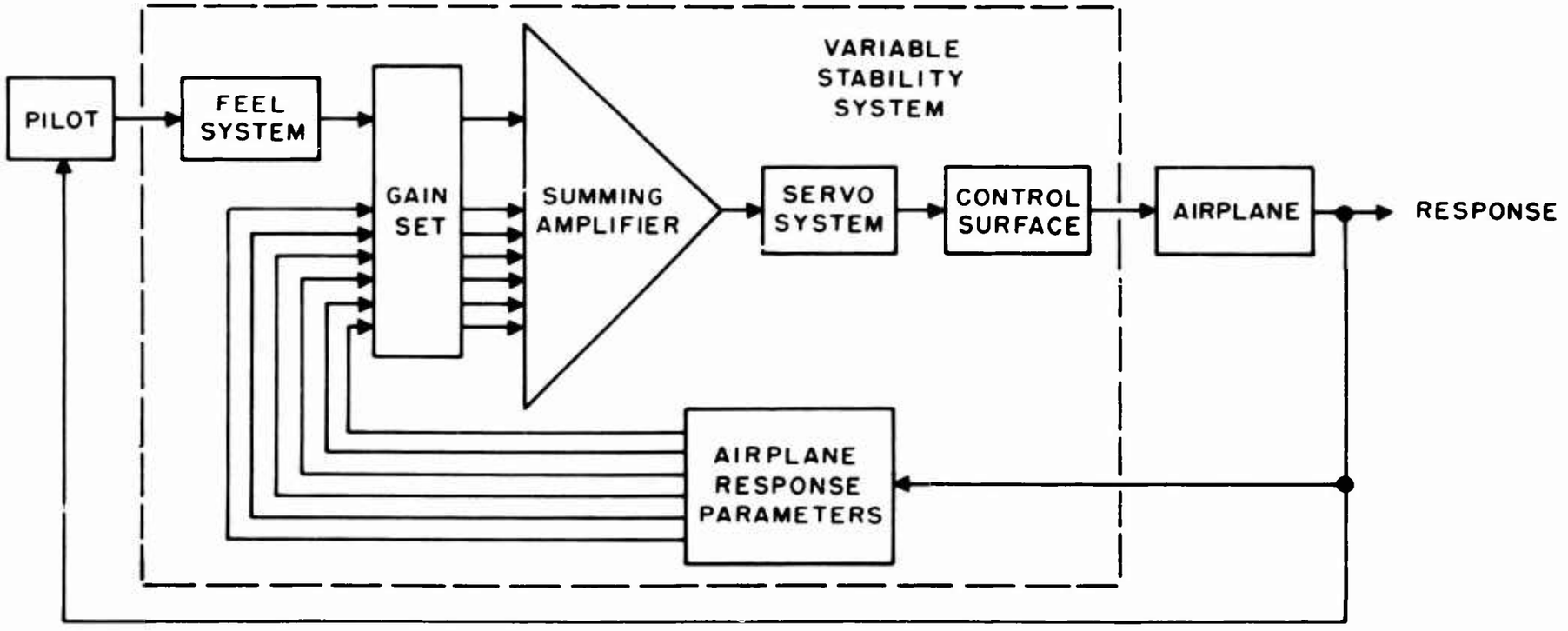

FIGURE 1 BASIC LOOPS OF A VARIABLE STABILITY SYSTEM

LIST OF TABLES

Table	
I	Ranges of Selected Stability and Control Parameters that have Been Shown Significant to Flying Qualities - Hover
II	Ranges of Selected Stability and Control Parameters that have Been Shown Significant to Flying Qualities - Conventional Flight
III	Maximum Control Power for Various VTOL Airplanes in Hover
IV	Function of Gains - Pitch Axis
V	Function of Gains - Thrust Axis
VI	Function of Gains - Roll Axis
VII	Function of Gains - Yaw Axis

FIGURE 4 FUNCTION GENERATOR

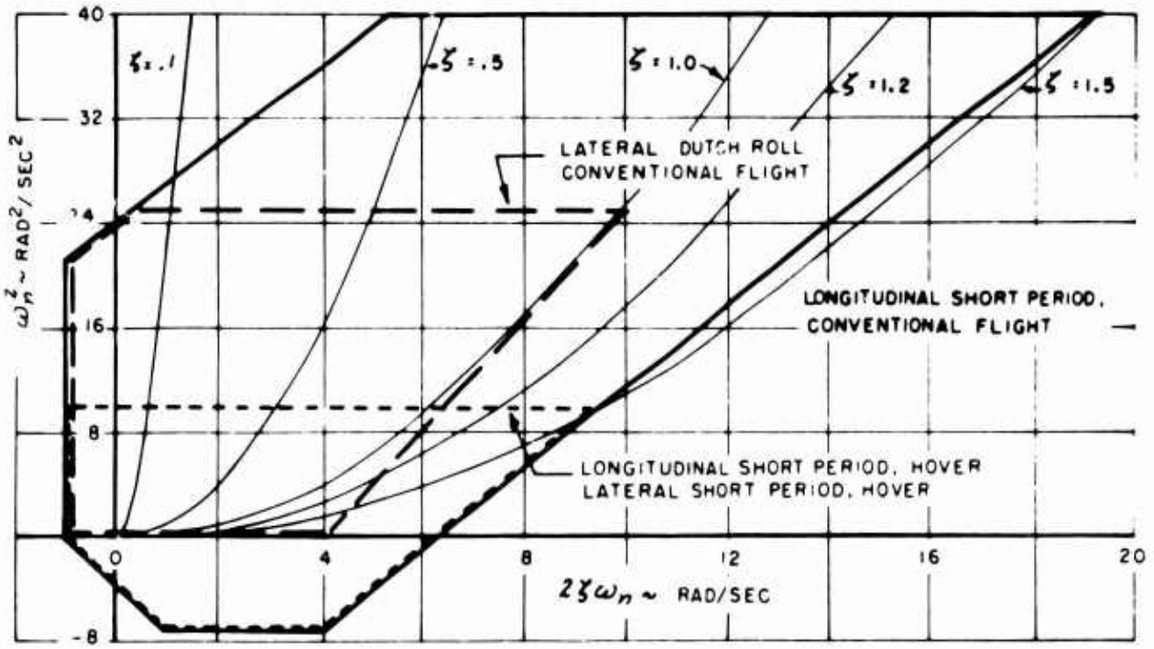

FIGURE 2 BOUNDARIES DEFINING FREQUENCIES, DAMPING RATIOS, AND TIME CONSTANTS SHOWN SIGNIFICANT TO FLYING QUALITIES

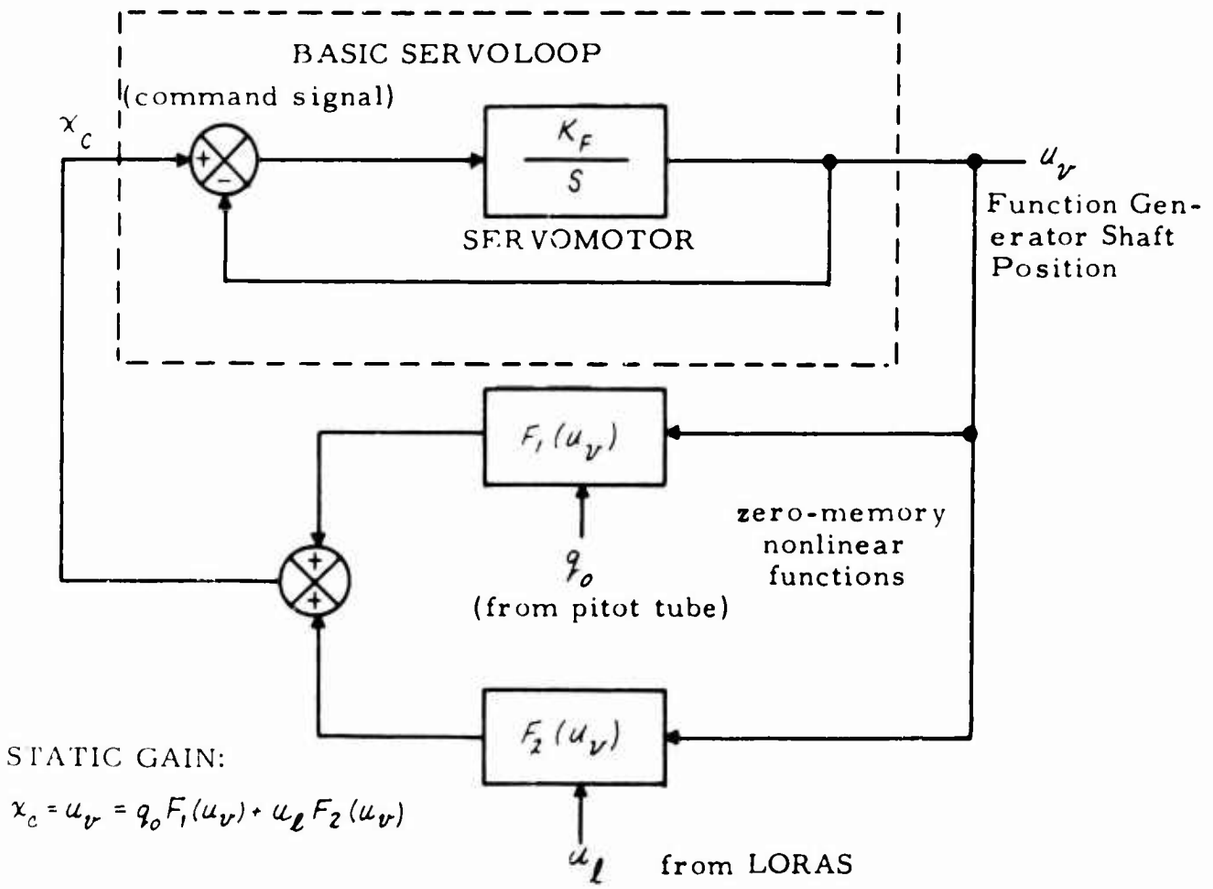

FIGURE 3 FUNCTIONAL BLOCK DIAGRAM OF THE VELOCITY MIXING SYSTEM

Figure 6 LORAS Installed on the X-22A Fin

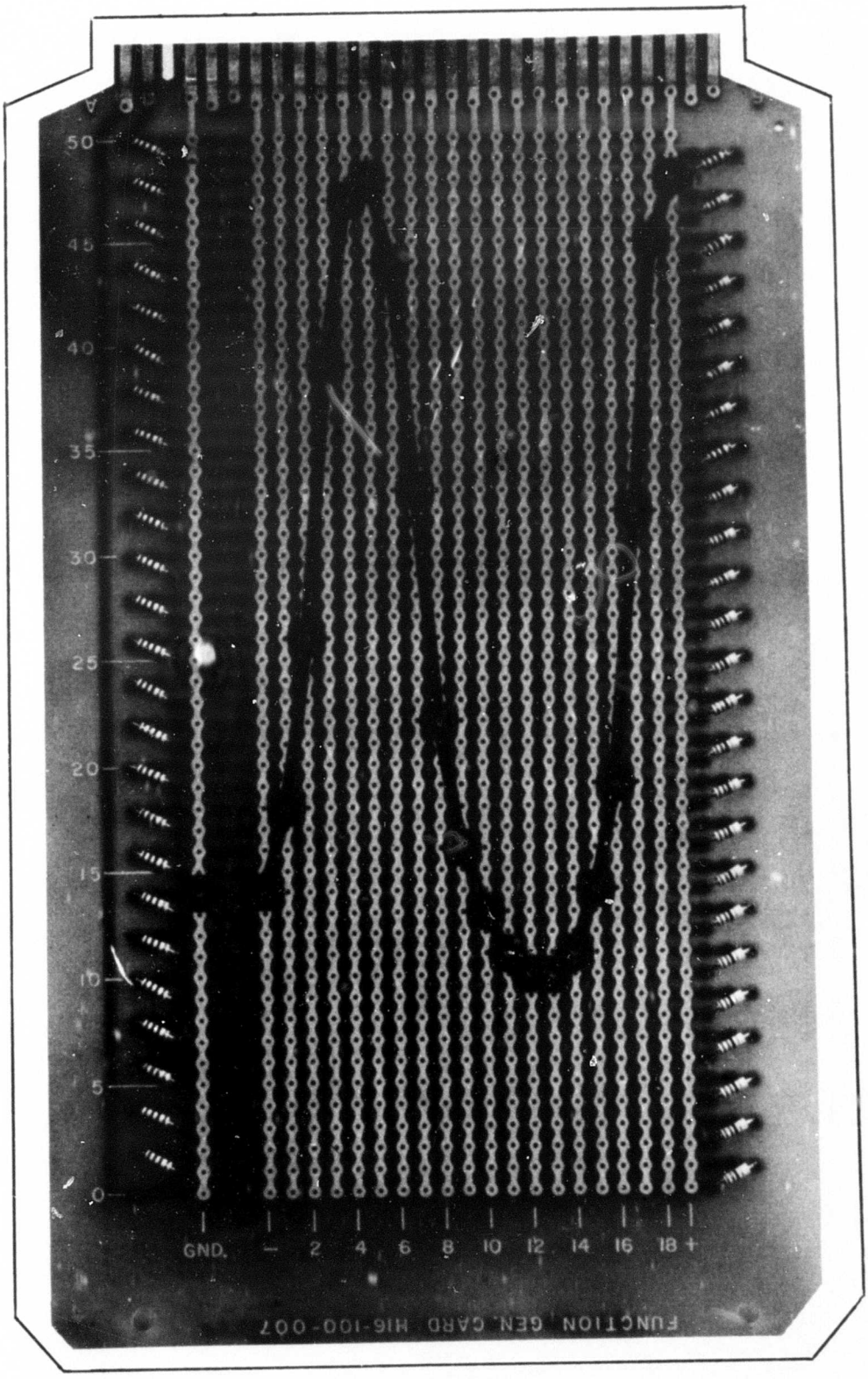

Figure 5 Function Generator Card

Figure 8 LORAS Test Vehicle

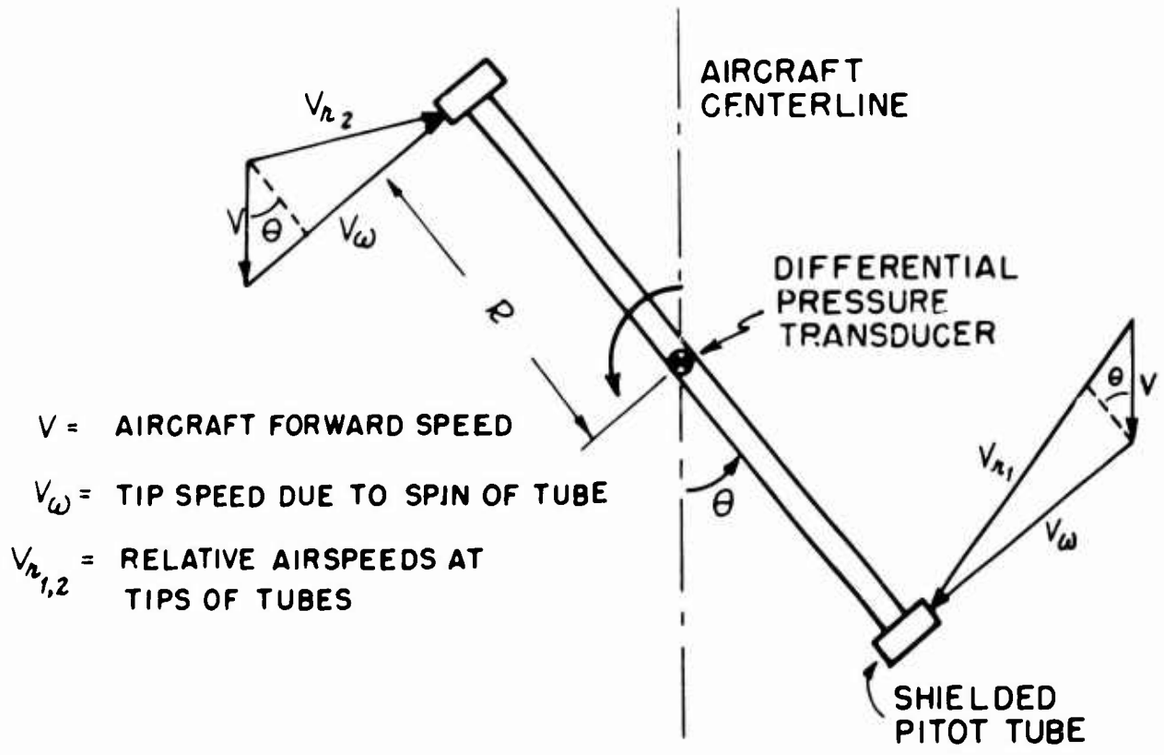

FIGURE 7 DIAGRAM FOR FINDING RELATIVE AIRSPEED AT TIPS OF SPINNING TUBE

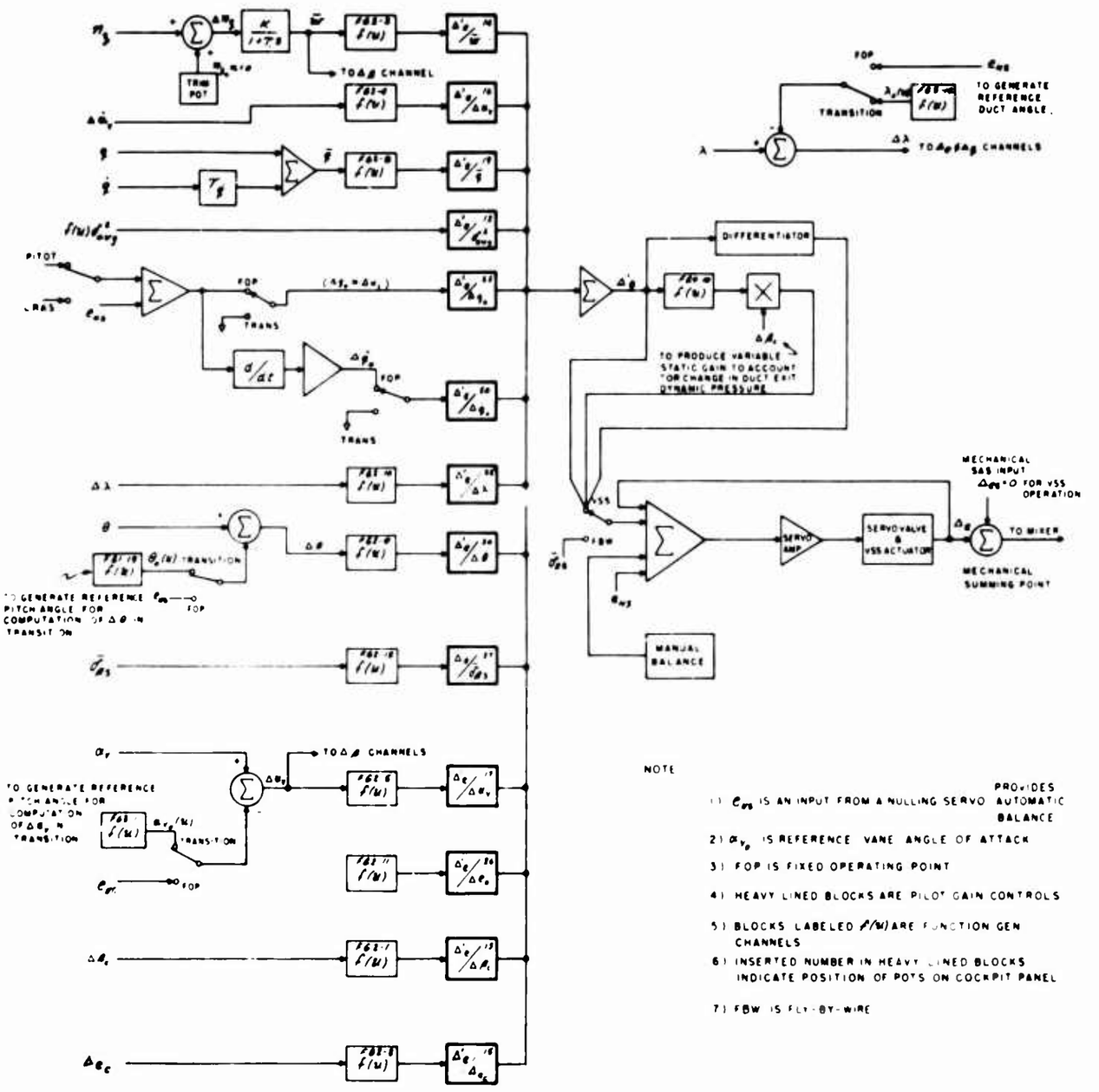

FIGURE 10 VARIABLE STABILITY AND CONTROL SYSTEM FUNCTIONAL BLOCK DIAGRAM - PITCH CONTROL

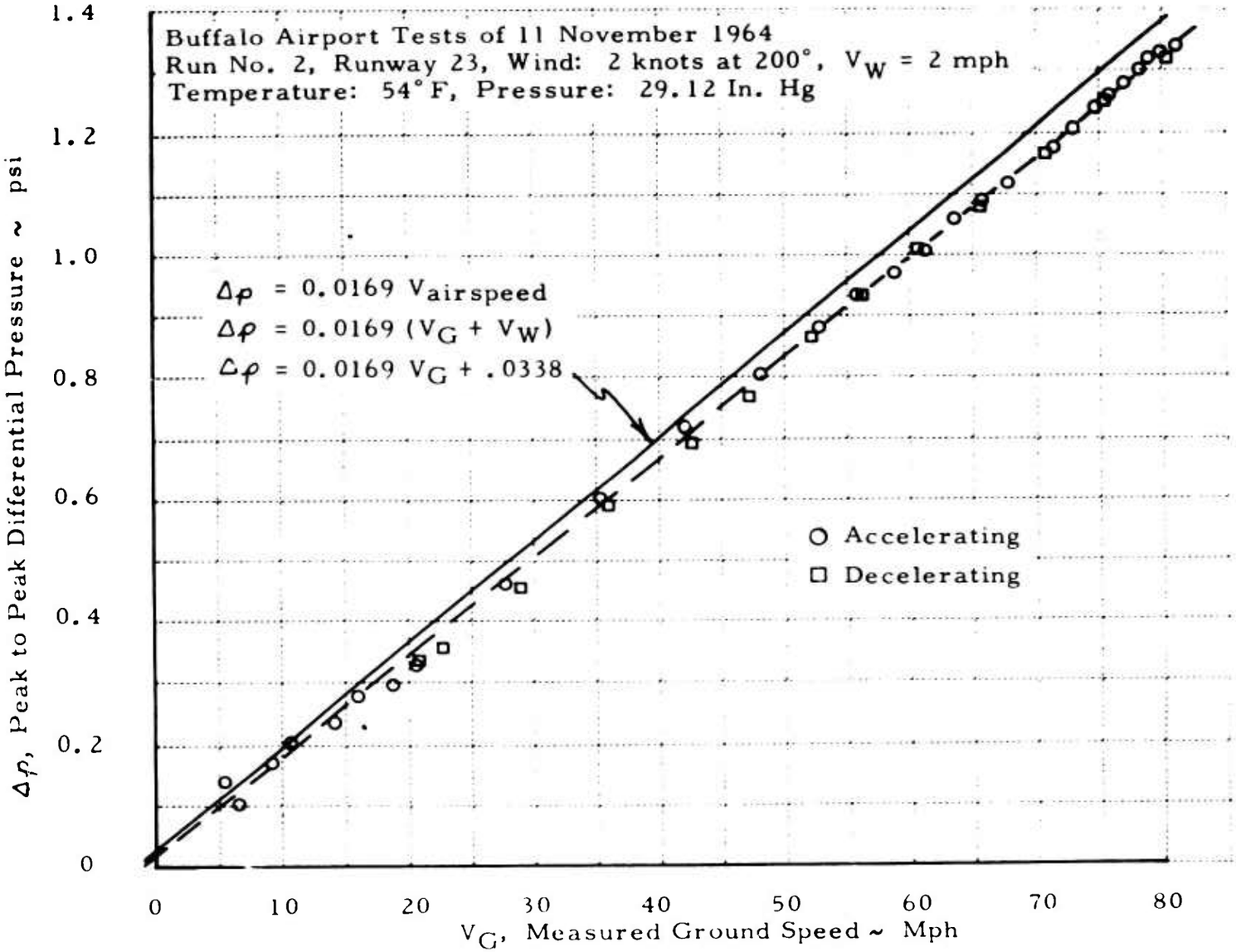

FIGURE 9 LOW RANGE AIRSPEED SYSTEM TEST RESULTS

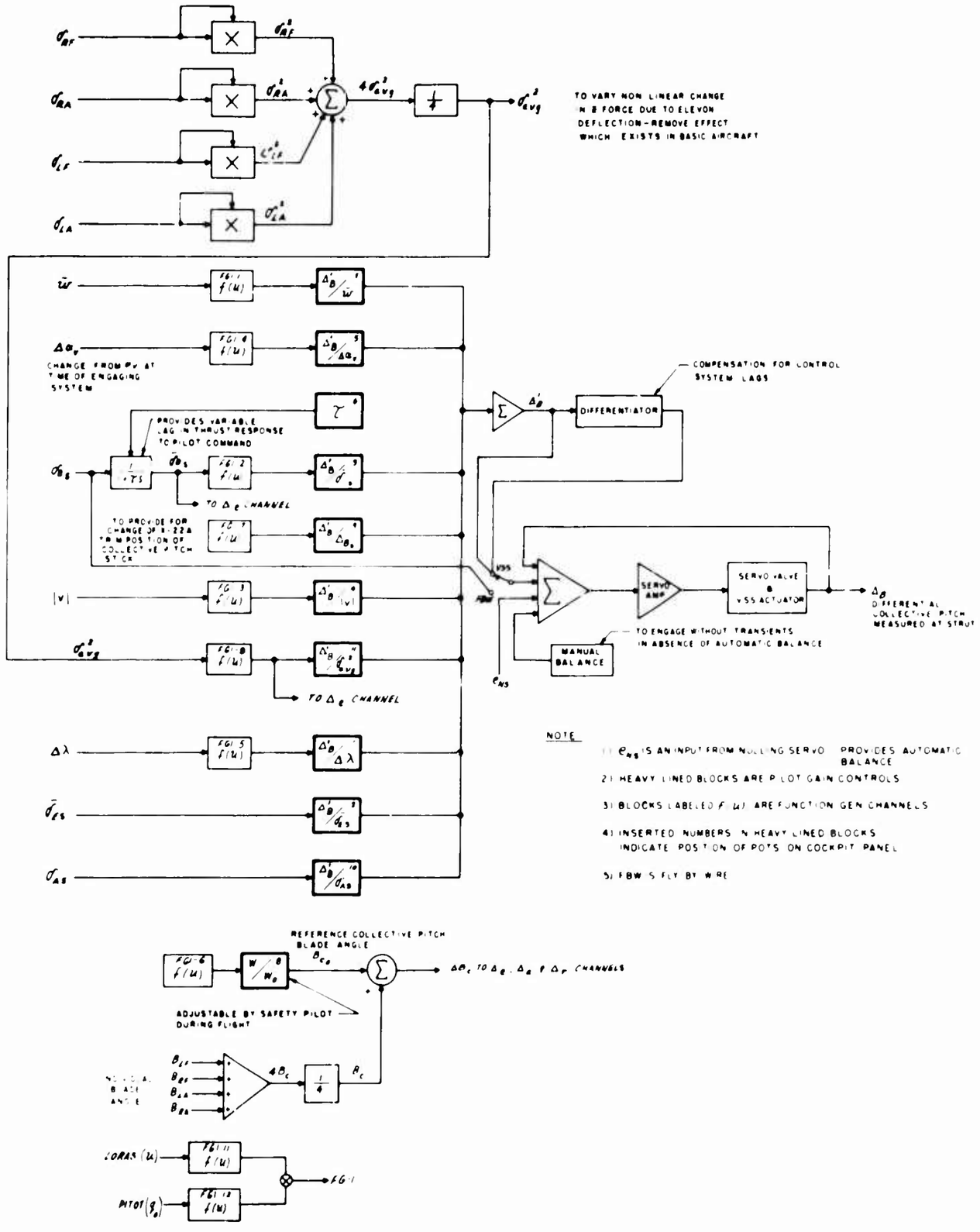

FIGURE 11 VARIABLE STABILITY AND CONTROL SYSTEM FUNCTIONAL BLOCK DIAGRAM – THRUST CONTROL

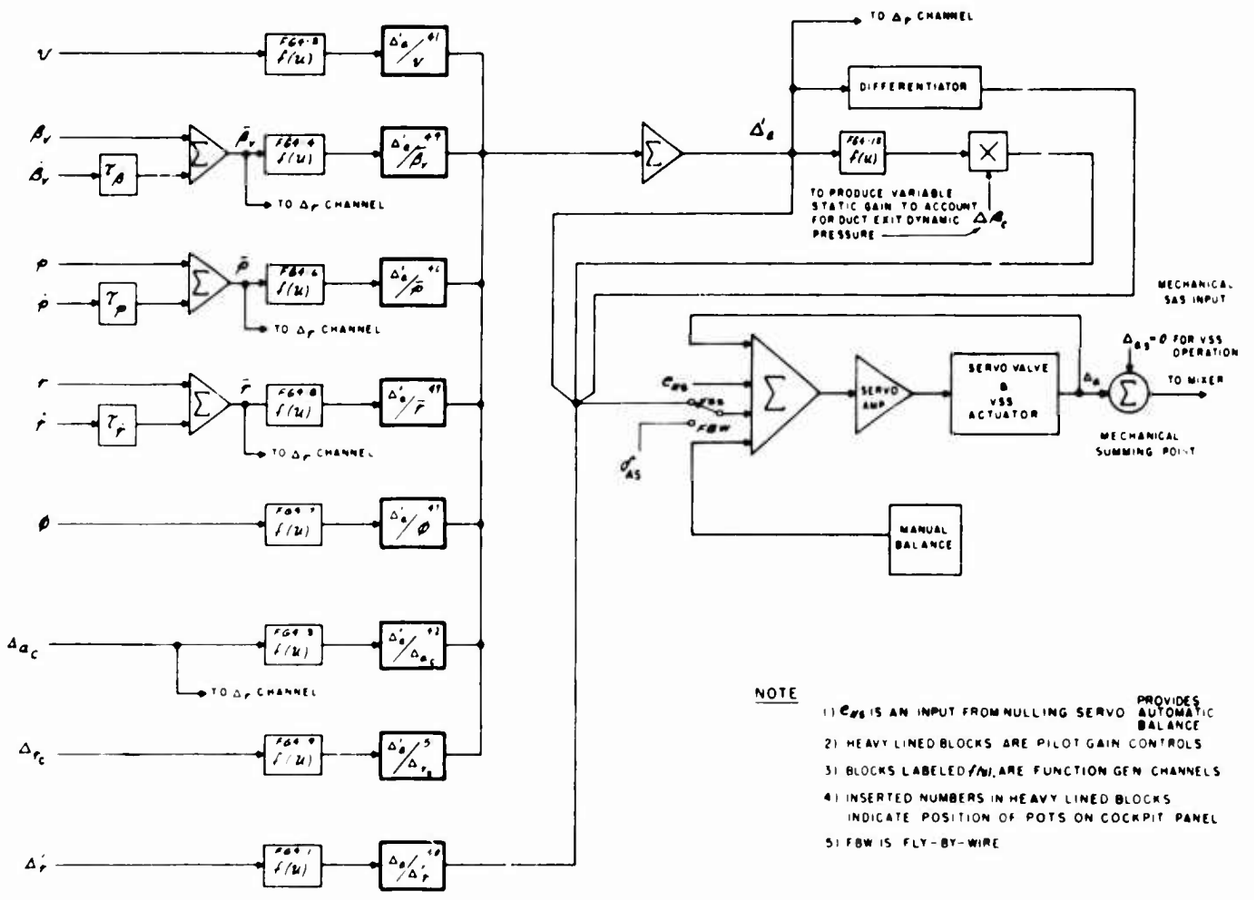

FIGURE 12 VARIABLE STABILITY AND CONTROL SYSTEM FUNCTIONAL BLOCK DIAGRAM - ROLL CONTROL

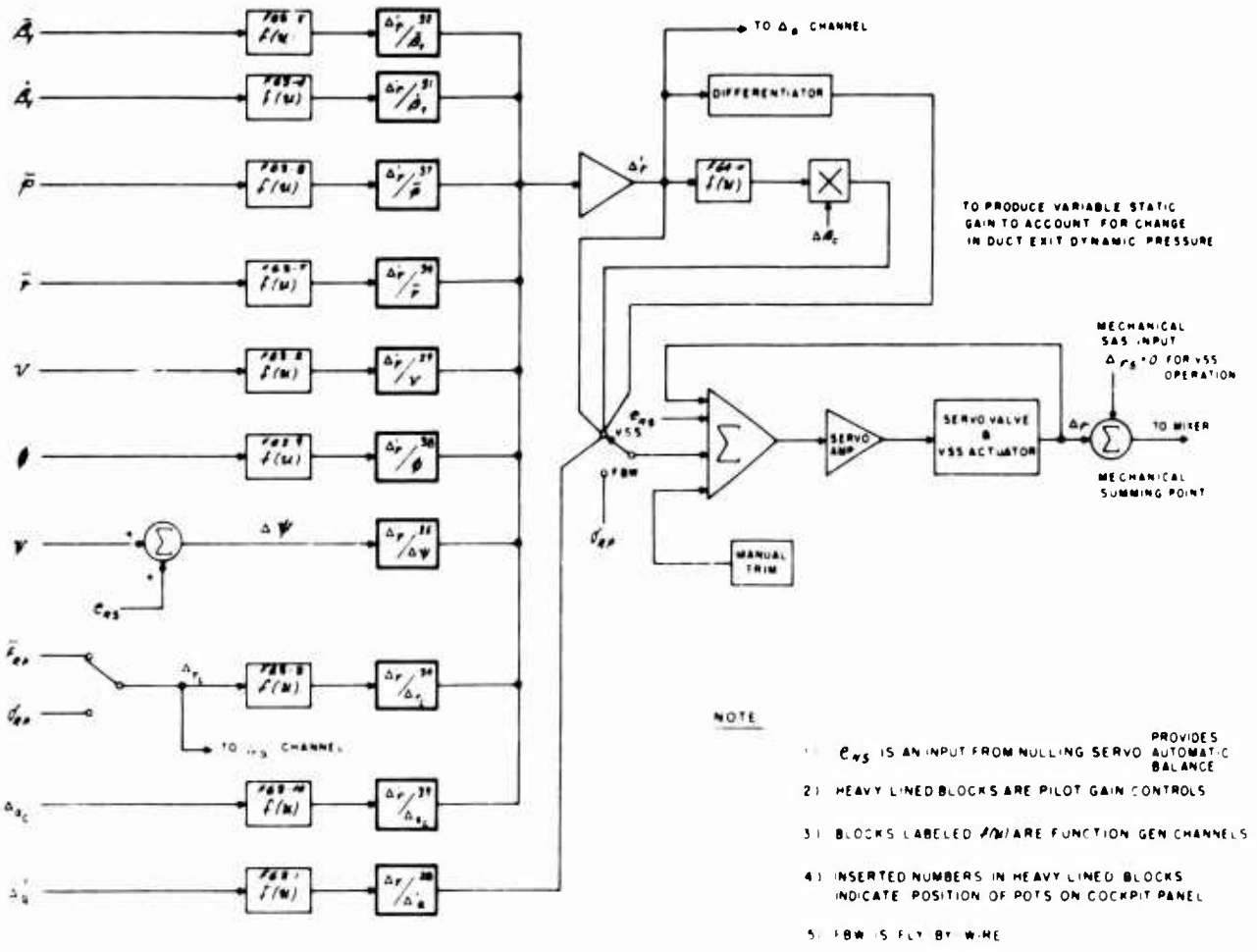

FIGURE 13 VARIABLE STABILITY AND CONTROL SYSTEM FUNCTIONAL BLOCK DIAGRAM - YAW CONTROL

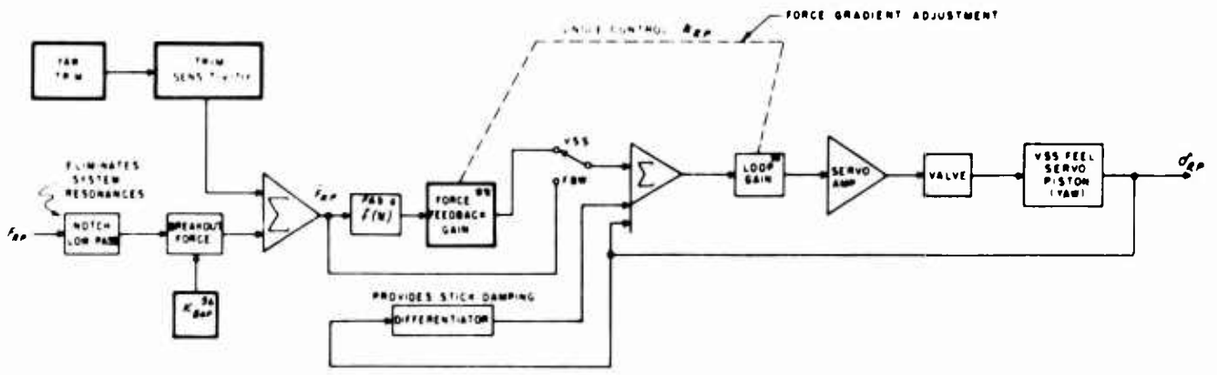

FIGURE 14 ARTIFICIAL FEEL SYSTEM YAW AXIS

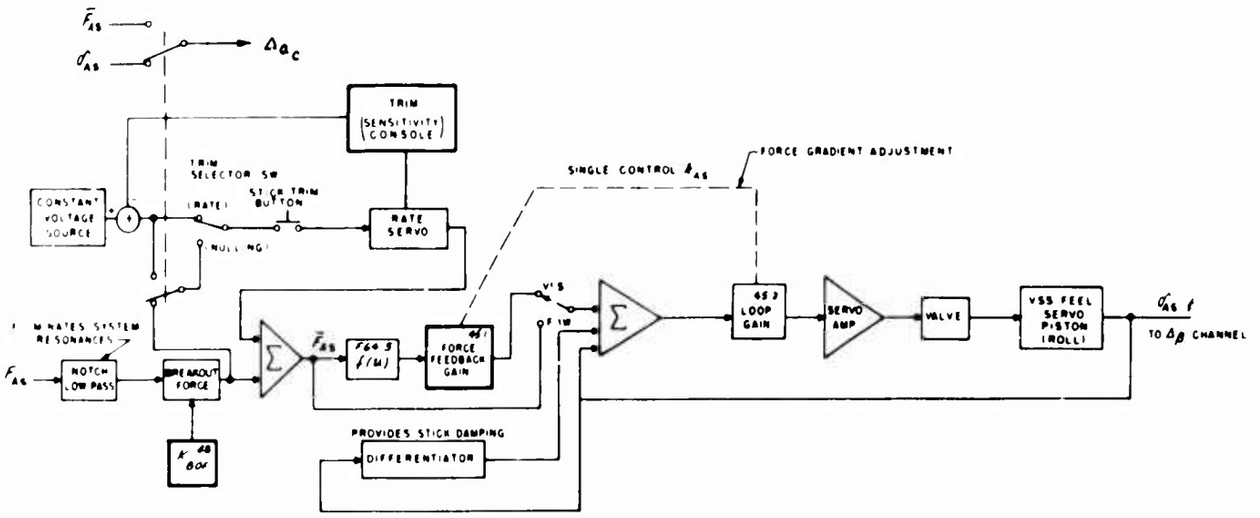

FIGURE 15 ARTIFICIAL FEEL SYSTEM ROLL AXIS

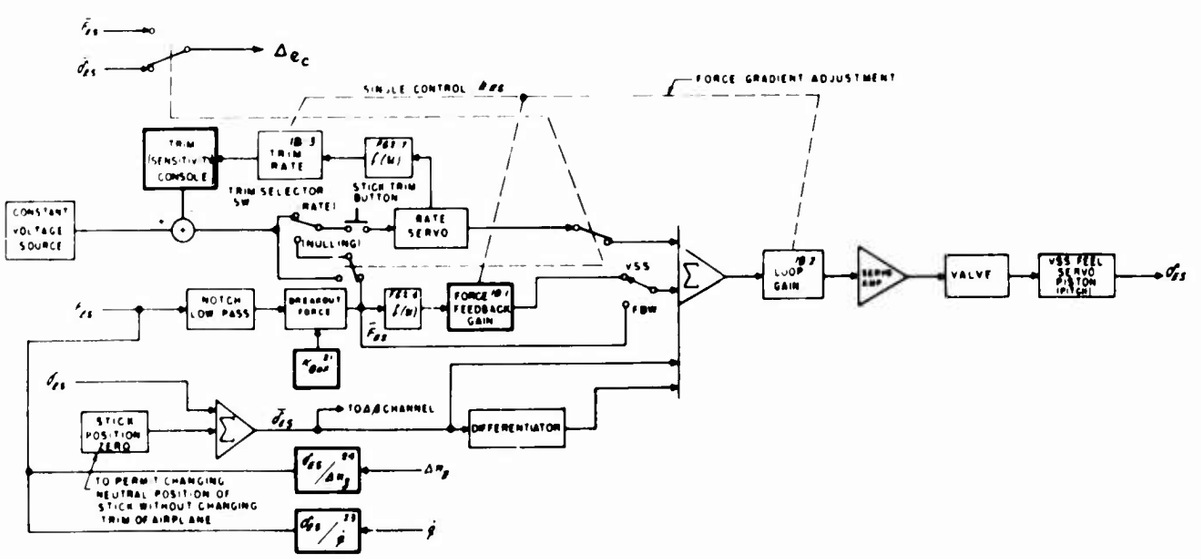

FIGURE 16 ARTIFICIAL FEEL SYSTEM PITCH AXIS

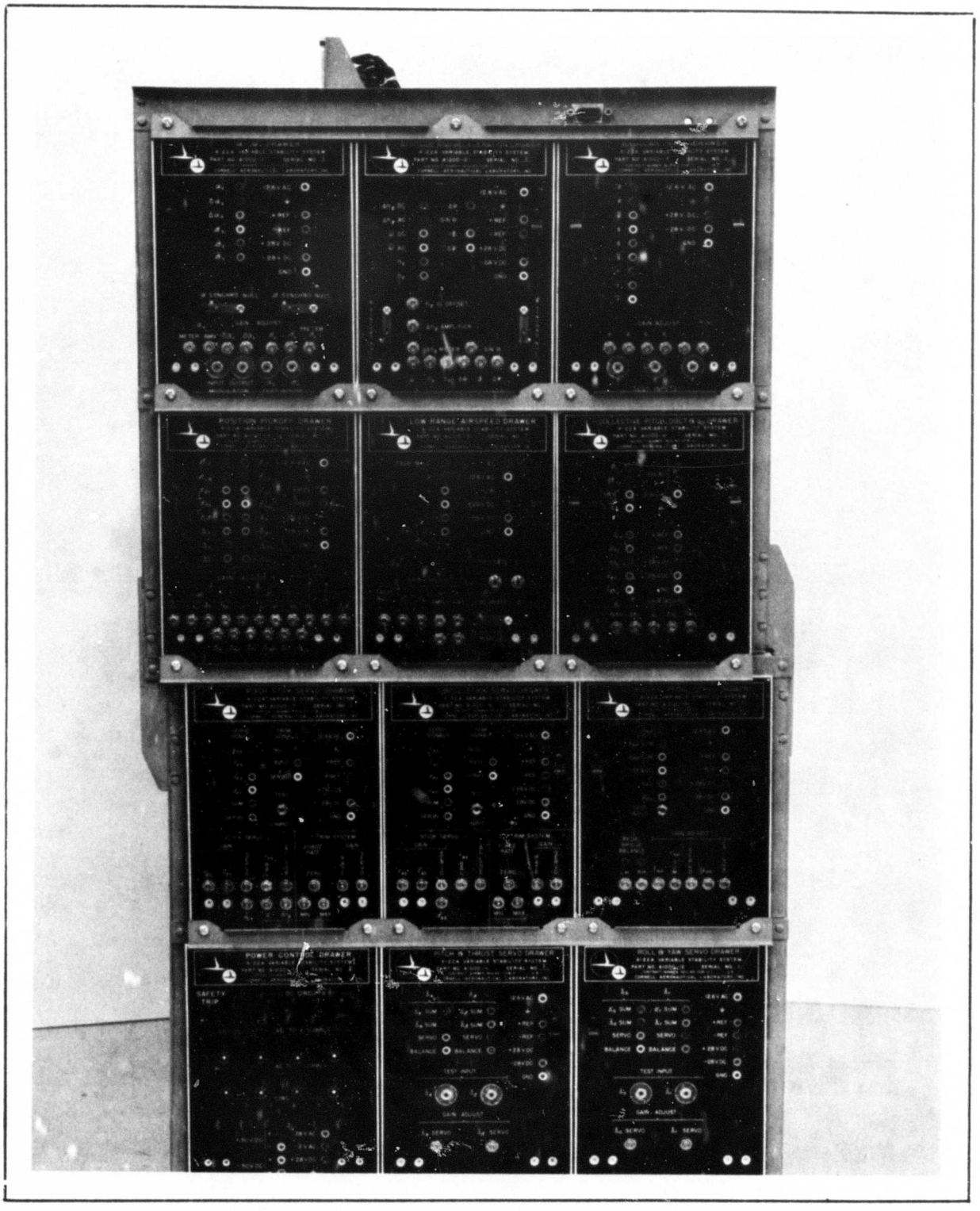

Figure 17 VSS Equipment Center - Front View

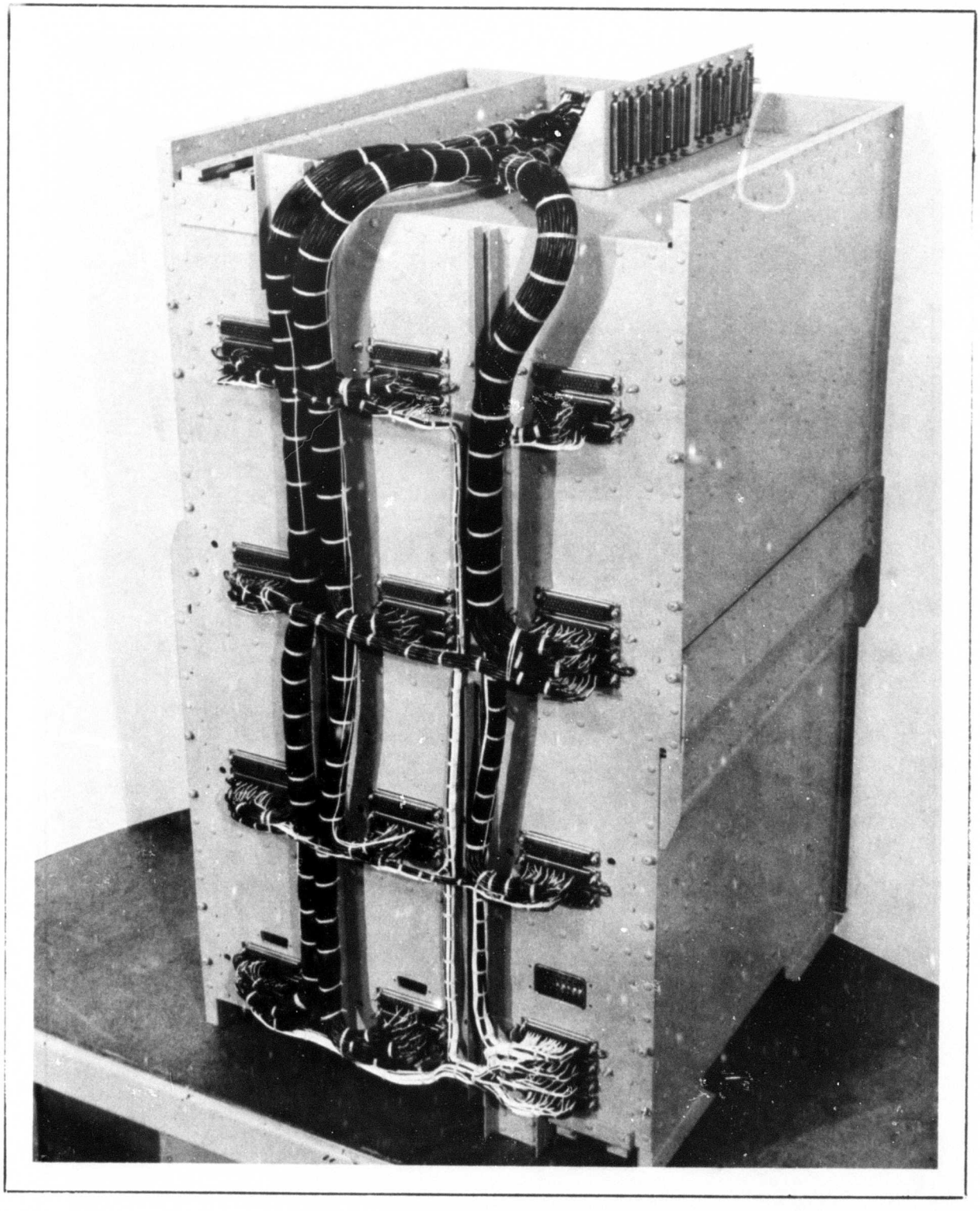

Figure 18 VSS Equipment Center - Rear View

Figure 20 Recording Control Unit

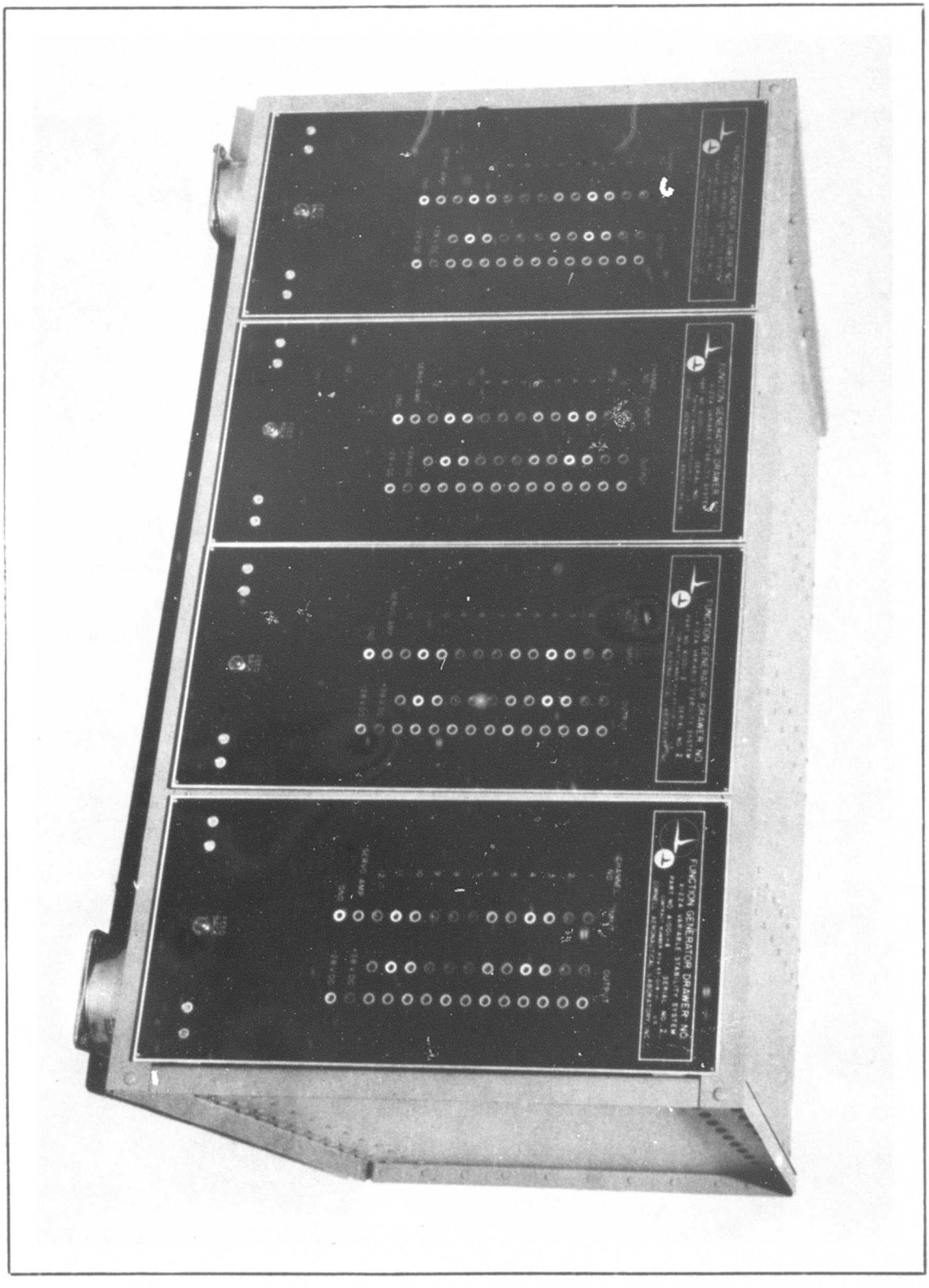

Figure 19 Function Generator

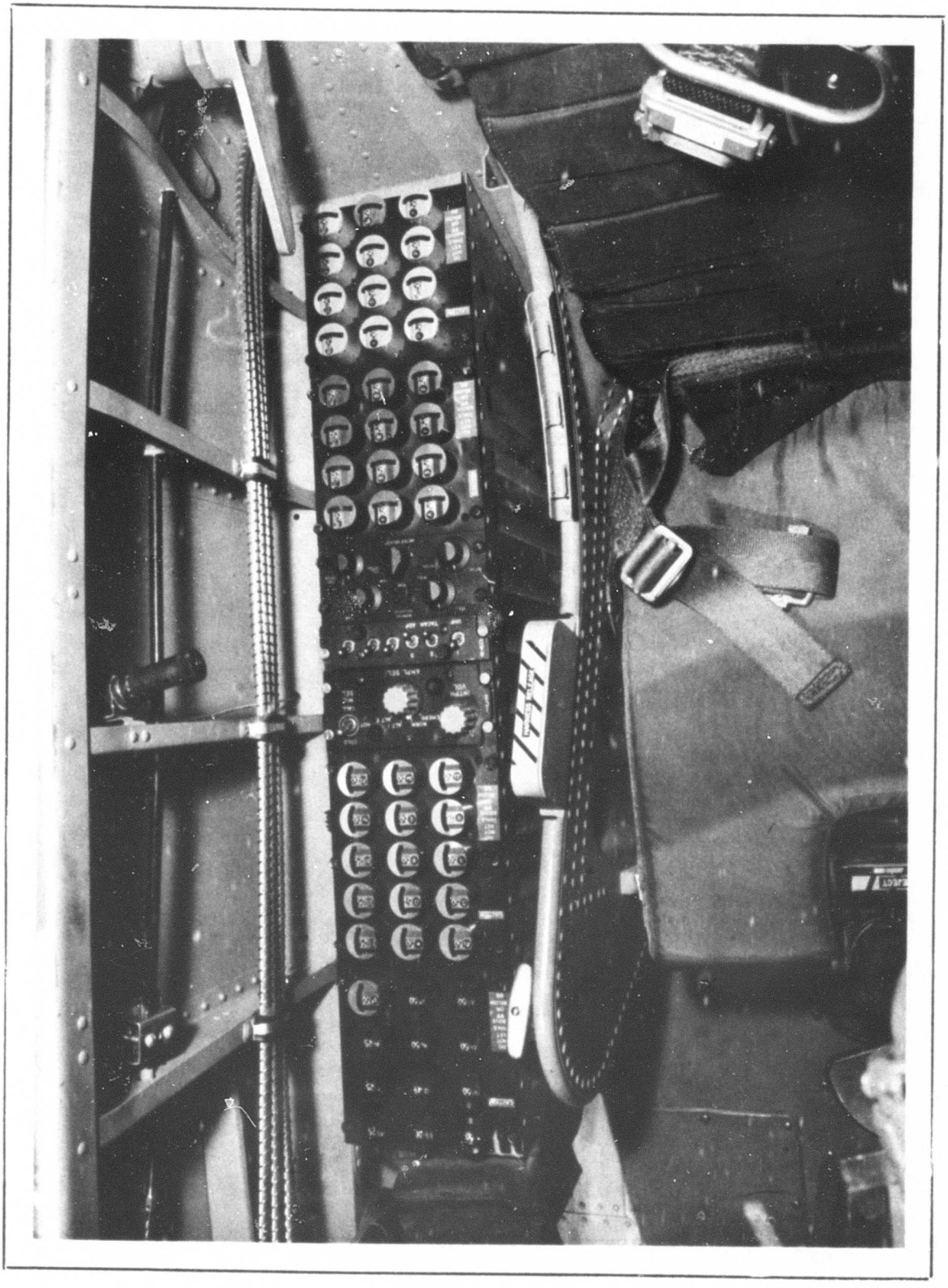

Figure 22 Right Hand Cockpit Console Gain Controls

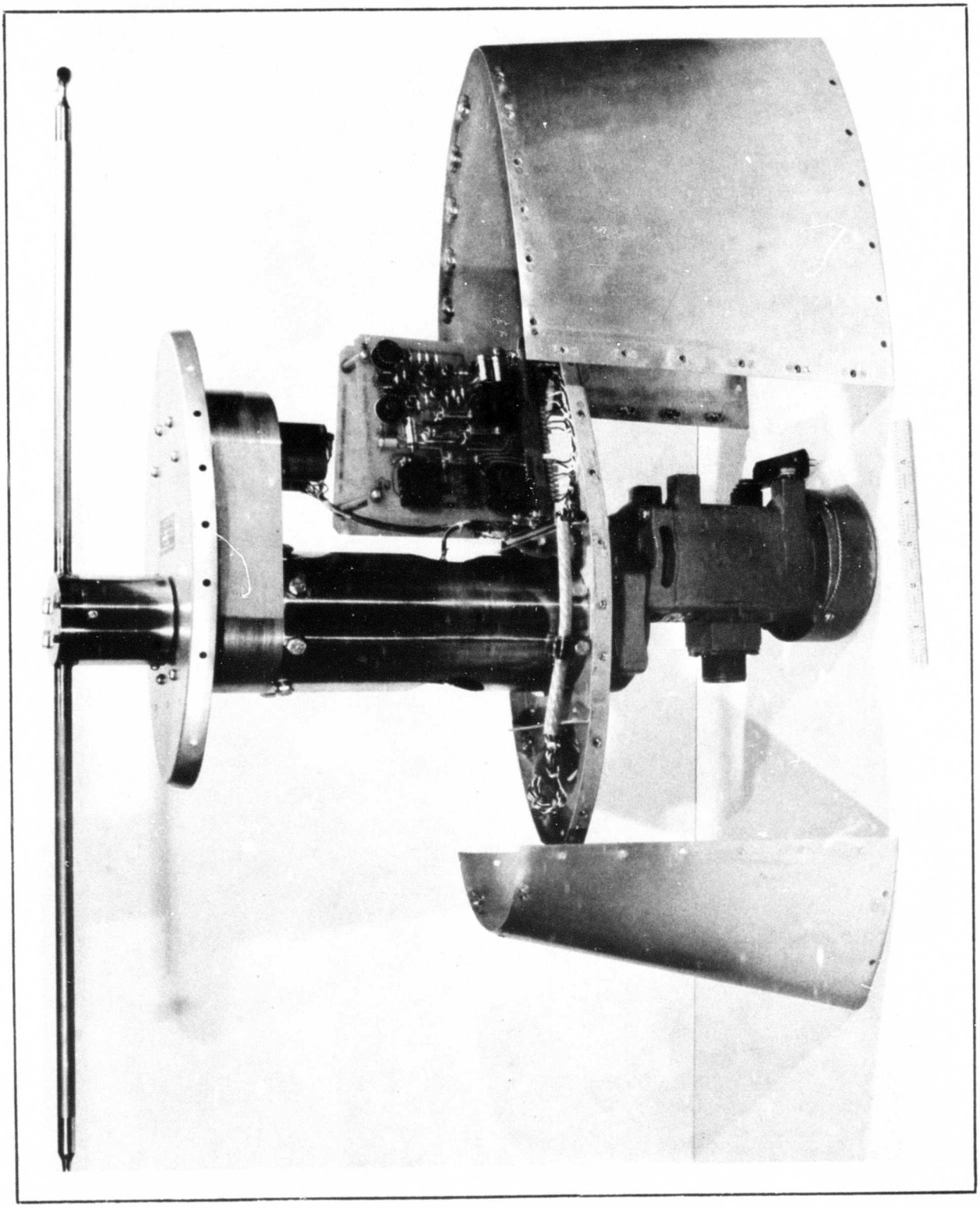

Figure 21 LORAS Rotating Hea l Assembly

Figure 24 VSS Modules

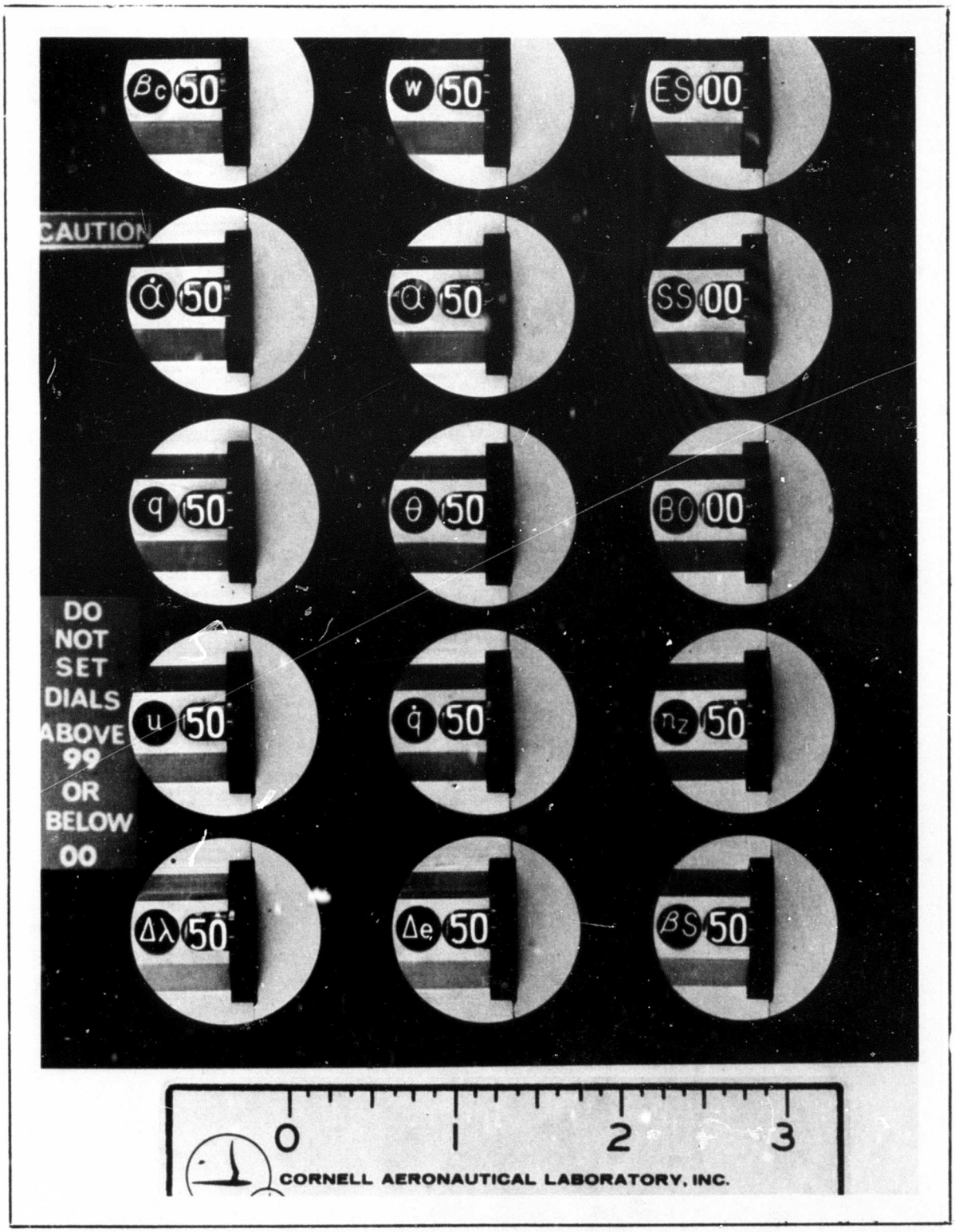

Figure 23 VSS Cockpit Gain Controls - Pitch Axis Panel

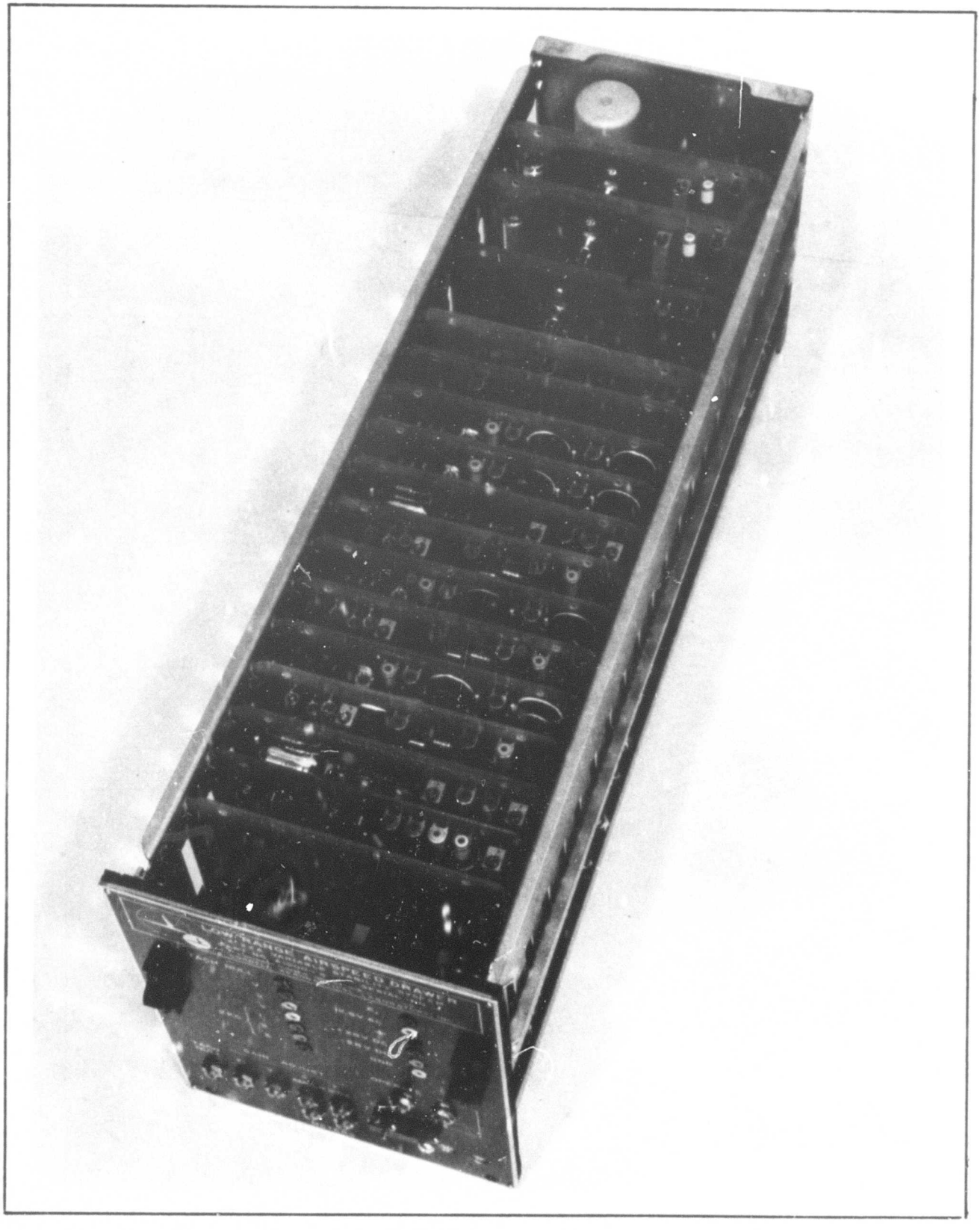

Figure 25 Typical Equipment Drawer

TABLE I

RANGES OF SELECTED STABILITY AND CONTROL PARAMETERS
THAT HAVE BEEN SHOWN SIGNIFICANT
TO FLYING QUALITIES - HOVER

Parameter	Units	Ranges
$\ell_{\delta_{AS}}$	$\frac{\text{rad/sec}^2}{\text{in.}}$	.1 to 1.0
$m_{\delta_{ES}}$	$\frac{\text{rad/sec}^2}{\text{in.}}$	.05 to 1.0
$n_{\delta_{RP}}$	$\frac{\text{rad/sec}^2}{\text{in.}}$	.05 to 3.0
ℓ_p	$\frac{\text{rad/sec}^2}{\text{rad/sec}}$	0 to -4
m_q	$\frac{\text{rad/sec}^2}{\text{rad/sec}}$	0 to -15
n_r	$\frac{\text{rad/sec}^2}{\text{rad/sec}}$	0 to -4
$\gamma_{\delta_{BS}}$	g/in.	.1 to 1
γ_w	$\frac{\text{g}}{\text{ft/sec}}$	0 to -.07
Longitudinal Short period		
ω_n, ζ		See Figure 2
Longitudinal Long Period		
ω_n^2	$\text{rad}^2/\text{sec}^2$	0 to 1
$2\zeta\omega_n$	rad/sec	-.5 to 1
Lateral Short Period		
ω_n, ζ		See Figure 2
Roll-Spiral		
ω_n Complex	rad/sec	0 to 1
ζ Roots	Non-dimensional	-.5 to 1
$1/\tau_R$ Real	sec^{-1}	-.4 to 10
$1/\tau_S$ Roots	sec^{-1}	-.2 to .2

TABLE II

RANGES OF SELECTED STABILITY AND CONTROL PARAMETERS
THAT HAVE BEEN SHOWN SIGNIFICANT
TO FLYING QUALITIES - CONVENTIONAL FLIGHT

Parameter		Units	Ranges
Longitudinal Snort Period			
ω_n , ζ			See Figure 2
Longitudinal Phugoid			
ω_n^2		rad^2/sec^2	0 to .1
$2\zeta\omega_n$		rad/sec	-.5 to .5
Lateral Dutch Roll			
ω_n , ζ			See Figure 2
Lateral Roll-Spiral			
ω_n	Complex	rad/sec	0 to .5
ζ	Roots	Non-Dimensional	0 to 1
$1/\tau_R$	Real	sec^{-1}	.2 to 10
$1/\tau_s$	Roots	sec^{-1}	-.2 to .2

TABLE III

MAXIMUM CONTROL POWER FOR VARIOUS VTOL AIRPLANES IN HOVER

Airplane	Maximum Acceleration for Full Control Deflection (rad/sec^2)		
	M_c	L_c	N_c
XV-4	0.80	1.3 1.7 (boundary layer control)	0.3
XV-5	0.85	0.75 (minimum collective pitch) 2.50 (maximum collective pitch)	0.4
X-19	1.05	1.10	0.25
X-22A	3.2	3.4	0.76 (single elevons) 2.0 (compound elevons)
XC-142	0.84	1.0	0.35 (h=0) 0.55 (h=40')

TABLE IV FUNCTION OF GAINS - PITCH AXIS

Feedback Variable	Source	Purpose
$\bar{\omega}$	Integrated incremental normal acceleration	To vary M_ω for all flight conditions. Changes short period frequency and damping ratio in cruise flight. Changes short period and long period modes in transition. Equivalent to M_α
$\dot{\alpha}$	Differentiated signal from angle of attack vane	To vary $M_{\dot{\alpha}}$. Changes short period damping in cruise and transition.
$\bar{q}$	Rate gyro signal plus derivative	To vary M_q . Pitch damper in cruise and transition. $\dot{q}$ used for lead compensation.
δ^2_{avg}	Elevon pickoff excited by elevon pickoff	Vary nonlinear change in pitching moments due to elevon deflection, especially to compensate (remove) effect present in basic aircraft.
Δu	Airspeed systems	To vary M_u in fixed operating point mode only. Influences phugoid frequency in cruise flight and both high and low frequency roots in hover.
$\dot{u}_i$	Differentiated signal from airspeed systems	To vary $M_{\dot{u}}$. Effective in stabilizing the long period mode in forward flight.
$\Delta\lambda$	Error between actual duct angle and reference duct angle	Variation of pitching moment with duct angle; provides linear variation with duct angle of trim stick position vs. velocity in transition.
θ	Attitude gyro	To vary M_θ . Very powerful in stabilizing the long period mode for all flight conditions. Increases frequency of short period mode. Pitch loop of attitude stabilization system.
$\bar{\delta}_{BS}$	Collective pitch stick with variable lag	Control cross-coupling. To vary M_{B_C}
α_V	Angle of attack vane	To vary M_α . Primary influence is on short period mode for all flight conditions. Affects stability of long period mode in transition.

TABLE IV FUNCTION OF GAINS - PITCH AXIS

(continued)

Feedback Variable	Source	Purpose
$\alpha_{V_0}(u)$	Function Generator	To generate a moment-required-to-trim function that differs from that of the basic aircraft. Influences elevator stick position through transition.
ΔB_c	Error between actual collective pitch and reference collective pitch	Dynamic control cross-coupling. Used for decoupling basic X-22A.
Δe_c	Pilot's control displacement or control force	Variable elevator gearing, M_{δ_e}

TABLE V FUNCTION OF GAINS - THRUST AXIS

Feedback Variable	Source	Purpose
$\bar{\omega}$	Integrated incremental normal acceleration	To vary time constant of one root of characteristic equation in hover; height damping.
$\Delta\alpha_V$	Angle of attack vane	To vary primary term in numerator of $\dot{\theta}/\delta_e$ and to change n_z/α.
δ_{BS}	Collective pitch stick position	Control input $\frac{\bar{\delta}_{BS}}{\delta_{BS}} = \frac{1}{1+\tau_s}$
τ	Integrator	Lag in thrust buildup
	Function Generator	Change from X-22A trim position of the collective pitch stick
$\|V\|$	LORAS	To change static gains in fixed operating point; change vertical force with forward speed and lateral speed.
δ^2_{avg}	Elevon pickoff excited by elevon pickoff	Vary nonlinear change in z - force due to elevon deflection, especially to compensate (remove) effect present in basic aircraft.
$\Delta\lambda$	Error between actual duct angle and reference duct angle	Variation of thrust with duct angle; provides linear variation with duct angle of thrust vs. velocity in transition.
δ_{ES}	Pitch stick position pickoff	Control input coupling. Thrust change due to elevator stick displacement.
δ_{AS}	Aileron stick position pickoff	Control input coupling. Thrust change due to aileron stick displacement.

TABLE VI FUNCTION OF GAINS - ROLL AXIS

Feedback Variable	Source	Purpose
v	LORAS	Provide for variable $\angle_v$ at low speed.
$\overline{\beta_v}$	Angle of sideslip vane	Provide for variable $\angle_\beta$ at high speed. Affects most dynamic characteristics. Also $\omega_\phi/\omega_{n_{DR}}$, $\phi/\beta \cdot \dot{\beta}_v$ used for lag compensation.
$\bar{p}$	Rate gyro signal plus derivative	Provide for variable $\angle_p$ derivative. Provide for variable roll root. $\dot{p}$ used for lag compensation.
$\bar{r}$	Rate gyro signal plus derivative	Provide for variable $\angle_r$. Affects spiral root, and ϕ/β . $\dot{r}$ used for lag compensation.
ϕ	Attitude gyro	Provide for variable $\angle_\phi$ derivative. Changes long period lateral mode at low speed, analogously to M_θ in longitudinal modes. Roll loop of attitude stabilization system.
Δa_c	Pilot's control displacement or control force	Variable aileron gearing, $\angle_{\delta_{AS}}$
Δr_c	Pilot's control displacement or control force	Variable rolling moment due to rudder pedal, $\angle_{\delta_{RP}}$. Control input coupling.
Δ'_r	Summing amplifier	Variable aileron roll control input due to yaw control to modify coupling (control phasing) of basic X-22A.

TABLE VII FUNCTION OF GAINS - YAW AXIS

Feedback Variable	Source	Purpose
$\bar{\beta}_V$	Angle of sideslip vane	Provide for variable N_β derivative. Change Dutch roll frequency, $\omega_\phi/\omega_{n_{DR}}$, ϕ/β . $\dot{\beta}_V$ used for lag compensation.
$\dot{\beta}_V$	Differentiated signal from angle of sideslip vane	Provide for variable $N_{\dot{\beta}}$ derivative. Change Dutch roll damping.
$\bar{p}$	Rate gyro signal plus derivative	Provide for variable N_p derivative. Affects most dynamic characteristics to some degree. Dutch roll damping and roll to yaw ratio, $\dot{p}$ used for lag compensation.
$\bar{r}$	Rate gyro signal plus derivative	Provide for variable N_r derivative. Change Dutch roll damping.
v	LORAS	Provide for variable N_v at low speed.
ϕ	Attitude gyro	Provide for variable N_ϕ derivative. Change spiral root. Coupling for attitude stabilization.
ψ	Compass system	Heading hold, attitude stabilization.
Δr_c	Pilot's control displacement or control force	Variable rudder gearing, N_{δ_r}.
Δa_c	Pilot's control displacement or control force	Variable yawing moment due to aileron stick, N_{δ_a} . Control input coupling.
Δ'_a	Summing amplifier	Variable rudder yaw control input from roll control to modify coupling (control phasing) of basic X-22A.

PRELIMINARY DEVELOPMENT

OF A

TRAILING ROTOR SYSTEM

J. A. DeTore

Bell Helicopter Company

PRELIMINARY DEVELOPMENT OF A TRAILING ROTOR SYSTEM

J. A. DeTore

Group Engineer, R&D Technical
Bell Helicopter Company
Fort Worth, Texas

INTRODUCTION

Continuing advancements in low-disc loading V/STOL aircraft technology may well lead into the 400+ knot speed range. To achieve this goal it is necessary that the rotor used for low speed lift not compromise the cruise efficiency nor create dynamic loading limitations of the aircraft in high speed flight. This paper presents results of a preliminary analytical and experimental investigation of a rotor stopping and folding process which offers promise as a means of accomplishing this goal. It is based on using the autorotative (zero shaft power) regime of the rotor during the stopping operation. Further, it is the special autorotation regime wherein the rotor operates at low thrust/weight ratios over an angle-of-attack range of approximately 90 degrees. The extensive research conducted by the NACA in the 30's on autogiro rotors (References 1 through 6) thoroughly defined the zero power rotor thrust characteristics over a wide range of speed and angle of attack. These investigations, however, concentrated on the high thrust/weight ratio regime. It is shown herein that these two regimes (high and low thrust autorotation) of operation are continuous from one to another and that a typical transition from one regime to the other occurs in the vicinity of maximum L/D for an unpowered rotor.

GENERAL CHARACTERISTICS IN AN APPLICATION

Before describing the results concerning the rotor as a subsystem, and for orientation purposes, some potential characteristics of the related vehicle will be presented.

The increasing interest in VTOL aircraft progress is based on the belief that ultimately vertical takeoff and landing capability, combined with efficient cruise flight at high speed, will be an important aspect of military and commercial aviation; and that such aircraft will also provide increased useful load capability in STOL or CTOL applications. This potential versatility is an important factor in the development of successful types. Also, there is a growing awareness that it is not the VFR takeoff, but rather the IFR landing that may well dictate

the most desirable type of low-speed lift system. Better accommodation of the critical conditions during the landing approach will be satisfied by lift systems which do not require more power to hover than cruise, but less. For example, a pilot can always slow down in cruise flight with partial loss of power but can he return and land where he took off? It is generally possible to predict the time to get from Point A to Point B during the cruise leg, but what about the unexpected time lost, fuel consumed and increased attention required prior to and during final approaches? Excessive design disc loadings can rapidly increase the reserve fuel requirements and pilot workload in these situations and thereby critically affect system economy.

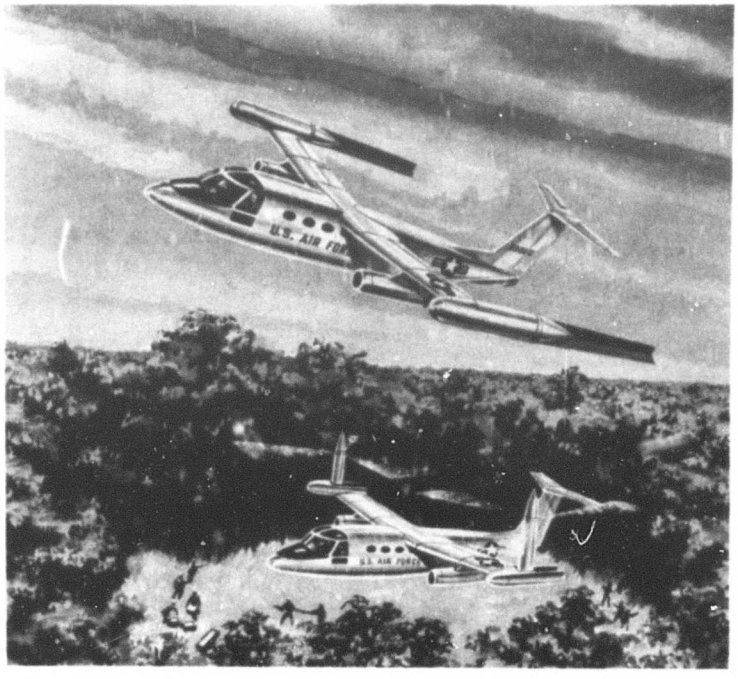

Figure 1 - Trailing Rotor V/STOL Aircraft

Based on considerations such as these, development of the low-disc loading approach to V/STOL design is certainly justified. Low-disc loading, as referred to here, means "rotors." The cleanest way to obtain 400+ knot speed capability with a rotorcraft is to stop the rotor and place it and its supporting pylon in a minimum drag configuration. Easily said, ... but how?

A possible solution is illustrated by the vehicle shown in Figure 1 in both hovering and cruise configuration. Powered by two compound fan jet engines in cruise flight, speeds in excess of 400 knots are possible. The two wing-mounted, low-disc loading rotors provide excellent hot day hovering ceilings or permit hovering with the shaft power output of one engine on a standard day. By making a conventional takeoff in the cruise configuration, with extra fuel, ferry ranges of at least 2200 n.mi. can be obtained.

TRANSITION PROCEDURE

The transition from helicopter to airplane configuration, Figure 2, would be executed at a flight speed above wing stall speed. The aircraft flies as a compound helicopter, (a), with the rotors sharing vehicle lift with a wing. The power output of the gas generators is split between the rotors and the cruise fans which provide the major portion of the propulsive thrust. As the transition continues, (b), the vehicle

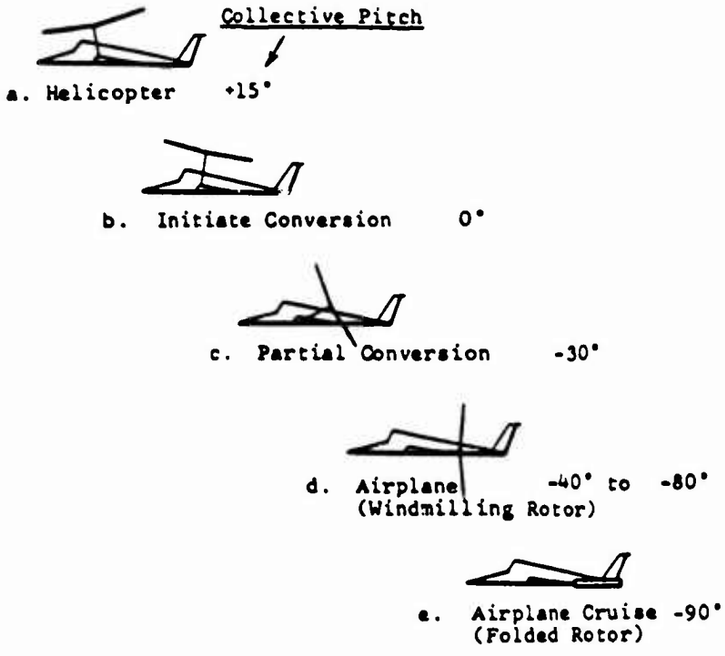

Figure 2 - Autorotative Conversion Sequence

angle of attack is slightly increased. The wing assumes a greater portion of the lift, and the rotor enters low-thrust autorotation at essentially full rpm. Since rotor shaft power is no longer required, the fans absorb engine output to maintain level flight. Further in the transition, (c), the rotor pylons are continuously tilted aft. As the remaining rotor lift is unloaded, the wing assumes full vehicle lift. When the rotor shafts arrive in a horizontal attitude (d), the rotors are windmilling behind the wing. The final phase of the transition, (e), consists of further reducing rotor rpm by coarsening the blade pitch, and as the rotor centrifugal field decays, folding the blades downstream by mechanical means. During the aft tilting, the drag of the rotor pylon is minimized. Also, the full transition procedure is reversible and can be stopped at any pylon tilt angle.

Important characteristics of the transition should be noted. First, the major portion takes place with no shaft power required by the rotor. Therefore, no sudden, rotor-induced trim changes result from loss of propulsive power during conversion, but rather, only the flight path angle changes. Second, the last portion of the conversion to airplane configuration, prior to blade folding, is accomplished with windmilling collective pitch settings rather than relatively flat "autogiro" blade pitch settings. The windmilling condition represents low rotor drag, within the thrust capability of a 400-knot vehicle, whereas autogiro pitch settings would represent prohibitive drag and rotor rpm at the conversion flight speed.

The change in vehicle configuration during the conversion process requires a shift in vehicle center of gravity. Depending on specific vehicle configuration, the remaining useful c.g. range is at least 10 to 15 percent of the mean aerodynamic chord.

AUTOROTATION AERODYNAMICS

High and low-thrust autorotation conditions are illustrated by the rotor blade element force diagram in Figure 3. With an inflow condition representing a moderate rotor angle of attack at a given rpm, two values of blade resultant thrust vector orientation which are parallel with the rotor shaft axis are possible; one at high thrust, the typical autorotation situation, and one at low thrust or windmilling. The specific values of blade pitch required to achieve these equilibrium conditions depend on the airfoil effective lift and drag characteristics.

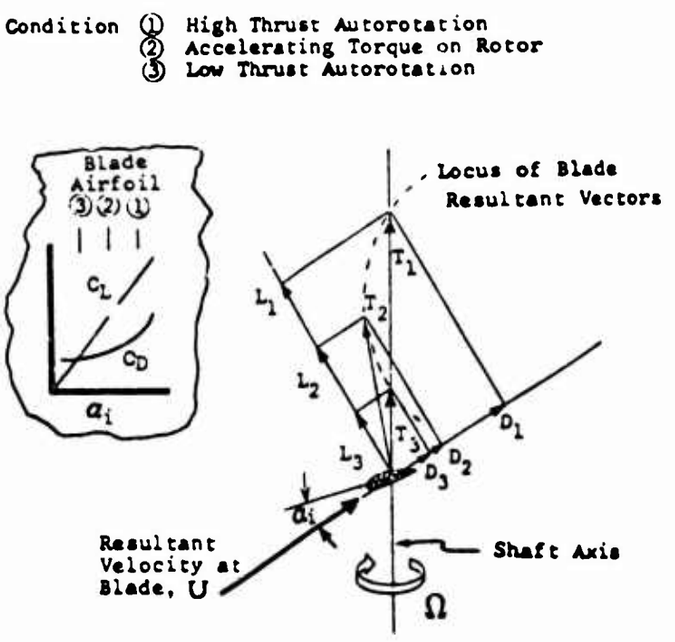

Figure 3 - Autorotation - High and Low Thrusts

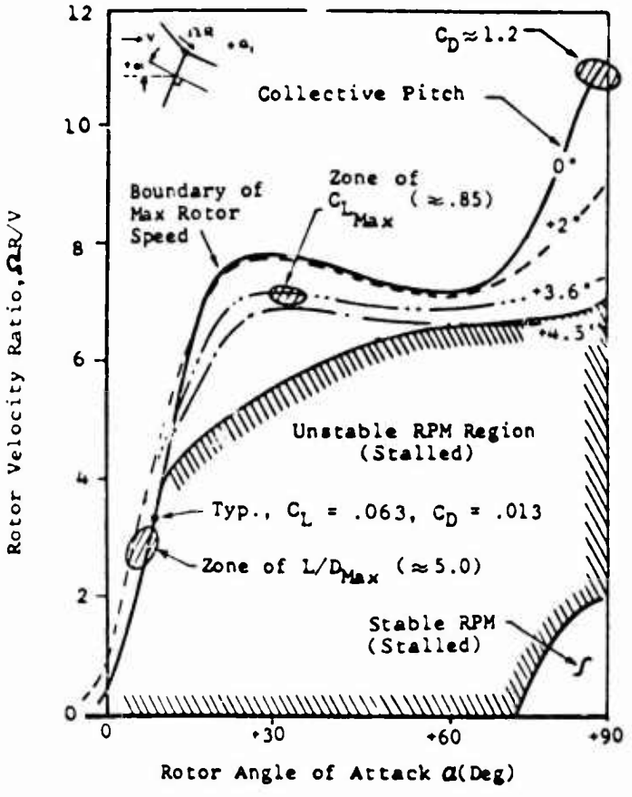

Figure 4
Conventional Autorotation
(High Thrust Equilibrium)

High Thrust Autorotation - The diagram shown in Figure 4 summarizes, for a typical rotor, the entire range of normal operating conditions from autorotation at high speed to autorotation in vertical descent. Rotor speed is expressed as $\Omega R/V$ (the reciprocal of the conventional rotor tip speed ratio) since speed of the unpowered rotor is governed by the flight velocity, rotor angle of attack and blade collective pitch. In vertical descent, the angle of attack of an autorotating rotor is 90 degrees and, in the high-thrust regime, the vehicle weight is supported entirely by the rotor drag. In high-speed flight, rotor angles of attack approach

zero. At a rotor angle of attack of 6 degrees and with blade collective pitch set for maximum rotor speed (in this case +2.0 degrees), the rotor lift coefficient (based on rotor disc area and flight dynamic pressure) is approximately .1 and the rotor L/D is maximized at approximately 5.0. Rotor tip speed will be approximately 3.0 times the flight velocity. For a given design rotor tip speed and rotor diameter, the vehicle design weight can be established. If flight speed is reduced to 50 percent ($\Omega R/V = 6.0$), the rotor resultant force coefficient will be found to be approximately four times greater. As indicated in References 1 and 6, the relationship of rotor velocity ratio, $\Omega R/V$, and rotor lift and drag coefficients is such that, at a given gross weight and collective pitch, rotor speed will remain essentially constant over the full angle of attack range. Over the greater portion of the range, a collective pitch setting of zero will produce the highest rotor speed. Any increase in pitch will tend to increase the rotor thrust and decrease the rotor speed. Too great an increase in pitch will tend to cause the rotor to stall and autorotation to cease. However, the unstalled operating band is both adequate and typical of everyday helicopter autorotation operation.

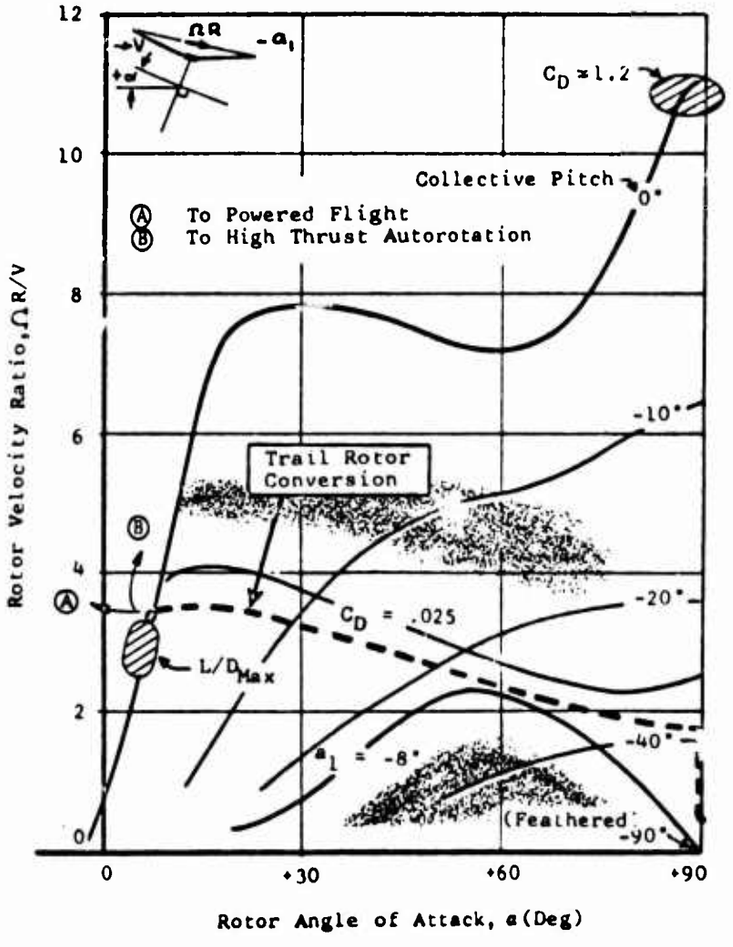

Figure 5 - Autorotative Conversion (Low Thrust Equilibrium)

Low-Thrust Autorotation - As collective pitch settings are reduced to negative values, the rotor speed will again drop off. Also, rotor thrust will drop off. This represents the low-thrust region of operation. At a rotor angle of attack of 90 degrees, for example, the condition analogous to a windmilling propeller exists, and in fact, with a collective pitch of -90 degree , the rotor speed can be brought to zero and rotor drag minimized. This low-thrust autorotation region is presented in Figure 5 and is continuous with the high-thrust region at the reference collective pitch of zero degrees.

A further exploration of this low-thrust autorotation region will indicate that rotor lift drops off quickly as collective pitch

is reduced from zero degrees; that equal drag coefficients parallel the one shown for C_D = .025, increasing toward the upper right, and that flapping rapidly gets excessive below the contour shown for -8 degrees (forward flapping relative to the control axis). If level flight is considered at constant speed above wing stall speed, it is feasible to tilt the autorotating rotor aft through approximately 90 degrees without encountering excessive rotor drag or flapping. This can be accomplished by mechanically varying blade collective pitch as a function of rotor shaft tilt ($\approx$ rotor angle of attack), according to the dashed path shown in Figure 5. In the case shown, rotor speed drops to approximately 50 percent its normal value as the rotor shaft becomes horizontal. Inflow is essentially axial and oscillatory aerodynamic excitations thereby are minimized.

As the autorotating rotor is converted back to the helicopter configuration, it arrives at a low angle of attack at an $\Omega R/V$ of approximately 3.5 and it shares lift with the wing. At this point it is possible to proceed into powered rotor flight by further reducing rotor angle of attack (Path A in Figure 5). Shaft power would be required to prevent rotor rpm from dropping as collective pitch is increased. Wing lift would be reduced if the vehicle angle of attack were also changed during this transition. In the event of power failure at this point, it would also be possible to enter high-thrust autorotation (Path B in Figure 5) by decreasing wing lift (e.g., by raising flaps) as normal autorotation collective setting is established. In this event, the rotor would be operating at about maximum L/D. Specific techniques for autorotation entry in the presence of a wing have been investigated in flight. Reference 7 defines the critical factors involved and the satisfactory techniques for obtaining good results regardless of wing size.

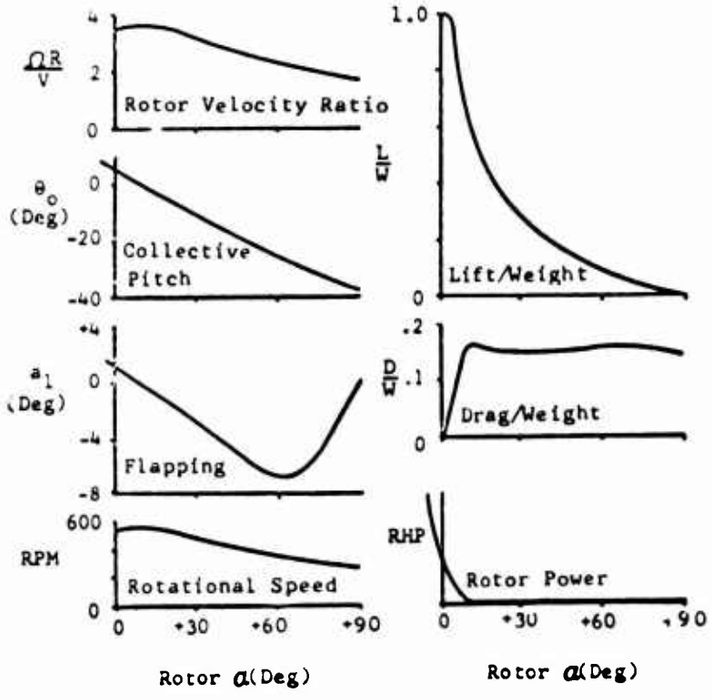

Figure 6 - Typical Rotor Characteristics in Conversion

Applying the non-dimensional characteristics, shown in Figure 5, to a specific rotor with a blade twist of zero degrees, solidity of .07, diameter of 25 feet and at a conversion flight speed of 120 knots, the variation of rotor characteristics through the conversion process as shown in Figure 6, is obtained.

During the conversion and with the rotor windmilling with shaft horizontal, the maximum drag of the rotor blades amounts to approximately 15 percent of the rotor hovering thrust.

BLADE DYNAMICS DURING CONVERSION

Due to the rotor speed range experienced during conversion, the rotor blades will pass through resonances. An examination of the dynamic natural frequenc characteristics of production-type blade construction for the range of rpm and collective pitch required during conversion results in the frequency diagrams, shown in Figure 7, for excitations through four-per-rev. It will be seen from the solid lines in Figure 7, that for a 25-foot diameter three-bladed rotor having stiff in-plane hub and blade geometry, a collective mode is excited by three-per-rev excitations at about 340 rpm and a cyclic mode is excited at four-per-rev, also by coincidence, at about 340 rpm. The first chordwise cantilever natural frequency which responds to cyclic excitations lies between one- and two-per-rev over the conversion rpm range due to the fortunate trend of frequency shift with scheduled pitch change. (The dashed lines in Figure 7 show the frequency trends with collective pitch fixed at zero degrees.) When the rotor arrives at its lowest rpm, the only excitation remaining is one-per-rev in-plane due to gravity. Aerodynamic harmonics are minimized due to the flow being axial.

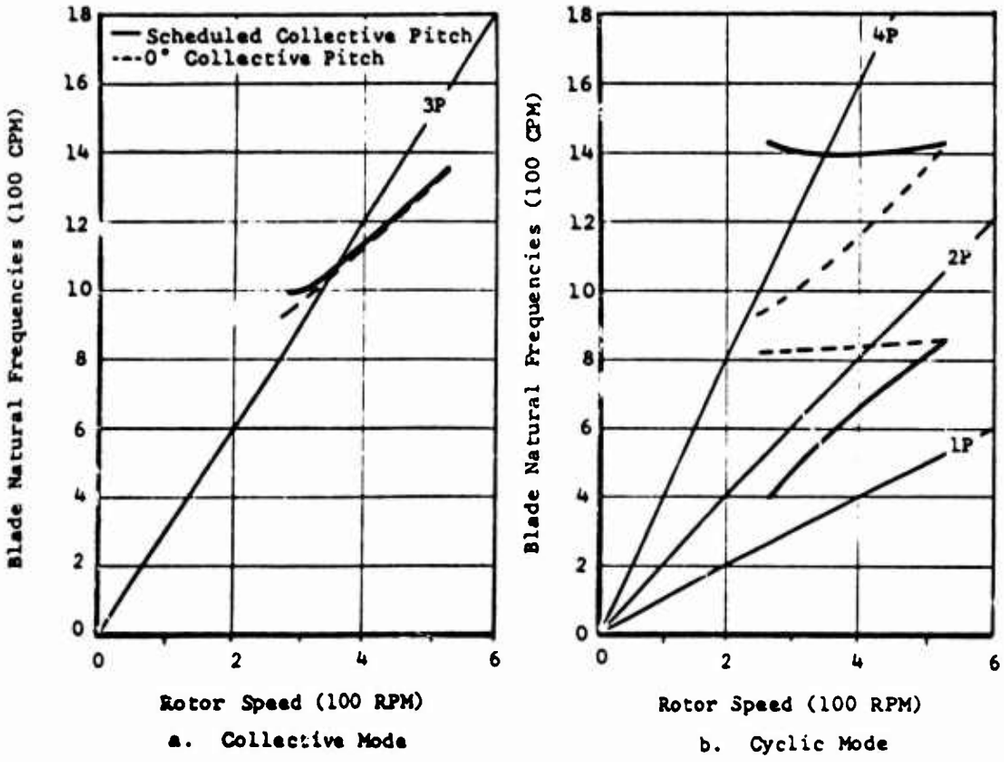

Figure 7
Blade Natural Frequencies - Autorotative Conversion at 120 Knots

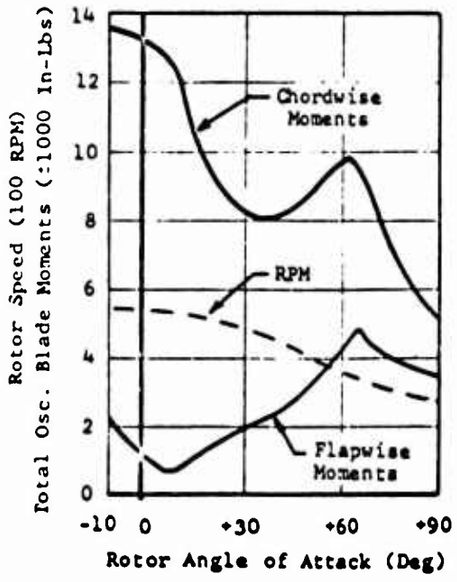

a. Blade Moments @ 15% R

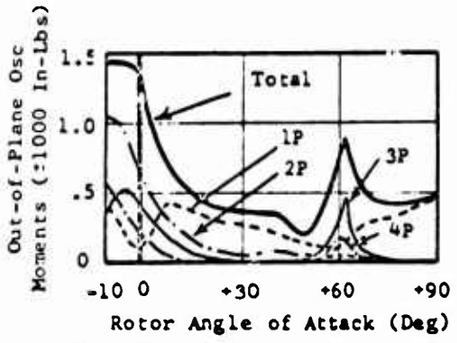

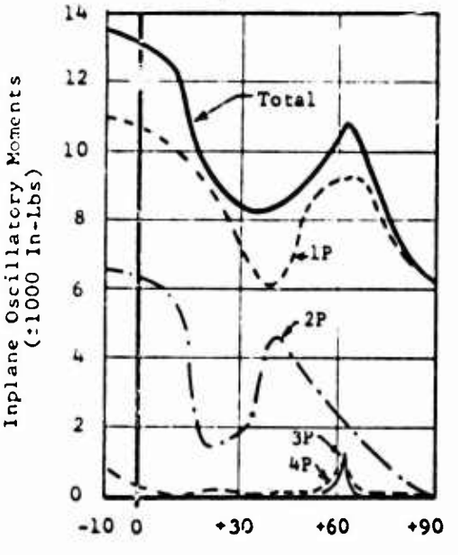

b. TPP Moments @ 15% R

Figure 8
Calculated Blade Loads
During Autorotative
Conversion

To determine the extent of the response of the rotor at these frequencies due to the aerodynamic and gravity excitations experienced during conversion, calculations of the oscillatory moments resulted in the blade loads shown in Figure 8a. To determine the origin of the primary loads, the total response was separated by harmonics in Figure 8b as they apply to in-plane and out-of-plane moments. The results indicate that the three-per-rev and four-per-rev loads at the resonant rpm (and in the presence of structural damping) are a minor part of the total oscillatory loads. When these loads are resolved into flapwise and chordwise loads on the blade, as shown in Figure 8a, it is apparent that one- and two-per-rev are the main components. The oscillatory flapwise moments at high rotor angle of attack are primarily due to the collective pitch setting. The resulting oscillatory moments shown in Figure 8a are well within the endurance limits for the blades.

The above analysis applies to the blade moments incurred through the conversion process and prior to blade folding. The folding (and opening) process, including the required rotor speed change between approximately 50 and zero percent rpm, takes place quickly. Any blade resonances in that speed range are rapidly traversed.

ROTOR OPENING

Figure 9 illustrates the characteristic variation of coning, blade pitch and rotor speed during the rotor opening process. To initiate rotor deployment, the feathered blades are mechanically opened partially into the airstream and pitch is changed. This initiates rotor rotation and as the rpm increases, the rotor opens. Once open, the rotor continues to accelerate until it reaches equilibrium windmilling speed...in this application

about 50 percent rpm, and the conversion to helicopter configuration can take place following the same pitch-tilt angle pattern as before.

Tests conducted with a rotor model of this concept have given opening times of approximately one second. The actual opening times of full-scale rotors would be controllable through the type of opening mechanism and the pitch-cone schedule used for deployment.

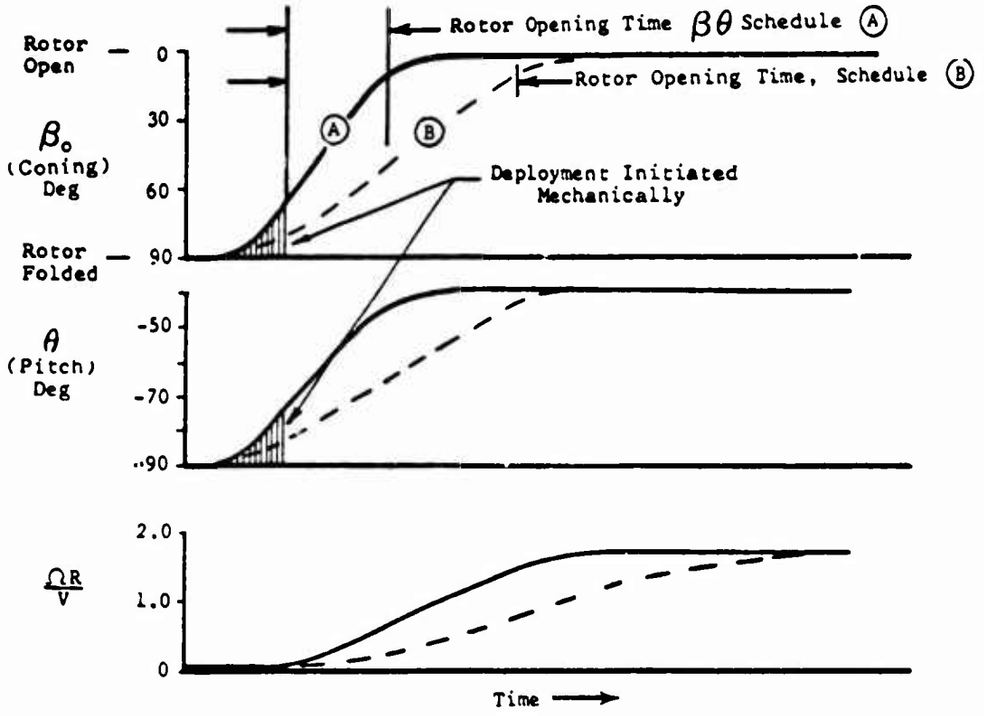

Figure 9
Rotor Opening Characteristics

EXPERIMENTAL MODEL PROGRAM

To explore experimentally the trailing rotor system conversion sequence including the blade folding and deployment phases, an unpowered three-bladed rotor system was tested in a 7 x 10-foot wind tunnel. The model was provided with the necessary mechanical functions for this purpose. These included a collective pitch range of 100 degrees, longitudinal and lateral cyclic pitch of 12 degrees, 100 degrees of coning freedom, inter-blade elastic flapping constraint, a pneumatic actuator for folding and initiating opening of the rotor and a self-contained pylon conversion actuator. Rotor diameter was four feet and blade chord was 1.63 inches giving a solidity of .065. The 4-inch diameter faired hub was of stiff, in-plane geometry with 5.4 percent radius offset flapping hinges. The collective and cyclic controls were of the servo-type to permit "flying" the rotor during conversions at constant pylon rates and thereby establish potential pitch-tilt coupling requirements.

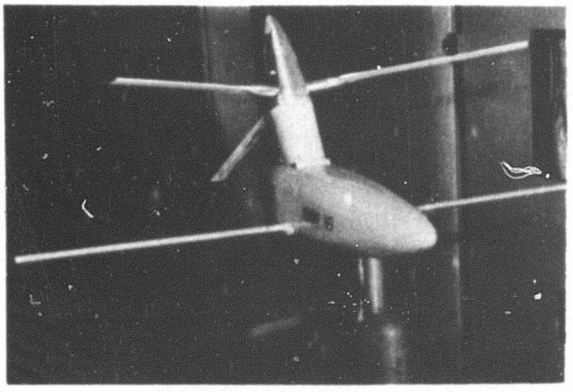

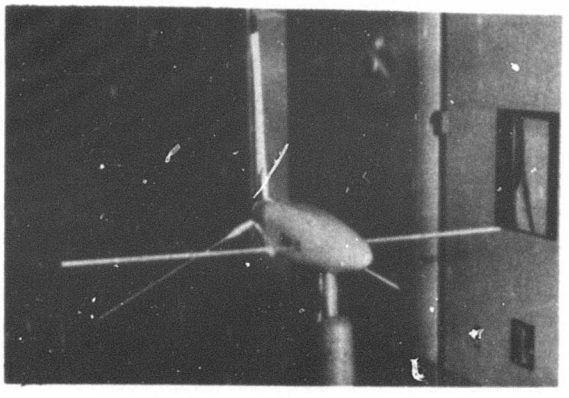

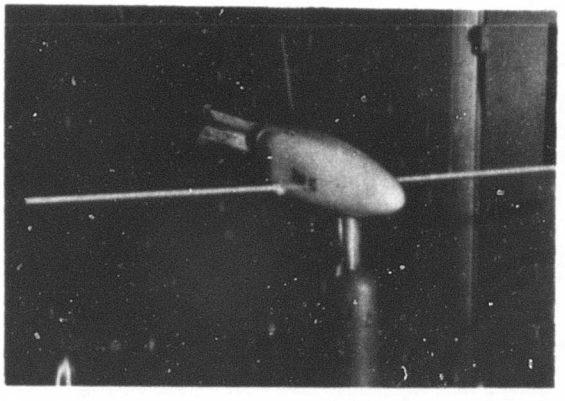

Figure 10
Trail Rotor Wind Tunnel Model

After initial powered hovering-type tests for checking tracking, balance, and control system behavior, the rotor was functionally tested without power through the autorotative conversion range, including the blade deployment and folding sequences. The pre-tunnel functional test was conducted from a pick-up truck test bed at speeds of approximately 40 knots. Rotor behavior was good even in gusty conditions.

The subsequent wind tunnel test, reported in Reference 8, was conducted to obtain force, moment, and flapping data and to explore the folding and opening process. Three positions of the model rotor are shown in Figure 10 The rotor was also tested in the presence of a wing wake where the wing operated at a C_L of 1.0. The wake had only a slight effect on the rotor flapping angles. Successful conversions were executed at 80 knots, deployments were conducted to speeds up to 140 knots, including deployments in yawed flow, and data were obtained with blades folded including yawed flow at speeds up to tunnel maximum of 200 knots. Conversions were made in step-by-step fashion to obtain data at various angles of pylon tilt. Typical test data obtained are shown in Figure 11 and show good agreement with analytical results. Continuous conversions were also made at 80 knots and consisted of deploying the blades from the folded position, converting the rotor to low angles of attack, returning the pylon to a horizontal position, slowing the rotor, then folding the blades.

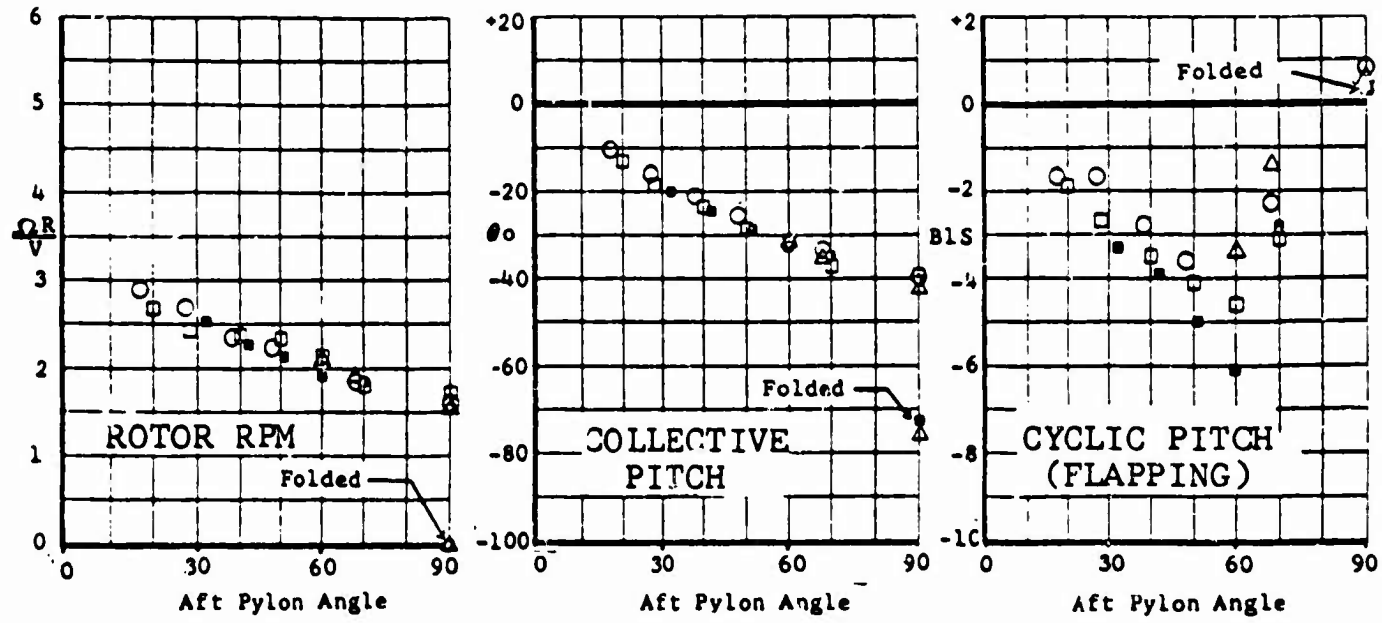

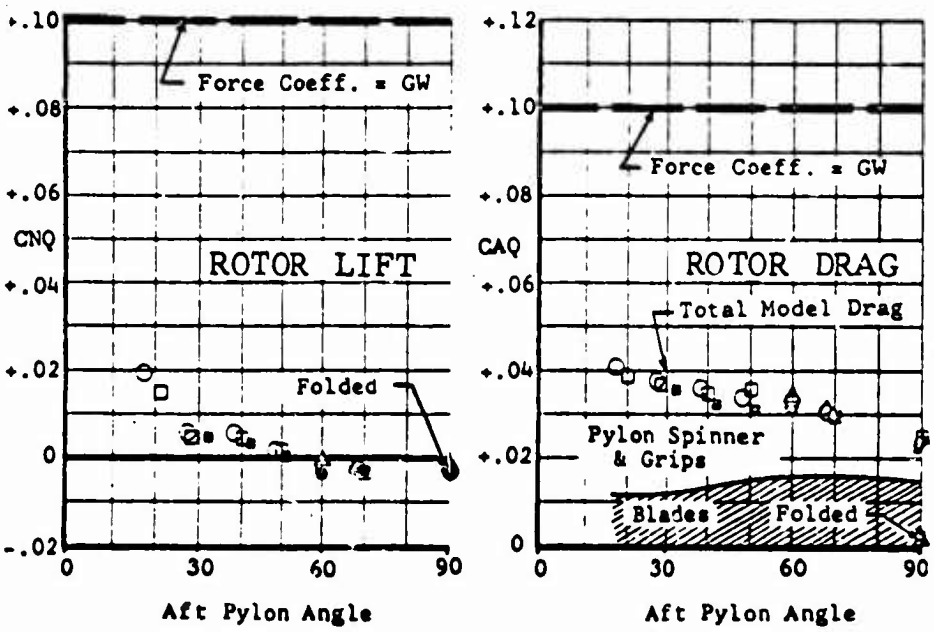

Figure 11
Trail Rotor Model
Wind Tunnel Test Data

From BHC
Rpt 859-099-001

Rotor Model Parameters
3 Blades
4-ft Diameter
.065 Solidity

CONCLUSIONS

1. The ability to convert an autorotating rotor to a (shaft-axis) trailing position without encountering excessive drag or flapping has been demonstrated analytically and experimentally. This is accomplished utilizing the low-thrust autorotative regime of the rotor.

2. Such a rotor system has potential application to high-speed V/STOL aircraft as a low-disc loading vertical lift system and is adaptable to placing in an aerodynamically clean configuration for cruise flight.

3. Demonstration of large-scale, flightworthy hardware is believed to be in order.

REFERENCES

1. Wheatley, John B., Lift and Drag Characteristics and Gliding Performance of an Autogiro as Determined in Flight, T.R. No. 434, NACA, 1932.

2. Wheatley, John B., An Aerodynamic Analysis of the Autogiro Rotor With a Comparison Between Calculated and Experimental Results, T.R. No. 487, NACA, 1934.

3. Wheatley, John B., and Hood, Manley J., Full-Scale Wind-Tunnel Tests of a PCA-2 Autogiro Rotor, T.R. No. 515, NACA, 1934.

4. Wheatley, John B., and Bioletti, Carlton, Wind-Tunnel Tests of a 10-Foot-Diameter Gyroplane Rotor, T.R. No. 536, NACA, 1935.

5. Wheatley, John B., and Bioletti, Carlton, Wind-Tunnel Tests of a 10-Foot-Diameter Autogiro Rotor, T.R. No. 552, NACA, 1935.

6. Wheatley, John B., An Analysis of the Factors that Determine the Periodic Twist of an Autogiro Rotor Blade with a Comparison of Predicted and Measured Results, T.R. No. 600, NACA, 1937.

7. Lynn, Robert R., Wing-Rotor Interactions, presented at the Symposium on the Noise and Loading Actions on Helicopter, V/STOL Aircraft and Ground Effect Machines, The University Southampton, Hampshire, England, September, 1965.

8. Sambell, Kenneth W., Trailing Rotor Convertiplane Model Rotor System Wind Tunnel Test, Bell Helicopter Company Report 859-099-001, August, 1964.

THE BREGUET 941/MCDONNELL 188 CROSS-SHAFT SYSTEM

H. J. DeGarcia

McDonnell Aircraft Company

(This paper was not received at press time. It is planned that this paper will be published and distributed at a later date.)

V/STOL AIRCRAFT TESTING & OPERATION

Lt. R. Rich, USN

Technical Session Chairman

BLANK PAGE

THE CANADAIR CL-84
V/STOL TILT-WING PROTOTYPE

F. C. Phillips

Canadair Limited

"THE CANADAIR CL-84 V/STOL PROTOTYPE - BACKGROUND AND EARLY TEST RESULTS".

F.C. Phillips

Program Manager CL-84, Canadair Limited

1. ABSTRACT

The Canadair CL-84, a 6-ton, two-engined V/STOL aircraft of the tilt-wing, deflected-slipstream type, is now being flight-tested at the home plant in Montreal. The Canadian Government and Canadair, in undertaking the program, intended to develop a prototype vehicle to the point where military demonstrations and evaluations could begin. The configuration is such that the CL-84 itself can be used directly in close support of ground forces and in a variety of utility roles. The program has proceeded straightforwardly through ground testing into the early stages of flight testing. This paper describes the CL-84 itself and outlines some of the reasoning that determined the airframe and equipment. Model testing and flight simulation activities are covered, especially as they relate to flying qualities. Component development and aircraft ground testing are discussed, with emphasis on problems encountered. Finally, flight testing - past and future - is outlined and commented upon.

2. INTRODUCTION

In August 1963 the Canadian Department of Defence Production and Canadair (wholly-owned subsidiary of the General Dynamics Corporation) agreed to develop the CL-84 tilt-wing V/STOL prototype aircraft. The program is jointly funded, approximately two-thirds by the Department of Defence Production and one-third by Canadair. The funding ceiling is 10,700,000 dollars (U.S.); about 8,800,000 dollars have been spent to date, which is very close to the program estimates. The U.S. Army is a participant in the program to the extent of four Lycoming T-53-L-11 turboshaft engines on loan to the Canadian Government.

The CL-84 program has proceeded on schedule (Figure 1) through ground testing into the current flight test stage. The intent of the program is to develop the prototype by the fall of next year to the point where military demonstrations as a close-support and utility transport vehicle can be made; we are confident that this intent will be fulfilled.

The hardware program is the culmination of a Canadair-Canadian Government V/STOL Research and Development program (Figure 2), carried

on continuously since 1956 by a relatively small group of specialists. During this period intensive analytical and design experience have been obtained in three competitions: tri-Service V/STOL transport (with McDonnell Aircraft Corp.); NATO NBMR-4 V/STOL transport; U.S. Army AAFSS. Throughout the period major emphasis has been placed upon experimental work associated with certain critical problems. Figure 3 shows a rig designed and built by Canadair in 1961 to help fill a virtual void in propeller literature with respect to static thrust; in Figure 4 we see a mobile rig, designed and built in 1958 used to investigate the low-speed aerodynamic characteristics of models, free of the severe flow constraints of the usual wind tunnel; Figure 5 illustrates the Canadair flight simulation facility, which has been particularly important to pilots and engineers in understanding flying qualities and control system design problems. This background work, plus a lengthy preliminary design stage for the CL-84 itself (reported in part in Reference 1), made it possible for the hardware program to get underway quickly and move forward at a fast pace. An additional advantage has been the organization of this developmental project as a largely-self-contained group (including shop and test operations) within the Engineering Division, reporting to a Project Manager with quite broad authority and responsibility.

3. THE AIRCRAFT ITSELF

The CL-84 was originally conceived as a research tool, of small size in order to keep costs to a minimum. As time went on, the V/STOL literature and the Canadair capability grew, such that the CL-84 evolved logically into a developmental vehicle with direct specific military applications in mind as soon as development had proceeded sufficiently. This change in intended usage required that the useful load be increased significantly, particularly for the hot-day condition. Likewise it became important to increase the maximum speed to a considerable extent. For these reasons the installed power was approximately doubled, to the level of 1400 SHP/ENG.

Figure 6 shows the general arrangement. The geometry of the fuselage will be explained later. The significant areas of the vehicle relative to its gross weight are generous, with the intent of providing good flying qualities. For example, the wing loading at design gross weight is about 45 lbs. per sq. ft. The disk loading based on total disk area is about 30 lbs. per sq. ft. The wing chord is half the propeller diameter. The wing is equipped with leading-and trailing-edge flaps across the entire span. The leading-edge Krueger flaps are 10% of the wing chord and the trailing-edge flaps 30% of the chord. The distances from wing to tail are generous, again for the reason of improving flying qualities; for example the wing to horizontal tail spacing is more than three wing chord lengths and the wing to vertical tail spacing is 1.3 semi-spans. While these generous parameters came at a price in terms of weight empty, we believe they have contributed greatly toward good flying qualities.

Several features of the CL-84 are particularly worthy of note. The

horizontal tail is placed relatively low so that it is below the wing wake during cruising flight and always within the slipstream regardless of wing-tilt angle. The placement within the slipstream is important in order to prevent large and abrupt changes in pitching moment as a function of wing-tilt angle. Three vertical tails are employed; wind tunnel tests indicated that at intermediate tilt angles the dynamic pressure over the lower portion of the vertical tail was sufficiently low that the directional stability became marginal to the point where poor lateral-directional characteristics (e.g., Dutch Roll) became highly probable. For this reason auxiliary fins were placed at the tips of the horizontal tail within the slipstream field, and by this means a good margin of static directional stability is provided throughout transition. The nacelles are placed low relative to the wing in order to assist in deflecting the slipstream to provide high lift in the STOL mode, and also to place the thrust line ahead of the center of gravity in VTOL flight in order to require favorable (up) balancing tail rotor loads. The propeller plane is placed well ahead of the wing leading-edge (0.5 chord or 0.25 diameter) to reduce vibratory loads in the propeller and Krueger flaps. The landing gear fairings are abnormally large for the reason that the tire pressures approach 40 lbs. per sq. in. with side-by-side wheels. While this is highly desirable in an Army support aircraft, it is nevertheless an aerodynamic difficulty. The fairings tend to cause a down-load in the slipstream and hence loss of gross weight in the VTOL mode, longitudinal stability loss, irregularities in directional stability, high drag, or a combination of all these things. The shape shown here is the optimum one on the basis of extensive wind tunnel testing.

The fuselage received considerable attention prior to decision on the lines shown in Figure 7. It had been decided that the prototype would be arranged to facilitate demonstration in Army support roles as well as utility transport roles. With respect to Army support roles, tandem-seating arrangement of the crew seemed to provide a series of advantages. However, such a fuselage arrangement would practically eliminate the possibility of demonstrating in the transport role. After considerable study and discussion with military people, we decided to use the side-by-side seating arrangement and to provide a substantial amount of cargo volume (200 cu. ft.) in the prototype fuselage, as shown in the Figure. It was also decided, however, to provide in the side-by-side transport fuselage a capability of carrying external stores beneath the fuselage and also for mounting a machine gun turret in the nose of the aircraft. These provisions are shown in Figure 8. The structural shell is capable of 4.0 g limit load factor while carrying 2000 lbs. of external stores beneath the fuselage and a 7.62 mm. high-rate-of-fire machine run turret in the nose of the aircraft. In order to do this the landing gear had to be lengthened so that the fuselage ground clearance would be adequate.

3.1 Control System.

The overall control system of the CL-84 necessarily involves a fixed-

wing system, a different system for hovering flight, and a means of changing gradually from one to the other through transition flight, so that the pilot can continuously command roll, pitch, yaw and height responses of the aircraft by movements of conventional airplane-type cockpit controls. Figure 9 shows the relationship of these cockpit controls to the control means used for the three phases of flight. Figure 10 shows the cockpit controls arrangement. The control for the Jarry Hydraulics wing tilt actuator is the speed brake switch on the standard cockpit power lever shown in the figure; it is used to command the tilt actuator on or off at a rate determined by wing tilt angle and direction of motion.

Figure 11 represents the elements of the control system deployed throughout the aircraft. Basically, the controls are power-operated, with servo, feel and trim units located close to the cockpit and servo-actuators near the control means. In the case of elevator and rudder, power operation would not be necessary but since these surfaces are always connected to the cockpit controls, it seemed preferable to divorce these controls from the pilot to prevent undesirable feedback to the pilot when hovering with tail to wind. The various powered controls are connected to primary and/or utility hydraulic system in an arrangement optimized with respect to degradation of the pilot's Cooper rating as a result of single hydraulic system failure.

The variation of control functions during transition is brought about by a control scheduling or "mixing" unit (Figure 11), which receives wing tilt angle as a mechanical input to rotate a series of plate cams which prescribe scheduled changes of control system gearings. By this straightforward means it is possible to provide, throughout the entire speed spectrum, an adequate and harmonious control system; the system can be modified readily by replacement of control cams - an important consideration for the flight test stage. In leaving this topic, it is appropriate to point out an important control system aspect: the power lever is always connected to the engine fuel control unit, but at higher tilt angles there is in addition a scheduled direct authority over propeller blade angle to provide immediate thrust response during hovering and low-speed flight.

The CL-84 control system contains an automatic control feature in the form of a stability augmentation system ("S.A.S.") by Sperry Phoenix. This S.A.S., which is active during hovering and transition flight, is made up of qualified elements of high reliability, packaged for the CL-84 usage and arranged so that the various parameters can be adjusted over ample ranges in flight, or switched to zero values. Aircraft upsets are sensed by rate gyros in pitch, roll and yaw; the gyro signals operate actuators through flapper-type hydraulic control valves. The S.A.S. actuator outputs are mechanically summed with the pilot's inputs at the control mixing unit. Since pitch is the most critical axis it was decided to dualize the pitch channel. A self-monitoring feature assures that in the event of a single gyro or actuator failure the overall dynamic performance of the pitch channel is unchanged. Another element of the S.A.S. is a pitch attitude gyro that can be set to

provide a difference signal relative to a reference fuselage pitch attitude; this signal is summed with the pitch rate gyro signals to drive the pitch actuators, and thus provide an artificial static stiffness. Further, the pitch and roll channels have a "lagged rate" capability which furnishes a pseudo-attitude signal. This is accomplished by operating on the rate gyro signal by a lag filter having a relatively large time constant. The "lagged rate" capability of the S.A.S. has not been used to date. While we do not believe all of these S.A.S. features will be required or even desired, nevertheless we feel it wise to have this large measure of flexibility in the S.A.S. for the flight test stage.

3.2 Lift Propulsion System.

The lift-propulsion system is shown in Figure 12. It includes, in each of the two nacelles, an engine and a propeller-gearbox unit. Also included are elements which connect the two propellers through their gearboxes, namely shafting and auxiliary gearboxes aligned with the wing-tilt axis. In the event of engine failure, the failed engine disengages by means of an overrunning clutch. The aircraft is then powered by the remaining engine through the cross-shafting, and the distribution of power corresponds to the relative blade angles of the two propellers. The lift-propulsion system also provides a central gearbox in the plane of symmetry, out of which extends a tail rotor shaft which continues aft in the fuselage to behind the vertical fin. At this point there is mounted a tail rotor and a gearbox for pitching control and lift during hover and transition flight. The hydraulic pumps are driven by the auxiliary gearboxes in the wing, and the fuselage gearbox drives the propeller governing system. The total number of gears in the lift-propulsion system is 30, which we believe compares quite favorably with corresponding data from helicopters of equivalent type.

The engine is the Lycoming T53-LTC1K-4A, which develops 1400 SHP under standard sea level conditions. This engine is closely related to the T-53 1100 SHP engines now in production for the UH-1 Iroquois helicopter and the OV-1 Mohawk fixed-wing airplane in the U.S. Army inventory. The 1400 h.p. level is obtained by means of a change to transonic compressor blading, a two-stage gas producer turbine, and a two-stage power turbine in the engine - developments which have been proceeding for some time at Lycoming. Changes have been made in the oil seals and lubrication system to ensure normal operation in the vertical as well as in the horizontal attitude. The engine passed a 50-hour PFRT to a rather demanding duty cycle in fall 1964, and has been operating very satisfactorily in the aircraft. This engine, slightly modified and less the VTOL modifications, is scheduled to pass its 150-hour qualification test at 1400 SHP next year as the T-53-L-13; it will be produced in quantity, and has a substantial growth prospect still.

The main propeller-gearbox units, auxiliary gearboxes and shafting have been developed specifically for the CL-84 application by the Curtiss-Wright Corporation. They have been designed to absorb the full output of both

engines, and have a growth potential to 2000 SHP/ENG from the present 1400 SHP/ENG. Several features of this hardware are worthy of mention here. The propeller is a 14-foot, 4-blade design incorporating blades of foam-filled fiberglas. The blade fabrication processes are essertially those used for the X-19 Tri-service transport blade, although the geometry involved is quite different. The propeller and its gearbox are integrated so that the propeller loads are transmitted directly into the gearcase and airframe via a large-diameter thrust bearing; nevertheless, propeller removal for servicing is easily accomplished in the field. The shafting is made by cold-working a forged stainless steel billet; it operates subcritically at about 6000 RPM, and is designed by shaft whirling considerations rather than stress levels. Thomas couplings are used to provide tolerance to misalignment between shafts; in this type of coupling the misalignment results in bending of a series of steel shims, which avoids fretting corrosion and other fatigue problems normally associated with pin-jointed or splined couplings. The shafting does not involve any welded material, as further insurance of freedom from fatigue. The RPM governing system is mounted on the fuselage gearbox and is driven by the shafting. It is hydromechanical, and controls RPM by operating upon the propeller blade angles in the usual manner. A standby governing system is actuated manually by the pilot or automatically by an overspeed switch, separate entirely from the engine topping governor. The governing system performance during throttle bursts at high RPM is improved by a cam which schedules propeller blade angle required to absorb engine torque as a function of power lever movement.

The tail rotor-gearbox unit has been developed in England by the combination of Servotec and C. F. Taylor companies. The design employed is essentially that of the main rotor of the Servotec "Grasshopper" helicopter. The tail-rotor gearbox absorbs its torque in two gear meshes, each of which is connected to a phase of the dual-rotation, rigid rotor. This system has the advantage of aerodynamic symmetry with respect to flying qualities, and it is lighter than the corresponding single-rotation tail rotor. There is an arrangement to declutch and stop the rotor as the wing is locked in the down position. Further, an indexing function is performed so that the two-blade rotors lie in the plane of symmetry. This feature reduces the CL-84 drag somewhat, and also lessens the tendency of the stopped rotor to diverge elastically at high forward speeds. It is worth noting that the tail rotor is used for lifting as well as for control purposes. The arrangement of the aircraft, in particular the relative locations of center of gravity and thrust line when the wing is vertical, requires the tail rotor to provide a steady upward balancing load. The magnitude of this load is such that even during extreme nose-up maneuvering, the tail rotor load will remain positive. Thus the power absorbed by the tail rotor is always favorable to performance; the low loading of the tail rotor gives it a lifting efficiency approximately that of the main propellers.

4. OTHER-THAN-FLIGHT TESTING

An outline of tests will be presented here in more or less chronological

order, leading to ground testing of the complete prototype. Very considerable care was required in making up and executing the test program because of the close association with flight safety and the threat to the limited funding.

Model testing has been a principal facet of CL-84 development (see Figure 13). Good-sized models have been used to approximate full-scale Reynolds Numbers for the transition regime. Propeller geometry and power loadings of the full-scale vehicle were duplicated in order to attain the true axial and rotational slipstream velocities important to flow-separation studies and flap development. Correlation between data from the wind tunnel and the open-air mobile rig has been good for the lower thrust coefficient regime where wind tunnel wall constraints upon the slipstream field are small. The mobile rig, with the model supported on the side arm as shown in Figure 4, is an excellent source of data within ground effect; comparative tests by Canadair showed that, for low heights above ground, the model must be supported above the true ground rather than a ground board, because of the errors introduced by the boundary layer of the ground board. The large half-model, with a 3-foot propeller, was found very convenient and useful, particularly for high-lift investigation; the model results indicated that airframe excitation of the propeller blade is reasonably low and that the blade stresses are slightly higher for the design dive case than for transition flight. The propeller rig investigations have been important to us in avoiding overoptimism in static thrust (see Section 5 below). The nacelle-propeller test demonstrated that static thrust is negligibly affected by the presence of the nacelle in the slipstream. Tests of the complete model in the hover rig showed that there is no measurable vertical load on the fuselage in the presence of the main and tail propellers, and a down-load of less than 1% of gross weight on the final landing gear fairings.

Flight simulation began as a fixed-base IFR operation because of cost considerations and previous experience with this form (Figure 14). In the interest of accuracy the extent of simulation was limited, for example as to degrees of freedom or airspeed. Thus, within the limits of the analog facility, extensive representation was made of non-linear characteristics, particularly as indicated by model test data for the low-speed regime. Control powers and sensitivities, stability augmentation system dampings, and like design criteria were developed with the fixed-base simulator. The use of the power lever for height control in hover was proven in the simulator, and final modifications to the cockpit arrangements were worked out. The Flight Research Section of the Canadian National Aeronautical Establishment (N.A.E.) had been consulted on flight simulation matters over a period of time; this contact led to a joint research program in which use was made of the variable-stability helicopter developed by them. References 2 through 5 document most of the investigations. A particularly important result of this program was the finding that quantitative pilot opinion ("Cooper rating"; Reference 6) is not critically affected by the degree of lateral-directional control cross-coupling. Figure 15, which is taken from Reference 2, shows the relationship between Cooper rating boundaries and degree of cross-

coupling in a VFR hovering and low-speed flight circuit exercise. The fixed aerodynamic parameters are tabulated; the CL-84 parameters for mid-transition speeds correspond well enough with these values that we feel the N.A.E. results relate to the CL-84 situation. The figure demonstrates clearly the limited amount of cross-coupling tolerated by the pilot for normal operation, but, perhaps more importantly, it shows the large amount of coupling permissible under emergency conditions. We take from this that the risk associated with an appreciable degree of cross-coupling, as may be the case in some configurations and/or the early stages of flight testing, is not as great as one might expect. Consequently, it seems feasible and safe to iterate the control mixing relationships in the flight test stage to progressively achieve the low Cooper ratings needed for normal operation. A further use of the N.A.E. variable-stability helicopter was as a calibrating device in effect for the fixed-base simulator; by adjusting the damping of the IFR representation of the aircraft over a spot on the ground, it was possible to obtain almost the same Cooper ratings for the fixed-base IFR hover simulator as for the moving-base VFR representation in the helicopter. We were then able to evaluate with confidence fairly sophisticated and detailed aspects not permitted by the limited capacity of the airborne analog. Prior to the first hover flights and after control dynamics tests on the aircraft, important simulation work was carried on to determine the sensitivity of Cooper rating to effects of backlash, friction and flexibility in the control system. Figure 16 shows the results of this sort of investigation; "lost motion" is defined as cumulative pseudo-static phase lag due to the three factors above. This work generated numerous small but important modifications; from it we have a good feeling for the criticality of control system deviations from the norm. We were very interested and pleased to compare pilot ratings for the first hover flight with those of the final hover simulation. The agreement was quite close, and we have used the simulator freely since, to investigate the effects of failures in the stability augmentation and hydraulic systems, and most recently to prepare for transition flight. We feel that V/STOL flight simulation, properly conducted, need not be terribly expensive and is extremely effective; the benefits in design cues, test program planning, flight safety and pilot training are outstanding.

Turning now to propulsion system development, we see in Figure 17 a list of the major tests performed prior to ground testing of the prototype. It was recognized at the start of the CL-84 program that the funding ceiling and scheduling considerations advised against an integrated propulsion test stand. Consequently, but recognizing that the only meaningful testing would be of the entire system, it was decided to do only ad hoc, specific testing of the various components as necessary to prepare them for extensive system testing in the actual aircraft. Only the engine was qualified in the usual sense as a component prior to propulsion system testing. There was of course some risk in this practice, but events have shown that the program was reasonably close to optimum in cost-effectiveness. The development of the propulsion components was accompanied by the usual number and variety of technical problems - for example, gearbox lubrication, bearing failures, excessive

gear deflection, breakdown of test rigs - and of course the associated management problems. A substantial overweight in the main gearbox will remain as a problem in the prototype, although in a production effort it probably could be eliminated.

4.1 Ground Testing

In January of this year we began ground testing of the aircraft, which was by this time nominally complete as to propulsion system. Testing was done with the ship tied down at the landing gear struts to a T-rig built up of I-beams, and equipped with a pivot and rollers so that the aircraft-rig ensemble could be re-oriented, if need be, when the wind shifted (Figure 18). During the deep-winter time period there were test days with sub-zero temperatures accompanied by winds up to 15 Knots. We were worried about damaging the aircraft by inducing abnormally-high loads in the presence of the ground. Some components have been overloaded somewhat, but no problem of any consequence has resulted from the test circumstances. The aircraft ground test program was paced in detail by the progress of the component development testing. As the various propulsive components were cleared for expansion of the test envelope, aircraft testing took advantage of the improved situation. At first there were limitations on power asymmetry and tail rotor operation. For a period there were restrictions on wind speed with the wing vertical, but for some time we have operated at low stress and vibration levels almost regardless of wind throughout the power and R.P.M. range. We have taken the usual precautions: the dynamics of the test rig are uncoupled as fully as possible from those of the aircraft; test instrumentation has been used freely where needed, e.g. oil temperatures and pressures, gearbox vibration and local stresses, propeller blade stresses, shaft torsion, bearing temperatures. Magnetic chip detection warnings were heeded religiously; although usually the metal particles were fine powder and inconsequential, there were a few times when the chip detectors warned of proper failures.

During February the engine-gearbox overrunning clutches malfunctioned and had to be rendered inoperative for some time while modification and additional testing were accomplished. Propulsion testing proceeded, so that by mid-February the system was shown to have acceptably-low vibration and stress levels throughout the operating range. During March the control system was completed and tested thoroughly without engines operating. Propeller governing tests showed that with wing up the scheduling cam arrangement relating power lever motion to propeller blade angle was not correct, as evidenced by inadequate R.P.M. governing during throttle bursts. While we have made progress with this problem, it is not fully satisfactory still. Also during March there were two local failures of the bond between the blade fiberglas shell and the foam-plastic fill (Figure 19); they were repaired in place overnight and these same blades are still in use on the aircraft.

In April with the propulsion system operating reasonably well, attention turned to control system proving. This was a most important task in that cost and schedule considerations had denied to the program a control system rig or other means of testing the system prior to installation in the prototype. The CL-84 could now be tied down to the test pad with strain-gaged arms to measure lift, pitching moment and rolling moment. The control dynamics work in March had shown rather higher impedances than expected, and the hovering flight simulator was indicating the importance of reducing these same impedances (Figure 16). With the help of dynamic records from the strain-gaged tiedowns on the rig, the control system was improved greatly for hover flight by a series of small modifications, consisting of anti-backlash springs, local stiffness increases, elimination of fouling and other causes of friction, and addition of an actuator to the propeller pitch control system. By this time (early May), the wing tilt actuator and stability augmentation systems were functioning dependably. It now appeared reasonable, after 36 hours of ground testing, to explore cautiously hover flight to determine if there were important flying qualities problems outstanding for the hover mode.

After 37 minutes of successful flight (see Section 5 below), ground testing was resumed in late May. Using a specially-instrumented power turbine, Lycoming and Canadair personnel tested to measure the turbine blade vibratory stress level. Excitation from propeller gearbox tooth impacts had been of concern at the start, and design work at Curtiss-Wright and Lycoming was closely coordinated. Measured turbine blade stresses were quite low, demonstrating a high degree of compatibility between engine and gearbox.

During most of June the CL-84 was in the hangar. The gearboxes, shafting and wing tilt actuator were removed after 56 hours of operation and replaced in order to extend operating limits with the new equipment and permit close examination of the old. Both engines were inspected and cleared by Lycoming for 75 hours before another check. The control system was modified in numerous details and completely re-rigged. Shortly after the start of testing in early July one of the propeller-gearbox overrunning clutches failed because of small foreign matter lodging in a critical clearance area. Within a week the clutch design had been modified and new clutches were installed in both gearboxes; no further trouble has been encountered with this component.

Additional instrumented testing of the propulsion system in July caused some concern as to stresses in a very localized region of the propeller gearbox casting, and in the large magnesium "adapter" casting which carries the propeller gearbox on its forward flange and the engine on its rear face (Figure 20). A local rework of the casting improved the stress level satisfactorily for the gearbox. Stresses in both components were found to be appreciably less in hovering flight than during ground test, and there is no present concern over fatigue life. The situation will be re-examined after the

stresses are known throughout the flight spectrum.

In late July systematic ground testing of the control system was done to determine its adequacy throughout the wing-tilt range. It was found quite satisfactory for wing tilts from 90° to 50°, below which several control programming cams were known not to correspond to criteria recently developed by model testing. During this period there were several incidences of fuselage gearbox clutch slippage at high torque, which induced high dynamic loads in the internal shaft of the tail rotor. The clutch appeared not to be developing the necessary coefficient of friction; increased clutch pressure provided an interim fix. In this period there were also several cases of fatigue failure in brackets and hydraulic fittings, and chafing of hydraulic lines. A close inspection was made and as a result additional tie-downs of lines, more flexible hoses, and modifications of fittings were introduced.

In the first week of August another series of successful flights were made, bringing total time to almost two hours. Shortly after, a 75-hour inspection was made without finding anything but local airframe failures and chafed lines. The engines were given an additional 25 hours of operation. In preparation for the PFRT, the ground test rig was "streamlined" somewhat to reduce the slipstream vorticity when the wing is down; this modification, plus removal of the horizontal tail from the aircraft reduced the airframe buffeting during ground testing to a reasonably low level (Figure 21).

On August 13, a period of concentrated propulsion system testing was begun, with the intent of simulating prototype flight duty so as to reveal weaknesses and establish appropriate inspection, overhaul and replacement times for the October flight test phase. For this purpose a one-hour duty cycle (Figure 22) was drawn up in the spirit of the helicopter 50-hour PFRT specification MIL-T-8679. Prototype aircraft duty was simulated rather than that of an operational V/STOL machine; since we expect to spend a lot of time in the low-speed flight regime, it was assumed arbitrarily that the tail rotor would be active fully 40% of the time. Considerable use of the non-aerodynamic controls was assumed, by the same reasoning, so that the transient loads on the propulsive system would be represented; for this purpose the stability augmentation system was fed synthetic upset signals in order to cycle the controls through the smaller amplitudes. While the detail of the duty cycle may seem burdensome, in practice it quickly became routine. The strict cycle was violated numerous times in order to keep the program moving as difficulties were encountered.

Figure 23 lists the major failures and malfunctions of this PFRT period, which is expected to end in the early part of October. As can be seen, none of these problems are of major concern in a development program. By intent or circumstance, several of the components started the PFRT with considerable operational time; at the time of writing, with about 40 PFRT hours accomplished, the engines and propellers originally installed were still in use. One engine had been out of PFRT service a short time for replacement

of first-row blades damaged by a bolt from the airframe intake duct. The tail rotor was removed late in the PFRT after 89 total running hours, because of calendar time required to replace a cracked part. Most of the problems experienced were easy to bear, because they were attributable to the developmental status of a component. For example, the fuselage gearbox bearing failure was almost certainly due to its reacting excessive pressure required in a substandard clutch; most of the tail rotor control problems were direct results of above-specification control loads. Design changes and/or developmental testing are already accomplished in most cases, and underway in others, so that the reliability will be increased to a satisfactory level. This action, plus establishment of appropriate inspection, overhaul and replacement times at the end of PFRT, will provide the propulsion system reliability required for further flight testing.

At the end of the PFRT, it is intended to conduct taxi tests. All propulsion system components will then be replaced by new or overhauled units. The control system will be brought to the latest modification standard, and carefully rigged throughout the entire wing-tilt range. The aircraft will be inspected very carefully and repaired as necessary. Several tests on the tiedown rig will be conducted to assure that all systems are functioning correctly and dependably, before flight test gets underway.

5. FLIGHT TESTING

The first flight of the CL-84 took place on May 7, 1965 with Canadair Chief Pilot W.S. Longhurst at the controls. "Bill" Longhurst has 25 years of piloting experience, including 10 years as an engineering test pilot of fixed-wing airplanes of all types and sizes to beyond 200,000 lbs. gross weight. These basic qualifications have been focused for CL-84 duty by many hours of fixed-base VTOL simulator piloting, acquisition of a helicopter rating, experience with three helicopter types, and considerable amounts of time during the variable-stability helicopter research program described earlier. I mention this to emphasize the critical need in V/STOL development flying for technically-trained pilots with adequate prior VTOL experience.

Four liftoffs of ten seconds each to 5 feet above the ground constituted the first flight. The gross weight was slightly in excess of the design gross weight, 10600 lb.; this same loading has been used generally for flight testing. At once on the first flight, pilot confidence was established. The Cooper ratings agreed so closely with the relevant simulator ratings that at once we were sure of our ability to proceed further without modification. During the next two weeks 37 minutes of flight were logged, in flights up to 7 minutes in duration. The envelope explored included the altitude band through ground effect to 15 feet, small velocities along and maneuvers about all axes, forward flight to 20 Knots, and vertical accelerations to about 1.15 g in height excursions. There was some difficulty in control initially below 5 feet in altitude, but during the two-week period the problem was resolved

by improvements in height control system backlash, and experience on the simulator and prototype. The wing tilt system was found to be jerky in flight, confirming suspicions from the test rig. On the positive side, it was found that, while below 5 feet the aircraft was excited in hovering by reflected slipstream, beyond that altitude the air was quite smooth. Further, there was a strong, positive ground effect on static thrust, amounting to about 15% increase over the free-air value when the ship's wheels were contacting the ground. Presence of the ground had no important effects on trim, and there were no tendencies toward instabilities, e.g. "digging in". Control was good all the way down to ground contact; yawing control at zero wheel height was surprisingly good - about 86% of the free-air value. Hence the CL-84 gave promise of very good flying qualities in hover with little additional development work.

A series of eight flights was accomplished between August 4 and 7. The longest of these flights was 26 minutes. The airborne time was one hour and a quarter, bringing total time to 1 hour 52 minutes. Hovering characteristics were well ahead of expectation for this stage of the program. The pilot felt that the CL-84 already compares quite favorably in flying qualities with the two operational helicopters of comparable size which he has flown. Specifically, the following had been accomplished:

(a) Forward flight from hover (wing tilt 88 degrees) to 33 Knots (wing tilt 48 degrees) and return to hover.

(b) Demonstration of quite acceptable flying qualities with the stability augmentation system completely deactivated.

(c) Demonstration of adequate control in winds gusting to 25 Knots.

(d) Flight at the targeted standard-day VTOL gross weight of 12,200 lb. with a ground temperature 8 degrees F. above the standard value.

(e) Rearward, sideward and turning flight in and out of ground effect.

(f) Sustained flight with hands free of the controls.

(g) Checkout of Canadair pilot G.D. Morrison to assist in the flight test program.

The acceleration to 33 Knots and return to hover was done twice at an altitude of about 20 feet without any difficulty, except for jerkiness in the wing tilt system. There were indications of reduced roll control sensitivity at the lower wing tilt angles, and also an indication that the power required

to fly reduces more rapidly with forward speed than expected.

The stability augmentation system (S.A.S.) deactivation was done in the manner and order developed in the simulator. Figure 24 represents the test sequence; for the test the artificial pitch attitude stiffness contribution was deactivated throughout. The yaw, roll and pitch modes of the S.A.S. were successively attenuated to zero effectiveness, interspersed in each case with the base condition to re-establish afresh the frame of reference. After deactivating the pitch mode, the roll mode was attenuated to zero and then the yaw channel was switched off. For each case, flight assessment was made on the basis of translations and rotations with respect to all three axes, in addition to hovering flight. Figure 24 shows in the right column the resulting Cooper ratings for the overall aircraft or for the particular channel, as applicable. Note that the Cooper rating improves with S.A.S. "failed" in yaw, because of the increase in control sensitivity and power. Loss of S.A.S. in roll was expected to deteriorate the rating because of over-sensitivity tendencies, but there seemed to be no great difficulty in correcting upsets and no tendency for pilot-induced oscillations to develop. Loss of S.A.S. in pitch necessitated use of large control displacements during longitudinal translations and for correction of upsets. During this particular flight the longitudinal control power was temporarily somewhat deficient; we believe that with the full control power the overall Cooper rating for the S.A.S.-off case would be 4 1/2 or perhaps better.

Figure 24 also gives for convenience the values of control, artificial stability and related parameters, based on analysis of the limited flight data available to date. The primary hovering control power in yaw is slightly in excess of that required by the AGARD yawing criterion of Reference 7, which has been used as the CL-84 flying qualities design requirement. It is indicated that the CL-84 will be able to satisfy the AGARD one-second yawing displacement criterion if the artificial yaw damping is deleted, as appears permissible. Note that the helicopter IFR flying qualities criterion of MIL-H-8501A is twice as demanding as the AGARD criterion in yaw. We think the MIL specification is unnecessarily demanding, for the CL-84 has developed steady yawing rates of 35 degrees/sec. and has made full turns in winds to 25 Knots, despite the present high level of yaw damping and S.A.S. authority. The control powers quoted in roll and pitch are roughly twice those needed to satisfy the hovering criteria of Reference which agree here with the IFR requirements of MIL-H-8501A, hence there is no doubt that both criteria can be satisfied without change in the CL-84 pitch and roll S.A.S. dampings and authorities. Incidentally, the roll and pitch control authorities can easily be increased by a substantial amount, the penalty being a tendency toward over-sensitivity of control.

The demonstration of controllability was made in a 10-Knot wind gusting frequently to 25 Knots. The ship was flown at low speed from point to point and return. Several 90° changes of heading and a full turn were made while hovering; the pilot was quite satisfied with control except that turning out of

wind against the S.A.S. was at a rather low rate. The photograph of Figure 25 was taken during this demonstration. Note the Krueger flap deployment at the reduced wing tilt used to fly into the wind. On other flights, and despite the adverse effects of the S.A.S., the following controllability indications have been obtained from hovering flight data; steady-state yawing velocities of 35 degrees/sec. with approximately full cockpit control displacement; peak rolling rates of about 25 degrees/sec. during banks to about ± 20 degrees with about 60% of full cockpit control displacement; peak pitching rates of 10 degrees/sec. with about half of full cockpit control displacement.

The flight at full standard sea level VTOL gross weight was made to obtain an indication of whether there is a significant static thrust deficiency. The test conditions were unfavorable, in that (a) the temperature was 8°F above standard, (b) 95% RPM was used rather than 100% (in order to reduce risk of possible overspeeding), and (c) the propeller blades were the first set and not typical aerodynamically because of airfoil deviations in the form of spanwise straingage wiring and a steel leading-edge anti-abrasion strip now being replaced by one of nicely-contoured plastic. The aircraft was hovered at about 8 feet height with little control activity using full available power. Retesting without the unfavorable conditions above would certainly provide some margin, but there will probably be a need for improved aerodynamics in the second blade design provided for in the program with Curtiss-Wright. We are satisfied that any thrust deficiency will prove to be reasonably small, and we know from model propeller testing that the CL-84 blade can be improved without extensive change. Further, we have indications that the thrust margin needed under limiting hovering conditions for the CL-84 may be less than expected; power losses due to control demands have been based effectively on liftoff and flight under very turbulent conditions without a favorable ground effect on static thrust. As mentioned earlier, only below 5 feet height is the CL-84 excited by slipstream-reflection, and at altitudes approaching zero there is a strong favorable ground effect on thrust trending to 15% increase at zero height. This combination of circumstances may prove in practice to boost the limiting gross weight by an appreciable amount.

6. FLIGHT TEST PLANS

Near the end of October the CL-84 will begin flight testing in earnest. After several flights to confirm the flight envelope outlined above, it is planned to explore briefly fixed-wing handling qualities at about 15° wing tilt. The wing will then be tilted from, say, 15° to 0°, and return, with flight characteristics being carefully studied at altitude. Having established good flying qualities in the region 90° to 48° to 90° wing tilt (see Section 5), and 15° to 0° to 15°, we would then close the gap and extend the range of continuous tilting by another flight or two. The next step would be a forward transition from hover out of ground effect over a long runway. Finally, the reverse transition would be accomplished down a slightly-inclined flight path into a long runway, ending in hover toward the far end of the runway. On

the basis of the good XC-142 flight experience, and considering the lower disk and wing loadings of the CL-84, there should be no broad area of difficulty during transition; recent flight simulation of the transition regime have shown that flight characteristics should be satisfactory in detail. After this has been established, transition procedures will be developed and optimized for various conditions, e.g. c.g. travel, longitudinal and normal acceleration, wing tilt rates, etc. Failures must be simulated, for example in the hydraulic system and S.A.S. Limits of operation can then be determined, so that the transition flight corridor can be drawn up. It is to be expected that during this transition development, some changes to controls programming will be required; this can be done readily by changes of cams in the controls mixing unit.

Hovering flight development work will be continued at convenient intervals during the program. Hydraulic system failures will be simulated. Noise measurements will be made. Problems of operating from a primitive site need to be investigated by flight testing. Required excess thrust margins, and the associated limiting gross weights, must be determined by hovering at various temperatures and altitudes.

Airplane flight would not appear to contain any serious flying qualities problems, and it is expected that the S.A.S. will be deactivated in this regime. Later this fall the landing gear retracting actuators and doors will be installed for high-speed flight. The V-g envelope will be extended. One matter that needs investigation at high speeds is the possible need for a means of modifying longitudinal control parameters as dynamic pressure builds up toward the end of the broad performance spectrum. While the CL-84 static longitudinal stability increases with airspeed, the stick movement and force per g nevertheless may need to be increased in high-speed flight. The control system has been designed with the possibility of this change in mind. Vibration, stress and noise levels will be measured in high speed. The design of the propeller blade was determined by the vibratory stresses of the design dive pull-up. With respect to noise, the propulsive system has been designed to make available full power at a rotational tip speed of only 810 fps (90% RPM), in order to favor propulsion efficiency and noise suppression.

Late in the program, attention will focus upon determination of performance. In particular, the STOL mode will be investigated, for the tilt-wing aircraft offers a large measure of safe overload operation in this mode. By the fall of next year we expect to be in a position to demonstrate the performance of Figure 26 in an aircraft that will be a point of reference for good V/STOL flying qualities.

OUTLINE OF CL-84 TEST PROGRAM

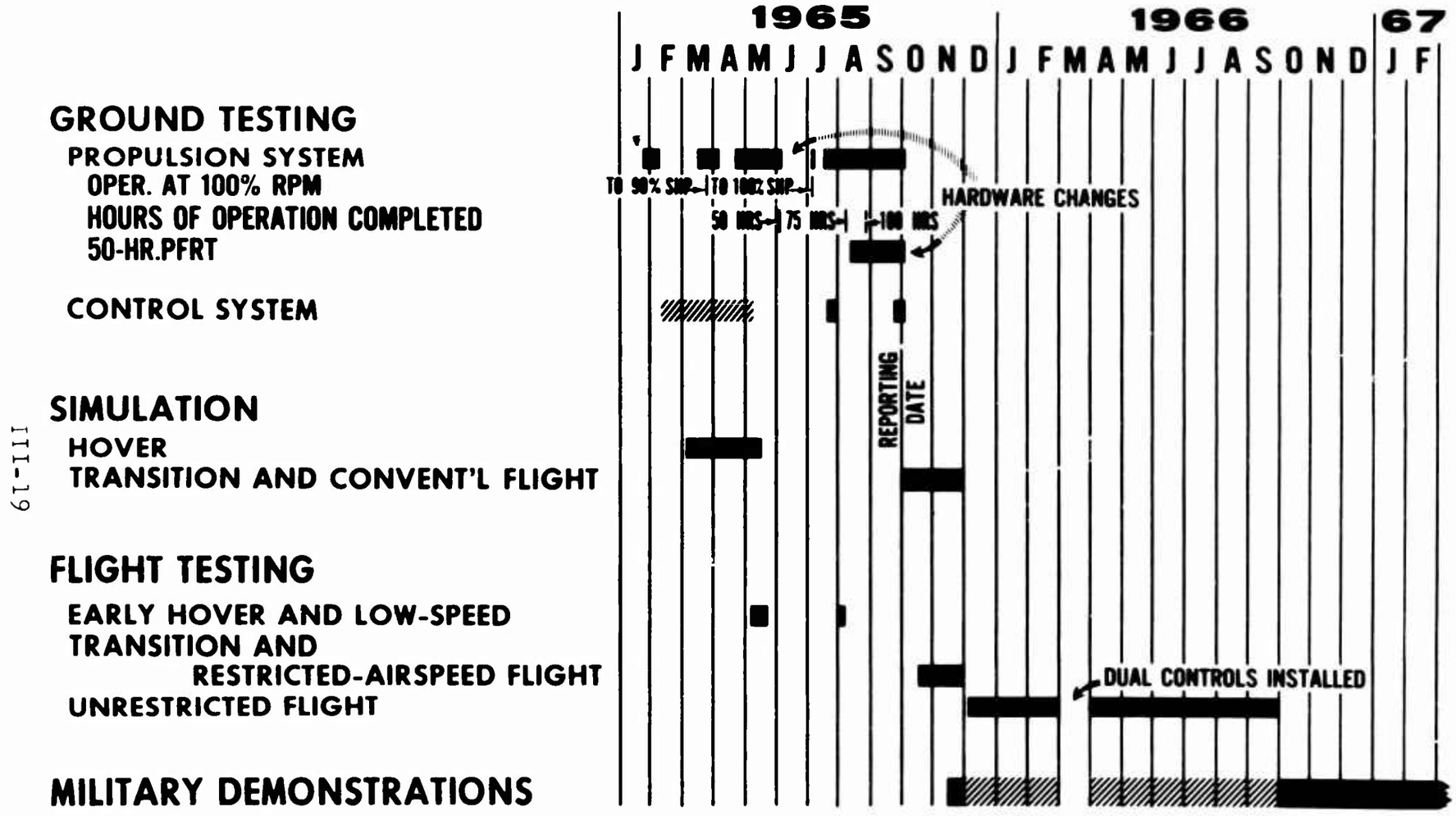

III-19

Fig. 1

REFERENCES

1. J.F. Martin and O.E. Michaelsen, "The Aerodynamic Approach to Improved Flying Qualities of Tilt-Wing Aircraft", AIAA Preprint 63-484 (Canadair paper presented at the AIAA/CASI/RAeS Ninth Anglo-American Conference, October 1963).

2. D.M. McGregor, "An Investigation of the Effects of Lateral-Directional Control Cross-Coupling on Flying Qualities Using a V/STOL Airborne Simulator", National Research Council (Canada) Aeronautical Report LR-390, December 1963.

3. D.F. Daw, D.G. Gould and D.M. McGregor, "A Flight Investigation of the Effects of Weathercock Stability on V/STOL Aircraft Directional Handling Qualities", National Research Council (Canada) Aeronautical Report LR-400, May 1964.

4. D.M. McGregor, "A Flight Investigation of the Influence of Various Levels of Dihedral Effect on V/STOL Aircraft Directional Handling Qualities", National Research Council (Canada) Aeronautical Report LR-412, November 1964.

5. D.M. McGregor, "Simulation of the Canadair CL-84 Tilt-Wing Aircraft Using an Airborne V/STOL Simulator", National Research Council (Canada) Aeronautical Report, July 1965 (to be published).

6. G.E. Cooper, "Understanding and Interpreting Pilot Opinion", Aeronautical Engineering Review, Vol.6, No.3, March 1957.

7. Anon., "Recommendations for V/STOL Handling Qualities", A.G.A.R.D. Report 408, October 1962.

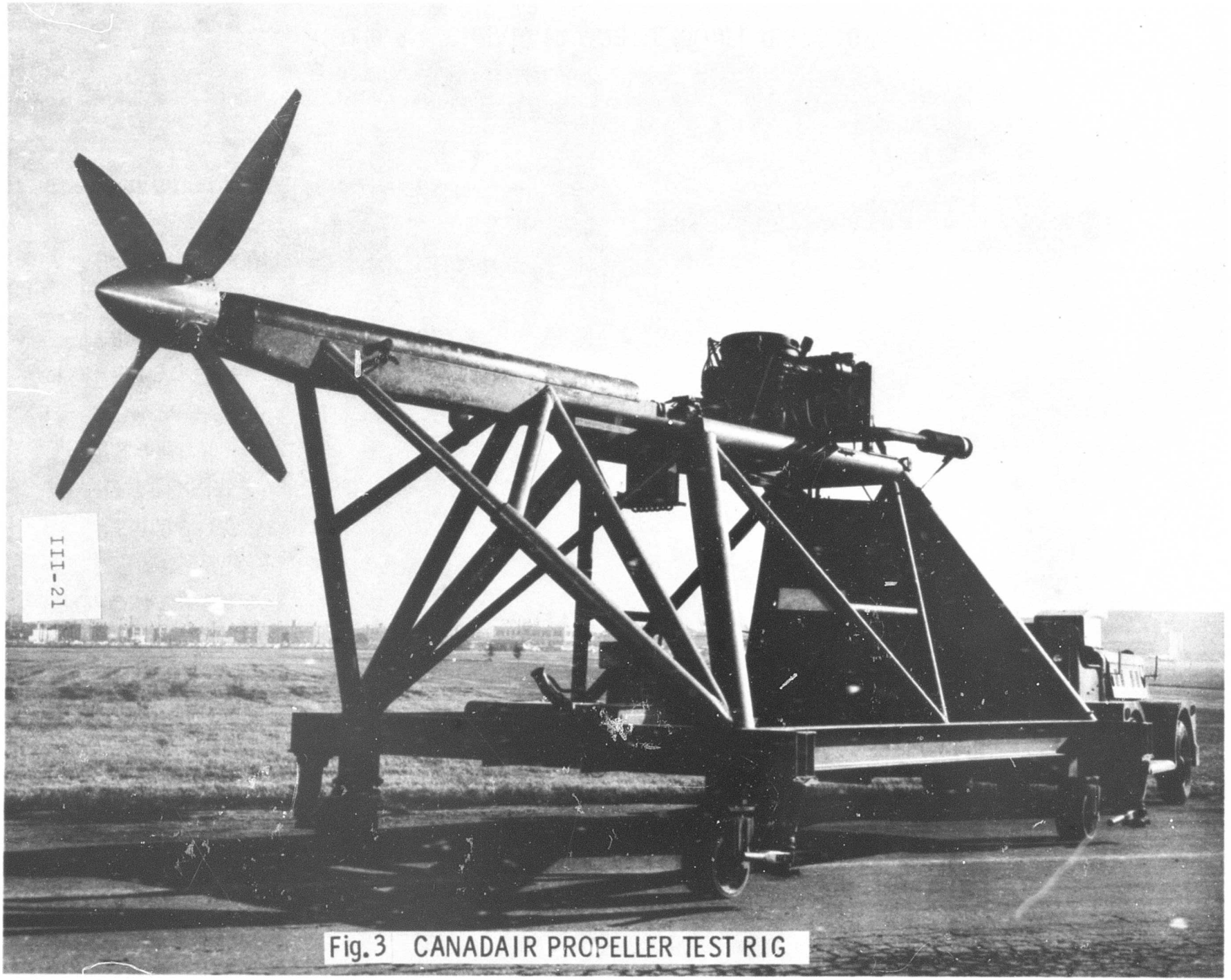

III-21

Fig. 3 CANADAIR PROPELLER TEST RIG

OUTLINE OF CANADAIR V/STOL PROGRAM

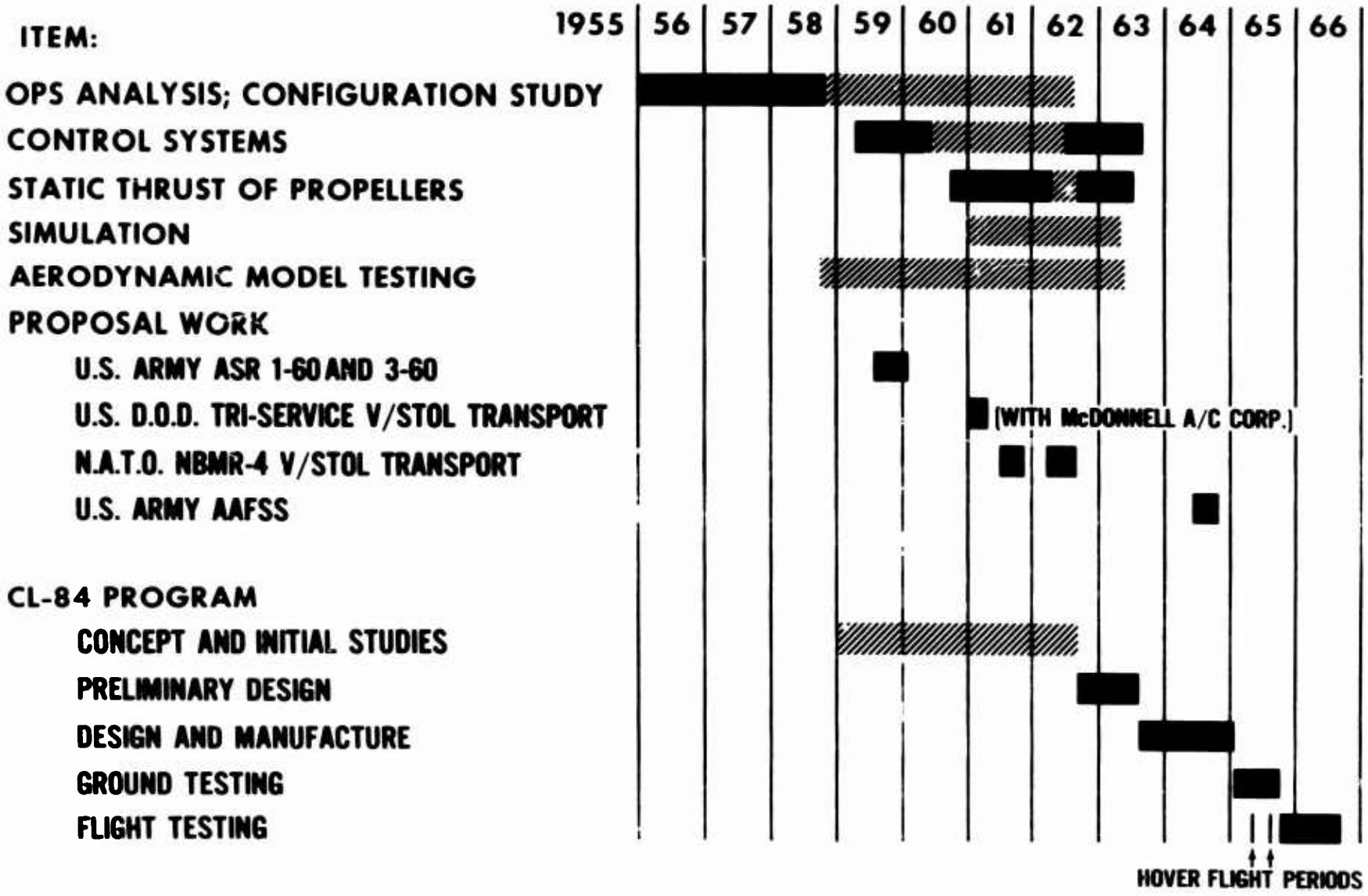

Fig. 2

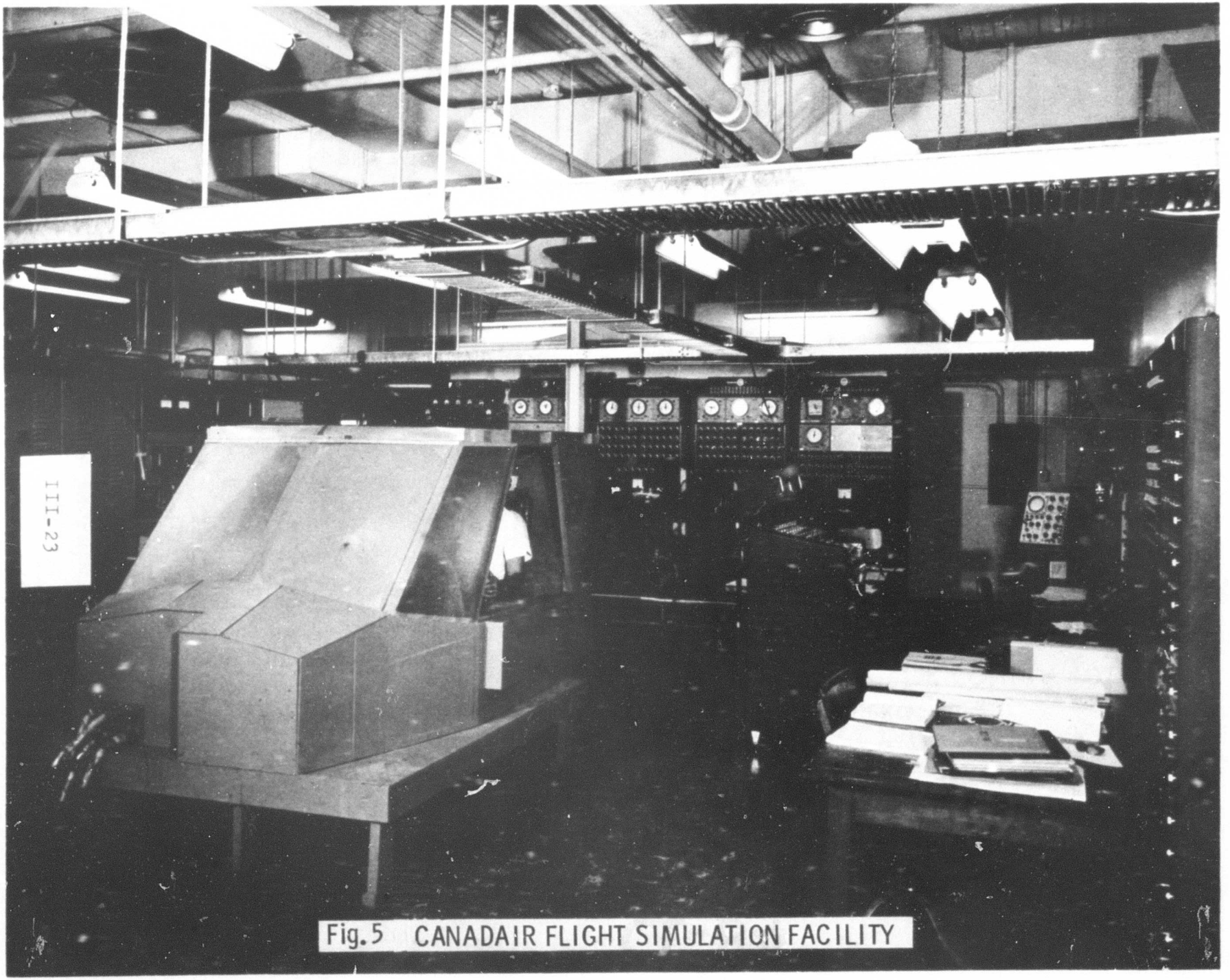

III-23

Fig.5 CANADAIR FLIGHT SIMULATION FACILITY

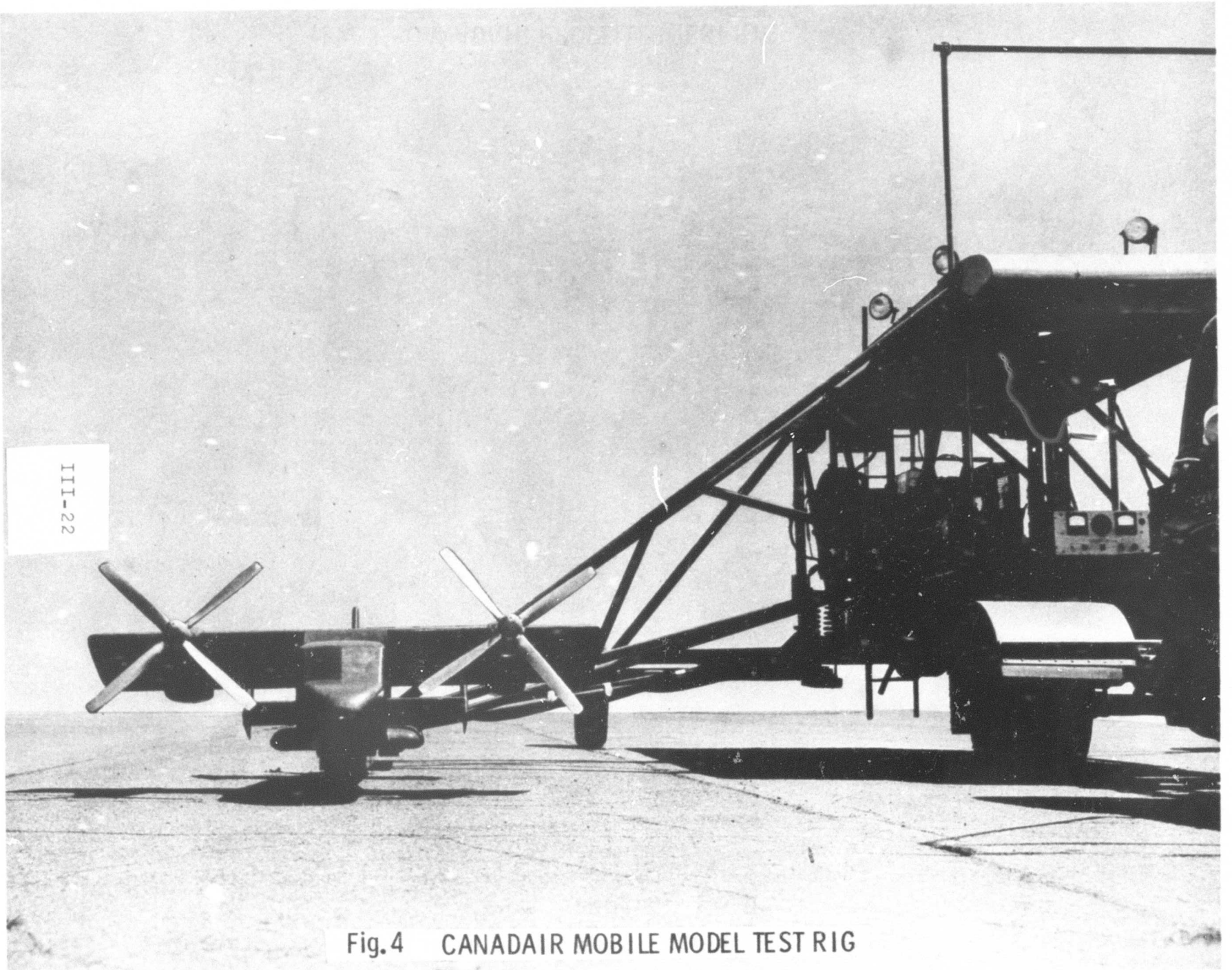

Fig. 4 CANADAIR MOBILE MODEL TEST RIG

CL-84 SPACE FOR CARGO OR PERSONNEL

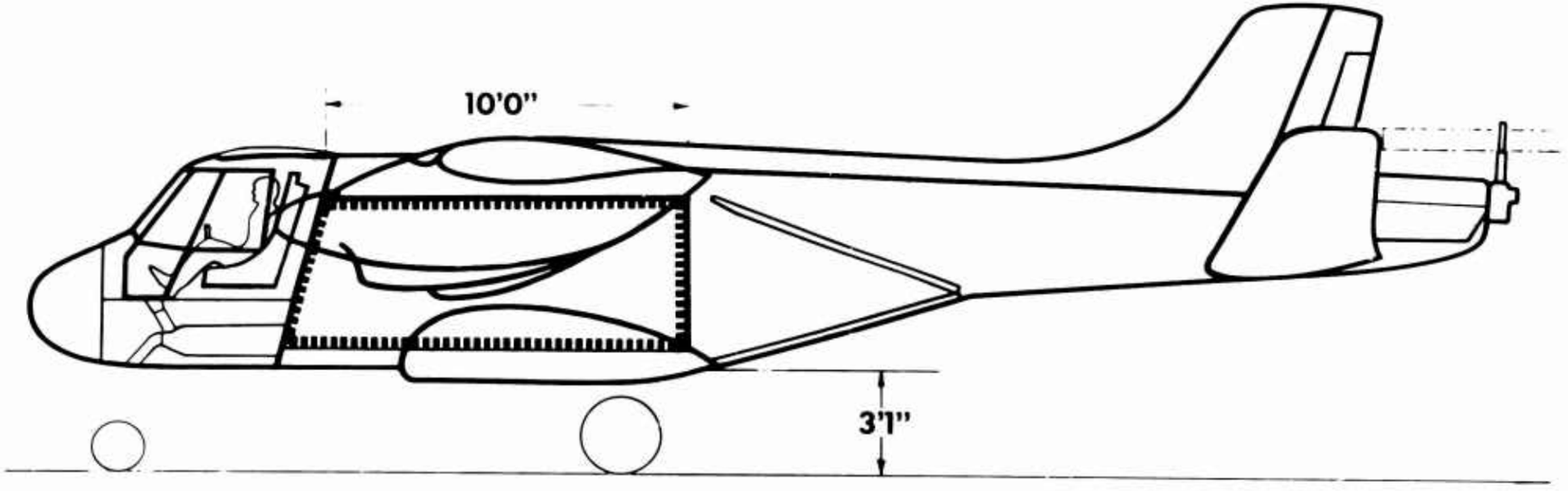

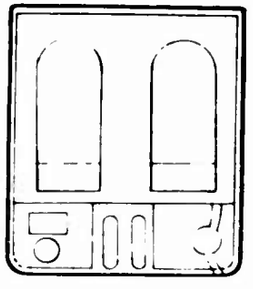

PILOTS COMPARTMENT

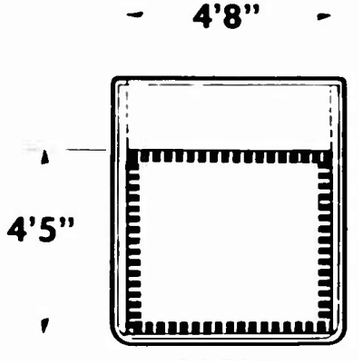

CABIN

84-1096C

Fig. 7

CL-84
GENERAL ARRANGEMENT

POWER PLANT - TWO 1400 SHP
LYCOMING T53 -LTC1K-4A
PROPELLER - 14' DIAMETER, 4 BLADES
OF FIBERGLAS
TAIL ROTOR - 7' DIAMETER CONTRA-ROTATING

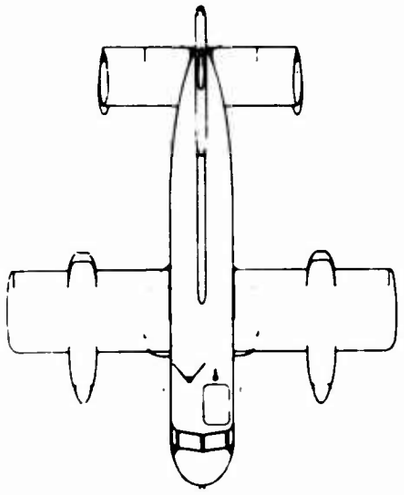

CONVENTIONAL

33'4"

45'6"

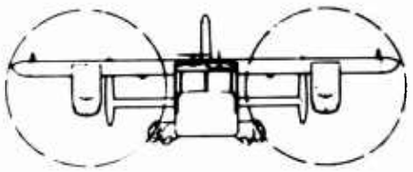

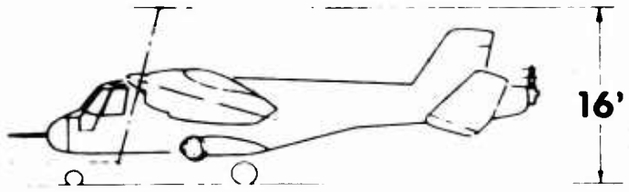

16'

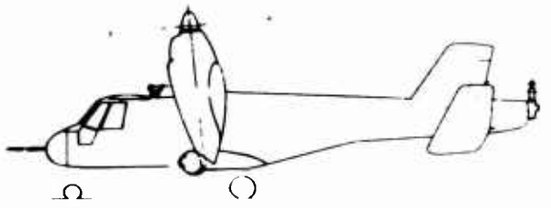

28" MIN.

STOL

VTOL

84-1637 A

III-24

Fig. 6

CL-84 CONTROL SYSTEM FUNCTIONS

AXIS	NORMAL AIRCRAFT FLIGHT	TRANSITION INBOUND	HOVERING
PITCH	STICK TO ELEVATOR	STICK TO ELEVATOR ACTIVE AND TAIL ROTOR ACTIVE	STICK TO TAIL ROTOR ACTIVE
ROLL	STICK TO FLAP/AILERONS	STICK TO FLAP/AILERONS PHASED OUT AND STICK TO DIFFERENTIAL PROPELLER PITCH PHASED IN	STICK TO DIFFERENTIAL PROPELLER PITCH
YAW	PEDALS TO RUDDERS	RUDDER PEDALS TO FLAP/AILERONS PHASED IN AND DIFFERENTIAL PROPELLER PITCH PHASED PROGRESSIVELY IN AND OUT	RUDDER PEDALS TO FLAP/AILERONS
HEIGHT	POWER LEVER TO ENGINE	POWER LEVER TO COLLECTIVE PROPELLER PITCH PHASED IN	POWER LEVER TO ENGINE AND COLLECTIVE PROPELLER PITCH

TRANSITION OUTBOUND - REVERSE OF TRANSITION INBOUND

III-27

84-1100A

Fig. 9

CL-84 EXTERNAL STORES POTENTIAL

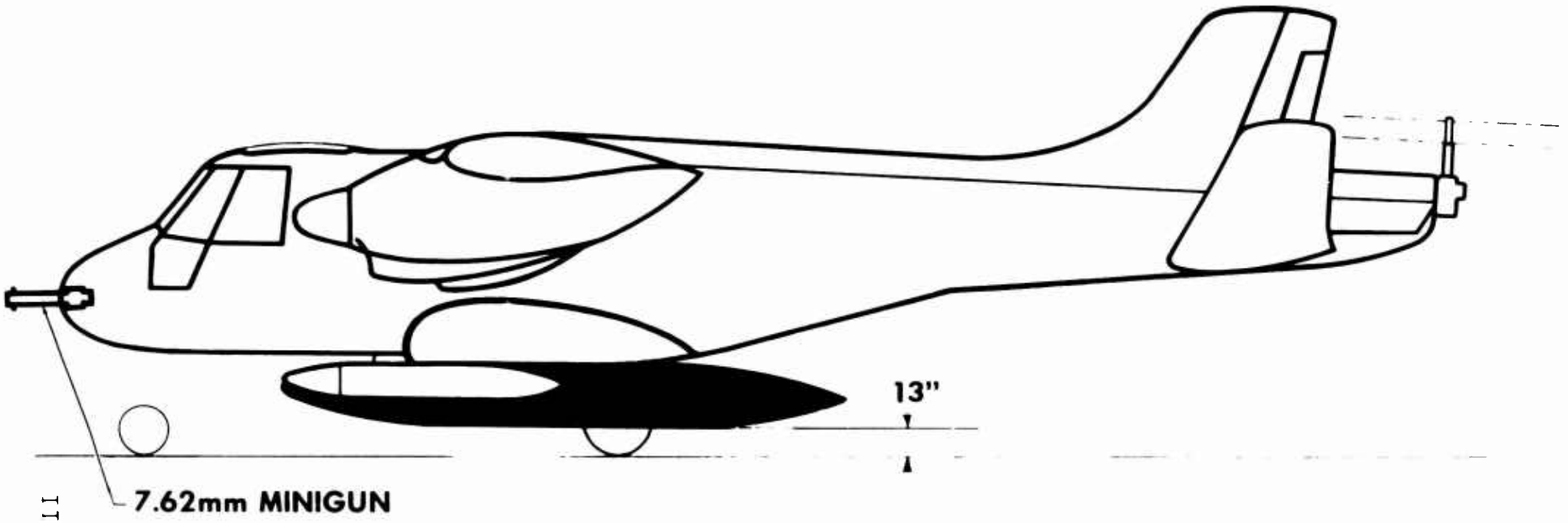

III-26

3 STRONG POINTS
21" APART

CAPACITY 1000 LB. EACH

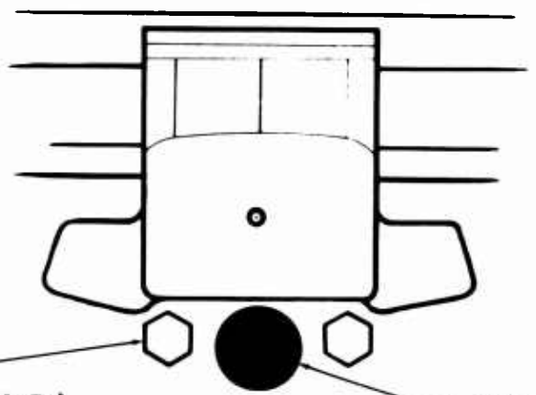

TYPES OF STORES:
FUEL, BOMBS, ROCKETS,
MISSILES, GUNPODS,
SENSORS, CARGO

84-10950

Fig. 8

CL-84 FLIGHT CONTROLS

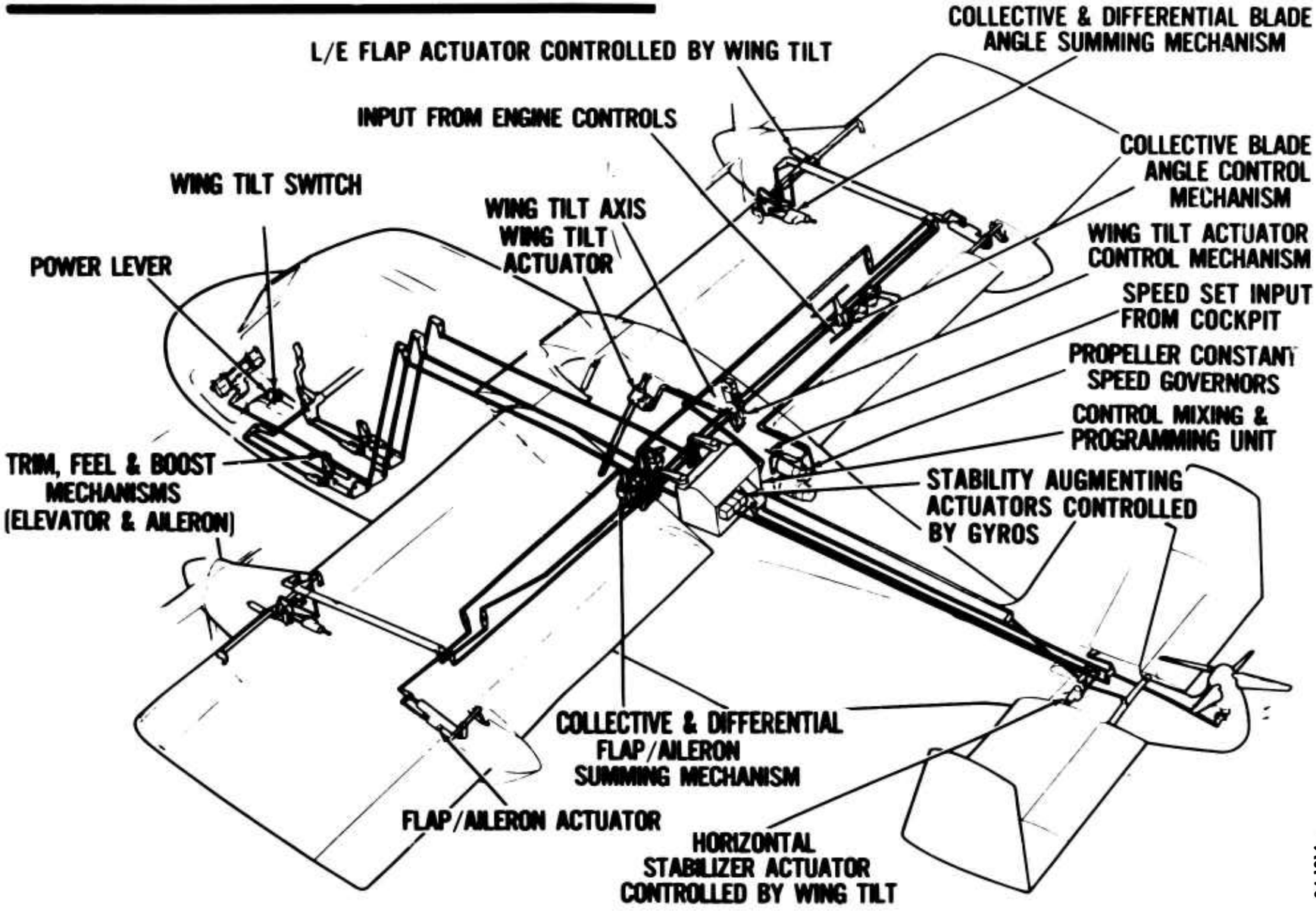

Fig. 11

Fig. 10 CL-84 COCKPIT ARRANGEMENT

CANADAIR CL-84 - OUTLINE OF MODEL TESTING

MODEL SCALE AND TYPE	TEST FACILITY	TYPE OF TEST
14% POWERED MODEL	WIND TUNNEL	AIRCRAFT CHARACTERISTICS IN INTERMEDIATE SPEED REGIME
18% POWERED MODEL	CANADAIR MOBILE RIG	LOW-SPEED AIRCRAFT CHARACTERISTICS
18% POWERED MODEL	CANADAIR HOVER RIG	STATIC AND DYNAMIC CHARACTERISTICS
22% POWERED HALF-MODEL	WIND TUNNEL	FLAP DEVELOPMENT AND OPERATING LOADS; WING FLOW SEPARATION STUDIES; PROPELLER VIBRATORY STRESSES AND EFFECTS ON STABILITY
18% UNPOWERED MODEL	WIND TUNNEL	HIGH-SPEED AIRCRAFT CHARACTERISTICS
36% PROPELLER MODEL	CANADAIR PROP RIG	STATIC THRUST MEASUREMENT AND BLADE DEVELOPMENT WORK
36% PROP-NACELLE MODEL	CANADAIR PROP RIG	INTAKE DEVELOPMENT AND EVALUATION OF LOSSES; EFFECT OF NACELLE ON STATIC THRUST

Fig. 13

CL-84 LIFT - PROPULSION SYSTEM

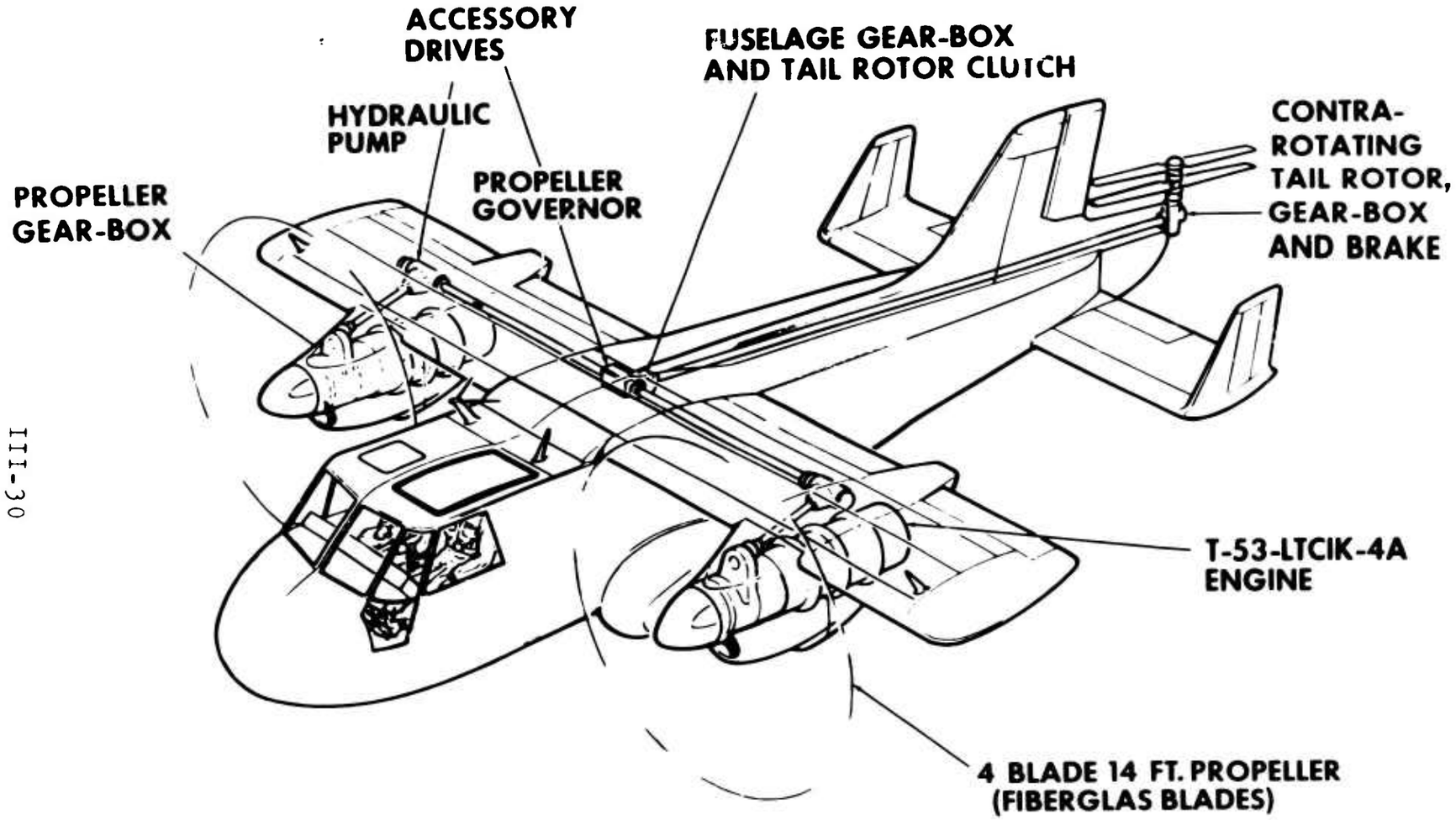

Fig. 12

LATERAL - DIRECTIONAL CONTROL
CROSS - COUPLING HANDLING QUALITIES BOUNDARIES

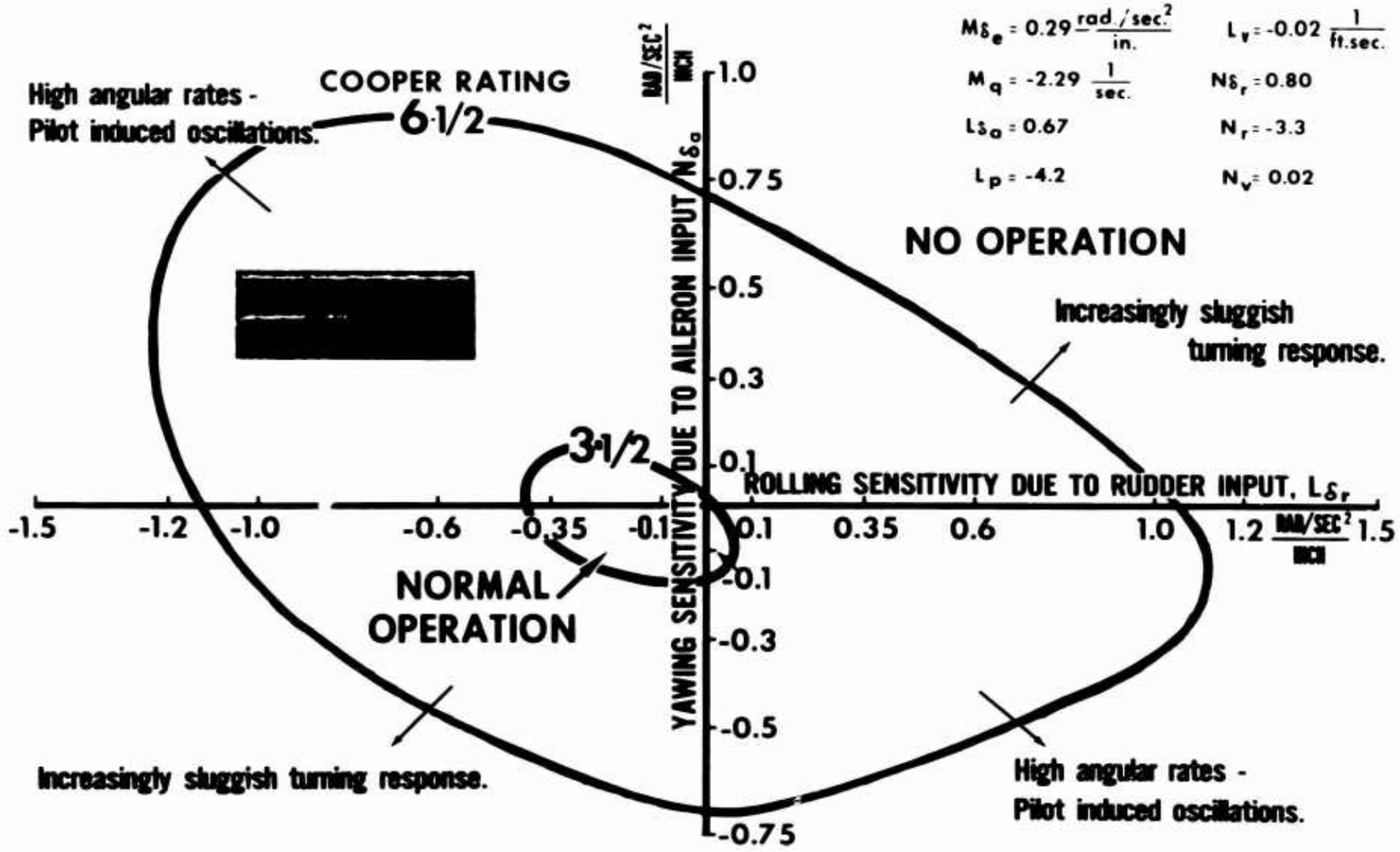

Fig. 15

CANADAIR CL-84 - OUTLINE OF FLIGHT SIMULATION

TEST FACILITY	TYPE OF SIMULATION
CANADAIR FIXED-BASE IFR	(a) LONGITUDINAL, WITH ADDED ROLL TASK (b) LATERAL-DIRECTIONAL; APPROX. LONG. SIMULATION (c) PITCH; STOL PERFORMANCE STUDY (d) TEN DEGREES OF FREEDOM; LAG AND BACKLASH; IN AND NEAR HOVER (e) TEN DEGREES OF FREEDOM; TRANSITION SPEED REGIME
NAT'L AERO.ESTABLISHMENT VARIABLE - STABILITY HELICOPTER	(a) LATERAL-DIRECTIONAL CROSS-COUPLING STUDY (b) LATERAL-DIRECTIONAL; EFFECTS OF STATIC LATERAL AND DIRECTIONAL STABILITY ON DIRECTIONAL DAMPING AND CONTROL POWER (c) HEIGHT CONTROL DYNAMICS USING POWER LEVER IN LIEU OF COLLECTIVE STICK (d) STUDY OF BACKLASH, PHASE LAGS, SAS GAINS AND FAILURES DURING HOVERING

Fig. 14

CANADAIR CL-84
MAJOR PROPULSION DEVELOPMENT TESTING

COMPONENT	TYPE OF TEST
ENGINE	50-HOUR PFRT TO TILTING DUTY CYCLE
MAIN, WING AND FUSELAGE GEARBOXES	LUBRICATION; ENVIRONMENTAL; CLUTCH TESTING; DEVELOPMENT RUNNING; SIMULATED 50-HOUR PFRT
PROPELLER LESS BLADES	ENDURANCE; ENVIRONMENTAL; CONTROL SYSTEM TEST
PROPELLER BLADE	FATIGUE; RETENTION STRENGTH; OVERSPEED; OVERPOWER; STATIC THRUST; FLUTTER BOUNDARY
SHAFTING AND COUPLINGS	RIG OVERSPEED TESTS
TAIL ROTOR	STATIC AND FATIGUE TESTS OF RETENTION STRAPS, SHAFTS, HUBS AND GEARCASE; STATIC THRUST; OVERSPEED; WIND TUNNEL STARTING AND STOPPING
TAIL ROTOR GEARBOX	GEAR MESHING AND WEAR; DEVELOPMENT RUNNING; CONTROL DYNAMICS; LUBRICATION; BRAKE AND ALIGNER PERFORMANCE

Fig. 17

CL-84 HOVER SIMULATION

EFFECT OF LOST MOTION IN ENGINE/PROP CONTROL SYSTEM ON HEIGHT CONTROL

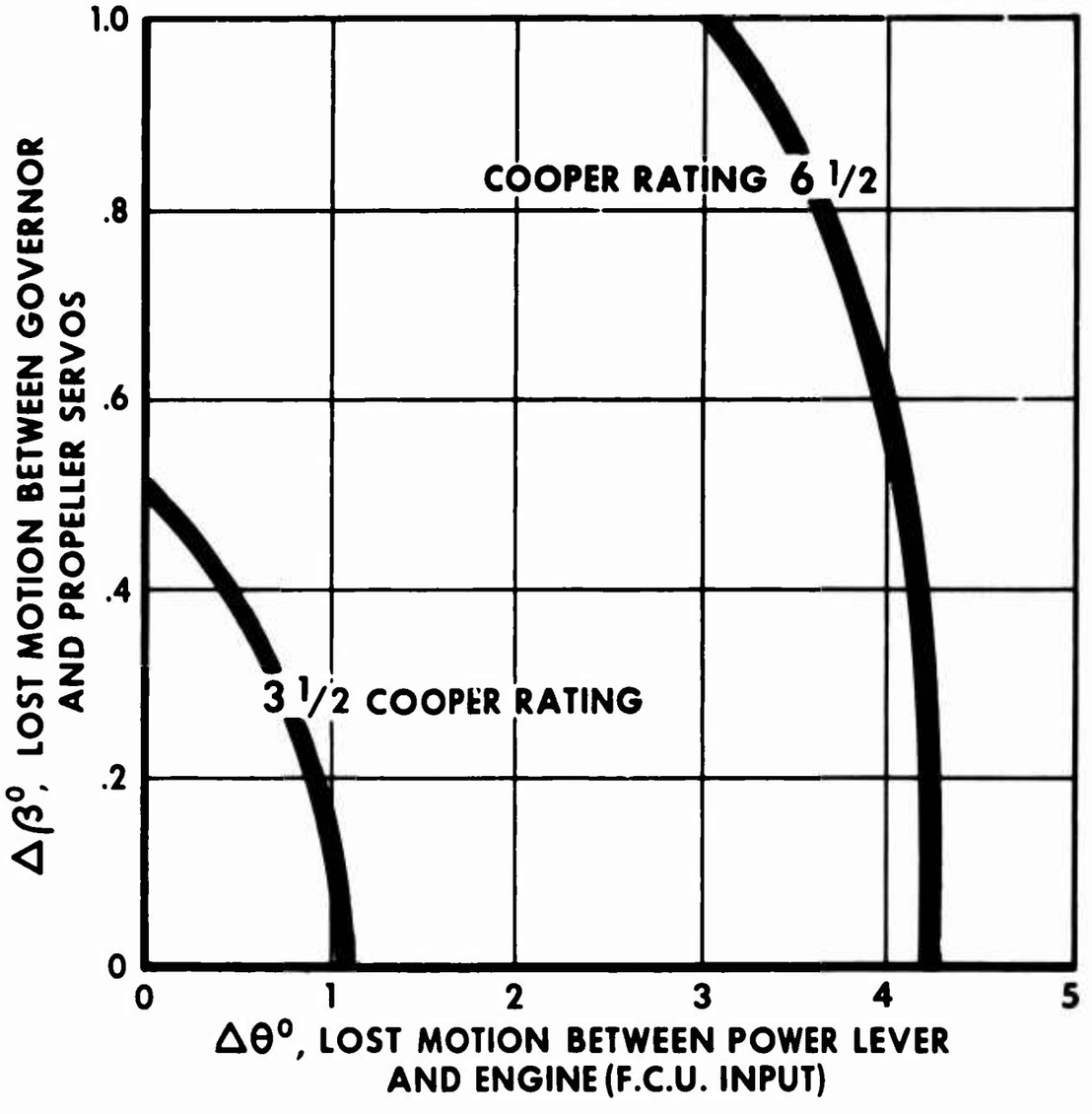

Fig. 16

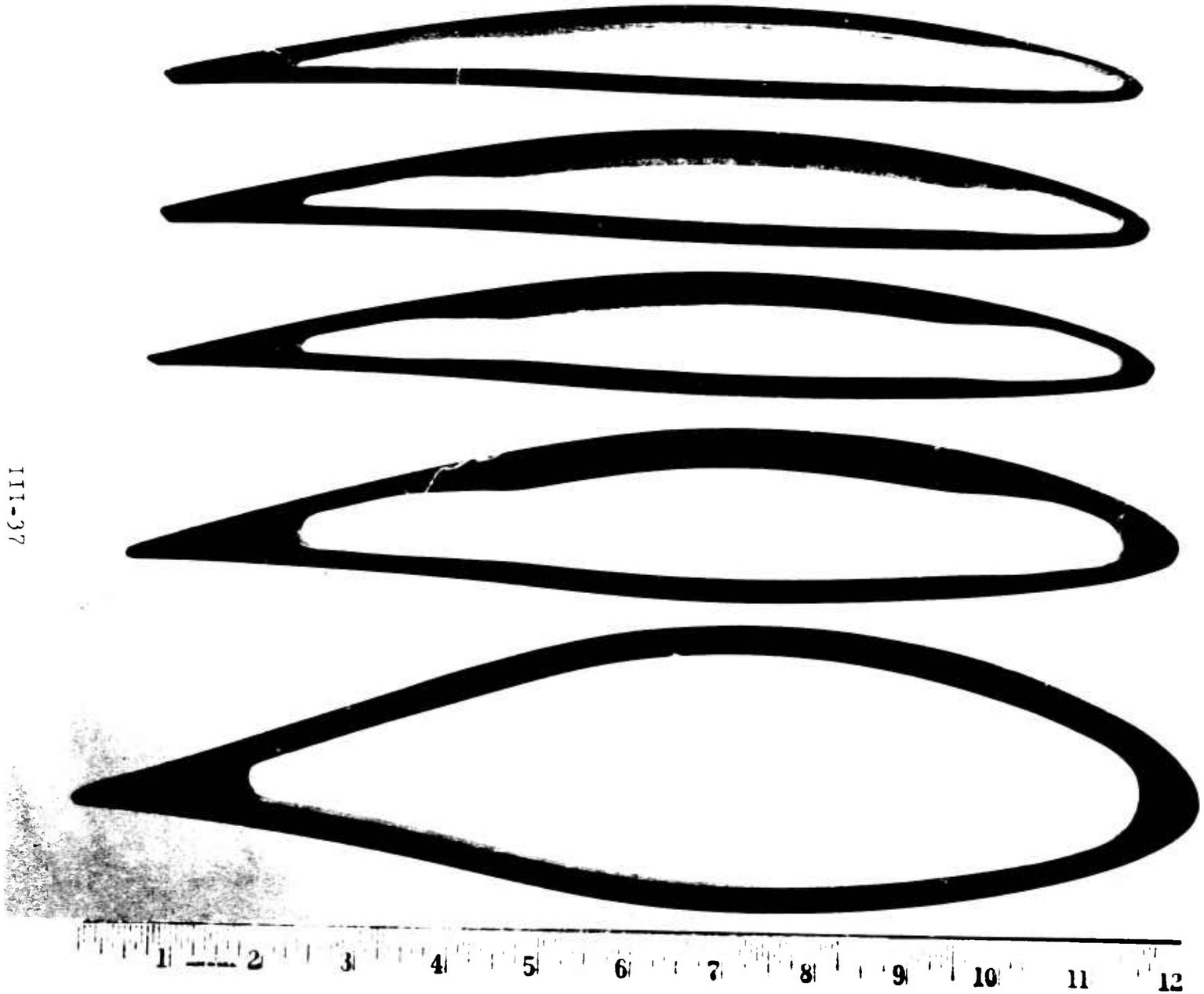

Fig. 19 SECTIONS OF CL-84 FIBERGLAS PROPELLER BLADE

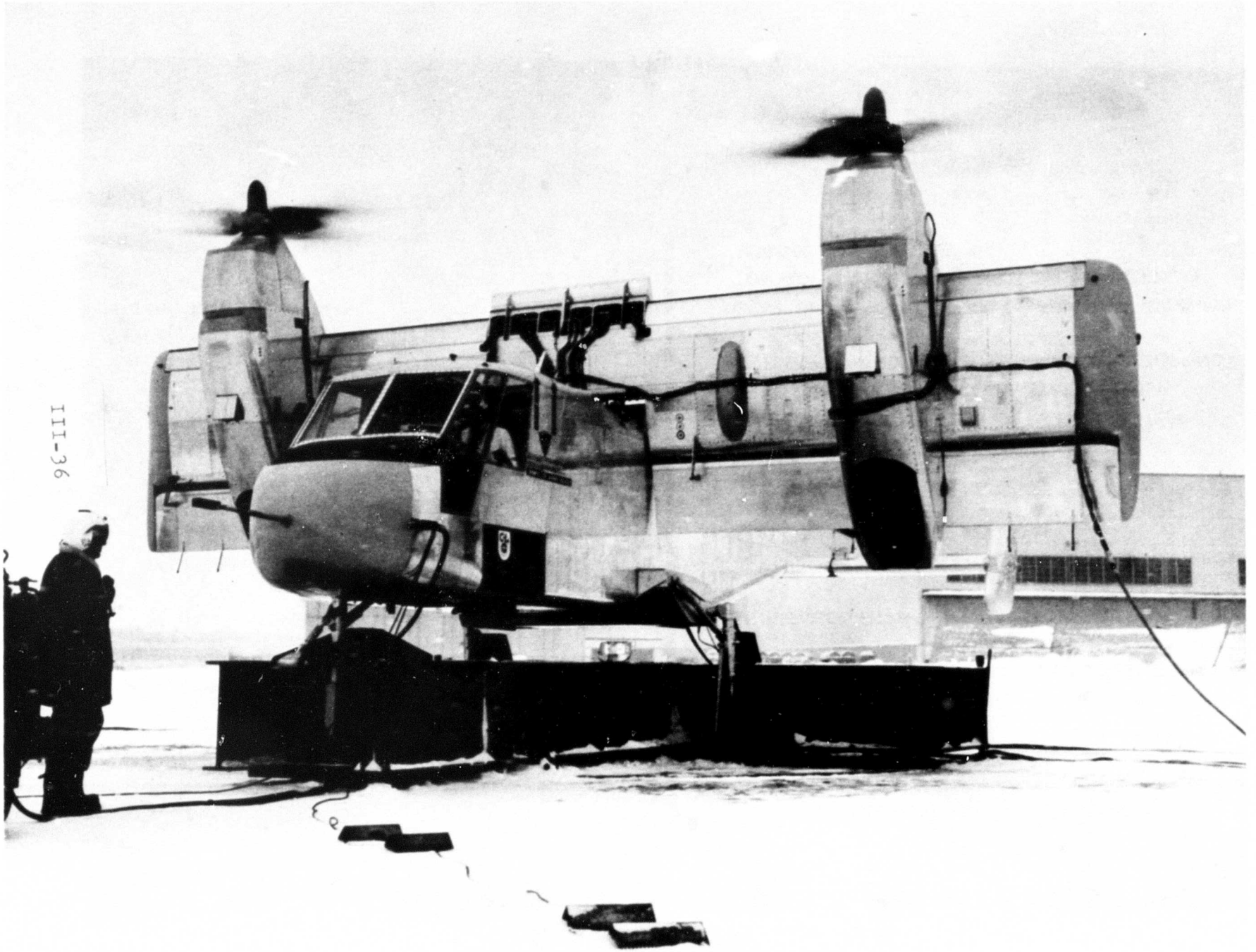

Fig. 18 CL-84 ON GROUND TEST RIG

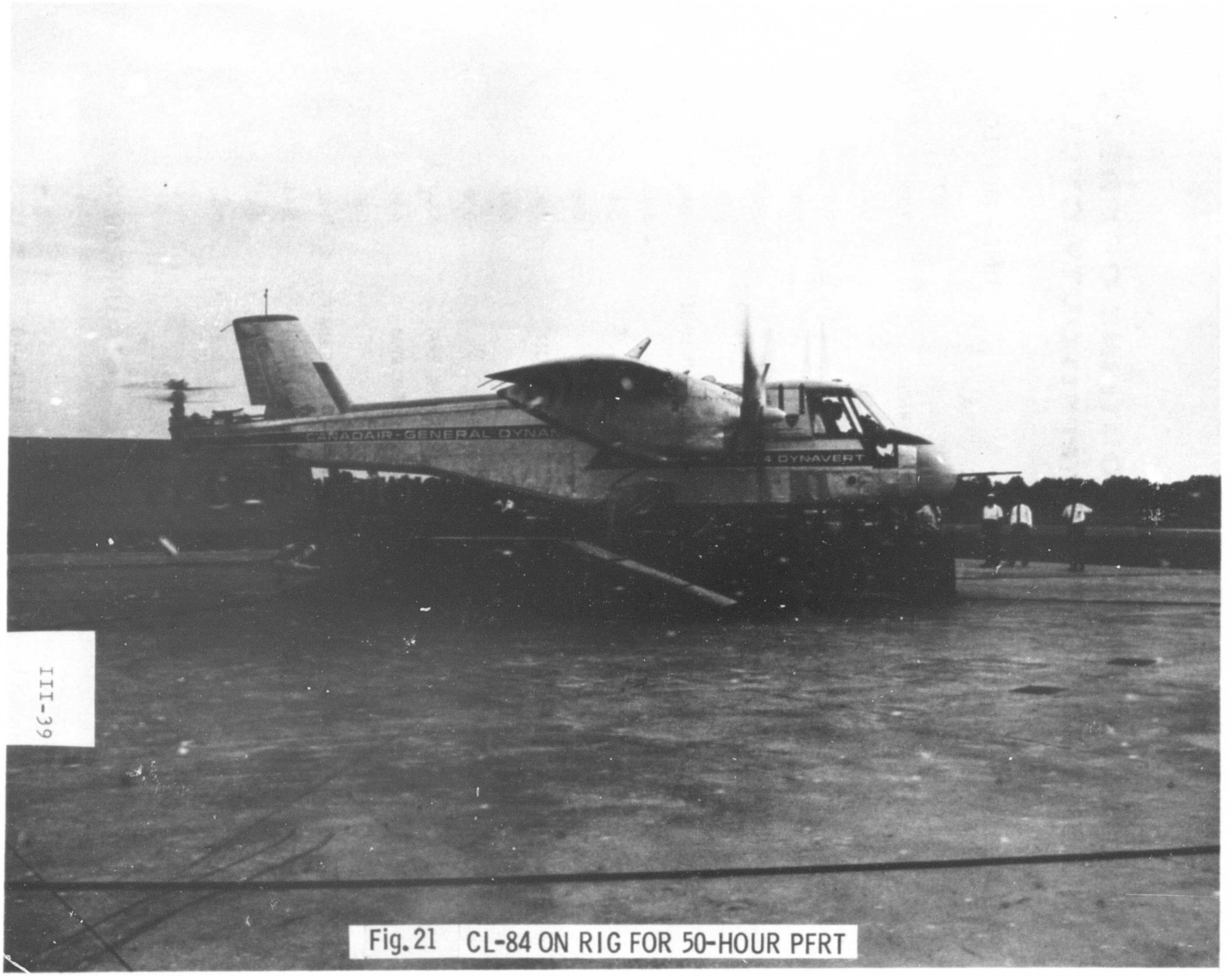

Fig. 21 CL-84 ON RIG FOR 50-HOUR PFRT

III-38

Fig. 20 CL-84 GEARBOX - "ADAPTER" - ENGINE ASSEMBLY

CANADAIR CL-84 OUTLINE OF PRE-FLIGHT RATING TEST (PFRT) DUTY CYCLE

ITEM	DESCRIPTION	TIME - MIN:SEC
A	START ENGINES; TILT WING UP	2:00
B	STEADY HOVER; TRANSIENT OVERSPEED	3:35
C	HOVER MANEUVERS	0:41
D	OUTBOUND TRANSITION	0:10
E	CRUISE AT 60% RPM	11:00
F	CRUISE AT 80% RPM	13:00
G	INBOUND TRANSITION	0:10
H	HIGH SPEED AT MILITARY RAM TORQUE LIMIT	1:30
J	STEADY HOVER	3:35
K	HOVER MANEUVERS	0:41
L	IDLE POWER; WING TILT FOR STO	0:15
M	SHORT TAKEOFF AND ASSOC. OPERATION	3:35
N	STOL MANEUVERS	0:41
O	OUTBOUND TRANSITION	0:10
P	CRUISE (ONE ENGINE IDLING) AT 80% RPM	5:00
Q	CRUISE (ONE ENGINE IDLING) AT 90% RPM	6:00
R	INBOUND TRANSITION	0:10
S	HIGH SPEED AT MILITARY RAM TORQUE LIMIT	1:30
T	SHORT LANDING AND ASSOC. OPERATION	3:45
V	STOL MANEUVERS	0:41
W	IDLE POWER; WING TO 15° TILT	0:45
X	IDLE AND SHUTDOWN	1:06

22 OPERATIONS **TOTALLING 60:00**

Fig. 22

CANADAIR CL 84 • MAJOR PROBLEMS ENCOUNTERED DURING PFRT

ITEM	CORRECTIVE ACTION
1. LOCAL SEPARATION BETWEEN PROP BLADE SHELL AND PLASTIC FILLER	REPAIRED IN PLACE AT START OF PFRT
2. PARTIAL FAILURE – TAIL ROTOR CONTROL	ALUMINUM PART REPLACED BY STEEL
3. FUSELAGE GEARBOX BEARING FAILURE	BEARING DUTY EXCESSIVE BECAUSE OF TAILSHAFT CLUTCH PRESSURE USED
4. PROPELLER PRELOAD BEARING FAILURES	REDESIGN OF BEARING RETENTION TO MINIMIZE VIBRATORY LOADS OF BEARING
5. TAILSHAFT BEARING OVERHEAT	GREASE SEAL FOUND DETERIORATED; REPLACED BEARING
6. STRAINED BOLT THREADS IN TAIL ROTOR CONTROL SYSTEM	PARTS REPLACED; EXCESSIVE CONTROL LOADS REQUIRE ADDITIONAL DEVELOPMENT WORK
7. PROPELLER CONTROL UNIT – BOLT FATIGUE	INSUFFICIENT BOLT TORQUE USED; BOLTS REPLACED
8. FUSELAGE GEARBOX CLUTCH SLIPPAGE	DAMAGE TO ALUMINUM ELEMENT; REPLACED BY STEEL
9. ENGINE FOREIGN OBJECT DAMAGE	WIRE LOCKING OF BOLTS AHEAD OF ENGINE INTAKE
10. PARTIAL FAILURE - TAIL ROTOR BLADE MOUNT HUB	REPLACED ROTOR; DESIGN STUDY IN PROGRESS

Fig. 23

Fig. 25 CL-84 FLYING IN WINDS GUSTING TO 25 KNOTS

CANADAIR CL-84 · PRELIMINARY EFFECTS OF SAS ON CHARACTERISTICS IN AND NEAR HOVER

SAS STATUS	SAS CHANNEL① YAW	ROLL	PITCH③	HEIGHT	OVERALL COOPER RATING
1. ACTIVE (BASE)②	✓	✓	✓	NONE	3 (AIRCRAFT)
2. BASE					3 } YAW PHASE
3. YAW ⟶O	×	✓	✓		2 ½ }
4. BASE					2 ½ } ROLL PHASE
5. ROLL ⟶O	✓	×	✓		4 ½ }
6. BASE					2 ½ } PITCH PHASE
7. PITCH ⟶O	✓	✓	×		5 }
8. PITCH ZERO; ROLL ⟶O ; YAW "FAILED"	×	×	×		5 (AIRCRAFT)
PRELIM. FLIGHT TEST PARAMETERS					
NATURAL RATE DAMPING	0.4 $\frac{\text{rad./sec.}^2}{\text{rad./sec.}}$	0.6	0.4	0.12 $\frac{\text{ft./sec.}^2}{\text{ft./sec.}}$	
ARTIFICIAL RATE DAMPING	1.8	3.7	4.0	—	
ARTIFICIAL ATTITUDE STIFFNESS	— $\frac{\text{rad./sec.}^2}{\text{rad.}}$	—	2.0	—	
S.A.S. AUTHORITY④	50%	37%	50%	—	
PRIMARY CONTROL POWER	± 0.45 rad./sec.^{2}	± 1.42	± 1.35	to 1.2g	
CONTROL SENSITIVITY	± 0.15 $\frac{\text{rad./sec.}^2}{\text{in.}}$	0.36	± 0.41	± 0.2g/in.	

NOTES: ① RATE DAMPING IN YAW, ROLL AND PITCH; ATTITUDE STIFFNESS IN PITCH DEACTIVATED FOR TEST
② BASE CONDITION 10600 LB. DESIGN GROSS WEIGHT; STD. S.L. DAY
③ SINGLE FAILURE IN PITCH CHANNEL DOES NOT DEGRADE PERFORMANCE ④ PERCENT OF PRIMARY CONTROL POWER

Fig. 24

ESCAPE AND RECOVERY SYSTEMS FOR V/STOL AIRCRAFT

James McCormack

S. Blair Poteate, Jr.

USAF

Fig. 26

CL-84 PROTOTYPE PERFORMANCE ESTIMATES

2 LYCOMING LTC1K-4A (1400 SHP) ENGINES

ITEM	VTOL MODE	STOL[1] MODE
GROSS WEIGHT AT SEA LEVEL, ISA - LB	12,200	14,700[3]
GROSS WEIGHT AT SEA LEVEL, 95°F - LB	10,600	12,700
GROSS WEIGHT AT 6,000FT, ISA - LB	10,600	12,700
FUEL LOAD INCL.(10%RESERVE) - LB	1600	1600
RANGE[2]AT S.L. AT 200K. - N.MI.	300	285
PAYLOAD FOR S.L. RANGE, ISA - LB	3100	5600[3]
PAYLOAD FOR S.L. RANGE, 95°F - LB	1500	3600
ENDURANCE AT S.L. AT 100-150K. - HR	2.0	1.9
ENDURANCE AT S.L. AT 50K.	1.4	1.1
HOVERING ENDURANCE AT S.L.	0.9	-
MAX. SPEED, MIL. POWER, S.L. ISA - K.	287	284
MAX. SPEED, NORMAL POWER, S.L. ISA - K.	274	270

NOTES

(1) CORRESPONDING TO TAKE-OFF AND LANDING OVER 50' OBSTACLE IN 500'.

(2) CONSIDERABLE IMPROVEMENTS POSSIBLE USING ONE ENGINE ONLY FOR CRUSING AND/OR HIGHER ALTITUDE.

(3) PERFORMANCE POTENTIAL ONLY; DEMONSTRATION LIMITED BY LOAD FACTOR AND CARGO SPACE.

ACKNOWLEDGEMENT

The authors wish to acknowledge the support and contributions of B. C. Solomonides, Group Leader, Escape and Recovery Systems, North American Aviation, Columbus Division, and members of this Group in the preparation of this paper.

ABSTRACT

V/STOL aircraft will spend relatively long time periods at very low altitude and very low speed. A power or control system failure can immediately result in high pitch and/or roll rates that would place the aircraft in an extremely adverse attitude relevant to escape and recovery. High sink rates can rapidly develop and further compromise this critical situation.

Escape and recovery under these conditions can be achieved only when the time from initiation of the escape sequence to full inflation of the recovery parachute is kept to a minimum. This paper describes an escape system that embodies this basic philosophy and meets the escape and recovery requirements for V/STOL aircraft.

TABLE OF CONTENTS

	PAGE
ACKNOWLEDGEMENT	i
ABSTRACT	ii
LIST OF FIGURES	iv
INTRODUCTION	1
DESIGN PHILOSOPHY	1
DESIGN APPROACH	1
ESCAPE SYSTEM DESIGN AND OPERATION	2
ESCAPE SYSTEM SEQUENCING	5
TEST PROGRAM	5
SUMMARY	7

LIST OF FIGURES

FIGURE		PAGE
1	LW-2 System Escape Recovery Envelope	9
2	Torso Positioning and Restraint	10
3	LW-2 Photo	11
4	LW-2 Photo	12
5	LW-2 Photo	13
6	Schematic - Ballistic Initiation System	14
7	Test Firing No. 16 - 498 KEAS	15
8	Test Firing No. 12 - 247 KEAS	16
9	Test Firing No. 13 - 211 KEAS	17
10	LW-2 Static Firing	18
11	Test Firing No. 18	19
12 thru 14	YAT-28E - LW-2 Sequence	20 21 22
15	Rocket Thrust Moment Arm Spread	23
16	Yaw Trajectory	24
17	Typical LW-2 Trajectories	25
18	Angle of Dive Recovery Capability	26
19	Sink Rate Recovery Capability	27
20	Live Inverted Ejections	28

ESCAPE AND RECOVERY SYSTEMS FOR V/STOL AIRCRAFT

James McCormack
Systems Engineering Group
Aeronautical Systems Division
Wright-Patterson Air Force Base, Ohio

S. Blair Poteate, Jr.
Aircraft Systems and Equipment Division
U. S. Army Aviation Materiel Laboratories
Fort Eustis, Virginia

INTRODUCTION

In 1960 the U. S. Air Force evaluated all escape systems to determine which systems would provide escape capability throughout the flight envelope of V/STOL aircraft being developed by this service. The study led to the decision to closely monitor the LW-2 Escape System Program, then being conducted by the U. S. Army Aviation Materiel Laboratories in conjunction with the Columbus Division of North American Aviation, Inc.

The LW-2 Escape System is unique in several ways. The personnel parachute is mounted on the outside of the seat back so that it can be positively deployed by a thruster slug immediately after seat-aircraft separation following a low altitude, low speed ejection. During a high altitude and/or high speed ejection, a stabilizing drogue chute is positively deployed by the thruster slug prior to seat-aircraft separation so that seat stability in an upright attitude is achieved immediately after seat-aircraft separation. Subsequent release of the drogue chute from the seat provides positive deployment for the personnel parachute. Thus this system is literally two escape systems in one.

DESIGN PHILOSOPHY

The basic design philosophy adhered to throughout the LW-2 Escape System Program was that of keeping the time from initiation of the escape sequence to full inflation of the recovery parachute to a minimum.

DESIGN APPROACH

A personnel parachute can be safely deployed at speeds up to 200 KEAS at all altitudes up to 10,000 feet. In turn, if the personnel

parachute is not deployed immediately after seat-aircraft separation when the aircraft is in this part of the flight envelope, the recovery capability of the system will be unduly compromised by the unnecessary time delay. For this reason, personnel parachute deployment immediately after seat-aircraft separation was established as a design requirement for the LW-2 Escape System, when the speed at the time of the ejection is less than 200 KEAS and the altitude less than 10,000 feet.

If an ejection occurs at high speed, the man or seat-man mass must be decelerated before the personnel parachute can be deployed. The higher the deceleration "G", the less the time required to decelerate. Man can sustain the highest deceleration force when the direction of this force is perpendicular to his spinal column. In turn, if the seat-man mass is not stabilized in an upright attitude, relative to the windstream, immediately after seat-aircraft separation following a high speed ejection, a longer time delay will be required for the deceleration, and the recovery capability of the system will be unduly compromised by the unnecessary time delay. For this reason, immediate seat stability in an upright attitude following a high speed ejection was also established as a design requirement for the LW-2 Escape System.

These requirements made the LW-2 Escape System a two-mode system.

ESCAPE SYSTEM DESIGN AND OPERATION

General - The LW-2 Escape System is an automatic, two-mode system. The mode is selected at the time of the ejection by a speed sensor. Figure 1 shows the altitudes and speeds at which each mode is used. At altitudes below 10,000 feet and at speeds less than 200 KEAS, the personnel parachute is ballistically deployed immediately after the seat leaves the aircraft. At speeds greater than 200 KEAS and/or at altitudes above 10,000 feet, the stabilizing drogue parachute is ballistically deployed before the seat leaves the aircraft so that it provides immediate seat stability after seat-aircraft separation. The drogue chute is separated from the seat at the time of seat-man separation and provides positive, forceful deployment of the personnel parachute. When ejection occurs at altitudes greater than 10,000 feet, the man descends to 10,000 feet in the drogue-stabilized seat before the harness release time delay is fired. In both the low and high speed mode, seat-man separation is effected by inflation of the personnel parachute.

The seat is equipped with an automatic ballistically powered retraction inertia reel which retracts and locks upon initiation of the ejection sequence. It provides automatic torso positioning and restraint prior to catapult firing. Its position relative to the

airman's shoulders is such that it also pulls him down onto his seat cushion should he be lifted off his seat (Negative G). Thus it prevents the vertebral injuries that normally occur as a result of improper body position and/or Negative G at the time the catapult fires. It also enables the pilot to eject his crewman without warning. The operation of the reel is illustrated in Figure 2.

The LW-2 Escape System is pictured in Figures 3 through 5. The entire escape sequence is completely automatic after D-ring initiation. The D-ring is located on the front of the seat bucket between the airman's legs. It can be reached and actuated by 3 through 97 percentile men while in the full back, locked position. Actuation of the D-ring fires two mechanical initiators (T-30E2) which in turn generate pressure to fire the catapult rocket. Actuation of either T-30E2 initiator is all that is required for escape system operation. The other is a redundant initiator with its own pressure line for increased reliability. The ballistic initiation system is schematically illustrated in Figure 6.

Escape system initiation jettisons the aircraft canopy, fires the 0.3 second delay in the catapult, and actuates the ballistic reel. The 0.3 second catapult delay allows the canopy to clear the aircraft and the ballistic reel to position and restrain the airman, before the catapult fires. Should for any reason the canopy jettisoning system malfunction, the airman will be ejected through the canopy without a delay in the escape sequence.

Peak catapult forces range from 9-12 G's with rates of onset of acceleration from 150-180 G's/sec.

High Speed Mode - The Escape System operates in the high speed mode at any time the ejection speed is greater than 200 KEAS or any time the ejection altitude is above 10,000 feet.

The drogue chute is ballistically deployed as the seat moves up the rails. It stabilizes the seat in an upright attitude immediately after the seat leaves the aircraft. A lanyard from the apex of the personnel parachute is attached to the upper drogue chute riser. The drogue chute is separated from the seat at the time of harness release and effects positive, forceful deployment of the personnel parachute. Inflation of the personnel parachute separates the man from the seat. This sequence following a 500 KEAS ejection is shown in Figure 7, and following a 247 KEAS ejection in Figure 8.

Leg restraint is provided by the sides of the seat bucket. Only lateral restraint is required for the legs in an escape system that is stabilized in an upright attitude immediately after the seat leaves the aircraft. The high "q" bends the legs at the knees and holds them against the front and underneath side of the seat bucket. This is also seen in Figure 7.

Low Speed Mode - The escape system operates in the low speed mode when the altitude at the time of ejection is less than 10,000 feet and the speed at the time of ejection less than 200 KEAS. The personnel parachute is ballistically deployed immediately after the seat clears the aircraft. Personnel parachute inflation separates the man from the seat. A low speed mode sequence following a 200 KEAS ejection is shown in Figure 9. Figure 10 presents a footprint of a static firing. Figure 11 shows a static firing through a 3/8 inch cast canopy, and Figures 12 through 14 show a static firing through the YAT-28E canopy.

The escape and recovery capability of this type of parachute deployment was demonstrated during a recent aircraft accident. Two pilots ejected from an aircraft in LW-2 seats while the aircraft was experiencing a violent, combination pitch-roll maneuver. Both seats left the aircraft almost simultaneously when it was inverted at an altitude of approximately 400 feet. Aircraft speed was estimated to be 118 knots. Both seats functioned as designed. Both pilots had fully inflated parachutes at altitudes in excess of 200 feet. Both parachutes were fully inflated less than 1.6 seconds after the seats left the aircraft.

This accident clearly demonstrated the importance of keeping the time from initiation of the escape sequence to full inflation of the recovery parachute to a minimum, and the recovery capability that can be achieved when this is accomplished in the design of an escape system.

At low speeds, the magnitude of aerodynamic forces is small; thus the rocket thrust moment arm about the seat-man CG affects initial stability. For seat adjustment, the LW-2 seat and man move up and down as a unit; therefore no shift in the CG relative to the rocket thrust vector results from seat adjustment. In this seat configuration, the total range of CG locations is about 1.3 inches. This relationship is shown in Figure 15. The moment arm spread was determined by actual measurements on twenty-two human subjects of numerous sizes and builds.

The rocket thrust is placed below the center of gravity of the ejected mass. Therefore at low speeds a mild head aft rotation is applied to the seat during rocket burning. Because of this rotation, more of the rocket thrust is directed upward during rocket burning. The increased vertical trajectory results in a greater sink rate and angle of dive recovery capability at low speeds.

The personnel parachute is mounted on the left-hand side of the seat back as seen in Figure 4. This provides a built-in, lateral, rocket-thrust moment arm, since the chute is not deployed until 0.20 second after rocket ignition. In turn, the man is always moving up and to the left of his deploying personnel parachute, as illustrated in Figure 16. Therefore, it is impossible for an airman ejecting in

the LW-2 Escape System to fall back into his chute canopy after chute inflation.

ESCAPE SYSTEM SEQUENCING

Nominal Operation Under 10,000 Ft.

High Speed		Low Speed	
Time-Sec.	Event	Time-Sec.	Event
0.00	Escape System Initiation Canopy Jettisoning System and Ballistic Inertia Reel Actuation	0.00	Escape System Initiation Canopy Jettisoning System and Ballistic Inertia Reel Actuation
0.3	Crewman Positioned	0.3	Crewman Positioned
	Catapult Ignition		Catapult Ignition
0.49	Drogue Gun Firing Drogue Chute Deployment	0.49	Drogue Gun Delay Ignition
0.55	Rocket Ignition	0.55	Rocket Ignition
0.56	Seat-Aircraft Separation	0.56	Seat-Aircraft Separation
0.83	Rocket Burn Out	0.70	Drogue Gun Firing Personnel Parachute Deployment
1.39	Harness Release Actuation Drogue Release Actuation	0.83	Rocket Burn Out
2.5	Full Parachute Inflation (Based on 600 KEAS ejection)	1.39	Harness Release Actuation
		1.8	Full Parachute Inflation (Based on 200 KEAS Ejection)

Figure 17 presents representative recovery trajectories. Figures 18 and 19 show angle of dive and sink rate recovery capabilities, respectively. Figure 20 presents the actual trajectories of the accident discussed above.

TEST ROGRAM

The LW-2 ejection seat has to date had a rather extensive test program conducted on both specific hardware components and total seat system

configuration. One seat was subjected to static structural loads to demonstrate the ability of the escape system to withstand loads resulting from 30 G ejection and crash loads of 40 G forward and aft. These loads applied in both instances were ultimate conditions; 1.5 times the maximum anticipated loads. To simulate the ejection requirement, a load of 9951 pounds was applied through a dummy survival kit in the seat and parallel to the egress path. The seat was placed in the test fixture such that the seat rails were in contact with the two upper bulkhead support fittings only. In the case of the crash load demonstration, the seat was loaded as follows: 5800 lbs. was applied to the seat through the survival kit; 3590 lbs. applied to the shoulder harness; 8200 lbs. applied to the lapbelt; and a load of 4600 lbs. simulating the inertia load of the seat and catapult-rocket was applied through the seat CG. All loads mentioned were applied simultaneously.

Various laboratory tests were conducted prior to full scale testing. For example, the harness and drogue riser release system and both the low and high mode parachute deployment systems were tested functionally to facilitate design and to insure proper operation. To insure that the Royalite chute riser protective cover design, mounted to the periphery of the headrest, would retain the risers at a maximum "q" ejection, windblast tests were conducted. Some 27 tests in all were performed with dynamic pressures between 830 to 1350 pounds per square foot directed at the Royalite cover.

To thoroughly prove the lockout configuration for the mode selector system, a series of thirty-two drop tests were conducted in the Structures Laboratory to evaluate the lockout system and to establish the configuration of the structural fuse. Weights varying from five to fifteen pounds were dropped from heights up to 24.8 feet on the striker arms, thereby simulating impact velocities as high as 40 feet per second. This represented the maximum impact velocity which could be imposed on the striker arm in the locked configuration.

A series of six full scale catapult ejections were conducted subsequent to the drop tests to evaluate the lockout configuration. Rocket motors were not necessary for these tests since the purpose was to duplicate the LW-2 escape sequence through the catapult phase and thruster slug firing with the lockout configuration.

Operational ground tests of the complete seat system were conducted in both the static and dynamic conditions. In the period between 6 September 1962 through 19 July 1963, six development firings and twelve demonstration firings for a total of eighteen full scale tests were conducted. In the twelve demonstration tests, three static (0-0) firings of which one was through a GE-Ryan XV-5A canopy, two sled runs at 200 KEAS with the seat's high-mode operation, and five

dynamic sled tests at the maximum design speed (500 KEAS), were performed.

All laboratory tests and static firings were conducted at the North American Aviation, Columbus Division facility. The sled test program was conducted at the FTFST Facility, Edwards Air Force Base, California. Throughout the test program, the extremes of all test variables were used rather than average values; that is, 5 and 95 percentile anthropomorphic dummies, minimum and maximum rocket thrust moment arms, and minimum and maximum speeds for the low and high speed mode were used.

Since July 1963, additional testing has been conducted on the LW-2 escape system due to its being placed in the North American Aviation YAT-28E type aircraft and the Curtiss-Wright X-19 VTOL Tri-Service transport. The tests conducted for the two programs to date have been ejections through the canopies, demonstrating the LW-2 seat's capability to penetrate the glass and recover the crewman. All tests have been successful. These tests were as follows:

November 8, 1963	YAT-28E Program - Static catapult firing only through canopy to demonstrate compatibility. Test Successful.
December 12, 1963	YAT-28E Program - Full scale firing through canopy. Test successful.
December 30, 1963	Curtiss-Wright X-19 Program - Full scale firing through canopy. Test successful.
January 22, 1964	Curtiss-Wright X-19 Program - Full scale firing through canopy (co-pilot side). Test successful.

SUMMARY

The LW-2 Escape System was designed for high performance V/STOL aircraft. This report describes its operation.

Outstanding recovery capabilities are provided throughout the aircraft flight envelope as a result of the two-mode system. At speeds less than 200 KEAS and at altitudes less than 10,000 feet, the recovery parachute is ballistically deployed immediately after the seat leaves the rails. At speeds greater than 200 KEAS, and at altitudes greater than 10,000 feet, a drogue chute effects seat stability immediately after the seat leaves the aircraft. Then release of the drogue chute from the seat provides positive deployment of the recovery parachute.

This North American LW-2 Escape System is considered to be a proven system capable of effecting safe escape and recovery from high performance V/STOL type aircraft.

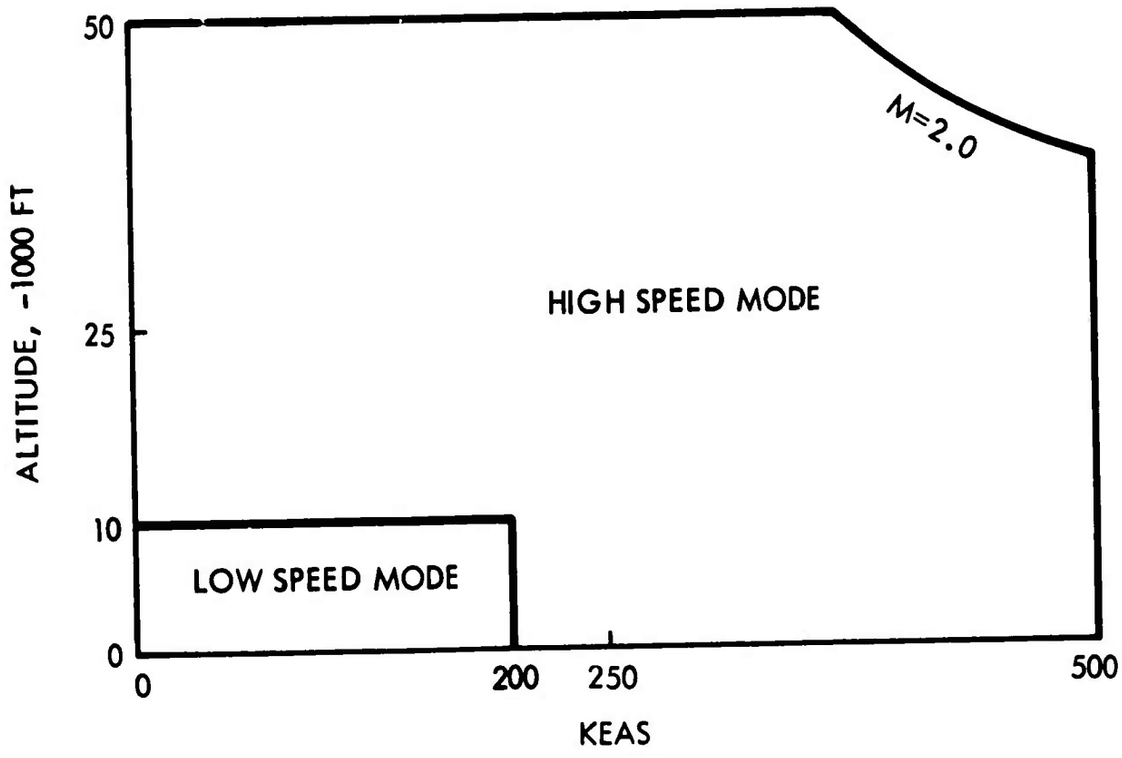

Figure 1. LW-2 System Escape Recovery Envelope

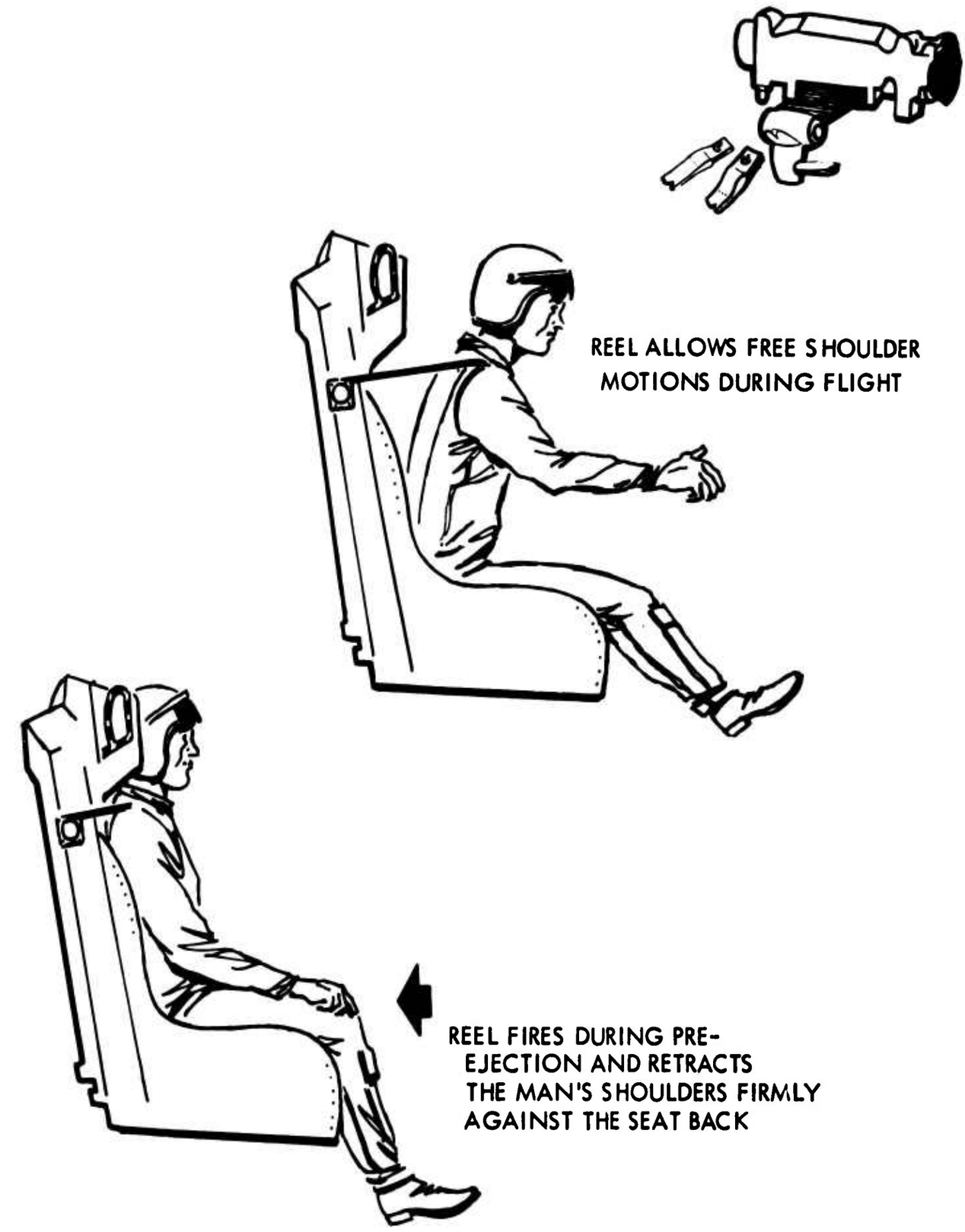

Figure 2. Torso Positioning and Restraint

Figure 3. LW-2 Ejection Seat

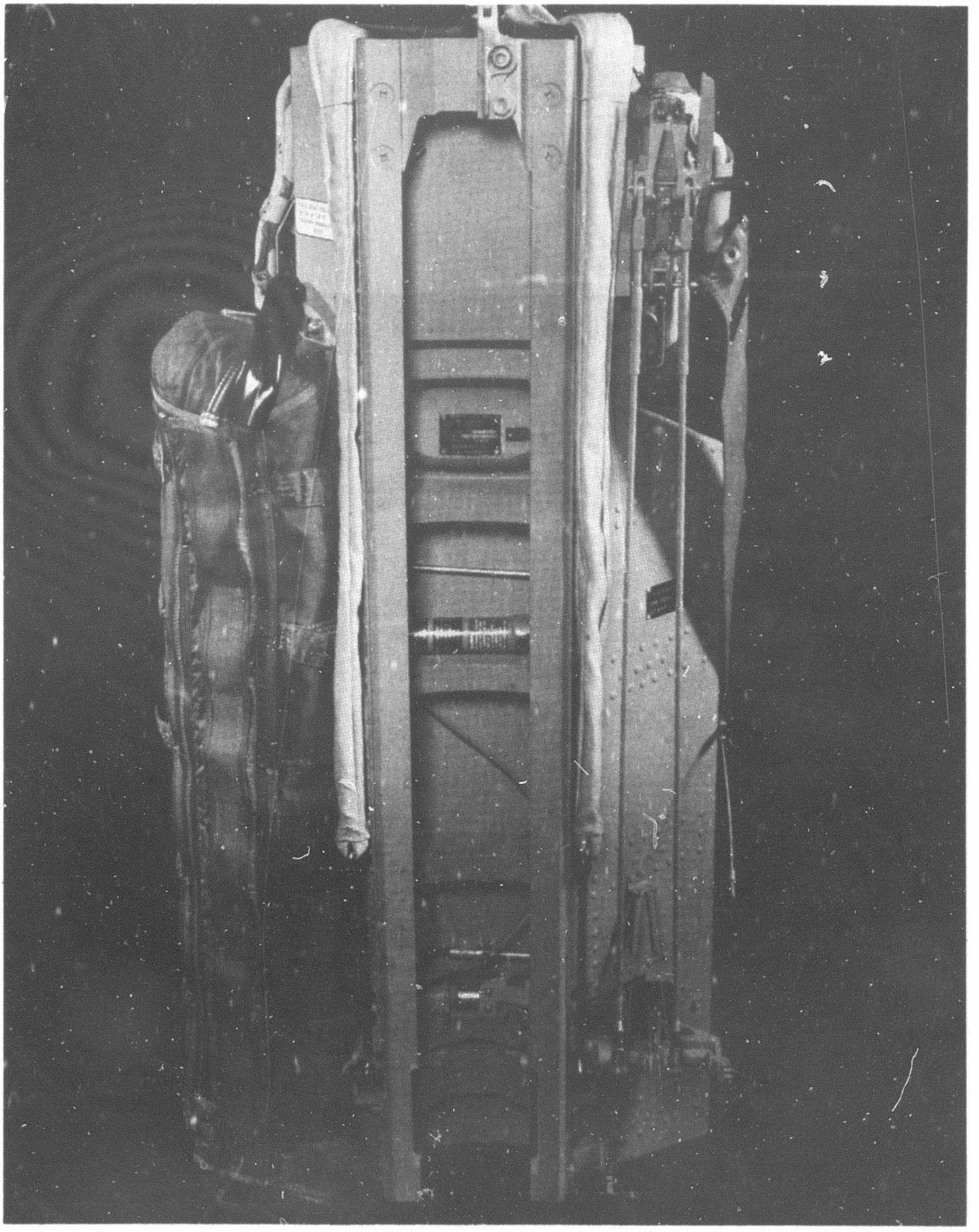

Figure 4. LW-2 Ejection Seat (Rear View)

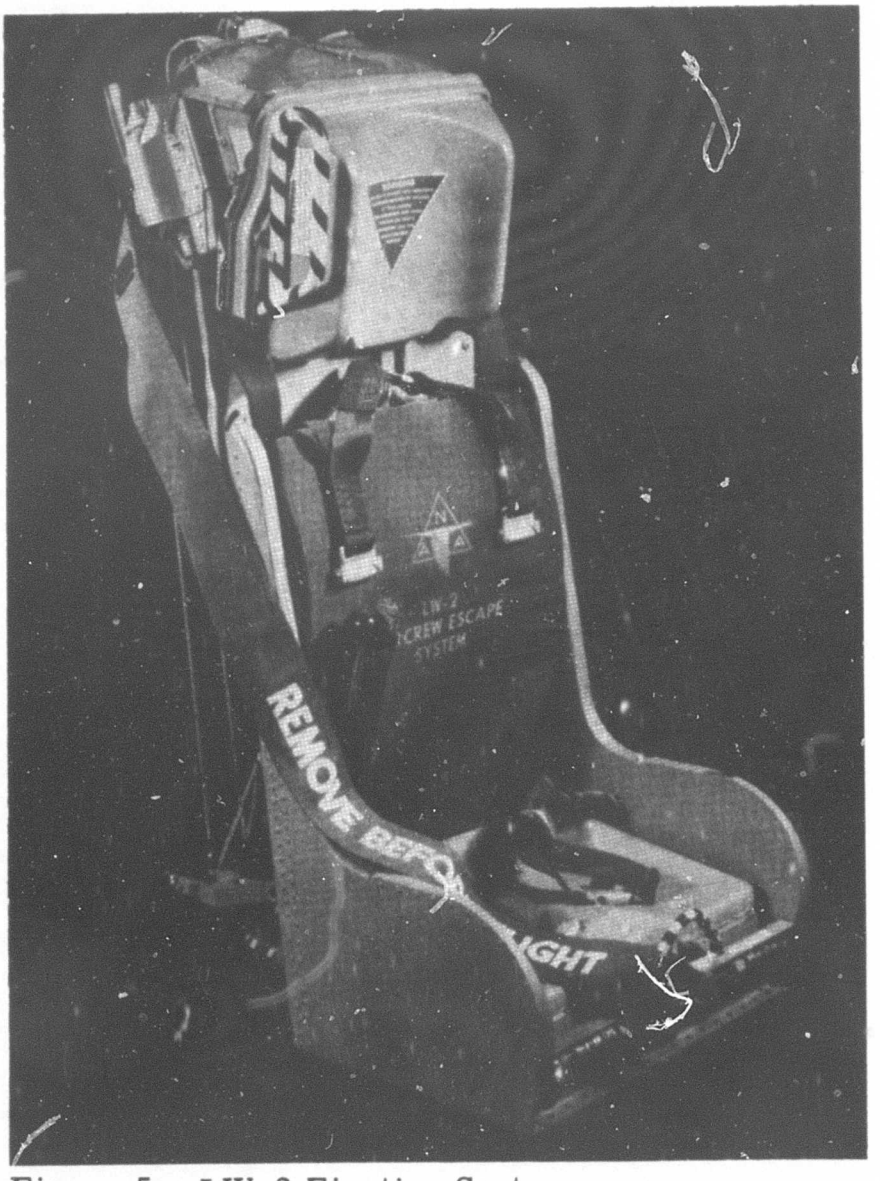

Figure 5. LW-2 Ejection Seat

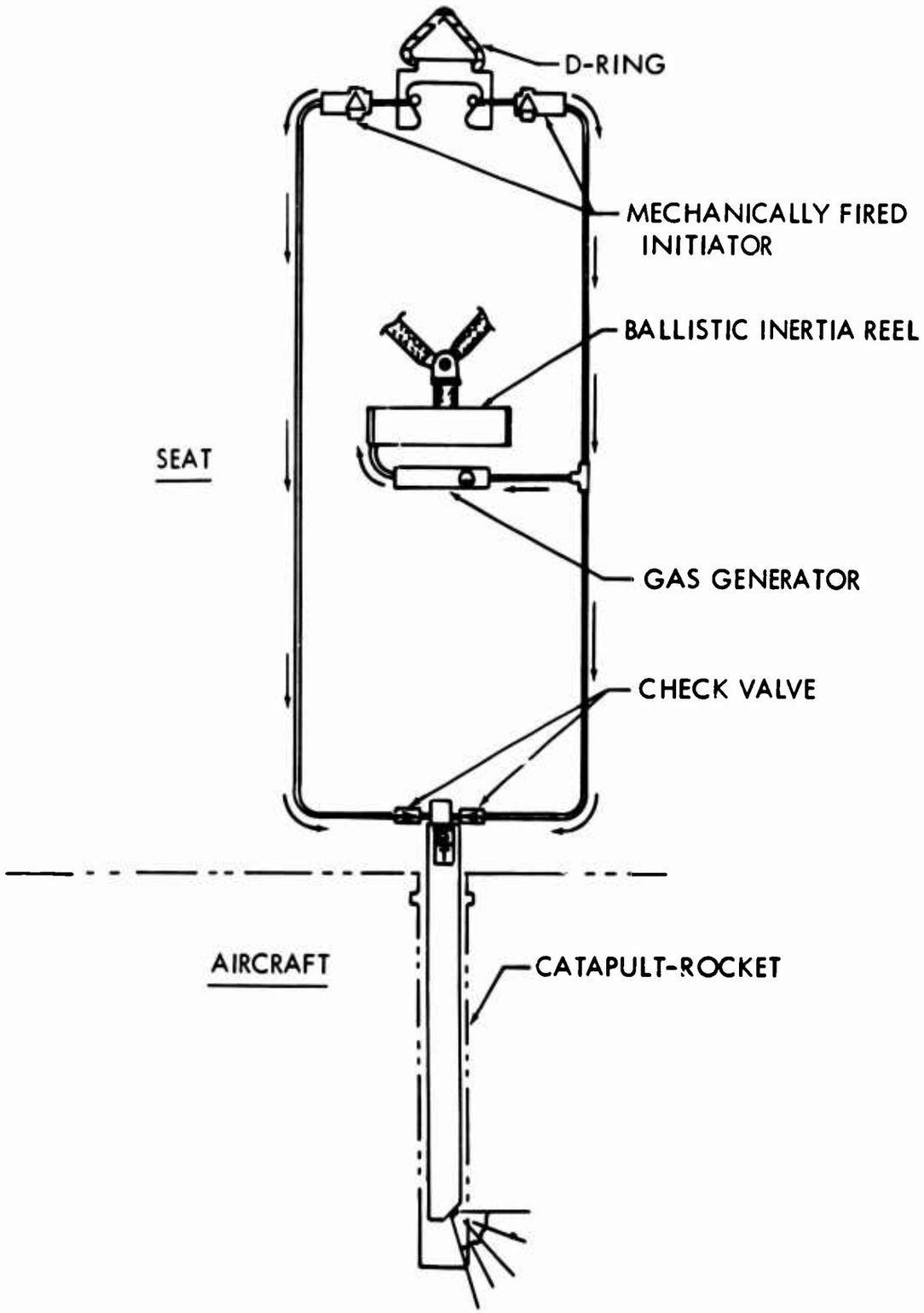

Figure 6. Schematic - Ballistic Initiation System

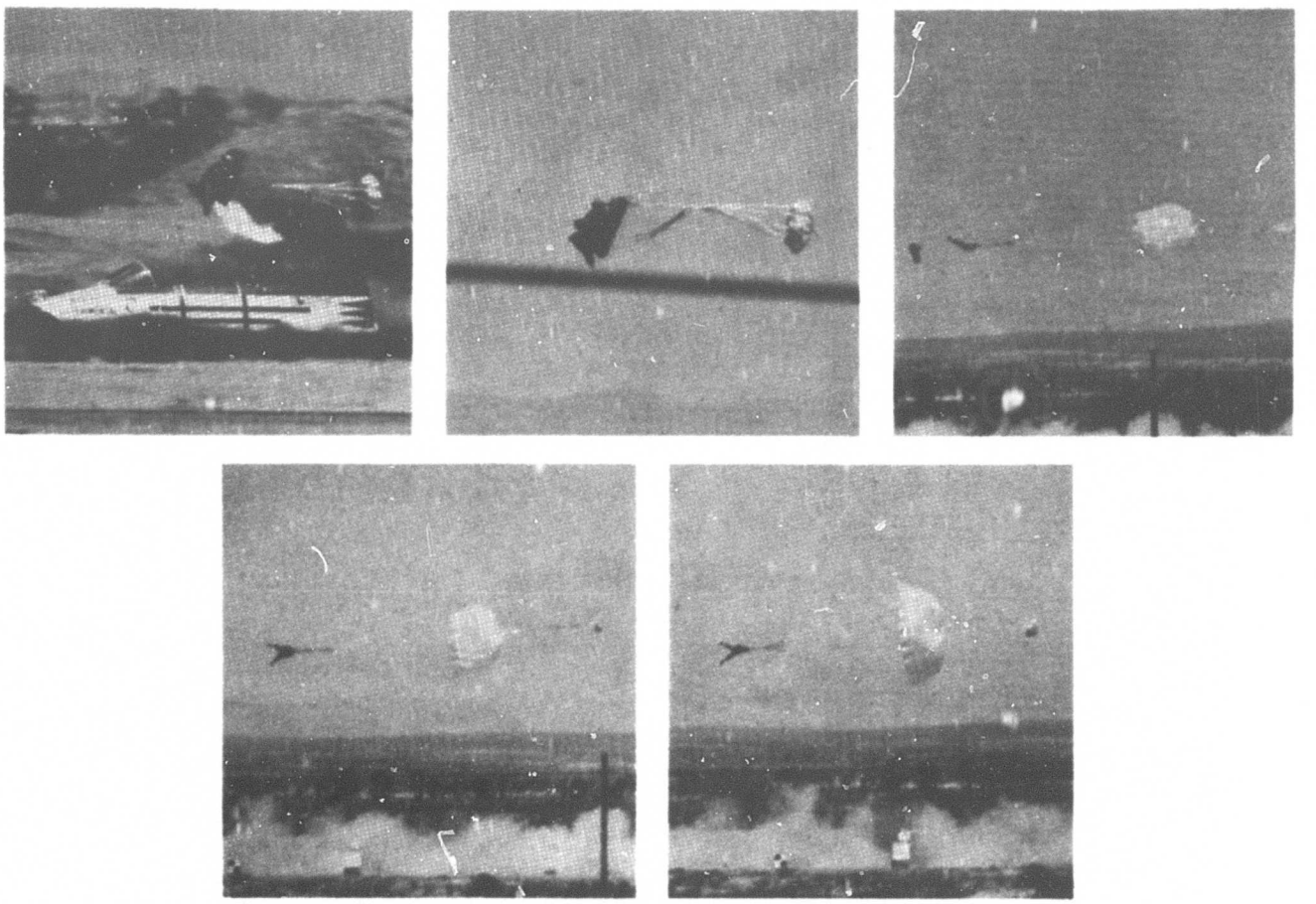

Figure 7. Test Firing No. 16 - 498 KEAS

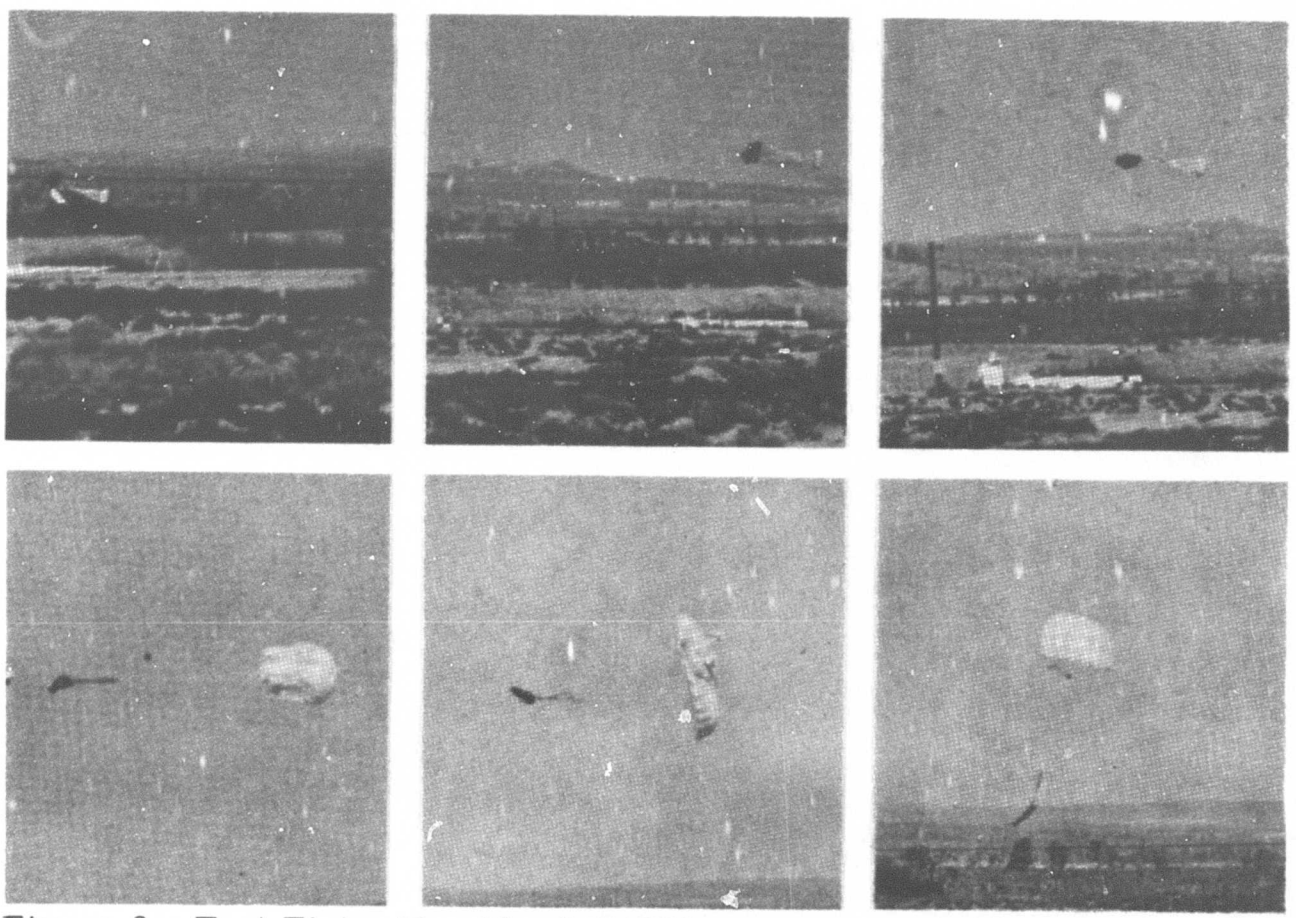

Figure 8. Test Firing No. 12 - 247 KEAS

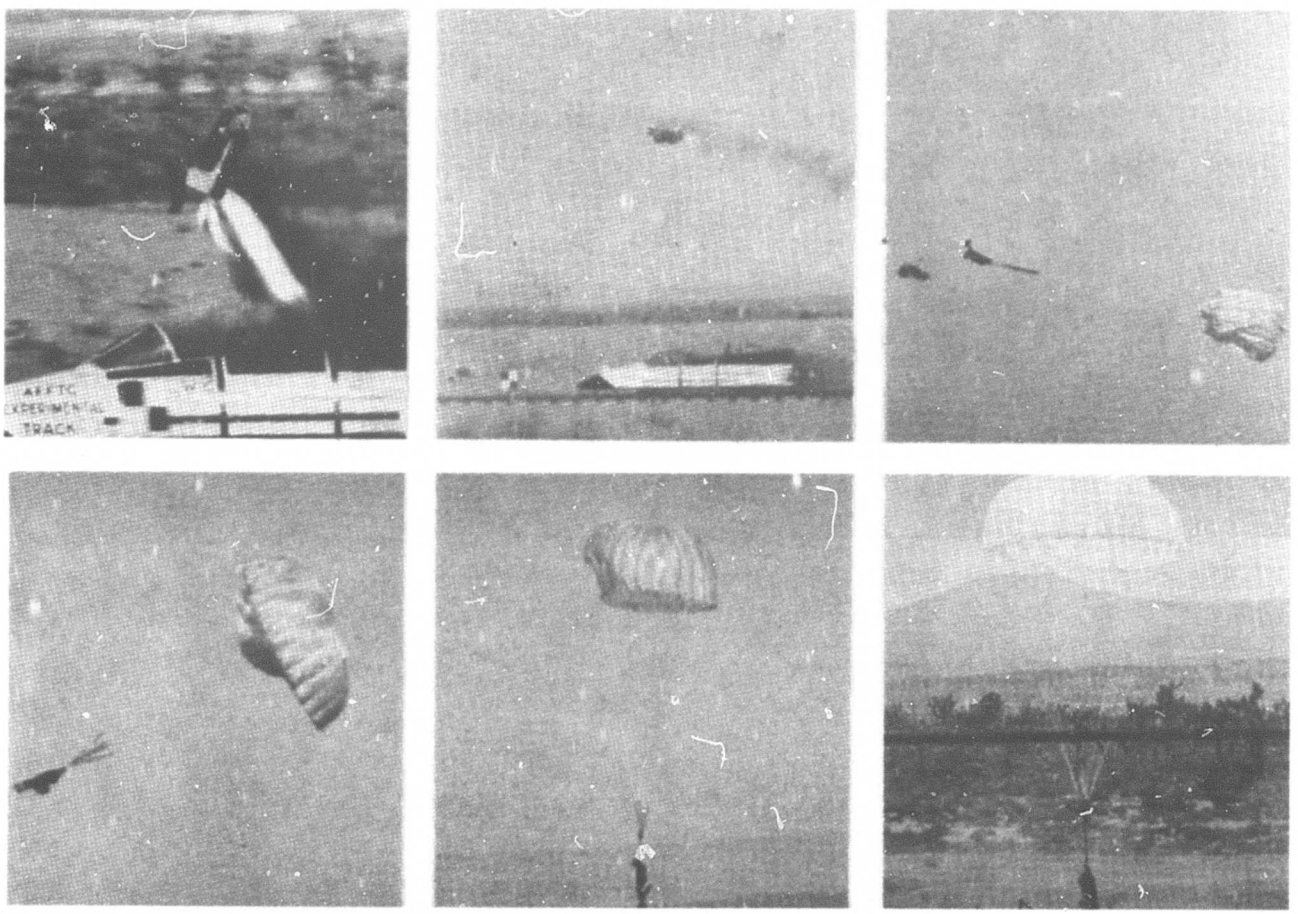

Figure 9. Test Firing No. 13 - 211 KEAS

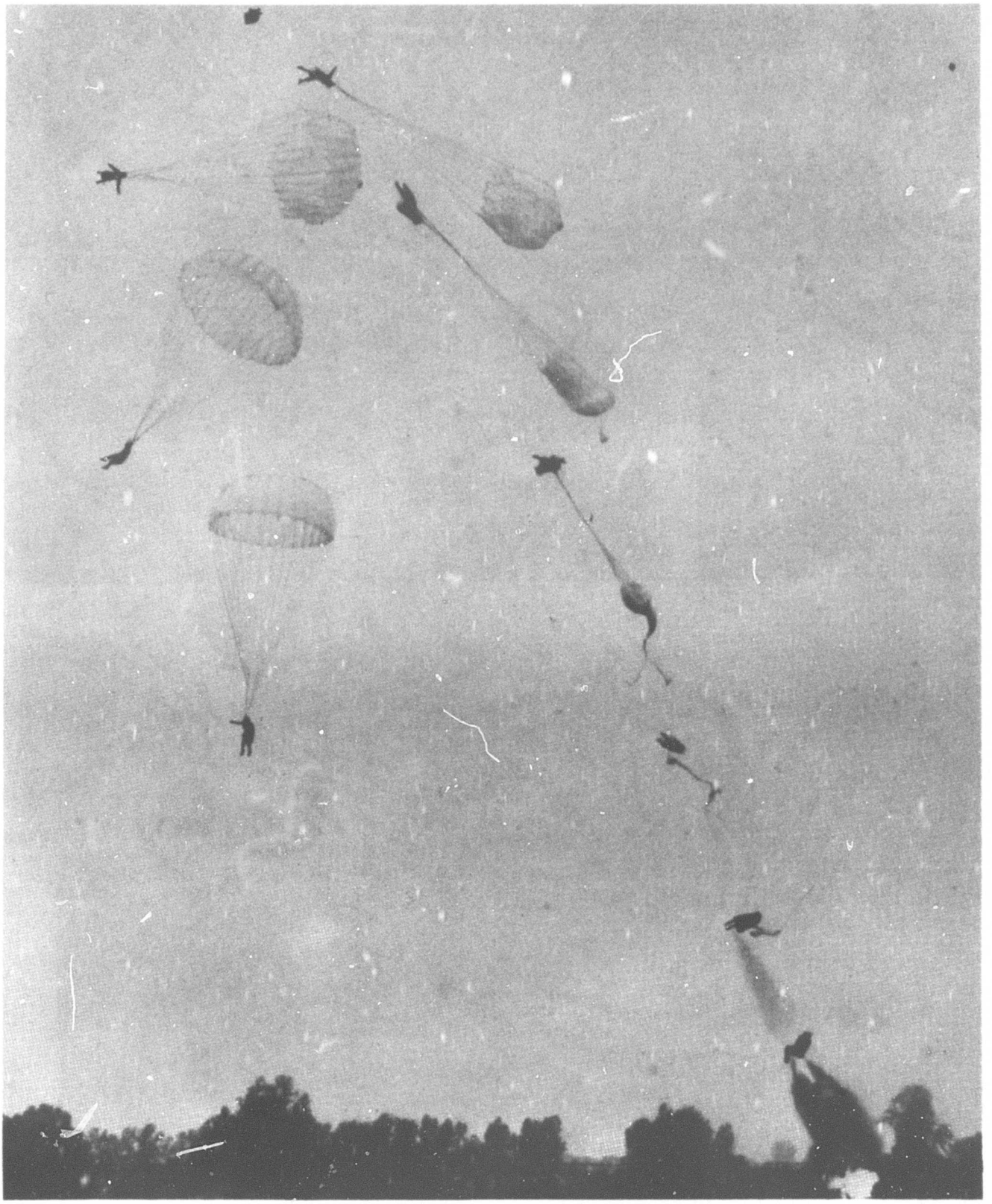

Figure 10. LW-2 Static Firing

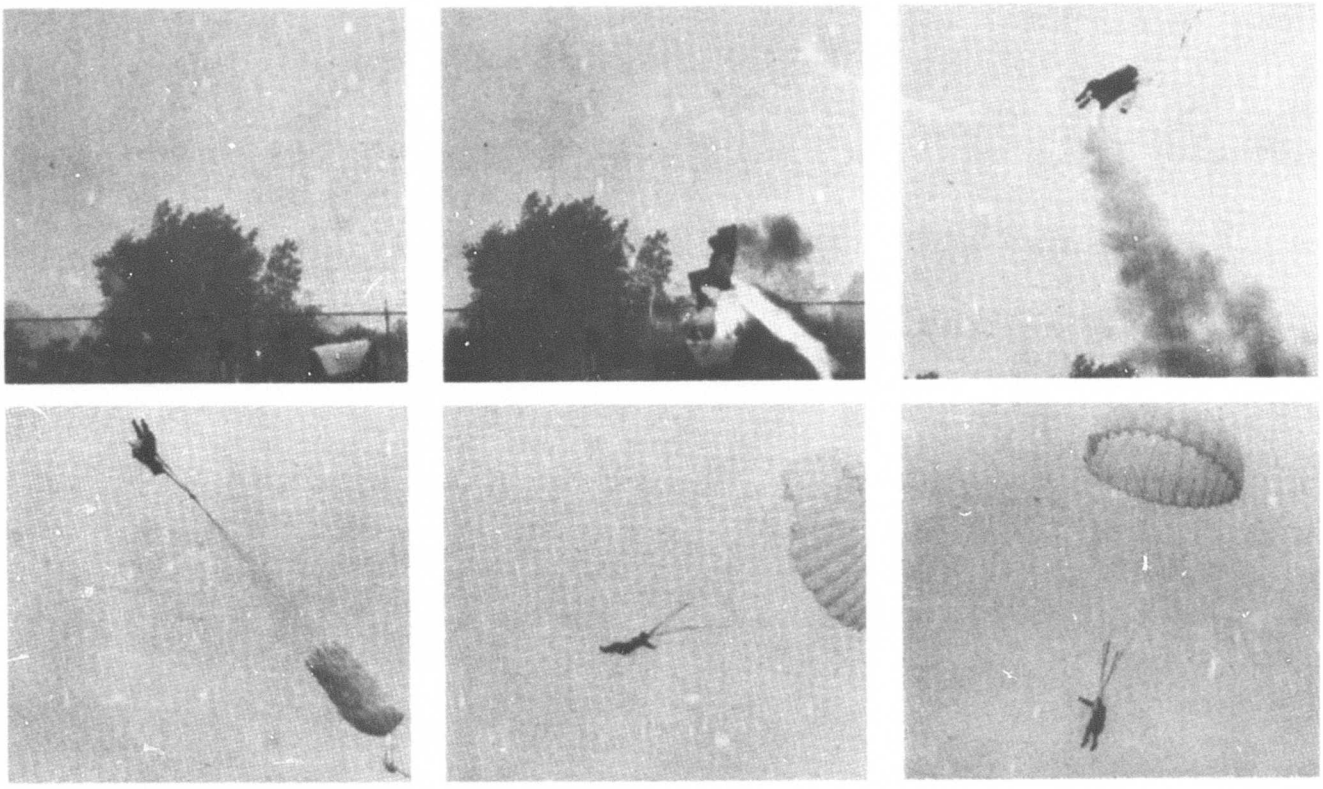

Figure 11. Test Firing No. 18

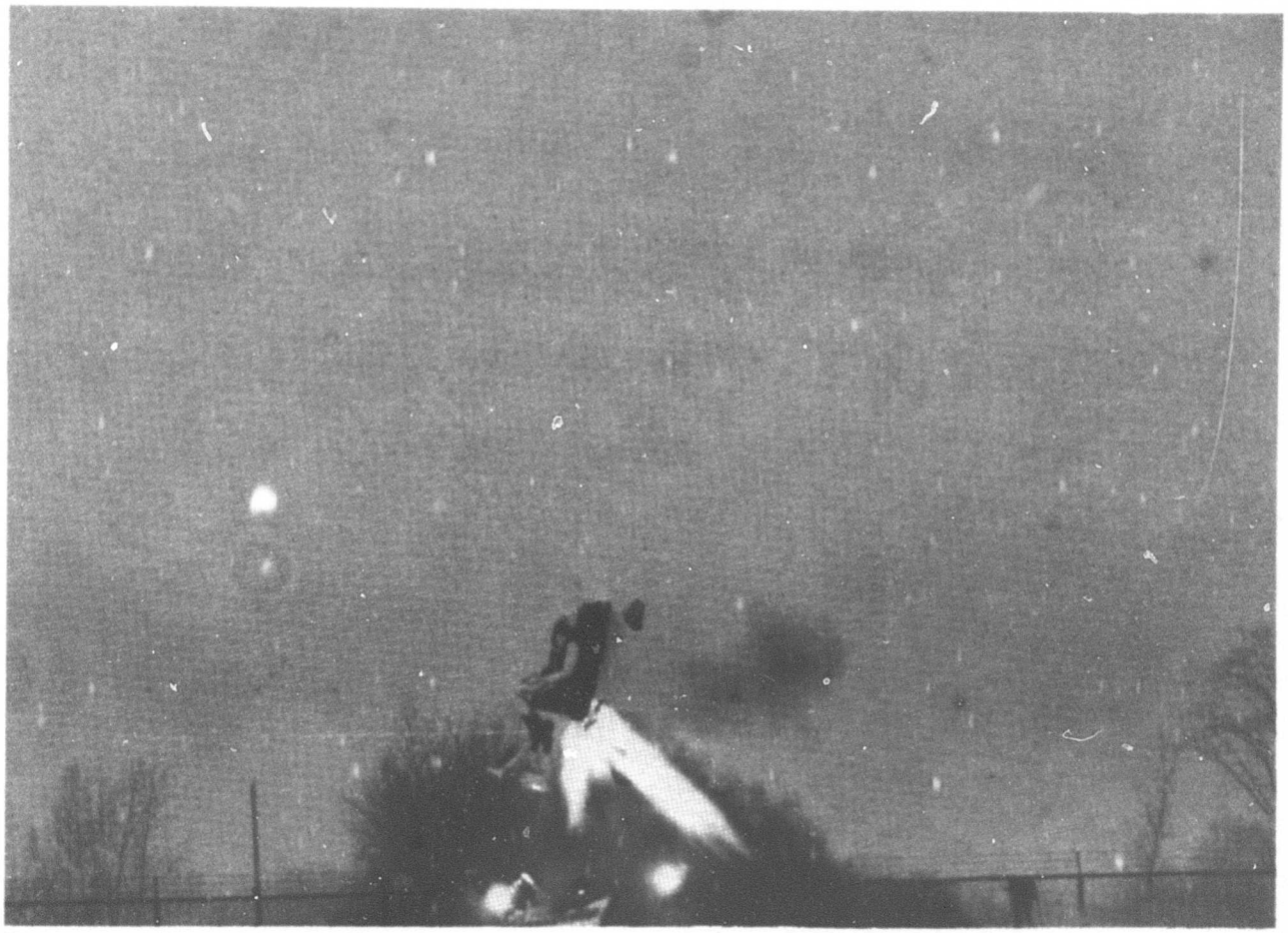

Figure 12. YAT-28E Static Firing - 12 December 1963

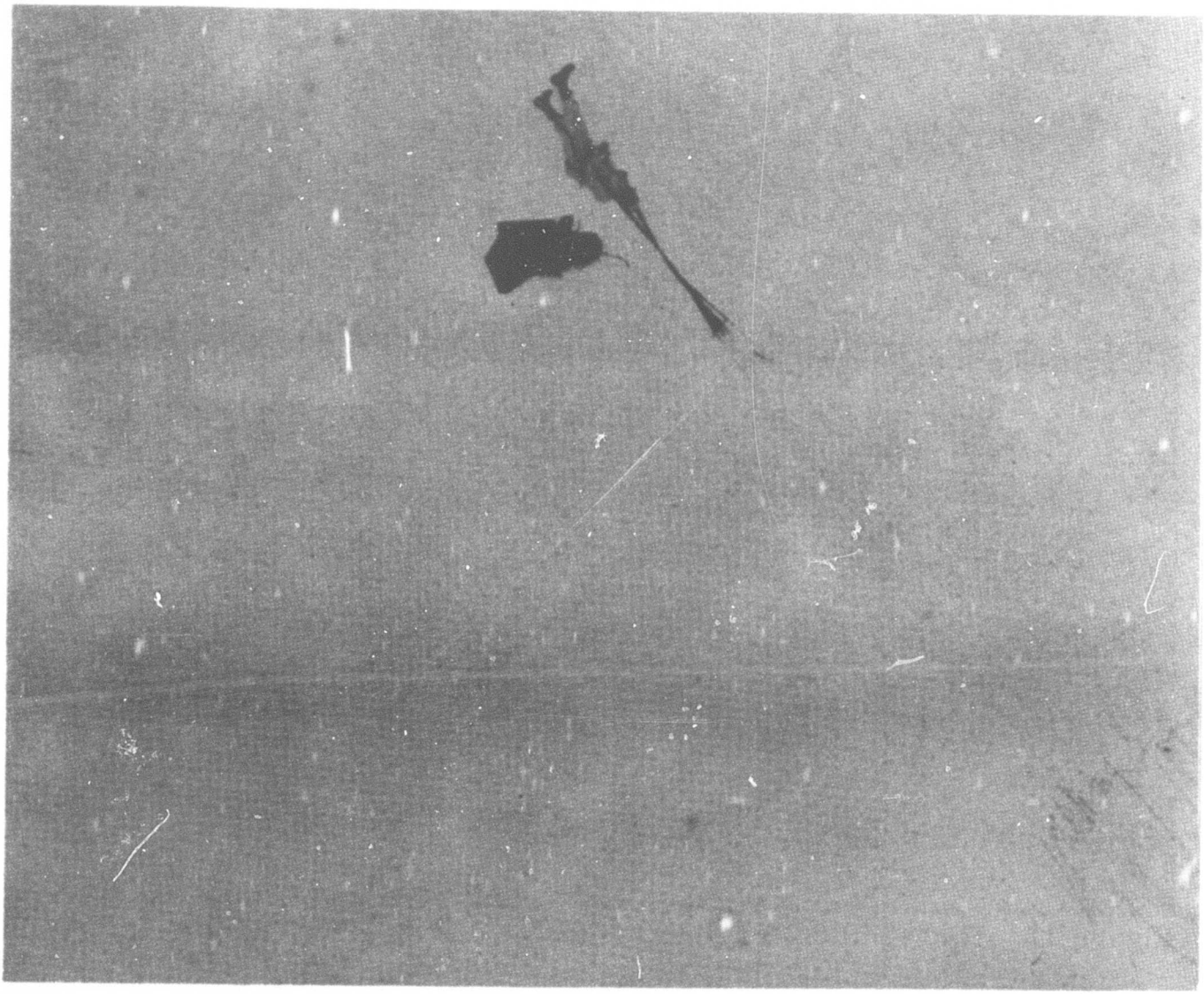

Figure 13. YAT-28E Static Firing - 12 December 1963

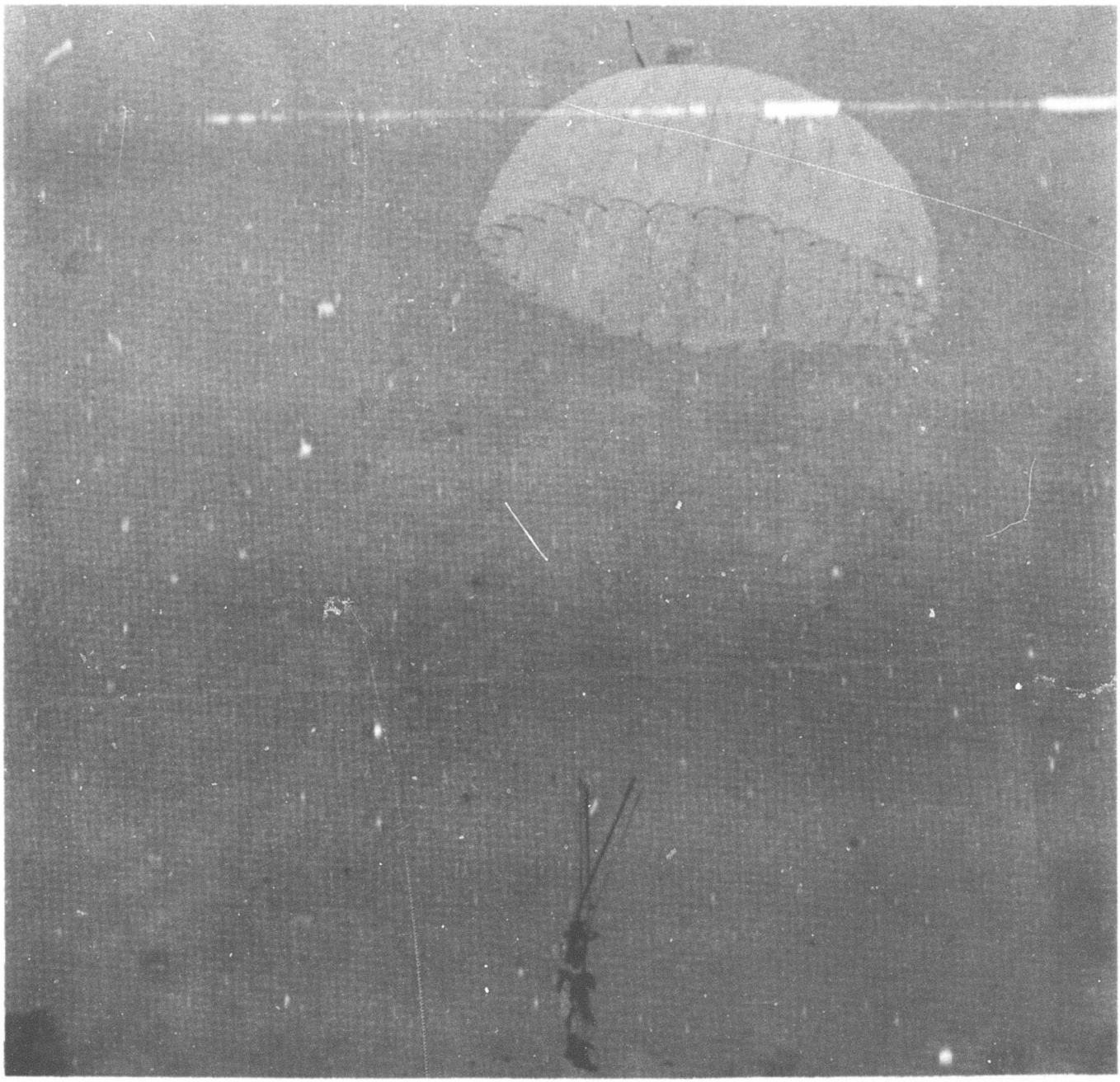

Figure 14. YAT-28E Static Firing - 12 December 1963

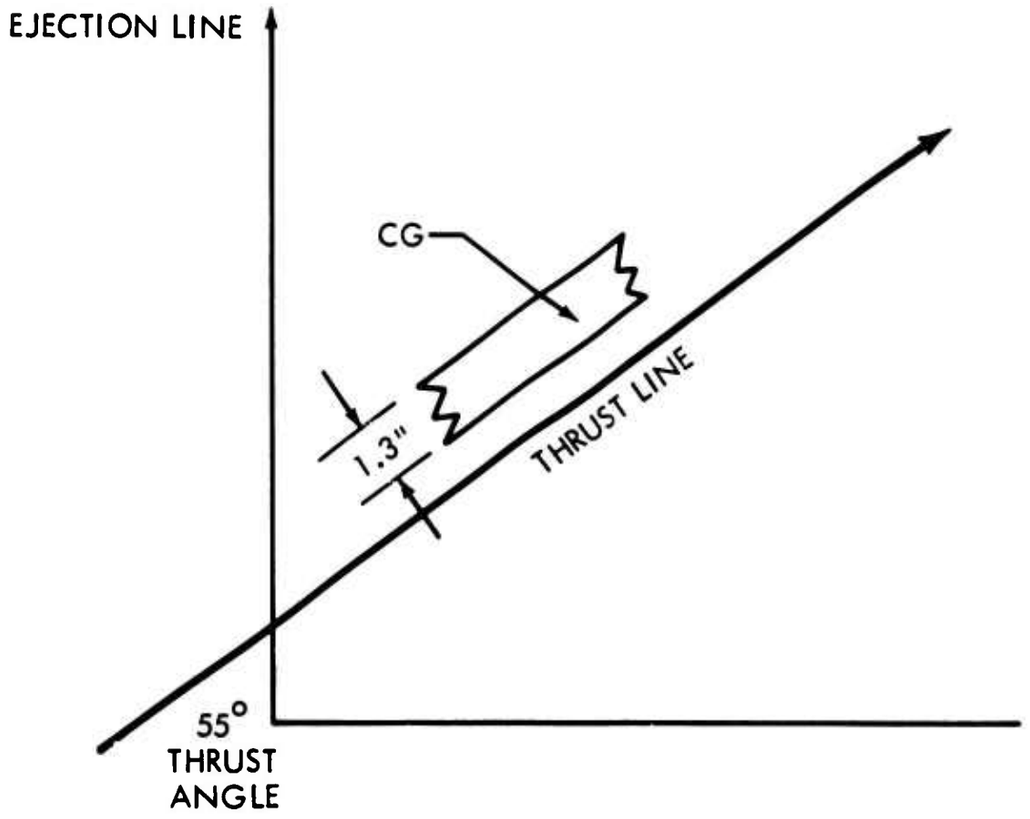

Figure 15. Rocket Thrust Moment Arm Spread

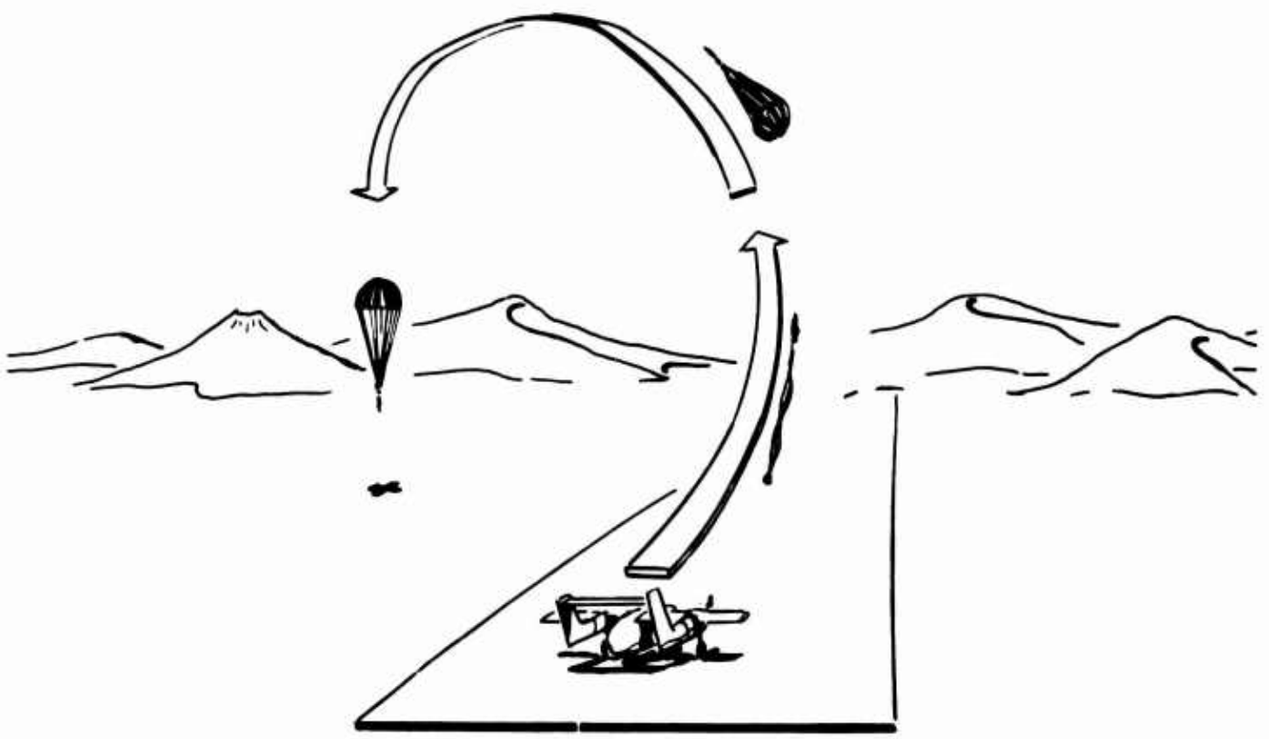

Figure 16. Low-speed Trajectory

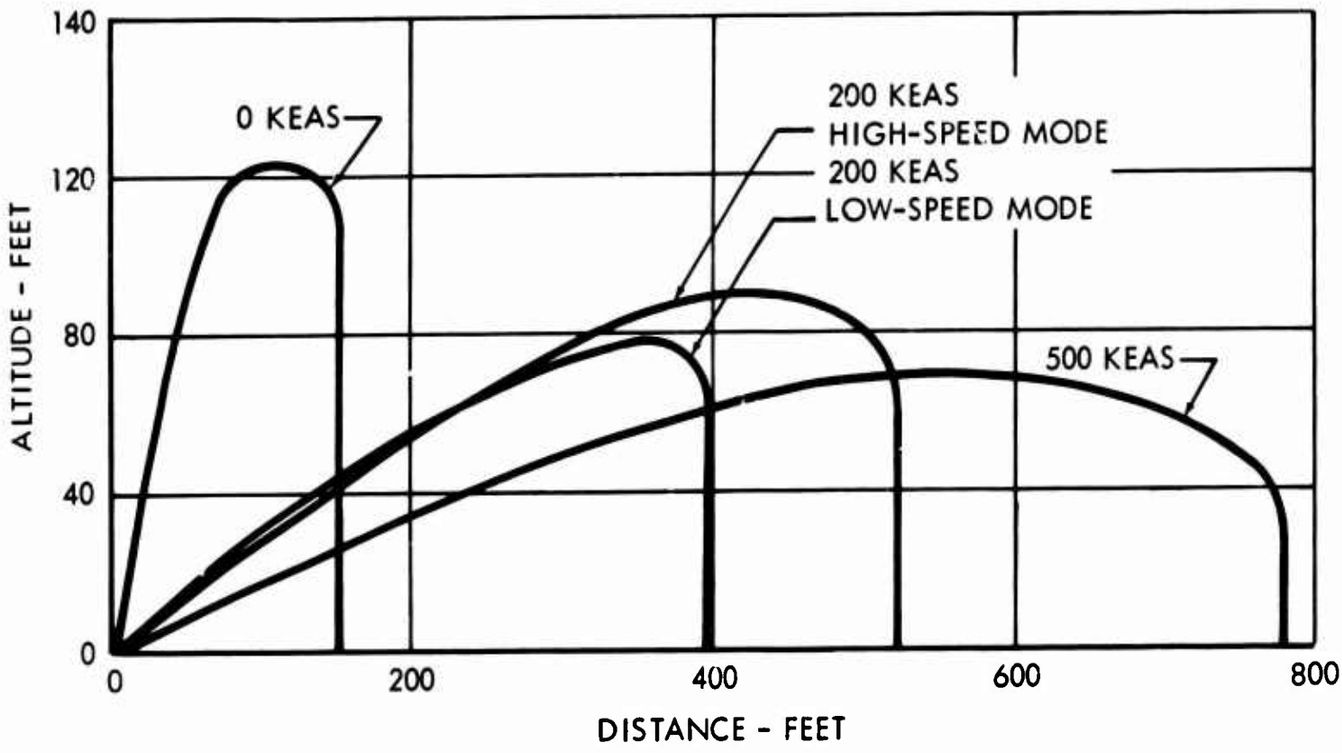

Figure 17. Typical LW-2 Trajectories

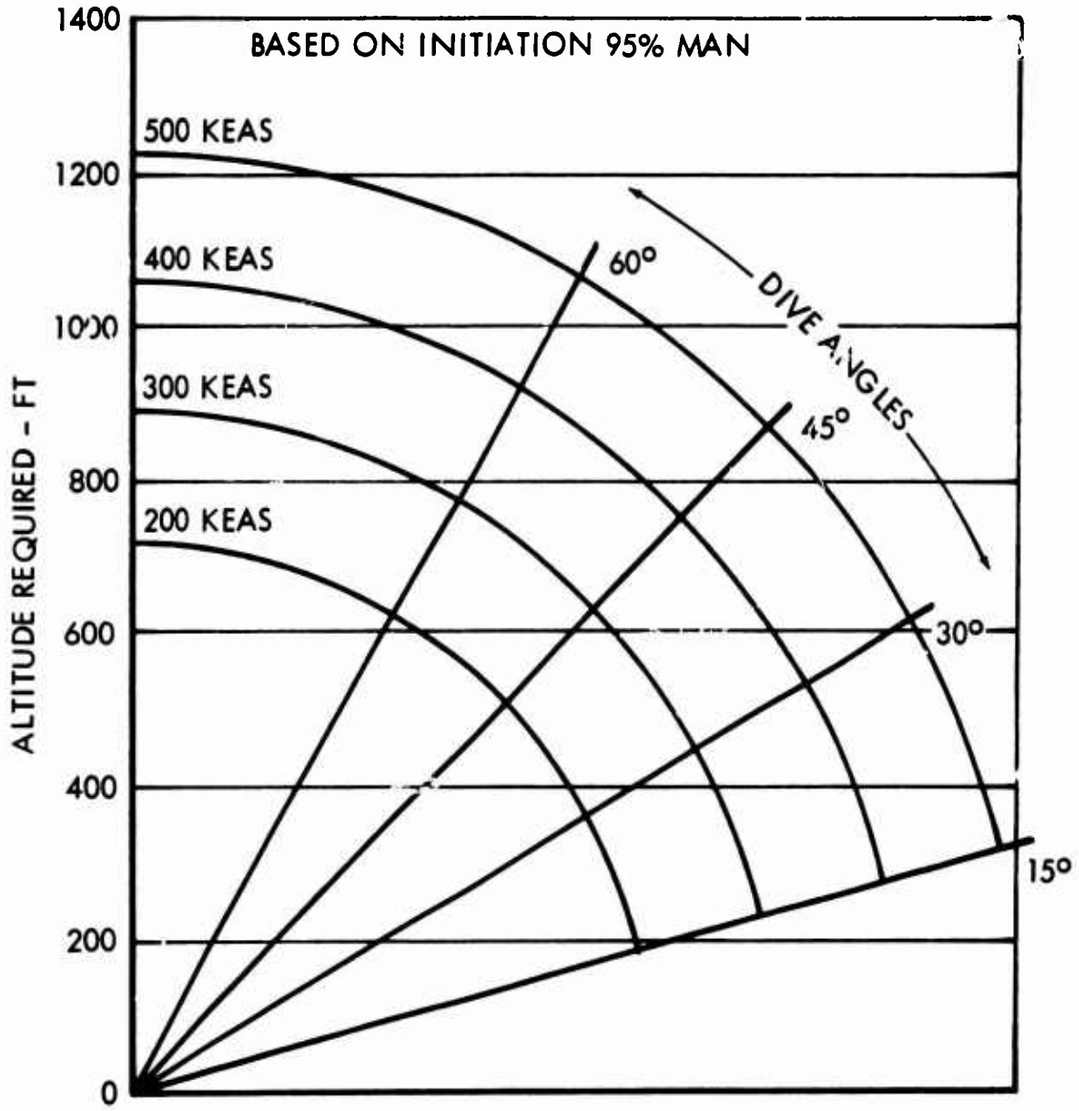

Figure 18. Angle of Dive Recovery Capability

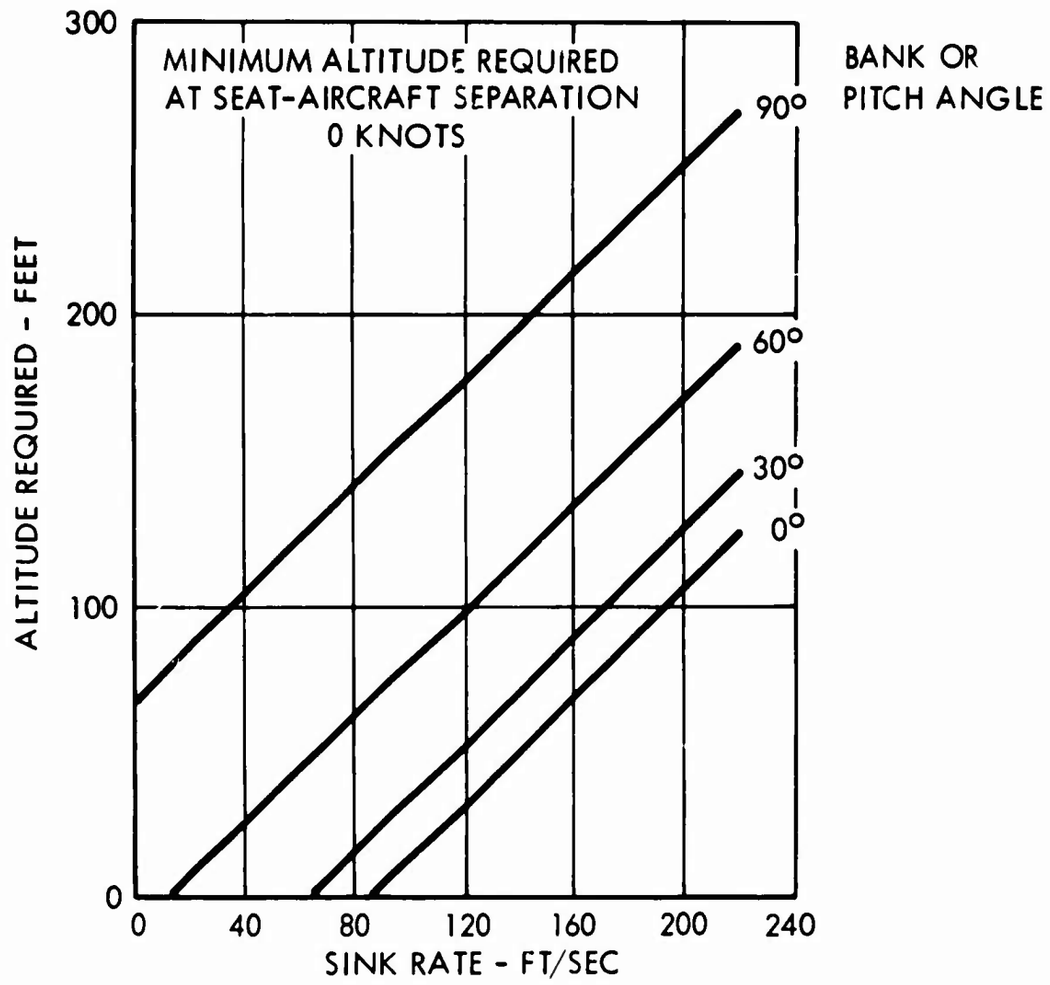

Figure 19. Sink Rate Recovery Capability

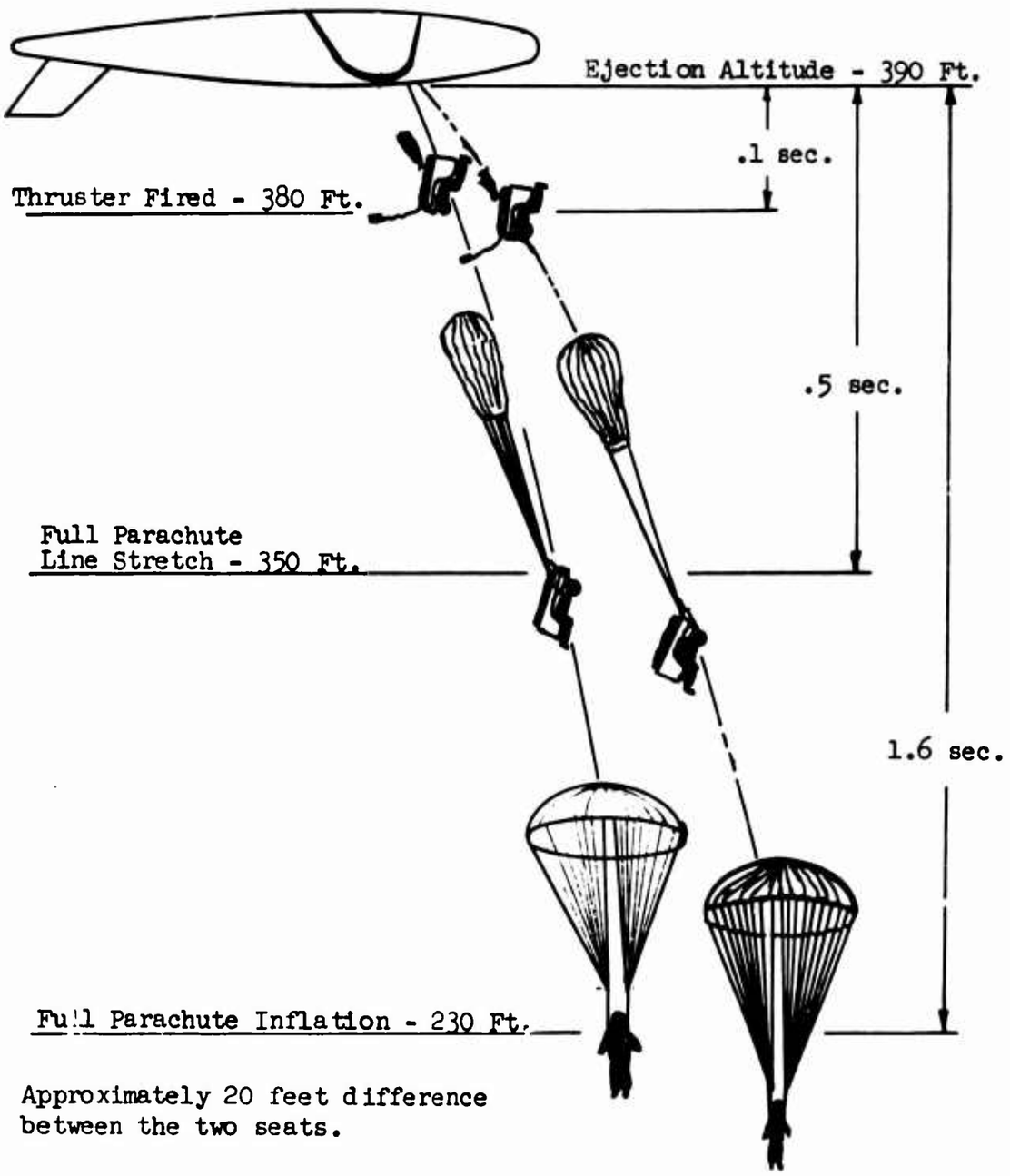

LIVE INVERTED EJECTION

FIGURE 20

THE KC-142A FLIGHT TEST PROGRAM

T. W. Shepard

Ling Temco Vought

THE XC-142A FLIGHT TEST PROGRAM

Thomas W. Shepard, Jr.

Flight Operations Department

LTV Aerospace Corporation

LTV Vought Aeronautics Division

ABSTRACT

The objectives of the XC-142A Flight Test Program are outlined. The philosophy used in planning the program is discussed and the original plan is reviewed. Events leading up to first flight, first hover and first transition are discussed. A comparison is then drawn between the plan and actual accomplishments. Accomplishments following initial conversion are then outlined. Program statistics are discussed and the aircraft instrumentation system and data reduction methods are outlined. Some results obtained to date are presented and compared with predictions. The discussion touches upon performance, structural demonstration and system performance but major emphasis is placed on flying qualities in the hover and transition flight regimes. Pilots comments are included.

THE XC-142A FLIGHT TEST PROGRAM

Thomas W. Shepard, Jr.

Flight Operations Department

LTV Aerospace Corporation

LTV Vought Aeronautics Division

The XC-142A aircraft has been in flight status for about 13 months. It is my purpose to review the highlights of the program to date. The discussion will cover early flight test planning, the events following first flight that led up to first hover and conversion and reconversion, and other accomplishments which followed. Also to be discussed are test program statistics and some of the results obtained to date. These results will be compared with predictions.

The primary objective of the Flight Test Program was to evaluate the XC-142 design and provide a flight envelope which would enable the Tri-Service Test Team to conduct an operational suitability evaluation of the tilt wing concept.

Before proceeding with the discussion of the flight test program, let us look at some of the features of the XC-142 which make it suitable for an operational evaluation.

The XC-142 is the world's largest VTOL flying today with a length of 58 feet, a wing span of 68 feet, a height of 26 feet. Figure 1 shows a comparison of the XC-142 with a familiar aircraft. With a cargo compartment of 7 x 7.5 x 30 feet, the XC-142 has in the VTOL mode a payload capability in the vicinity of 8,000 pounds or 32 fully equipped combat troops. This payload and capacity permits the XC-142 to be used for various supply and assault transport missions. The operational evaluation will demonstrate how well the XC-142 can perform these missions.

The task of preparing the XC-142 for the Category II flight tests and for operational evaluation is being accomplished during the Category I Flight Test Program. Obtaining the objective previously stated has been broken down into three interrelated tasks.

The first of these is to evaluate and/or demonstrate the flying qualities, performance, structural adequacy, systems and emergency procedures.

The second is developmental in nature and involves defining problems found during evaluation and demonstration and then evaluating fixes installed to solve the problem.

The third task which results in part from the first and second is the determination of an adequate and safe envelope and the publication of restrictions which define the envelope.

How best to accomplish these tasks was the subject of many planning sessions. In this planning work, the XC-142 was examined as three separate aircraft. First, with apologies to the rotary wing people, it was considered as a helicopter, then as a conventional fixed wing aircraft and finally as an undefined "you name it" in the in-between area where all, some, or none of the criteria for evaluation of flying qualities of helicopter and conventional aircraft applied. The approach finally settled on was to start out with a conventional mode series of shakedown flights to examine conventional flying qualities and to evaluate critical system performance. Then the plan called for exploring flying qualities at a safe altitude at progressively slower speeds by raising the wing incrementally. This procedure would be repeated at lower altitude and in ground effect. This work would be followed by hover flight after completion of VTOL test stand tests at Edwards Air Force Base. After hover work and the investigation of handling qualities in ground effect at progressively lower wing angles starting from 90 degrees, complete transition was then to follow. This was, of course, the major goal of the early flight test program. Once accomplished, the program of filling out the envelope would be pursued along conventional lines.

The time table for first hover and first conversion was as follows:

First hover 15 weeks after first flight
First conversion one week after first hover

After some delay due to the prerequisite of completing a 50-hour ground run on the propulsion system (i.e. engines, propellers and transmission system) first flight of the XC-142A was made on 29 September 1964.

After four system shakedown flights which were flown in the conventional mode except for take-offs and landings where 10 degrees of wing and 30 degrees of flaps were used, the aircraft was put into work status for incorporation of several changes. These changes were found necessary during ground test programs conducted prior to first flight and were required to clear the aircraft for operation at wing angles above ten degrees. Also incorporated were changes found necessary during the shakedown. Included in these changes was a rework to improve nacelle cooling.

On the next six flights, flying qualities were investigated at various steady state wing positions between zero and 40 degrees using both take-off and landing flap programs. The short take-off or conversion maneuver was investigated in approximately 5 degree wing increments using the take-off flap program which limits flap travel to 30 degrees. The short landing or reconversion maneuver was investigated in increments to a maximum wing angle of 40 degrees using the landing flap program which permits the flaps to travel to a maximum at 60 degrees. The 40 degree wing, 60 degree flap configuration produced a fuselage level trim speed of 26 knots which at 8,000 feet made the pilots a little unhappy. This stemmed from the lack of adequate visual references at the test altitude. The pilots were unable to perceive yaw rates or sideward accelerations and were forced to use the yaw meter in performing tests below approximately 50 knots. Although the yaw meter was an aide, it was not a good substitute for outside references.

One of the next two flights was devoted to clean configuration work up to an altitude of 20,000 feet. The other was used to extend, at 8,000 feet, the investigation of flying qualities to 47 degrees of wing and 30 degrees of flaps.

While flying at the higher wing angles during these first 12 flights, the pilots were able to obtain a good feel for the hover characteristics of the aircraft. With the wing at 90 degrees, further knowledge in the area of the hovering flying qualities of the XC-142 was obtained by applying only sufficient power to "get light" on the gear. With this experience, customer clearance to hover was obtained prior to initiation of the VTOL test stand program. On the 13th flight on 29 December 1964, 13 weeks after first flight, the XC-142A was hovered for the first time.

On the next five flights, flying qualities in ground effect and short take-offs and landings were evaluated at various fixed wing angles. During this time, a wing and flap setting of 50 and 30 degrees respectively was investigated at an altitude of 8,000 feet and resulted in a level flight trim speed of 29 knots. This is the highest wing angle explored at altitude. Three hundred sixty degree hover turns were evaluated. Also following hover take-off, forward translations were accomplished by lowering the wing in increments to 50 degrees. This closed the gap in the evaluation of flying qualities at various wing angles and in fact provided an overlap in flight speed between hover and complete transition. In getting to and from the various steady state wing angles at which flying qualities were evaluated, the pilots gained considerable practice for the continuous transition maneuver. The lower wing angles were frequently traversed providing maximum experience in the area where aircraft acceleration per degree of wing is greatest.

On flight 19 on 11 January 1965, 13 days after first hover, the first complete conversions and reconversions were accomplished by the XC-142A. Figure 2 summarizes the scheduled and accomplished milestones leading up to first transition. As indicated under accomplishments, the first military participation occurred on 19 December 1964 when the Air Force Project pilot occupied the co-pilot's seat. It is also pertinent to note that the XC-142 was first operated by a full military crew on 26 March 1965 in the 13th week after first hover. In a little more than 12 months since first flight, 15 pilots have flown the XC-142A.

Since the first transitions, or verti circuits as some have called them, we have continued to expand the flight envelope. Currently, the aircraft has been operated to the conditions listed in Table 1.

Let us look at a few statistics which show where the program stands at the end of September 1965. Figure 3 graphically shows the percentage complete of a number of parameters by which flight test progress may be measured. The two numbers on each bar represent the planned and completed quantities from which the percentages were calculated. Note that the percentage of test points accomplished is running slightly ahead of the percentage of aircraft months expended. This is pertinent in measuring progress. Because total test points planned best defines the scope of the program to be accomplished, most weight is given to test points successfully completed. The excellent

progress in completing test points is the result of two factors: one, the excellent data recovery rate from the instrumentation system installed in the three flight test aircraft; and, two, a continuing careful evaluation to insure that multiple objectives met at any given flight condition are accounted for. Because of excellent correlation between predicted and actual performance in certain areas, more rapid progress to specific end objectives has been possible, and tests at certain build-up points have not been required. Credit for all such points has also been accounted for. The progress toward completing all the planned test points has been made with the expenditure of less flight time than planned, that is the productivity per flight hour has been higher than planned. This has resulted in a significant savings in valuable transmission system time with attendant savings in transmission overhaul expense.

The data recovery rate bears some further mention. The aircraft are heavily instrumented using high and low level pulse duration modulation switches, FM/FM subcarrier oscillators and straight FM channels. Most data is recorded during maneuvers on a 14 track airborne tape recorder. Part of these data are also recorded during the entire flight on a ground tape recorder which receives its intelligence through telemetry. Eighteen parameters are stripped from the telemetry signal, scaled, and presented on the ground to engineering and flight test observers in real time on strip charts. This system has provided the ability for quick decision making and has contributed significantly to the progress of the program. In addition, photographs are taken of engine instruments in the cockpit and a photo observer is used for certain parameters where rapid response is not required. The total system has the capability of recording approximately 275 separate parameters. After a flight, the airborne tape is stripped and converted to digital format compatible with IBM 7090 language by an SDS 910 data processor. Scaling and selected computations are performed by the 7090. Tabulated data and a tape for use by automatic plotters are available within less than 24 hours. Scaled plots of selected parameters are then made available within another 24 hours. A typical flight on an instrumented aircraft will produce about 20 minutes of airborne tape which will contain over 3 million data samples. This system provides large quantities of data in a reasonably short time and permits an early thorough engineering evaluation of actual data versus predictions.

From all this data and the flying that has produced it, what are some of the results that have been obtained?

In general, system performance has been excellent. The electrical and hydraulic power distribution systems have been relatively trouble free.

Throughout the life of the program, the GE T64-1 powerplant has performed well. Installed performance is as predicted; in fact, limits have been raised to permit operation for short periods up to 3080 horsepower.

The transmission system shown schematically in Figure 4 consists of the four main integral gearcase propellers, the interconnecting wing shafting, the tri-directional gearcase, the pivot gearcase, the fuselage shafting and the tail integral gearcase propeller. This system has been pleasingly trouble free throughout the flight test program. This is the result of a rather thorough development and ground test program which included component tests, back to

back tests, engine-IGC system compatibility tests, a 50-hour ground run on No. 1 aircraft and a 150 hour system qualification test program on the system test stand. When updated, after 50 hours of operation, all system components will have a 150 hour time between overhaul.

The control and stability augmentation systems have performed in accordance with design predictions. Adjustments and changes have been minor. This is largely due to the test program conducted on the flight control simulator shown in Figure 5.

A few words about this powerful test tool and its effect on the flight test program are in order. The simulator consists of a steel frame, wing and tail surfaces into which all the control system components were installed. All components are in the same location relative to one another as in the flying aircraft. The various controls and surfaces were instrumented. These instruments fed a combination analog-digital computer system which contained the various equations of motion. A cockpit display provided cues to the pilot. The computer setup permitted the pilot to fly the complete envelope from hover to conventional flight as one continuous maneuver. The simulator served to confirm many of the predicted flying qualities and provided excellent training for the pilots both in normal and emergency operation prior to flight. Differences in simulator results and flight results were minor even though the simulator is a fixed base device and provides only IFR type cues.

Probably of most interest is the aerodynamic behaviour and flying quality characteristics in the hover and transition modes of operation. Looking at aerodynamic behaviour first, figures 6 and 7 illustrate the excellent correlation between predicted and actual wing and flap position versus equivalent level flight trim speed. The data points obtained prior to flight 19 represent a spread of weights and center-of-gravity between 35,600 and 38,700 pounds and 18.3 and 21.3 percent MGC respectively. Figure 6 represents data for a conversion, that is, from hover to cruise flight. Figure 7 presents data for a reconversion, that is, from cruise flight to hover. The difference between these two curves is the flap angles attained at various wing angles. Although manually controllable, flap angles are normally automatically programmed as a function of wing angle. For take-off or conversion the flap angle is restricted to 30 degrees as illustrated in figure 6, and permitted to travel to 60 degrees for landing or reconversion as illustrated in Figure 7. Similarly, the correlation between the predicted and actual tail prop angle and unit horizontal tail (UHT) angle required for trim is very close. Since the UHT and tail prop angles are automatically trimmed as a function of wing position, the execution of a conversion requires very little stick motion. In fact, the whole fuselage level conversion or reconversion is accomplished through the manipulation of essentially only two controls, the collective lever and the wing position control which is located on the collective grip. Only minor lateral and longitudinal control inputs are required. The airspeed indicator is of little importance during transition because wing stall will not occur with sufficient power on the aircraft. This is the result of having the wing fully immersed in the slip stream. Descent or ascent rate can be changed instantly with power.

Speaking of descent rate, how has the XC-142A flight test data stacked up against design? Figure 8 provides the answer. The buffet on-set point

has been found to be at 50 to 100 feet per minute higher sink speeds than predicted. Significantly greater sink rates can be obtained in moderate buffet. The controlling factors are the individual pilots tolerance to buffet and/or the point at which lateral flying qualities become unsatisfactory.

What do the pilots have to say about the flying qualities of the XC-142A? In general, all have had high praise for the aircraft in all modes of flight and in all axes.

In the hover mode with the stability augmentation system on, the aircraft has been described as easier to fly than most helicopters. Response to inputs in all axes is positive. Pilots have hovered on their first flight. Cooper ratings of 2 have been applied to the hover mode. The excellent characteristics in hover are due in part to the stabilization system and in part to the control sensitivity and control power provided. For hover the design calls for the following control powers expressed in radians per second squared: Yaw, 0.55; Roll, 1.01; Pitch up, 0.94; and Pitch down, 0.78. Measurements to date indicate that these values are being very nearly obtained. In the longitudinal axis the control power provided may be more than required. Control power used for hover in gusty wind conditions, in the vicinity of 20 to 25 knots, has not produced a noticeable effect on height control at thrust to weight ratios as low as 1.05. This thrust to weight ratio provides satisfactory single engine out safety.

The aircraft has been hovered with various combinations of SAS off from one-half off in one axis to full off in all axes. From this work it has been verified that the roll axis most requires augmentation and the need becomes less in the following order: pitch, yaw, and height. Pilots have assigned a Cooper rating of 6 to the all SAS off hover. By way of explanation each axis except the height axis is dualized and monitored such that a failure in one channel results in that axis locking out. In addition to damping, the pitch and roll axes have an attitude stabilization function which is selectable by the pilot. This mechanization is due to a specification requirement which calls for an instrument hover capability.

In the STOL configuration, the aircraft is much easier to handle than most conventional or STOL aircraft. Both take-off and landing are fuselage level maneuvers. For take-off, power is applied and without need for rotation the aircraft is airborne. For landing, the approach is established at a constant fuselage level altitude. Because of the excellent speed stability of the aircraft only very small changes in collective lever position are necessary to control the approach angle. With the wing completely immersed in the propeller slip stream, small increases or decreases in power produce instantaneous changes in lift and, therefore, cause immediate changes in glide slope angle. No flaring is necessary.

During STOL, and the transition maneuver previously discussed, SAS off operation displays the same characteristics as were observed during hover except that at lower wing angles the task becomes less demanding. This is to be expected since as a result of the simulator program SAS gains are progressively reduced, reaching zero at zero wing angle. The ease of converting

XC-142A ACCOMPLISHMENTS

LTV AEROSPACE CORPORATION
VOUGHT AERONAUTICS DIVISION

THRU 30 SEPTEMBER 1965

MAX SPEED TAS	386 KN	MAX GROSS WEIGHT	41,500 LB
MAX SPEED EAS	326 KN	MAX FORWARD C. G.	15% MGC
MAX ALTITUDE	25,000 FT	MAX AFT C. G.	28% MGC
MAX HOVER ALTITUDE (EAFB)	5,000 FT	MAX LATERAL SPEED	25 KN
MAX HOVER ASCENT RATE (EAFB)	1,800 FT/MIN	MAX REARWARD SPEED	20 KN
MAX RATE OF DESCENT	8,200 FT/MIN	MAX RATE CONVERSIONS	12 SEC
MAX RATE OF CLIMB (TO 25,000 FT IN LESS THAN 6 MIN)	6,400 FT/MIN	LONGEST FLIGHT TO DATE (DALLAS TO PHOENIX)	3.3 HR
		MAX NORMAL ACCELERATION	2.7 'G'

III-87

TABLE 1

and reconverting the XC-142A is possibly best illustrated by the fact that one of the three military pilots flew his first conversion with the SAS intermittently off throughout the maneuver.

During transition the control power available is equal to or more than the predicted values. Transitions in gusty wind conditions have been entirely satisfactory to the pilots.

In the conventional mode, with the wing down and on throttle control, i.e., the collective stowed, the XC-142A handles in a conventional manner. Maneuvering characteristics have been described as "crisp" by one military pilot. The stick rather than the column and wheel for longitudinal and lateral control and the aircraft response about any axis during conventional flight make the pilots feel like the XC-142A is a fighter rather than a transport.

An example of the envelope currently available to the military for the Category II program is given by the V-H diagram of figure 9. Many more points, not shown for clarity, have been flown within this envelope. The 80 percent structural data has been obtained, leaving the structural demonstration to 100 percent as the major work remaining to be accomplished.

If LTV has another V/STOL flight test program to conduct, and we hope we will, it will be planned in much the same manner as the XC-142A program.

XC-142A MILESTONES

LTV AEROSPACE CORPORATION
VOUGHT AERONAUTICS DIVISION

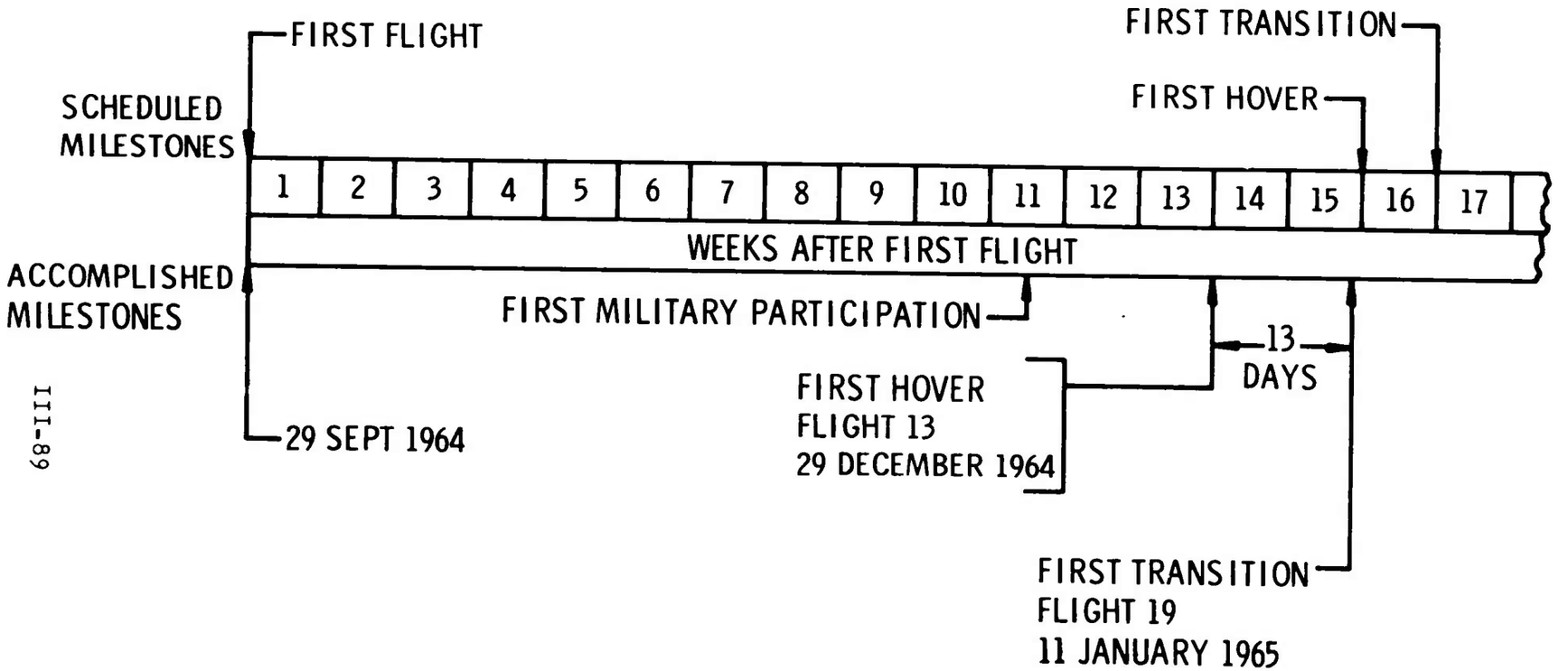

FIGURE 2

XC-142A vs DC-3
A SIZE COMPARISON

LTV AEROSPACE CORPORATION
VOUGHT AERONAUTICS DIVISION

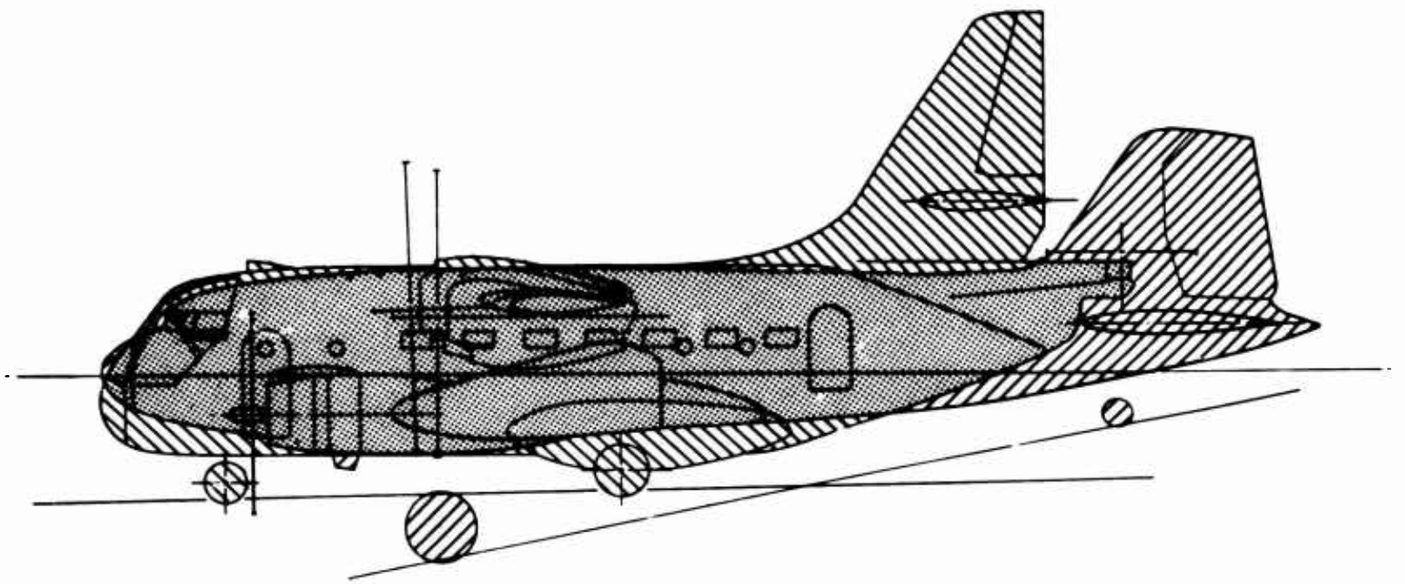

III-88

FIGURE 1

XC-142A TRANSMISSION SYSTEM

LTV AEROSPACE CORPORATION
VOUGHT AERONAUTICS DIVISION

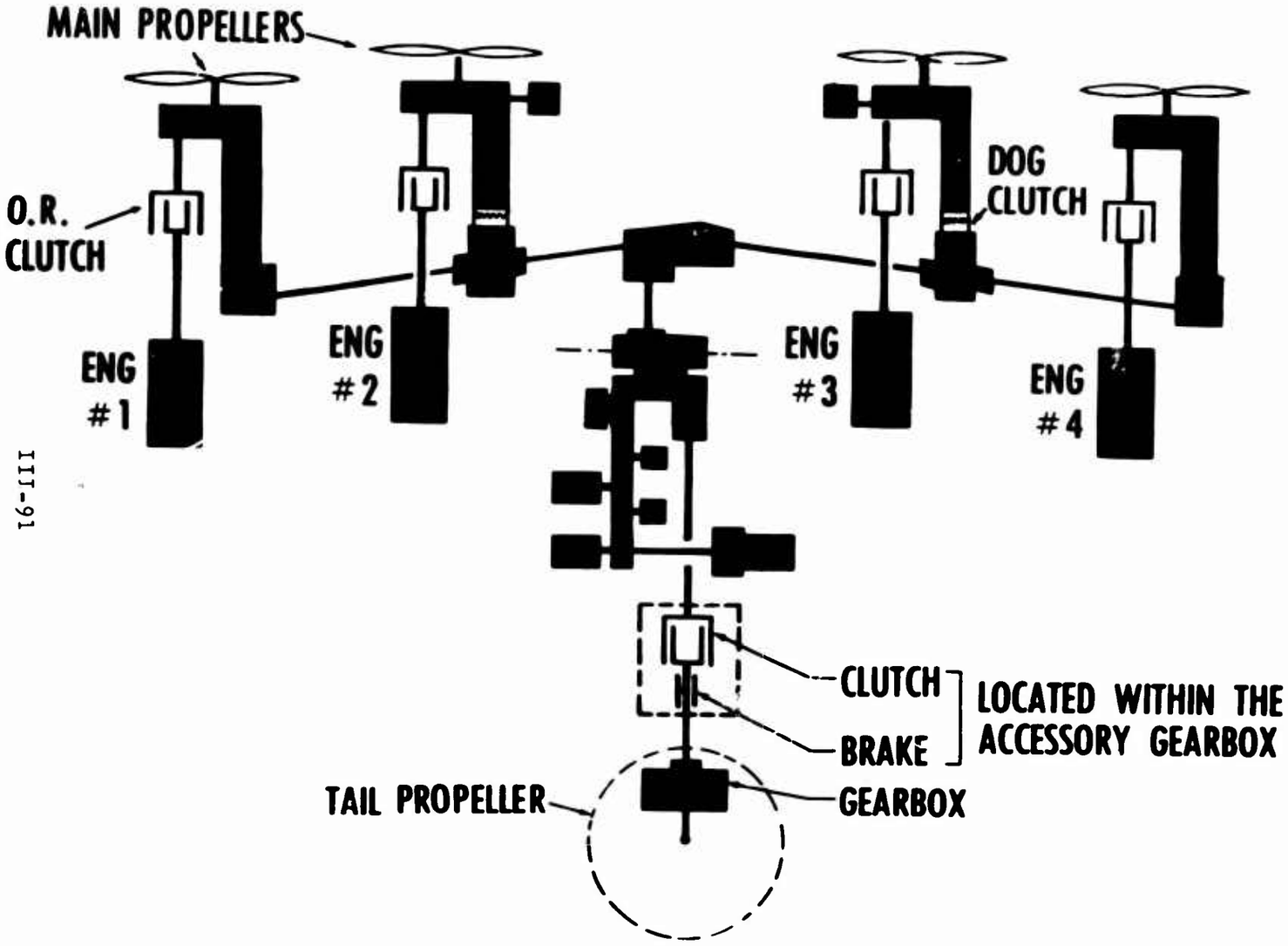

III-91

FIGURE 4

XC-142A FLIGHT TEST PROGRESS

LTV AEROSPACE CORPORATION
VOUGHT AERONAUTICS DIVISION

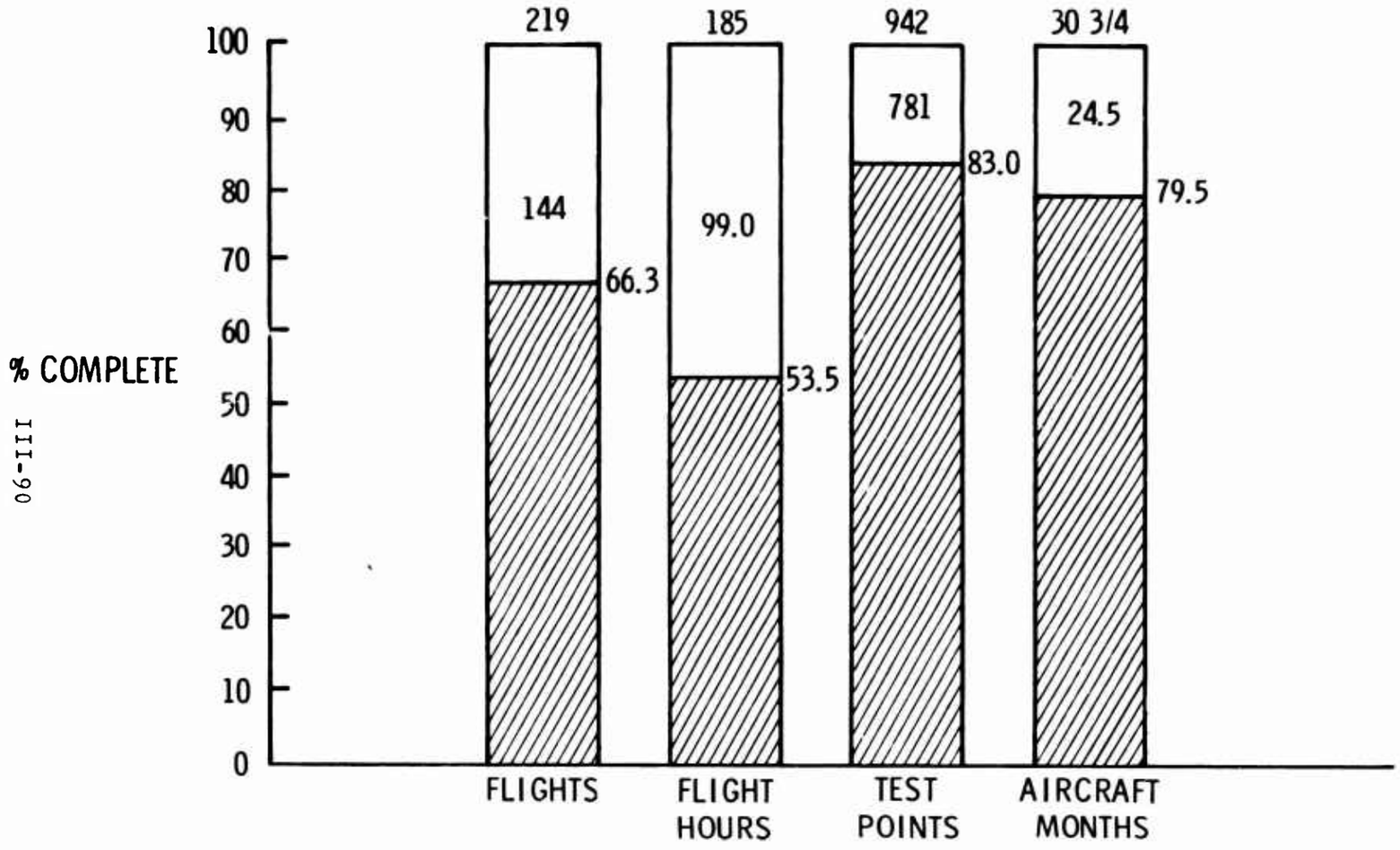

III-90

FIGURE 3

XC-142A CONVERSION UNACCELERATED FLIGHT

LTV AEROSPACE CORPORATION
VOUGHT AERONAUTICS DIVISION

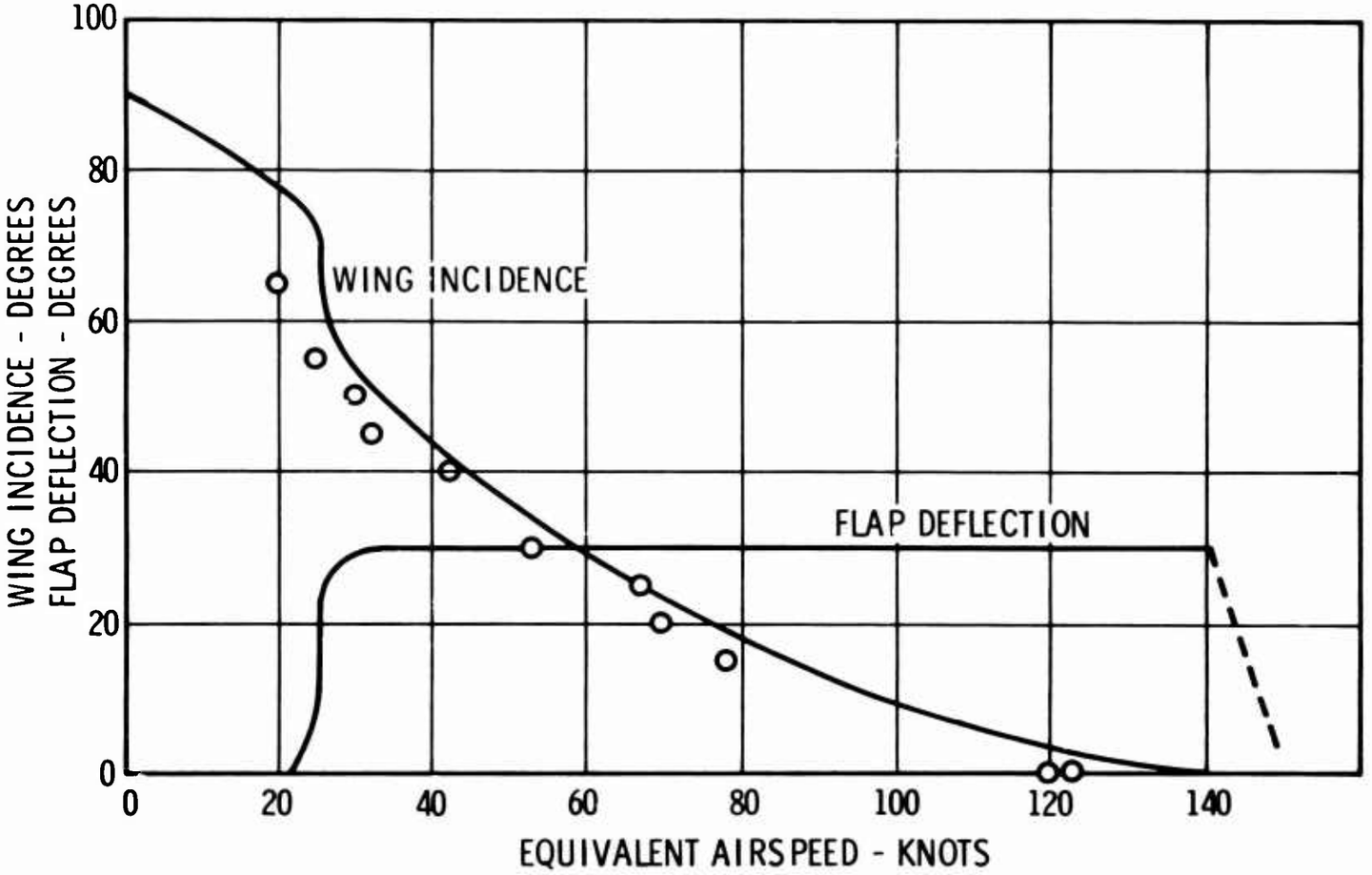

III-63

FIGURE 6

XC-142A FLIGHT CONTROL SIMULATOR

LTV AEROSPACE CORPORATION
VOUGHT AERONAUTICS DIVISION

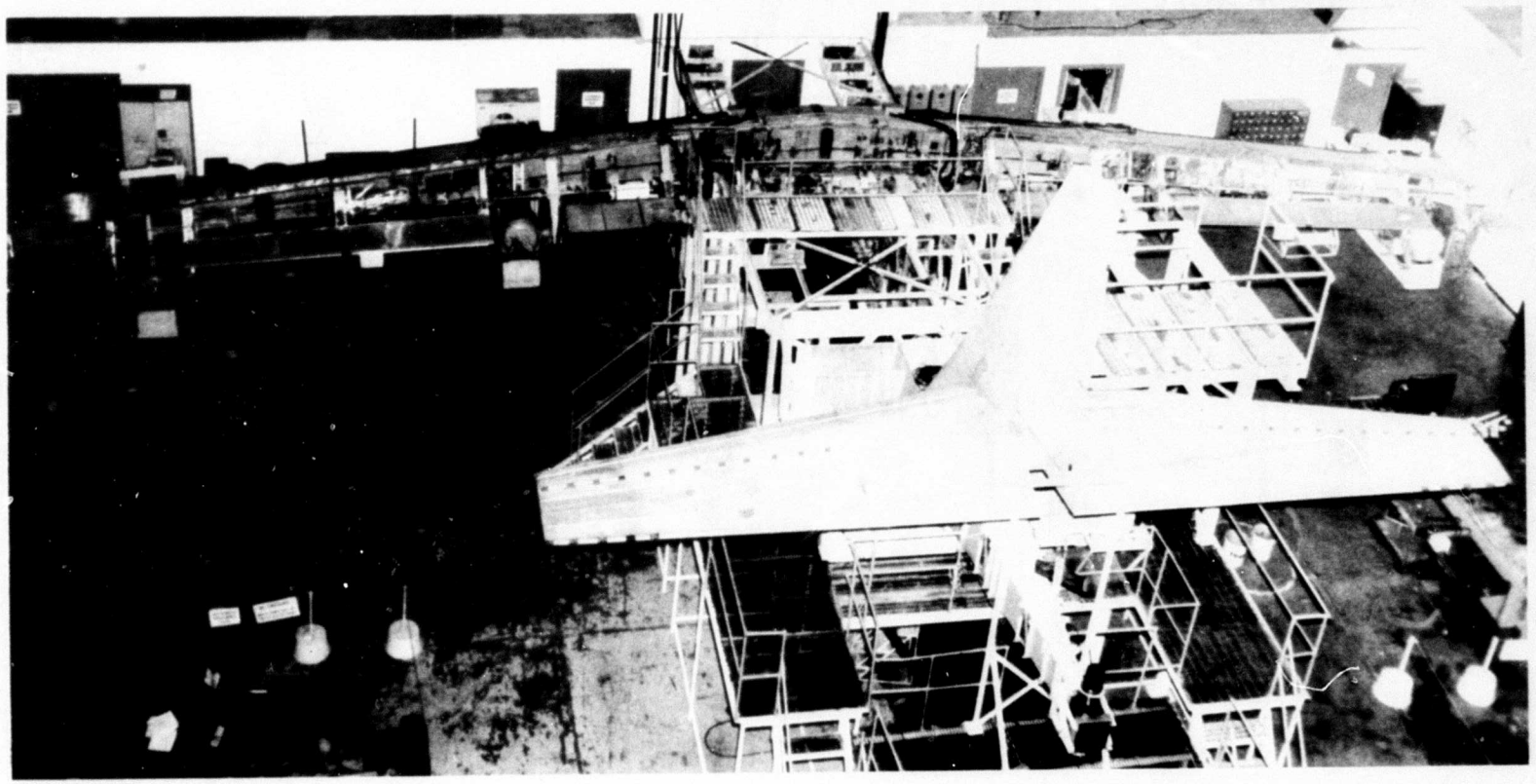

III-92

FIGURE 5

FIGURE 7

XC-142A RECONVERSION DESCENT BOUNDARY

LTV AEROSPACE CORPORATION
VOUGHT AERONAUTICS DIVISION

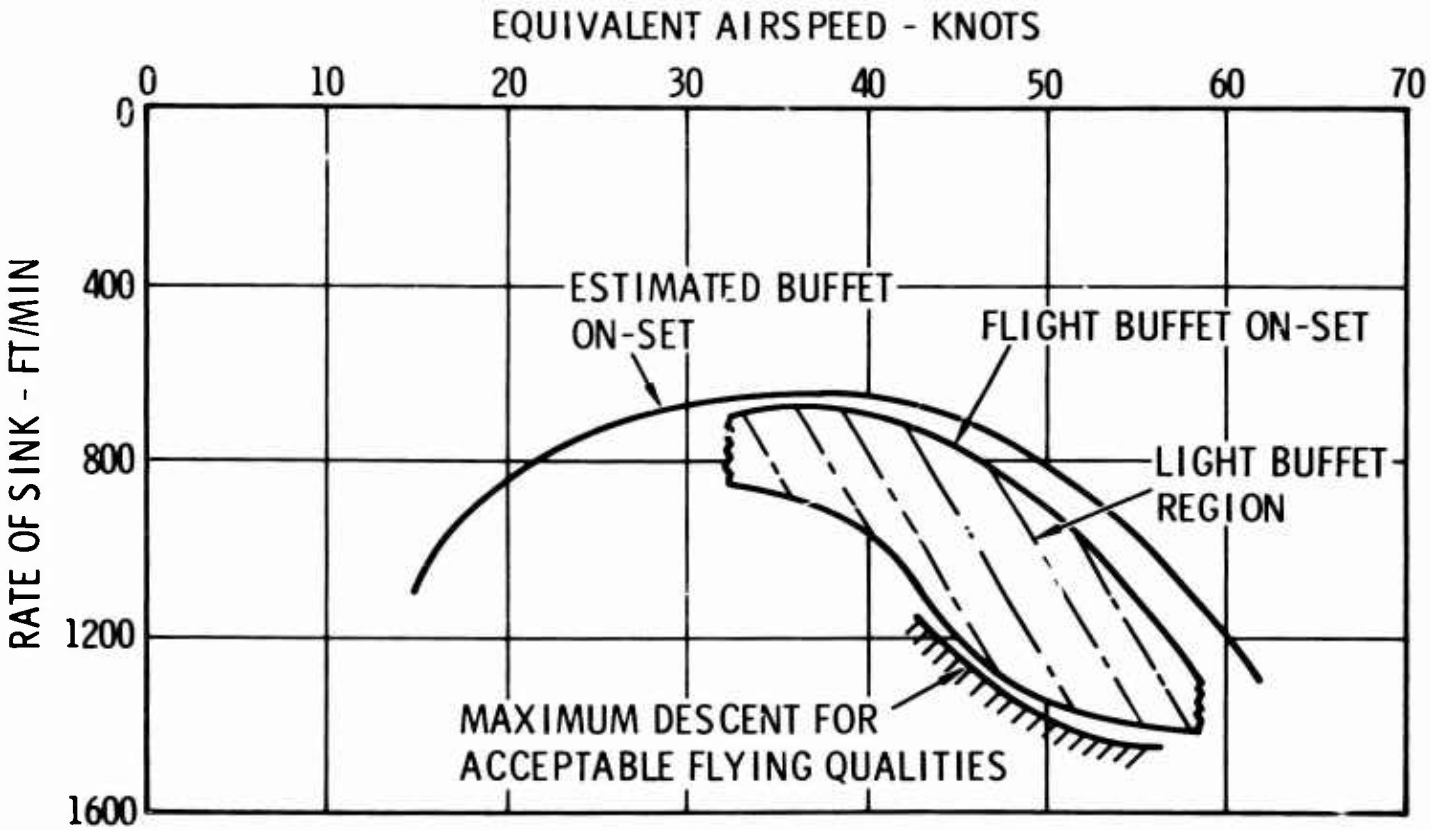

FIGURE 8

XC-142A
RECONVERSION
UNACCELERATED FLIGHT

LTV AEROSPACE CORPORATION
VOUGHT AERONAUTICS DIVISION

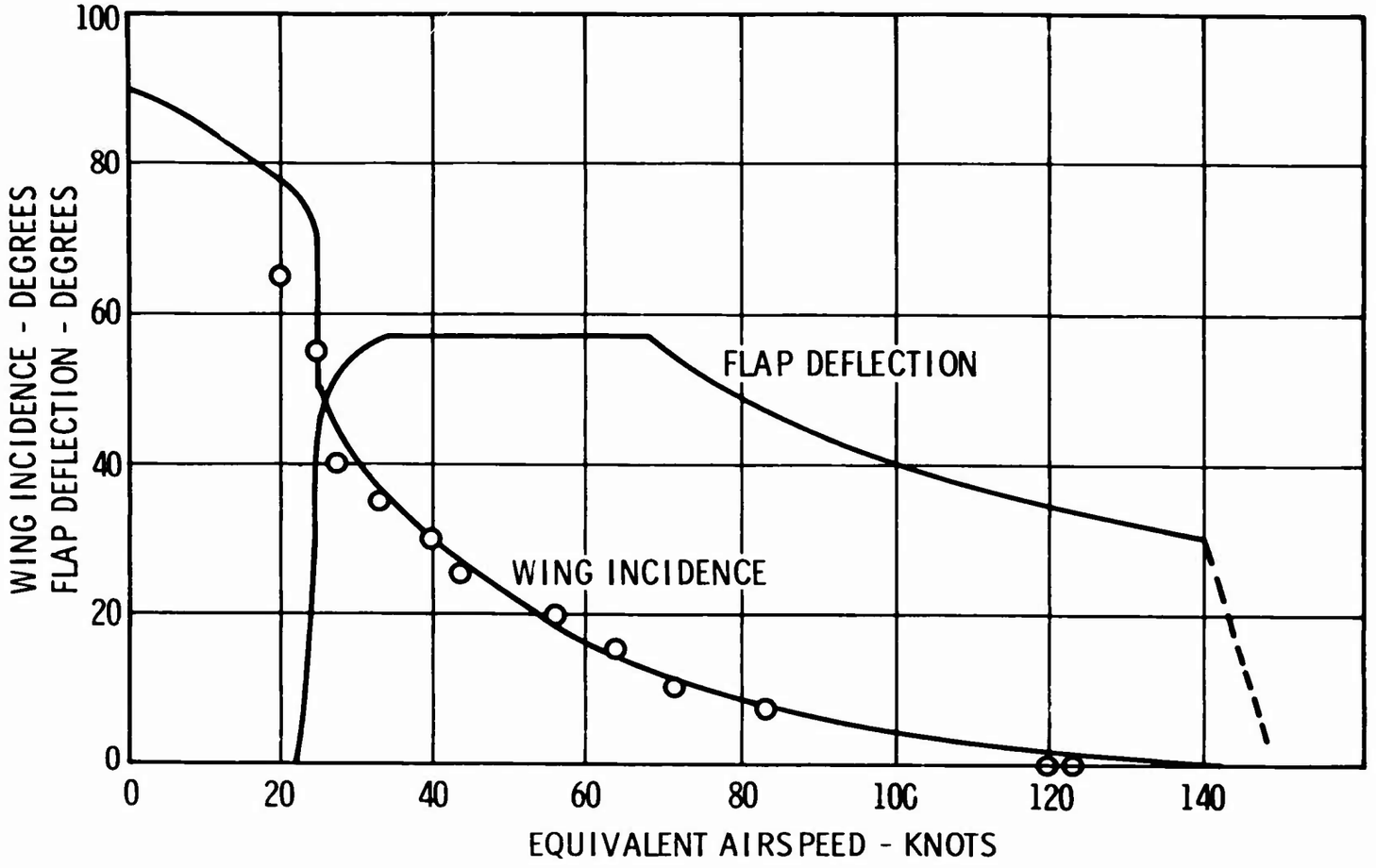

46-III

LIFT FAN, V/STOL

D. R. Geehring

S. H. Spooner

General Electric Company

(This paper was not received at press time. It is planned that this paper will be published and distributed at a later date.)

XC-142A OPERATIONAL ENVELOPE

LTV AEROSPACE CORPORATION
VOUGHT AERONAUTICS DIVISION

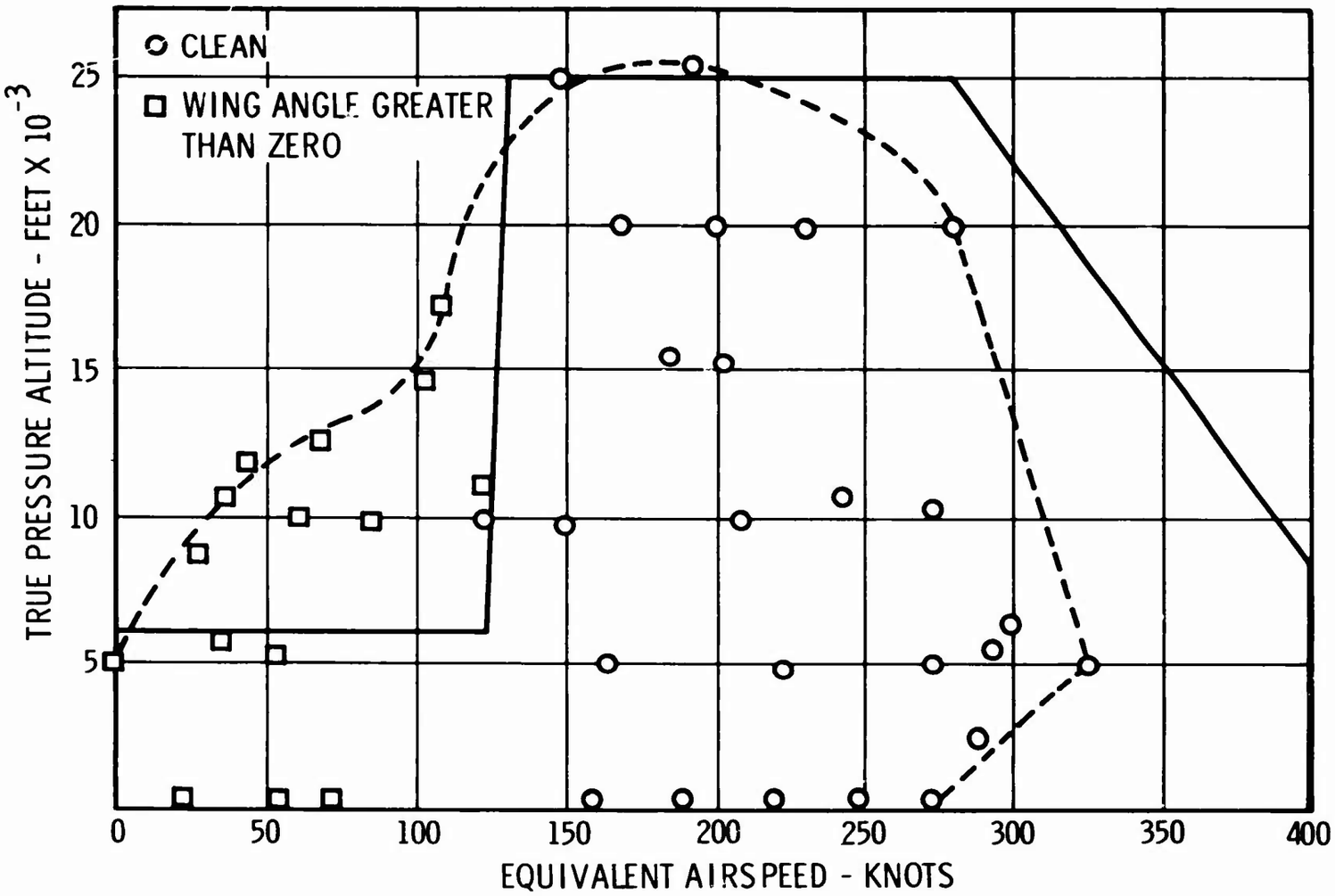

96-111

FIGURE 9

X-22A FLIGHT TEST PROGRAM

R. L. Pfeiff

Bell Aerosystems Company

(This paper was not received at press time. It is planned that this paper will be published and distributed at a later date.)